Screening, Optimization of Process Parameters and Scale-Up of Native and Recombinant Thermophilic Xylanases and Their Application in Chicken Feed Hydrolysis

by Priyashini Dhaver

Submitted in fulfilment of the academic requirements of Doctor of Philosophy in the Discipline of Microbiology School of Life Sciences, College of Agriculture, Engineering and Science University of KwaZulu-Natal Durban, South Africa

PREFACE

The research contained in this thesis was completed by the candidate while based in the Discipline of Microbiology, School of Life Sciences of the College of Agriculture, Engineering and Science, University of KwaZulu-Natal, Westville Campus, South Africa, under the supervision of Dr. R. Govinden and the co-supervision of Prof. B. Sithole and Prof. B. Pletschke. The research was financially supported by the Technology and Innovation Agency (TIA) and the Centre for Scientific and Industrial Research (CSIR).

The contents of this work have not been submitted in any form to another university and, except where the work of others is acknowledged in the text, the results reported are due to investigations by the candidate.

Dr. R. Govinden

Date: 20/11/2023

Prof. B. Sithole

Date: 20 November 2023

Prof. B. Pletschke

Date: 20/11/2023

DECLARATION 1: PLAGIARISM

I, Priyashini, declare that:

(i) the research reported in this thesis, except where otherwise indicated or acknowledged, is my original work;

(ii) this thesis has not been submitted in full or in part for any degree or examination to any other university;

(iii) this thesis does not contain any other persons' data, pictures, graphs or other information, unless specifically acknowledged as being sourced from other persons;

(iv) this dissertation does not contain other persons' writing, unless specifically acknowledged as being sourced from other researchers. Where other written sources have been quoted, then:

a) their words have been re-written but the general information attributed to them has been referenced;

b) where their exact words have been used, their writing has been placed inside quotation marks, and referenced;

(v) where I have used material for which publications followed, I have indicated in detail my role in the work;

(vi) this thesis is primarily a collection of material, prepared by myself, published as journal articles or presented as a poster and/or oral presentations at conferences. In some cases, additional material has been included;

(vii) this dissertation does not contain text, graphics or tables copied and pasted from the Internet, unless specifically acknowledged, and the source being detailed in the in the References sections.

Signed: Priyashini Dhaver

Date: 20 November 2023

DECLARATION 2: PUBLICATIONS

My role in each paper and presentation is indicated. The * indicates the corresponding author.

CHAPTER 2

Dhaver, P.*, Pletschke, B., Sithole, B. & Govinden, R. (2022). Isolation, screening and partial optimization of thermostable xylanase production under submerged fermentation by fungi in Durban, South Africa. *Mycology*. 13(4): 271-292. doi.org/10.1080/21501203.2022.2079745

Published online: 20 June 2022

This paper is a research chapter based on the isolation and screening of xylanases, the analysis of data was conducted and written by Dhaver, P.

CHAPTER 3

Dhaver, P.*, Pletschke, B., Sithole, B., Govinden, R. (2022). Optimization, purification, and characterization of xylanase production by a newly isolated *Trichoderma harzianum* strain by a two-step statistical experimental design strategy. *Scientific Reports*. 12, 17791. doi.org/10.1038/s41598-022-22723-x

Published online: 18 October 2022

The scope of this chapter was the optimization of xylanase production using statistical methods, purification and characterization of the xylanase. The laboratory work, data analysis and writing of the manuscript was carried out by Dhaver, P.

CHAPTER 4

Dhaver, P.*, Sithole, T., Pletschke, B., Sithole, B., & Govinden, R. (2023). Enhanced production of a recombinant xylanase (XT6): Optimization of production and purification, and scaled-up batch fermentation in a stirred tank bioreactor. Manuscript ID: 9705f889-cf4b-470f-8596-95c611d456c2

Date of submission: 15 August 2023

Date of corrections received for possible acceptance: 26 October 2023

The scope of this chapter was the optimization of cell lysis and expression of the recombinant XT6 xylanase using statistical methods, its purification and scaled-up production in 5-L bioreactors. The laboratory work, data analysis and writing of the manuscript was carried out by Dhaver, P. Assistance with bioreactors included the help of interns at the Technology Innovation Agency (TIA).

CHAPTER 5

Dhaver, P, Pletschke, B., Sithole, B., & Govinden, R*. (2023). Optimization of the production of xylooligosaccharides by native and recombinant xylanases from chicken feed substrates, and toxicity testing. Manuscript ID: ijms-2708967

Date of submission: 25 October 2023

Date of corrections received for possible acceptance: 17 November 2023

The scope of this chapter was the optimization of chicken feeds hydrolysis by xylanases using Response surface methodology followed by toxicity testing of the hydrolysates on human embryonic kidney cells. The laboratory work, data analysis and writing of the manuscript was carried out by Dhaver, P. The analysis (HPLC) of hydrolysis products was carried out by Dr Adarsh Puri in the department of Biotechnology at the Durban University of Technology, Steve Biko campus. The toxicity studies were carried out by Dhaver, P with the assistance of Prof Niesler and Dr Ray Hewer in the Department of Biochemistry, at the Pietermaritzburg campus, UKZN.

CHAPTER 4- Was presented at the Postgraduate Research and innovation Symposium (PRIS) 2022 and won third place for the School of Life Science, Flash presentations. Certificate attached.

CHAPTER 5- Was presented at PRIS 2023 and won first place for the School of Life Science, Flash presentations. Certificate attached.

Signed: Priyashini Dhaver

Date: 20 November 2023

ABSTRACT

Lignocellulosic biomass is a renewable raw material that has gained industrial interest due to its abundance, low cost, and potential to mitigate greenhouse gas emissions. Biomass is treated with various microbial enzymes to produce desired products under ideal conditions. Thermophilic microorganisms are excellent sources of thermostable enzymes that can tolerate extreme conditions. Optimized xylanases can be produced through genetic engineering, and recombinant DNA techniques. The biotechnological potential of xylanases from thermophilic microorganisms is discussed and the ways they are being optimized and expressed for industrial applications. Monogastric animal farming relies on grain feedstocks with non-starch polysaccharides (NSP's) and anti-nutritive factors that cause adverse effects like increased digesta viscosity and nutrient inaccessibility which leads to reduced feed conversion, energy metabolism, and growth. Exogenous enzymes have been used to reduce viscosity and increase nutrient absorption in poultry and pigs. Xylooligosaccharides (XOS) are functional feed additives that are attracting growing commercial interest due to their ability to modulate the composition of the gut microbiota. This study aimed to isolate and screen potential xylanolytic fungi from soil and tree bark samples in South Africa and to determine their growth conditions for maximum xylanase production. The highest xylanase activity was produced by *Trichoderma harzianum.* The enzyme with a molecular weight of 72 kDa retained >70% activity after 4 h at pH 6.0 and 70°C. The study also identified multiple isoforms of xylanase, which could be beneficial for animal feed and biofuel industries. The xylanase was purified from the submerged culture and displayed maximum xylanolytic activity at pH 6.0 and 65°C and the enzyme was activated by Fe^{2+}, Mg^{2+}, and Zn^{2+}. Enzyme production was then optimized for maximal xylanase production strain using the Plackett-Burman Design (PBD) and Box Behnken Design (BBD), screening, and optimization design strategies, respectively. Xylanase

production was enhanced to 153.80 U/ml by BBD representing a 3.99-fold increase and a 2.24-fold increase, respectively compared to the preliminary one-factor-at-a-time (OFAT) activity of 68.7 U/ml. The experimental design effectively provided conditions for the production of an acidic enzyme based on pH and incubation time. This is an exciting prospect for the application of enzymes in animal feed improvement (pH 5.0). The *Geobacillus stearothermophilus* glycoside hydrolase family 10 xylanase, endoxylanase XT6, is a promising candidate for industrial application. This gene was cloned and expressed and the xylanase was applied as an additive to locally produced chicken feeds. Optimization of cell lysis and expression conditions led to enhanced recombinant XT6 xylanase production. The recombinant XT6 xylanase was purified using cobalt chromatography, resulting in a 43 kDa protein with 15.69-fold purity. Cellulose, hemicelluloses, and lignin are the primary sources of fermentable sugars in lignocellulosic feedstock. Carbohydrate-active enzymes which can help release functional compounds from the carbohydrate matrix, such as phenolics are used to modify polysaccharides for industrial purposes. However, it should be noted that the primary action of carbohydrate enzymes like cellulases or xylanases is specific to the carbohydrate structure and may involve the hydrolysis of polysaccharides like xylan or other complex carbohydrate-lignin compounds, rather than being directly responsible for the release of phenolic compounds. Corn, with its antioxidant potential, is used in animal feed production, thus improving its quality for animal feed supplementation is crucial.

The crude and purified *T. harzianum* xylanases as well as the recombinant XT6 xylanase were applied to locally produced chicken feeds in an experimental BBD design to optimize hydrolysis to monosaccharides and XOS. The Response Surface Methodology (RSM) results showed that higher (8.05 U/ml) levels of reducing sugars were produced for the crude *T. harzianum* xylanase and starter feed, than on the grower feed (3.11 U/ml). Treatment with the

purified *T. harzianum* and recombinant XT6 xylanases produced lower levels of reducing sugars with similar levels for both feed types of starter feed (2.81 U/ml) and (2.98 U/ml), compared to the grower feed (2.41 U/ml) and (2.62 U/ml), respectively. Profiling of the hydrolysis products by thin-layer chromatography (TLC) and high-performance liquid chromatography (HPLC) revealed that the chicken feed enzymatic hydrolysates contained a range of monosaccharides (mannose, glucose and galactose) and XOS, with xylobiose being the predominant XOS. Toxicity studies showed that the higher dilutions of the feed enzymatic hydrolysates were not toxic to HEK293 cells. Therefore, the *T. harzianum* and recombinant XT6 xylanase are appropriate for application in the feed industry to produce XOS. These results are promising for future studies and application in the poultry feed industry as additives. The novelty of this study was the identification and characterization of a thermostable xylanase from a South African *T. harzianum* isolate, the application of experimental design to optimize its production and as well as that of a recombinant XT6 xylanase. The recombinant XT6 xylanase exhibited high yields in bioreactor production with activity superior to that of a commercial xylanase preparation, further emphasizing its potential for commercialization through scaling-up techniques and its industrial application. Moreover, the enzymes investigated in this research hold promise for the production of prebiotics in animal feed applications.

ACKNOWLEDGEMENTS

I am grateful to have reached this significant milestone, and there are numerous individuals who deserve recognition for their unwavering support, inspiration, and guidance throughout my PhD journey. Firstly, I would like to express my deepest gratitude to God for granting me the strength, wisdom and patience to pursue and successfully complete my PhD degree. I would like to express my profound appreciation to my supervisor, Dr Roshini Govinden, whose unwavering support, encouragement and insightful suggestions have been instrumental in the completion of this thesis. I would like to express my gratitude to my co-supervisors, Professor Brett Pletschke and Professor Bruce Sithole, for their guidance, expertise, and support throughout my PhD journey. Your commitment and dedication to my academic and professional development helped shape my research and personal growth in equal measure. I am indebted to the funders, Technology Innovation Agency (TIA), CSIR, Prof Bruce Sithole, Dr Roshini Govinden and Prof Brett Pletschke whose generous financial support not only enabled me to undertake this research project but also allowed me to broaden my educational opportunities, thereby empowering me to grow both personally and professionally. I would like to thank the following academics for their assistance; Dr Hewer, Prof Niesler and the students at UKZN PMB campus for assistance with toxicity studies; Dr Adarsh Puri and team at DUT for assistance with HPLC; and TIA platform, Vuyi and Vukile Zulu for their help with the bioreactors. To my beloved parents, thank you for being my constant source of motivation, love, and emotional support. To my special someone, Shravan, thank you for understanding, supporting, and believing in me. Your unwavering love, patience, occasional humour, and countless moments of encouragement and support played a significant role in keeping me sane through the research process and in achieving this significant milestone. I'm also appreciative of the supportive community that I worked with - my peers and colleagues from the

microbiology department, who helped me to discuss and troubleshoot many research ideas and challenges. Thank you to my lab colleague and friend, Nivisti, your unwavering support, and encouragement have been pivotal in keeping me motivated. Last but not least, I would like to express my gratitude to my best friends; Leah and Deveshni, whose outstanding support, love, and humour kept me sane, provided a break from the rigors of research, and made the long journey worthwhile.

TABLE OF CONTENTS

LIST OF FIGURES

LIST OF TABLES

CHAPTER ONE

INTRODUCTION AND LITERATURE REVIEW

1.1 Introduction

Enzymes are present in animals, plants, and microorganisms. However, due to the short life cycles, low fermentation costs, high concentrations of enzymes that may be acquired by genetic manipulation, and the diversity of enzymes available that catalyze the same reaction, microbes as an enzyme source are a favourable option [1]. Enzymes are biocatalysts containing globular tertiary or quaternary protein structures. The structural components of proteins are α-L-amino acids, except glycine, which is not chiral [2]. Enzymes comprise long chains of amino acids with peptide bonds and can react with the substrates in various ways, under moderate temperature and pH conditions [3]. One of the most essential aspects in determining a process's economics is the cost of an enzyme. However, in the industrial sector, the key objective of the research is to lower the enzyme production costs by optimizing the fermentation medium.

1.2 Structure of xylan and function of xylanolytic enzymes

1.2.1 Xylan and its Structure

Hemicelluloses, the second most abundant terrestrial polysaccharide, are located in the middle lamella and cell walls of plant cells and are known as hemicelluloses. Hemicellulose includes a variety of polysaccharides, specifically non-cellulosic, composed of monosaccharide units in different proportions [4]. Classes of hemicellulose are named according to their main sugar unit. Xylan is a homopolysaccharide having acetyl, -O-methyl-D-glucuronosyl, and α-

arabinofuranosyl residues attached to the backbone of β-1,4 linked xylopyranose units with binding qualities that mediate interactions (covalent and non-covalent) with cellulose, lignin, as well as other polymeric materials (Figure 1.1) [5]. Xylans are categorized into glucuronoxylan in hardwoods and arabinoxylan and glucuronoarabinoxylan in grasses. Arabinoxylans have their main chain substituted with α-arabinosyl residues, while glucuronoxylans have 4-O-methyl glucuronic acid linked by α-(1→2) linkages. Glucuronoarabinoxylans consist of 1,4-linked-β-D-xylose residues with heterogenous substitutions. Hydrolysis of the xylan backbone is achieved by the synergistic action of β-xylosidase (EC 3.2.1.37) and endoxylanase (EC 3.2.1.8) activities. β-Xylosidase hydrolyses xylooligosaccharides from the non-reducing ends to produce xylose while endoxylanase cleaves the β-bonds in the xylan main chain polysaccharides and liberate a mixture of xylooligosaccharides [4]. Accessory enzymes such as feruloyl esterase (EC 3.1.1.73), acetyl xylan esterase (EC 3.1.1.72), *p*-coumaric esterase (EC 3.1.1.B10), α-arabinofuranosidase (EC 3.2.1.55), and α-glucuronidase (EC 3.2.1.139) are required for the complete saccharification of the xylan molecule. The action of α-glucuronidase and acetyl xylan esterase removes the acetyl and phenolic side branches. The elimination of side groups is catalyzed by α-L-arabinofuranosidases. The action of *p*-coumaric esterase and ferulic acid esterase cleaves the ester bonds on the xylan. [7,8,9]. The structure of xylan illustrating the bonds that are attacked by hemicellulolytic enzymes for the complete hydrolysis of xylan to its constituent monomeric units is represented in Figure 1.2. The xylanolytic system exists in bacteria, fungi, and actinomycetes.

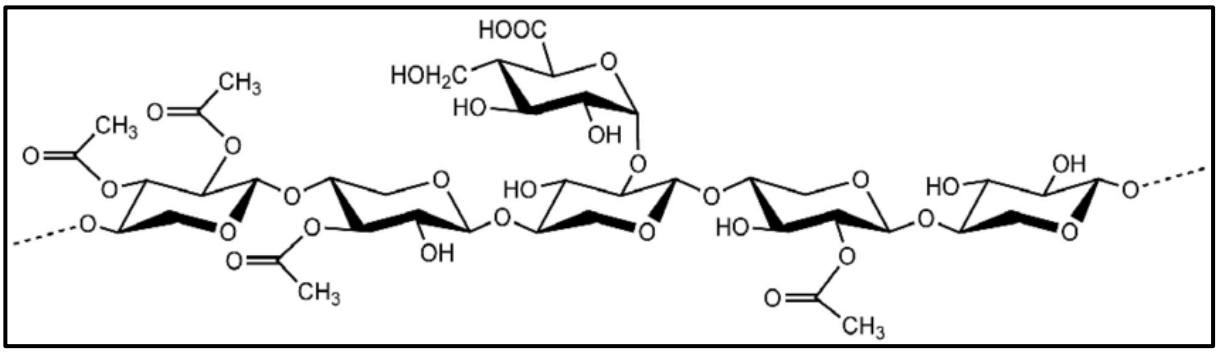

Figure 1.1: Molecular structure of xylan [modified from 6].

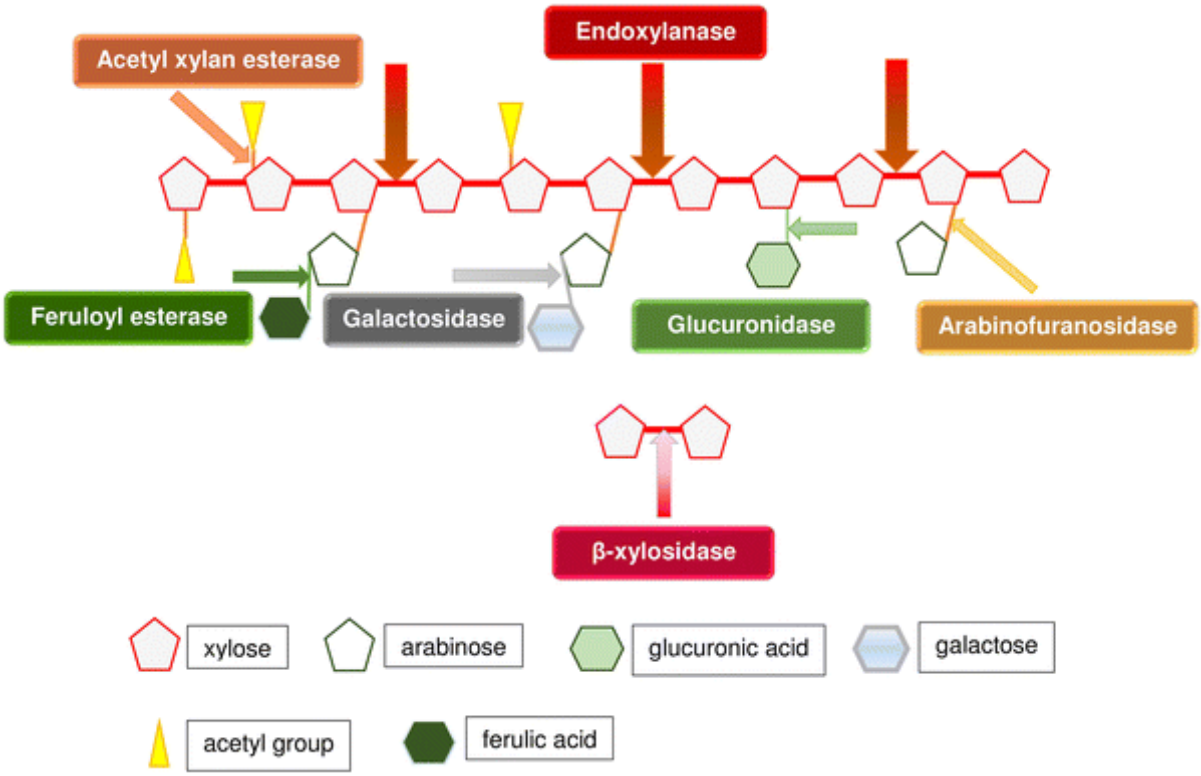

Figure 1.2: Schematic overview of hemicellulose and cleavage sites of hemicellulose-degrading enzymes [modified from 10].

1.2.2 Xylanases

Xylanases are a unique group of enzymes that break down xylan. These enzymes can cleave the xylan chain in a random manner, which causes a reduction in the degree of polymerization of the substrate and liberates shorter oligomers, xylobiose, and xylose, as shown below in Figure 1.3 [12].

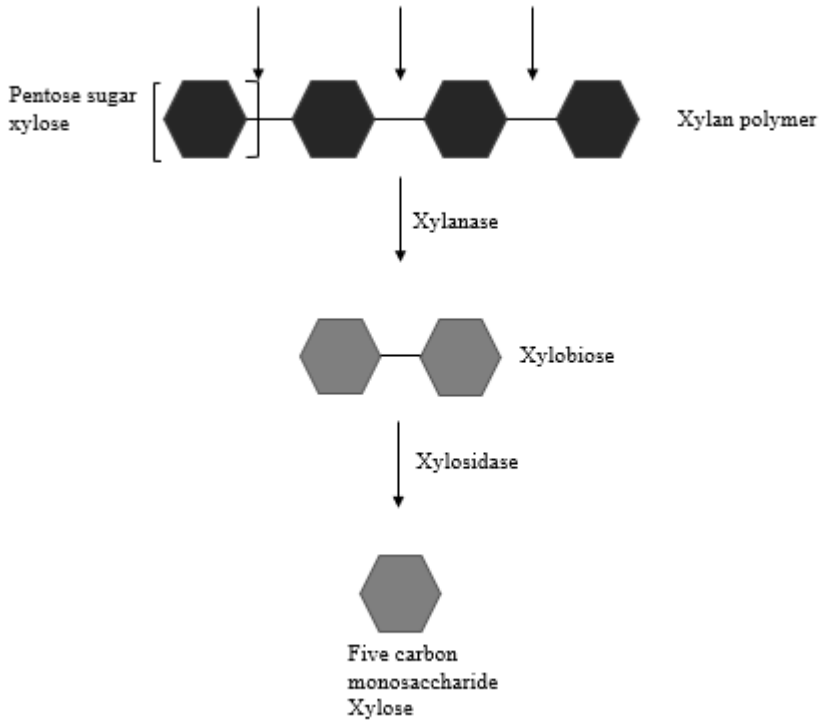

Figure 1.3: A modified xylanolytic enzyme scheme breaks down xylan to xylose. Bonds between xylose structures are β-1,4 linkages [13].

1.2.3 Classification of xylanases

Xylanases may be divided into three classes based on their kinetic and/or catalytic properties, isoelectric point, and molecular weight [14]. Over the years a variety of xylanases have evolved due to the complex composition of xylans. The evolution of the classification system was inadequate; therefore, a more complete form of classification was required and established. The primary structure of the catalytic domain aided in classification, and the enzymes that share similar sequences have been grouped [15]. The genomic, functional, and structural information of xylanase is available on the carbohydrate-active enzyme (CAZy) database under glycoside hydrolase (GH) families [15]. The hydrophobic cluster analysis of the catalytic domains and related investigations of amino acid sequences are used to identify the key GH families

associated with xylanases [7]. Xylanases are divided into two groups: GH families 10 (GH10) and 11 (GH11). Xylanolytic activities have also been discovered in other classes.

1.3 The mechanism of action of xylanases belonging to multiple GH families

Members of the GH families have a variety of action mechanisms, physiochemical characteristics, substrate specificities, and structures. Retention and inversion are two modes of action by which xylanases hydrolyze xylan [16].

1.3.1 Retention as a mode of action

As seen in Figure 4, this process is represented by a 2-fold displacement mechanism, with the synthesis of α-glycosyl and oxo-carbonium intermediates followed by hydrolysis [17]. The catalytic mechanism relies heavily on glutamate residues. First, two carboxylic acid residues in the active site result in the production of α-glycosyl enzyme intermediate. A carboxylic acid residue forms the intermediate as an acid catalyst protonating the substrate and causing the leaving group to move due to a nucleophilic attack generated by another carboxylic acid. Due to the production of α-glycosyl enzyme intermediates, this leads to the β to α inversion. Second, the first carboxylate group abstracts a proton from a nucleophilic water molecule and attacks the anomeric carbon, resulting in the second substitution, where the anomeric carbon gives rise to a product with the configuration (to inversion) via an oxo-carbonium ion transition state [18], as shown in Figure 1.4. Enzymes from families 5, 7, 10, and 11 mostly act on the retention principle.

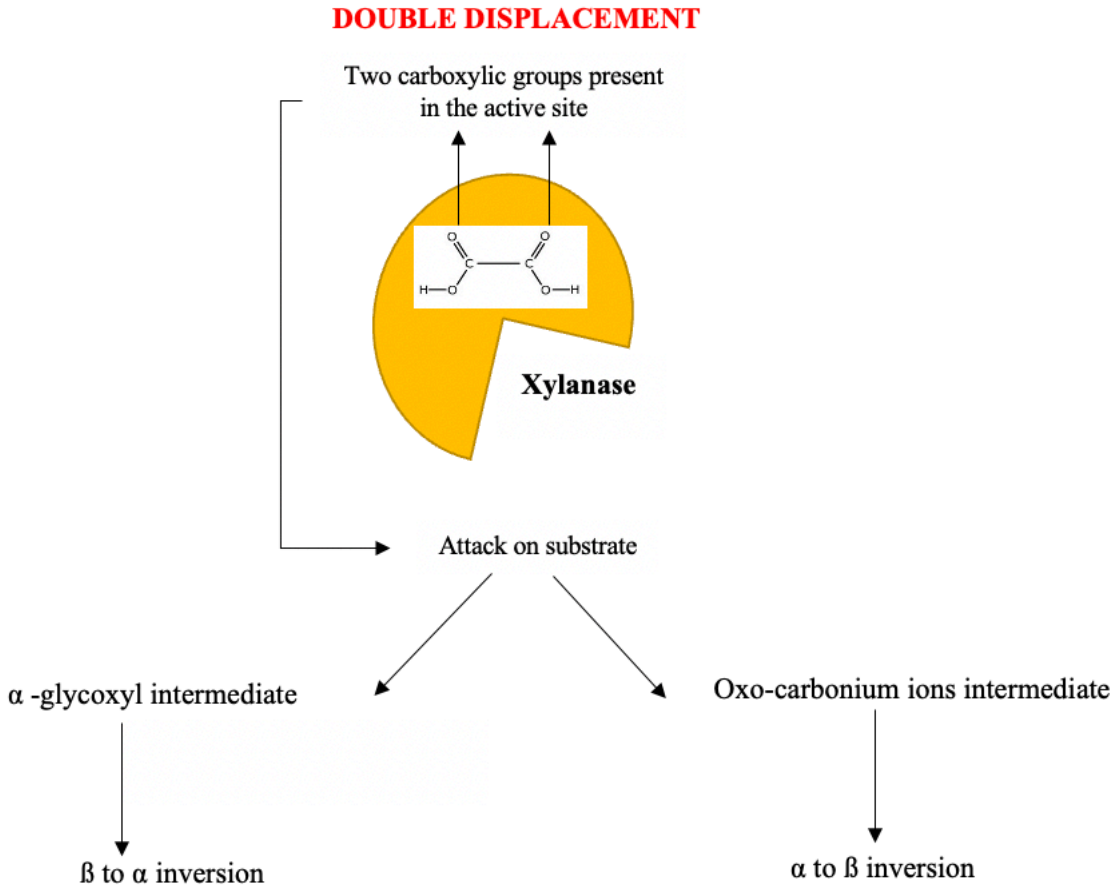

Figure 1.4: A modified scheme of the mode of action: Retention [17].

1.3.2 Inversion as a mode of action

Families 8 and 43 enzymes work by inverting the anomeric core, with glutamate and aspartate as the primary catalytic residues. Figure 1.5 shows this is a single displacement mechanism in which only one carboxylate ion is available for total acid-catalyzed group departure [17]. This enzyme also serves as a base for activating a nucleophilic water molecule to attack the anomeric carbon, disrupting glycosidic bonds and inducing an inversion of anomeric carbon configuration (depending on the distance between the two molecules) [7,18].

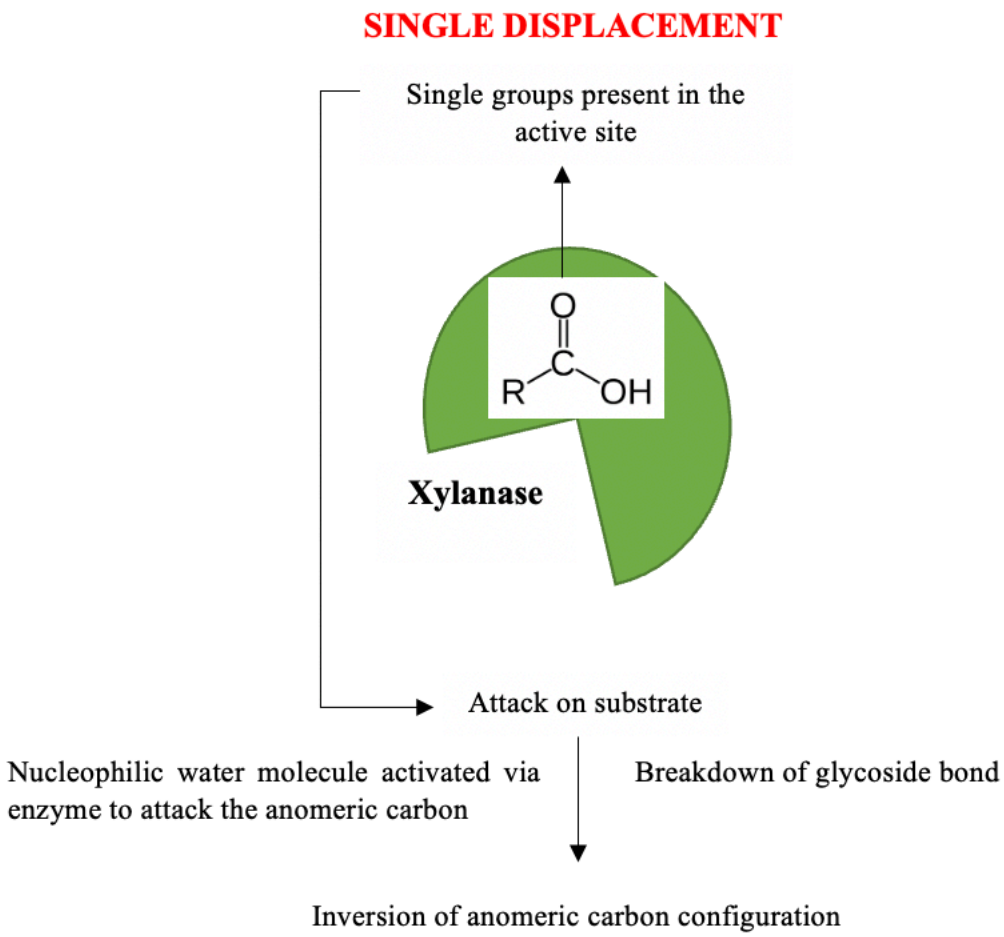

Figure 1.5: A modified scheme of the mode of action: Inversion [17].

Family GH10 comprises endo-2,4-β-xylanases and endo-1,3-β-xylanases [19]. The aryl β-glucosides of xylobiose and xylotriose can likewise be hydrolyzed at the aglyconic linkage by members of this family. Structural analysis shows that members of this family have 4-5 substrate-binding sites, high molecular mass, a low pI, and display an α/β barrel fold [7]. GH11 comprises xylanase with high pI and low molecular weight and a catalytic mechanism similar to that of the GH10 family. Studies show high substrate selectivity and catalytic efficiency [20,21]. These enzymes can hydrolyse the aryl-β-glycosides of xylobiose and xylotriose at the aglyconic bond; however, they are inactive on aryl cellobioses [22,23]. In lignocellulosic matrices, xylan is closely associated with cellulose fibrils and lignin.

To some extent, xylan covers the fibre surfaces, thereby limiting the access of cellulases to the cellulose surface [24]. It has been reported that enzymatic removal of xylan enhances cellulose hydrolysis by removing xylan covering or entrapping cellulose. The addition of xylanases has been shown to significantly improve cellulases' performance and increase cellulose conversion of many lignocellulosic materials. Thus, the solubilization of xylan in lignocellulosic materials is important for efficient enzymatic hydrolysis [24].

1.4 Microbial Sources

Xylanases are ubiquitous and present in diverse living organisms such as bacteria, fungi, yeast, insects, etc. [8]. Bacteria and fungi have been reported as notable species for producing high levels of xylanases [25,26]. Filamentous fungi can thrive on recalcitrant substrates. These species of fungi display a diverse group of enzymes required for the hydrolysis and utilization of complex organic substrates [27]. Previous studies have shown that fungal xylanases displayed higher activity and were produced in higher concentration than bacterial xylanases. Table 1.1 lists several microbiological sources of xylanase.

Table 1.1: Xylanases from microbial sources

Microorganisms that produce xylanase			
Main types	**Genus**	**Species**	**References**
Bacteria			
	Bacillus	*Bacillus subtilis, Bacillus stearothermophilus, Bacillus firmus, Bacillus licheniformis, Bacillus amyloliquifaciens, Bacillus arseniciselenatis*	[28], [29], [30], [31], [32]
	Pseudomonas	*Pseudomonas* sp., *Pseudomonas aeruginosa, Pseudomonas fluorescens* subsp. *cellulase, Pseudomonas boreopolis, Pseudomonas stutzeri*	[33], [34], [35], [36]
Fungi			
	Thermomyces	*Thermomyces lanuginosus*	[37]
	Aspergillus	*Aspergillus niger, Aspergillus flavus, Aspergillus niveus, Aspergillus ochraceus, Aspergillus foetidus, Aspergillus terreus, Aspergillus tamarii, Aspergillus fumigatus*	[38]
	Trichoderma	*Trichoderma harzianum, Trichoderma viride*	[39], [40]
Actinomycetes	*Streptomyces*	*Streptomyces lividans, Streptomyces* sp.	[41]

1.5 Strategies used for xylanase production

The fermentation procedure utilized, the substrate used, and the various media components impact xylanase production. Table 1.2 shows the production methods, distinctive traits, and applications of xylanases from various organisms.

1.5.1 Fermentation processes employed for xylanases production

Different fermentation procedures such as submerged fermentation (SmF) and solid-state fermentation (SSF) involving diverse microorganisms are used to produce xylanases. The technique chosen is determined by the producer microorganisms. The SmF process involves growing microorganisms in a liquid medium composed of the required nutrients. Various agro-wastes such as rice or wheat bran can be used as nutrient media, or defined chemical components can be used, either in the dissolved or suspended form in liquid [42,43]. Bacteria usually require high amounts of water, therefore, SmF is usually preferred. The benefits of SmF include the uniform conditions across the medium, the well-characterized approach, and the ease with which it may be scaled up. SmF also has some disadvantages, such as high maintenance costs, energy-intensive, and complex downstream processes. The SSF process involves growing microorganisms on a solid medium with a high nutrient content, large surface area, and additional mineral salt solution [44]. Fungi require less moisture and fungal mycelia can penetrate substrates to access nutrients and are preferred in SSF [45]. SSF has numerous benefits, including a lower rate of contamination, low cultivation operation and capital costs, productivity improvements per reactor capacity, and simple enzyme recovery [44]. A few drawbacks of SSF are that the process is not suitable for all microorganisms, scaling up is complex, and requires proper aeration and humidity control.

1.5.2 Suitable choice of substrate

The quality and quantity of a product can vary depending on the substrate utilised. A range of commercial substrates such as xylan, pectin, and starch are available; however, due to their high cost, they are not economically feasible as a fermentation feedstock. Thus, researchers have been working to find alternatives. Organic wastes such as agro-wastes and industrial wastes have been employed as carbon sources to produce enzymes [46]. Wood pulp, rice straw, wheat bran, vegetable waste, and other agro-residues are the most often utilized to synthesize xylanases.

1.5.3 Media components and their role in xylanase production

The production of xylanolytic enzymes is induced by many intermediate products [9]. Although xylan is known as the greatest xylanase inducer, it cannot induce xylanase synthesis as this high molecular weight polymer cannot penetrate microbial cells. A small amount of constitutive enzymes is generally released into the medium, resulting in the formation of low molecular weight fragments namely xylobiose, xylotriose, xylooligosaccharides of xylose and glucose and their positional isomers, which in turn induce the production of xylanolytic enzymes, resulting in increased productivity [9]. Nitrogen is a key structural element in microbial systems necessary for metabolic activities. As a result, the nitrogen source used is critical for microorganism development and, as a result, enzyme production. Peptone, tryptone, yeast extract, and other nitrogen sources are appropriate [39]. Trace minerals, amino acids, and vitamins are also essential for microbial growth; thus ensuring their presence at appropriate concentrations in the media helps xylanase production.

Table 1.2: Xylanases from various species with diverse production processes, characteristics, and applications.

Microorganisms	Substrates	Fermentation type	Production optima				Enzyme characteristics				Applications	References
							Optima		Stability			
			Molecular weight (kDa)	Time (h)	Temp (C°)	pH	Temp (C°)	pH	Temp (C°)	pH		
Bacteria												
Geobacillus stearothermophilus	Peptone	SmF	86	24	60	6.0	60	6.0	60-80	6-7.5	Pulp and paper	[47], [48]
Pseudomonas boreopolis	Wheat bran	SmF	20	96	30	7.0	65	6.0	55-75	5-9	Thermo- alkaline stable xylanase for industrial applications	[34]
Fungi												
Trichoderma piluliferum	Wheat bran	SSF	-	96	45	6.0	50	4.5	30-60	3.0-10.0	Additives for bovine feeding	[49]
Aspergillus oryzae	Rice straw	SmF	35	-	25	5.0	25	5.0	25-60	3.0-10.0	Hydrolysis of agro residues	[17], [50]

SmF: Submerged fermentation; SSF: solid-state fermentation

1.6 Selecting a design protocol for optimal xylanase production

Typically, a medium that provides essential nutrients for the growth of microorganisms is utilized. This aids in determining if the strains are capable of producing the desired enzyme. The study is optimized to increase the strain's enzyme production [9]. Different approaches are employed for increasing the yield of the desired product, such as adjusting physical growth factors, optimizing medium components, and enhancing the strain using various biotechnological tools [2,51]. Not selecting a design protocol for optimal production can result in several drawbacks. Without a structured protocol, there is a risk of suboptimal enzyme production, leading to lower yields and potentially higher production costs. Inconsistent quality of the xylanase may also arise, impacting its performance in various industrial applications. The absence of a design protocol can result in inefficient resource utilization, as well as a lack of standardization in the production process. This can ultimately lead to decreased competitiveness in the market, as well as higher overall manufacturing costs. Therefore, the implementation of a well-defined design protocol is crucial for maximizing efficiency and ensuring high-quality xylanase production.

1.6.1 Enhancing xylanase production: One-factor-at-a-time (OFAT)

For the screening of significant parameters that impact xylanase production, the OFAT method is applied [50]. One factor is used as the variable while the others are kept constant. The factor may be a key physical or nutritional factor that controls microbial growth and product formation [50].

This method is time-consuming and involves a high number of experiments. Recent research has revealed a trend in using this strategy to design trials with many variables and then undertake interaction studies between various nutritional and physical characteristics. The

statistical design technique has been employed to optimize fungal and bacterial xylanase production, using a small number of runs in the experimental set [50].

1.6.2 Statistical approach

1.6.2.1 Plackett-Burman Design (PBD)

The PBD, created by R.L. Plackett and J.P. Burman in 1946, is a prominent type of screening design. It was developed to enhance the quality assurance process so that rational selections could be made after studying the impacts of design parameters on the given system. This design produces reliable estimates of the critical effects in the smallest design possible [52]. This statistical approach is beneficial in identifying the most important components of a process. The design is used to screen the essential factors and does not consider the interaction effects between the variables [53]. One major disadvantage is that it does not allow for the estimation of interaction effects between factors. This means that it is only suitable for identifying main effects, but not for studying the complex interactions that may exist between factors. Additionally, the design assumes that all factors have a linear relationship with the response variable, which may not always be the case in real-world scenarios. A successful application of the PBD can be found in a study conducted by Rashid et al. [53] who aimed to optimize the production of xylanase by using different pre-treated sugarcane bagasse feedstocks. They utilized the Plackett-Burman Design to screen 8 factors (including temperature, incubation time, inoculum size, medium, pre-treatment, substrate concentration, agitation, and pH) that potentially influenced the production of the desired xylanase. The design allowed the researchers to efficiently identify the significant factors affecting production and their optimal levels. Subsequent analysis and optimization based on the PBD results led to a significant increase in the yield of the xylanase. The study demonstrates how the PBD can be successfully applied to identify key factors and optimize production processes in various fields.

1.6.2.2 Box-Behnken Design: Response Surface Methodology (RSM)

The RSM design may offer mathematical models that explain how enzyme activity is influenced by independent factors, as well as predicted responses and probable levels of linked independent variables. Interactions aid in showing the significant effect on the production of the enzyme of interest [54]. Another example of a successful application of the RSM can be found in a study conducted by Khusro et al. [54]. In this study, the researchers aimed to optimize the thermo-alkali stable xylanase production from *Bacillus tequilensis* strain ARMATI. RSM was employed to statistically screen medium constituents and the physical factors affecting xylanase and biomass yield of the isolate. The design showed 3.7 fold and 1.5 fold increased xylanase production and biomass yield of the isolate respectively compared to OFAT approach.The researchers designed a set of experiments based on a central composite design, and the obtained response data was subsequently analyzed using RSM. Through the optimization process, RSM helped identify the optimal conditions for enzyme production, resulting in a significantly higher yield compared to previous methods.

There are some drawbacks of RSM such as it requires a relatively large number of experimental runs compared to other designs, which can be time-consuming and costly. Secondly, the design assumes a quadratic relationship between the factors and the response, making it less suitable for capturing non-linear or complex relationships. This limitation can result in inaccurate predictions and suboptimal process optimization.

1.7 Genetically modified microorganisms for increased xylanase production

Typically, chemical mutagenesis or radiation strain enhancement have been utilized to increase xylanase production from the producer strain culture [55]. Recombinant DNA technology has

sparked great interest in developing strains overexpressing enzymes for complete lignocellulose degradation [56]. Several researchers have cloned xylanases from various microbial sources and genetically modified microbial strains to produce xylanases [57, 58, 59]. Many have selected *E. coli* as the expression host [60]. Even though the xylanases produced in *E. coli* are functional, they lack N-glycosylation which tends to lower their specific activity and stability [61]. Gram-positive bacteria, such as *Lactobacillus* species and *B. subtilis*, have also been employed as heterologous hosts for xylanase production [62].

Compared to *E. coli,* these species are capable of N-glycosylation and greater protein production levels. Goswami et al. [57] showed successful cloning and heterologous expression of cellulose free thermostable xylanase from *Bacillus brevi* in *E. coli.* Elgharbi et al. [60] report the successful expression of the *Aspergillus niger* US368 xylanase in *E. coli*. Yeasts, which can grow to very high cell densities and release proteins into the fermentation media, are also suitable hosts for xylanase expression. Lu et al. [56], showed high-level expression of improved thermostable alkaline xylanase variant in *Pichia pastoris* through codon optimization, multiple gene insertions, and high-density fermentation. Filamentous fungi are attractive expression systems because they are easy to cultivate, have undergone strain improvement and secrete the proteins [58]. Recombinant protein expression has some disadvantages, including the complexity and time-consuming nature of the production process, issues with protein misfolding or aggregation, and potential regulatory hurdles [63]. However, native production of proteins offers some promising opportunities. Native production involves harnessing natural protein production pathways and systems within an organism without introducing foreign DNA. This approach can circumvent many of the challenges associated with recombinant expression, as it relies on the organism's inherent ability to produce the desired protein. Native production can offer advantages such as improved protein folding and functionality, reduced likelihood of contamination from foreign components, and potentially lower production costs

[63]. Additionally, native production may be more environmentally sustainable and avoid public concerns surrounding genetically modified organisms. Exploring native production strategies can provide alternative avenues for protein production that address some of the downsides of recombinant expression.

1.8 Scaling up production in stirred tank bioreactors

Industrial fermentation utilizes microorganisms to produce various products, including antibiotics [1], organic acids [2], pharmaceutical proteins [3], and industrial enzymes [4]. It is estimated that biotechnology products cover one-third of the worldwide market, with a value of more than 300 million USD [5]. Industrial fermentation is advantageous because it involves relatively moderate pressures and temperatures, and is more sustainable in terms of exploiting natural resources. Thus, it has attracted considerable interest and promoted the emergence of a bio-economy. Furthermore, with the progress in metabolic engineering and synthetic biology, it is easier to obtain engineered cell factories with improved product yield, even producing new products [6,7]. High-throughput screening techniques have been developing at great speed. It has been noted that scaling up a fermentation process from a shake flask to an industrial fermenter may be challenging [11,12], as non-homogeneous conditions in industrial fermenters may negatively impact strains. Even though it is customary to keep specific parameters constant during scale-up. In practice, it is crucial to establish the key influential parameters, however, it is impossible to keep those properties (such as flow dynamics or fluid kinetics) similar or synchronized at different scales [11]. Fermentation performance is mainly determined by the capacity of the strain. However, the environment around the cell inside a bioreactor may hinder the ability of the strain. The interrelationship between the environment in the bioreactor and the cell physiological properties is a key that determines the outcome of bioreactors at different scales. Malhotra et al. [64] successfully optimized and scaled up

xylanase production in stirred tank bioreactors by a *Bacillus licheniformis* strain isolated from a hot water geyser , resulting in a 3-fold increase in the xylanase yield.

1.9 Downstream processing and purification strategies of xylanases for industrial application

Microbial systems produce a high proportion of biochemicals throughout their various growth and development phases. These biochemicals include enzymes, secondary metabolites, reaction intermediates, etc., which are important in many biotechnological applications [50]. DSP – solid- liquid separation of cells from fermentation liquor depends on the product being intracellular or extracellular. Intracellular proteins are synthesized within the cytoplasm or other organelles of the cell and accumulate within the cell. Examples of intracellular proteins include enzymes involved in metabolism and structural proteins that give cells their shape. In contrast, extracellular proteins are secreted by the cell and accumulate outside the cell. Examples of extracellular proteins include antibodies, cytokines, and growth factors. The choice of protein production system depends on the desired application and functionality of the protein. Intracellular protein production can be beneficial for the production of enzymes, while extracellular protein production is important for proteins that interact with external environments such as therapeutic proteins. Purification is a prerequisite for acquiring an enzyme with few or no contaminants. Purification involves concentrating and desalting the crude extract before chromatographic analysis. The protein samples can be concentrated using organic polymers, organic solvents, and salts to reduce the dilution effect created by other subsequent purification steps. The selection of methods will depend on the properties, the sample's nature, and the chromatographic techniques employed. An array of chromatography techniques, as shown in Table 1.3 are available depending on the properties of the protein to

be purified [65, 66]. Several xylanases of fungal origin have been purified using various methods. Ammonium sulphate precipitation, followed by dialysis, gel permeation chromatography, ion-exchange chromatography, and more recently discovered techniques such as aqueous phase chromatography and ultrafiltration are some of the enzyme purification methodologies applicable to xylanases [17,67]. The required level of purity for enzymes used in enzyme studies and animal feed studies can vary depending on the specific application and objectives of the research. In general, enzyme studies often require a high level of purity to ensure that the observed effects or catalytic properties can be attributed solely to the enzyme of interest [68]. For animal feed studies, the required level of purity may be less stringent compared to enzyme studies. In these cases, the focus is often on the functional properties of the enzyme, such as its ability to improve digestion or nutrient utilization in animals [69].While a certain level of impurities may be acceptable, it is still essential to ensure that the enzyme is sufficiently pure to avoid any adverse effects or unintended interactions with the animals' digestive processes. Regulatory bodies often set specific guidelines for the purity and quality of enzymes used in animal feed, which must be adhered to in order to ensure safety and efficacy [69].

Table 1.3: List of chromatographic techniques and the protein properties

Chromatographic techniques	**Protein property**
Affinity chromatography	Specific ligand recognition
Ion exchange chromatography	Charge
Immobilized metal ion affinity chromatography	Metal ion binding
Reversed-phase chromatography	Hydrophobicity
Hydrophobic interaction chromatography	Hydrophobicity
Gel filtration chromatography	Size

1.9.1 Ammonium sulphate precipitation and dialysis

The crude xylanase extracellular extract is fractionated using a series of ammonium sulphate concentrations (30–90%) to select the suitable salt concentration for enzyme precipitation [70]. The salt is subsequently removed from the precipitated enzyme using dialysis [71]. One of the limitations is that further processing is required for salt removal. Further, for dialysis, it is important to understand protein solubility. Since they have hydrophilic amino acid side chains facing outwards that may interact with water, they are soluble in aqueous conditions. Essential amino acids (arginine, histidine, arginine, and lysine), acidic amino acids (aspartate and glutamate), and neutral hydrophilic amino acids (asparagine, glutamine, serine, threonine, tyrosine, and cysteine) all contribute to these [72]. By limiting the accessible water, any substance that interferes with these interactions between amino acid side chains and water reduces the protein's solubility. As interactions with water become less evident, protein-protein interactions become more important, and the protein will aggregate and come out of the solution. It's also suggested that ammonium precipitation concentrates it rather than purifying the protein. As a result, contaminants in the crude sample may also be present in the protein sample after precipitation and dialysis [73]. Trichloroacetic acid (TCA) and acetone can also concentrate or precipitate xylanases. However, TCA may denature the protein; thus, it is not recommended to employ TCA when the protein must be folded, and TCA's toxicity further restricts its applicability [74].

1.9.2 Purification and chromatography methods for increased xylanase yield

Following concentration of the protein by ammonium acetate/TCA/acetone precipitation or ultracentrifugation , a single step or series of chromatography procedures may be employed for xylanase purification [75]. Traditional multistep purification processes are time-consuming, raising the overall cost of the process while also causing protein loss at each step [76,77]. In

the downstream processing of the enzyme, the purification phase accounts for 60–70% of the total processing cost [78,17]. As a result, numerous single-step liquid fractionation approaches have been developed, such as the aqueous two-phase system (ATPS) [79, 80, 81]. ATPS has several benefits over traditional purification methods, including low-cost components, reduced energy consumption with high yield, and improved resolution [80, 81]. The ATPS technique is unaffected by protein concentration and does not affect the protein's native properties [76, 77].

Table 1.4 summarizes multiple purification procedures for xylanases from various microorganisms and the process efficiency in terms of recovery kinetic and potential features.

Table 1.4: Purification techniques for xylanases

Source organism	Purification technique	Specific activity (IU/mg)	Fold purification	Recovery (%)	K_m (mg/ml)	V_{max} (µmol/mg/ min)	Application of purified enzyme	References
Combination of purification techniques								
Aspergillus flavus	Ammonium sulphate fractionation (40-60%)	621.4	2.7	46.7	-	-	Efficiently hydrolysed pre-treated corncobs for generation of XOS	[82]
	Gel filtration (Hiprep 16/60 Sephacryl S-100 HR column) chromatography	838.2	3.7	34.8				
The single-step purification technique								
Aspergillus tamarii kita	CM- cellulose chromatography	1215.89	7.43	36.72	7.59-8.13	1178.56-1330.20	XOS generation	[83]

1.10 Application of xylanases

The biotechnological use of xylans and xylanases has risen significantly in recent years, with xylan degradation products playing a significant role in commercial applications. In the 1980s, xylanases were first utilized in animal feed manufacturing, then in the food, textile, and paper sectors [84]. Xylanases, cellulases, and pectinases currently account for 20% of the global enzyme market [7].

1.10.1 Treating animal feed

Animal feed is nearly entirely made up of barley, maize, rye, oats, and sorghums [85]. Animal feed can be provided whole or ground, and be supplemented with by-products, minerals, and other ingredients to make a complete meal for chickens, pigs, ruminants, and horses [86]. Corn is utilized in animal feed diets worldwide, but as with any feed component, price, availability, quality, and accessibility within an area, all play a significant role [87]. Co-products from the dry and wet milling of maize are used instead of grain to save on feed costs. The most common coproduct is corn distiller's dried grains with solubles (DDGS) [88]. Corn's energy comes primarily from starch, with specific non-starch polysaccharides (NSP) contributing as well. When corn DDGS are incorporated into animal feed diets, the starch content will be reduced, which is attributed to effective enzymatic digestive mechanisms along the small intestine [89], and an increase in NSP levels will occur (Figure 1.6). Altering the profile of the diets would increase the viscosity in the intestine by their high water-binding capacity. Consequently, this slows down the migration and absorption of nutrients, lowers feed intake, and reduces access to digestive enzymes synthesized and released by the animal [90,91].

Carbohydrases have gained interest over the years, as they are enzymes that hydrolyse carbohydrates [92]. The NSP found in corn and corn DDGS is comprised of arabinoxylans [93], and therefore xylanase, which hydrolyses the β-1,4-glycosidic bonds of arabinoxylans, may be used to mitigate the impact of corn-based NSP [94].

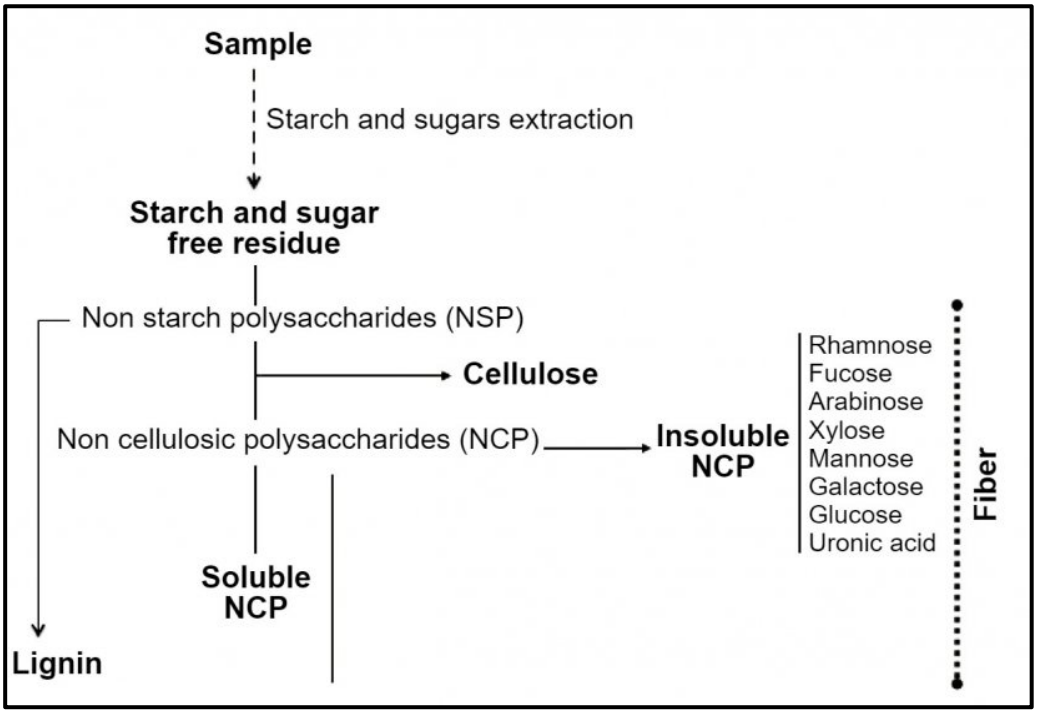

Figure 1.6: Determination of non-starch polysaccharides, lignin, and fibre by the enzymatic-chemical procedure [91].

For decades, a decline in weight gain of broilers and feed conservation efficiency has been a concern [95]. Xylanases are described in several research publications as feed additives that increase the nutritional content of the animal feed, resulting in better animal growth and weight gain [96]. Insoluble polysaccharides are solubilized and degraded by xylanases and their accessory enzymes which liberate oligosaccharides and monosaccharides (arabinose, xylose, mannose, etc.). Because of the improved arabinoxylan digestibility in monogastric animal diets, they serve an essential function in animal feed by lowering raw material viscosity and

increasing the feed conversion ratio [97]. With modest doses of enzyme treatment, some researchers postulate that xylanases may have a prebiotic impact due to xylooligosaccharide production, which benefits *Lactobacillus* spp. proliferation, *E. coli* reduction, gut morphology, and cecal volatile fatty acid concentrations [86].

1.10.1.1 Xylooligosaccharide (XOS)

Xylooligosaccharide (XOS) refers to sugar oligomers made from the xylan component found in plant fibers [98]. Hydrolysis of xylan produces xylose, xylobiose, xylotriose, and xylotetraose, along with some residual oligosaccharides. XOS with a lower degree of polymerization (2-10 monomers) are considered non-digestible sugars, while those with < 4 monomeric units have prebiotic applications as they support beneficial bacteria in the gut. Japan initially explored the use of XOS as a food ingredient and its positive effects on gastrointestinal health [98].

1.10.1.2 Applications of Xylooligosaccharides

Xylobiose in particular is now recognized as an effective prebiotic with beneficial effects on animal and human digestion. XOS not only promote the growth of the right type of commensals, but also help to improve the structural components of the gut [99]. XOS are protected from degradation while passing through the stomach due to their acid stability and the presence of β-bonds. Recent studies have shown that linear XOS and arabino-xylooligosaccharides (AXOS) are fermented more quickly than oligosaccharides containing uronic acid (UXOS) [100]. In addition, XOS support the growth of a greater number of intestinal bacteria compared to AXOS and UXOS [101,102], which can only be utilized by a few strains.

XOS have an potential for a variety of applications such as in the food pharmaceutical and agriculture industries (Figure 1.7). Currently, the most significant applications of XOS based

on the market demand correspond to functional food ingredients, for example nutritive preparations, as supplements in yogurt, soymilk, cocoa drinks, tea, jam, jellies, dairy products, candies, pastries, cakes, puddings, biscuits and fortified food for children and adults. Due to the prebiotic characteristics of XOS, symbiotic nourishment foods (a combination of a prebiotic and a probiotic) have also been manufactured [103].

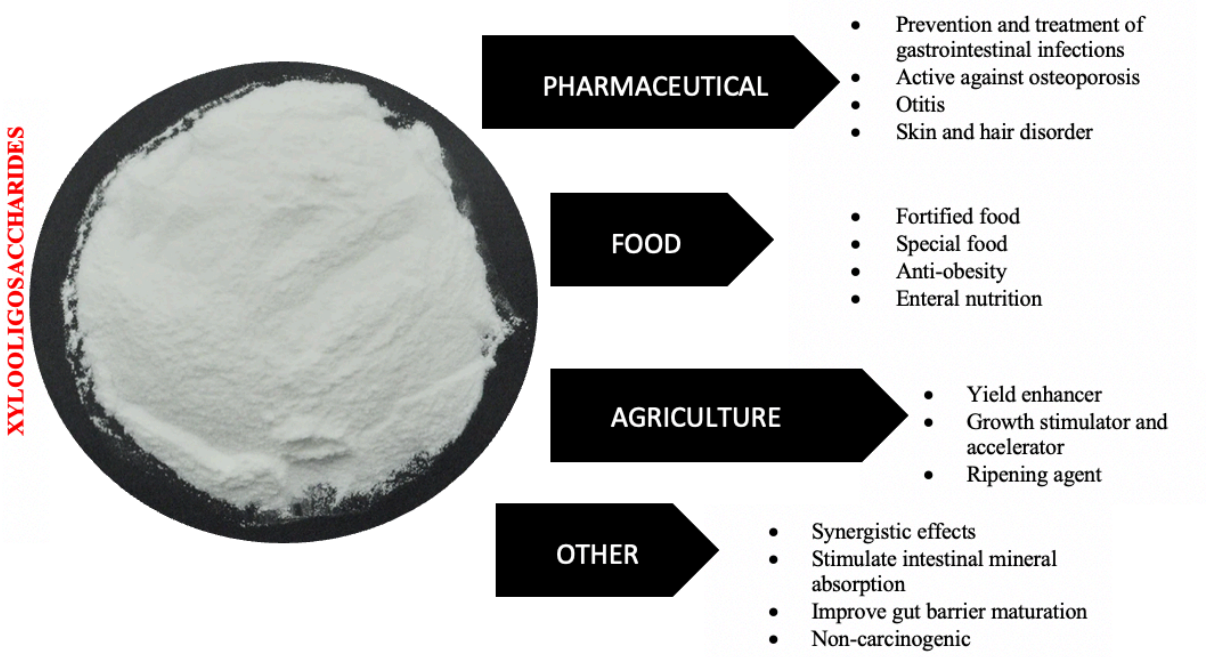

Figure 1.7: Modified diagram of applications of XOS in industry [104].

1.10.2 Applications in the baking industry

Xylanases are utilized in the food sector for processes such as baking. Wheat, which contains hemicelluloses like arabinoxylan, is used to make bread. Xylanases may solubilize water-insoluble arabinoxylan and convert it to water-extractable arabinoxylan [105]. This assists with the regular distribution of water and the formation of a gluten network throughout the dough. Adding xylanase to the dough increases rheological qualities, e.g., softness, extensibility, and elasticity, as well as breed-specific volume and crumb hardness [105]. The arabinoxylan breakdown products in bread are beneficial [106].

1.10.3 Paper and pulp industry

In paper mills, the bleaching property of xylanases, especially endo-β-xylanases are exploited in the kraft pulp pre-bleaching step [107] where they hydrolyse the reprecipitated xylan on the paper pulp fibres. Xylanase treatment increases the permeability of the fibres allowing for easier removal of lignin from the fibres. The use of xylanases also reduces the need for polluting chlorine bleaches [108]. However, Prior to the enzymatic treatment, the temperature and pH of the pulp must be adjusted. This necessitated the development of xylanases with a higher pH tolerance and temperature stability to reduce processing costs. Xylanases are genetically modified to change their enzymatic activity in harsh environments, although their overexpression is still being investigated [108].

1.10.4 Degradation of lignocellulose

The conversion of agricultural and other lignocellulose residues into value-added products is another use of xylanases, as shown in Figure 1.8 below.

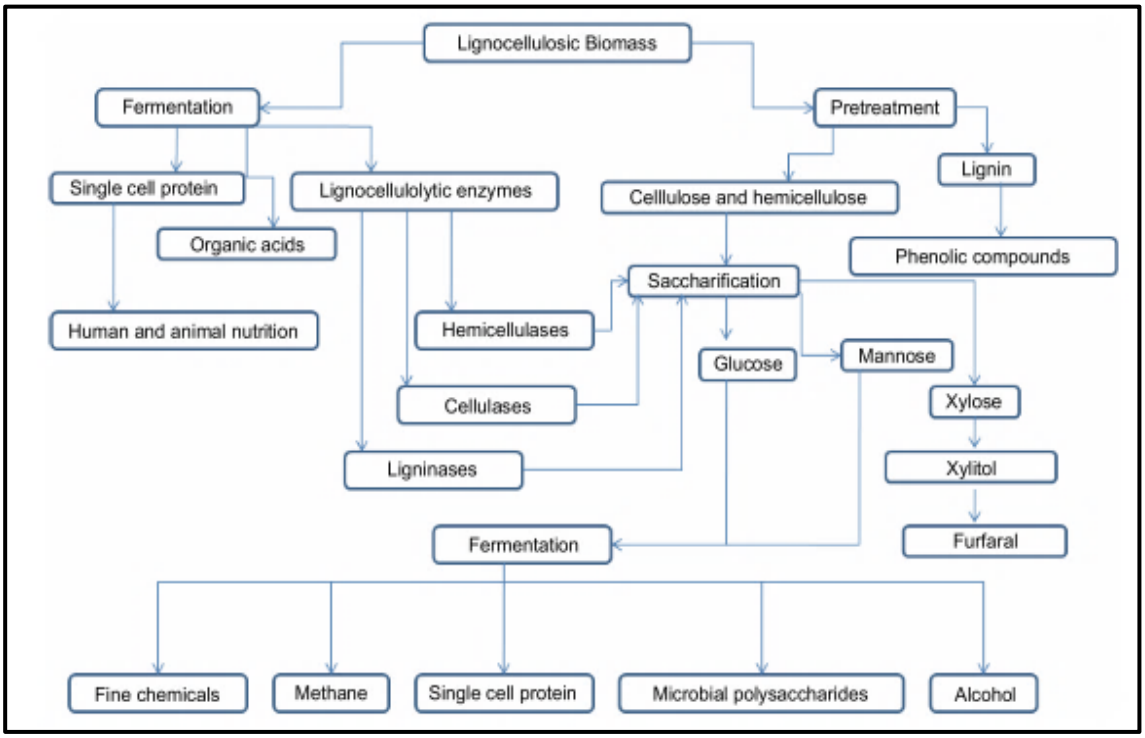

Figure 1.8: Lignocellulosic biomass bioconversion into value-added goods, xylanases being hemicellulases will saccharify the hemicellulose component [10].

The delignification of lignocelluloses involves the freeing of lignin from cellulose and hemicelluloses from lignin. It is followed by carbohydrate polymer depolymerization to produce sugars and then simple sugar fermentation to produce ethanol [109]. Many lignocellulose pre-treatment procedures, such as acid and alkali treatments or steam explosions have been devised to render the cellulose accessible to hydrolysis due to the global interest in creating sustainable technology. Cellulose is known to be shielded by xylan against the hydrolytic activity of cellulolytic enzymes. By enhancing fibre swelling and porosity, xylanase treatment enhances the accessibility of cellulose to hydrolysis [21].

1.10.5 Xylanase application in the chemical and pharmaceutical industries

Xylanases are added in combination with a complex of enzymes and pharmaceutical goods as a dietary supplement or to treat poor digestion [110]. β-D-Xylopyranosyl residues, hydrolytic products of xylan, may be converted into combustible materials, solvents, and artificial low-calorie sweeteners. The first step is to delignify xylan-rich hemicellulose, which is then hydrolyzed by xylanases and hemicellulases to generate sugars like β-D- xylopyranosyl units. As depicted in Figure 1.9, the products are then fermented, primarily by yeasts, to ethanol or xylitol. Although enzymatic xylan hydrolysis is a potential way of generating β-D-xylopyranosyl units, commercial xylitol is now generated on a large scale using chemical catalysis. This is a high-cost procedure because the xylose must first be refined in many stages. Furthermore, chemical reactions frequently produce by-products that are toxic to fermentation; e.g., during the decomposition of lignocellulosic material, in addition to the liberation of sugars, products derived from the degradation of glucose (hydroxymethylfurfural), xylose (furfural), and lignin may be formed (aromatic and phenolic compounds and aldehydes). Microbial

activity can be inhibited by substances liberated from the lignocellulose structure, such as acetic acid and extracted material. The advancement of more suitable xylitol manufacturing technologies has sparked optimism for its widespread usage in the culinary and pharmaceutical industry [111,112,113]. The production of xylitol and ethanol by bacteria and yeasts from lignocellulosic materials is depicted in Figure 1.9.

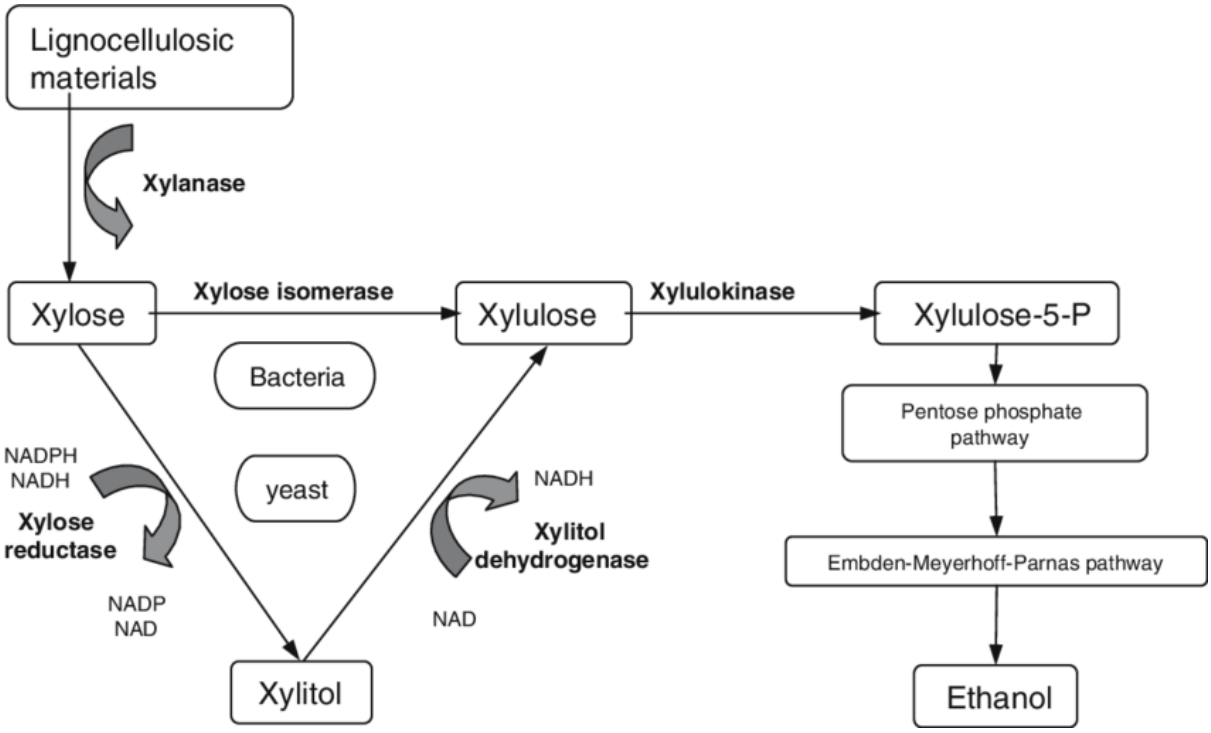

Figure 1.9: Simplified xylitol and ethanol production scheme by bacteria and yeasts from lignocellulosic materials [modified from 114].

1.11 Rationale of the study

Xylanases open up an extensive variety of biotechnological applications in different industrial sectors. Commercial applications require cheaper enzymes thus there is a need for improved enzyme production. The breakdown of xylan is restricted due to its heterogeneous nature and can be overcome by xylanases which are capable of cleaving these β-1,4-glycoside linkages. Microbial xylanases display varying substrate specificities and biochemical properties which makes them suitable for various applications in industrial and biotechnological sectors. Robust

xylanases with the necessary properties to survive the harsh industrial level processing are required in large quantities for industrial application. Therefore, there is a need to select the required microorganisms for xylanase production, followed by optimization of media components for enhanced production. Microbial xylanase production is affected by the fermentation process employed, choice of substrate and different media components. These components are often regulated by different process optimization for enhanced production of the enzyme for its application at a large scale. Hydrolysis of chicken feed to produce XOS is an important area of research due to its potential health and economic benefits for the poultry industry. XOS have been shown to have prebiotic properties which can improve gut health and overall immune system function of the chickens. This is because XOS acts as a food source for beneficial bacteria in the gut, leading to the enhancement of their population and subsequently, the suppression of harmful bacteria. Thus, the consumption by chickens of feed with increased levels of XOS can lead to improved digestive function, nutrient absorption, and overall health of the chickens. Therefore, this study was focused on the production optimization and scale-up of native and recombinant xylanases and their application in local chicken feed hydrolysis.

1.12 General aim of the study

The initial aim of the study was to search for fungal producers of xylanases from soil and tree bark samples. Fungi were preferred as they are known to be higher producers of xylanases compared to bacteria. Soil and tree bark samples were selected as these are environments that are most likely to be inhabited by microorganisms that secrete xylanases. The study focused on searching for a strain that produced xylanases at high temperatures and at an acidic pH. The study also included a recombinant XT6 xylanase that was obtained from Rhodes University.

In order to achieve the first goal of the study, the focus was on optimizing production of the *T. harzianum* and recombinant xylanases using statistically designed experiments followed by purification and characterization the xylanase enzymes. He next crucial step was the assessment of their potential application as poultry feed supplements, by determining the hydrolytic efficiency of the crude and purified *T. harzianum* xylanase and the purified recombinant *G. stearothermophilus* xylanase on chicken feeds using RSM. The XOS and monosaccharides in the feed hydrolysates were profiled and quantified. By conducting such detailed investigations, the study sought to provide valuable insights into the potential of these enzymes for industrial-scale XOS production from lignocellulosic biomass. Finally, the toxicity of the hydrolysates was assessed.

1.13 Specific aims and objectives

1. To isolate xylanase-producing fungi

    - To screen the cultures for xylanase activity using xylanase and substrate agar plates
    - To quantify the xylanase activity of each isolate displaying activity, and proceeding with the five highest producers in further studies.

2. To optimize xylanase production and identify the five selected isolates

    - To conduct OFAT experiments
    - To identify the isolates using BLAST

3. To characterize the *T. harzianum* crude xylanase

    - To determine the optimal pH, temperature and stability of the crude xylanases

- To conduct SDS-PAGE and NATIVE PAGE on the crude xylanase

4. To optimize production of the *T. harzianum* and recombinant XT6 xylanase

- To obtain the recombinant XT6 xylanase strain from the laboratory of Prof. Brett Pletschke, at Rhodes University
- To optimize the lysis of the *E. coli* cells
- To conduct PBD and RSM of BBD experiments
- To produce xylanase from *T. harzianum* and recombinant XT6 xylanase in bulk using the optimized growth conditions determined by the OFAT, PBD and RSM

5. To purify and characterize the *T. harzianum* xylanase

- To purify the xylanase from *T. harzianum* using ammonium sulphate precipitation, and anion exchange chromatography.
- To determine the optimal pH, temperature and stability of the purified xylanase
- To determine the effect of metal ions and different solvents on the xylanase activity of the purified xylanase
- To determine the effect of different substrates on the xylanase activity of the purified
- To determine the enzyme kinetics of the purified xylanase
- To conduct SDS-PAGE and NATIVE PAGE on the purified xylanase

6. To scale up the production of the recombinant XT6 xylanase

- To optimize aeration rates and monitor pH and dissolved oxygen content in 5-L stirred tank bioreactors

- To produce bulk recombinant XT6 xylanase production under optimized conditions
- To purify the recombinant XT6 xylanase and characterize the xylanase enzyme

7. To optimize and determine the effectiveness of the crude and purified *T. harzianum* xylanase and purified recombinant XT6 xylanase on chicken feed hydrolysis

- To conduct RSM using the BBD to optimize the hydrolysis conditions for xylanases on local chicken feed
- To analyse the hydrolysis products using quantitative and qualitative analysis methods such as high-performance liquid chromatography (HPLC) and thin layer chromatography (TLC)

8. To perform cytotoxicity studies to determine toxic effects of the hydrolysis products on Human Embryonic Kidney cells (HEK293)

- To analyse toxicity of hydrolysis products using the MTS assay

1.14 References

[1] Nigam, P.S. (2013). Microbial enzymes with special characteristics for biotechnological applications. *Biomolecules.* 3(3): 597-611.

[2] Sharma, H.P., Patel, H., & Sughanda, S.P. (2017). Enzymatic added extraction and clarification of fruit juices- A review. *Critical Reviews in Food Science and Nutrition.* 57(6): 1215-1227**.**

[3] Robinson P. K. (2015). Enzymes: principles and biotechnological applications. *Essays in Biochemistry*. 59, 1–41.

[4] Zhou, X., Li, W., Mabon, R., & Broadbelt, L. (2017). A critical review on hemicellulose pyrolysis. *Energy Technolog*y. 5, 52–79.

[5] S**mith, P. J., Wang, H. T., York, W. S., Peña, M. J., & Urbanowicz, B. R.** (2017). Designer biomass for next-generation biorefineries: leveraging recent insights into xylan structure and biosynthesis. *Biotechnology for Biofuels*. 10, 286.

[6] Rogowski, A. *et al.* (2014). Evidence that GH115α -glucuronidase activity, which is required to degrade plant biomass, is dependent on conformational flexibility. *Journal of Biological Chemistry.* 289(1): 53-64.

[7] Motta, F.L., Andrade, C.C.P., & Santana, M.H.A. (2013). A review of xylanase production by the fermentation of xylan: classification, characterization, and applications. *Intech*. 251–275.

[8] Chakdar, H., Kumar, M., & Pandiyan, K. (2016). Bacterial xylanases: biology to biotechnology. *Journal of Biotechnology*. 6, 1–15.

[9] Walia, A., Guleria, S., & Mehta, P. (2017). Microbial xylanases and their industrial application in pulp and paper biobleaching: a review. *Biotechnology.* 7, 1–12.

[10] Malhotra, G., & Chapadgaonkar, S.S. (2019). Productions and applications of xylanases- an overview. *Journal of Biotechnology, Computational Biology, and Bionanotechnology.* 99(1): 59-72.

[11] Yi, Z. *et al.* (2022). Xylan deconstruction by thermophilic *Thermoanaerobacterium bryantii* hemicellulases is stimulated by two oxidoreductases. *Catalysts*. 12(2): 182.

[12] Maitan-Alfenas, G.P., Oliveira, M.B., Nagem, R.A., de Vries, R.P., & Guimaraes, V.M. (2016). Characterization and biotechnological application of recombinant xylanases from *Aspergillus nidulans. International Journal of Biology and Macromolecules*. 91, 60–67.

[13] Held, P. (2012). Enzymatic digestion of polysaccharides (part II). Applications Department, *BioTek Instruments*.

[14] Meng, D.D. *et al.* (2015). Distinct roles for carbohydrate-binding modules of glycoside hydrolase 10 (GH10) and GH11 xylanases from *Caldicellulosiruptor* sp. strain F32 in thermo-stability and catalytic efficiency. *Applied and Environmental Microbiology*. 81, 2006–2014.

[15] Uday, U.S.P., Choudhury, P., Bandopadhyay, T.K., & Bhunia, B. (2016). Classification, mode of action, and production strategy of xylanase and its application for biofuel production from water hyacinth. *International Journal of Biological Macromolecules*. 82, 1041-1054.

[16] Liu, X. *et al.* (2019). Biochemical characterization of a novel exo-oligoxylanase from *Paenibacillus barengoltzii* suitable for monosaccharification from corncobs. *Biotechnology and Biofuels*. 12, 190.

[17] Bhardwaj, N., Kumar, B., & Agarwal, K. (2019). Purification and characterization of a thermo-acid/alkali stable xylanases from *Aspergillus oryzae* LC1 and its application in xylooligosaccharides production from lignocellulosic agricultural wastes. *International Journal of Biology and Macromolecules*. 122, 1191–1202.

[18] Lombard, V., Golaconda, Ramulu, H., & Drula, E. (2014). The carbohydrate-active enzymes database (CAZy) in 2013. *Nucleic Acids Research.* 42, 490–495.

[19] Pavarina, G.C. *et al.* (2021). Characterization of a new bifunctional endo-1,4-β-xylanase/esterase found in the rumen metagenome. *Scientific Reports.* 11, 10440.

[20] Faulds, C.B., Mandalari, G., & Lo Curto, R.B. (2006). The synergy between xylanases from glycoside hydrolase family 10 and family 11 and a feruloyl esterase in the release of phenolic acids from cereal arabinoxylan. *Applied Microbiology and Biotechnology*. 71, 622–629.

[21] Hu, J., Arantes, V., & Saddler, J.N. (2011). The enhancement of enzymatic hydrolysis of lignocellulosic substrates by the addition of accessory enzymes such as xylanase: is it an additive or synergistic effect? *Biotechnology for Biofuels*. 36, 1–13.

[22] Zhang, D., Wang, Y., & Zheng, D. (2016a). New combination of xylanolytic bacteria isolated from the lignocellulose degradation microbial *consortium* XDC-2 with enhanced xylanase activity. *Bioresources Technology*. 221, 686–690.

[23] Zhang, Y., & An, J., & Yang, G. (2016b). Structure features of a GH10 xylanase from *Caldicellulosiruptor bescii*: implication for its thermophilic adaption and substrate binding preference. *Acta Biochimica et Biophysica Sinica.* 48, 948–957.

[24] Zhang, J., Siika-Aho, M., Tenkanen, M., & Viikari, L. (2011). The role of acetyl xylan esterase in the solubilization of xylan and enzymatic hydrolysis of wheat straw and giant reed. *Biotechnology for Biofuels.* 4(1): 60.

[25] Chadha, B.S., Kaur, B., Basotra, N., Tsang, A., & Pandey, A. (2019). Thermostable xylanases from thermophilic fungi and bacteria: current perspective. *Bioresource Technology*. 277, 195–203.

[26] Singh, S., Sidhu, G.K., & Kumar, V. (2019). Fungal xylanases: sources, types, and biotechnological applications. Recent advancement in white biotechnology through fungi. *Springer*. 405–428.

[27] Garcia-Huante, Y., Cayetano-Cruz, M., & Santiago-Hernández, A. (2017). The thermophilic biomass-degrading fungus *Thielavia terrestris* Co3Bag1 produces a hyper thermophilic and thermostable β-1, 4-xylanase with exo-and endo-activity. *Extremophiles.* 21, 175–186.

[28] Bajaj, B.K., & Manhas, K. (2012). Production and characterization of xylanase from *Bacillus licheniformis* P11(C) with potential for fruit juice and bakery industry. *Biocatalytic Agricultural and Biotechnological Journal.* 1, 330–337.

[29] Kamble, R.D., & Jadhav, A.R. (2012). Isolation, purification, and characterization of xylanase produced by a new species of *Bacillus* in solid-state fermentation. *International Journal of Microbiology*. 683193.

[30] Amore, A., Parameswaran, B., & Kumar, R. (2015). Application of a new xylanase activity from *Bacillus Amyloliquifaciens* XR44A in brewer's spent grain saccharification. *Journal of Chemical Technology and Biotechnology*. 90, 573–581.

[31] Kotzekidou, P. (2014). *Geobacillus stearothermophilus* (formerly *Bacillus stearothermophilus*). *Encyclopedia of Food Microbiology*. 129-134.

[32] Yardimci, G.O., & Cekmecelioglu, D. (2018). Assessment and optimization of xylanase production using co-cultures of *Bacillus subtilis* and *Kluyveromyces marxianus*. *3 Biotech.* 8(7): 290.

[33] Iloduba, M.I., Milala, M.A., & Ali, A. (2016). Isolation and partial characterization of crude cellulase-free xylanase from *Pseudomonas aeruginosa* and *Staphylococcus aureus* for possible use in the paper industry. *International Journal of Microbiology*. 3, 8.

[34] Lin, C., Shen, Z., Zhu, T., & Qin, W. (2017). Bacterial xylanase in *Pseudomonas boreopolis* LUQ1 is highly induced by xylose. *Journal of Biotechnology*. 1, 73–79.

[35] Purkan, P., Huruniawati, E., & Sumarsih, S. (2017). Xylanase enzyme from a local strain of *Pseudomonas stutzeri*. *Journal of Chemical Technology*. 52, 1079–1085.

[36] Lee, J.H., Kim, Y.G., & Lee, J. (2018). Thermostable xylanase inhibits and disassembles *Pseudomonas aeruginosa* biofilms. *Biofouling*. 34, 346–356.

[37] Seemakram, W., Boonrung, S., Kokaew, U., Aimi, T., & Boonlue, S. (2020). Optimization of culture conditions for xylanase production from cellulase-free xylanase-producing thermophilic fungus, *Thermomyces dupontii* KKU−CLD−E2−3. *Chiang Mai Journal of Science*. 47, 391-402.

[38] Ang, S.K., & Ariyani, L.P. (2013). Production of cellulases and xylanase by *Aspergillus fumigatus* SK1 using untreated oil palm trunk through solid-state fermentation. *Process Biochemistry*. 48, 1293–1302.

[39] Irfan, M., Nadeem, M., & Syed, Q. (2014). One-factor-at-a-time (OFAT) optimization of xylanase production from *Trichoderma viride*-IR05 in solid-state fermentation. *Journal of Radiation Research and Applied Sciences*. 7, 317-326.

[40] Syuan, Y., Ong Gaik Ai, L., & Kim Suan, T. (2018). Evaluation of cellulase and xylanase production from *Trichoderma harzianum* using acid-treated rice straw as a solid substrate. *Materials Today: Proceedings*. 5(10): 22109-22117.

[41] Rahmani, N., Kahar, P., & Lisdiyanti, P. (2018). Xylanase and feruloyl esterase from *actinomycetes* cultures could enhance sugarcane bagasse hydrolysis in the production of fermentable sugars. *Bioscience Biotechnology and Biochemistry*. 82, 904–915.

[42] Jain, A., Morlok, C.K., & Henson, J.M. (2013). Comparison of solid-state and submerged-state fermentation for the bioprocessing of switchgrass to ethanol and acetate by *Clostridium phytofermentans*. *Applied Microbiology and Biotechnology*. 97, 905 –917.

[43] Roy, S., Dutta, T., & Ghosh. (2013). Novel xylanases from *Simplicillium obclavatum* MTCC 9604: a comparative analysis of production, purification, and characterization of the enzyme from submerged solid-state fermentation. *Springer plus*. 2, 382–392.

[44] Shrivastava, N. (2019). Solid-state fermentation strategy for microbial metabolites production: *Microbial Secondary Metabolites Biochemistry and Applications.* 23, 345–354.

[45] Bück, A., Casciatri, F.P., Thomeo, J.C., & Tsotsas, E. (2015). Model-based control of enzyme yield in solid-state fermentation. *Procedia Engineering.* 102, 362–371.

[46] Kumar, B.A, Amit, K., Alok, K., & Dharm, D. (2018). Wheat bran fermentation for the production of cellulase and xylanase by *Aspergillus niger* NFCCI 4113. *Research Journal of Biotechnology.* 13, 5.

[47] Adhyaru, D.N., Bhatt, N.S., Modi, H.A., & Divecha, J. (2017). Cellulase-free-thermo-alkali-solvent-stable xylanase from *Bacillus altitudinis* DHN8: over-production through

statistical approach, purification, and bio-deinking/bio-bleaching potential. *Bio-catalytical Agriculture and Biotechnology*. 12, 220–227.

[48] Bibi, Z., Ansari, A., Zohra, R.R., Asman, A., & Ul Qader, S.H. (2014). Production of xylan degrading endo-1,4-b-xylanase from thermophilic *Geobacillus stearothermophilus* KIBGE-IB29. *Journal of Radiation Research and Applied Science*. 7, 478-485.

[49] da Costa, A.C., Cavalheiro, G.F., & de Queiroz Vieira, E.R. (2019). Catalytic properties of xylanases produced by *Trichoderma piluliferum* and *Trichoderma viride* and their application as additives in bovine feeding. *Biocatalytic Agriculture and Biotechnology*. 19, 101161.

[50] Bhardwaj, N., Chanda, K., & Kumar, B. (2017). Statistical optimization of nutritional and physical parameters for xylanase production from newly isolated *Aspergillus oryzae* LC1 and its application in the hydrolysis of lignocellulosic agro-residues. *BioResources*. 12, 8519–8538.

[51] Walia, A., Mehta, P., Guleria, S., & Shirkot, C.K. (2015). Modification in the properties of paper by using cellulase-free xylanase produced from alkalophilic *Cellulosimicrobium cellulans* CKMX1 in biobleaching of wheat straw pulp. *Canadian Journal of Microbiology*. 61, 671–681.

[52] Shinde, M.B., Shinde, G.V., Patel, R.S., & Dharmasi, A.T. (2021). Computational predictability of polyethylene glycol encapsulated modified-release multiple unit pellets

formulation of metoprolol succinate using different multivariate models. *Materials Technology.* 1-12.

[53] Rashid, R. *et al.* (2020). Combined pre-treatment of sugarcane bagasse using alkali and ionic liquid to increase hemicellulose content and xylanase production. *BMC Biotechnology*. 20.

[54] Khusro, A., Kaliyan, B.K., & Al-Dhabi, N.A. (2016). Statistical optimization of thermo-alkali stable xylanase production from *Bacillus tequilensis* strain ARMATI. *Electronic Journal of Biotechnology*. 22, 16–25.

[55] Abdel-Aziz, M.S., Talkhan, F.N., Fadel, M., Abou Zied, A.A., & Abdel-Razik, AS. (2011) Improvement of xylanase production from *Streptomyces pseudogriseolus* via UV mutagenesis. *Australian Journal of Basic and Applied Science.* 5, 1045–1050.

[56] Lu, Y. *et al.* (2016). High-level expression of improved thermostable alkaline xylanase variant in *Pichia Pastoris* through codon optimization, multiple gene insertions, and high-density fermentation. *Scientific Reports.* 6, 1–10.

[57] Goswami, G.K. *et al*. (2015). Cloning and heterologous expression of a cellulose-free thermostable xylanase from *Bacillus brevis*. *SpringerPlus.* 3, 1–6.

[58] Zafar, A. *et al.* (2016) Cloning, expression, and purification of a xylanase gene from *Bacillus licheniformis* for use in saccharification of plant biomass. *Applied Biochemistry and Biotechnology*. 178, 294–311.

[59] Meng, X. *et al.* (2022). Developing fungal heterologous expression platforms to explore and improve the production of natural products from fungal biodiversity**.** *Biotechnology Advances*. 54, 107866.

[60] Elgharbi, F. *et al.* (2015). Expression of US368 xylanase in purification, characterization, and copper activation. *International Journal of Biology and Macromolecules*. 74, 263–270.

[61] Chang, X. *et al.* (2017). Role of N-linked glycosylation in the enzymatic properties of a thermophilic GH 10 xylanase from *Aspergillus fumigatus* expressed in *Pichia pastoris*. *PLoS ONE.* 12(2): 1-13.

[62] Verma, D., & Satyanarayana, T. (2013). Production of cellulase-free xylanase by the recombinant *Bacillus subtilis* and its applicability in paper pulp bleaching. *Biotechnology Process.* 29, 1441–1447.

[63] Beygmoradi, A., Homaei, A., Hemmati, R., & Fernandes, P. (2023). Recombinant protein expression: Challenges in production and folding related matters. *International Journal of Biological Macromolecules*. 233, 123407.

[64] Malhotra, G., & Chapadgaonkar, S.S. (2020). Taguchi optimization and scale up of xylanase from *Bacillus licheniformis* isolated from hot water geyser. *Journal of Genetic Engineering and Biotechnology*. 18(1): 65.

[65] Smith, D.M. (2017). Protein separation and characterization procedures. *Food Science Text Series*. 431-453.

[66] Gómez-garcía, R. *et al*. (2018). Production of xylanase by *Trichoderma harzianum* (*Hypocrea lixi*i) in solid-state fermentation and its recovery by an aqueous two-phase system. *Canadian Journal of Biotechnology*. 2, 108–115.

[67] Guleria, S., Walia, A., Chauhan, A., & Shirkot, C.K. (2016). Purification and characterization of detergent stable alkaline protease from *Bacillus Amyloliquifaciens* SP1 isolated from apple rhizosphere. *Journal of Basic Microbiology*. 56, 138–152.

[68] Robinson, P.K. (2015). Enzymes: principles and biotechnological applications. *Essays in Biochemistry*. 59:1-41.

[69] Bedford, M.R., & Apajalahti, J.H. (2022). The role of feed enzymes in maintaining poultry intestinal health. *Journal of Science and Food Agriculture*. 102(5):1759-1770.

[70] Bhardwaj, N., Kumar, B., & Verma, P. (2019). A detailed overview of xylanases: an emerging biomolecule for current and future prospective. *Bioresources and Bioprocessing.* 6, 40.

[71] Coman, G., Georgescu, L., & Bahrim, G. (2013). *Streptomyces* p12-137 endoxylanase characteristics evaluation to obtain xylooligosaccharides. *Romanian Biotechnology Letters.* 18, 8086–8096.

[72] Deshmukh, R.A. *et al.* (2016). Purification, biochemical characterization, and structural modeling of alkali-stable β-1,4-xylan xylanohydrolase from *Aspergillus fumigatus* R1 isolated from soil. *BMC Biotechnology*. 16, 11.

[73] Biosciences G (2019). Ammonium sulfate protein precipitation-the key to salting-out. https://info.gbiosciences.com/blog/ammonium-sulfate accessed 01/06/22.

[74] Koontz, L. (2014). TCA precipitation. *Methods in Enzymology*. Elsevier, New York, 3–10.

[75] Yadav, P., Maharjan, J., & Korpole, S. (2018). Production, purification, and characterization of thermostable alkaline xylanase from *Anoxybacillus kamchatkensis* NASTPD13. *Frontiers in Bioengineering and Biotechnology*. 6, 65.

[76] Iqbal, M., Tao, Y., & Xie, S. (2016). Aqueous two-phase system (ATPS): an overview and advances in its applications. *Biological Procedures Online.* 18, 18.

[77] Ramakrishnan, V., Goveas, L.C., & Suralikerimath, N. (2016). Extraction and purification of lipase from *Enterococcus faecium* MTCC5695 by PEG/ phosphate aqueous-two phase system (ATPS) and its biochemical characterization. *Biocatalytic Agricultural Biotechnology*. 6, 19–27.

[78] Loureiro, D.B., Braia, M., Romanini, D., & Tubio, G. (2017). Partitioning of xylanase from *Thermomyces lanuginosus* in PEG/NaCit aqueous two-phase systems: structural and functional approach. *Protein Expression and Purification*. 129, 25–30.

[79] Glyk, A., Scheper, T., & Beutel, S. (2015). PEG-salt aqueous two-phase systems: an attractive and versatile liquid-liquid extraction technology for the downstream processing of proteins and enzymes. *Applied Journal of Microbiology and Biotechnology*. 99, 6599–6616.

[80] Xu, H. *et al.* (2021). An aqueous two-phase system formed in a single-component solution of α-ketooctanoic acid. *RSC Advances*. 11(54): 34245–34249.

[81] Saddique, H. *et al.* (2020). Aqueous two-phase systems for the isolation and partial purification of lipases from soil bacteria. *Iranian Journal of Chemistry and Chemical Engineering* (IJCCE). 39(6): 281-292.

[82] Chen, Z., Zaky, A.A., & Liu, Y. (2019). Purification and characterization of new xylanase with excellent stability from *Aspergillus flavus* and its application in hydrolysing pre-treated corncobs. *Protein Expression and Purification*. 154, 91–97.

[83] Heinen, P.R., Bauermeister, A., & Ribeiro, L.F. (2018). GH11 xylanase from *Aspergillus tamarii* Kita: purification by one-step chromatography and xylooligosaccharides hydrolysis monitored in real-time by mass spectrometry. *International Journal of Biology and Macromolecules*. 108, 291–299.

[84] Harris, A.D., & Ramalingam, C. (2010). Xylanases and its application in food industry: a review. *Journal of Experimental Sciences*. 1(7): 01-11.

[85] Humer, E., & Zebeli, Q. (2017). Grains in ruminant feeding and potentials to enhance their nutritive and health value by chemical processing. *Animal Feed Science and Technology.* 226, 133–151.

[86] Van Hoeck, V. *et al.* (2021). Xylanase impact beyond performance: a prebiotic approach in broiler chickens. *Journal of Applied Poultry Research.* 2021(30): 100193.

[87] Popp, J.M. *et al.* (2016). Biofuels and their coproducts as livestock feed: global economic and environmental implications. *Molecules*. 21(3): 285.

[88] Shurson, G.C., Zijlstra, R.T., Kerr, B.J., & Stein, H.H. (2012). Feeding biofuels co-products to pigs. In: Makkar, H., editor. Biofuel co-products as livestock feed: opportunities and challenges. Rome (Italy): Food and Agriculture Organization of the United Nations; p. 175–207.

[89] Li, Y. *et al.* (2015). In vitro and in vivo digestibility of corn starch for weaned pigs: effects of amylose: amylopectin ratio, extrusion, storage duration, and enzyme supplementation. *Journal of Animal Science.* 93, 3512–3520.

[90] Acosta, J.A., Stein, H.H., & Patience. J.F. (2020). Impact of increasing the levels of insoluble fibre and the method of diet formulation on measures of energy and nutrient digestibility in growing pigs. *Journal of Animal Science*. 98,1–9.

[91] Mohamed, E.A.E., Mahmoud, A., Mayada, R.F., & Kuldeep, D. (2015). Use of maize distiller's dried grains with solubles (DDGS) in laying hen diets. *Asian Journal of Animal and Veterinary Advances*. 10, 690-707.

[92] Zier-Rush, C.E., Groom, C., Tillman, M., Remus, J., & Boyd, R.D. (2016). The feed enzyme xylanase improves finish pig viability and carcass feed efficiency. *Journal of Animal Science*. 94, 115.

[93] Jaworski, N.W., Laerke, H.N., Bach Knudsen, K.E., & Stein, H.H. (2015). Carbohydrate composition and in vitro digestibility of dry matter and non-starch polysaccharides in corn, sorghum, wheat, and coproducts from these grains. *Journal of Animal Science*. 93, 1103–1113.

[94] Torres-Pitarch, A., Manzanillaac, E.G., Gardiner, G.E., O'Doherty, J.V., & Lawlor, P.G. (2019). Systematic review and meta-analysis of the effect of feed enzymes on growth and nutrient digestibility in grow-finisher pigs: effect of enzyme type and cereal source. *Animal Feed Science and Technology*. 251, 153–165.

[95] Abdollahi, M. R., F. Zaefarian, & V. Ravindran. (2018). Feed intake response of broilers: Impact of feed processing. *Animal Feed Science and Technology.* 237:154–165.

[96] Jha, R., & Mishra, P. (2021). Dietary fibre in poultry nutrition and their effects on nutrient utilization, performance, gut health, and on the environment: a review. *Journal of Animal Science and Biotechnology.* 12, 51.

[97] Whiting, I.M., Rose, S.P., & Mackenzie, A.M. (2019). Effect of wheat distillers dried grains with solubles and exogenous xylanase on laying hen performance and egg quality. *Poultry Science.* 98, 3756–3762.

[98] Rashid, R., & Sohail, M. (2021). Xylanolytic *Bacillus* species for xylooligosaccharides production: a critical review. *Bioresources and Bioprocessing.* 8, 16.

[99] Finegold, S.M. *et al.* (2014). Xylooligosaccharide increases bifidobacteria but not *lactobacilli* in human gut microbiota. *Food and Function*. 5: 436–445.

[100] Karina, L.R., Winnie, D., Karolien, V., Harivony, R., & Caroline R. (2021). Enzymatic production of xylo-oligosaccharides from destarched wheat bran and the impact of their degree of polymerization and substituents on their utilization as a carbon source by probiotic bacteria. *Journal of Agricultural and Food Chemistry.* 69 (44): 13217-13226

[101] Nordberg Karlsson, E. *et al.* (2018). Endo-xylanases as tools for production of substituted xylooligosaccharides with prebiotic properties. *Applied Microbiology and Biotechnology*. 102, 9081–9088.

[102] Stuivenberg, G.A, Burton, J.P., Bron, P.A., & Reid, G. (2022). Why are bifidobacteria important for infants? *Microorganisms*. 10(2): 278.

[103] Jagtap, S., Deshmukh, R.A., Menon, S., & Das, S. (2017). Xylooligosaccharides production by crude microbial enzymes from agricultural waste without prior treatment and their potential application as nutraceuticals. *Bioresource Technology*. 245: 283–288.

[104] Rashid, R., & Sohail, M. (2021). Xylanolytic *Bacillus* species for xylooligosaccharides production: a critical review. *Bioresources and Bioprocessing.* 8, 16.

[105] De Queiroz Brito Cunha, C.C., Gama, A.R., & Cintra, L.C. (2018). Improvement of bread-making quality by supplementation with recombinant xylanase produced by *Pichia pastoris*. *PLoS ONE*. 13, 1–14.

[106] Bajpai, P. (2014). Sources, production, and classification of xylanases. *Xylanolytic Enzyme Academic Press (Imprint Elsevier).* 43–52.

[107] Zhang, K., Zhang, Y., Yan, D., Zhang, C., & Nie, S. (2018). The enzyme-assisted mechanical production of cellulose nanofibrils: thermal stability. *Cellulo*se. 25(9), 5049–5061.

[108] Tao, P. *et al.* (2019). Effect of enzymatic treatment on the thermal stability of cellulose nanofibrils. *Cellulose.* 26, 7717–7725.

[109] Kucharska, K. *et al.* (2018). Pre -treatment of lignocellulosic materials as substrates for fermentation processes. *Molecules*. 23(11): 2937.

[110] Gupta, P.K., Agrawal, P., Hedge, P., & Akhtar, M.S. (2018). Xylooligosaccharides and their anticancer potential: an update. Anticancer plants: natural products and biotechnological implements. *Springer.* 255–271.

[111] Otieno, D.O., & Ahring, B.K. (2012). A thermochemical pre-treatment process to produce xylooligosaccharides (XOS), arabinooligosaccharides (AOS), and mannooligosaccharides (MOS) from lignocellulosic biomasses. *Bioresources Technology*. 112, 285–292.

[112] Chapla, D., Dholakiya, S., Madamwar, D., & Shah, A. (2013). Characterization of purified fungal endoxylanase and its application for production of value-added food ingredients from agro residues. *Food and Bioproducts Processing*. 91, 682–692.

[113] Gowdhaman, D., & Ponnusami, V. (2015). Production and optimization of xylooligosaccharides from corncob by *Bacillus aerophilous* KGJ2 xylanase and its antioxidant potential. *International Journal of Biology and Macromolecules*. 79, 595–600.

[114] Polizeli, M. L. T. M. *et al.* (2005). Xylanases from fungi: properties and industrial applications. *Applied Microbiology and Biotechnology*. 67, 577–591.

CHAPTER TWO

ISOLATION, SCREENING, PRELIMINARY OPTIMIZATION AND CHARACTERIZATION OF THERMOSTABLE XYLANASE PRODUCTION UNDER SUBMERGED FERMENTATION BY FUNGI IN DURBAN, SOUTH AFRICA

2.1 Abstract

Fungi are renowned for their ability to produce extracellular enzymes into their surrounding environment. Xylanases are hydrolytic enzymes capable of xylan degradation. The objectives of this study were to isolate, screen for potential xylanolytic fungi from soil and tree bark samples from three locations in South Africa and to determine their growth conditions for maximum xylanase production. Forty six isolates were obtained based on clearing zone formation on xylan-enriched agar plates using Congo red indicator. Xylanase activity was quantified in the submerged fermentation (SMF) broth of these isolates. Isolate MS5 which identified as *Trichoderma harzianum* with the highest enzyme activity (38.17 U/ml) was selected for further studies based on thermophilic properties (70°C) and pH (5.0). The culture conditions such as incubation period (5 days), agitation speed (160 rpm) wheat bran (1%) and ammonium sulphate (1.2%) were optimized further for xylanase production. Biochemical characterization of the crude enzyme revealed two pH and temperature optima (pH 6.0 at 60 and 70°C, pH 8.0 at 55 and 75°C). The enzyme retained > 70% activity after 4 h at pH 6.0 at 70°C. SDS-PAGE revealed multiple protein bands with a prominent band at 70 kDa. Substrate Native PAGE revealed multiple isoforms as xylanase activity was observed between 55-130 KDa. This enzyme will be beneficial for applications in the animal feed and biofuel industries. The other isoform has suitable properties for application in enzymatic pulp bleaching as the requirements are high temperature and basic (pH 8.0) conditions during that process.

Key words: *Fungi; xylanase; screening; isolation; xylan plate assay*

2.2 Introduction

Lignocellulosic materials are widespread in nature and xylan is a polysaccharide found in the hemicellulose fraction of lignocellulose, a major component of the plant cell wall. Xylan is a significant resource of renewable biomass, suitable as a substrate for the production of many commodities such as biofuels, affordable energy sources for fermentation and improved animal feeds. However, xylan must be converted to xylose and XOS for most bioconversion processes. The conversion of xylan can be performed by acid hydrolysis or by xylanolytic enzymes (xylanases) that deconstruct plant structural material thus breaking down hemicellulose [1].

Xylanase production by fungi, bacteria, yeast, marine algae, etc. has been studied and reported by several authors, but the main sources of industrial enzymes are fungi and bacteria [2,3,4,5] through intracellular or extracellular secretions by the microorganisms [5]. Depending on the source, xylanases have different characteristics which make them useful for several applications. Microbial enzymes are preferred in industrial applications due to their ability to be produced in large volumes over a short period [6,7]. Fungi are highly diverse in nature and have been recognised as an unrivalled target for enzyme screening [8]. Filamentous fungi are producers of xylanases and other xylan degrading enzymes, with the noteworthy characteristics of secreting enzymes into the surrounding medium, thus avoiding the need for cell lysis, and with much higher activities compared to yeasts and bacteria [8]. Thus fungal enzymes are very attractive for various industrial processes [9]. On an industrial scale, xylanases are produced mainly by *Aspergillus and Trichoderma* spp. in solid-state fermentation (SSF). *T. harzianum* is present in all soil types and is the most prevalent culturable fungi [10].

The application of xylanases in industrial processes has had many limitations for its commercial feasibility due to several factors [11]. These include the inaccessibility of substrate to the xylanases caused by physical limitations, the incomplete hydrolysis of xylan due to its diverged branched nature, the narrow pH optimum range and thermal instability of the enzymes, end-product inhibition, and cost of enzyme production [11]. Fungal xylanases are effective in a pH range of 4.0-6.0 and temperatures below 50°C, thus their use in industrial applications is restricted. Previous studies also showed that mesophilic organisms are not ideal for xylanase production as these enzymes generally become denatured at temperatures above 55°C [12]. As a consequence, the efficiency of hydrolysis decreases during the catalytic application, requiring supplementation during the process or higher enzyme yields to overcome this problem, thus increasing the process costs. Therefore, the use of thermostable enzymes is essential for hydrolysis at high temperatures.

Xylanases have been used in the feed industry to reduce the viscosity of food and improve nutrient absorption in the digestive tracts of animals [13]. The enzymes could be applied when the feeds are being processed, before the pellet process (70°C-95°C, pH 4.0-6.0), indicating the requirement for thermostable enzymes that are also active in acidic conditions [14,15]. Numerous studies have been conducted to isolate thermophilic enzymes with superior enzyme stability from fungi [12,16]. Thermophilic xylanases are characterised by temperature optima between 50 and 80°C and are stable in this range [16]. Chadha et al. [17] published a review on thermophilic fungal and bacterial xylanases that details that these enzymes have a multiplicity of isoforms (in excess of 15 for *Myceliophothora sepedonium*) in some instances that was revealed by transcriptomic and proteomic studies. However, due to the yield of enzymes required for large-scale applications, the search for microorganisms able to produce thermostable xylanases with high yields and characteristics desired for industrial applications

is still ongoing. Considering the industrial importance of xylanase, the aim of this study was to isolate, screen, and identify fungal isolates from the soil and bark of trees from three locations in KwaZulu-Natal, South Africa (29°49'01"S 30°56'41" E; 29°49'03"S 30°56'29" E and 29°16'13"S 31°22'06" E). This paper describes the isolation and screening of thermophilic xylanolytic fungi, as well as the growth parameters for optimal xylanase production by the highest xylanase producer, which was identified as a *T. harzianum* ZNH14 strain with appropriate physico-chemical properties for potential industrial application.

2.3 Materials and methods

2.3.1 Isolation, growth, and maintenance of bacteria and fungi

Soil and tree bark samples were collected from three local sites i.e., the University of KwaZulu-Natal (Westville) close to the Chemistry (29°49'01"S 30°56'41" E) and Microscopy (29°49'03"S 30°56'29" E) disciplines and a town known as Darnall in the north coast region (29°16'13"S 31°22'06" E) in KwaZulu-Natal, South Africa. Soil microbial properties vary widely, both spatially and temporally. Therefore, soil still remains an attractive source of microorganisms with desirable properties. It is important to carefully collect soil samples for bioprospecting microbial enzyme producers according to a given objective or hypothesis. However, in the interest of obtaining many different types of organisms, isolation was thus conducted from soil and tree bark samples that were obtained from different sites as simple random sampling [18]. Using sterile beakers and spatulas, 1 g of soil and bark samples were transferred to 10 ml sterile tubes. Ten-fold serial dilutions was performed, thereafter 0.1 ml aliquots from each dilution were spread plated on potato dextrose agar (PDA) and incubated at 30°C for 5 to 7 d. Pure isolates were obtained from each dilution plate [19]. Short term (working) stocks were prepared by with fungal isolates at 4°C that were previously inoculated and grown for 5 d at 30°C. For

the medium term stocks, PDA slants were prepared and left to solidify at room temperature in 15 ml falcon tubes. Fungal cultures were streaked on the PDA slants, grown for 5 d at 30°C followed by addition of sterile mineral oil to cover the fungal mycelium and storage at 4°C. Long term stocks were prepared by washing fungal spores from the 5 d PDA plates with distilled water and adding 50% glycerol in a 1:1 ratio to the spore suspension and storing at -20°C and -80°C.

2.3.2 Screening for enzyme activity

The screening strategy used was based on a combination of approaches reported in literature [20,21].

2.3.2.1 Primary screening of isolates

Qualitative screening was conducted by first growing the fungi on substrate agar plates containing (g/L): 0.5 g NaCl, 1 g KH_2PO_4, 0.5 g $MgSO_4$, 0.01 g $MnSO_4$, 0.3 g NH_4NO_3, 0.01 g $FeSO_4$, 6 g bacteriological agar supplemented with 1% (w/v) beechwood xylan. Plates were inoculated in the centre with the microorganism and incubated at 30°C for 5 to 7 d, then stained with 0.1% Congo red for 10 min and destained with 1 M NaCl for 15 min to observe and measure halo diameters for xylanase activity [21].

2.3.2.2 Secondary screening of isolates

The selected xylanase-producing isolates (after primary screening) were inoculated into potato dextrose broth and incubated at 30°C for 7 d at 200 rpm in a shaking incubator (New Brunswick Scientific, incubator shaker series, Innova 44). The cultured media was then centrifuged (Eppendorf Centrifuge 5418, Germany) at 16 873 × *g* for 10 min. Using sterile pipette tips, 5 mm wells were made on substrate agar plates as prepared above. The supernatants containing

the crude enzymes were dispensed into the wells and the plates incubated at 30°C for 2 to 3 d, after which they were stained, destained, and analysed as described previously in 2.3.2.1.

2.3.2.3 Tertiary (quantitative) screening of isolates

The isolates that showed high xylanase activity were subjected to quantitative screening after cultivation in a nutrient salt solution (NSS) medium [(g/L): 0.005 g CaCl, 0.23 g KH_2PO_4, 0.05 g $MgSO_4$, 0.005 g $NaNO_3$, 0.002 g $ZnSO_4$, 0.009 g $FeSO_4$, 0.23 g KCl, 7 g peptone, and 20 g wheat bran]. Erlenmeyer flasks (250 ml) containing 50 ml of the medium were each inoculated with two 5 mm fungal plugs from a 5 d old plate culture and incubated at 30°C at 200 rpm for 7 d in a shaking incubator (New Brunswick Scientific, incubator shaker series, Innova 44, Germany). Cultured media were removed after the incubation period and the cell-free supernatant was recovered by centrifuging samples at 16873 × *g* for 10 min (Eppendorf Centrifuge 5418, Germany). Xylanase activity was determined as described below 2.3.2.4.

2.3.2.4 Xylanase assay

Xylanase activity was quantified using the DNS assay for reducing sugars according to the method of Miller [23]. The reaction included 600 µl of 1% (w/v) beechwood xylan (1 g in 100 ml of 50 mM citrate buffer pH 5) which was placed in 15 ml test tubes and 66.67 µl of the enzyme was added. The reaction mixture was incubated in a water bath at 55°C for 15 min and terminated by adding 1 ml 3,5-Dintrosalicylic acid (DNS) reagent to the reaction mixture and then heated for 5 min at 100°C in a water bath. The absorbance was read at 540 nm using a spectrophotometer (Shimadzu UV-1800, Japan) to determine the concentration of sugar released by the enzyme. One unit (U) of xylanase was defined as the amount of enzyme that released 1 µmol xylose as reducing sugar equivalents per min under the specified assay conditions. All enzyme assays were performed in duplicate. The identification of the unknown

isolates was accomplished by: isolation of the genomic DNA; and amplification of the 18S rRNA ITS2 region; sequencing and BLAST analysis of the 18S rRNA gene.

2.3.3 Identification of unknown isolates

2.3.3.1 Genomic DNA extraction

Genomic DNA isolation was performed using the ZR Soil Microbe DNA Miniprep^{TM} kit (Zymo Research, USA) according to the instructions provided by the manufacturer. After extraction, gDNA samples were stored at -20°C. A gDNA concentration of 58.6 (CB1), 13.1 (CB2), 33.9 (PB7), 8.1 (PS3) and 44.7 µg/ml (MS5) was indicative of a successful DNA extractions and was used as template DNA in PCR reactions.

2.3.3.2 Polymerase chain reaction amplification of the 18S ribosomal RNA ITS2 region and identification

Universal fungal primers for the ITS2 region of the 18S rRNA were used for the PCR reaction. The ITS primer pair used were: forward: ITS5F (5'- GGAAGTAAAAGTCGTAACAAGG -3') and reverse: ITS4R (5'CTCCTCCGCTTATTGATATGC -3') [24]. The PCR reaction consisted of template DNA, 2.5 µM forward and reverse primers, 25 mM $MgCl_2$, 10 mM dNTPs, Taq DNA polymerase from *Thermus aquaticus* (Sigma-Aldrich, USA), 10 mM buffer (Thermo Scientific, USA). The reaction mixture was brought up to a volume of 50 µl using nuclease-free water. Amplification was conducted in a T100 Thermal Cycler (Bio-Rad, USA) under the following thermal cyclic conditions: initial denaturation at 95°C for 2 min followed by 25 cycles of denaturation at 95°C for 30 s, annealing at 53°C for 45 s, and extension at 72°C for 1 min. Thereafter, a final extension step was performed at 72°C for 8 min. The PCR products were then subjected to electrophoresis on a 1% agarose gel, which was run at 90 V for 45 min and then stained with ethidium bromide (0.5 µg/ml). The presence of the PCR amplicon was

confirmed and sent to Inqaba for sequencing. The sequences cleaned using DNA Man and thereafter the consensus sequence was used to identify the isolates by BLAST analysis, using the NCBI database [25].

2.3.4 Effect of pH and incubation temperature on xylanase production from MS5

The effect of pH and incubation temperature on xylanase production was studied according to Bhavsar et al. [26] to aid in the selection of the most promising isolate. High temperatures could result in evaporation and drying of the wheat bran. This was avoided by using a larger total volume of media and an equivalent inoculum size. The effect of pH on xylanase production was determined in NSS media prepared in buffers ranging from pH 4.0 to 10.0 by adjusting the pH using 1 M HCl and 1 M NaOH. Erlenmeyer flasks (250 ml) containing 50 ml of the medium were each inoculated with two 5 mm fungal plugs from 5 d old plate cultures and incubated at 30°C at 200 rpm for 7 d in a shaking incubator (New Brunswick Scientific, incubator shaker series, Innova 44, Germany). The pH was not maintained however to verify that the pH was the same as the initial, the pH was measured towards the end of fermentation and compared to the initial pH (4.0-10.0).

The effect of temperature on xylanase production was studied by inoculating a 5 d old culture into the NSS medium prepared with the pH buffer that resulted in the best enzyme activity determined previously and incubated at 20 to 80°C for 7 d at 200 rpm. Xylanase assays were performed as described previously and results were reported. The catalytic temperature during the assays was controlled by a CPS Controller (Shimadzu CPS-240A, Kyoto Japan) attached to the spectrophotometer. The isolate that resulted in the highest enzyme activity was selected for further studies.

2.3.5 Phylogenetic analysis and morphological studies of MS5

2.3.5.1 Phylogenetic analyses

The 18S rRNA sequence of the isolate was compared with other closely related strains using BLAST and NCBI GenBank data base. Alignment and the phylogenetic tree were constructed using MEGA 11 software. The neighbour-joining (NJ) tree of the isolate was evaluated using 100 bootstrap replications [27]. The phylogenetic tree included 51 nucleotide sequences obtained from NCBI Blast.

2.3.5.2 Morphological characterization using light microscopy

The morphological characteristics of the *T. harzianum* strain were examined using a 5 d old fungal culture. A lactophenol cotton blue wet mount slide was prepared using the method of Leck [28]. The slide was examined using a light microscope (Primostar 415500-0057-000, Germany) to examine the structures. The photomicrographs were recorded with an iPhone 6s camera.

2.3.6 Time course for optimal enzyme production

To determine the time required for optimal enzyme production, 50 ml NSS (pH 5.0) was dispensed into 250 ml Erlenmeyer flasks, inoculated with two 5 mm plugs of a 5 d old fungal culture, and incubated at 200 rpm at 70°C in a shaking incubator (New Brunswick Scientific, incubator shaker series, Innova 44, Germany). Samples were collected every 24 h and centrifuged at 16 873 × *g* for 10 min and xylanase activity quantified. All experiments and analytical assays on samples were carried out in duplicate yielding quadruplicate results [29].

2.3.7 Effect of agitation on xylanase production

The effect of agitation conditions on xylanase production during submerged shake flask fermentation was studied in Erlenmeyer flasks (250 ml) containing 50 ml of the medium (pH 5.0) inoculated with two 5 mm fungal plugs from a 5 d old plate culture and incubated at 70°C in a shaking incubator (New Brunswick Scientific, incubator shaker series, Innova 44, Germany) at different rpm (120, 140, 160, 180 and 200). All experiments and analytical assays on samples were carried out in duplicate yielding quadruplicate results [29].

2.3.8 Effect of different carbon and nitrogen sources on xylanase production

The effect of carbon and nitrogen sources in the NSS was determined. Different carbon sources (1% w/v) such as wheat bran, glycerol (v/v), glucose, sucrose, maltose, and lactose [30,31] and different nitrogen sources (1% w/v) such as peptone, ammonium sulphate, ammonium acetate, casein, glycine, and yeast extract [32,33] were used to determine maximal enzyme production under optimized conditions for the other parameters. Once the optimal carbon and nitrogen sources were determined, concentrations between 0.5 and 2% (w/v) were used to determine the optimal concentration for maximum xylanase production.

2.3.9 Biochemical characterization of crude enzyme

2.3.9.1 Determination of pH and temperature optima of crude xylanase

To determine the optimum pH values for xylanase activity, different pH buffers were required with 1% substrate for the enzyme reaction at 55°C. The following buffers were used: 0.1 M sodium citrate buffer (pH 3.0-5.0), 0.1 M potassium phosphate buffer (pH 6.0-8.0) and 0.1 M Glycine-NaOH buffer (pH 9.0-10.0) [34]. All buffers were adjusted to the required pH by using 0.1 M HCl and 0.1 M NaOH as the acid and base. Thereafter, the reaction was stopped by adding DNS and incubating assays at 100°C [23].The optimum temperature of xylanase activity

was determined by incubating the enzyme with the optimum pH buffer (pH 6.0 and 8.0) and substrate (1%) in a temperature range between 40 and 90°C for the reaction time. Thereafter, the enzyme was assayed using the DNS method [23].

2.3.9.2 pH and temperature stability of crude xylanase

The pH stability of the enzyme was determined at both pH optima (pH 6.0 and 8.0) by incubating the enzyme in the respective buffers for 4 h at optimum temperature with aliquots removed every 30 min [35]. Thereafter, xylanase activity was assayed using the DNS method [23] and reported as residual activity (%). Temperature stability of xylanase was determined by preincubating the enzyme at the different temperature optima (55, 60, 70 and 75°C) with aliquots collected every 30 min for 4 h for determination of residual activity that was reported as a mean (n=3) ± SD.

2.3.9.3 SDS-PAGE

SDS-PAGE was carried out according to Laemmli [36]. A 12% denaturing polyacrylamide gel which contained SDS was prepared. Following electrophoresis at 50 V for 4 h, the gel was stained with Coomassie Brilliant Blue for 15 min and destained overnight in a de-staining solution. In order to visualize the proteins and determine the molecular mass of the proteins using standard molecular weight markers. To allow for the protein to be more visible, sliver staining was performed according to the manual instructions (SilverQuest^{TM} Silver Staining kit, Thermo Fisher Scientific, LC6070).

2.3.9.4 Substrate Native PAGE

Native-PAGE was conducted at room temperature using a 15% polyacrylamide gel supplemented with 1% (w/v) beechwood xylan. Following electrophoresis at 50 V for 4 h, the

xylan gel was incubated at optimum temperature (70°C) in pH 5.0 citrate buffer for 1h. The gel was stained with 0.1% (w/v) Congo red for 15 min at room temperature and destained with 1M NaCl for 10 min. The protein bands associated with xylanase activity were visualized as clearing zones against a background [37].

2.3.10. Statistical analysis

Data presented in this paper showed the mean of four replicates with their standard deviation (mean ± SD). Results were analyzed statistically by Microsoft Excel.

2.4 Results and discussion

2.4.1 Screening for enzyme activity

A total of 48 isolates were obtained from the three sites, with similar isolates obtained from soil and bark samples within the three sites. From all the isolates, 33 were selected for secondary screening based on the size of the clear zones on xylan agar plates (Appendix I, Supplementary Tables 1-3). The unhydrolyzed, Congo red-stained xylan medium appeared dark red as seen in the negative control (Table 2.1).

Table 2.1: Fungal isolates substrate agar screening results for xylanase activity

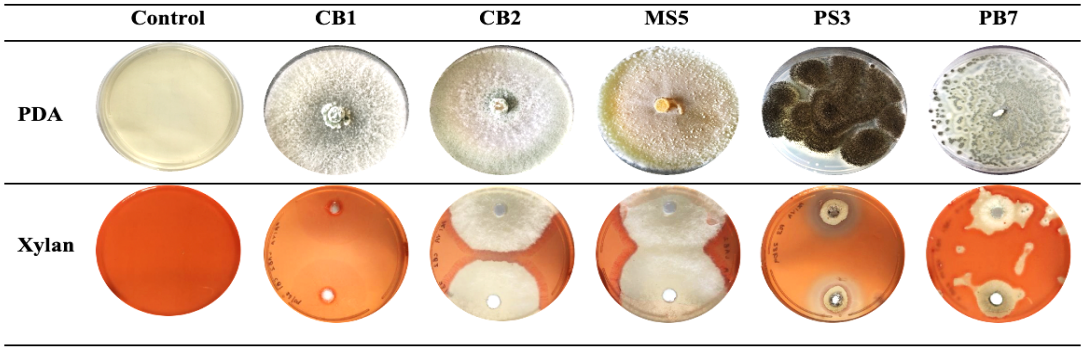

In spite of advanced knowledge of microbial xylanases garnered over the past decades, bioprospecting for organisms with xylanases with potentially ideal characteristics for industrial application is ongoing and to this end several factors (location, desired qualities, characteristics of microorganism, etc.) are still significant for the choice of such an organism. In the present study 46 filamentous fungal isolates were obtained from soil and tree bark samples and screened for their xylanase activity under submerged fermentation. During the isolation, the growth of bacteria was not intentionally prevented, instead sub culturing was performed from the original plates to obtain pure fungal cultures. Primary screening using qualitative methods is a powerful tool that allows rapid and easy screening of microorganisms for enzyme production. This qualitative substrate agar test indicates positive or negative enzyme production and is invaluable when screening a large number of isolates and quantitative analysis is not required [38]. The xylanase-producing isolates displayed clearing zones from a dark red to a light red colour representing efficient xylanase activity. The low enzyme activity displayed by some isolates may be due to the presence of contaminants or enzyme activities being too low for complete hydrolysis of the substrate for visualization on the substrate agar [39].

The 23 isolates (Appendix I, Supplementary Tables 4-6) with the largest zones of clearance (Figure 2.1) were selected for quantitative analysis. In Figures 2.1a-c, isolates CB1 (21.67 U/ml), CB2 (16.98 U/ml), MS5 (22.98 U/ml), PS3 (15.64 U/ml) and PB7 (14.22 U/ml) produced the highest xylanase activity.

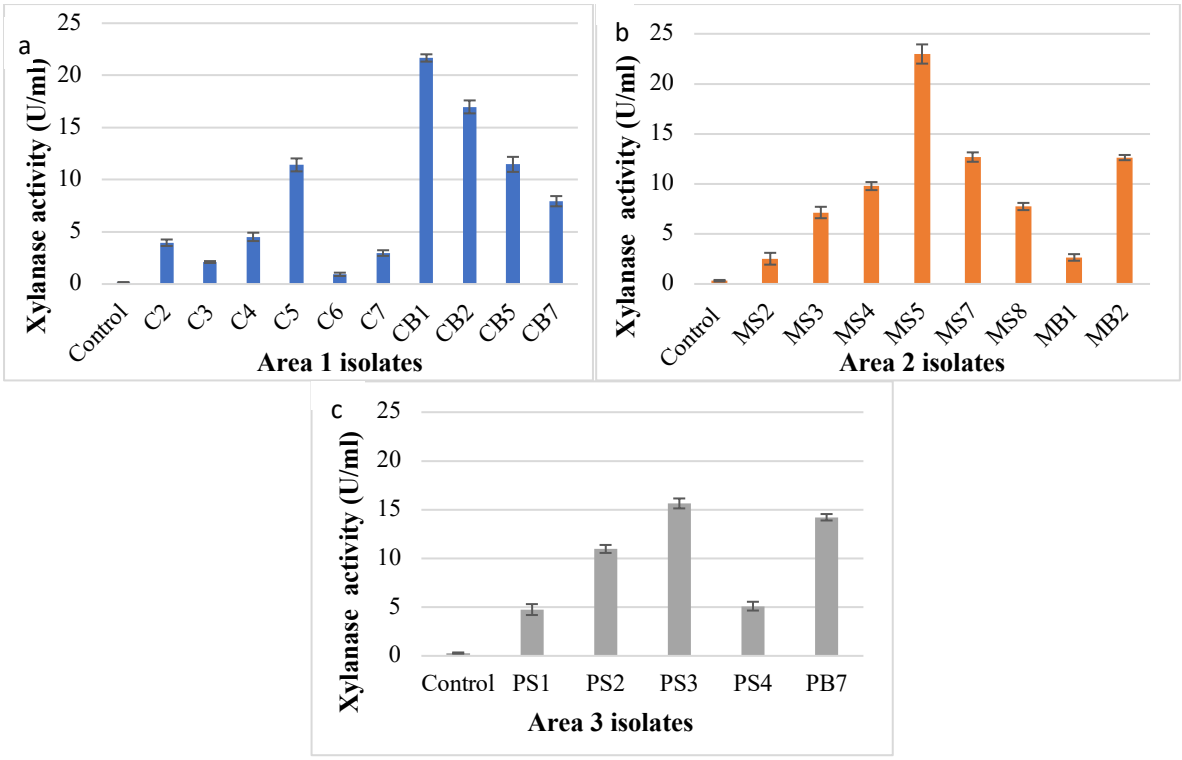

Figure 2.1: Xylanase activity of the fungal isolates from the different sample areas based on the DNS method for reducing sugars. a: Area 1, b: Area 2, and c: Area 3.

2.4.2 Effect of pH and incubation temperature on xylanase production

Five of the 23 isolates, with the highest activities (CB1, CB2, MS5, PS3, and PB7) were selected for pH and temperature studies in order to determine the best isolate for future studies. To determine the best conditions for enzyme production, the effect of pH was determined between pH 4.0 and 10.0 (Figure 2.2). Isolate CB1 produced the highest enzyme activity (38.32 ±0.89 U/ml) when grown in the medium at pH 10.0, with elevated enzyme activity at pH 7.0 and 9.0. Isolates CB2 and MS5 produced the highest enzyme activities of 38.49 ±1.16 U/ml and 38.50 ±0.76 U/ml at pH 6.0 and 5.0, respectively. Isolate PB7, produced highest enzyme activity (38.12 ±0.79 U/ml) at a neutral pH. Lastly, for isolate PB7, the highest enzyme activity (36.96 ±0.32 U/ml) was observed at pH 6.0.

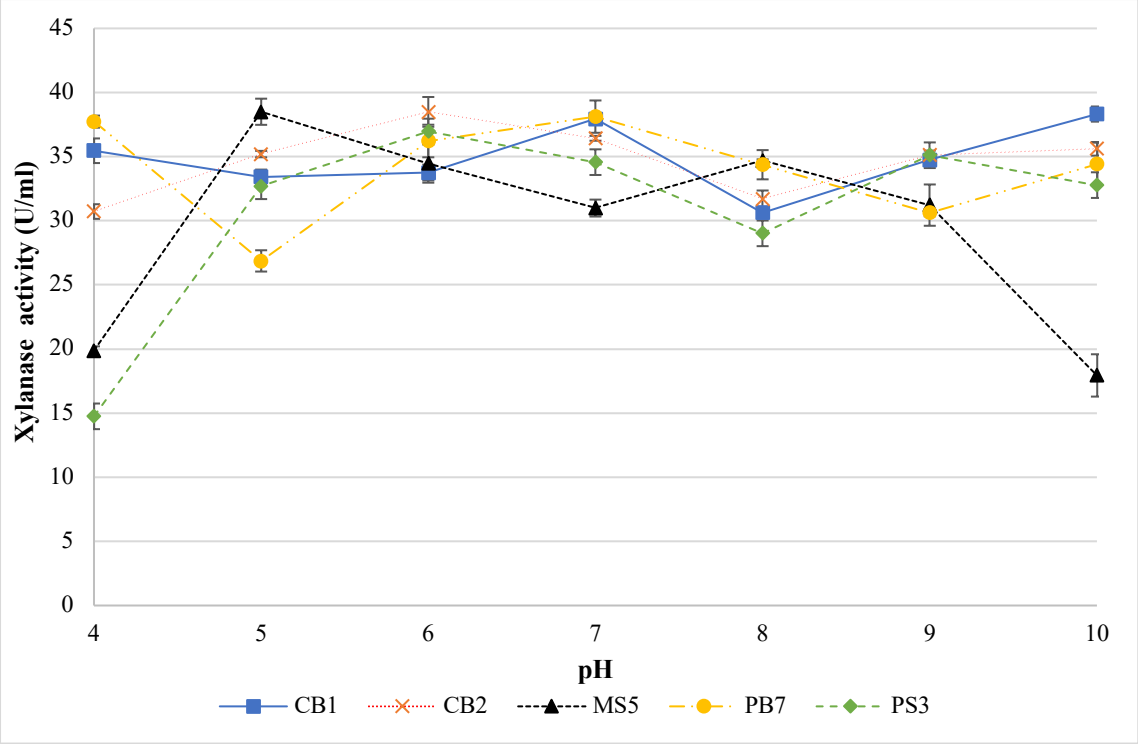

Figure 2.2: Effect of pH on xylanase production for the five selected fungal isolates, produced during submerged fermentation at 30°C and 200 rpm. Data points represent the means ± SD (n=4).

The effect of temperature on enzyme production is shown in Figure 2.3. Temperatures between 20-80°C were tested as this was the range tested in previous studies [40]. For isolate CB1, enzyme activity was highest (36.17 ±1.65 U/ml) at 60°C and for isolates, CB2 and PB7, the highest activities of 37.77 ±0.85 U/ml and 37.69 ±0.82 U/ml, respectively were observed at 50°C. Isolate MS5 produced the highest enzyme activity (38.17 ±0.86 U/ml) at 70°C, and isolate PS3 appeared to be an extreme thermophile and produced the highest (35.96 ±1.16 U/ml) enzyme activity at 80°C with similar activities at 40°C and 50°C (35.61 ±0.84 U/ml and 35.01 ±0.84 U/ml). Isolate MS5 was selected for further studies due to its thermophilic properties and acidic conditions.

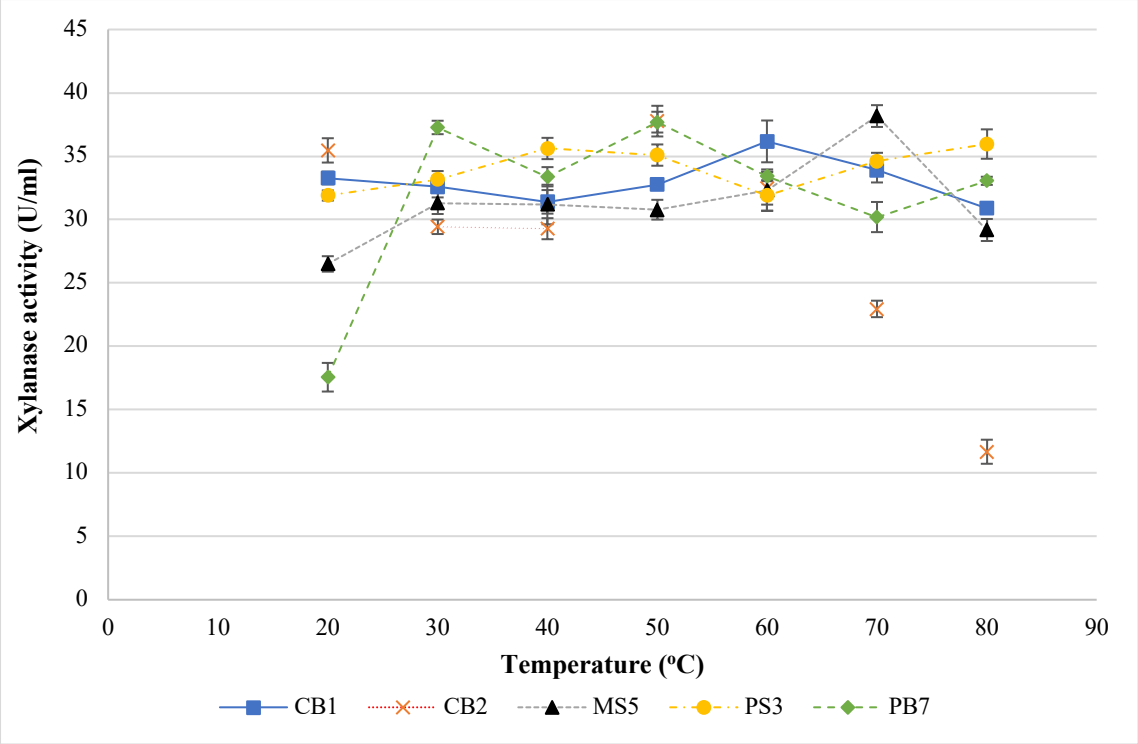

Figure 2.3: Effect of temperature on xylanase production by the five selected fungal isolates, during submerged fermentation at their optimum pH and 200 rpm. Data points represent the means ± SD (n=4).

The pH plays a crucial role in nutrient transport across the membrane and the functioning of the microorganism's enzyme systems and thus influences the growth rate and the levels of enzyme produced [41]. The temperature of the fermentation medium is a vital factor that has a strong influence on product formation [42]. Isolate CB1 identified as *Hypocrea lixii* (a teleomorph of *T. harzianum*), exhibited the highest activity at pH 10.0 with several other peaks indicating the organism, is possibly an alkaliphile that also produced isoforms with different pH and temperature optima or could be different gene encoding a different GH enzyme. Temperatures between 20-80°C were tested and all five isolates produced the highest activities at temperatures between 50 and 70°C. Again, a second enzyme activity peak observed would indicate the presence of more than one isoform. de Oliveira et al. [43] also reported the presence of isoforms at 55°C at pH 5.0 and at 44°C at pH 3.6 for xylanases produced by *Hypocrea lixii*. Isolate CB2, identified as *Trichoderma atroviride,* appeared to be an acidophile and produced the highest activity at pH 6.0. Isolates PS3 and PB7 displayed highest activity at neutral pH and

at pH 6.0, respectively indicating that the latter could possibly be an acidophile. Both these isolates are *Aspergillus* spp. and Hombalimath et al.[44] reported similar studies where optimal activity was obtained at pH 7.0. Isolate MS5 showed optimal results at pH 5.0 with a second peak at pH 8.0, this was similar to a report by Amore et al. [45] who obtained maximal activity at pH 7.0 and a second peak at pH 9.0. Most fungi can grow in a wide pH range of 5.0–10.0 [39, 46]. Generally, the higher xylanase titres (2701 U/g substrate) in fungal systems have been reported to occur at pH 5.0 [47]. However, their reported activity was expressed per gram substrate utilized which was reported for lignocellulosic biomass whereas the current study reports it in the conventional manner (U/ml). In addition, many studies report on the purified enzymes or on recombinant enzymes thus activities are higher [48,49,50]. Xylanases produced by these isolates may have a potential in applications in different sectors, including food and feed, paper and pulp and textile industries that require enzyme to work at high temperatures. The highest xylanase titres in fungal systems have generally been reported to occur at temperatures that are optimal for the growth of cultures in submerged fermentation [51]. The majority of fungal isolates produce one to three xylanase isoforms [52,53]. Lenartovicz et al. [54] reported that three xylanase isoforms were produced by *Aspergillus fumigatus*. However, *Thermomyces stellatus* and *Scytalidium thermophilium* are reported to have 10 isoforms while *Pseudocercosporella* and *Myceliophthora themophilum* have 14 and 13 isoforms, respectively [27]. Multiple forms of xylanases differ in stability, catalytic efficiency, absorption, and activity on substrates [55]. Badhan et al. [56] reported that ten different functionally diverse xylanases were resolved electrophoretically using PAGE/IEF from *Myceliophthora* sp. and they also showed characteristically different activity against unsubstituted xylans, arabinoxylans and methyl-glucuronoxylan.

Isolate MS5 was selected for further studies due to its thermophilic properties (temperature optimum of 70°C) and acidic pH optimum of 5.0; these properties were deemed favourable to

the conditions for its targeted application in the hydrolysis of animal feed [57]. The advantages of thermophilic enzymes for conducting biotechnological processes at elevated temperatures are; reducing the risk of contamination by mesophilic microorganisms, decreasing the viscosity of the reaction medium, increasing the bioavailability and solubility of organic compounds, increasing the diffusion coefficient of substrates and products resulting in higher reaction rates [58]. Azimova et al. [59] reported that the *T. harzianum* strain UzCF-28 produced xylanases which was also confirmed by Abbas et al. [60].

2.4.3 Identification of the five fungal isolates and morphological studies of the selected isolate

2.4.3.1 Identification of fungal isolates

The PCR amplicon was sent to Inqaba for sequencing and the consensus sequences were submitted to National Centre for Biotechnology Information (NCBI) database to determine the identity of the unknown isolates. Isolate CB1 had a 99.83% identity with *Hyprocrea lixxi* strain TU Graz 3TSM1 and CB2, a 100% identity to *Trichoderma atroviride* strain CUZFVG243. Isolates PB7 and PS3 are both *Aspergillus* sp. with a 99.49 and 99.83% identity to *Aspergillus fumigatus* CK392 and *Aspergillus welwitschiae* SFC102281, respectively. Although sequencing and BLAST analysis resulted in a low (45%) percentage coverage the ID of the unknown isolate MS5, it was revealed to be *T. harzianum* strain with a 99.83% identity to *T. harzianum* ZNH14 strain (Table 2.2). The ITS2 region of the 18S ribosomal RNA was amplified as shown in Figure 2.4, in which an expected 600 bp amplicon was obtained.

Table 2.2: Identification of unknown isolates

Isolate	Identity	Max score	Total score	% Coverage	E.value	% Identity	Accession number
CB1	*Hypocrea lixii* TU Graz 3TSM1	1096	2096	94	0	99.83	EU871017.1
CB2	*Trichoderma atroviride* CUZFVG243	1075	2107	96	0	100	KC884783.1
PB7	*Aspergillus fumigates* CK392	1066	2111	98	0	99.49	MK439477.1
PS3	*Aspergillus welwitschiae* SFC102281	1068	2046	94	0	99.83	MH374611.1
MS5	*Trichoderma harzianum* ZNH14	1110	2129	45	0	99.83	KR868336.1

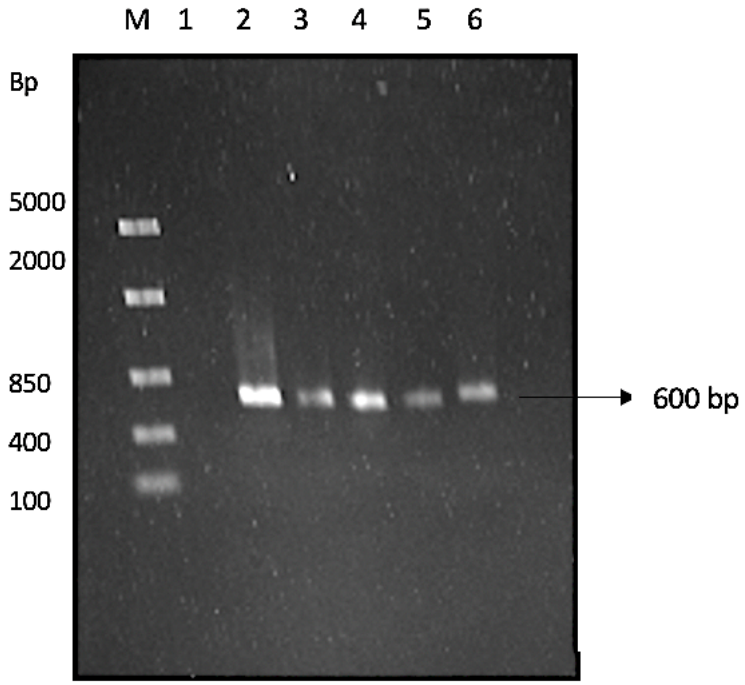

Figure 2.4: Agarose (1%) gel showing 18S rRNA amplicon. Lane M: Marker, FastRuler Middle Range Molecular Weight Ladder (Thermo Scientific, USA), Lane 1: Negative control, Lane 2: CB1, Lane 3: CB2, Lane 4: PB7, Lane 5: PS3, and Lane 6: MS5, 600 bp between ITS5 and

The BLAST analysis returned a low percentage coverage (45%) however, the ITS2 amplicon was of the recommended size, the E value (Table 2.2) is 0 despite the low percentage coverage there was a 99.8% similarity to *T. harzianum* ZNH14 [61]. Filamentous fungi that belong to the *Trichoderma* genus are attractive [62] due to their inducible enzyme systems, the considerable quantities of enzymes secreted by these fungi, including cellulase and hemicellulase cocktails. As a result of their wide spectrum of metabolic activities, *Trichoderma* sp. fungi have found numerous practical applications such as enzyme producers, as bio-fungicides [63], and in the food industry [64].

2.4.3.2 Phylogenetic analysis of isolate MS5

The phylogenetic tree was constructed using the Neighbour-joining method [65] (Figure 2.5). Phylogenetic analysis plays an important role in understanding the current research in biological

processes (the evolution of species, populations and genes) and became an important data source for how traits evolve over time, the order in which interrelated traits evolve and the influence of an ecology on the evolution of traits. The evolutionary relationship between species is generally reflected in the form of phylogenetic trees [10]. There were 46 branches originating from the original root. All the *T. harzianum* isolates do not form a single taxon but form sister taxa with other *Trichoderma* species. The isolate reported in the current study forms sister taxa with 2 other *T. harzianum* strains as well as a third branch that splits into 2 sister taxa, one being a *Trichoderma* sp. and the other *T. lixii*.

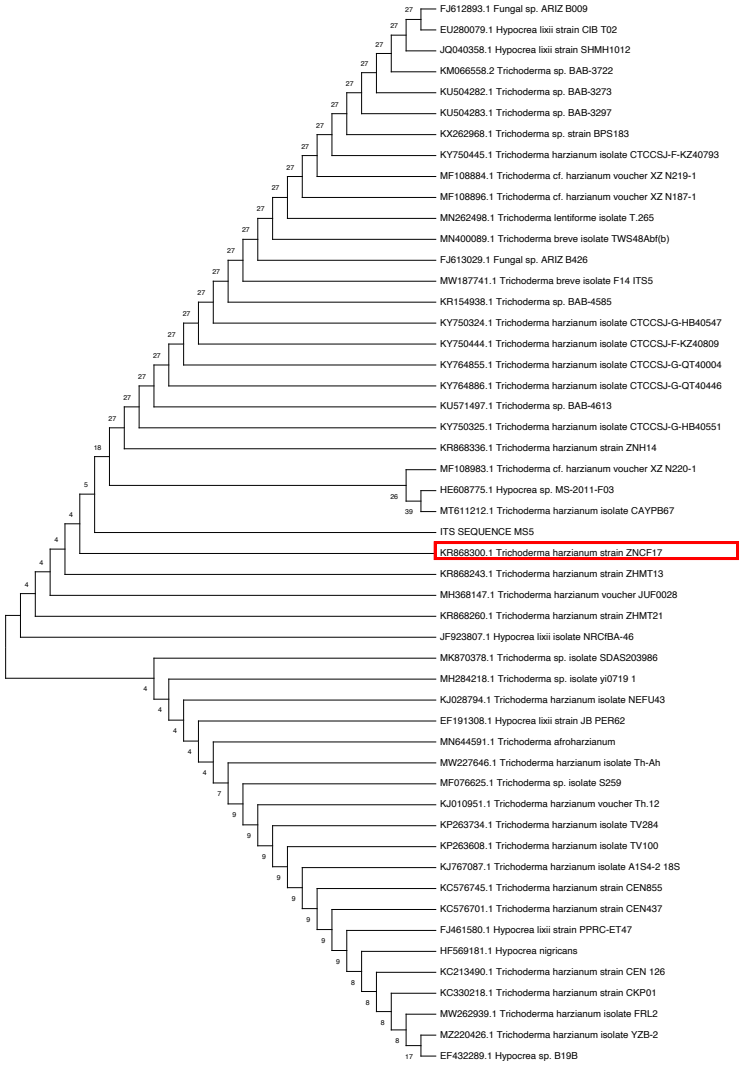

Figure 2.5: Phylogenetic analysis of the 50 isolates based on alignment of the nucleotide sequences of xylanases including the ITS sequence of selected MS5 isolate with Mega11. The microbial species, strain name and accession number are presented.

Sequences were assembled and aligned using the Mega11 software. All species of the related taxa from BLAST analysis were included in the phylogenetic tree, all *T. harzianum* strains were not grouped together and the species were either scattered among the clades or showed separate terminal branches. Chen and Zhuang [10] discovered several new *Trichoderma* sp. during a screening exercise conducted on several hundred soil samples in China. They reported that *T. harzianum* formed the largest clade among the green-spored groups that formerly contained 41 species. The abbreviated tree was constructed using 50 different microorganisms, mostly *T.*

harzianum strains. Two predominant sister clades emerge from the root. Both consist of strains of *T. harzianum* but with *Hypocrea* strains forming part of the same sister clades. such as *T. harzianum* strains as well as *T. lixii* NRCfBA-46 in terms of distance [10]. Chaverri and Samuels [66] reported cultures derived from ascospores of *H. lixii* (*T. lixii*) cultures produced the morphological species *T. harzianum.* Studies showed *H. lixii* isolates were shown to group with isolates of *T. harzianum* based on phylogenies of four genes, translation elongation factor-1 α, calmodulin, actin and ITS rDNA, and morphological data [67]. This could explain the genetic link between the two morphotypes.

2.4.3.3 Morphological studies of MS5

Microscopic examination of the 5 d old culture using light microscopy showed septate hyphae, conidiospores and phialides (Figure 2.6). The morphological analysis indicates that isolate MS5 belongs to the *Trichoderma* genus.

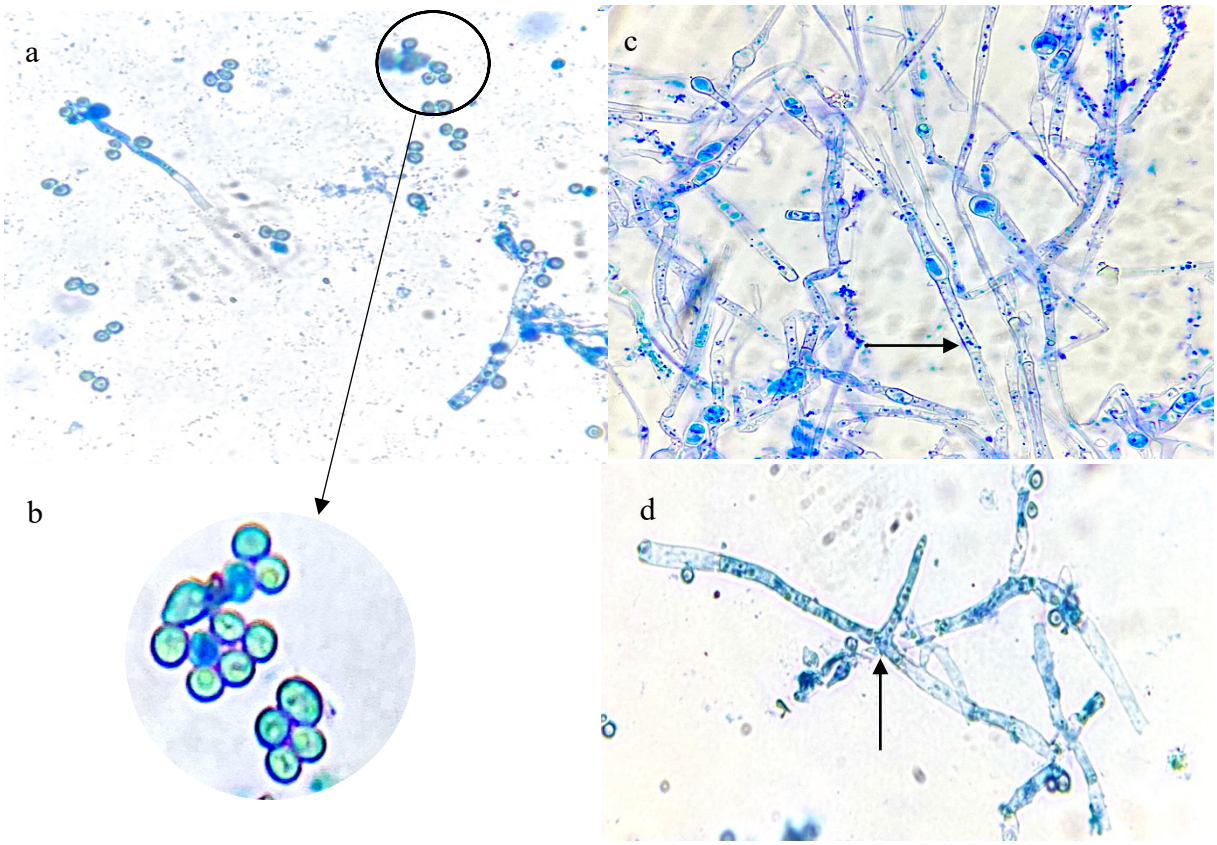

Figure 2.6: Photomicrographs of a lactophenol cotton blue strain preparation of the identified *T. harzianum* strain at 1000 X magnification. The black arrows represent, (a) Conidia (b) an enlarged image of the conidiospores (c) Hyphae, and (d) Phialides.

When grown on PDA, the *T. harzianum* strain initially produced a fast-growing white downy mycelium (Table 2.1) which then changed to yellowish-green and later deep green as it matured. The conidiation predominantly effuse which appear powdery and granular due to dense conidiation producing woolly and floccose compact tufts and rings with green coloured spores fringed by sterile white mycelium [68]. Microscopic examination of the 5 d old culture using light microscopy showed septate hyphae, conidiospores and phialides (Figure 2.6). Conidiospores of *T. harzianum* were formed in pairs along the main branches and axis (Figure 2.6a). The hyphae were thin and branched (Figure 2.6c).The phialides branching patterns were verticillate, broad, and branching frequently at approximately 90° one branching verticillate had two to three phialides (Figure 2.6d). Phialides were characteristically elongate lageniform

in shape. At the end of the phialides, conidia were formed with a globose or subglobose shape to obovoid and are smooth-walled, subhyaline to pale green (Figure 2.6b). These structures are similar to those described in previous studies [68].

2.4.4 Time course studies for optimal xylanase production by *T. harzianum*

The effect of time required for maximal xylanase production was determined by growing the isolate at 70°C at 200 rpm for 1 to 8 d. The highest activity (39.01 ±0.75 U/ml) was obtained after 5 d. A further increase in the incubation period resulted in a decrease in the enzyme production (Figure 2.7).

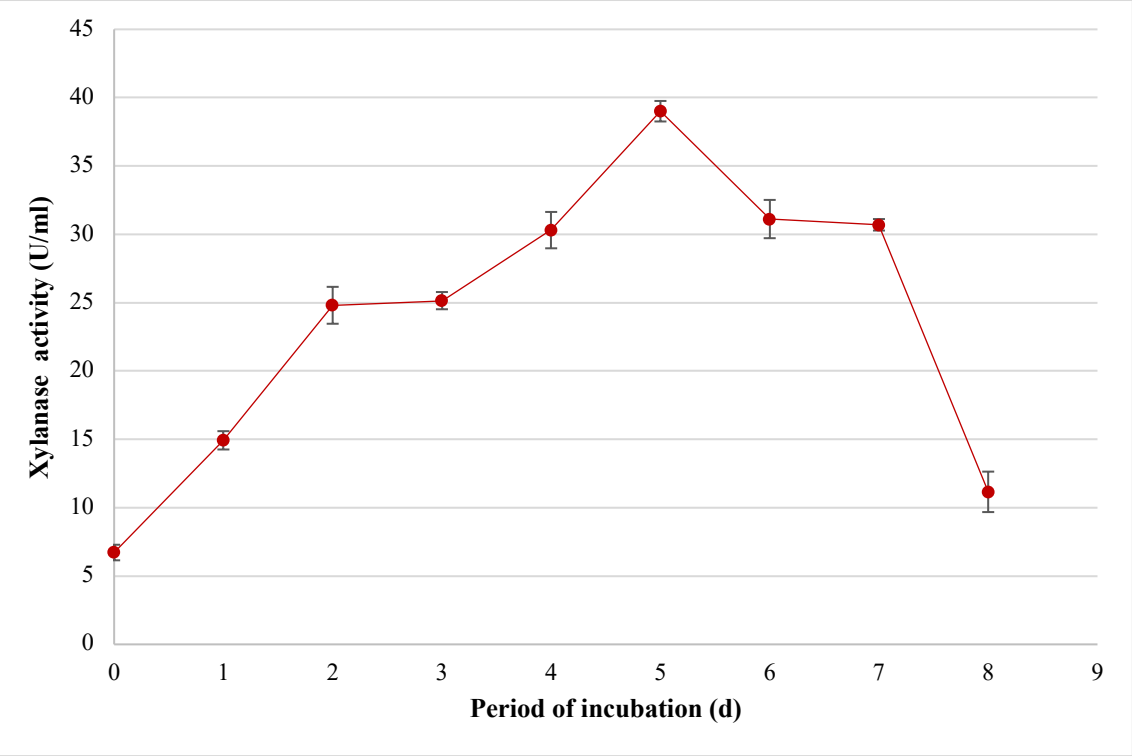

Figure 2.7: Time course studies showing the optimal period of incubation for maximum xylanase production by identified *T. harzianum* isolate during submerged fermentation at 70°C, pH 5.0 and standard agitation (200 rpm). Data points represent the means ± SD (n=4).

Production of microbial enzymes is dependent upon various cultural and nutritional factors such as fermentation incubation period, agitation, carbon and nitrogen sources and hence these were

studied in order to optimize xylanase production from *T. harzianum*. For the optimal period for enzyme production, the fungal isolate was incubated for a period of 8 d at optimal pH and temperature obtained previously. The highest enzyme activity (39.01 U/ml) was obtained after 5 d. Similar results were reported by Goyal et al. [69] where optimal xylanase activity (139.82 U/ml) was obtained between 5 to 7 d of incubation for *T. viride*. After 5 d of incubation, the enzyme activity declined, this could be due accumulation of toxic products in the medium that inhibit fungal growth, repression of enzyme expression by metabolic products or by multiple regulatory mechanisms [70].

2.4.5 Effect of agitation on xylanase production by *T. harzianum*

The effect of agitation speeds on xylanase production was studied between 120 and 200 rpm at 70°C for 5 d. At the lower agitation rates tested, enzyme production was directly proportional to agitation speed with the highest xylanase activity (39.19 ±0.83 U/ml) observed at 160 rpm (Figure 2.8). However, a further increase in agitation speed resulted in a sharp and steady decrease in enzyme activity.

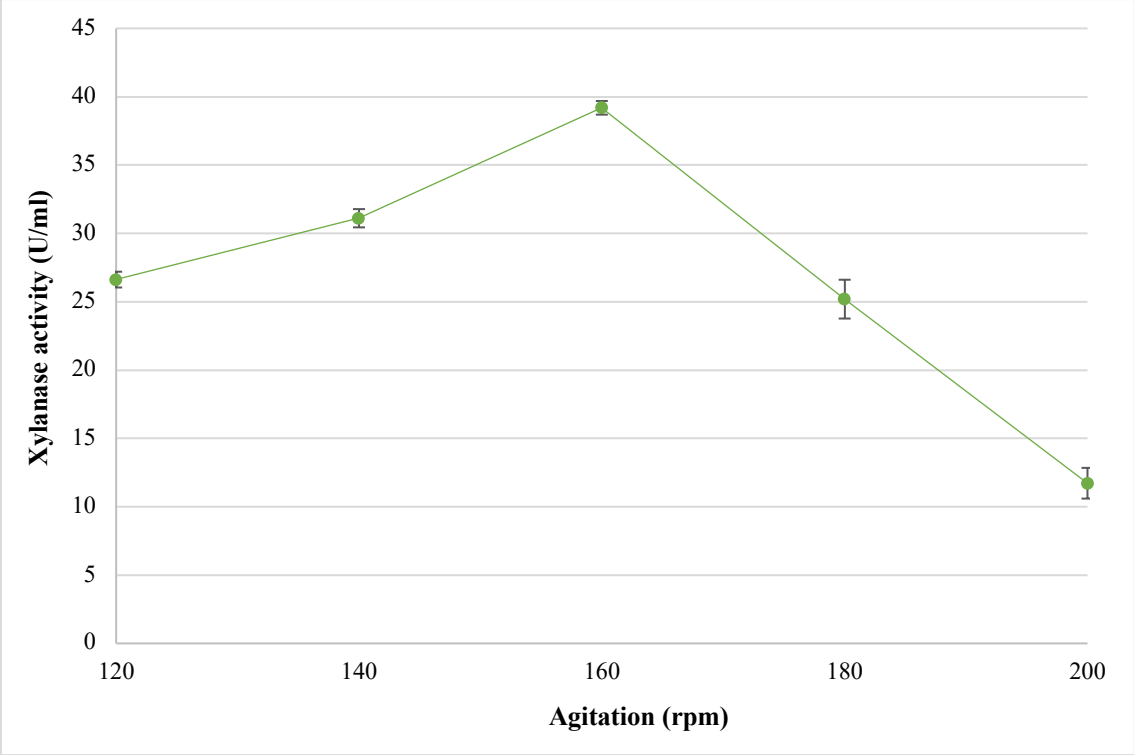

Figure 2.8: The effect of agitation on xylanase production by the identified *T. harzianum* isolate, produced during submerged fermentation at 70°C, pH 5.0 for 5 days. Data points represent the means ± SD (n=4).

Agitation is considered an important factor for microbial growth as it controls the transfer of oxygen, heat, and nutrients from the medium to the microorganism and prevents the clumping together of the mycelia [71]. Highest enzyme activity (39.19 U/ml) was observed at 160 rpm (Figure 2.8) with higher agitation speeds resulting in lower xylanase activity. These higher agitation levels may have aggravated cell damage which, in turn, could have led to enzyme production falling off [72]. Several reports link increased agitation speeds to high shear stress leading to mycelial rupture and destruction of cellular structures which decreases both mycelial growth and enzyme production [73,74]. At high agitation rates, laminar flows are generated in a flask which do not allow absorption of oxygen into the medium although rpm is high which may cause reduced growth and enzyme production. However, below a certain threshold, lower

agitation rates result in reduced mixing of the medium and as a consequence lower oxygen supply to the microorganism, lower growth rates and thus enzyme production.

2.4.6 Effect of different carbon and nitrogen sources on xylanase production by *T. harzianum*

The effect of carbon (Figure 2.9a) and nitrogen sources (Figure 2.9b) in the growth medium were studied to order to maximize enzyme production. It was clear that the *T. harzianum* strain produced the highest xylanase levels when supplemented with glucose (36.76 ±0.97 U/ml) compared to the control, followed by wheat bran (35.44 ±0.86 U/ml) and sucrose (24.77 ±0.71 U/ml). Glycerol had a large negative effect on enzyme production (6.86 ±0.44 U/ml). Wheat bran was selected as the carbon source for further studies.

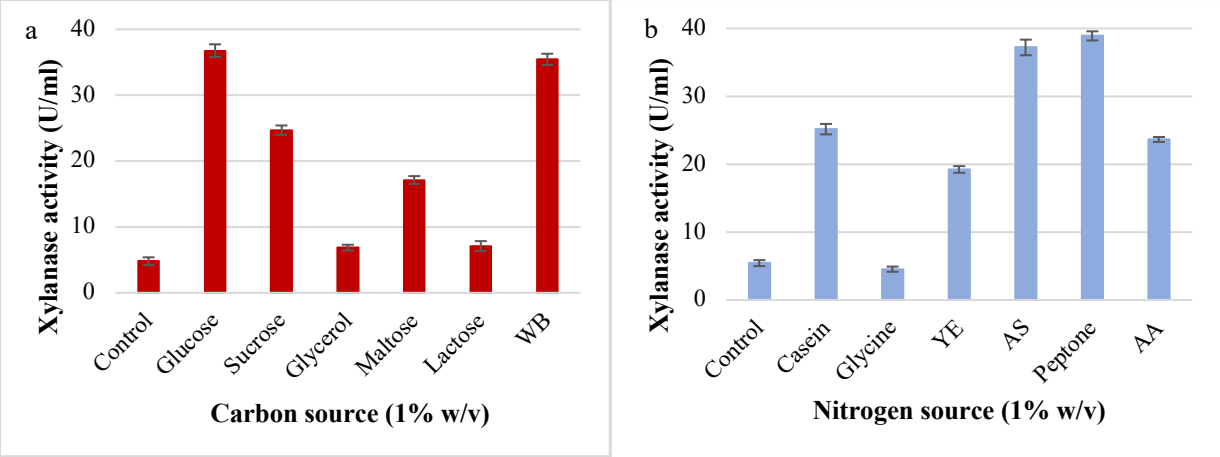

Figure 2.9: Effect of various carbon (a) and nitrogen (b) sources on xylanase production by identified *T. harzianum* isolate during submerged fermentation at 70°C, pH 5.0, for 5 d at 160 rpm. WB: wheat bran, YE: yeast extract, AS: ammonium sulphate, and AA: ammonium, and AA: ammonium acetate. Bars represent the means ± SD (n=4).

Carbon and nitrogen sources are necessary for the growth and metabolism of microorganisms. The use of affordable C and N sources is important as these can reduce the cost of production significantly. Surprisingly the best carbon source for xylanase production from *T. harzianum*

was glucose. Carbon catabolite repression (CCR) has to be overcome for expression of hydrolytic enzymes [75]. Basal expression levels of *xyn1* coding for xylanase is affected by glucose and repression is reported to be mediated by the binding of the catabolite repressor protein *Cre1* to the promoter of *xyn1*. Mutants with truncated *Cre1* escape CCR [76]. Segato Rizzatti et al. [77] studied xylanase regulation in *Aspergillus phoenicis* by growing the organism in media supplemented with 1% glucose, xylan or xylose. In the first few hours glucose repressed xylanase production but after 72 h the level of glucose in the culture medium had dropped below 0.05 mg/ml, and some xylanolytic activity was already detectable in this carbon-derepressed culture. We believe that the levels of xylanase obtained in our study were during the de-repressed phase. The next best substrate was wheat bran while glycerol resulted in the lowest xylanase levels. Low activity could be due to the inability of the fungus to metabolize some substrates. Seyis and Aksoz [78] tested xylanase production by *T. harzianum* 1073 D3 and reported maximum activity on melon peel (26.5 U/mg of protein) Wheat bran was selected as carbon source as glucose is not cost-effective. Other enzyme production studies have also shown that wheat bran is a good carbon source for maximal xylanase production [79]. The organic nitrogen source, peptone resulted in the maximum yield of xylanase from *T. harzianum* followed by ammonium sulphate (Figure 2.9) while xylanase production decreased in the presence of glycine. A review of the literature showed that ammonium sulphate (37.2 U/ml) is an appropriate source of nitrogen for *T. harzianum,* so it was selected as peptone (38.9 U/ml) is not cost-effective [79,80]. Glycerol had the greatest catabolic repression as the carbon source due to its minimal enzyme activity (6.86 U/ml). da Silva Delabona et al. [81] reported that the use of glycerol to bulk up biomass is a good strategy followed by induction for cellulase production. Glycine as the nitrogen source had the greatest catabolic repression as minimal enzyme activity (4.53 U/ml).

A range of wheat bran and ammonium sulphate concentrations were tested in order to establish the best concentrations for xylanase production. As shown in Figure 2.10a and 2.10b the highest xylanase levels were produced in 1% (w/v) wheat bran (35.49 ±0.72 U/ml) and 1.2% (w/v) ammonium sulphate (37.01 ±1.24 U/ml).

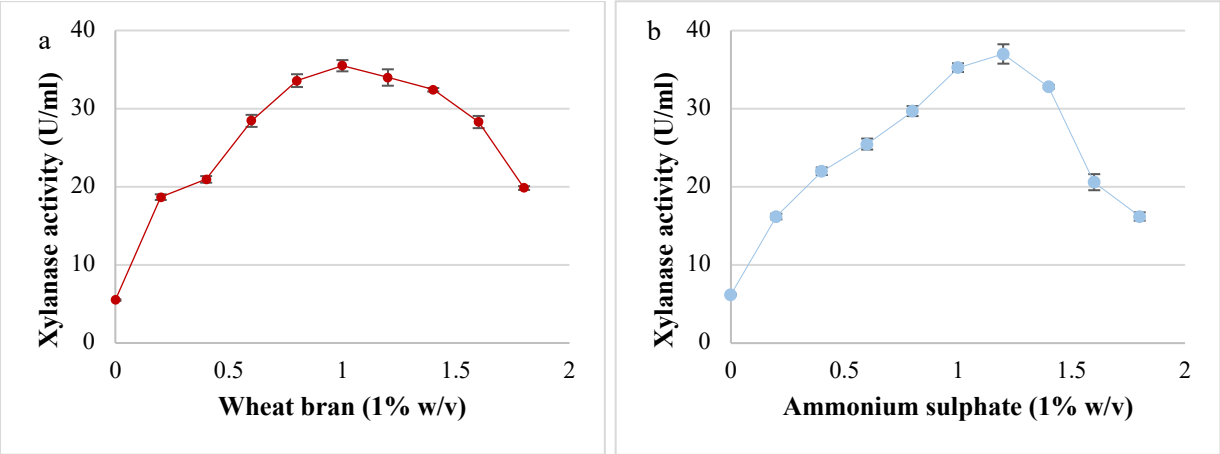

Figure 2.10*:* Effect of different wheat bran (a) and ammonium sulphate (b) concentrations (w/v) on xylanase production by the identified *T. harzianum* isolate during submerged fermentation at 70°C, pH 5.0, for 5 d at 160 rpm. Data points represent the means ± SD (n=4).

2.4.7 Biochemical characterization of crude xylanase

2.4.7.1 Determination of pH and temperature optima for enzyme activity

Various pH affected the activity of xylanase from *T. harzianum*. The highest xylanase activity was seen at pH 8.0 (37.80 ±1.53 U/ml) and second peak of increasing activity was showed at pH 6.0 (36.13±1.44 U/ml), respectively (Figure 2.11a). Enzyme activity assays were performed at various temperatures at both pH optima. Figure 2.11b shows that the xylanase activity was the highest at 60°C (39.37 ±0.86 U/ml) and showed a second peak of increasing activity 70°C (31.66 ±0.41 U/ml) at pH 6.0, whereas at pH 8.0, the xylanase activity was the highest at 75°C (39.08 ±1.92 U/ml) and peaked at 55°C (38.24 ±2.11 U/ml).

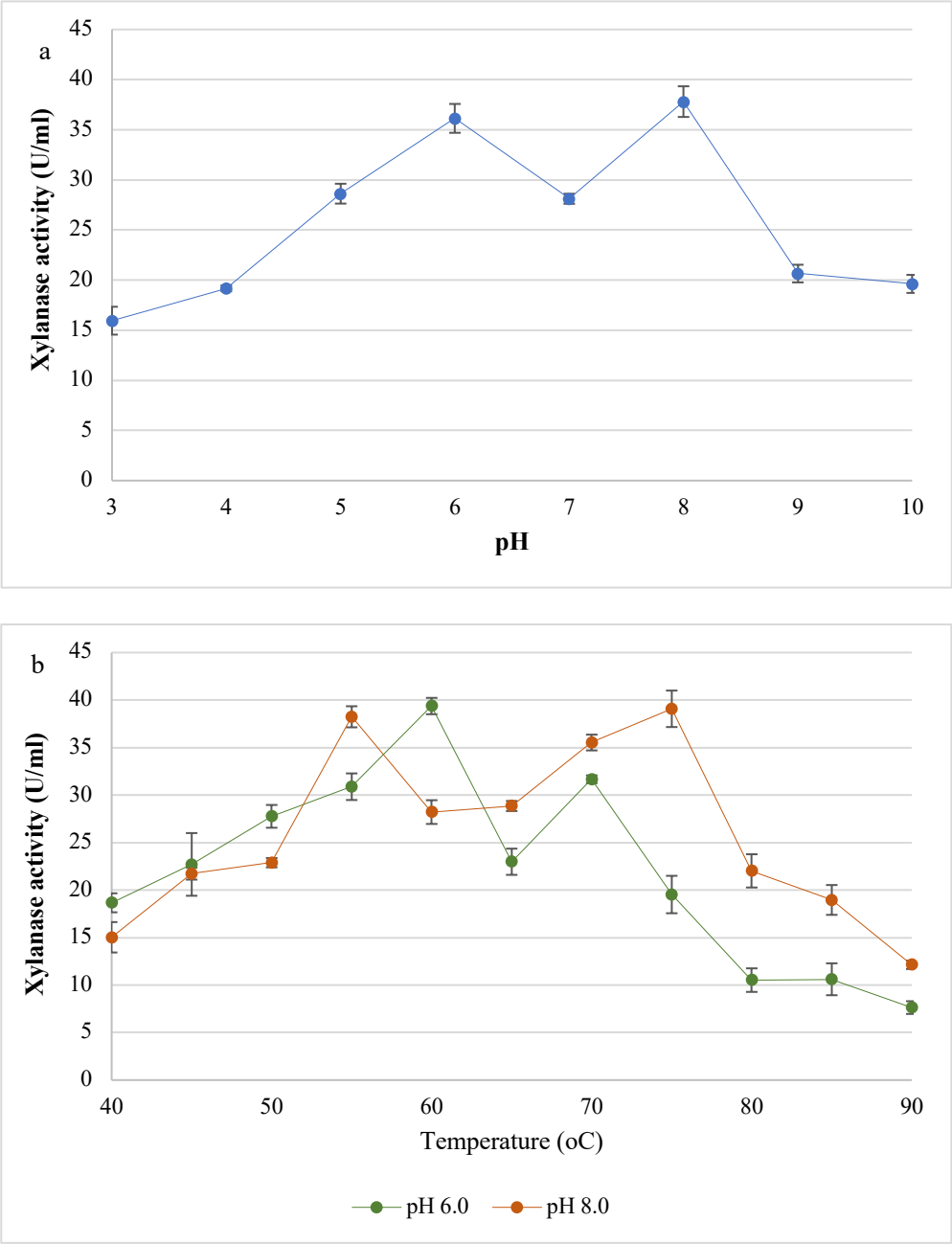

Figure 2.11: Effect of pH (A) and temperature (B: At pH 6.0 and pH 8.0)) on the activity of xylanase from the identified *T. harzianum* isolate crude extracellular supernatants. Data points represent the means ± SD (n=3).

Biochemical characterization of xylanase revealed an enzyme with promising properties (high enzyme activity at various pH and temperatures) for future studies. The crude xylanase from *T. harzianum* demonstrated two pH optima: at 6.0 and 8.0 meaning that at least two different

isoforms present. The enzyme displayed greater stability at pH 6.0 and retained more than 50% of its activity over 4 h. However, it was not very stable at pH 8.0, as it lost activity after 1.5 h. These results are similar to those reported by Costa et al. [82] and Sharma et al. [2] for xylanase from *T. viride* and thermostable *Fusarium* sp. XPF5. Abo-Elmagd [35] found that the xylanase from *T. harzianum* MH-20 had highest activity at pH 5.5 and was stable from pH 5.5-6.5. Temperature can influence the reaction rate of an enzyme. Thermal stability of the enzyme was observed at higher temperatures than expected, with the xylanase retaining > 50% of its activity at 60, 70 and 75°C.

Thermostable and neutrally-stable xylanases are beneficial for large scale production as the process would be simplified and save cooling time and energy as well as reduce the problems of possible contamination [83] thus reducing costs. However, the target enzyme in the current study is produced under mildly acidic conditions, yet the cost impact may be minimised if acid lysed lignocellulose is used as the carbon source. The multiple high activities at various temperature and pH optima observed suggests that this organism produces multiple xylanases. This has been reported previously [84], multiple xylanases and endoglucanases produced by *Simplicillium obclavatum* MTCC 9604 during growth on wheat bran. Each xylanase may have diverse structures, physicochemical properties and rate of activities.

2.4.7.2 Determination of pH and temperature stability

The *T. harzianum* xylanase showed > 50% maximal activity at pH 6 after 4 h (Figure 2.12a) whereas at pH 8.0 the enzyme retained activity for 0.5 h and thereafter activity declined for 2.5 h and showed a further sharper decline in activity between 2.5-4 h. In Figure 2.12b, at pH 6.0, the enzyme retained > 50% activity after 4 h at both 60 and 70°C. At pH 8.0 the enzyme retained > 50% activity at 75°C for 4 h and lost activity after 4 h at 55°C.

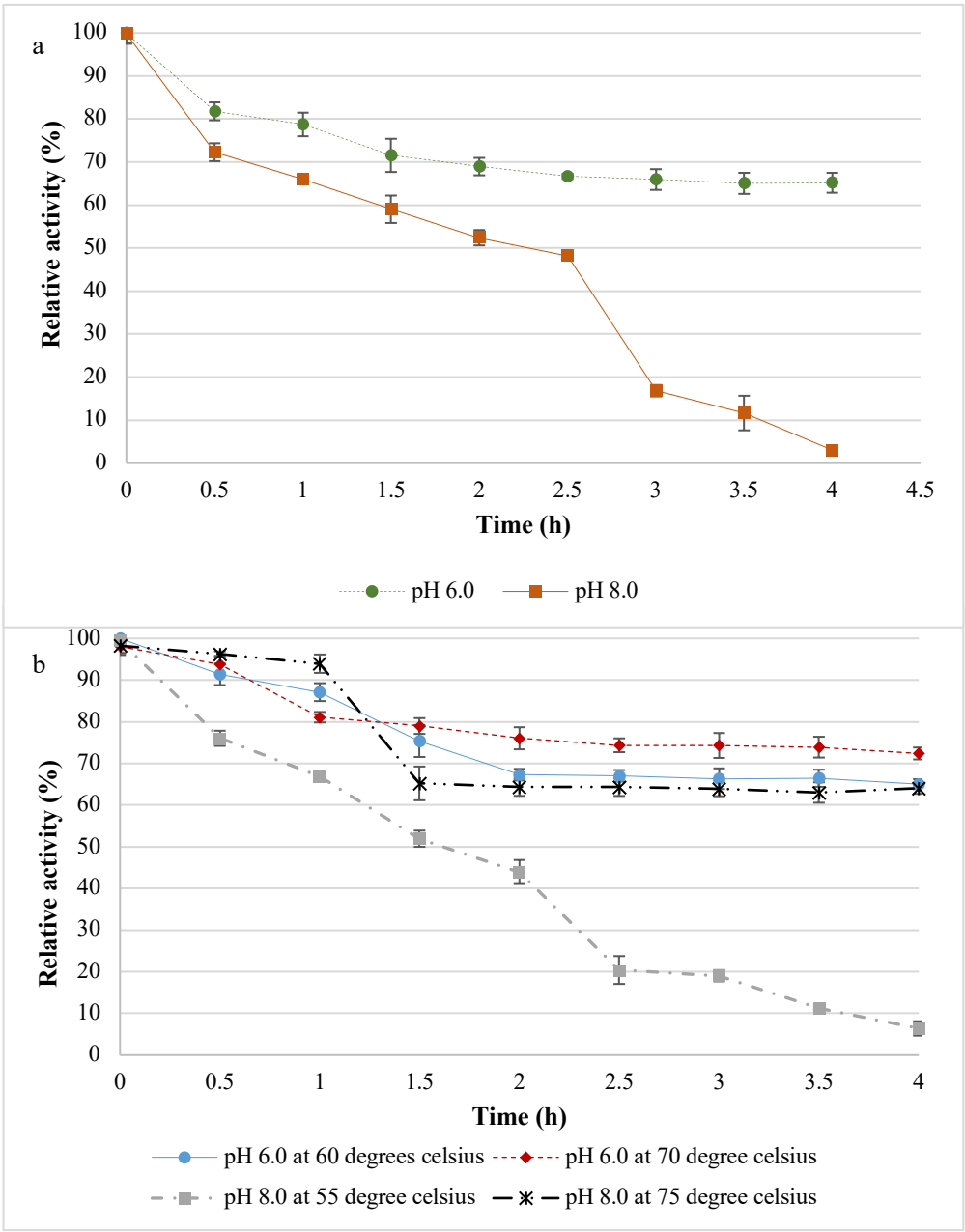

Figure 2.12: pH (a) and temperature (b) stability of crude xylanases produced by the identified *T. harzianum* isolate. Data points represent the means ± SD (n=3).

2.4.7.3 Polyacrylamide Gel Electrophoresis

SDS PAGE gel of the crude xylanase enzyme (Figure 2.13) was stained using silver staining which revealed multiple protein bands in the crude extract. A prominent band with a molecular weight of 70 kDa was observed. The native Page gel supplemented with 1% (w/v) beechwood

xylan revealed hydrolysis of the substrate as evidenced by the areas with a slightly yellow hue. The majority of the xylanase activity corresponded to the mass of proteins in the top half of the gel between 34-130 kDa in molecular weight where brighter bands were observed at a higher molecular weight (55-130 kDa).

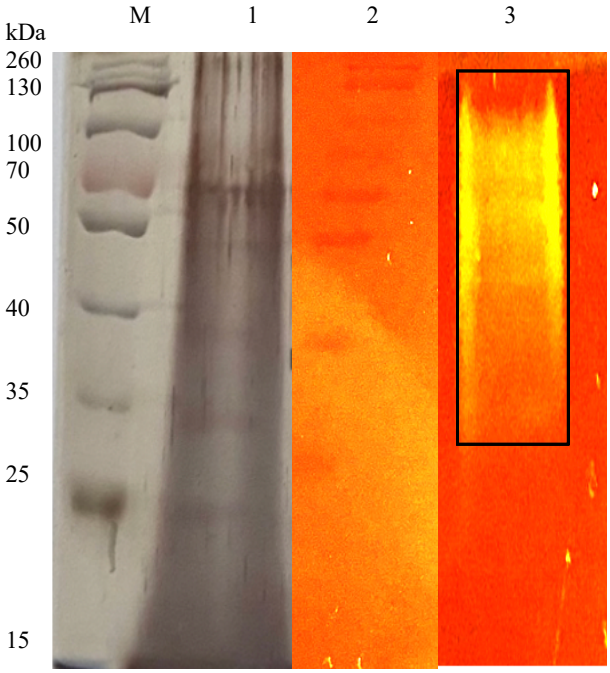

Figure 2.13: SDS PAGE gel (silver stained) and Native Substrate PAGE gel (1% xylan) of the identified *T. harzianum* crude xylanase. Lanes M: Spectra Multicolour Broad Range marker (Thermoscientific, USA), Lane 1: Crude extract, Lane 2: Spectra Multicolour Broad Range marker (Thermoscientific, USA) (Stained with congo red) and Lane 3: Crude xylanase extract showing zones of clearance.

Several bands at approximately 70 kDa, 49 kDa, 39 kDa, and 25 kDa (Figure 2.13) were apparent for the crude *T. harzianum* xylanase. de Paula Silveira et al. [85] and Silva et al. [86] reported xylanase at 14-19 kDa from *T. inhamatum and T. harzianum.*. Nathan et al. [87] reported molecular weights between 14-66 kDa for xylanases from *T. viride* VKF3. Native substrate PAGE was performed using a native gel supplemented with xylan substrate and stained with Congo red. This approach and zymogram analysis are widely used for confirmation of xylanolytic activity and to identify the fractions that possess the activity during purification. A range of isoforms were detected (55-130 kDa) as the crude enzyme migrated through the

Native PAGE gel and hydrolysed the xylan forming bands of hydrolysis. Nathan et al. [87] reported xylanase activity at 14 kDa and between 43-66 kDa.

2.5 Conclusion

T. harzianum xylanases with various pH and temperature optima and activities have been studied previously, e.g., one with a lower temperature optimum (22°C) [88]. Bhalla et al. [89] reported maximal xylanase activity from *Geobacillus* sp. strain WSUCF1 at 60°C (pH 6.0). However, the current study is the first report of a *T. harzianum* strain isolated in South Africa with thermophilic isoforms displaying high activities and different pH optima which are suitable for applications in animal feed improvement and biofuels production. The isoform produced at acidic optimum (pH 5.0) was targeted in this study for future applications in the feed industry. The growth conditions of the isolate in submerged fermentation was performed to find the best conditions for highest xylanase production. Future studies using statistical experimental design (PBD and BBD), scaled up production in bioreactors, purification and characterization of the pure enzyme will be conducted.

2.6 References

[1] Bhardwaj, N., Kumar, B., & Verma, P. (2019). A detailed overview of xylanases: an emerging biomolecule for current and future prospective. *Bioresources and Bioprocessing.* 6, 40.

[2] Prade, R.A. (1996). Xylanases, from biology to biotechnology. *Biotechnology, Genetics and Engineering Reviews*. 13, 101–131.

[3] Wong, K.K.Y., Tan, L.U.L., & Saddler, J.N. (1988). The multiplicity of β-1,4-xylanase in micro-organisms: functions and applications. *Microbiology Reviews.* 52, 305–317.

[4] Mandla, A. (2015). Review on microbial xylanases and their applications. *International Journal of Life Science.* 4(3): 178-187.

[5] Lee, S.H., Lim, V., & Lee, C.K. (2018). Newly isolate highly potential xylanase producer strain from various environmental sources. *Biocatalysis and Agricultural Biotechnology*. 16, 669-676.

[6] Adesina, F.C., & Onilude, A.A. (2013). Isolation, identification, and screening of xylanase and glucanase-producing micro fungi from degrading wood in Nigeria. *African Journal of Agricultural Research.* 8(34): 4414-4421.

[7] Motta, F.L., Andrade, C.C.P., & Santana, M.H.A. (2013). A review on xylanase production by the fermentation of xylan: Classification, characterization, and applications. In sustainable degradation of lignocellulosic biomass – techniques, applications and commercialization. [place unknown]: InTechOpen.

[8] Nair, S.G., & Shashidhar, S. (2008). Fungal xylanase production under solid-state and submerged fermentation conditions. *African Journal of Microbiology Research.* 2(4): 82-86.

[9] Prasad Uday, U.S., Bandyopadhyay, T.K., Goswami, S., & Bhunia, B. (2017). Optimization of a physical and morphological regime for improved cellulase-free xylanase

production by fed-batch fermentation using *Aspergillus niger* and its application in bio-bleaching, *Bioengineered.* 8, 137–146.

[10]Chen, K., & Zhuang, W.Y. (2017). Discovery from a large-scaled survey of *Trichoderma* in soil of China. *Science*. 7, 9090.

[11] Walia, A., Mehta, P., Chauhan, A., & Shirkot, C.K. (2013). Optimization of cellulase-free xylanase production by alkalophilic *Cellulosimicrobium* sp. CKMX1 in solid-state fermentation of apple pomace using central composite design and response surface methodology. *Annals of Microbiology*. 63, 187–198.

[12] Robledo, A. *et al.* (2016). Production of thermostable fungal strains isolated from maize silage. *Journal of Food.* 14(2): 302-308.

[13] Bedford, M.R. (2018). The evolution and application of enzymes in the animal feed industry: the role of data interpretation. *British Poultry Science*. 59(5): 486-493.

[14] Collins, T., Gerday, C., & Feller, G. (2005). Xylanases, xylanase families and extremophilic xylanases. *FEMS Microbiology Review.* 29(1): 3-23.

[15] Pariza, M.W., & Cook, M. (2010). Determining the safety of enzymes used in animal feed. *Regulatory Toxicology and Pharmacology*. 56(3): 332-342.

[16] Haki, G.D., & Rakshit, S.K. (2003). Developments in industrially important thermostable enzymes: A review. *Bioresource Technology.* 89, 17-34.

[17] Chadha, B.S., Kaur, B., Basotra, N., Tsang, A., & Pandey, A. (2019). Thermostable xylanases from thermophilic fungi and bacteria: current perspective. *Bioresource Technology.* 277, 195–203.

[18] Lorenz, N., & Dick, R. (2011). Sampling and pre-treatment of soil before enzyme analysis. *Methods of Soil Enzymology*. 85-100.

[19] Mohammed, I.J. (2013). Screening of fungi isolated from environmental samples for xylanase and cellulase production. *International Scholarly Research Notices: Microbiology.* 283423.

[20] Gautam, A., Kumar, A., & Dutt, D. (2015). Production of cellulase-free xylanase by *Aspergillus flavus* ARC- 12 using pearl millet stover as the substrate under solid-state fermentation. *Journal of Advanced Enzyme Research.* 1, 1-9.

[21] da Silva Menezes, B., Rossi, D.M., Ayub, M.A. (2017). Screening of filamentous fungi to produce xylanase and xylooligosaccharides in submerged and solid-state cultivations on rice husk, soybean hull, and spent malt as substrates. *World Journal of Microbiology and Biotechnology*. 3, 58.

[22] Mosina, N.L., Naidu Krishna, S.B., Ramnath, L., & Govinden, R. (2017). Screening, production, and partial characterization of xylanases from woodchips fungi with potential application in bioethanol production. *Current Trends in Biotechnology and Pharmacy.* 11(4): 2230-7303.

[23] Miller, G.L. (1959). Use of dinitrosalicylic acid reagent for determination of reducing sugar. *Analytical Chemistry.* 31, 426–428.

[24] White, T.J., Bruns, T., Lee, S.B., & Taylor, J. (1990). Amplification and direct sequencing of fungal ribosomal RNA genes for phylogenetics. PCR protocols: a guide to methods and application. New York (NY): Academic Press.

[25] Tuohy, M.G., Puls, J., Claeyssens, M., anská, M.V.R., & Coughlan, M.P. (1993). The xylan-degrading enzyme system of *Talaromyces emersonii*: novel enzymes with activity against aryl -D-xylosides and unsubstituted xylans. *Biochemistry Journal.* 290, 515-523.

[26] Bhavsar, N.H., Raol, B.V., Raol, G.G., & Bhatt, P.R. (2016). Isolation, screening, and optimization of xylanase-producing fungi from compost pit. *International Journal of Impotence Research.* 2(11): 44-68.

[27] Tamura, K. *et al.* (2011). MEGA5: molecular evolutionary genetics analysis using maximum likelihood, evolutionary distance and maximum parsimony methods. *Molecular Biology and Evolution.* 28, 9-2731.

[28] Leck, A. (1999). Preparation of lactophenol cotton blue slide mounts. *Community Eye Health.* 12(30): 1-24.

[29] Cunha, L. *et al.* (2018). Optimization of xylanase production from *Aspergillus foetidus* in soybean residue. *Hindawi Enzyme Research*. (2): 1-7.

[30] Okafor, U.A., Okochi, V.I., Onyegeme-okerenta, B.M., & Nwodo-Chinedu, S. (2007). Xylanase production by *Aspergillus niger* ANL 301 using agro-wastes. *African Journal of Biotechnology*. 6, 1710-1714.

[31] Pandey, S. *et al.* (2012). Isolation and optimized production of xylanase under solid-state fermentation condition from *Trichoderma* sp. *International Journal of Advanced Research.* 2(3): 263-273.

[32] Gomaa, E.Z. (2013). Optimization and characterization of alkaline protease and carboxymethyl-cellulase produced by *Bacillus pumillus* grown on *Ficus nitida* wastes. *Brazilian Journal of Microbiology*. 44(2): 529-537.

[33] Ajijolakewu, A.K., Leh, C.P., Wan Abdullah, W.N., & Lee, C.K. (2017). Optimization of production conditions for xylanase production by newly isolated strain *Aspergillus niger* through solid state fermentation of oil palm empty fruit bunches. *Biocatalysis and Agricultural Biotechnology*. 11, 239-247.

[34] Franco, P.F., Ferreira, H.M., & Filho, E.X. (2004). Production and characterization of hemicellulase activities from *Trichoderma harzianum* strain T4. *Biotechnology and Applied Biochemistry.* 40(3): 255-9.

[35] Abo-Elmagd HI. (2014). Optimization and biochemical characterization of exracellular xylanase from *Trichoderma harzianum* MH-20 under solid state fermentation. *Life Science Journal.* 11(3): 188-195.

[36] Laemmli, U.K. (1970). Cleavage of structural proteins during the assembly of the head of bacteriophage T4. *Nature*. 227, 680–685.

[37] Goluguri, T.C., Addepally, U., & Shetty, P.R. (2016). Novel alkali-thermostable xylanase from *Thielaviopsis Basicola* (MTCC 1467): purification and kinetic characterization. *International Journal of Biological Macromolecules.* 82, 823–829.

[38] Pointing, S.B. (1999). Qualitative methods for the determination of lignocellulosic enzyme production by tropical fungi. *Fungal Diversity*. 2, 17-33.

[39] Singh, R., Gupta, V., Kumar, V., & Gupta, R. (2006). A simple activity staining protocol for lipases and esterases. *Journal of Applied Microbiology and Biotechnology.* 70, 679-682.

[40] Yadav, P. *et al.* (2018). Production, purification, and characterization of thermostable alkaline xylanase from *Anoxybacillus kamchatkensis* NASTPD13. *Frontiers in Bioengineering and Biotechnology*. 6, 65.

[41] Gupta, U., & Kar, R. (2009). Xylanase production by thermotolerant *Bacillus* species under solid state and submerged fermentation. *Brazilian Archives of Biology and Technology.* 52(6): 1363-1371.

[42] Pathak, P., Bhardwaj, N.K., & Singh, A.K. (2014). Production of crude cellulase and xylanase from *Trichoderma harzianum* PPDDN10 NFCCI-2925 and its application in photocopier waste paper recycling. *Applied Biochemistry and Biotechnology,* 172(8): 3776-97.

[43] de Oliveira, Q. *et al.* (2014). *Trichoderma atroviride* 102C1 mutant: a high endoxylanase producer for assisting lignocellulosic material degradation. *Journal of Microbial Biochemistry and Technology*. 5-6.

[44] Hombalimath, V.S., Achappa, S., Patil, L.R., Shet, A.R., & Desai, S.V. (2021). Optimization of xylanase production from *Aspergillus* spp. under solid-state fermentation using lemon peel as substrate. *Journal of Pharmaceutical Research International*. 33, 35-43.

[45] Amore, A. *et al*. (2015). Application of a new xylanase activity from *Bacillus amyloliquefaciens* XR44A in brewer's spent grain saccharification. *Journal of Chemical Technology and Biotechnology.* 90(3): 573–581.

[46] Abubakar, A. *et al.* (2013). Effect of pH on mycelial growth and sporulation of *Aspergillus parasiticus*. *Journal of Plant Science.* 1(4): 64-67.

[47] Shah, A., & Datta, M. (2005). Xylanase production under solid-state fermentation and its characterization by an isolated strain of *Aspergillus foetidus* in India. *World Journal of Microbiology and Biotechnology*. 21, 233–243.

[48] Zhang, M., Jiang, J., Yang, S., Hua, C., & Li, L. (2010). Cloning and expression of a *Paecilomyces thermophila* xylanase gene in *E. coli* and characterization of the recombinant xylanase. *Bioresource Technology.* 101(2): 688-695.

[49] Yang-yuan, L. *et al.* (2015). High-level expression and characterization of a thermostable xylanase mutant from *Trichoderma reesei* in *Pichia pastoris*. *Protein Expression and Purification*. 108, 90-96.

[50] Deshmukh, R.A., Jagtap, S., Mandal, M.K., & Mandal, S.K. (2016). Purification, biochemical characterization and structural modelling of alkali-stable β-1,4-xylan xylanohydrolase from *Aspergillus fumigatus* R1 isolated from soil. *BMC Biotechnology.* 16, 11.

[51] Sanghvi, G.V., Koyani, R.D., & Rajput, K.S. (2010). Thermostable xylanase production and partial purification by solid-state fermentation using agricultural waste wheat straw. *Mycology*. 1(2): 106-112.

[52] Polizeli, M.L.T.M. *et al.* (2005). Xylanases from fungi: properties and industrial applications. *Applied Microbiology and Biotechnology.* 67(5): 577-591.

[53] Gong, W., Dai, L., Zhang, H., Zhang, L., & Wang, L. (2018). A highly efficient xylan-utilization system in *Aspergillus niger* An76: a functional-proteomics study. *Frontiers in Microbiology*. 9, 430.

[54] Lenartovicz, V., Marques De Souza, G., Moreira, F., & Peralta, R. (2002). Temperature effect in the production of multiple xylanases by *Aspergillus fumigatus*. *Journal of Basic Microbiology.* 42(6): 388-395.

[55] Liao, H. *et al.* (2015). Functional diversity and properties of multiple xylanases from *Penicillium oxalicum* GZ-2. *Scientific Reports*. 5, 12631.

[56] Badhan, A.K., Chadha, B.S., Kaur, J., Saini, H.S., & Bhat, M.K. (2007). Production of multiple xylanolytic and cellulolytic enzymes by thermophilic fungus *Myceliophthora* sp. IMI 387099. *Bioresource Technology*. 98, 504–510.

[57] Rigoldi, F., Donini, S., Redaelli, A., Parisini, E., & Gautieri, A. (2018). Review: Engineering of thermostable enzymes for industrial applications. *APL Bioengineering*. 2(1): 011501.

[58] Kambourova, M. (2018). Thermostable enzymes and polysaccharides produced by thermophilic bacteria isolated from Bulgarian hot springs. *Engineering in Life Science*. 18(11): 758–767.

[59] A**zimova, N.S., Khamidova, K.M., Turaeva, B.I., Karimov, H.K., & Shakirov, Z.S.** (2020). Properties of the cellulase and xylanase enzyme complexes of *Trichoderma harzianum* UzCF-28. *Eurasian Journal of Biosciences.* 14, 5803-5808.

[60] Abbas, A., Ahmad, S., Mushtaq, Z., & Jamil, A. (2012). Partial purification and characterization of a xylanase from *Trichoderma harzianum*. *Journal of the Chemistry Society in Pakistan*. 34(6): 1455-1459.

[61] BLAST Command Line Applications User Manual. Bethesda: National Centre for Biotechnology Information (US). 2008.

[62] Marecik, R., Błaszczyk, L., Biegańska-Marecik, R., & Piotrowska-Cyplik, A. (2018). Screening and identification of *Trichoderma* strains isolated from natural habitats with potential to cellulose and xylan degrading enzymes production. *Polish Journal of Microbiology.* 67(2): 181–190.

[63] Mulatu, A., Alemu, T., Megersa, N., & Vetukuri, R.R. (2021). Optimization of culture conditions and production of bio-fungicides from *Trichoderma* species under solid-state fermentation using mathematical modelling. *Microorganisms.* 9(8): 1675.

[64] Harris, A.D., & Ramalingam, C. (2010). Xylanases and its application in food industry: a review. *Journal of Experimental Sciences.* 1(7): 1–11.

[65] Telles, G.P., Araújo, G.S., Walter, M., Brigido, M.M., & Almeida, N.F. (2018). Live neighbour-joining. *BMC Bioinformatics*. 19(1): 172.

[66] Chaverri, P., & Samuels, G. (2002). *Hypocrea lixii*, the teleomorph of *Trichoderma harzianum*. *Mycological Progress.* 1, 283-286.

[67] Chaverri, P., Castlebury, L., Samuels, G., & Geiser, D. (2003). Multilocus phylogenetic structure within the *Trichoderma harzianum/Hypocrea lixii* complex. *Molecular Phylogenetics and Evolution*. 27, 302-13.

[68] Gams, W., & Bissett, J. (2002). Morphology and identification of *Trichoderma.* In Christian, P.K., & Gary, G.H. *Trichoderma and Gilocladium.* Basic biology, taxonomy and genetics. *Taylor & Francis,* London. 1, 3-31.

[69] Goyal, M., Kalra, K., Sareen, V., & Soni, G. (2008). Xylanase production with xylan rich lignocellulosic wastes by a local soil isolate of *Trichoderma viride*. *Brazilian Journal of Microbiology*. 39(3): 535– 541.

[70] Shulami, S. *et al.* (2014). Multiple regulatory mechanisms control the expression of the *Geobacillus stearothermophilus* gene for extracellular xylanase. *Journal of Biological Chemistry*. 289(37): 25957–25975.

[71] Ibrahim, D., Weloosamy, H., & Lim, S. (2015). Effect of agitation speed on the morphology of *Aspergillus niger* HFD5A-1 hyphae and its pectinase production in submerged fermentation. *World Journal Biology Chemistry*. 6(3): 265-271.

[72] Zhu, H., Liu, W., Tian, B., & Zhang, C. (2012). Fluid flow induced shear stress affects cell growth and total flavone production by *Phellinus igniarius* in stirred-tank bioreactor. *Chiang Mai Journal of Science.* 39, 69–75.

[73] Bhattacharyya, M.S., Singh, A., & Banerjee, U.C. (2008). Production of carbonyl reductase by *Geotrichum candidum* in a laboratory scale bioreactor. *Bioresource Technology*. 99, 8765-8770.

[74] Singhania, R.R. *et al.* (2011). Properties of a major beta-glucosidase-BGL1 from *Aspergillus niger* NII-08121 expressed differentially in response to carbon sources. *Process Biochemistry.* 46, 1521-1524.

[75] Hu, Y. *et al.* (2021). Carbon catabolite repression involves physical interaction of the transcription factor CRE1/CreA and the Tup1–Cyc8 complex in *Penicillium oxalicum* and *Trichoderma reesei. Biotechnology for Biofuels.* 14, 244.

[76] Mach, R.L., Strauss, J., Zeilinger, S., Schindler, M., & Kubicek, C.P. (1996). Carbon catabolite repression of xylanase I (xyn1) gene expression in *Trichoderma reesei. Molecular Microbiology*. 21(6): 1273- 1281.

[77] Segato Rizzatti, A.C. *et al.* (2008). Regulation of xylanase in *Aspergillus phoenicis*: a physiological and molecular approach, *Journal of Industrial Microbiology and Biotechnology*. 35(4): 237–244.

[78] Seyis, I., & Aksoz, N. (2005). Effect of carbon and nitrogen sources on xylanase production by *Trichoderma harzianum* 1073 D3. *International Journal of Biodeterioration.* 55, 115-119.

[79] Biswas, P., Bharti, A.K., Kadam, A., & Dutt, D. (2019). Wheat bran as substrate for enzyme production and its application in the bio-deinking of mixed office waste (MOW) paper. *BioResources.* 14(3): 5788-5806.

[80] Abdullah, R., Nisar, K., Aslam, A., Iqtedar, M., & Naz, S. (2015). Enhanced production of xylanase from locally isolated fungal strain using agro-industrial residues under solid-state fermentation. *Natural Product Research*. 29(11): 1006-11.

[81] da Silva Delabona, P. *et al.* (2016). Enhanced cellulase production by *Trichoderma harzianum* by cultivation on glycerol followed by induction on cellulosic substrates. *Journal of Industrial Microbiology and Biotechnology.* 43, 617–626.

[82] Costa, A. *et al.* (2019). Catalytic properties of xylanases produced by *Trichoderma piluliferum* and *Trichoderma viride* and their application as additives in bovine feeding. *Biocatalysis and Agricultural Journal*. 19, 101-161.

[83] Liang, Y., Feng, Z., Yesuf, J., & Blackburn, J.W. (2010). Optimization of growth medium and enzyme assay conditions for crude cellulases produced by a novel thermophilic and cellulolytic bacterium, *Anoxybacillus* sp. 527. *Applied Biochemistry and Biotechnology.* 160, 1841–1852.

[84] Raj, A., Kumar, S., Singh, K.S., & Kumar, M. (2013). Characterization of a new *Providencia* sp. strain x1 producing multiple xylanases on wheat bran. *The Scientific World Journal.* 6(1):1-10.

[85] de Paula Silveira, F. *et al.* (1999). A new xylanase from a *Trichoderma harzianum* strain. *Journal of Indian Microbiology and Biotechnology*. 23, 682–685.

[86] Silva, L.A.O., Terrasan, F., Rafael, C., & Carmona, E. (2015). Purification and characterization of xylanases from *Trichoderma inhamatum*. *Electronic Journal.* 18(4): 307-313.

[87] Nathan, V., Mary, R., Gunaseeli, R., & Dhiraviam, K. (2017). Low molecular weight xylanase from *Trichoderma viride* VKF3 for bio-bleaching of newspaper pulp. *Bioresources.* 12.

[88] Azzouz, Z., Bettache, A., Boucherba, N., Amghar, Z., & Benallaoua, S. (2020). Optimization of xylanase production by newly isolated strain *Trichoderma afroharzianum* isolate az 12 in solid state fermentation using response surface methodology. *Cellulose Chemistry and Technology.* 54 (5-6): 451-462.

[89] Bhalla, A., Bischoff, K.M., & Sani, K.R. (2015). Highly thermostable xylanase production from a thermophilic *Geobacillus* sp. Strain WSUCF1 utilizing lignocellulosic biomass. *Frontiers in Bioengineering and Biotechnology*. 3, 84.

CHAPTER THREE

OPTIMIZATION, PURIFICATION, AND CHARACTERIZATION OF XYLANASE PRODUCTION BY A NEWLY ISOLATED *TRICHODERMA HARZIANUM* STRAIN BY A TWO-STEP STATISTICAL EXPERIMENTAL DESIGN STRATEGY

3.1 Abstract

Xylanases are hydrolytic enzymes with a wide range of applications in several industries such as biofuels, paper and pulp, food, and feed. The objective of this study was to optimize the culture conditions and medium components for maximal xylanase production from a newly isolated *Trichoderma harzianum* strain using the Plackett-Burman Design (PBD) and Box Behnken Design (BBD) experimental strategies. Xylanase production was enhanced to 153.80 U/ml by BBD compared to a preliminary one-factor-at-a-time (OFAT) activity of 37.01 U/ml, representing a 4.16- fold increase. The BBD resulted in a 2.24-fold increase when comparing activities to the PBD (68.70 U/ml). The optimal conditions for xylanase production were obtained as follows: 6 d of fermentation, incubation temperature of 70°C, pH 5.0, agitation at 160 rpm, and 1.2% wheat bran and ammonium sulphate – under such conditions, xylanase activity increased from 37.01 U/ml to 153.80 U/ml. The experimental design effectively provided conditions for the production of an acidic-thermostable enzyme. This is an exciting prospect for the application of enzyme in animal feed improvement (pH 5.0). The acidic-thermostable xylanase was purified from the submerged culture and the SDS-PAGE analysis of xylanase showed a molecular weight of 72 kDa. This protein had maximum xylanolytic activity at pH 6.0 and 65°C and was stable for 4 h retaining >70% activity and exhibited substrate specificity, including xylan from beechwood, birchwood, and Larchwood with K_m of 5.56 mg/ml and V_{max} of 1052.63 µmol/min/mg towards beechwood xylan. The enzyme was

activated by Fe^{2+}, $Mg^{2,+,}$ and Zn^{2+}. There was an absence of strong inhibitors of xylanase. Overall, these characteristics indicate the potential for at least two industrial applications and the experimental designs have proven to be an effective method for determining the optimal parameters for enzyme production.

Keywords: *Xylanase; Plackett-Burman Design; Box-Behnken Design; Response Surface Methodology; Purification.*

3.2 Introduction

After cellulose, hemicellulose is the most abundant terrestrial polysaccharide composed of ß-1,4-D-xylopyranoside residues and ß-1,4-xylan as main constituents with arabinosyl and acetyl side chains [1]. Xylan is a renewable biomass resource that has the potential as a substrate in many production processes. However, it must be hydrolysed to xylose and xylooligosaccharides (XOS) for most processes and this can be accomplished by xylanolytic enzymes. However, the complete degradation of heterogeneous xylan into simple sugars requires the synergistic action of several hemicellulases [2]. The main enzymes involved are endo-1,4-β-xylanase and β-xylosidase. Among them, xylanases deserve special attention as they degrade major hemicellulosic polysaccharides by catalyzing the hydrolysis of xylopyranosyl linkages of ß-1,4-xylan [3].

Microbes are ubiquitous in nature [4] and these enzymes are produced by several microorganisms such as bacteria, fungi, and actinomycetes. Endogenous and exogenous microbial enzymes have been widely explored for a variety of microorganisms that are commonly employed as the primary source of enzymes as they are the most significant and convenient source that can be easily produced in large quantities in a short period on

inexpensive media. Xylanase production for industrial applications is based on microbial biosynthesis [5,6]. Thermophilic fungi are promising candidates for biotechnological applications due to their strong ability to degrade plant polysaccharide components and their higher stability under harsh environmental conditions [2]. Several filamentous fungi have been studied because they have high xylan-degrading ability and thus produce several xylanases. *Trichoderma* sp. And *Aspergillus* sp. Are the most dominant among the high xylanase producers and are the most frequently employed for industrial applications [2]. These applications include the bioconversion of plant biomass into animal feed, plant fertilizers, and chemicals for the food industry.

The production of enzymes is costly, thus, to meet industrial demand, a low-cost growth medium is required for enzyme production. There are two possible cultivation methods for microbial xylanase production: solid-state and submerged fermentation [7]. Submerged fermentation technology has the advantage of short production periods to achieve high yields at low costs. Both the nutrient medium composition and culture conditions have a strong influence on xylanase production. The physical and chemical factors known to influence xylanase production are temperature, pH, incubation period, carbon and nitrogen sources and concentration, and agitation speed [8]. Temperature effects on enzyme production are predominantly related to the growth of the organism (mesophilic, psychrophilic, or thermophilic). The pH is one of the most important factors governing microbial growth due to its sensitivity to the hydrogen ion concentration in the medium [9]. It is also key to enzyme activity as it can alter the ionic charges on the molecule, which could cause changes to the enzyme's shape (they may denature), and that usually leads to a reduction or loss of the catalytic properties of the enzymes and cessation of metabolic activity [10].

Supplementation of the growth medium with carbon and nitrogen sources usually increases enzyme production as this provides an enriched environment for microbial growth [11]. Therefore, screening of the most influential factors and optimization of the growth conditions are essential to ensure maximal enzyme production, potentially significantly reducing production costs for xylanases [12]. There are two ways by which optimization of the fermentation process can be addressed; classical and statistical approaches. The classic approach is based on the OFAT and the statistical approach includes PBD and RSM.

The OFAT approach is a conventional single-dimensional investigation that involves changing one independent variable at a time while the others remain at their optimal level [13,14]. This is the main strategy used for selecting optimal conditions, which continues to be widely used in preliminary optimization studies [15]. The main disadvantages of OFAT are the partial explanation regarding the effect of the factors on the response and the absence of the interaction effects between the variables [16]. This method also involves a relatively high number of experiments, which makes it laborious and time-consuming [15]. Moreover, it may lead to unreliable results and inaccurate conclusions.

To resolve this problem, optimization studies can be carried out by using multivariate statistical methods [15], PBD and RSM can potentially eliminate the limitations of a single factor optimization process [17]. PBD is a powerful statistical technique for screening medium components in shake flask fermentation and reduces the total number of experiments [18]. This technique is useful and has been widely used as the first step of an optimization procedure, however, it cannot determine the interaction effects [17] but allows the evaluation of the importance of each factor in few experiments [19]. RSM using a BBD is an effective optimization tool. The RSM design can provide the dependence of enzyme activity on

independent variables, predicted results for responses, and levels for independent variables in the form of mathematical models [20,21].

Hydrolysis of xylan and hemicellulosic materials to various XOS has been accomplished using crude xylanase. However, to meet the desired requirements of industries, xylanase with specific qualities such as pH and thermostability, high specific activity, and resistance to metal ions and chemicals are required, which could be obtained through enzyme purification [22]. Purification is necessary to remove contamination from other proteins and enzymes such as cellulases in the culture medium, as well as compounds derived from the substrate. This contamination can cause challenges with activity assays, protein quantification, and physicochemical properties [23]. Purification and physicochemical characterization (activity and stability at various pH and temperatures) of pure xylanase offer information on the enzyme's structure and functional features, which may be used to assess its application potential [23]. Purification should be centred on attaining the best feasible yield while keeping the highest possible enzymatic activity and purity [24].

Xylanases are required in large quantities for industrial-level applications because it has the necessary characteristics to withstand harsh industrial-level processing. As a result, there is a need to select strong microorganisms for xylanase synthesis, followed by medium component modification for increased production [7]. There are several reports available on the optimization of media components and physical growth parameters for the production and purification of xylanase for various applications using different substrates [8,12,15]. Xylanase production by *Trichoderma reesei* SAF3 [25], *Trichoderma stromaticum* AM7 [26] and several other species has been optimized however, there were scant reports for thermostable *T. harzianum* in the literature.

Therefore, in the present study, a recently isolated and characterized *T. harzianum*, producing thermophilic and acidic xylanase was the subject of study with the major focus and novelty of this study being to statistically optimize experiments to identify the significant factors affecting xylanase production by PBD and determine their optimal levels in the culture using a factorial BBD methodology to enhance xylanase production levels. The purification and physicochemical characterization of this xylanase produced by submerged fermentation was described to determine its suitability for future application studies in animal feed improvement.

3.3 Materials and methods

3.3.1 Microbial strain

The *T. harzianum* strain was selected from a previous screening study as the candidate for xylanase production [27]. Fungal cultures were streaked on the PDA plates and slants, grown for 5 d at 30°C followed by the addition of sterile mineral oil to cover the fungal mycelium and storage at 4°C. Long-term stocks were prepared by washing fungal spores from the 5 d PDA plates with distilled water and adding 50% glycerol in a 1:1 ratio to the spore suspension and storing at -20°C and -80°C.

3.3.2 Medium and cultivation

Nutrient salt solution (NSS) used for xylanase production comprised [(g/L): (0.005 g) $CaCl_2$, (0.23 g) KH_2PO_4, (0.05 g) $MgSO_4$, (0.005 g) $NaNO_3$, (0.002 g) $ZnSO_4$, (0.009 g) $FeSO_4$, (0.23 g) KCl, (7 g) peptone, and (20 g) wheat bran]. Erlenmeyer flasks (250 ml) containing 50 ml of the medium were each inoculated with two 5 mm fungal plugs from a 5 d old plate culture and incubated at 30°C at 200 rpm for 7 d in a shaker (New Brunswick Innova 44, Germany).

Cultured media were removed after the incubation period and the cell-free supernatant was recovered by centrifuging samples at 16873 × *g* for 10 min (Eppendorf centrifuge 5418, Germany). Xylanase activity was determined as described below in the xylanase assay method (section 3.3.3).

3.3.3 Xylanase assay

Xylanase activity was quantified using the 3,5-Dintrosalicylic acid (DNS) assay for reducing sugars according to the method by Miller [28]. The reaction included 600 µl of 1% (w/v) beechwood xylan (1 g in 100 ml of 50 mM citrate buffer pH 5.0) in 15 ml test tubes to which 66.67 µl of the culture supernatant was added. The reaction mixture was incubated in a water bath at 55°C for 15 min and terminated by the addition of 1 ml DNS reagent followed by heating for 5 min at 100°C in a water bath. One unit (U) of xylanase was defined as the amount of enzyme that released 1 µmol xylose as reducing sugar as equivalents per min under the specified assay conditions.

3.3.4 Optimization of xylanase production: OFAT

To optimize the growth parameters, OFAT was used to evaluate the effect of a single parameter at a time performed in earlier studies [22]. For each step, the enzyme activity was obtained to determine the optimal yield and reported in previous studies [27].

3.3.5 Statistical optimization, experimental design, and data analysis

3.3.5.1 PBD

Six variables were selected for this study: Incubation temperature (X1), Incubation time (X2), pH (X3), Agitation (X4), Wheat bran (X5), and Ammonium sulphate (X6) (Table 3.1). The

total number of experimental runs carried out for the six variables was twelve [29]. Each variable was represented by a high level denoted by '+' and a low level denoted by '-'.

Table 3.1: Experimental variables and levels used in the PBD for optimal xylanase production by the *T. harzianum* strain

Variables	**Symbol code**	**Units**	**Experimental values**	
			Low level (-1)	**High level (+1)**
Incubation Temperature	X1	°C	40	80
Incubation time	X2	Days (d)	2	6
pH	X3	-	4	8
Agitation	X4	rpm	140	180
Wheat bran (carbon source)	X5	%	0.8	1.2
Ammonium sulphate (nitrogen source)	X6	%	1.0	1.4

The high level of each variable was sufficiently far from the low level so that any significant effect would be observed. The experimental runs were performed in duplicate and an average of the results was reported based on the first-order polynomial model equation (I):

$$Y=\beta 0 \sum \beta i\ Xi \qquad (I)$$

Where Y is the response (peak area and retention factor), β_0 is the model intercept, β_i is the linear coefficient and X_i is the level of the independent variable. The PBD was analyzed using R studio

software [30] to estimate the significant factors. Analysis of variance (ANOVA) was performed to determine the p-values as well as the R coefficients to check the significance and fit of the regression model. Screened parameters were represented on a Pareto chart of standardized effects. The effect of each variable was analyzed and the ones with the highest influence on the production of xylanase were selected for the second level optimization by BBD of RSM.

3.3.5.2 Optimization of the significant variables using Response Surface Methodology (RSM)

The BBD was used to elucidate the main interaction and quadratic effects of the three significant variables arising from the PBD, with replicated centre points [15]. The experimental design and statistical analysis were performed using R Studio [30]. A three-level three-factor BBD was used to evaluate the combined effect of the three significant independent variables, Incubation time (X2), pH (X3), and wheat bran (X5) (Table 3.2). The design consisted of 16 combinations, including three replicates of the centre point as shown in Table 3.2.

Table 3.2: Experimental codes and levels of independent variables in the RSM for optimal xylanase production by the *T. harzianum* strain

Variables	**Symbol code**	**Experimental codes**		
		Lower (-1)	*Zero (0)	Higher (+1)
Incubation time (d)	X2	4	5	6
pH	X3	4	5	6
Carbon source	X5	0.8	1	1.2

*Optimum level

After the experimental runs were completed, the average xylanase activities were taken as the response (Y). A multiple regression analysis of the data was carried out to obtain an empirical

model that relates the response measured to the independent variables [31]. The second-order polynomial equation II is shown below:

$$Y=\beta 0 +\sum \beta i\ X1+\sum \beta ii\ X22 +\sum \beta ij\ X1X2 \qquad (II)$$

where Y represents the response variable (peak area), β0 is the interception coefficient, β1 is the coefficient for the linear effects, β2 is the coefficient for the quadratic effect, β12 interaction coefficient and X1 X2 is the coded independent variables that influence the response variable Y. The response in each run was the average of duplicates. In this experimental design, data were analyzed by one-way ANOVA with Tukey's multiple comparison test ($p \leq 0.05$) using R studio [30], and ggplot2 was used for the generation of 3D response surface and contour plots [32].

3.3.6 Scale-up production in optimized media

From the statistical design experiments, the optimized parameters for each factor were considered. The NSS was prepared as previously mentioned in the medium and cultivation protocol (section 3.3.2). However, the optimized parameter for wheat bran and ammonium sulphate concentrations were used. Erlenmeyer flasks (2 L) containing 400 ml of the medium were each inoculated with two 5 mm fungal plugs from a 5 d old plate culture and incubated at the optimized parameters in a shaker (New Brunswick Innova 44, Germany). Cultured media were removed after the incubation period and the cell-free supernatant was recovered by centrifuging samples at 16873 × *g* for 10 min (Eppendorf centrifuge 5418, Germany). Xylanase activity was determined as described below in the xylanase assay method (section 3.3.3).

3.3.7 Purification of xylanase

All purification steps were carried out at 4°C. Partial purification of xylanase was carried out by ammonium sulphate precipitation (20-80%). The pellets were dissolved in 50 mM citrate buffer pH 5.0 and subjected to dialysis overnight in the same buffer. The fractionation that resulted in the highest activity, was concentrated in 3 kDa Amicon centrifugal tubes. The protein precipitate was dissolved in 50 mM citrate buffer pH 5.0 buffer and was loaded onto an anion exchange column (HiTrap Q FF 5 ml) which was connected to the AKTA Purifier (AKTA Purifier, GE Healthcare Bio-Science, AB75184, Uppsala Sweden). Before loading the sample, the column was equilibrated with 20 mM Tris buffer, pH 8.0. The elution of the enzyme was done using a sodium chloride gradient from 0 to 2 M. The fractions were collected at a flow rate of 1.5 ml/min. Active fractions were pooled, concentrated, and dialyzed against a 50 mM citrate buffer (pH 5.0), to be used for further characterization of the enzyme. Protein concentration was measured by the Bradford method [33] using bovine serum albumin (BSA) as the standard and enzyme activity was determined as per the xylanase assay protocol in section 2.3. SDS- polyacrylamide gel with 12% gel was performed according to Laemmli [34]. Native PAGE was performed with 1% xylan as the substrate. Once electrophoresis was completed, the gel was incubated in 50 mM citrate buffer pH 5.0 at optimum temperature (70°C) for 20 min and thereafter stained with 0.1% Congo red solution for 30 min and destained in 1M NaCl until clearance bands of xylanase activity were obtained.

3.3.8 Characterization of purified xylanase

3.3.8.1 Effect of pH and temperature on xylanase activity

The pH optimum was determined by incubating the enzyme during the reaction in the enzyme assay at various pH values between 4.0-10.0. The following buffers were used: 0.1 M sodium citrate buffer (pH 3.0-5.0), 0.1 M potassium phosphate buffer (pH 6.0-8.0) and 0.1 M Glycine

NaOH buffer (pH 9.0-10.0) [35]. Enzyme assays were done as described in section 3.3.3. For determination of the optimum temperature, the reactions were carried out at 40 to 80°C with an interval of 5°C at the optimum pH.

3.3.8.2 pH and thermostability

The pH stability of the enzyme was determined by incubating the enzyme in an optimal pH buffer for 4 h at 55°C with aliquots removed every 30 min. A substrate control was also incubated for 4 h. Thereafter, xylanase activity was assayed using the DNS method and reported as residual activity (%). Temperature stability was determined by incubating the enzyme in optimal pH buffer at optimal temperature for 4 h and aliquots were collected every 30 min. The activity was reported as residual activity (%).

3.3.8.3 Effect of metallic ions and different solvents on xylanase activity

The effect of metallic ions ($CaCl_2$, $CoCl_2$, $FeSO_4$, $MgSO_4$, $MnSO_4$, and $ZnSO_4$) and chemical agents (SDS, DMSO, and EDTA) on enzyme activity was evaluated at two concentrations: 2 mM and 10 mM. The residual activity was measured using the standard assay conditions. The activity found in the absence of metallic ions or inhibitors was taken as the control (100%) [36].

3.3.8.4 Substrate specificity

The specificity of the purified xylanase was verified by determining it's activity against various substrates, i.e., beechwood xylan, birchwood xylan, xylan from Larchwood, wheat arabinoxylan (soluble and insoluble), carboxymethylcellulose (CMC) and Avicel. Substrates (1% w/v) were suspended in 50 mM citrate buffer pH 6.0 and incubated with the purified enzyme at 65°C for 15 min and thereafter the xylanase activity was determined by the DNS method as described in section 3.3.3 [37].

3.3.8.5 Kinetic parameters

The K_m and V_{max} values for the xylanase were determined by measuring the enzymatic activity using different concentrations of the xylan substrate (1-20 mg/ml). The activity was measured under standard assay conditions as described above. The Michaelis-Menton and Lineweaver-Burk plots were acquired to determine K_m and V_{max}.

3.3.9 Equipment and settings

No image acquisition tools and image processing software packages were used for the figures in this study. For figure 3.7, processing such as changing brightness and contrast was used and was applied equally across the entire image and applied equally to the controls. The contrast does not allow for any data to disappear. There were no excessive manipulations, such as processing to emphasize one region in the image at the expense of others.

3.4 Results and discussion

3.4.1 Screening of significant medium constituents for xylanase production

The rows in Table 3.3 represent the twelve different experiments. The data obtained from the PBD runs indicate a wide variation in xylanase activity from 9.8 U/ml to 68.7 U/ml across the twelve runs.

Table 3.3: PBD matrix for screening of six medium components for xylanase production by the *T. harzianum* strain

	Variable level						Enzyme activity (U/ml)	
Run no.	**X1**	**X2**	**X3**	**X4**	**X5**	**X6**	**Observed**	**Predicted**
1	80 (+)	6 (+)	4 (-)	180 (+)	1.2(+)	1.4 (+)	27.1	32.3
2	40 (-)	6 (+)	8 (+)	140 (-)	1.2 (+)	1.4 (+)	68.7	68.4
3	80 (+)	2 (-)	8 (+)	180 (+)	0.8 (-)	1.4 (+)	19.3	17.5
4	40 (-)	6 (+)	4 (-)	180 (+)	1.2 (+)	1.0 (-)	29.3	27.8
5	40 (-)	2 (-)	8 (+)	140 (-)	1.2 (+)	1.4 (+)	32.5	32.6
6	40 (-)	2 (-)	4 (-)	180 (+)	0.8 (-)	1.4 (+)	8.8	9.9
7	80 (+)	2 (-)	4 (-)	140 (-)	1.2 (+)	1.0 (-)	25.6	20.5
8	80 (+)	6 (+)	4 (-)	140 (-)	0.8 (-)	1.4 (+)	23.1	18.2
9	80 (+)	6 (+)	8 (+)	140 (-)	0.8 (-)	1.0 (-)	16.2	21.2
10	40 (-)	6 (+)	8 (+)	180 (+)	0.8 (-)	1.0 (-)	34.8	30.0
11	80 (+)	2 (-)	8 (+)	180 (+)	1.2 (+)	1.0 (-)	16.7	18.3
12	40 (-)	2 (-)	4 (-)	140 (-)	0.8 (-)	1.0 (-)	9.8	15.2

X1: Incubation temperature

X_2: Incubation time

X3: pH

X4: Agitation

X5: Wheat bran concentration

X6: Ammonium sulphate concentration

The medium and culture conditions significantly influenced ($p<0.05$) xylanase production. The R^2, or coefficient of determination, is the percentage of response variance that can be ascribed to the model rather than a random error [38]. According to Xie et al. [39], R^2 should be at least

90% for a model to fit well. The determination coefficient (R^2) indicates that the independent variables were responsible for 97 percent of the sample variance in xylanase output, and just roughly 3% of the overall variation was not explained by the model. The greater the correlation between experimental and anticipated values, the closer R (correlation coefficient) is to 1. The value of R (0.97) indicated that the experimental data and the theoretical values predicted by the model equation were in close agreement. As indicated in Table 3.4, the p-value was used to verify the significance of each of the coefficients. The incubation period (X2), pH (X3), and Wheat bran. (X5) were all shown to have a significant amount ($p<0.05$) of effect on xylanase output.

Table 3.4: ANOVA for six variables by PBD experiment

	df	**Sum of Squares**	**Mean Square**	**F-value**	***p*-value**
Model	6	2521.08	420.18	12.59	0.00700*
Incubation time (X1)	1	610.6	610.6	20.473	0.00626*
Incubation temperature (X2)	1	119.1	119.1	3.992	0.10220
pH (X3)	1	280.1	280.1	9.392	0.02796*
Agitation (X4)	1	166.0	166.0	5.566	0.06481
Wheat bran(X5)	1	1277.7	1277.7	42.839	0.00125*
Ammonium sulphate (X6)	1	66.3	66.3	2.222	0.19622
Residuals	5	166.92	33.39		

df: degree of freedom

* Significant p-value at $p \leq 0.05$

Adjusted R^2 (mean coefficient of determination) = 0.97

The Pareto chart of standardization histogram graph (Figure 3.1) confirmed that these three factors had a significant level ($p<0.05$), as they crossed the p-line and thus were considered to significantly influence xylanase production. However, the other independent factors ($p>0.05$) were generally considered insignificant.

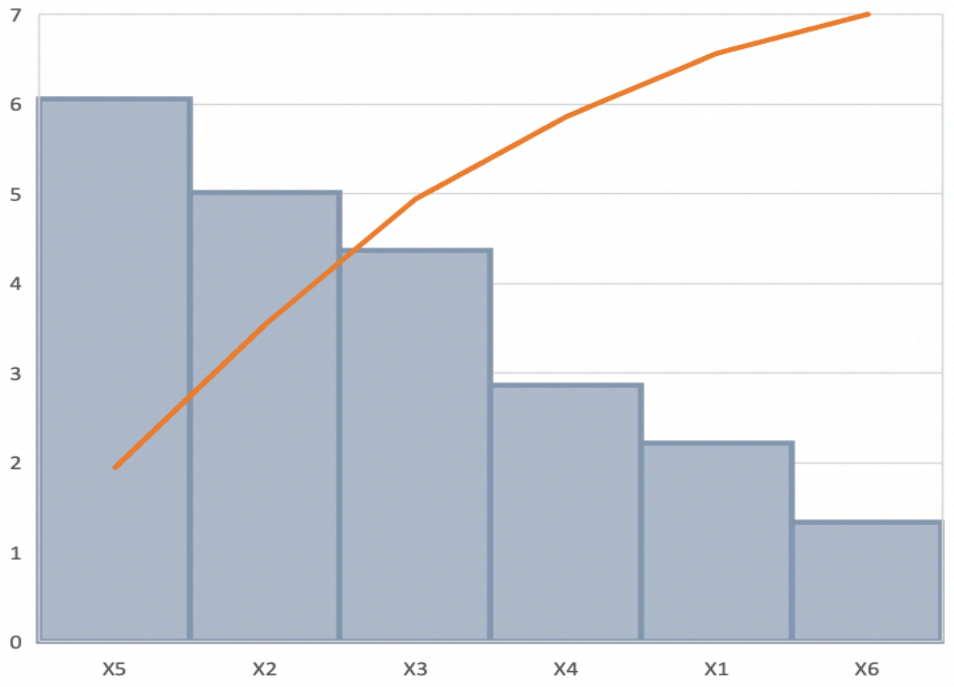

Figure 3.1: Pareto chart standardized effects of six factors screening design for the production of xylanase. Incubation temperature (X1), incubation time (X2), pH (X3), agitation (X4), wheat bran (X5), ammonium sulphate (X6). Orange line represents p= 0.05.

There is a 97% chance that the model explains the measured variations in response. The magnitude and direction of the factor coefficient in the equation clarify the influence of the six variables for xylanase production. The higher the magnitude indicated a large effect on the response. The corresponding response of xylanase production was expressed in terms of the following regression equation (III) derived from the Unstandardized Beta values (Table 3.5):

$$Y=X1 +X2 +X3+X4 +X5 +X6$$

(III)

$$Y = 20.58 +4.28X1 -0.47X2 + 1.51X3 – 0.16X4 + 23.99X5 + 4.56X6$$

Table 3.5: Effect estimates for xylanase production from the results of PBD

	Unstandardized Beta	**Coefficients Std. Error**	**Standardized coefficients Beta**	**t-value**
Model	20.58	14.45		1.42
Incubation time (X1)	4.28	0.85	0.57	5.02
Incubation temperature (X2)	-0.47	0.11	-0.61	-2.22
pH (X3)	1.51	0.68	0.25	4.37
Agitation (X4)	-0.16	0.06	-0.33	-2.87
Wheat bran (X5)	23.99	3.96	0.80	6.06
Ammonium sulphate (X6)	4.56	3.41	0.15	1.34

3.4.2 Optimization of significant variables using RSM for xylanase production

3.4.2.1 BBD

A total of 16 runs were performed to determine the conditions for optimal xylanase production by *T. harzianum*. A matrix was run with the three significant variables as per PBD. The results for the BBD matrix runs (Table 3.6) show that run 8 resulted in the highest xylanase activity of 153.80 U/ml under the following conditions: 6 d of incubation, pH 5.0, and 1.2% wheat bran, while the lowest activity of 27.38 U/ml was obtained under zero level (optimal) conditions (5 d, pH 5.0, and 1% wheat bran) in run 15. This was significantly and markedly higher ($p \geq 0.05$),

compared to the highest enzyme activities obtained during OFAT (38.50 U/ml). Long et al. [15] confirmed a similar influence of optimized parameters on the xylanase production (174.46 U/ml-266.70 U/ml). Using the quadratic equation, the predicted values were determined (Table 3.6).

Table 3.6: Experimental design for the BBD model for three independent variables (Incubation time, pH, and Wheat bran concentration) tested and predicted responses for xylanase production

Experimental value (Coded value)				Enzyme activity (U/ml)	
Run order	**Incubation time (d)**	**pH**	**[Wheat bran] %**	**Observed**	**Predicted**
1	4 (-)	4 (-)	1 (0)	97.09	86.35
2	6 (+)	4 (-)	1 (0)	89.76	87.11
3	4 (-)	6 (+)	1 (0)	98.65	107.01
4	6 (+)	6 (+)	1 (0)	109.22	102.35
5	4 (-)	5 (0)	0.8 (-)	90.82	97.68
6	6 (+)	5 (0)	0.8 (-)	101.32	108.72
7	4 (-)	5 (0)	1.2 (+)	103.37	88.34
8	6 (+)	5 (0)	1.2 (+)	153.80	134.75
9	5 (0)	4 (-)	0.8 (-)	60.01	58.78
10	5 (0)	6 (+)	0.8 (-)	66.92	74.32
11	5 (0)	4 (-)	1.2 (+)	82.99	69.65
12	5 (0)	6 (+)	1.2 (+)	116.74	64.98
13	5 (0)	5 (0)	1 (0)	29.68	37.85
14	5 (0)	5 (0)	1 (0)	33.23	37.85
15	5 (0)	5 (0)	1 (0)	27.38	37.85
16	5 (0)	5 (0)	1 (0)	42.30	37.85

The R^2 of 0.9647 (close to 1) confirmed the validity of the model. The value of the coefficient of adjusted determination, adjusted R^2, was 0.9112 confirming that the actual values were close to the predicted values [40,41]. The correlation was confirmed by plotting the actual value curve

as a function of the predicted values (Figure 3.2) which shows the points distributed around the regression line. Figure 3.2 shows that the actual response values agreed well with the predicted response values, thus the predicted xylanase production is within the limits of the experimental factors. Therefore, the model is considered of sufficient quality [40] with a 96.47% chance that it explains the measured variations in response.

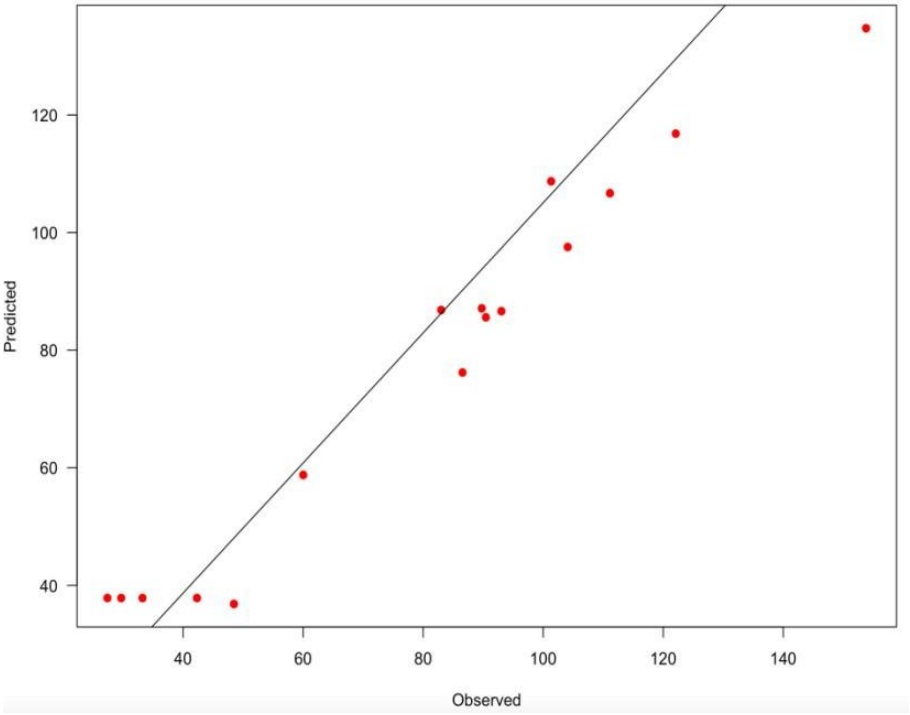

Figure 3.2: Graphical representation of the minimal difference between the actual (straight line) and predicted responses (circles) for the RSM Design for optimal xylanase activity.

Maximum xylanase production (153.80 U/ml) by the *T. harzianum* strain occurred in BBD run 8 under acidic conditions (pH 5.0), the higher wheat bran (1.2%), and a 5 d incubation period. Similar results were observed for run 12 (116.74 U/ml) where the incubation period was 5 d, the wheat bran was at 1.2% and the pH was 6.0. Similar enzyme activities were obtained for runs 6 (101.32 U/ml) and 7 (103.37 U/ml) where either the incubation time (4 or 6 d) or wheat

bran (0.8 or 1.2 %) was at its low or high levels, respectively compared to run 8 where both these parameters were at their high levels (6 d and 1.2%). In the presence of xylan, most microorganisms can produce multiple types of xylanases. Fungi are well-known for producing a wide range of xylanases (up to 30 multiple forms) [5,42]. Zhang et al. [43] reported that three xylanase isoforms were produced by *Aspergillus fumigatus*. The multiple forms of xylanases differ in stability, catalytic efficiency, absorption, and activity on substrates [44]. Okafor et al. [45] isolated a strain of *Penicillium chrysogenum* PCL501 from wood wastes and found that after 4 d of fermentation, wheat bran had the highest xylanase activity of 6.47 U/ml. Abdel-Sater et al. [46] obtained maximum xylanase production from *T. harzianum* after 8 d of fermentation whereas, Thomas et al. [47] achieved maximum xylanase production in 4 d of fermentation by an *Aspergillus* sp. strain.

Multiple forms of xylanases can be influenced by many factors, including the presence of various alleles of the same gene, variable mRNA processing, proteolytic digestion post secretion, and post-translational modifications such as glycosylation and autoaggregation [48]. Because xylanases have varying catalytic efficiencies, the production of several xylanases is particularly beneficial for the complete hydrolysis of hemicellulosic substances [49]. Hemicellulose is a short crosslinked polymer compared to cellulose, which is a long chain homopolymer. Xylans have a β-(1,4) linked backbone made of D-xylose and there are three subtypes of xylan based on the side chain. The subtypes are homoxylan, glucuronoxylan, and arabinoxylan. Homoxylan is only found in two or three types of plants and is mostly cross-linked by β-(1,4)-glycosidic bonds. Generally, xylanase production is directly proportional to the duration of the fermentation time up to a certain level and then decreases, thus, incubation time affects xylanase production by fungi [50].

3.4.2.2 Second order regression and prediction

The second-order regression equation provides the xylanase activity produced by the *T. harzianum* strain as a function of incubation time (X2), pH (X3), and wheat bran (X5) which can be presented in the following equation (IV):

$$Y= 44.91-0.004X2 +0.012X3 +42.09X5 -0.004X22 +0.012X32 +42.09X52 +X2X3 + X2X5+ X3X5 \quad (IV)$$

Where Y is the peak area, X2 is the incubation time, X3 is the pH and X5 is the wheat bran. The statistically insignificant parameters ($p > 0.05$) and their interactions were omitted from the equation. The model constants and coefficients were generated using the unstandardized beta values.

3.4.2.3 ANOVA

The "Lack of fit p-value" (Table 3.7) was insignificant as the p-value was greater than 0.05, however, literature shows this p-value (>0.05) is considered acceptable [51]. According to Bezerra et al. [52], significant regression and a non-significant lack of fit present in the model were well fitted to the experiments. Based on this, the regression equation can be validated [53]. ANOVA was performed to determine the p-values (Table 3.7). This showed the model, the linear and square terms for X2 (Incubation time), and the interaction between X3 (pH) and X5 (Wheat bran) as well as the linear terms of X3 (pH) to be significant as the p-values were 0.0490, 0.001, 0.0019, 0.0395 and 0.0447, respectively.

Table 3.7: ANOVA: and regression coefficients of the response surface quadratic model for the response variables for xylanase production by *T. harzianum* strain

	Estimate	Std. Error	t value	p-value
Model	2736.80	227.41	12.03	0.00001*
Incubation time (X2)	-555.80	43.97	-12.64	0.00001*
pH (X3)	-178.57	49.62	-3.60	0.01137*
[Wheat bran] (X5)	-1897.16	219.83	-8.63	0.00013
Incubation time (X2): pH (X3)	4.48	3.78	1.18	0.28169
Incubation time (X2): [Wheat bran] (X5)	12.08	25.78	0.47	0.65598
pH (X3): [Wheat bran] (X5)	33.55	18.92	1.77	0.12655*
Incubation time (X2)^2	52.50	4.17	12.59	0.00005*
pH (X3)^2	13.04	4.17	3.13	0.02042
[Wheat bran] (X5)^2	887.04	104.24	8.51	0.00014

* Significant p-value at $p \leq 0.05$

Adjusted R^2= 0.9117

Lack of fit p-value= 0.3741

The Pareto chart of standardization histogram graph (Figure 3.3) also showed that Incubation time (X2, $X2^2$), the interaction between pH and wheat bran concentration (X3, X5), and pH (X3) was significant ($p<0.05$), as it crosses the p-line.

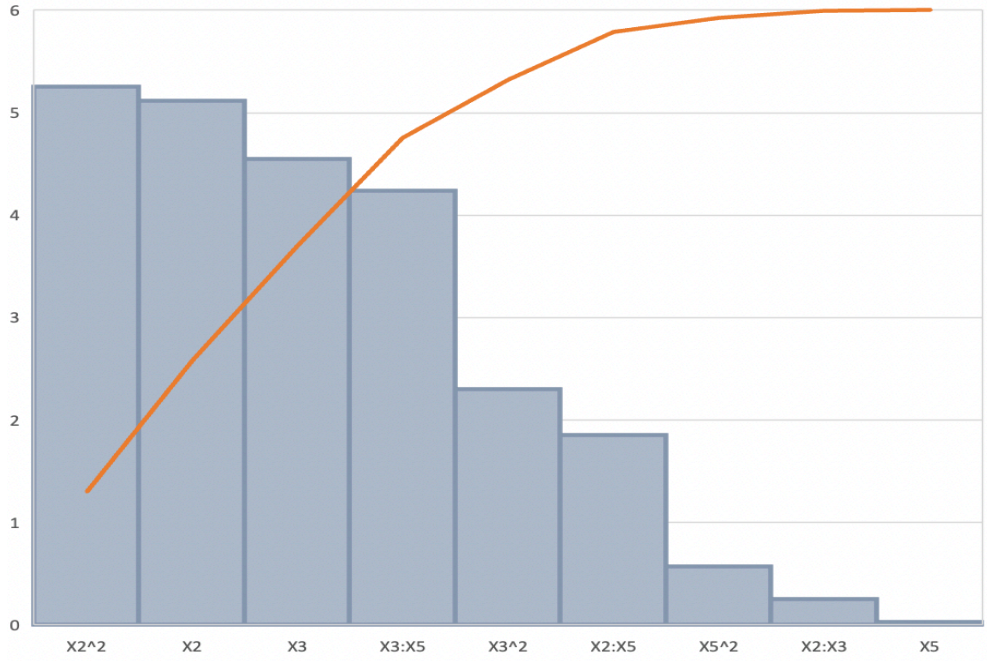

Figure 3.3: Pareto chart standardized effects of nine interactive factors affecting the production optimization of xylanase. Incubation temperature (X1), incubation time (X2), pH (X3), agitation (X4), wheat bran (X5), ammonium sulphate (X6). Orange line represents p= 0.05.

3.4.2.4 Interaction of variables

The relationship between the parameters and the responses can be understood by studying the three-dimensional (3D) response surface plots for xylanase activity; this response was generated from the quadratic model. The 3D response surface plot can also be used to determine the optimum level of each variable for xylanase activity (Figure 3.4-3.6). While maintaining other variables at their optimal level, the Z-axis (referring to xylanase activity) versus any two variables was constructed in the response surface plot.

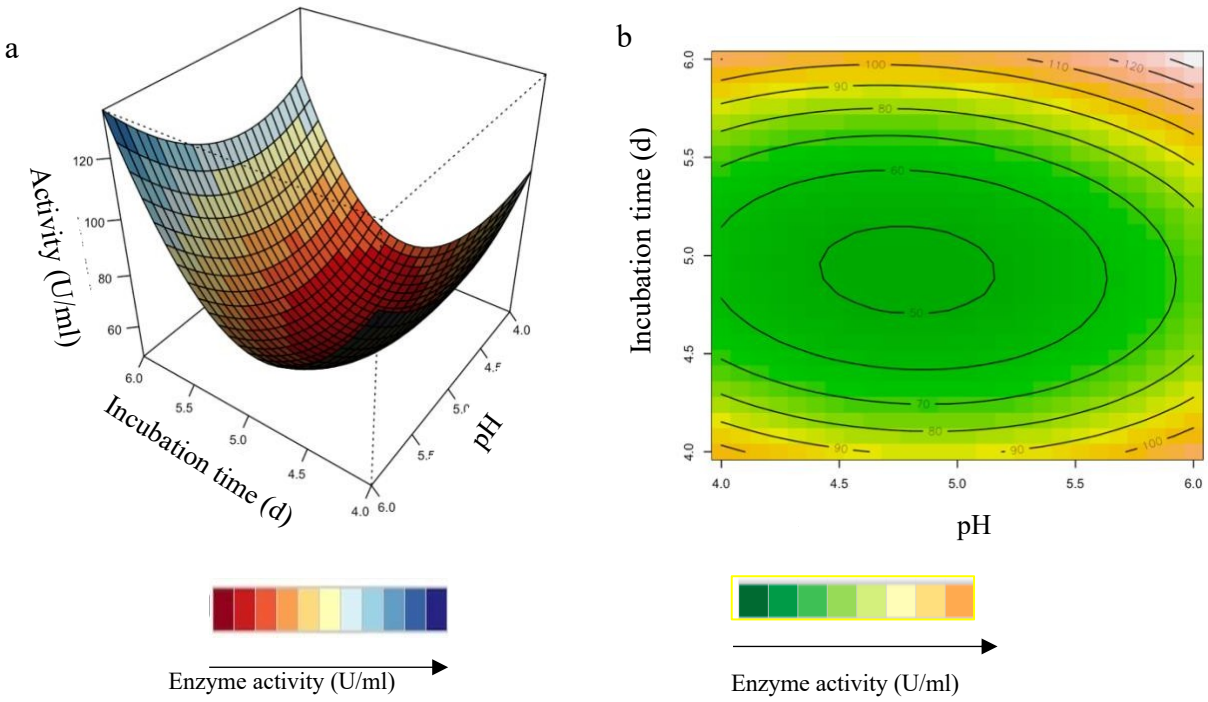

Figure 3.4: Response surface plots (a) and contour plots (b) of the combined effects of Incubation time (X2) and pH (X3) on xylanase production by *T. harzianum* strain.

Figures 3.4a and 3.4b illustrate the combined effects of incubation time and pH. As shown in the 3D response surface plot, the xylanase activity increases at a high pH and shorter incubation time. Figure 3.4b illustrates the contour plot, which shows that high enzyme activity is obtained at the shortest (4 d) and longest period (6 d) of incubation in acidic (4.0 to 6.0) conditions.

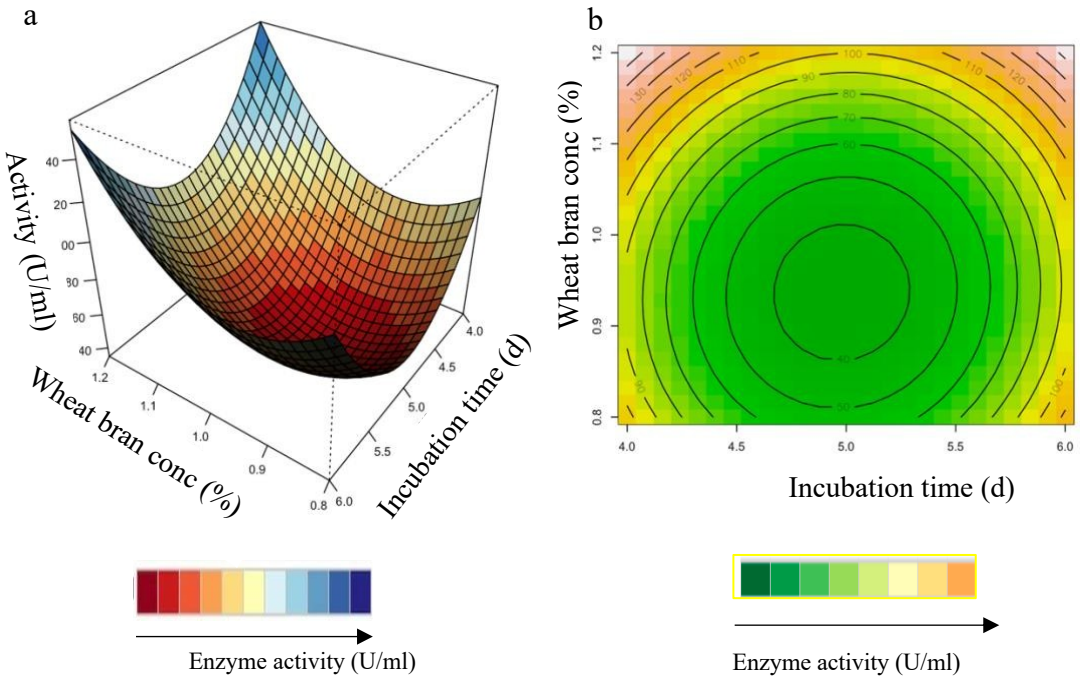

Figure 3.5: Response surface plots (a) and contour plots (b) of the combined effects of Incubation time (X2) and wheat bran concentration (X5) on xylanase production by *T. harzianum* strain.

Figures 3.5a and 3.5b show that xylanase production is directly proportional to incubation time and wheat bran. This could be due to higher levels of degradation of xylan present in the wheat bran by *T. harzianum*. In Figure 3.5b, it is apparent that the xylanase activity is the highest at high concentrations of wheat bran with the shortest (4 d) and longest period (6 d) of incubation. Previous studies showed the time course during the OFAT approach, being favourable at 4 d and 6 d of incubation with the optimum being at 5 d [27]. The RSM plots correspond with OFAT results, as the plots show the highest xylanase activity obtained at high wheat bran concentration between 4 to 6 d. Simultaneously, it was highlighted by Beg et al. [54] that wheat bran could effectively induce higher xylanase production for xylanase production by *Aspergillus awamori.* Li et al. [55] also reported the importance of the substrate concentrations for xylanase production by *A. awamori.* The facts mentioned here, are accounted for by the reports made by Cui and Zhao et al. [56], as they mention that the enzymes involved in substrate

degradation, were generally inducible. These were formed only when the relevant substrate was present in the nutrient salt solution.

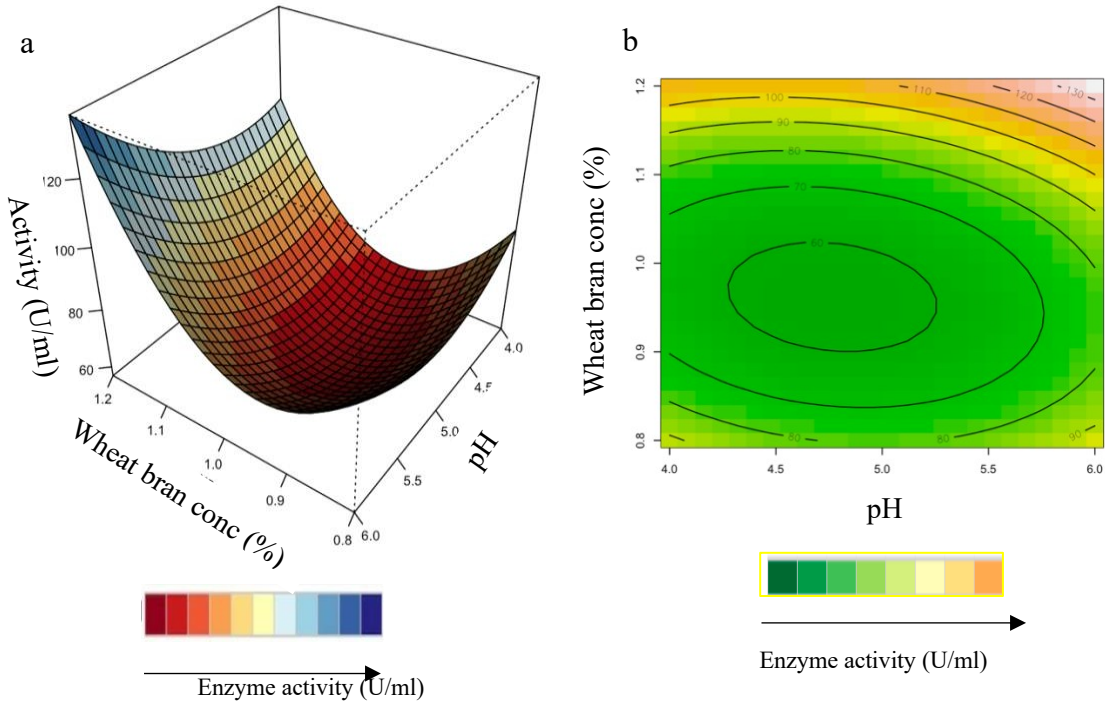

Figure 3.6: Response surface plots (a) and contour plots (b) of the combined effects of pH (X3) and wheat bran concentration (X5) on xylanase production by *T. harzianum* strain.

Figure 3.6 shows the highest xylanase activity obtained with high wheat bran and pH. Figure 3.6b demonstrates that the highest xylanase activity was obtained at high wheat bran and over a wide pH range with the highest activity obtained at the highest pH and wheat bran. The interaction between the pH and wheat bran (130 U/ml) and between incubation time and wheat bran (130 U/ml) had the highest effect on xylanase activity compared to the interaction between incubation time and pH (120 U/ml).

The studies showed that there was a large increase in enzyme activity using the statistical design experiments compared to the OFAT approach. The studies also showed that there were multiple forms of xylanase present (isoforms) with various growth and media conditions. Based on Table 3.6, there are approximately 5 different isoforms present in this study related to the RSM results

obtained. High xylanase activity was observed on runs 4, 6, 7, 8, and 12. Appendix II, supplementary figure 6 represents these RSM runs which indicate the presence of isoforms by the zones of clearance of the substrate native PAGE gels. Multiple forms of xylanases with different pH optima could be beneficial for animal feed improvement [7]. Xylanase is used to reduce the viscosity of the feed and improve the absorption of nutrients in the digestive tract of animals. Before the pelleting process, the enzyme could be applied which requires a pH range of between 4.0 and 6.0. Most xylanases reported to date are optimally active in the acidic or neutral pH range. Xylanases with acidic pH optima could potentially also be useful for applications containing waste, as a method of waste management, and as a feedstock of fermentable sugars [57].

3.4.3 Optimized bulked-up medium for further studies

The xylanase enzyme was produced at pH 5.0 for 6 d of incubation and with 1.2% wheat bran on a larger scale for further studies. The enzyme activity was determined to compare the activities to the smaller scale production. The enzyme activity obtained was 152.78 U/ml which was similar to the enzyme production on a smaller scale (153.80 U/ml).

3.4.4 Purification and zymography of the *T. harzianum* xylanase

The xylanase from *T. harzianum* was purified using ammonium sulphate precipitation, dialysis, and chromatographic methods in combination. Table 3.8 summarizes the purification stages. The enzyme was fractionated with the following ammonium sulphate saturations: (0-20%, 20-30%, 30-40%, 40-50%, 50-60%, 60-70% and 70-80%).

Table 3.8: Purification table for xylanase from *T. harzianum* strain

AS fraction(%)	Total protein (mg)	Total activity (U)	Specific Activity (U/mg)	Yield (%)	Fold purity
Crude extract	95	9593	101.21	100	1.0
Ammonium sulphate fraction:					
50%	12.77	2394.51	187.53	24.96	1.85
60%	10.45	1796.44	171.91	18.73	1.70
70%	10.11	1676.73	165.85	17.48	1.64
80%	7.02	1947.93	277.48	20.31	2.74
Anion exchange chromatography:					
50%	0.40	999.90	2499.75	10.42	24.70
60%	0.28	636.88	2274.57	6.64	22.47
70%	0.16	313.67	1960.44	3.27	19.37
80%	0.32	700.60	2189.38	7.30	21.63

The 50-60%, saturation fraction resulted in significantly high xylanase activity with a recovery of 24.96 % enzyme activity. The 80-90% and fractions also showed relatively high recovery of enzyme activity (20.31%, 18.73%, and 17.48%, respectively) (Table 3.8), therefore these fractions were further studied to confirm if they were isoforms. The active fractions were then dialyzed at 4°C overnight to remove the salts, and the enzyme was loaded onto DEAE Sephadex for further purification. A sodium chloride concentration gradient was used to elute the bound protein (0- 2 M). Xylanase activity was measured in both bound and unbound protein fractions. The primary peak eluted at a 0.5 M sodium chloride gradient, and the corresponding fraction had a specific activity of 254.62 U/mg, resulting in 2.52-fold purity. Furthermore, a single band with a molecular weight of 72 kDa was evident on SDS-PAGE gels of the purified enzyme (50%) (Figure 3.7a). The other ammonium sulphate fractions (60-80%) also have the same molecular weight protein (72 kDa). To assess the activity/purity, the purified xylanase was

subjected to zymogram analysis by substrate native-PAGE (1% beechwood xylan). The xylanolytic activity of the enzyme was indicated by clear zones in the gel after Congo-red staining (Figure 3.7b).

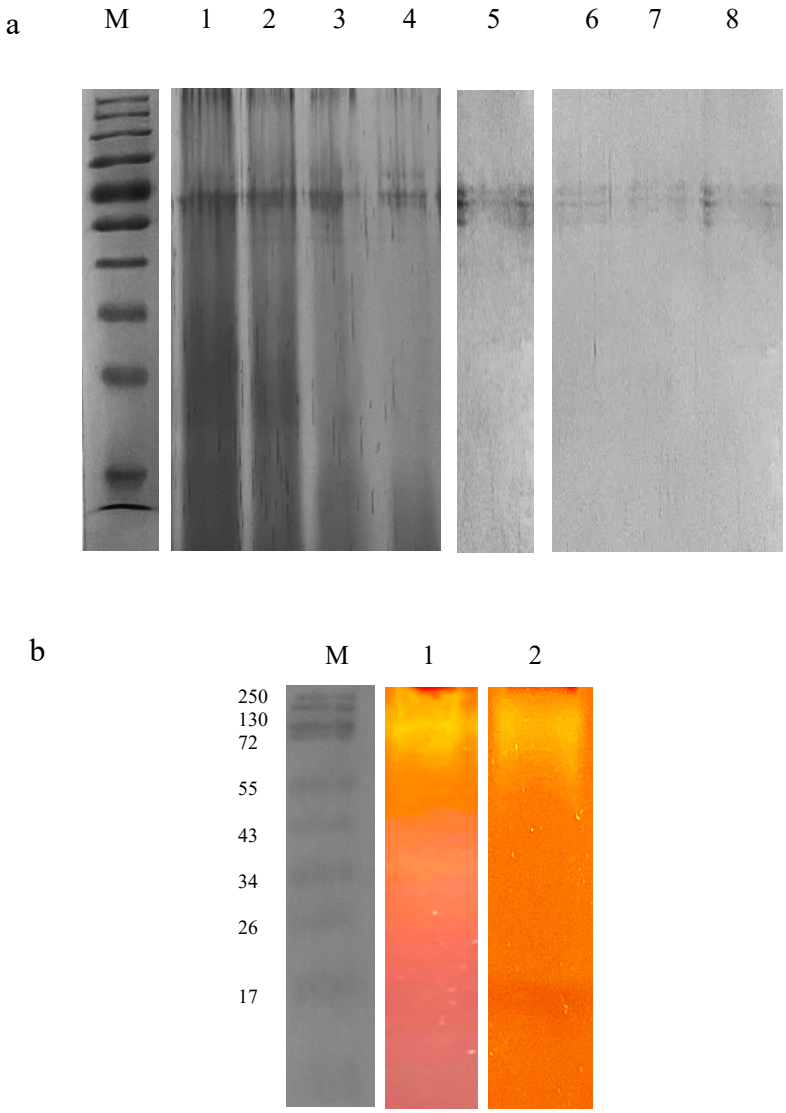

Figure 3.7: 12% SDS PAGE (a) and Native substrate-PAGE (b) analysis of purified xylanase. 12% SDS PAGE (cropped) represents Lane M: Molecular weight marker (Thermoscientific, USA), 1-4: 50, 60, 70 and 80% ammonium sulphate fractions (Coomassie-stained), and 5-8: Purified xylanase from *T. harzianum*. Native substrate-PAGE (cropped) represents Lane M: Molecular weight marker (Thermoscientific, USA), 1: 50% Ammonium sulphate fraction showing zone of clearance, and Lane 2: Purified xylanase from *T. harzianum* on native substrate gel showing zone of clearance. The original gels are presented in Appendix II, Supplementary Figures 1-5.

Purified preparations of enzymes are requisite for their application as well as decoding their basic characteristics and mechanisms. Based on the high molecular weight of the purified enzyme, it can be inferred that it may belong to the GH10 family since enzymes belonging to this family feature a larger molecular weight [57]. Enzymes are also classified based on their catalytic reactions. Based on the sequence similarities of amino acids, xylanases are classified into glycosyl hydrolase (GH) families 10 (GH10) and 11 (GH11). GH 10 contains xylanases of high molecular mass (>30 kDa) with a (β/α)8 barrel structure and acidic pI values. GH11 are the low-molecular-weight endoxylanase which are divided into alkaline pI and acidic pI xylanases [3].

3.4.5 Characterization of purified xylanase

3.4.5.1 pH optima and stability

The enzyme activity is greatly affected by pH, because substrate binding and catalysis are dependent on the charge distribution of both the substrate and the enzyme molecules. The reaction pH was adjusted to 4.0-10.0 with various buffers as described above. The optimum pH of *T. harzianum* xylanase is pH 6.0 with an activity of 40 U/ml (Figure 3.8a). The enzyme is fairly stable at pH 6.0 and remains active (Figure 3.9) retaining >70% of its activity over 4 h. Souza et al. [58] reported that the xylanase from *Thermoascus aurantiacus* expressed in *E. coli* showed optimum values at a similar pH. The purified 60-80% ammonium sulphate fraction was further confirmed to be the same protein purified as the 50% fraction, due to the same pH optimum obtained (pH 6.0) (Figure 3.8a). Thus, the purified fractions of the 50-80% ammonium sulphate fractions can be combined to increase the yield (%).

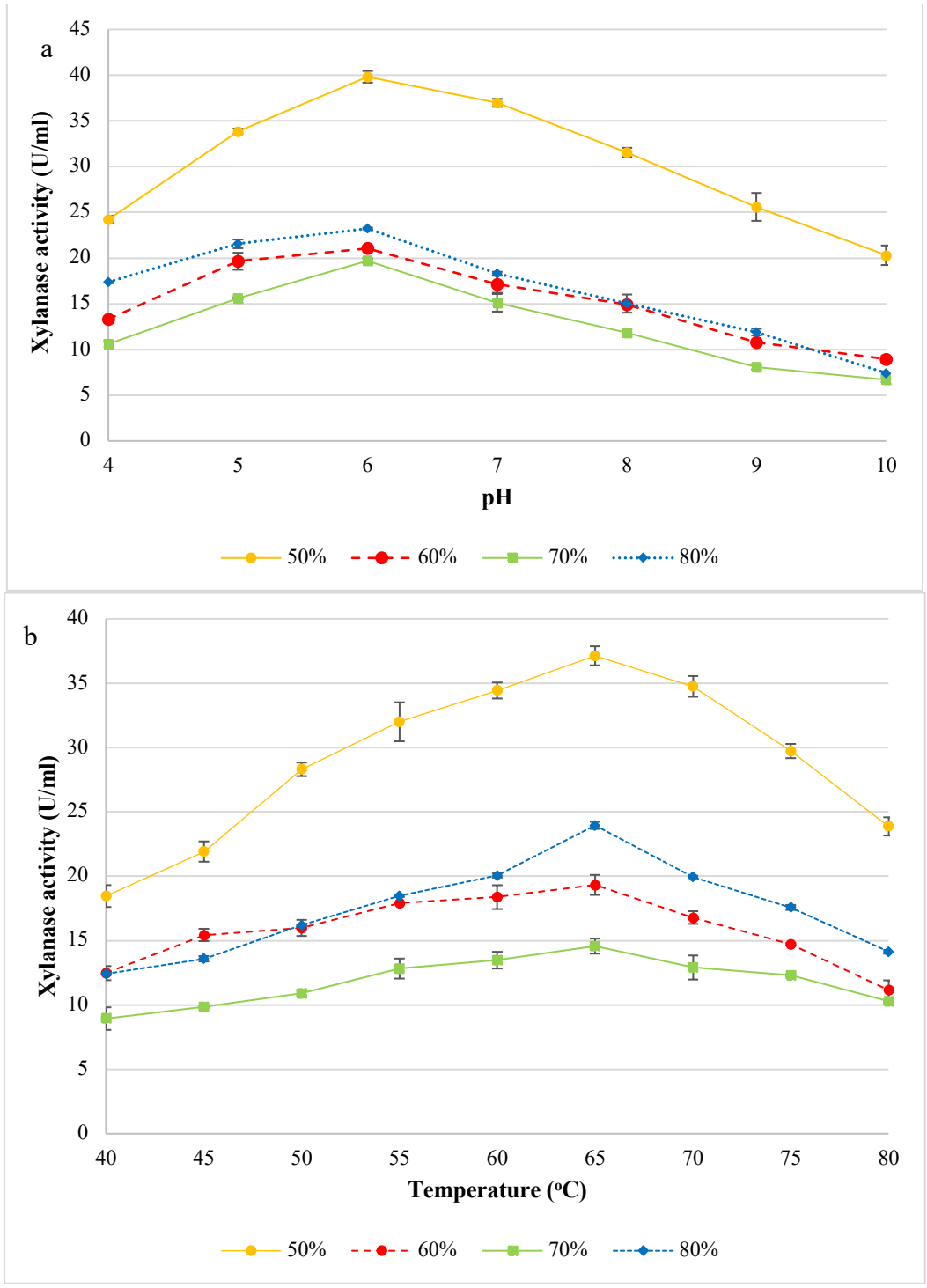

Figure 3.8: Effect of pH (a) and temperature (b) on the activity of purified xylanases (50%, 60%, 70%, and 80% ammonium sulphate fractions). Data points represent the means ± SD (n=4).

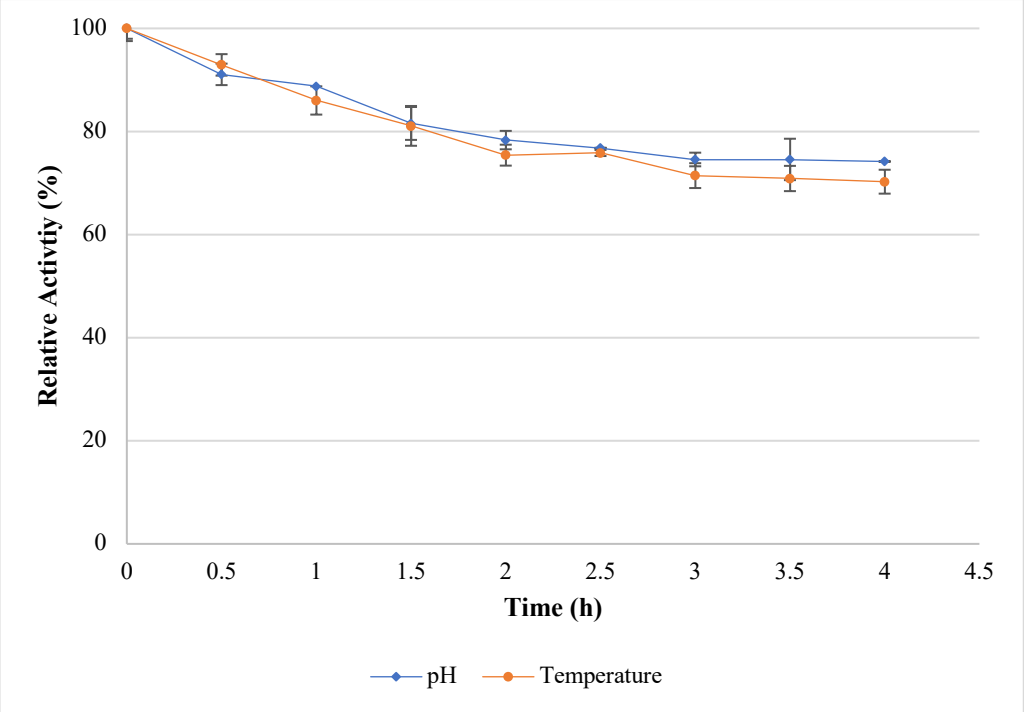

Figure 3.9: pH and temperature stability of purified xylanases (50% ammonium sulphate fraction) produced by the *T. harzianum* isolate. Data points represent the means ± SD (n=4).

3.4.5.2 Optimum temperature and thermal stability

The experiment was carried out at different reaction temperatures ranging from 40 to 80°C to find the optimal temperature of the xylanase. The highest activity of xylanase was observed at 65°C (Figure 3.8b). Thermal stability data illustrated in Figure 3.9 shows that the enzyme retained >70% activity at 65°C for 4 h. A similar result was reported by de Oliveira Simões et al. [59]. However, in that study, the enzyme was subjected to treatment for 24 h and was stable for 1 h. The purified 60-80% ammonium sulphate fraction was further confirmed to be the same protein purified as the 50% fraction, due to the same temperature optima obtained (65°C) (Figure 3.8b). This confirms that these fractions are not isoforms of the xylanase produced. However, the shape of the curve for the 50% ammonium sulphate fraction is different from the other fractions, which seem to show an optimum rather than a broad bell shape.

The advantages of enzymes that prefer high temperatures are well known because the solubility of the reagents and products is increased, the viscosity is reduced, and the mass transfer rate is higher [60]. When looking for enzymes for industrial uses, stability, and activity at high temperatures are highly desirable.

3.4.5.3 Effect of metal ions and inhibitors

The effects of 8 metal ions (Ca^{2+}, Co^{2+}, Fe^{2+}, Mg^{2+}, Mn^{2+}, Zn^{2+}, K^{+}, and Na^{+}) at a final concentration of 2 mM and 10 mM on xylanase activity were determined (Table 3.9) at the optimal pH and temperature (6.0 and 65°C).

Table 3.9: Effect of metal ions on purified xylanase activity. (Relative activity %)

	Concentration (mM)	
Metal ions	**2 .0**	**10.0**
None	100	100
CaCl	84.71	104.27
$CoCl_2$	100.20	104.59
$FeSO_4$	97.62	110.89
$MgSO_4$	96.56	109.44
$MnSO_4$	101.77	100.96
$ZnSO_4$	94.05	108.55
KH_2PO_4	101.98	110.91
NaCl	101.11	98.76

Enzyme activity was slightly increased by 2 mM Mn^{2+}, K^{+}, and Na^{+} (101.11 -101.77 U/ml) whereas the enzyme activity was the highest with 10 mM Ca^{2+}, Co^{2+}, Fe^{2+}, Mg^{2+}, Zn^{2+} (104.27-

110.89 U/ml) ($p \geq 0.05$) and thus, these ions act as cofactors for the enzyme. Inhibitory effects were observed for certain metal ions at each concentration; however, this inhibition of xylanase was weak (<50%). Co^{2+} and Ca^{2+} had no effect on xylanase activity (100%) at 2 and 10 mM. Maximum enhancement was observed for Fe^{2+} (10.88%) followed by Mg^{2+} (9.43%) and Zn^{2+} (8.43%) at 10 mM. Fu et al. [37] reported similar findings for xylanase from *Trichoderma* sp.TPS-36.

3.4.5.4 Substrate specificity of purified xylanase

To determine the substrate specificity of the xylanase for polysaccharide degradation, potential substrates, including birchwood xylan, beechwood xylan, wheat arabinoxylan (soluble and insoluble), xylan from Larchwood, CMC and Avicel were tested under optimal conditions (pH 6.0 and temperature 65°C) using the purified xylanase. Higher hydrolytic activity was observed for the xylans from beechwood, birchwood, and Larchwood compared to wheat arabinoxylan (Table 3.10).

Table 3.10: Substrate specificity of the purified xylanase

Substrates	Relative activity
Beechwood xylan	100
Birchwood xylan	174.07
Xylan from Larchwood	131.03
Wheat arabinoxylan (soluble)	70.54
Wheat arabinoxylan (Insoluble)	46.62
CMC	ND
Avicel	ND

Each data point represents mean ±SD (n=3), ND is not detected

The xylanase most actively degraded birchwood xylan (174.07 %), followed by Larchwood xylan (131.03%), and presented the lowest activity towards wheat arabinoxylan (soluble 70.54% and insoluble 46.62%). The purified xylanase exclusively hydrolyzed xylans, with no activity on CMC and Avicel. This suggested that xylanase's substrate-binding domain has a high affinity for xylans from softwood (birchwood and beechwood) [61]. This might be due to differences in xylan polymer structures and the presence of reactive groups on the surface that are more readily bound. The purified xylanase exhibited significant hydrolytic activity on the diverse xylan substrates, indicating that it might be classified as an endo-1,4-xylanase [62].

3.4.5.5 Kinetic analysis

The Michaelis constant, K_m, may be determined by measuring the substrate concentration at half the maximum velocity. K_m is a constant that remains fixed for every given enzyme and substrate combination. As a result, a low K_m improves the enzyme's affinity for the substrate [63]. The concentration range of the substrate under investigation was 1 to 20 mg/ml, the study revealed K_m and V_{max} were 5.56 mg/ml and 1052.63 µmol/min/mg (Figure 3.10).

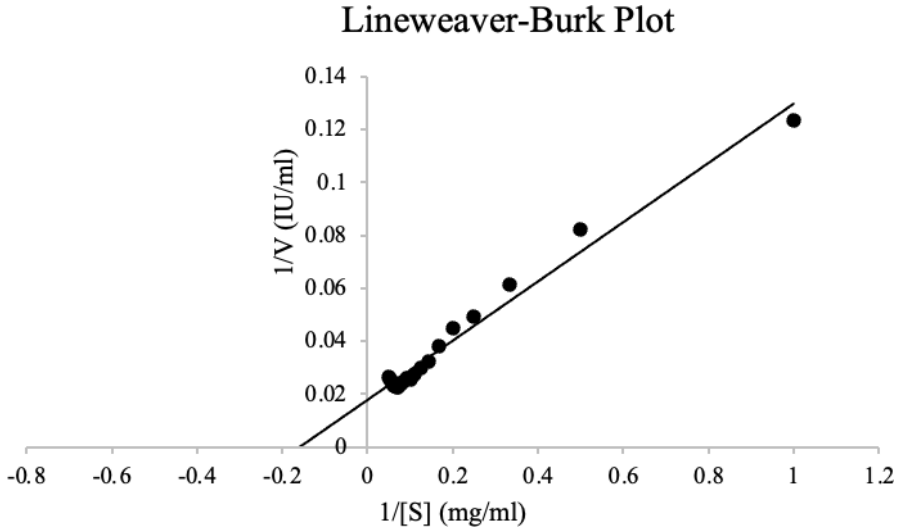

Figure 3.10: Double reciprocal plot of the purified (50% ammonium sulphate fraction) xylanase from *T. harzianum* on beechwood xylan. Data points represent the means ± SD (n=3).

The value of K_m is within the range of fungal xylanases reported in literature (0.14 to 14 mg/ml). Raj et al. [64] obtained similar values (4.96 mg/ml and lower V_{max} 402 µmol/mg/ml) for xylanase from alkaliphilic *Bacillus licheniformis*. Fu et al. [37] reported high V_{max} (1250 µmol/min/mg) similar to this study. Because xylanase has a high V_{max} value and a low K_m value, it has a high affinity for the substrate, beechwood xylan, and can catalyze it more efficiently and quickly than other substrates. Xylanases from *Caldicoprobacter algeriensis* sp. nov. strain TH7C1T were shown to have high selectivity for beechwood xylan [36].

3.5 Conclusion

The current study describes the successful optimization of xylanase production via statistical modelling using PBD and BBD by a *T. harzianum* strain in submerged fermentation. The most influential independent variables were identified and optimized - resulting in a 4.16-fold and 2.24-fold increase in enzyme activity with BBD compared to the OFAT and PBD, respectively. PBD allowed for the consideration of various variables and avoided loss of information, which might be essential in the optimization of the fermentation process. The predictions of the mathematical models were validated by experimental results. Quadratic models with three independent variables were shown to accurately define xylanase production, with high R^2 values for correlations between the actual and predicted values of the response variables. Results showed high enzyme activities obtained within a high pH range which indicates the potential of the xylanase for use over a wide range of applications. The acidic-thermostable xylanase was purified with a 10.42% recovery and 2.52-fold purity. The specific activity of purified xylanase was 254.63 U/mg. The acidic-thermostability of *T. harzianum* xylanase is advantageous for animal feed manufacturing. Future studies will include scaling up the production of xylanase from *T. harzianum* under optimized conditions, which include the

factors and their variables that resulted in the highest xylanase activity (RSM, run 8). Studies will also include sequencing the xylanase protein to understand the structure-guided function of this enzyme.

3.6 References

[1] Broeker, J. *et al.* (2018). The hemicellulose-degrading enzyme system of the thermophilic bacterium *Clostridium stercorarium*: comparative characterisation and addition of new hemicellulolytic glycoside hydrolases. *Biotechnology for Biofuels.* 11, 229.

[2] Yi, Z. *et al.* (2022).Xylan deconstruction by thermophilic *Thermoanaerobacterium bryantii*, hemicellulases is stimulated by two oxidoreductases. *Catalysts*. 12, 182.

[3] Bagewadi, Z.K., Mulla, S.I. & Ninnekar, H.Z. (2016). Purification, characterization, gene cloning and expression of GH-10 xylanase (*Penicillium citrinum* isolate HZN13). *3 Biotech.* 6, 169.

[4] Golgeri, M.D.B. *et al.* (2022). A systematic review on potential microbial carbohydrases: current and future perspectives. *Critical Reviews in Food Science and Nutrition.* (2022).

[5] Chadha, B.S., Kaur, B., Basotra, N., Tsang, A., & Pandey, A. (2019). Thermostable xylanases from thermophilic fungi and bacteria: current perspective. *Bioresource Technology.* 277, 195–203.

[6] Intasit, R., Cheirsilp, B., Suyotha , W., & Boonsawang, P. (2021). Synergistic production of highly active enzymatic cocktails from lignocellulosic palm wastes by sequential solid state submerged fermentation and co-cultivation of different filamentous fungi. *Biochemical Engineering Journal*. 173, 108086.

[7] Walia, A., Guleria, S., Mehta, P., Chauhan, A., & Parkash, J. (2017). Microbial xylanases and their industrial application in pulp and paper biobleaching: a review. *3 Biotech.* 7, 11.

[8] Kereh, H., Mubarik, N.R., Palar, R., Santoso, P., & Yopi. (2018). Optimization of process parameters and scale-up of xylanase production using corn cob raw biomass by marine bacteria *Bacillus subtilis* LBF M8 in stirred tank bioreactor. *Pakistani Journal of Biotechnology.* 15(3): 707-714.

[9] Jain, P. & Pundir, R.K. (2011). Effect of fermentation medium, pH and temperature variations on antibacterial soil fungal metabolite production. *Journal of Agriculture, Science and Technology*. 7(2): 247-269.

[10] Kurrataa, Y., & Meryandini, A. (2015). Characterization of xylanase activity produced by *Paenibacillus* sp. XJ18 from TNBD Jambi, Indonesia**.** *Journal of Biosciences*. 22, 20-26.

[11] Wang, X. *et al.* (2019). Growth strategy of microbes on mixed carbon sources. *Nature Commununications.* 10, 1279.

[12] Nasr, S., Soudi, M. R., Hatef Salmanian, A., & Ghadam, P. (2013). Partial optimization of endo-1, 4-B-xylanase production by *Aureobasidium pullulans* using agro-industrial residues. *Iranian Journal of Basic Medical Sciences*. 16(12): 1245–1253.

[13] Uhoraningoga, A., Kinsella, G. K., Henehan, G. T., & Ryan, B. J. (2018). The goldilocks approach: a review of employing design of experiments in prokaryotic recombinant protein production. *Bioengineering.* 5(4): 89.

[14] Khusro, A., & Aarti, C. (2015). Molecular identification of newly isolated *Bacillus* strains from poultry farm and optimization of process parameters for enhanced production of extracellular amylase using OFAT method. *Research Journal of Microbiology.* 10(9): 393-420.

[15] Long, C., Liu, J., Gan, L., Zeng, B., & Long, M. (2019). Optimization of xylanase production by *Trichoderma orientalis* using corn cobs and wheat bran via statistical strategy. *Waste and Biomass Valorization.* 10 (1): (2019).

[16] Zhang, H., & Wu, J. (2021). Statistical optimization of aqueous ammonia pre-treatment and enzymatic hydrolysis of corn cob powder for enhancing sugar production. *Biochemical Engineering Journal.* 174, 108106.

[17] Irfan, M. *et al.* (2016). Statistical optimization of saccharification of alkali pretreated wheat straw for bioethanol production. *Waste Biomass Valorization.* 7(6): (2016).

[18] Ekpenyong, M. G., Antai, S. P., Asitok, A. D., & Ekpo, B. O. (2017). Plackett-Burman Design and response surface optimization of medium trace nutrients for glycolipopeptide biosurfactant production. *Iranian Biomedical Journal.* 21(4): 249–260.

[19] Sun, T. *et al.* (2019). The optimization of fermentation conditions for *Pichia pastoris* GS115 producing recombinant xylanase. *Engineering in Life Sci*ence. 20, 216-228.

[20] Wu, W.J., & Ahn, B.Y. (2018). Statistical optimization of medium components by response surface methodology to enhance menaquinone-7 (vitamin k2) production by *Bacillus subtilis*. *Journal of Microbiology and Biotechnology.* 28(6): 902-908.

[21] Momeni, M.M., Kahforoushan, D., Abbasi, F., & Ghanbarian, S. (2018). Using chitosan/chpatc as a coagulant to remove colour and turbidity of industrial wastewater: optimization through RSM design. *Journal of Environmental Management.* 211, 347–355.

[22] Kiran, E.U., Akpinar, O., & Bakir, U. (2013). Improvement of enzymatic xylooligosaccharides production by the co-utilization of xylans from different origins. *Food and Bioproducts Processing*. 91, 565–574.

[23] Yadav, P. *et al.* (2018). Production, purification, and characterization of thermostable alkaline xylanase from *Anoxybacillus kamchatkensis* NASTPD13. *Frontiers in Bioengineering and Biotechnology.* 6, 65.

[24] Periyasamy, K., Santhalembi, L., & Mortha, G. (2017). Production, partial purification and partial characterization of enzyme cocktail *Trichoderma citrinoviride* AUKAR04 through solid- state fermentation. *Arabian Journal of Science and Engineering.* 42, 53–63.

[25] Kar, S.S. *et al.* (2012). Process optimization of xylanase production using cheap solid substrate by *Trichoderma reesei SAF3* and study on the alteration of behavioural properties of enzyme obtained from SSF and SmF. *Bioprocessing and Biosystems Engineering*. 36, 2012.

[26] Carvalho, E.A. *et al.* (2017). Optimization of Xylanase production by *Trichoderma stromaticum* in solid state fermentation. *Proceedings.* 3, (2017).

[27] Dhaver, P., Pletschke, B., Sithole, B. & Govinden, R. (2022). Isolation, screening and partial optimization of thermostable xylanase production under submerged fermentation by fungi in Durban, South Africa. *Mycology.* 13(4): 271-292.

[28] Miller, G.L. (1959). Use of dinitrosalicylic acid reagent for determination of reducing sugar. *Analytical Chemistry.* 31, 426–428.

[29] Ghosh, P., & Ghosh, U. (2019). Statistical optimization of laccase production by isolated strain *Aspergillus flavus* PUF5 utilizing ribbed gourd peels as the substrate and enzyme application on apple juice clarification. *Indian Journal of Chemical Engineering.* 61, 1-12.

[30] R Core Team. R: A language and environment for statistical computing. R Foundation for Statistical Computing, Vienna, Austria. URL http://www.R-project.org/. (2020).

[31] Coman, G., & Bahrim, G. (2011). Optimization of xylanase production by *Streptomyces* sp. P12-137 using response surface methodology and central composite design. *Annals of Microbiology.* 61(4): 773–779.

[32] Wickham, H. (2009). Ggplot2: elegant graphics for data analysis. 2nd Edition, Springer New York. 10.1007/978-0-387-98141-3.

[33] Bradford, M.M. (1976). A rapid and sensitive method for the quantitation of microgram quantities of protein utilizing the principle of protein-dye binding. *Analytical Biochemistry.* 72(12): 248–254.

[34] Laemmli, U.K. (1970). Cleavage of structural proteins during the assembly of the head of bacteriophage T4. *Nature.* 227, 680–685.

[35] Franco, P.F., Ferreira, H.M., & Filho, E.X. (2004). Production and characterization of hemicellulase activities from *Trichoderma harzianum* strain T4. *Biotechnology and Applied Biochemistry.* 40(3): 255-9.

[36] Amel, B.D. *et al.* (2016). Characterization of a purified thermostable xylanase from *Caldicoprobacter algeriensis* sp. nov. strain TH7C1. *Carbohydrate Research.* 419, 60-68.

[38] Fu, L.H. *et al.* (2019). Purification and characterization of an endo-xylanase from *Trichoderma* sp., with xylobiose as the main product from xylan hydrolysis. *World Journal of Microbiology and Biotechnology.* 35, 171.

[38] Said, K., & Afizal, M. (2016). Overview on the response surface methodology (RSM) in extraction processes. *Journal of Applied Science and Process Engineering.* 2, 1.

[39] Xie, Y. *et al.* (2019). Collaborative optimization of ground source heat pump-radiant ceiling air conditioning system based on response surface method and NSGA-II. *Renewable Energy*. 147(1): 249-264.

[40] Azzouz, Z., Bettache, A., Boucherba, N., Amghar, Z., & Benallaoua, S. (2020). Optimization of xylanase production by newly isolated strain *Trichoderma afroharzianum* isolate AZ12 in solid-state fermentation using Response Surface Methodology. *Cellulose.* 2020.

[41] Chicco, D., Warrens, M. J., & Jurman, G. (2021). The coefficient of determination R squared is more informative than SMAPE, MAE, MAPE, MSE, and RMSE in regression analysis evaluation. *PeerJ Computer Science.* 7, 623.

[42] Roy, S., Dutta, T., Sarkar, T. S., & Ghosh, S. (2013). Novel xylanases from *Simplicillium obclavatum* MTCC 9604: comparative analysis of production, purification, and characterization of enzyme from submerged and solid state fermentation. *SpringerPlus*. 2, 382.

[43] Zhang, S. *et al.* (2013). Synergistic mechanism of GH11 xylanases with different action modes from *Aspergillus niger* An76. *Biotechnology and Biofuels*. 14, 118.

[44] Liao, H. *et al.* (2015). Functional diversity and properties of multiple xylanases from *Penicillium oxalicum* GZ-2. *Scientific Reports.* 5, 12631.

[45] Okafor, U.A., Okochi, V.I., Onyegeme-okerenta, B.M., & Nwodo-Chinedu, S. (2007). Xylanase production by *Aspergillus niger* ANL 301 using agro-wastes. *African Journal of Biotechnology.* 6, 1710-1714.

[46] Abdel-Sater, M.A., & El-Said, A.H.M. (2001). Xylan-decomposing fungi and xylanolytic activity in agricultural and industrial wastes. *International Biodeterioration and. Biodegradation.* 47, 15-21.

[47] Thomas, L., Parameswaran, B., & Pandey, A. (2016). Hydrolysis of pretreated rice straw by an enzyme cocktail comprising acidic xylanase from *Aspergillus* sp. for bioethanol production. *Renewable Energy*. 98, 9-15.

[48] Maity, C. *et al.* (2012). Xylanase isozymes from the newly isolated *Bacillus* sp. CKBx1D and optimization of its deinking potentiality. *Applied Biochemistry and Biotechnology.* 167(5): 1208-1219.

[49] Choudhury, B. *et al.* (2006). Biobleaching of nonwoody pulps using xylanase of *Bacillus brevis* BISR-062. *Applied Biochemistry and Biotechnology.* 128, 159–169.

[50] Ribeiro Sales, M. *et al.* (2011). Cellulase and xylanase production by *Aspergillus* species. *Annals of Microbiology.* 61, 917–924.

[51] Abu, M.L., Nooh, H.M., Oslan, S.N., & Salleh, A.B. (2017). Optimization of physical conditions for the production of thermostable T1 lipase in *Pichia guilliermondii* strain SO using response surface methodology. *BMC Biotechnology.* 17, 78

[52] Bezerra, M.A., Santelli, R.E., Oliveira, E.P., Villar, L.S., & Escaleira, L.A. (2018). Response surface methodology (RSM) as a tool for optimization in analytical chemistry. *Talanta*. 76(5): 965-977.

[53] He, X. *et al.* (2018). Efficient degradation of azo dyes by a newly isolated fungus *Trichoderma tomentosum* under non-sterile conditions. *Ecotoxicology and Environmental Safety*. 150, 232-239.

[54] Beg, Q.K., Bhushan, B., Kapoor, M., Hoondal, G.S. (2000). Production and characterization of thermostable xylanase and pectinase from *Streptomyces* sp. QG-11-3. *Journal of Industrial Microbiology and Biotechnology.* 23, 396–402.

[55] Liu, W., Lu, Y.L., & Ma, G.R. (1999). Induction and glucose repression of endo-beta-xylanase in the yeast *Trichosporon cutaneum* SL409. *Process Biochemistry.* 34, 67–72.

[56] Cui, F., & Zhao, L. (2012). Optimization of xylanase production from *Penicillium* sp.WX-Z1 by a two-step statistical strategy: Plackett-Burman and Box-Behnken experimental design. *International Journal of Molecular Sciences.* 13(8): 10630-10646.

[57] Bhardwaj, N., Kumar, B. & Verma, P. (2019). A detailed overview of xylanases: an emerging biomolecule for current and future prospective. *Bioresources and Bioprocessing.* 6, 40.

[58] Souza, A.R. *et al.* (2016). Engineering increased thermostability in the GH-10 endo-1, 4-β-xylanase from *Thermoascus aurantiacus* CBMAI 756. *International Journal of Biological Macromolecules.* 93, 20–26.

[59] de Oliveira Simões, L.C. *et al.* (2019). Purification and physicochemical characterization of a novel thermostable xylanase secreted by the fungus *Myceliophthora heterothallica* F.2.1.4. *Applied Biochemistry and Biotechnology.* 188(4): 991-1008.

[60] Vieille, C., & Zeikus, G. J. (2001). Hyper thermophilic enzymes: sources, uses, and molecular mechanisms for thermostability. *Microbiology and Molecular Biology Reviews.* 65(1): 1–43.

[61] Yin, L., Lin, H., Chiang, Y., & Jiang, S.T. (2010). Bio properties and purification of xylanase from *Bacillus* sp. YJ6. *Journal of Agricultural and Food Chemistry.* 58(1): 557-562.

[62] Fang, Z., Smith, J., Richard, L., & Tian, X. (2019). Isolation, purification, and potential applications of xylan. *Sustainable Biomass Resources.* 9(1): 3-35.

[63] Deshmukh, R.A. *et al.* (2016). Purification, biochemical characterization and structural modelling of alkali-stable β-1,4-xylan xylanohydrolase from *Aspergillus fumigatus* R1 isolated from soil. *BMC Biotechnology.* 16, 11.

[64] Raj, A.S., Kumar, S., Singh, S.K., & Prakash, J. (2018). Production and purification of xylanase from alkaliphilic *Bacillus licheniformis* and its pre-treatment of eucalyptus kraft pulp. *Biocatalysis and Agricultural Biotechnology.* 15, 199-209.

CHAPTER FOUR

ENHANCED PRODUCTION OF A RECOMBINANT XYLANASE (XT6): OPTIMIZATION OF PRODUCTION AND PURIFICATION, AND SCALED-UP BATCH FERMENTATION IN A STIRRED TANK BIOREACTOR

4.1 Abstract

The endoxylanase XT6 produced by *Geobacillus stearothermophilus* is a desirable candidate for industrial applications. In this study, the gene encoding XT6 was cloned using the pET-28a expression vector and expressed in *Escherichia coli* BL21 (DE3) cells. Recombinant XT6 production was improved by optimizing cell lysis (sonication, chemical, and enzymatic lysis) and expression conditions. Sonication in a 0.05 M sodium phosphate (pH 6.0) buffer resulted in the highest xylanase activity (16.48 U/ml). Screening and optimization of induction conditions using the Plackett-Burman Design (PBD) and Box-Behnken Design (BBD) approaches revealed that cell density pre-induction (OD_{600nm}), post-induction incubation time, and IPTG concentration significantly ($p<0.05$) influenced the expression levels of XT6 (16.48 U/ml to 40.06 U/ml) representing a 3.60-fold increase. BBD resulted in a further 8.74-fold increase in activity to 144.02 U/ml. Batch fermentation in a 5-l stirred tank bioreactor at 1 vvm aeration boosted recombinant xylanase production levels to 165 U/ml suggesting that heterologous expression of the XT6 enzyme is suitable for scaled-up production. The pure enzyme with a molecular weight of 43 kDa and a 15.69-fold increase in purity was obtained using affinity chromatography and a cobalt column. Future studies will include application of the purified recombinant xylanase to animal feed.

Keywords: *expression; Geobacillus stearothermophilus; Plackett-Burman Design; purification; Response Surface Methodology; scale-up*

4.2 Introduction

Interest in xylan-degrading enzymes has escalated over the last few years due to their applications in pulp processing and the biodegradation of lignocellulosic materials [1]. Hemicellulose, which makes up 30-40% of lignocellulosic biomass, is mainly constituted of xylan [1]. Xylan is a polysaccharide made up of β-1,4-xylose units or β-1,4-mannose units with arabinose, methylglucuronic acid, and acetate substitutions[2, 3]. The complex chemical composition of xylan requires the concerted action of several enzymes, collectively known as hemicellulases, including endo-β-D-xylanases, β-xylosidases, α-L-arabinofuranosidases, α-D-glucuronidases, acetyl xylan esterases, ferulic and *p*-coumaric acid esterases. These enzymes work together to produce xylooligosaccharides (XOS) and xylose, which are the end products of their synergistic action on the linear and side chains [4]. Endo-1,4-β-xylanase is an important enzyme that operates on the xylan backbone of hemicellulose with high specificity, minimum substrate loss, and few side products [2] compared to the commonly used chemical hydrolysis techniques. Xylanase acts synergistically in conjunction with other accessory enzymes to degrade xylan to component sugars.

In nature, filamentous fungi such as *Aspergillus* spp. [5] and *Trichoderma* spp. [6] produce xylanases rapidly. Some bacteria, such as *Bacillus stearothermophilus, Bacillus subtilis* [7], and *Paenibacillus* spp., produce extracellular thermostable xylanase enzymes [8]. These thermostable xylanases are more suitable for industrial bioprocesses than those produced by mesophilic bacteria [3]. The species *Geobacillus* has been widely examined among numerous thermophilic bacteria studied for xylanase production due to its ability to produce highly thermostable enzymes and ability to use a variety of carbon sources [9]. In thermophilic niches, the genus evolved several species, whose genomes encode highly thermostable enzymes that can be applied in several industrial bioprocesses such as in lignocellulosic biomass hydrolysis [6], pulp and paper production [10], bioethanol production [11], etc. In recent years, xylanases

with specific properties have been identified from bacterial and fungal sources, and numerous strategies have been developed to engineer them for different industrial applications [12]. Due to product inhibition and catabolite repression, microbial xylanases are produced in low titres. Researchers have introduced recombinant DNA technology to solve this challenge which has led to the development of xylanolytic enzymes that are more appropriate for industrial applications. To attain overproduction of the enzyme to suit commercial purposes, the xylanase-encoding genes have been cloned into homologous and heterologous hosts [13]. *Escherichia coli* is the first-line system for the heterologous production of particularly non-glycosylated proteins [14]. Cloning of genes in *E. coli* is considered advantageous for high enzyme production levels as it can be easily grown and rapidly on inexpensive substrates to high cell density under favourable growth conditions to achieve high-level expression of the desired recombinant protein [15]. Moreover, *E. coli* can be easily manipulated and has several available cloning and expression vectors, and is amenable to various cultivation techniques. [14]. In view of these advantages, *E. coli* can be a suitable host for the large-scale manufacturing of heterologous proteins [14] in bioreactors that provide a well-controlled culture environment [16]. One of the most significant disadvantages of using *E. coli* to produce desired products is that these bacteria do not ordinarily release proteins into the environment [17]. Proteins produced remain confined within the constraints of the cellular framework requiring disruption of the cell walls for the release of proteins into the surrounding environment. Techniques such as sonication, chemical lysis, enzymatic lysis, bead milling, and high-pressure homogenization are reported to be effective for the recovery of proteins from *E. coli* cells [18].

The reaction of cells to their surroundings can also influence the host's expression level [19]. As a result, fermentation factors such as temperature, cell density, induction period, and inducer concentrations must be optimized for the host cells, to maintain favorable conditions to ensure

high enzyme activity and protein production efficiency [14]. The traditional method for optimizing the fermentation process is the one-factor-at-a-time (OFAT) approach, where one parameter is varied, while the others are kept constant. However, this approach is laborious due to many factors and the inability to identify the interactions between variables, which can cause misinterpretation of the results [20]. Such challenges may be overcome by using statistical approaches. PBD and RSM approaches were used in this study to optimize the expression of the *G. stearothermophilus* XT6 in *E. coli* to produce high yields of the functional recombinant XT6 protein. Significant steps in the production of a recombinant protein after cloning include fermentation to produce high biomass yields, cell lysis to release intracellular proteins, and the recovery of the protein of interest using a targeted separation technique such as Immobilized Affinity Chromatography (IMAC). All steps are paramount for the success and economic viability of the process.

This study aimed to optimize cell lysis (sonication, chemical lysis, and enzymatic lysis) which is critical to achieving the highest possible yield of soluble protein, the expression of XT6 by *E. coli* in shake flask studies, and the scale-up of production in large-scale bioreactors. The expressed recombinant XT6 protein was then purified and used for further studies in an application to improve the digestibility of animal feed by assessing the effect of the recombinant XT6 xylanase on the hydrolysis of feed substrates.

4.3 Materials and methods

4.3.1 Obtaining *E. coli* harbouring pET28(+)/XT6 and expression of the recombinant XT6 xylanase.

E. coli BL21(DE3) cells were transformed with the pET28(+)-XT6 plasmid DNA [22]. The recombinant cells were grown on 2× YT plates containing 50 µg/ml kanamycin (SIGMA, China)

and were incubated with shaking (Heraeus B6120 Incubator, Gemini BV) for 24 h at 37°C [22]. Single colonies of the recombinant *E. coli* cells harboring XT6 were cultured in 5 ml of 2× YT broth (50 µg/ml kanamycin) and incubated at 37°C for 24 h. The culture was transferred into fresh 2× YT broth (50 µg/ml kanamycin) and grown at 37°C until the mid-log phase at OD_{600nm} was between 0.4-0.7. Protein expression was induced by the addition of 1 mM isopropyl-β-D-thiogalactopyranoside (1 M IPTG) (Glentham Life Science, Corsham). Samples were taken every hour for up to 4 h, and the OD_{600nm} readings of the bacterial cells were recorded each hour. Collected samples were centrifuged (Eppendorf centrifuge 5418, Germany) at 16 060 ×*g* for a minute. The supernatant was discarded, and the pellet resuspended in 2× SDS sample buffer (0.004% (v/v) bromophenol blue, 10% (v/v) 2-mercaptoethanol, 20% (v/v) glycerol, 4% (v/v) SDS and 0.125 mM Tris-HCl, Sigma, South Africa). The volume of sample buffer used to resuspend the pellet was obtained using the formula: [resuspension volume (ml) = OD_{600nm} /6]. Samples were boiled for 5 min and then incubated on ice before SDS-PAGE analysis [22].

4.3.2 Optimization of cell lysis

Lysis is a critical stage in the purification of intracellular bioproducts. There are several factors and challenges to consider when selecting the correct lysis protocol as there is no standard procedure applicable for the recovery of all types of recombinant proteins [18]. It is thus, advisable to thoroughly study and test various lysis protocols to ensure the highest possible recovery of the desired product. The different lysis protocols that were tested to maximize recovery of the intracellular recombinant xylanase from the *E. coli* expression host are described below.

4.3.2.1 Methods of lysis

4.3.2.1.1 Enzymatic lysis (lysozymes)

After induction, the cells were harvested by centrifugation (Eppendorf Centrifuge 5418, Germany) (10000 ×*g* at 4°C for 10 min), and the pellet was resuspended in phosphate-buffered saline (PBS) buffer (20 ml/g of cells). Lysozyme (1 mg/ml) (Sigma, Switzerland) was added to the cell suspension and incubated with shaking at room temperature for 2 h. Samples were stored at -80°C overnight and thereafter centrifuged as described above, and the protein was obtained in the supernatant (soluble fraction) [18].

4.3.2.1.2 Enzymatic and chemical lysis

The procedure described above in 2.3.1.1 was followed. However, TritonX-100 (1% v/v) (Merck chemicals, England) was used in conjunction with lysozyme, as TritonX-100 is reported to assist in the disruption of the cellular membrane leading to enhanced cell lysis [23].

4.3.2.1.3 Sonication

The harvested cells were centrifuged, and the pellets were resuspended in 0.05 M sodium phosphate (pH 6.0), 0.05 M Tris-HCl (pH 8.0) buffer, and 0.05 M Tris-HCl (pH 8.0) with 8 M urea. The cell suspensions were lysed using a probe sonicator (OMNI Sonic Ruptor 400, 220V 6A, 18- 200, United Kingdom) at 50 kHz for 30 s. The samples were kept on ice to prevent heating and denaturation during sonication. The lysate was centrifuged for 10 min at 10 000 ×*g* at 4°C, and the soluble fraction was expected to contain the target protein [18].

4.3.2.2 Quantification of the extent of lysis

There are several techniques which can be used to quantify the extent of cell lysis. These can be categorized as direct and indirect analysis of cellular lysis.

4.3.2.2.1 Direct cellular analysis: optical density at 600 nm

The extent of the lysis of *E. coli* cells can be determined by measuring and comparing the OD_{600nm} before and after cell lysis treatments [24].

4.3.2.2.2 Indirect analysis (quantification of cellular products)

The indirect techniques of cellular lysis quantification are based on separating several cellular products resulting from cell lysis.

4.3.2.2.2.1 Quantification of total protein

The total protein content was determined using the Bradford technique using bovine serum albumin (BSA) (Sigma, USA) as the standard at values ranging from 0 to 50 mg/ml. In a reaction vessel, aliquots of 1 ml Bradford reagent (Sigma, USA were well mixed with 33.33 µl of protein and allowed to stand for 5 min at room temperature. A spectrophotometer was used to detect the absorbance at 595 nm (Shimadzu UV-1800, Japan). The blank was comprised of 33.33 µl of distilled water mixed with Bradford reagent [26]. The degree of cell lysis was evaluated by measuring the concentration of proteins in the supernatant of a lysate sample before and after lysis.

4.3.2.2.2.2 Xylanase protein quantification

The concentration of the xylanase protein was determined before and after cell lysis using a spectrophotometer (Nanodrop 2000c spectrophotometer, Thermo Scientific). The molar extinction coefficient used was 80 790 $M^{-1}cm^{-1}$ at 280 nm, with a theoretical molecular weight (46 763 Da) for the enzyme [25].

4.3.2.2.2.3 Quantification of xylanase activity

Xylanase activity was quantified using the 3,5-dinitro salicylic (DNS) (Sigma, India) acid assay for reducing sugars [27]. The reaction included 600 µl of 1% (w/v) of beechwood xylan (1 g in 100 ml of 50 mM citrate buffer, pH 5) (Sigma, India), to which 66.67 µl of the enzyme. The reaction mixture was incubated in a water bath at 55°C for 15 min and terminated by adding 1 ml DNS acid reagent to the reaction mixture and then heating for 5 min at 100°C in a water bath. The absorbance was read at 540 nm using a spectrophotometer (Shimadzu UV-1800, Japan) to determine the concentration of sugar released by the enzyme. One unit (U) of xylanase was defined as the amount of enzyme that released 1 µmol xylose as reducing sugar equivalents per min under the specified assay conditions. All enzyme assays were performed in triplicate.

4.3.2.2.2.4 SDS-PAGE

The molecular weight of the recombinant XT6 xylanase was confirmed by 12% SDS-PAGE [28]. The gel was run at a constant voltage (50 V) (BioRad, Power Pac™ HV, USA) until the dye front reached the bottom of the gel. Following electrophoresis, the gel was stained in Coomassie Brilliant Blue (Merck, Germany) for 15 min and destained overnight in a destaining solution (10% acetic acid (Merck, Germany), 20% methanol (Merck, Germany), and 70% dH_20) to visualize the proteins and determine the molecular weight of the proteins using standard molecular weight markers. To determine the degree of lysis samples representing the total lysate proteins, both the insoluble phase(pellet), and lysate supernatant (soluble phase) were run on the gel. The greater the number of proteins (represented by the number of bands as well as the intensity of bands) released to the soluble phase, the greater the cellular lysis efficiency.

4.3.3 Experimental design and optimization of cultivation parameters

4.3.3.1. One-factor-at-a-time (OFAT) optimization of the recombinant XT6 xylanase production

The factors tested included cell density pre-induction (OD_{600nm}) [31], induction temperature [30], time, [13] IPTG concentration [13], as well as yeast extract, and tryptone concentration [29].

4.3.3.2 Statistical optimization, experimental design, and data analysis

4.3.3.2.1 PBD

In this study, tube cultivation was employed, and six variables were selected as shown in Table 4.1: Incubation temperature (X1), cell density pre-induction (OD_{600nm}) (X2), post-induction time (X3), yeast extract concentration (X4), tryptone concentration (X5), and IPTG concentration (X6). The total number of experimental runs carried out for the six variables was twelve [32]. Each variable was represented by a high level denoted by '+' and a low level denoted by '-.' The high level of each variable was sufficiently far from the low level so that any significant effect would be observed. The experimental runs were performed in duplicate, and an average of the results was reported. Table 1 represents the PBD based on the first-order polynomial model equation I.

Table 4.1: : Experimental variables and levels used in the PBD for optimal recombinant XT6 xylanase production.

	Symbol code	Units	Experimental Values	
			Low level (-1)	**High level (+1)**
Induction temperature	X1	°C	25	37
Cell density pre-induction (OD_{600nm})	X2	-	0.4	0.6
Post induction time	X3	Hours (h)	3	5
Yeast extract	X4	%	0.5	1.5
Tryptone	X5	%	1	2
IPTG	X6	mM	0.5	2.5

Table 4.1 represents the PBD based on the first-order polynomial model equation I.

$$Y=\beta_0 \sum\beta_i X_i \qquad [I]$$

Where Y is the response (peak area and retention factor), β_0 is the model intercept, βi is the linear coefficient, and X_i is the level of the independent variable. The PBD was analyzed using R studio software [33] to estimate the significant factors. Analysis of variance (ANOVA) was performed to determine the p-values and the *R* coefficients to check the significance and fit of the regression model. Screened parameters were represented on a Pareto chart of standardized effects. The effect of each variable was analyzed, and the variables with the highest influence on the production of xylanase were selected for the second-level optimization by BBD of Response Surface Methodology (RSM).

4.3.3.2.2 Optimization of significant variables using RSM

The BBD was used to elucidate the primary interaction and quadratic effects of the three significant variables arising from the PBD, with replicated centre points. The experimental design and statistical analysis were performed using R Studio [33]. Table 4.2 represent a three-level, three-factor BBD was used to evaluate the combined effect of the three independent variables, cell density pre induction (OD_{600nm}) (X2), post-induction time (X3), and IPTG concentration (X6).

Table 4.2: Experimental codes and levels of independent variables in the RSM for optimal recombinant XT6 xylanase production

Variables	**Symbol code**	**Experimental values**		
		Lower (-1)	*Zero (0)	Higher (+1)
Cell density pre-induction (OD_{600nm})	X2	0.4	0.5	0.6
Post-induction time (h)	X3	3	4	5
[IPTG] (mM)	X6	0.5	1.5	2.5

* Optimum level

The design consisted of 16 combinations, including three replicates of the centre point. After the experimental runs, the average xylanase activities were taken as the response (Y). A multiple regression analysis of the data was carried out to obtain an empirical model relating the response to the independent variables.

The second-order polynomial equation is shown below in Equation II:

$$Y=\beta_0 + \sum\beta_i X_1 + \sum\beta_{ii} X_2 + \sum\beta_{ij} X_1X_2 \quad [II]$$

Where Y represents the response variable (peak area), β_0 is the interception coefficient, β_i is the coefficient for the linear effects, β_{ii} is the coefficient for the quadratic effect, β_{ij} are interaction coefficient, and X_1 X_2 is the coded independent variables that influence the response variable Y. The response in each run was the average. In this experimental design, data were analyzed by one-way ANOVA with Tukey's multiple comparison tests ($p < 0.05$) using R studio [33], and ggplot2 was used for the generation of 3D response surface and contour plots.

4.3.4 Scale-up of enzyme production in a stirred tank bioreactor

This study was carried out in a Sartorius BioStat®B-DCU fermenter with a working volume of 3-l with 2x YT medium supplemented with kanamycin (50 µg/ml) in a UniVessel® Glass 5 L (260 mm diameter and 690 mm height). The fermenter was sterilized at 121°C for 15 min. Optimal conditions from the lab-scale production were used to set up fermentation in the bioreactor. A BioStat®B twin control tower with MFCS was used to monitor all the relevant parameters and data. The pH and Dissolved Oxygen (DO) probes were first calibrated according to the standard procedure given by the manufacturer. Fermentation was carried out at 30°C, 200 rpm with one impeller (Rushton blade disc impeller). Three different aeration rates: 0.5, 1, and 2 volume of air per volume of liquid per min (vvm) were tested. Growth was monitored every 30 min and after 2 h, cells reached the expected OD_{600nm} (0.5), and IPTG was added to the fermentation. After 4 h of fermentation, the content of the bioreactor was harvested, and down streaming was carried out with the separation of the pellet and supernatant using the centrifuge (Beckman Coulter™, Avanti® J-26XPI, USA) at 4°C, 16 873 × *g* for 10 min.

4.3.4.1 Specific Growth Rate

The specific growth rate is the most important parameter to be determined during fermentation, as it represents the dynamic behavior of microorganisms. The specific growth rate period is

defined as the rate of increase of biomass of a cell population per unit of biomass concentration. This can be determined by obtaining the gradient of the growth curve shown in Figure 3.8 [34].

$$\textbf{Specific growth rate } (\mu) = \frac{\textbf{ODx} - \textbf{ODy}}{\textbf{Tx} - \textbf{Ty}}$$

4.3.4.2 Productivity

Productivity is defined as the final product concentration divided by the time from inoculation to batch delivery. This is determined by the final biomass concentration subtracted from the inoculum concentration divided by the cultivation time (h).

$$\mathbf{P_o} = (\mathbf{X_F} - \mathbf{X_O})/\mathbf{t_c}$$

Where X_F is the final biomass concentration (g/l), X_o is the inoculum (g/l), and t_c is the cultivation time (h).

4.3.4.3. Biomass yield coefficient

The biomass yield coefficient could be defined as the mass of microorganisms produced per mass of a substrate utilized, known as the growth yield coefficient [35].

$$\textbf{Yield coefficient} = \frac{\textbf{Biomass produced}}{\textbf{Substrate utilized}}$$

4.3.5 Purification of recombinant XT6 xylanase

Purification was conducted using affinity chromatography. A column was packed with the appropriate amount of HisPur cobalt resin, and gravity flow allowed the storage buffer to drain from the resin. Two resin bed volumes of the equilibration /wash buffer (50 mM NaH_2PO_4, 300

mM NaCl, 0.03% (w/v) sodium azide, 10 mM imidazole, and 50 mM Na_2HPO_4, pH 8.0) were added. The buffer was allowed to drain from the resin at a flow rate of 0.5-1 ml/minute. Two resin bed volumes of the prepared protein extract (supernatant) were loaded directly into the column containing the HisPur cobalt resin (SIGMA, USA). The flow-through was collected and reapplied to maximize the yield. The supernatant was decanted and kept as the flow-through fraction (FT- unbound protein sample). The resin was washed with two resin-bed volumes of equilibration/wash buffer to remove all non-specifically bound proteins on the resin. This was repeated until the absorbance of the flow-through fraction, at 280 nm, reached baseline. The flow-through was collected each time in a new collection tube and labeled as the "wash" fractions (W1-W3). Two-resin bed volumes of elution buffer (50 mM NaH_2PO_4, 300 mM NaCl, 0.03% (w/v) sodium azide, 250 mM imidazole, and 50 mM Na_2HPO_4, pH 8.0, SIGMA, USA) were added to the resin and repeated three times (E1-E3), to elute His-tagged proteins and any remaining protein. A final wash step (W4) was conducted to remove residual imidazole using the wash buffer from the column. The three elution fractions were pooled together and concentrated using 30 kDa Amicon filters by centrifugation (4000 ×*g* at 4℃ for 20 min) (Eppendorf centrifuge 5418, Germany). The concentrate was then constituted in a final glycerol concentration of 20% (v/v) for XT6 stabilization during storage at -20℃. To store the cobalt column appropriately for regeneration, it was washed with ten resin-bed volumes of 20 mM 2-(N-morpholino)ethanesulfonic acid (MES) buffer (SIGMA, South Africa), 0.05 M NaCl, pH 5.0, followed by ten resin-bed volumes of ultrapure water and stored in 30% ethanol at 4°C.

4.4 Results and discussion

4.4.1 Expression of the recombinant XT6 xylanase

Induction and expression of the recombinant XT6 xylanase were performed by growing the cells until the OD_{600nm} was between 0.4 and 0.6, then adding 1 mM IPTG, followed by hourly sampling (1 to 4 h). The insoluble fractions were analyzed using 12% SDS-PAGE and illustrated in figure 1, with the uninduced cell lysate serving as a control. More highly contrasted bands of 43 kDa were observed in the cell lysate of samples after induction, while less contrasted bands were observed for the control (uninduced), indicating successful expression of the cloned XT6 gene. Gomez Garcia et al. reported a similar molecular weight (45 kDa) for a xylanase from *Geobacillus* sp. DUSELR13 [6].

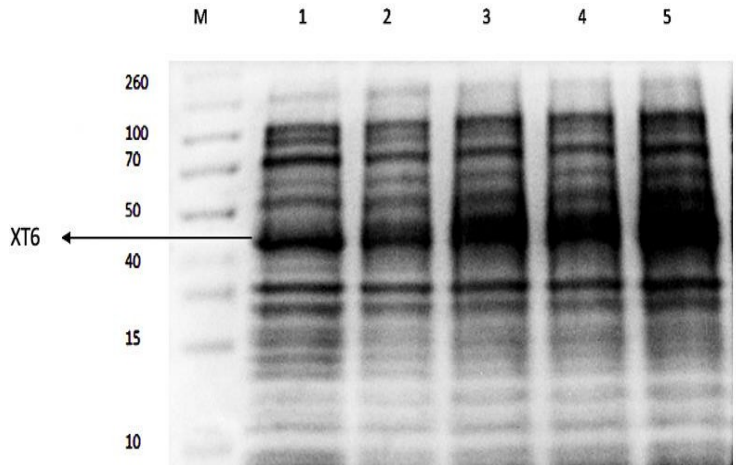

Figure 4.1: 12% SDS-PAGE gel showing expression of the recombinant XT6 xylanase in *E. coli* BL21 (DE3) cells. Lane M: Molecular weight marker (Thermo Scientific, USA), Lane 1: uninduced sample, and Lanes 2-5: Induction samples at 1-4 h, respectively. (Original image shown in appendix III, supplementary Figure 1).

A series of experiments were performed to determine the most efficient method for lysing the recombinant *E. coli* cells. The SDS-PAGE gel in figure 4.2 showed that sonication with a 0.05 M sodium phosphate (pH 6.0) buffer resulted in the highest protein concentrations compared to the other lysis procedures.

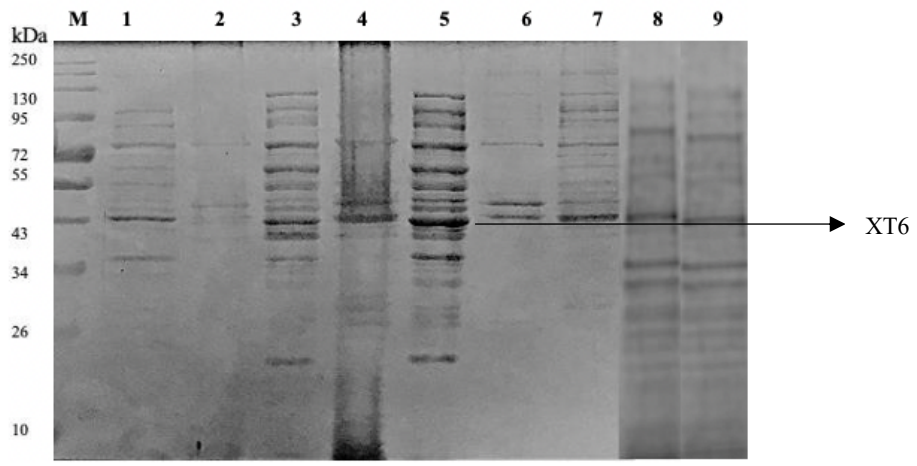

Figure 4.2: 12% SDS-PAGE gel showing the recombinant XT6 xylanase expressed in *E. coli* BL21 (DE3) cells after various lysis techniques. Lane M: Broad range molecular weight marker (Thermo Scientific, USA), Lane 1: uninduced sample, Lanes 2 and 3: insoluble and soluble fractions after lysis with lysozyme + 1% TritonX-100, Lanes 4 and 5: insoluble and soluble fractions following sonication in 0.05 M sodium phosphate (pH 6.0) buffer, Lane 6: insoluble fraction sonicated in 0.05 M Tris-HCl and 8M urea, Lane 7: soluble fraction sonicated in Tris-HCl buffer, and Lanes 8 and 9: insoluble and soluble fraction treated with lysozyme. (Original image shown in Appendix III, supplementary Figure 2).

Figure 4.3 shows the various direct and indirect analysis methods to monitor cell lysis. Sonication was effective with 0.05 M sodium phosphate buffer (pH 6.0) as high enzyme activity was obtained after cell lysis (16.48 U/ml) compared to the other techniques (9.40, 9.36, 9.03, and 9.53 U/ml) ($p < 0.05$). There was a significant difference ($p<0.05$) between the "Before" and "After" cell lysis fractions for each analysis and method of lysis.

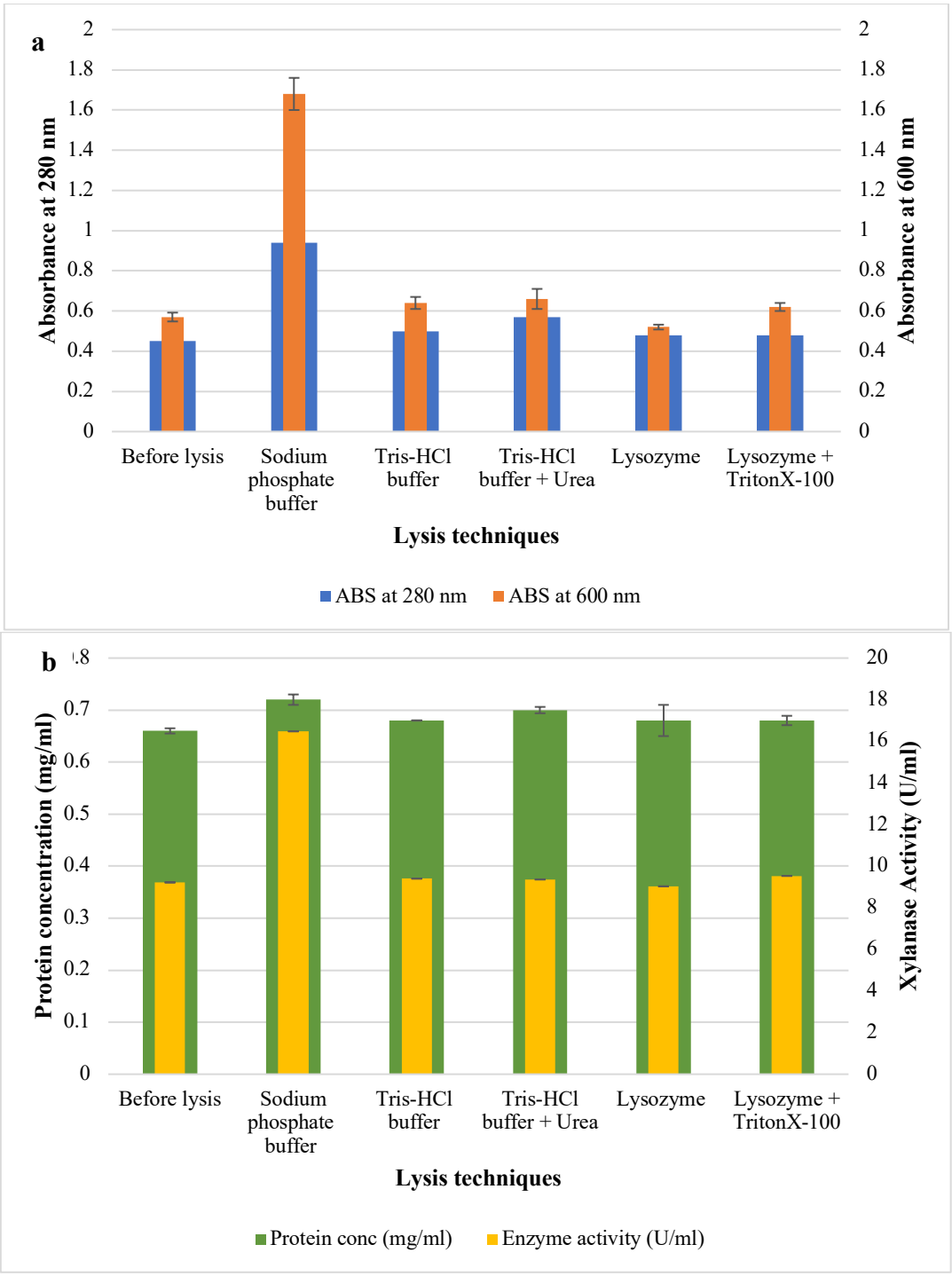

Figure 4.3: Analysis of the lysis methods to assess the efficiency of lysis of recombinant *E. coli* cells expressing the XT6 xylanase representing (a) OD280nm and OD600nm, and (b) protein concentration, and xylanase activity after different lysis techniques.

Sonication has been shown to be an effective method for lysing bacterial cell walls [21]. Sonication, using a probe to generate sound energy, usually within a range of 20-50 kHz, can

disrupt the structure of cells through the formation of violent implosions of small bubbles and cavitation within the sample. The energy of the sonic waves can disrupt the intramolecular forces that provide the integrity for the cellular wall [21]. Tris-HCl has an effective pH range of 7.0 to 9.0 and can be used to extract soluble cytoplasmic proteins. However, the preferred pH of the enzyme in this study is pH 6.0; thus, this may be a reason for the low enzyme activity. The components of cell disruption buffers are critical for efficient disruption and will affect subsequent purification steps, including targeting the stability and recovery of the protein. Criteria such as pH, ionic strength, additives to prevent degradation and improve stability, and the buffer-to-cell weight ratio, are required to achieve efficient cell disruption. The pH selected for the lysis buffer should be one pH unit below or above the protein isoelectric point, as this will maintain a positive or negative charge on the protein and prevent isoelectric precipitation [36]. The ionic strength inside the cytoplasm of a typical cell is 0.15-0.2 M, with high concentrations of charged biomolecules available for ionic protein interaction. The lysis buffer should contain at least 0.05-0.1 M NaCl; if the ionic strength of the lysis buffer is increased, it will reduce the ionic interactions [36]. The isoelectric point of XT6 is 9, and therefore at lower pH values, the enzyme will have a positive net charge [22,37]. However, the cell lysis was most effective with 0.05 M sodium phosphate buffer at pH 6.0 compared to Tris-HCl (+/- 8 M urea) at pH 8.0.

The synergistic effect of lysozyme and TritonX-100 has previously been shown to increase the amount of cellular lysis substantially; however, in this study, it was not observed [23]. Lysozyme breaks down the polysaccharide chains of peptidoglycan, which surround the inner membrane of the *E. coli* cells [18]. Gram-positive bacteria can be directly exposed to lysozyme; however, the outer membrane of the Gram-negative bacteria needs to be removed before exposing the peptidoglycan layer to the enzyme. TritonX-100 is a non-ionic detergent that can solubilize the outer and inner membranes of *E. coli* cells [38]. The cost of purchasing

lysozymes may be a deterrent to enzymatic lysis, as this additional cost may make the operating costs unfeasible. Thus, sonication of cells resuspended in 0.05 M sodium phosphate buffer (pH 6.0) is recommended for cells lysis in future studies.

4.4.2 Statistical optimization of the recombinant XT6 xylanase production in batch fermentation

4.4.2.1 Screening of significant medium constituents for the recombinant XT6 xylanase production

Each row in Table 4.3 represents one of twelve experiments, and each column has a different variable tested at high (+) and low (-) levels. The data obtained from the PBD runs indicate a wide variation in xylanase activity from 13.97 U/ml to 40.06 U/ml across the twelve runs. ANOVA demonstrated that this variation due to the effect of the medium and culture conditions on xylanase production was significant ($p<0.05$).

Table 4.3: PBD matrix for screening of six medium components

Variable level							Enzyme activity (U/ml)	
Run no.	**X1**	**X2**	**X3**	**X4**	**X5**	**X6**	**Observed**	**Predicted**
1	25 (-)	0.4 (-)	3 (-)	1.5 (+)	1 (-)	2.5 (+)	25.88	14.61
2	37 (+)	0.6 (+)	3 (-)	0.5 (-)	1 (-)	2.5 (+)	18.81	11.58
3	37 (+)	0.4 (-)	3 (-)	0.5 (-)	2 (+)	0.5 (-)	28.30	15.41
4	25 (-)	0.6 (+)	3 (-)	1.5 (+)	2 (+)	0.5 (-)	17.82	10.32
5	25 (-)	0.6 (+)	5 (+)	1.5 (+)	1 (-)	0.5 (-)	23.65	12.73
6	37 (+)	0.6 (+)	5 (+)	0.5 (-)	1 (-)	0.5 (-)	20.73	13.56
7	37 (+)	0.4 (-)	5 (+)	1.5 (+)	2 (+)	0.5 (-)	31.36	18.19
8	25 (-)	0.4 (-)	5 (+)	0.5 (-)	2 (+)	2.5 (+)	13.97	8.06
9	25 (-)	0.4 (-)	3 (-)	0.5 (-)	1 (-)	0.5 (-)	40.06	32.70
10	37 (+)	0.6 (+)	3 (-)	1.5 (+)	2 (+)	2.5 (+)	21.35	12.22
11	25 (-)	0.6 (+)	5 (+)	0.5 (-)	2 (+)	2.5 (+)	16.83	8.89
12	37 (+)	0.4 (-)	5 (+)	1.5 (+)	1 (-)	2.5 (+)	27.07	16.47

X1: Induction temperature

X2: Cell density pre-induction (OD600nm)

X3: Post-induction time

X4: Yeast extract

X5: Tryptone

X6: IPTG

A previous study suggested for a good fit of a model [40], R^2 should be at least 90% [39]. The closer *R* (correlation coefficient) value is to 1, the better the correlation between the experimental and predicted values. Here, the *R* value (0.94) shown in Table 4.4 indicated a close agreement between the experimental results and the theoretical values predicted by the model equation.

Table 4.4: Analysis of variance (ANOVA) for six variables by PBD

	df	Sum of Squares	Mean Square	F-value	*p*-value
Model	6				
Induction temperature	1	70.71	70.71	3.44	0.1126
Cell density pre-induction (OD_{600nm})	1	149.46	149.46	7.82	0.0429*
Post induction time	1	300.63	300.63	14.65	0.0123*
[Yeast extract]	1	19.89	19.89	0.96	0.3701
[Tryptone]	1	26.08	26.08	1.27	0.3108
[IPTG]	1	136.74	136.74	6.66	0.0494*
Residuals	5	102.62	102.62		

df: degree of freedom

*Significant p-value at $p < 0.05$

R2(mean coefficient of determination) = 0.9419

The p-value served as a tool for checking the significance of each of the coefficients, as is shown in Table 4.4, and indicates that cell density pre-induction (OD_{600nm}) (X2), post-induction time (X3), and IPTG concentration (X6) had a significant effect ($p<0.05$) on xylanase production. The Pareto chart of standardization illustrated in Figure 4.4 confirmed that these three factors significantly influenced xylanase production ($p < 0.05$) as the factors crossed the p-line. However, the other independent factors ($p > 0.05$) were considered insignificant. It has been demonstrated in a previous study that the four most relevant variables influencing recombinant protein expression were cell density pre-induction (OD_{600nm}), IPTG concentration, post-induction temperature, and duration of induction [20].

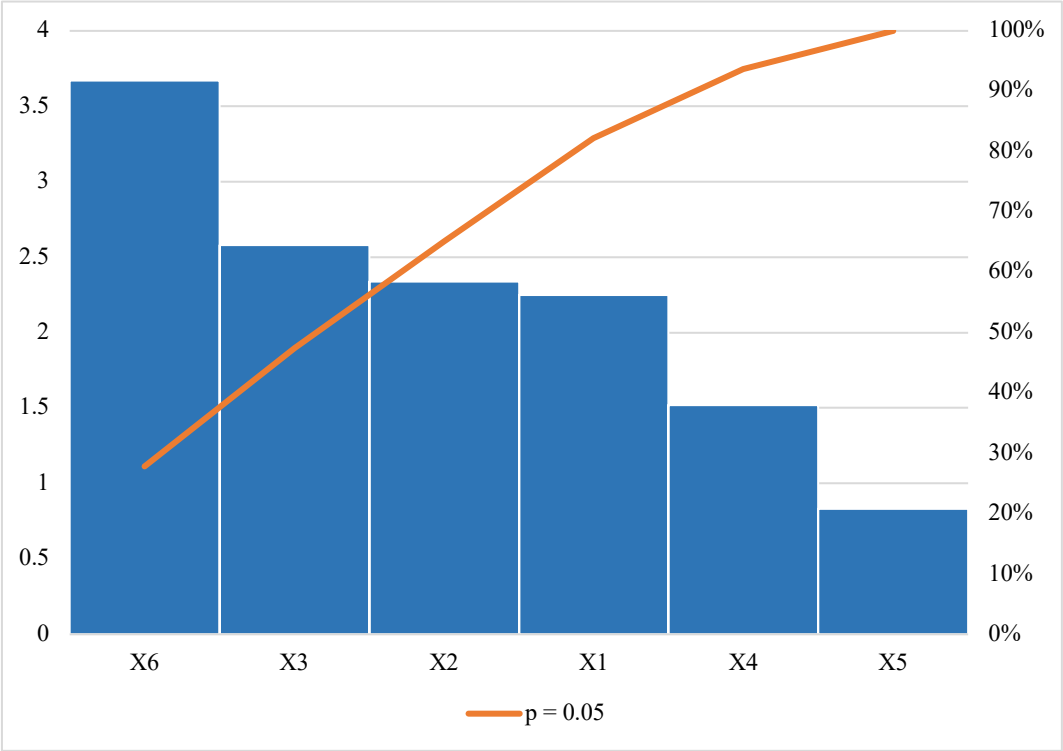

Figure 4.4: Pareto chart of standardized effects for the production of the recombinant XT6 xylanase by *E. coli* BL21. Induction temperature (X1), Cell density pre-induction (OD600nm) (X2), post-induction time (X3), yeast extract concentration (X4), tryptone concentration (X5), IPTG concentration (X6).

There was a 94% chance that the model explained the measured variations in response. The magnitude and direction of the factor coefficient in the equation clarified the influence of the six variables for xylanase production. The higher magnitude indicated a large effect on the response. The corresponding response of xylanase production was expressed in terms of the following regression equation III derived from the Unstandardized Beta values shown in Table 4.5:

$$Y = X_1 + X_2 + X_3 + X_4 + X_5 + X_6$$

$$Y = 48.49 - 0.28X_1 - 33.37X_2 - 3.74X_3 - 4.93X_4 - 2.35X_5 - 0.98X_6 \quad [III]$$

Table 4.5: Effect estimates for recombinant XT6 xylanase production from the results of PBD

	Unstandardized beta	Coefficient std. error	Standardized coefficient beta	t-value
Model	48.49	9.57		5.66
Induction temperature (X_1)	0.28	0.13	0.36	2.25
OD_{600nm} (X_2)	-33.37	14.25	-0.40	-2.34
Post-induction time (X_3)	-3.74	1.45	0.46	-2.58
[Yeast extract] (X_4)	-4.93	3.24	-0.28	-1.52
[Tryptone] (X_5)	-2.35	2.84	-0.14	-0.83
[IPTG] (X_6)	-0.98	0.27	-0.60	-3.67

4.4.2.2 Optimization of significant variables using RSM for recombinant XT6 xylanase production

4.4.2.2.1 BBD

A total of 16 runs were performed to determine the conditions for optimal xylanase production. A matrix was run with the three significant variables as per PBD. The results for the BBD matrix runs in Table 4.6 showed that run 13 resulted in the highest xylanase activity of 144.02 U/ml under the following conditions: Cell density pre-induction (OD_{600nm}) 0.5, post-induction time of 4 h, and 1.5 mM IPTG, while the lowest activity of 10.18 U/ml was obtained under conditions (cell density pre-induction (OD_{600nm}) of 0.5, post-induction time of 3 h and 0.5 mM IPTG) in run 9. This was markedly higher ($p > 0.05$) compared to the highest enzyme activities obtained during OFAT (16.48 U/ml). Farliahati et al. [41] confirmed a similar influence of

optimized parameters on the enhanced xylanase production by recombinant *E. coli* DH5α (1.526-2.655 U/ml).

Table 4.6: Experimental design obtained for the BBD model for three independent variables tested and predicted responses for recombinant XT6 xylanase production by *E. coli* BL21

	Experimental value (Coded value)			Enzyme activity (U/ml)	
Run no.	**X2**	**X3**	**X6**	**Observed**	**Predicted**
1	0.4 (-)	3 (-)	1.5 (0)	44.72	47.24
2	0.6 (+)	3 (-)	1.5 (0)	10.96	10.45
3	0.4 (-)	5 (+)	1.5 (0)	11.65	10.09
4	0.6 (+)	5 (+)	1.5 (0)	31.42	28.51
5	0.4 (-)	4 (0)	0.5 (-)	13.42	12.55
6	0.6 (+)	4 (0)	0.5 (-)	51.37	50.02
7	0.4 (-)	4 (0)	2.5 (+)	71.59	64.28
8	0.6 (+)	4 (0)	2.5 (+)	26.23	27.68
9	0.5 (0)	3 (-)	0.5 (-)	10.18	9.85
10	0.5 (0)	5 (+)	0.5 (-)	16.24	14.45
11	0.5 (0)	3 (-)	2.5 (+)	101.37	118.01
12	0.5 (0)	5 (+)	2.5 (+)	86.27	86.11
13	0.5 (0)	4 (0)	1.5 (0)	144.02	151.50
14	0.5 (0)	4 (0)	1.5 (0)	127.84	127.47
15	0.5 (0)	4 (0)	1.5 (0)	131.77	126.93
16	0.5 (0)	4 (0)	1.5 (0)	120.72	124.70

X2: Cell density pre-induction (OD_{600nm})

X3: post-induction time

X6: IPTG concentration

For the regression analysis of the experimental data, a quadratic equation was generated for the BBD for optimal xylanase production, as shown in equation IV:

$$Y = \beta 0 + X2 + X3 + X5 + X22 + X32 + X52 + X2X3 + X2X5 + X3X5 \qquad [IV]$$

The predicted values were determined using the regression equation (Table 4.6). The R^2 or coefficient of determination (0.9357, close to 1) confirmed the model's validity. The coefficient of adjusted determination, adjusted R^2, was 0.9383, confirming that the actual values were close to the predicted values [42, 43]. The correlation was established by plotting the actual value curve as a function of the predicted values (Figure 4.5), which shows the points distributed around the regression line.

Figure 4.5 shows that the actual response values agreed well with the predicted response values. Thus, the predicted xylanase production was within the limits of the experimental factors. Therefore, the model was considered of sufficient quality [42] with a 93.57% chance that it explained the measured variations in response. Maximum xylanase production (144.02 U/ml) by the recombinant XT6 xylanase occurred in BBD run 13 under optimal conditions (Cell density pre-induction (OD600nm) 0.5, 4 h post-induction time, and 1.5 mM IPTG concentration).

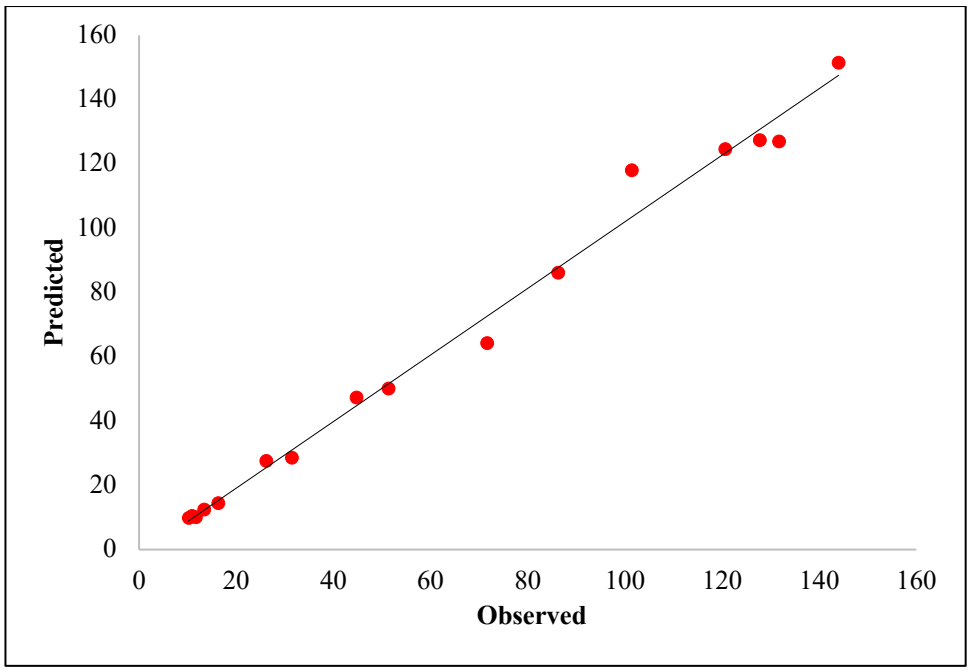

Figure 4.5: Graphical representation of the minimal difference between the actual (straight line) and predicted responses (circles) for the RSM design for optimal recombinant xylanase activity.

4.4.2.2.2 Second-order regression and prediction

The second-order regression equation provides the xylanase activity produced by XT6 from *G. stearothermophilus* as a function of cell density pre-induction (OD_{600nm}) (X2), post-induction time (X3), and IPTG concentration (X6) which is presented in equation VI:

$$Y= 50.26 – 26.75X2 -2.71X3 +X6 + X2^2 +X3^2 + X6^2 +X2X3 +X2X6 +X3X6 \quad [VI]$$

Where Y is the peak area, X2 is the OD_{600nm}, X3 is the post-induction time, and X6 is the IPTG concentration. The statistically insignificant parameters ($p>0.05$) and the interactions were omitted from the equation. The model constants and coefficients were generated using the unstandardized beta values.

4.4.2.2.3 ANOVA and Pareto chart

The "Lack of fit p-value" represented in Table 4.7, was insignificant as the p-value was greater than 0.05; in accordance with literature (>0.05)[44] and also that significant regression and a non-significant lack of fit of the model were well-fitted to the experiments [44]. The regression equation was validated on this basis [45] and ANOVA performed to determine the p-values. As evident in Table 4.7.

Table 4.7: ANOVA for the RSM parameters for the recombinant xylanase

Variable	Estimates	Std. Error	t value	p-value
Model	-2109.82	364.36	-5.79	0.0011614*
X2 (OD_{600nm})	5713.49	1077.59	5.30	0.0018261*
X3 (Post-induction time)	312.47	94.72	3.30	0.0164311*
X6 [IPTG]	241.99	70.27	3.44	0.0137398*
X2:X3	133.83	98.88	1.35	0.2247133
X3:X6	-208.28	98.88	-2.11	0.0797899
X2:X6	-5.29	9.89	-0.54	0.6119137
X2^2	-5963.13	988.86	-6.03	0.0009394*
X3^2	-46.77	9.89	-4.73	0.0032260*
X6^2	-30.80	9.89	-3.12	0.0207146*

*Significant p-value at $p < 0.05$

Adjusted R^2= 0.9357

Lack of fit p-value= 0.0694

This showed the model, the linear and square terms for X2 (Cell density pre-induction (OD_{600nm})), X3 (post-induction time), and X6 (IPTG concentration) to be significant as p-values were 0.0018261, 0.0164311, 0.0138398, 0.0009394, 0.0032260 and 0.0207146, respectively. The Pareto chart of standardization histogram graph (Figure 6) also showed that terms were significant ($p < 0.05$), as the factors crossed the p-line (cumulative % = 50%).

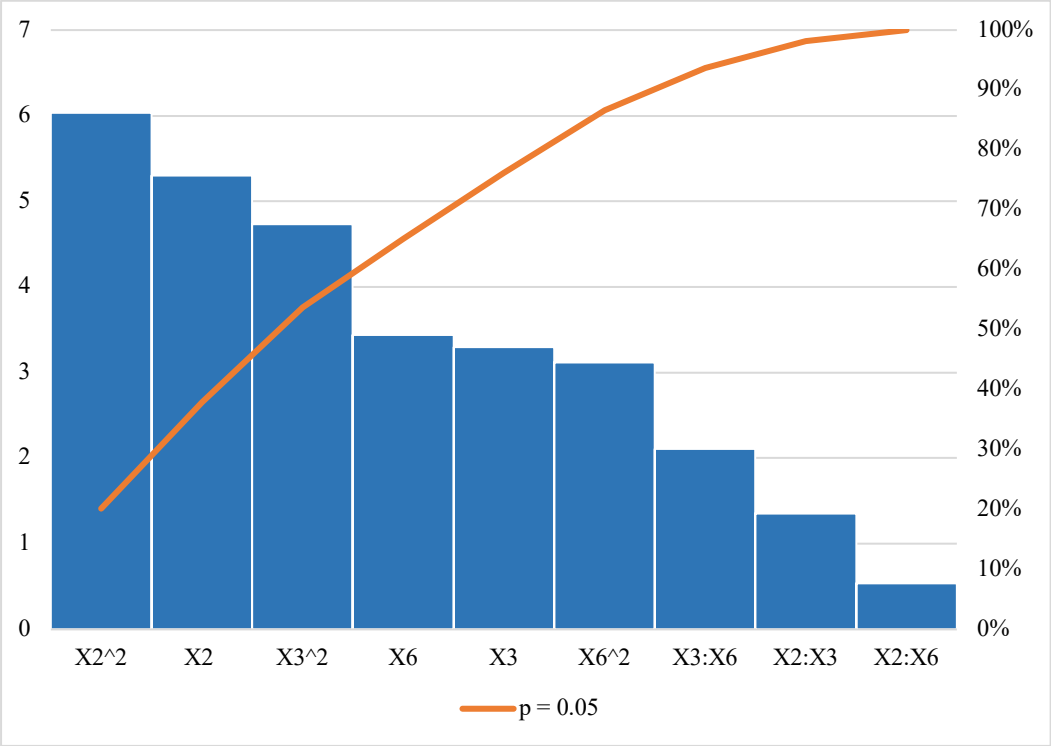

Figure 4.6: Pareto chart of standardized effects for the nine interactive factors affecting the optimization of xylanase production. Interactions, linear and square terms for cell density (X2), post-induction time (X3), and IPTG concentration (X6).

4.4.2.2.4 Interaction of variables

The interaction effects of the variables on xylanase production were also studied by plotting response surface plots and 3D-contour plots against any two independent variables while having another variable at its central level. These plots were drawn to illustrate the combined

effect of each independent variable on the response variable and is shown in Figure 4.7. The Z-axis refers to the xylanase activity versus any two variables.

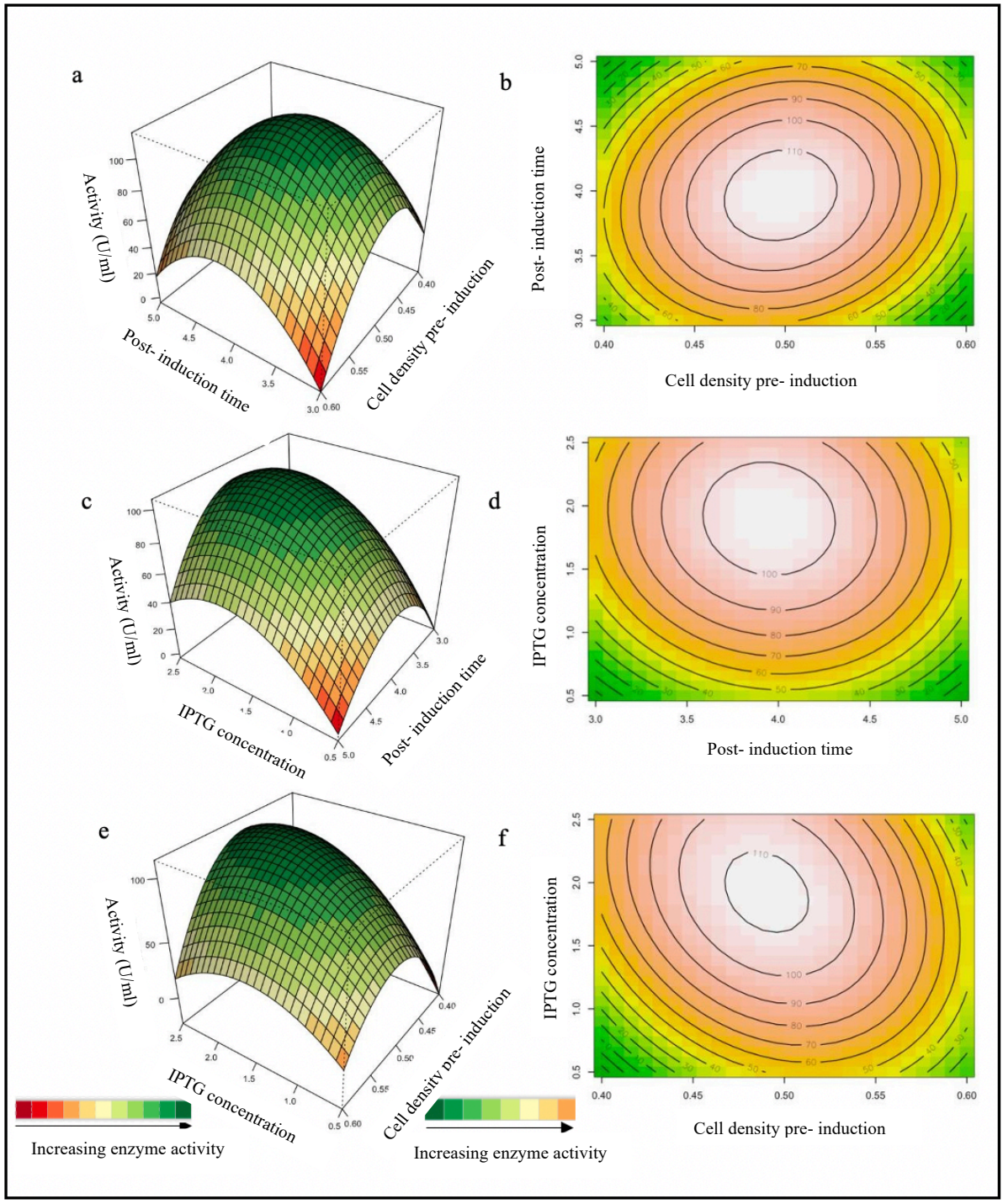

Figure 4.7: Response surface plots (a, c, e) and contour plots (b, d, f) of the combined effects of; a and b: Cell density pre-induction (OD600nm) (X2) and post-induction time (X3), c and d: Post-induction time (X3) and IPTG concentration (X6) and e and f: Cell density pre-induction (OD600nm) (X2) and IPTG concentration (X6) on recombinant XT6 xylanase production.

4.4.2.2.4.1 Effect of cell density pre-induction (OD_{600nm}) and post-induction time

The overexpression of the recombinant XT6 xylanase was influenced by the post-induction time and pre-induction cell density (OD_{600nm}) [20,46]. The interactive effect of cell density pre-induction ($OD_{600\ nm}$) (X2) and post-induction time (X3) was examined, and the results are illustrated in Figures 4.7a and b. For this analysis, the other parameter was kept constant at the optimal level. The mutual interaction of both factors (X2X3) was not significant ($p>0.05$), indicating that there is no synergistic interaction favoring the expression of recombinant XT6. The highly elliptical response surface plot Figure 4.7a shows the highest activity (110 U/ml) of the recombinant XT6 when both variables, cell density pre-induction (OD_{600nm}) (X2) and post-induction time (X3), were close to the optimal values, cell density pre-induction (OD_{600nm}) of 0.5 and 4 h, respectively. The findings accentuated that post-induction time was a key factor influencing the expression of XT6 xylanase. In the present study, the post-induction time of 4 h optimally induced production of active recombinant XT6 presumably because this duration was suitable for the correct folding and accumulation of the of recombinant XT6 in *E. coli*. This finding is in accordance with previous reports [20,47,48].

4.4.2.2.4.2 Effect of post-induction time and IPTG concentration

Considering that IPTG is costly and is potentially toxic to cells, it is essential to determine the optimum concentration for induction [49]. The interactive effect of post-induction time (X3) and IPTG concentration (X6) was examined, and the results are illustrated by both surface and contour plots as illustrated in Figures 4.7c and 7d. The mutual interaction of both factors (X2X3) was not significant ($p>0.05$), indicating that there is no synergistic interaction favoring the expression of recombinant XT6 xylanase. The expression of the recombinant XT6 increased with time up to 4 h and IPTG concentration up to its midpoint (1.5 mM), reaching the highest xylanase activity of 100 U/ml.

4.4.2.2.4.3 Effect of cell density pre-induction (OD_{600nm}) and IPTG concentration.

The dependency of the recombinant XT6 xylanase production on IPTG concentration (mM) and cell density pre-induction is presented in Figures 4.7e and f. The interaction between these two parameters was insignificant based on the high p-value (0.6119) represented in Table 6. At the zero levels (optimal levels) of cell density (OD_{600nm}) and IPTG concentration, the production of recombinant XT6 xylanase will improve as depicted by Figure 4.7e. Figure 4.7f illustrated that with a higher IPTG concentration; the xylanase activity was the highest (110 U/ml) demonstrating that the induction of recombinant XT6 in the middle log phase leads to higher protein expression levels. In this phase, most recombinant bacteria are growing rapidly, and cells are in an ideal environment for the expression of recombinant proteins. A previous study by Batumalaie et al. [20], also reported that induction at the mid-log phase led to overexpression of lipase KV1 in *E. coli.*

4.4.3 Scaled-up production of recombinant XT6 xylanase

Similar or higher enzyme activities are expected when scaling up the production of enzymes from shake flasks to bioreactors [50]. This was observed for the 5-l stirred tank bioreactor run using the same production parameters. The bioreactor maintains a more consistent and homogenous environment with more efficient aeration rates, pH, better mixing, and heat transfer [51]. Table 4.8 compares xylanase production in shake flask and a stirred tank bioreactor (at different aeration rates). In stirred tank bioreactors, agitation and aeration are essential operational parameters in scaling up aerobic biosynthesis systems and industrial bioprocess development [52]. In aerobic fermentation, the presence of oxygen influences enzyme secretion, which may be attributed to increased metabolic activities of the organism

[53] as has been reported that amylase production by *Bacillus* spp. is strongly affected by the presence of dissolved oxygen.

Table 4.8: Analysis of protein concentration, enzyme activity and specific activity of recombinant XT6 xylanase produced in batch shake flask and in bioreactor fermentations at different aerations rates

Samples	Protein concentration (mg/ml)	Enzyme activity (U/ml)	Specific activity (U/mg)
Expression in shake flasks	3.01	145.13	48.22
Expression in a 5-l bioreactor (0.5 vvm)	1.57	146.32	93.20
Expression in a 5-l bioreactor (1 vvm)	0.50	165.18	330.36
Expression in a 5-l bioreactor (2 vvm)	1.14	159.44	139.86

Consequently, providing air to the fermentation medium using a compressor under sterile conditions is more efficient by combining agitation with aeration [54]. Higher aeration rates implies improved oxygen supply in the fermenter thus enhanced growth of bacteria and enzyme production. Higher xylanase activities were obtained in the 5-l bioreactor at all the oxygen transfer rates tested [(146.32 U/ml (0.5 vvm), 165.18 U/ml (1 vvm) and 159.44 U/ml (2 vvm)], compared to shake flask studies (145.83 U/ml) under the same production parameters (30°C, cell density pre-induction (OD_{600nm}) 0.5, 4 h post-induction time, 1% yeast extract, 1.5% tryptone, and 1.5 mM IPTG). Overall, at 1 vvm aeration, the xylanase activity was observed to be the highest (165.18 U/ml). A similar study reported optimal xylanase activity from *Bacillus amyloliquifaciens* at 1 vvm (56.80 U/ml) in a stirred tank bioreactor [48]. Another study showed aeration rates to be a significant factor for high enzyme yields in a stirred tank bioreactor [55].

4.4.3.1 Effect of aeration rates on pH, dissolved oxygen, biomass, and xylanase activity

Figure 4.8 shows the fermentation kinetics at 200 rpm and the different aeration rates (0.5, 1, and 2 vvm). Increasing the aeration rate increased biomass, and xylanase production rates and decreased dissolved oxygen. There was more of a change in the fermentation media pH during the growth phase as aeration rates increased. After 6 h, the pH changed from an initial value of 7.00 to 6.42, 6.38 and 6.62 with aeration rates of 0.5, 1, and 2 vvm (Figure 4.8a-c), respectively. This can be attributed to higher growth and metabolism rates at the higher aeration rates [56, 57]. DO% at 2 h was 63.4, 71.3, and 78.65 % at 0.5, 1, and 2 vvm, respectively, and then decreased after 4 h (at 6 h on graph) of expression to 1.1, 0.6 and 2.3 % at 0.5, 1, and 2 vvm, respectively shown in Figures 4.8a-c. However, as mentioned earlier this had no effect on xylanase activity in the bioreactor. Given the low solubility of oxygen in aqueous solutions [58], DO in the broth can be limiting, so it is an important influencing factor in aerobic microbial fermentations and can be manipulated up to a point by agitation and aeration rates. The drop in DO levels is due to the active growth phase of the culture when it rapidly consumes oxygen, thus decreasing the oxygen levels in the reactor. While the shake flask culture system allowed oxygen transfer, it was expected to be lower than the 1 vvm achieved in the bioreactor.

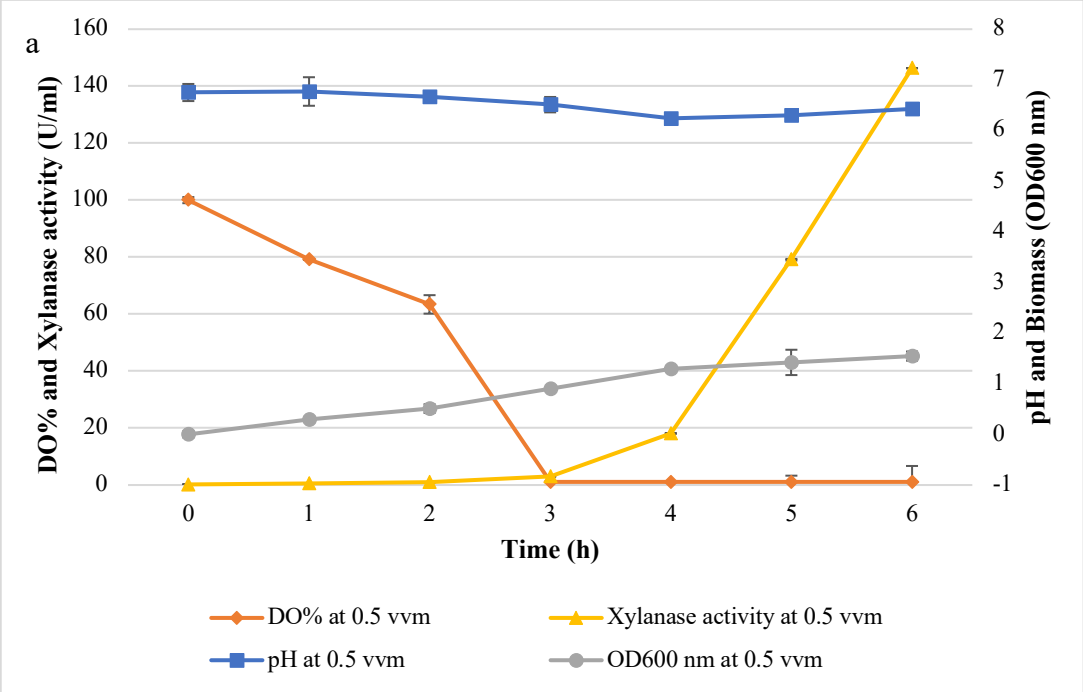
a
DO% and Xylanase activity (U/ml)
pH and Biomass (OD600 nm)
Time (h)
DO% at 0.5 vvm
Xylanase activity at 0.5 vvm
pH at 0.5 vvm
OD600 nm at 0.5 vvm

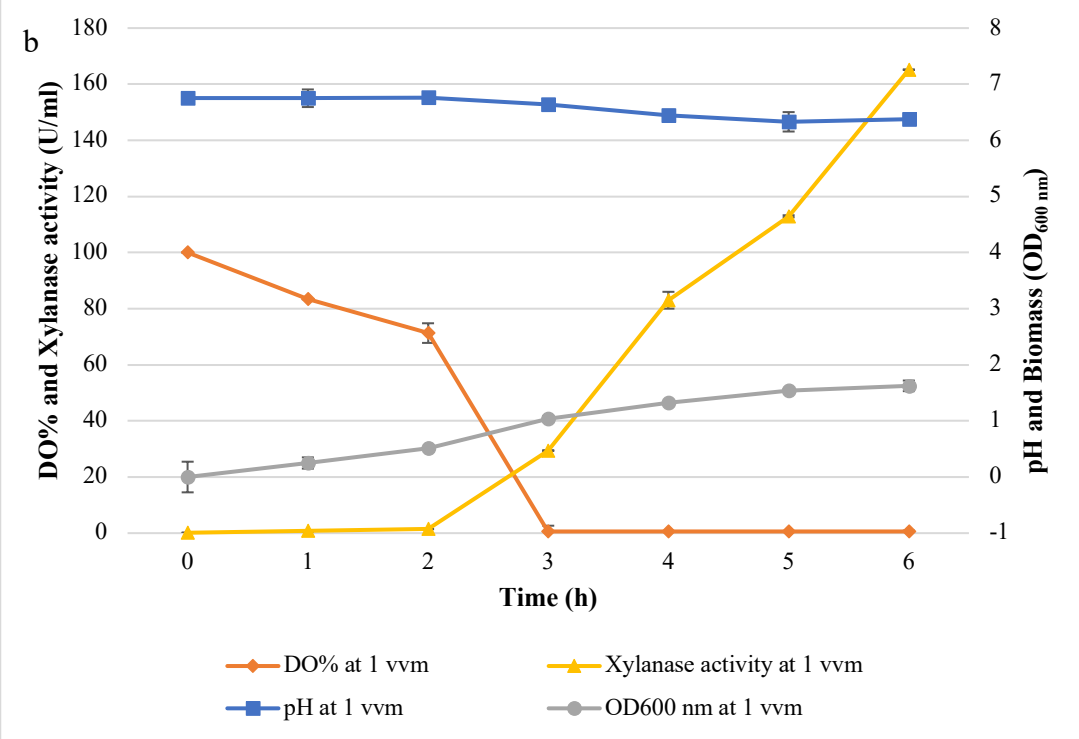
b
DO% and Xylanase activity (U/ml)
pH and Biomass (OD600 nm)
Time (h)
DO% at 1 vvm
Xylanase activity at 1 vvm
pH at 1 vvm
OD600 nm at 1 vvm

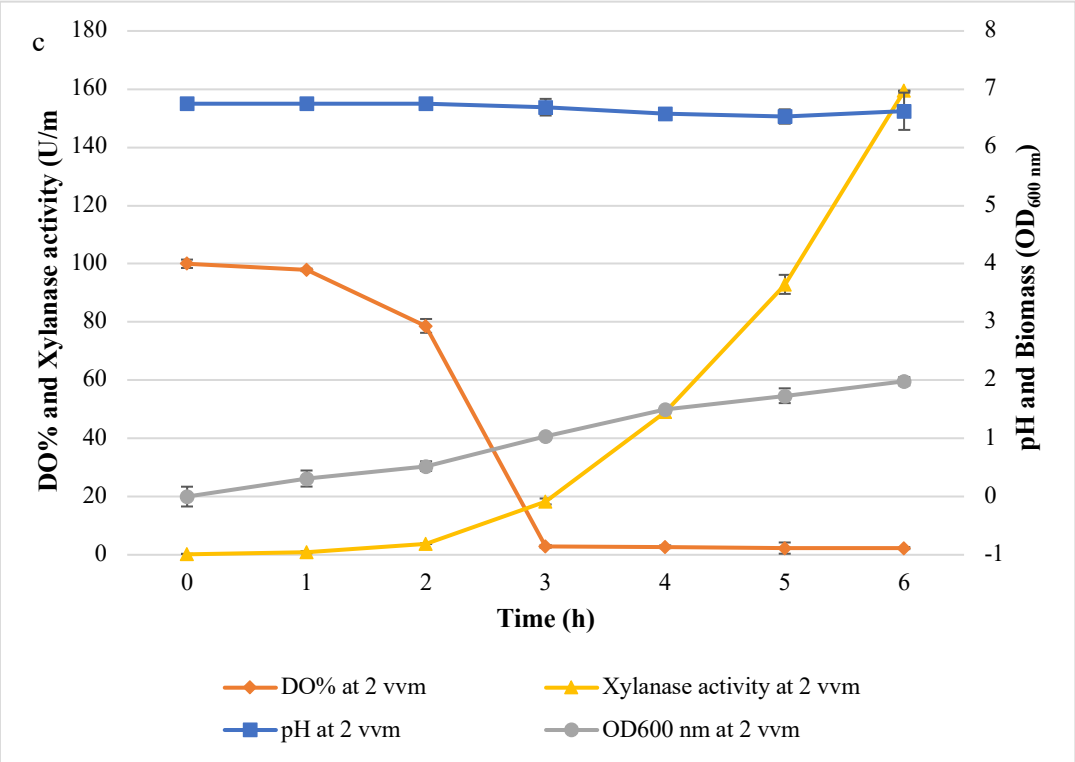

Figure 4.8: Analysis of pH, dissolved oxygen (DO%), biomass, and xylanase activity at 0.5 vvm (a), 1 vvm (b), and 2 vvm (c) aeration rates, during batch fermentation in a stirred tank bioreactor at 200 rpm. 0-2 h represents the time before induction.

4.4.3.2 Effect of aeration rate on specific growth rate, productivity and yield coefficient

Table 9 demonstrates that an increase in the aeration rate resulted in improvements in the specific growth rate, biomass productivity, and yield coefficient.

Table 4.9: Effect of aeration rates on specific growth rate, biomass yield, and productivity

Aeration rates (vvm)	Specific growth rate (h^{-1})	Productivity ($g/l.h^{-1}$)	Yield coefficient
0.5	0.25	66	2.71
1	0.27	78	2.82
2	0.36	34	1.28

Higher aeration increases the oxygen available to cells, which promotes respiration and the efficient use of the oxidative phosphorylation pathway for energy generation and growth which naturally manifests in a higher growth rate and more significant biomass formation. A change in the aeration rate from 0.5 to 2 vvm resulted in a 1.44-fold increase in the specific growth rate. A similar trend was also observed with the productivity and yield coefficient; however, at 2 vvm, the productivity and yield coefficient decreased. This indicates that the optimum aeration rate for xylanase production in the stirred tank bioreactor is 1 vvm. Similar findings were obtained by Ronda et al. [59]. The highest aeration rate at 2 vvm increased the shear stress on the bacterium, leading to lower biomass productivity and yield coefficient.

4.4.4 Purification of recombinant XT6 xylanase

The T-7-based pET vector for the *E. coli* expression system was selected for the production of the recombinant XT6 xylanase, as this expression system has been reported to be fast-growing and produces a high yield of the target protein [20]. This vector is recognized for its expression efficiency and, most importantly, for facilitating purification due to the presence of the His6-tag sequence. The recombinant XT6 xylanase was then purified to homogeneity by HisPur cobalt resin affinity chromatography. SDS-PAGE in figure 4.9 showed that the expressed protein band was 43 kDa in size.

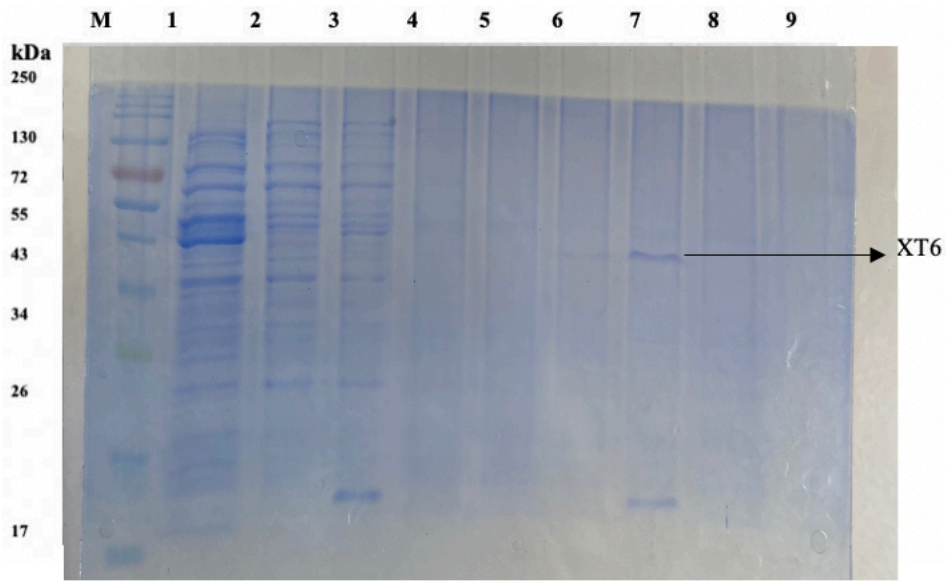

Figure 4.9: 12% SDS PAGE gel of purification fractions of the heterologously produced recombinant XT6 xylanase after affinity chromatography purification in a cobalt column. Lane M: Molecular weight marker (Thermo Scientific, USA), Lane 1: Crude (expressed XT6), Lane 2: Flow-through, Lanes 3-5: Wash 1-3, Lanes 6-8: Eluted fractions 1-3, and Lane 9: Wash 4. (Original image shown in Appendix III, supplementary as Figure 3).

These findings were consistent with a previous study [60] optimizing recombinant protein expression and purification. The His6-tag sequence aids in the selective binding of the expressed protein to the cobalt beads without impact on protein structure [61]. Therefore, the results from the present study are in accordance with the well-established concept that *E. coli* BL21 (DE3)/pET28a is an excellent expression host/system [15,25,62]. The specific activity of the purified recombinant XT6 xylanase was 4388.55 U/mg (Table 4.10), 28.97-fold higher than that of the crude lysate (151.50 U/mg) with a 67.04% recovery of the enzyme.

Table 4.10: Purification of the recombinant XT6 xylanase

Purification step	Total protein (mg)	Total activity (U)	Specific activity (U/mg)	Yield (%)	Fold purity
Recombinant crude lysate	9.50	1440.20	151.50	100.0	1.0
Cobalt column	1.35	1038.15	769.00	72.08	5.08
Ultrafiltration	0.22	965.48	4388.55	67.04	28.97

The higher purification fold (28.97) compared to the recombinant crude lysate shows that the recombinant tagged protein remained in its active conformation [24]. The commercial endo-1,4-β-xylanase (*Bacillus stearothermophilus* T6) has a specific activity of 12-65 U/mg on wheat arabinoxylan, according to Megazyme (CAS number: 9025-57-4). This study yielded a xylanase with a 67.5 to 365 -fold higher specific activity (4388.55 U/mg) albeit on beechwood xylan.

4.5 Conclusions

Multiple lysis techniques were tested in this study to release the intracellular protein, including sonication and synergistic lysis with lysozyme and TritonX-100. Based on our analysis, a mechanical technique; sonication of cells resuspended in 0.05 M sodium phosphate (pH 6.0) buffer was recommended for further studies as resulted in 3.21 fold increase compared to the other lysis techniques. In this study, optimization of the expression of the recombinant XT6 xylanase using PBD and RSM was successfully carried out as these statistical designs showed that under the optimized induction conditions of an induction temperature of 30°C, cell density pre-induction (OD_{600nm}) at 0.5, post-induction time of 4 h, yeast extract concentration of 1%

(w/v), tryptone concentration of 1.5% (w/v), and IPTG concentration of 1.5 mM, the enzyme activity increased from 16.48 U/ml to 144.02 U/ml. The large-scale production of xylanase was successful at 1 vvm aeration and improved the production of the recombinant XT6 xylanase. Compared to commercial XT6 xylanase from megazyme, the specific activity obtained from the scaling up production is 5.23 fold higher. Future applications involving this enzyme will include testing on animal feed substrates for the production of xylooligosaccharides, which are used as prebiotics in the feed industry, to reduce the viscosity and improve the gut microbiota.

4.6 References

[1] **Chen, *Z. et al.*** (2023). Exploitation of lignocellulosic-based biomass biorefinery: A critical review of renewable bioresource, sustainability and economic views. *Biotechnology Advances*. 69, 108265.

[2] **Marcolongo, L. *et al*.** (2015). Properties of an alkali-thermo stable xylanase from *Geobacillus thermodenitrificans* A333 and applicability in xylooligosaccharides generation. *World Journal of Microbiology and Biotechnology.* 31, 633–648.

[3] **Bhalla, A., Bischoff, K.M., & Sani, R.K.** (2015). Highly thermostable xylanase production from a thermophilic *Geobacillus* sp. strain WSUCF1 utilizing lignocellulosic biomass. *Frontiers in Bioengineering and Biotechnology*. 3, 84.

[4] Linares-Pasten, J.A., Aronsson, A., & Karlsson, E.N. (2018). Structural considerations on the use of endo-xylanases for the production of prebiotic xylooligosaccharides from biomass. *Current Protein and Peptide Science.* 19(1): 48–67.

[5] Cunha, L., Martarello, R., Souza, P., & Freitas, M. (2018). Optimization of xylanase production from *Aspergillus foetidus* in soybean residue. *Enzyme Research.* 12, 10–17.

[6] Gómez García, R. *et al.* (2018). Production of a xylanase by *Trichoderma harzianum* (*Hypocrea lixii*) in solid-state fermentation and its recovery by an aqueous two-phase system. *Canadian Journal of Biotechnology.* 2(9): 108-115.

[7] Bibra, M., Kunreddy, V.R., & Sani, R.K. (2018). Thermostable xylanase production by *Geobacillus* sp. strain DUSELR13, and its application in ethanol production with lignocellulosic biomass. *Microorganisms*. 6(3): 93.

[8] Wang, L. *et al.* (2019). Identification and characterization of a thermostable GH11 xylanase from *Paenibacillus campinasensis* NTU-11 and the distinct roles of its carbohydrate-binding domain and linker sequence. *Colloids and Surfaces B: Biointerfaces.* 209(1): 112167.

[9] Carlson, C., Singh, N.K., Bibra, M., Sani, R.K., & Venkateswaran, K. (2018). Pervasiveness of UVC 254-resistant *Geobacillus* strains in extreme environments. *Applied Microbiology and Biotechnology*. 102, 1869–1887.

[10] Gupta, G.K. *et al.* (2022). Xylanolytic enzymes in pulp and paper industry: new technologies and perspectives. *Molecular Biotechnology*. 64, 130–143.

[11] Raita, M., Ibenegbu, C., Champreda, V., & Leak, D.J. (2016). Production of ethanol by thermophilic oligosaccharide utilizing *Geobacillus thermoglucosidasius* TM242 using palm kernel cake as a renewable feedstock. *Biomass and Bioenergy*. 95, 45–54.

[12] Walia, A. *et al.* (2017). Microbial xylanases and their industrial application in pulp and paper biobleaching: a review. *3 Biotech.* 7, 11.

[13] Zafar, A. *et al.* (2016). Cloning, expression, and purification of xylanase gene from *Bacillus licheniformis* for use in saccharification of plant biomass. *Applied Biochemistry and Biotechnology*. 178, 294–311.

[14] Zare, H., Mir Mohammad Sadeghi, H., & Akbari, V. (2019). Optimization of fermentation conditions for reteplase expression by *Escherichia coli* using response surface methodology. *Avicenna Journal of Medical Biotechnology*. 11(2): 162–168.

[15] Choi, T.G., & Geletu, T.T. (2018). High-level expression and purification of recombinant flounder growth hormone in *E. coli*. *Journal of Genetic Engineering and Biotechnology.* 16, 347-355.

[16] Tripathi, N.K., & Shrivastava, A. (2019). Recent developments in bioprocessing of recombinant proteins: expression hosts and process development. *Frontiers in Bioengineering and Biotechnology.* 7, 420.

[17] Kleiner-Grote, G., Risse, J.M., & Friehs, K. (2018). Secretion of recombinant proteins from *E. coli. Engineering in Life Sciences*. 18(8): 532–550.

[18] Shehadul Islam, M., Aryasomayajula, M., & Selvaganapathy, P.R. (2018). A review on macroscale and microscale cell lysis methods. *Micromachines*. 8(3): 83.

[19] Dehnavi, E., Ranaei Siadat, S.O., Fathi Roudsari, M., & Khajeh, K. (2016). Cloning and high-level expression of beta-xylosidase from *Selenomonas ruminantium* in *Pichia pastoris* by optimizing pH, methanol concentration and temperature conditions. *Protein Expression and Purification.* 124, 55–61.

[20] Batumalaie, K., Khalili, E., Mahat, N.A., Huyop, F.Z., & Wahab, R.A. (2018). A statistical approach for optimizing the protocol for overexpressing lipase KV1 in *Escherichia coli*: purification and characterization. *Biotechnology and Biotechnological Equipment*. 32(1): 69-87.

[21] Kwon, YC., & Jewett, M. (2015). High-throughput preparation methods of crude extract for robust cell-free protein synthesis. *Scientific Reports.* 5, 8663.

[22] Sithole, T. Cloning, expression, partial characterization and application of a recombinant GH10 xylanase, XT6, from *Geobacillus stearothermophilus* T6 as an additive to chicken feeds. (ORCID ID: 0000-00030-2058-5571) Master's thesis, Rhodes University, Grahamstown (EC), 2022.

[23] Grigorov, E., Kirov, B., Marinov, M.B., & Galabov, V. (2021). Review of microfluidic methods for cellular lysis. *Micromachines*. 12(5): 498.

[24] Newton, J. M., Schofield, D., Vlahopoulou, J., & Zhou, Y. (2016). Detecting cell lysis using viscosity monitoring in *E. coli* fermentation to prevent product loss. *Biotechnology Progress.* 32(4): 1069–1076.

[25] Lu, Y. *et al.* (2016). High-level expression of improved thermostable alkaline xylanase variant in *Pichia pastoris* through codon optimization, multiple gene insertion and high-density fermentation. *Scientific Reports*. 6, 37869.

[26] Bradford M.M. (1976). A rapid and sensitive method for the quantitation of microgram quantities of protein utilizing the principle of protein-dye binding. *Analytical Biochemistry*. 72(12): 248–254.

[27] Miller, G.L. (1959). Use of dinitrosalicylic acid reagent for determination of reducing sugar. *Analytical Chemistry*. 31, 426–428.

[28] Laemmli, U.K. (1970). Cleavage of structural proteins during the assembly of the head of bacteriophage *T4. Nature.* 227, 680–685.

[29] Zhang, Z., Xiaoqiong, P., & Wu, Z. (2010). De novo synthesis and expression of a thermostable xylanase from *Geobacillus stearothermophilus* in *Escherichia coli*. *Chinese Journal of Applied and Environmental Biology*. 2, 271-275.

[30] Mühlmann, M. *et al.* (2017). Optimizing recombinant protein expression via automated induction profiling in microtiter plates at different temperatures. *Microbial Cell Factories.* 16, 220.

[31] Kaur, J., Kumar, A., & Kaur, J. (2018). Strategies for optimization of heterologous protein expression in *E. coli:* roadblocks and reinforcements. *International Journal of Biological Macromolecules*. 106, 803-822.

[32] Ghosh, P., & Ghosh, U. (2019). Statistical optimization of laccase production by isolated strain *Aspergillus flavus* PUF5 utilizing ribbed gourd peels as the substrate and enzyme application on apple juice clarification. *Indian Journal of Chemical Engineering.* 61, 1-12.

[33] R Core Team (2020). R: A language and environment for statistical computing. R Foundation for Statistical Computing, Vienna, Austria. Available online: URL http://www.R-project.org/.

[34] Zwietering, M.H., Jongenburger, I., Romburts, F.M., & Van't Riet, K. (1990). Modeling the bacterial growth curve. *Applied and Environmental Microbiology.* 56, 1875-1881.

[35] Kahm, M., Hasenbrink, G., Lichtenberg-Fraté, H., Ludwig, J., & Kschischo, M. (2010). Fitting biological growth curves with R. *Journal of Statistical Software*. 33, 1–21.

[36] Tokmakov, A.A., Kurtani, A., & Sato, K.I. (2021). Protein pI and intracellular localization. *Frontiers in Molecular Bioscience.* 29(8): 775736.

[37] Fishman, A., Berk, Z., & Shoham, Y. (1995). Large-scale purification of xylanase T-6. *Applied Microbiology and Biotechnology.* 44, 88-93.

[38] Orwick-Rydmark, M., Arnold, T., & Linke, D. (2016). The use of detergents to purify membrane proteins. *Current Protocols in Protein Science*. 8, 4481-4835.

[39] Said, K., & Afizal, M. (2016). Overview on the response surface methodology in extraction processes. *Journal of Applied Science and Process Engineering*. 2, 1.

[40] Xie, Y. *et al.* (2019). Collaborative optimization of ground source heat pump-radiant ceiling air conditioning system based on response surface method and NSGA-II. *Renewable Energy.* 147(1): 249-264.

[41] Farliahati, M.R. *et al.* (2010). Enhanced production of xylanase by recombinant *Escherichia coli* DH5α through optimization of medium composition using Response Surface Methodology. *Annals of Microbiology*. 60, 279–285.

[42] Azzouz, Z., Bettache, A., Boucherba, N., Amghar, Z., & Benallaoua, S. (2020). Optimization of xylanase production by newly isolated strain *Trichoderma afroharzianum* isolate AZ12 in solid-state fermentation using Response Surface Methodology. *Cellulose Chemistry and Technology*. 54(5-6): 451-462.

[43] Chicco, D., Warrens, M. J. & Jurman, G. (2021). The coefficient of determination R squared is more informative than SMAPE, MAE, MAPE, MSE, and RMSE in regression analysis evaluation. *PeerJ Computer Science.* 7, 623.

[44] Bezerra, M.A., Santelli, R.E., Oliveira, E.P., Villar, L.S., & Escaleira, L.A. (2018). Response surface Methodology (RSM) as a tool for optimization in analytical chemistry. *Talanta.* 76(5): 965-977.

[45] He, X. *et al.* (2018). Efficient degradation of Azo dyes by a newly isolated fungus *Trichoderma tomentosum* under non-sterile conditions. *Ecotoxicology and Environmental Safety*. 150, 232-239.

[46] Akbari, V. *et al.* (2015). Optimization of a single-chain antibody fragment overexpression in *Escherichia coli* using response surface methodology. *Research in Pharmaceutical Science*. 10(1): 75–83.

[47] Kanno, A.I. *et al.* (2019). Optimization and scale-up production of Zika virus ΔNS1 in *Escherichia coli:* application of Response Surface Methodology. *AMB Express.* 10(1): 1.

[48] Kumar, S., Gulati, P., & Singha, T. (2020). Kinetic study and optimization of recombinant human tumor necrosis factor-alpha (rhTNF-α) production in *Escherichia coli*. *Preparative Biochemistry and Biotechnology*. 51(3): 267-276.

[49] Gomes, L., Monteiro, G., & Mergulhão, F. (2020). The impact of IPTG induction on plasmid stability and heterologous protein expression by *Escherichia coli* biofilms. *International Journal of Molecular Science*. 21(2): 576.

[50] Kereh, H., & Mubarik, N. (2018). Optimization of process parameters and scale-up of xylanase production using corn cob raw biomass by marine bacteria *Bacillus subtilis* LBF M8 in stirred tank bioreactor. *Pakistani Journal of Biotechnology*. 15, 707-714.

[51] Kumar, S., Sharma, N., & Pathania, S. (2015). Optimization of process parameters and scale-up of xylanase production from *Bacillus amyloliquifaciens* Sh8 in a stirred tank bioreactor. *Cellulose Chemistry and Technology*. 51(5-6): 403-415.

[52] Bandaiphet, C., & Prasertsan, P. (2015). Effect of aeration and agitation rates and scale-up on oxygen transfer coefficient, KLa in exopolysaccharide production from *Enterobacter cloacae* WD7. *Carbohydrate Polymers*. 66(2): 216-228.

[53] Zotta, T., Parente, E., & Ricciardi, A. (2017). Aerobic metabolism in the genus *Lactobacillus*: impact on stress response and potential applications in the food industry. *Journal of Applied Microbiology*. 122(4): (2017).

[54] Elmansy, E.A., Asker, M., El-Kady, E.M., Hassanein, S.M., & El-Beih, F.M. (2018). Production and optimization of α-amylase from thermo-halophilic bacteria isolated from different local marine environments. *Bulletin of the National Research Centre*. 42(1): 31.

[55] **Núñez, E.G. *et al.*** (2014). Influence of aeration-homogenization system in stirred tank bioreactors, dissolved oxygen concentration and pH control mode on BHK-21 cell growth and metabolism. *Cytotechnology.* 66(4): 605–617.

[56] **Abdella, A., Mazeed, T.E.S., Yang, S.T., & El-Baz, A.F.** (2014). Production of β-glucosidase by *Aspergillus niger* on wheat bran and glycerol in submerged culture: factorial experimental design and process optimization. *Current Biotechnology*. 3(2): 197-206.

[57] **Kumar, V., & Shukla, P.** (2018). Extracellular xylanase production from *T. lanuginosus* VAPS24 at pilot scale and thermostability enhancement by immobilization. *Process Biochemistry*. 71, 53-60.

[58] **Garcia-Ochoa, F., & Gomez, E.** (2009). Bioreactor scale-up and oxygen transfer rate in microbial processes: an overview. *Biotechnology Advances.* 27(2): 153-76.

[59] **Ronda, S.R., Bokka, C.S., Ketineni, C., Rijal, B., & Allu, P.R.** (2012). Aeration effect on Spirulina platensis growth and γ-Linolenic acid production. *Brazilian Journal of Microbiology.* 43(1): 12-20.

[60] **Rosano, G.L, & Ceccarelli, E.A.** (2017). Recombinant protein expression in *Escherichia coli:* advances and challenges. *Frontiers in Microbiology.* 5, 172.

[61] **Kielkopf, C.L., Bauer, W., & Urbatsch, I.L.** (2020). Expressing cloned genes for protein production, purification, and analysis. *Cold Spring Harbor Protocols.* 2, 43-69.

[62] **Shilling, P.J. *et al*.** (2020). Improved designs for pET expression plasmids increase protein production yield in *Escherichia coli*. *Communications in Biology.* 3, 214.

CHAPTER FIVE

OPTIMIZATION OF THE PRODUCTION OF XYLOOLIGOSACCHARIDES BY NATIVE AND RECOMBINANT XYLANASES USING CHICKEN FEED SUBSTRATES, AND TOXICITY TESTING

5.1 Abstract

Poultry production faces several challenges, with feed efficiency being the main factor that could be influenced through the use of different nutritional strategies. Proper use of exogenous enzymes, such as xylanases, could improve feed conversion, gut health, growth performance, and improve environmental problems as fewer undigested nutrients are excreted.

Xylooligosaccharides are functional feed additives that are attracting growing commercial interest due to their excellent ability to modulate the composition of the gut microbiota. The aim of the study was to apply crude and purified fungal xylanases from *Trichoderma harzianum* as well as a recombinant glycoside hydrolase family 10 xylanase (XT6), derived from *Geobacillus stearothermophilus* T6, as additives to locally produced chicken feeds. A Box Behnken Design (BBD) experimental design was used to optimize the enzymatic hydrolysis of feeds to monosaccharides and XOS. Response Surface Methodology revealed that reducing sugars were higher (8.05 U/ml) for the starter feed treated with the crude *T. harzianum* xylanase compared to the treated grower feed (3.11 mg/ml). Treatment with the purified *T. harzianum* xylanase and recombinant XT6 xylanase produced higher reducing sugar for the starter feed (2.81 mg/ml and 2.98 U/ml) compared to the grower feed (2.41 mg/ml and 2.62 U/ml). The study included analysing the hydrolysis products and performing toxicity assays. Thin-layer chromatography and high-performance liquid chromatography analysis showed that the enzymes hydrolysed the chicken feeds, producing a range of monosaccharides

(arabinose, mannose, glucose, and galactose) and XOS, with xylobiose being the predominant XOS. Toxicity studies resulted in more viable HEK293 cells with higher dilutions of the enzyme-treated feed thus the enzymatic treatments were not toxic to HEK293 cells. Therefore, the xylanases from *T. harzianum* and the recombinant XT6 xylanase could potentially be utilized for the production of prebiotics and anti-inflammatory XOS from chicken feeds. These results show promising data for future studies as additives to poultry feeds.

Keywords: *xylooligosaccharides; chicken feed, lignocellulosic biomass; Response Surface Methodology; xylanase*

5.2 Introduction

Hemicellulose is the second most common renewable terrestrial polysaccharide in nature after cellulose. Non-starch polysaccharides (NSPs) like xylan cannot be hydrolyzed by endogenous enzymes in monogastric animals like poultry [1]. This leads to an environment favourable for these NSPs to encapsulate the other nutrients, thus acting as a barrier in the small intestine and resulting in the increased viscosity of the digesta [2]. Recent studies [3,4] have shown that a decreased growth performance due to increased digesta viscosity has been commonly seen in chickens that ingest diets containing high levels of NSPs.

In response to this, livestock producers have incorporated exogenous enzymes such as xylanases into poultry feeds in order to degrade the xylan into short-chain sugars, thereby reducing intestinal viscosity and enhancing the digestive utilization of nutrients [5]. Research suggests that the presence of certain enzymes, such as xylanase, or the combination of enzymes with dietary components, like xylanase with hybrid rye, can have an impact on the integrity of the chicken intestinal barrier, specifically affecting the tight junction proteins [6].

Xylan, derived from lignocellulosic biomass, can be hydrolyzed through the use of exogenous chemical and enzymatic processes to generate a mixture of xylooligosaccharides (XOS) and monosaccharides [7,8]. The resulting XOS mixture is recognized as a prebiotic [1]. The XOS are oligosaccharides made up of repeating xylose units linked by β-(1–4)-linkages - examples are xylobiose, xylotriose, xylotetraose, xylopentaose and xylohexaose [9]. XOS has a promising market potential as food additives, feed additives, health care products, and pharmaceuticals [10], because of its prebiotic [11], antioxidant [12], and anticancer activity [13]. Hemicelluloses are efficiently hydrolyzed into monosaccharides or XOS with minimal enzyme loading which is important for the lignocellulosic bioenergy and biorefinery industry [8].

Lignocellulosic biomass is the most cost-efficient and sustainable natural resource available globally. It is comprised of terrestrial vegetation like shrubs and grasses, as well as agricultural biomass by-products like corn stover, straw, saw-dust wastes, paper mill discards, and energy-yielding vegetation [14]. The hydrolysis products have been widely adopted as prebiotics and carbohydrases in feed additives in broiler chickens, to enhance intestinal health and stimulate performance [15]. However, hydrolysis conditions affect the production of the hydrolysis products. Therefore, it is vital to understand the effects of enzyme dosage, feed substrate loading, incubation time, temperature, and pH during hydrolysis [16,17]. An efficient way to understand the impact of various process variables and their interactions on the process's outcome and to identify the ideal conditions for maximizing the process output is to use RSM, a mathematical and statistical technique [18]. RSM using a BBD is an effective optimization tool. The RSM design can provide the dependence of enzyme activity on independent variables,

predict results for responses, and levels for independent variables in the form of mathematical models [19].

Following optimization to enhance yields, the analysis of the hydrolysates products are usually carried out by two techniques: thin-layer chromatography (TLC) and high-performance liquid chromatography (HPLC) [20,21,22]. HPLC employs detectors [such as refractive index (RI) and diode array detector (DAD)] for the determination of total component sugars produced after hydrolysis [23]. The 3-4,5-dimethylthiazol-2-yl)-5-(3-carboxymethoxyphenyl)-2-(4-sulfophenyl)-2H-tetrazolium) MTS assay has been widely used to assess cell viability and cytotoxicity [24]. The cellular reduction of tetrazolium salts to their formazan crystal forms is the foundation of the MTS assay [25]. It is important to identify the cell concentration range where the optical density and the total number of counted cells are directly correlated. The number of cells at the beginning and end of the incubation time should be within the calibration curve's linear range. HEK293 cells are a specific, immortalised cell line obtained from human embryonic kidneys which are cultured in vitro [26]. In addition to the kidney's role as the body's filter for toxic substances, HEK293 cells were selected for the study because of their reputation for consistent development and a proclivity for transformation [27].

The addition of xylanases to chicken cereal feed diets can enhance NSP hydrolysis and the production of prebiotic XOS. Considering the potential market demand for XOS in the agricultural and pharmaceutical industry, the aim of the present study was to optimize the hydrolysis of chicken feed using crude and purified fungal xylanases produced by *Trichoderma harzianum* and the recombinantly produced XT6 xylanase (from *Geobacillus stearothermophilus* cloned and expressed in *E. coli*) of starter and grower chicken feeds, to enhance the production of reducing sugars. By analysing the product profiles using chromatographic techniques, XOS and monosaccharides were monitored qualitatively and

quantitatively. The viability of the hydrolysates were examined using HEK293 cells in cytotoxic analysis.

5.3 Materials and methods

5.3.1 Feed samples and enzymes

Chicken starter and grower feed substrates were obtained from Rhodes University, Grahamstown, Eastern Cape. According to Biasato et al. [46] the feeds for monogastric animals such as chickens and pigs in South Africa primarily consist of corn as the main energy source and soybean as the main protein source. Studies by El-Deek et al. [47] and Saleh and Watkins [48] have reported that the formulations of starter and grower feeds for broilers often vary in terms of the ratio of corn to soybean. It is observed that starter feeds generally contain more soybean and less corn compared to grower feeds. The fungal xylanase from *T. harzianum* has been previously isolated and purified [19,49]. The recombinant XT6 xylanase was obtained from a student at Rhodes university and expression was optimized and the xylanase was purified. Quantification of reducing sugars in the samples was carried out according to a previously described method [19]. All the analyses were performed in triplicate.

5.3.2 Optimization of the hydrolysis of feed using the crude and purified fungal *T. harzianum* and recombinant XT6 xylanase

Crude and purified *T. harzianum* xylanases and purified recombinant XT6 xylanase were used in this study to hydrolyse xylan in starter and grower chicken feed substrates. RSM using the BBD was used to study the influence of six variables on the hydrolysis of chicken feeds by xylanases to statistically determine the optimum combination of dosage, feed, time, pH, and temperature for enhanced reducing sugars. The main interactions and the quadratic effects of

the variables on the enzymatic hydrolysis of the feed were also assessed, and a five-factor, three-level design was applied to investigate the quadratic response surfaces and construct secondary polynomial models. Each variable was coded and run at three independent levels, (−), (0), and (+) levels (Table 5.1). The significant relationships in the model were assessed and the 3,5-Dinitrosalicylic acid (DNS) assay was used to determine the reducing sugars (mg/ml) after incubation. All the statistical analyses were carried out using the R Studio software [50]. The effect of each factor and their interactions on the dependent variables was assessed by the Two-way Analysis of variance (ANOVA) technique [19]. The optimization data were analyzed for the determination of regression coefficients to arrive at the regression equation. The regression model containing coefficients including the linear and quadratic effect of factors and linear effect of interactions was assumed to describe relationships between response (Y) and the experimental factors (A1, A2, A3, A4, and A5).

The second-order polynomial equation is shown below in Equation I:

$$Y=\beta_0 + \sum\beta_i\, A1 + \sum\beta_{ii}\, A2 + \sum\beta_{ij}\, A1A2 \qquad [I]$$

where β0 is the constant coefficient, βi is the linear coefficient of main factors, βii is the quadratic coefficient for main factors, and βij is the second-order interaction coefficient. The response variable was assigned at low and high of the observed values for the desirability of 0 and 1, respectively, to get the overall desirability [51].

Table 5.1: The BBD model matrix for reducing sugars by enzymatic hydrolysis if chicken feed substrates

Run order	A1 (U/ml)	A2 (%)	A3 (h)	A4 (°C)	A5 (pH)	Starter chicken feed			Grower chicken feed		
						Crude *T. harzianum* xylanase	Purified *T. harzianum* xylanase	Recombinant XT6 xylanase	Crude *T. harzianum* xylanase	Purified *T. harzianum* xylanase	Recombinant XT6 xylanase
1	5 (-)	0.5 (-)	24 (0)	65 (0)	5 (0)	3.16	0.82	2.36	**3.21**	2.09	2.37
2	15 (+)	0.5 (-)	24 (0)	65 (0)	5 (0)	3.10	1.90	1.68	2.92	1.59	2.17
3	5 (-)	1.5 (+)	24 (0)	65 (0)	5 (0)	2.78	1.99	2.12	2.56	1.73	2.62
4	15 (+)	1.5 (+)	24 (0)	65 (0)	5 (0)	1.95	2.22	2.46	2.96	2.21	2.34
5	5 (-)	1 (0)	12 (-)	65 (0)	5 (0)	2.02	2.23	2.10	2.85	1.68	2.20
6	15 (+)	1 (0)	12 (-)	65 (0)	5 (0)	2.74	2.25	2.57	2.84	1.93	2.14
7	5 (-)	1 (0)	36 (+)	65 (0)	5 (0)	2.86	2.15	2.03	2.69	1.49	2.22
8	15 (+)	1 (0)	36(+)	65 (0)	5 (0)	3.23	2.21	1.97	2.50	1.97	2.12
9	10 (0)	0.5 (-)	12 (-)	55 (-)	5 (0)	2.60	1.87	2.18	2.46	2.00	2.16
10	10 (0)	1.5 (+)	12 (-)	55 (-)	5 (0)	2.82	2.13	2.05	2.51	2.10	2.45
11	10 (0)	0.5 (-)	36 (+)	75 (+)	5 (0)	2.21	2.11	2.27	2.40	2.17	2.53
12	10 (0)	1.5 (+)	36 (+)	75 (+)	5 (0)	2.93	**2.81**	**2.98**	2.83	2.31	**2.79**
13	10 (0)	1 (0)	24 (0)	55 (-)	4 (-)	2.74	2.05	2.17	2.79	1.85	2.62
14	10 (0)	1 (0)	24 (0)	75 (+)	4 (-)	2.68	2.00	1.97	2.59	1.73	1.99
15	10 (0)	1 (0)	24 (0)	55 (-)	6 (+)	2.38	1.68	1.67	2.57	1.55	1.81
16	10 (0)	1 (0)	24 (0)	75 (+)	6 (+)	2.56	1.80	1.81	2.60	1.65	1.92

	Variable Level					Reducing sugars (mg/ml)					
Run order	**A1 (U/ml)**	**A2 (%)**	**A3 (h)**	**A4 (°C)**	**A5 (pH)**	**Starter chicken feed**			**Grower chicken feed**		
						Crude *T. harzianum* xylanase	**Purified *T. harzianum* xylanase**	**Recombinant XT6 xylanase**	**Crude *T. harzianum* xylanase**	**Purified *T. harzianum* xylanase**	**Recombinant XT6 xylanase**
17	10 (0)	0.5 (-)	24 (0)	65 (0)	4 (-)	2.60	1.88	1.71	2.28	1.29	1.94
18	10 (0)	1.5 (+)	24 (0)	65 (0)	4 (-)	2.52	1.78	1.71	2.46	1.03	1.69
19	10 (0)	0.5 (-)	24 (0)	65 (0)	6 (+)	2.50	1.80	1.57	2.28	1.65	1.73
20	10 (0)	1.5 (+)	24 (0)	65 (0)	6 (+)	2.08	1.91	1.72	2.31	1.68	1.99
21	10 (0)	1 (0)	24 (0)	65 (0)	5 (0)	1.92	2.01	1.86	1.95	1.81	1.41
22	10 (0)	1 (0)	24 (0)	65 (0)	5 (0)	2.32	1.88	1.92	1.82	1.92	2.44
23	10 (0)	1 (0)	24 (0)	65 (0)	5 (0)	2.21	2.13	1.94	1.77	1.91	1.95
24	10 (0)	1 (0)	24 (0)	65 (0)	5 (0)	2.18	2.27	2.10	2.46	**2.41**	2.11
25	5 (-)	1 (0)	24 (0)	55 (-)	5 (0)	3.03	1.78	2.20	3.07	1.77	1.92
26	15 (+)	1 (0)	24 (0)	55 (-)	5 (0)	2.66	1.59	1.64	2.63	1.60	1.73
27	5 (-)	1 (0)	24 (0)	75 (+)	5 (0)	2.56	1.63	1.85	2.45	1.89	1.75
28	15 (+)	1 (0)	24 (0)	75 (+)	5 (0)	2.51	1.60	1.73	2.22	1.87	1.80
29	5 (-)	1 (0)	24 (0)	65 (0)	4 (-)	2.33	1.86	1.87	2.16	1.25	1.65
30	15 (+)	1 (0)	24 (0)	65 (0)	4 (-)	2.47	1.91	1.86	2.36	1.63	1.51
31	5 (-)	1 (0)	24 (0)	65 (0)	6 (+)	2.41	1.90	1.89	2.22	1.51	1.89
32	15 (+)	1 (0)	24 (0)	65 (0)	6 (+)	2.05	1.71	1.80	2.13	1.76	1.90

	Variable Level					Reducing sugars (mg/ml)					
Run order	A1 (U/ml)	A2 (%)	A3 (h)	A4 (°C)	A5 (pH)	Starter chicken feed			Grower chicken feed		
						Crude *T. harzianum* xylanase	Purified *T. harzianum* xylanase	Recombinant XT6 xylanase	Crude *T. harzianum* xylanase	Purified *T. harzianum* xylanase	Recombinant XT6 xylanase
33	10 (0)	0.5 (-)	12 (-)	65 (0)	5 (0)	2.36	1.78	1.74	2.03	1.70	2.13
34	10 (0)	1.5 (+)	12 (-)	65 (0)	5 (0)	-5.86	1.71	1.89	1.76	1.85	2.24
35	10 (0)	0.5 (-)	36 (+)	65 (0)	5 (0)	2.28	1.90	1.69	1.58	1.72	1.91
36	10 (0)	1.5 (+)	36(+)	65 (0)	5 (0)	2.48	2.16	1.92	2.10	1.89	2.48
37	10 (0)	0.5 (-)	24 (0)	55 (-)	5 (0)	2.97	1.80	1.84	2.89	1.96	2.03
38	10 (0)	1.5 (+)	24 (0)	55 (-)	5 (0)	4.45	1.60	2.07	2.56	1.79	1.92
39	10 (0)	0.5 (-)	24 (0)	75 (+)	5 (0)	2.51	1.52	1.79	2.31	1.35	1.59
40	10 (0)	1.5 (+)	24 (0)	75 (+)	5 (0)	2.61	1.49	1.66	2.22	1.91	1.36
41	10 (0)	1 (0)	12 (-)	65 (0)	4 (-)	2.49	1.60	1.67	2.24	1.71	1.93
42	10 (0)	1 (0)	36 (+)	65 (0)	4 (-)	2.40	1.80	1.69	2.48	1.77	1.60
43	10 (0)	1 (0)	12 (-)	65 (0)	6 (+)	2.07	1.77	1.67	2.21	1.74	1.61
44	10 (0)	1 (0)	36 (+)	65 (0)	6 (+)	2.41	1.73	1.64	2.22	1.60	1.83
45	10 (0)	1 (0)	24 (0)	65 (0)	5 (0)	**8.05**	1.60	1.65	1.98	1.75	2.03
46	10 (0)	1 (0)	24 (0)	65 (0)	5 (0)	4.91	1.51	1.80	1.81	1.75	2.16
47	10 (0)	1 (0)	24 (0)	65 (0)	5 (0)	1.90	1.52	1.74	1.62	1.89	2.29
48	10 (0)	1 (0)	24 (0)	65 (0)	5 (0)	7.84	1.95	2.11	1.96	2.18	2.33

5.3.3 Chromatographic analysis of hydrolysed products

The qualitative and quantitative analyses of monosaccharides and XOS resulting from the feed hydrolysis were carried out using 2 µl aliquots from each hydrolysate for TLC and HPLC. The treatment sample was applied to Silica Gel 60 F254 TLC plates (Merck, Darmstadt, Germany). The plates were then developed with a 1-butanol: acetic acid: water (2: 1: 1, v/v/v) mobile phase. The plates were left to air dry for 1 h and were then stained by soaking in Molisch's Reagent (0.3% (w/v) α-naphthol dissolved in sulfuric acid: methanol solution (5: 95, v/v)). The sugars developed on the plates were finally visualized by heating the plates at 110°C (using the oven) for 15 min. A mixture of the XOS standard [xylobiose (X2), xylotriose (X3), xylotetraose (X4), xylopentaose (X5), and xylohexaose (X6)] was obtained from Professor Kugen Perumal at Durban University of Technology. Monosaccharide standards (xylose, arabinose, mannose, glucose, and galactose) were purchased from Sigma, Aldrich. The yield of monosaccharides and XOS were estimated by HPLC. The supernatant fractions from the hydrolysates were filtered using a 0.2 µm filter. The XOS and monosaccharides in the samples were quantified with a Shimadzu RID-20A HPLC system (Shimadzu Scientific Instruments, North America) using a BioRad Aminex HPX-87H column (Transgenomic, Inc., Omaha, North America) at 50°C with a mobile phase of 5 mM H_2SO_4 and a flow rate of 0.5 ml/min and samples were analysed with a refractive index (RI) detector.

5.3.4 Cytotoxicity study of feed hydrolysed products

HEK293 cells were grown in scrum-containing media (SCM) in a Roux culture bottle. The liquid was discarded and the excess liquid on the surface of the Roux culture bottle was rinsed with PBS. For detaching, 2-3 ml of trypsin (in PBS) was added to the Roux culture bottle and incubated (ESCO CelCulture CO_2 Incubator, Singapore, 2018) for 10 min at 37°C. An equal

volume of fresh SCM was added and mixed to remove clumps. Cells were viewed under an automated cell counter and further diluted to obtain 10000 cells/ml. Aliquots of 100 µl of the cells were added into flat-bottomed 96-well plates at a loading of 10 000 cells per well, and cultured in full growth SCM. The plates were incubated (ESCO CelCulture CO_2 Incubator, Singapore, 2018) at 37°C for 3 h to allow the cells to settle. The hydrolysate samples were diluted with SCM to test the toxic effects on the HEK293 cells. The plates were incubated (ESCO CelCulture CO_2 Incubator, Singapore, 2018) at 37 °C for 48 h. After the treatment, 20 µL of MTS labelling reagent was added to each well, and the plates were incubated (ESCO CelCulture CO_2 Incubator, Singapore, 2018) at 37 °C for another 3 h. Following MTS incubation, the spectrophotometric absorbance of the samples was detected by using a SpectraMax ABS Plus microplate reader (Separations, Waltham, MA, USA) at 490 nm.

5.4 Results and discussion

5.4.1 Optimization of feed hydrolysis for enhanced reducing sugars

5.4.1.1 Hydrolysis of starter and grower feeds with crude T. harzianum xylanase

This study focused on the conditions favouring the hydrolysis of chicken feeds. Production of XOS from various sources of xylan such as wheat bran, birchwood, corncob, tobacco stalk, etc. using commercial xylanases has been reported previously [28]. However, relatively few studies have involved the xylanases from *T. harzianum* and the recombinant XT6 xylanase. The runs that produced the highest reducing sugars for the starter feed with the crude *T. harzianum* xylanase was run 45 (8.05 mg/ml) with all variables at their optimal levels (Table 5.1). For the grower feed, the highest reducing sugars was produced at run 1 (3.21 mg/ml) with the enzyme dosage (5 U/ml) and feed percentage (0.5%) at their low levels and time, pH, and temperature at their optimal levels. Run 25 also produced similar high yields of reducing sugars (3.07 U/ml)

with the only difference being the feed percentage at its optimal level (1%) and temperature at its low level (55°C). The ANOVA was performed to determine the p-values (Table 5.2-5.4). The model was significant ($p \leq 0.05$) for all enzymatically treated feed samples. Table 5.2 shows the results for the starter feed treatment with crude *T. harzianum* xylanase, the interactions between the feed and time including the time and temperature ($p \leq 0.05$) and the square terms for feed and time ($p \leq 0.03$) were significant . The grower feed treatment showed the square terms for enzyme dosage ($p \leq 0.0001$) and temperature ($p \leq 0.005$) to be significant including the linear terms for temperature ($p \leq 0.004$). The Pareto charts of standardization histogram graphs (Figure 5.1) also showed that the above mentioned terms were significant ($p \leq 0.05$), as they crossed the p-line (cumulative% = 50%).

Table 5.2: The ANOVA and regression coefficients of the response surface quadratic model for the response variables for optimizing reducing sugars by crude *T. harzianum* xylanase

Variable	Estimate		Std. Error		t value		p-value	
	Starter feed	Grower feed	Starter feed	Grower feed	Starter feed	Grower feed	Starter feed	Grower feed
Model	-23.24	27.40	49.43	8.95	-0.47	3.06	0.05*	0.005*
Dosage	0.48	-0.45	1.68	0.30	0.28	-1.47	0.78	0.15
Feed	14.41	-2.59	14.11	2.55	1.02	-1.02	0.32	0.32
Time	-0.61	-0.01	0.77	0.14	-0.79	-0.01	0.43	0.99
Temperature	0.30	-0.53	0.94	0.17	0.32	-3.10	0.75	0.004*
pH	6.51	-1.70	9.13	1.65	0.71	-1.03	0.48	0.31
Dosage: Feed	-0.08	0.07	0.37	0.07	-0.21	1.03	0.84	0.31
Dosage: Time	-0.01	-0.01	0.02	0.02	-0.10	-0.26	0.92	0.80
Dosage: Temperature	0.01	-0.01	0.02	0.01	0.09	0.32	0.93	0.75
Dosage: pH	-0.02	-0.01	0.18	0.03	-0.14	-0.43	0.89	0.67
Feed: Time	0.26	0.02	0.13	0.02	2.07	1.06	0.03*	0.30
Feed: Temperature	-0.18	0.00	0.15	0.02	-1.18	0.03	0.25	0.98
Feed: pH	-0.17	-0.07	1.84	0.33	-0.09	-0.22	0.93	0.83
Time: Temperature	0.01	-0.01	0.01	0.01	1.18	-0.15	0.05*	0.88
Time: pH	0.01	-0.01	0.08	0.01	0.12	-0.34	0.91	0.73
Temperature: pH	0.01	0.01	0.09	0.02	0.06	0.33	0.95	0.74
Dosage^2	-0.02	0.02	0.02	0.01	-0.69	4.41	0.50	0.0001*
Feed^2	-4.12	0.81	2.43	0.44	-1.70	1.86	0.04*	0.07
Time^2	-0.01	0.01	0.01	0.01	-2.08	0.72	0.03*	0.48
Temperature^2	-0.01	0.03	0.01	0.01	-0.59	3.02	0.56	0.005*
pH^2	-0.68	0.02	0.61	0.11	-1.12	1.47	0.27	0.15

* $p \leq 0.05$ shows significance , Lack of fit = 0.98, Lack of fit = 0.16

a

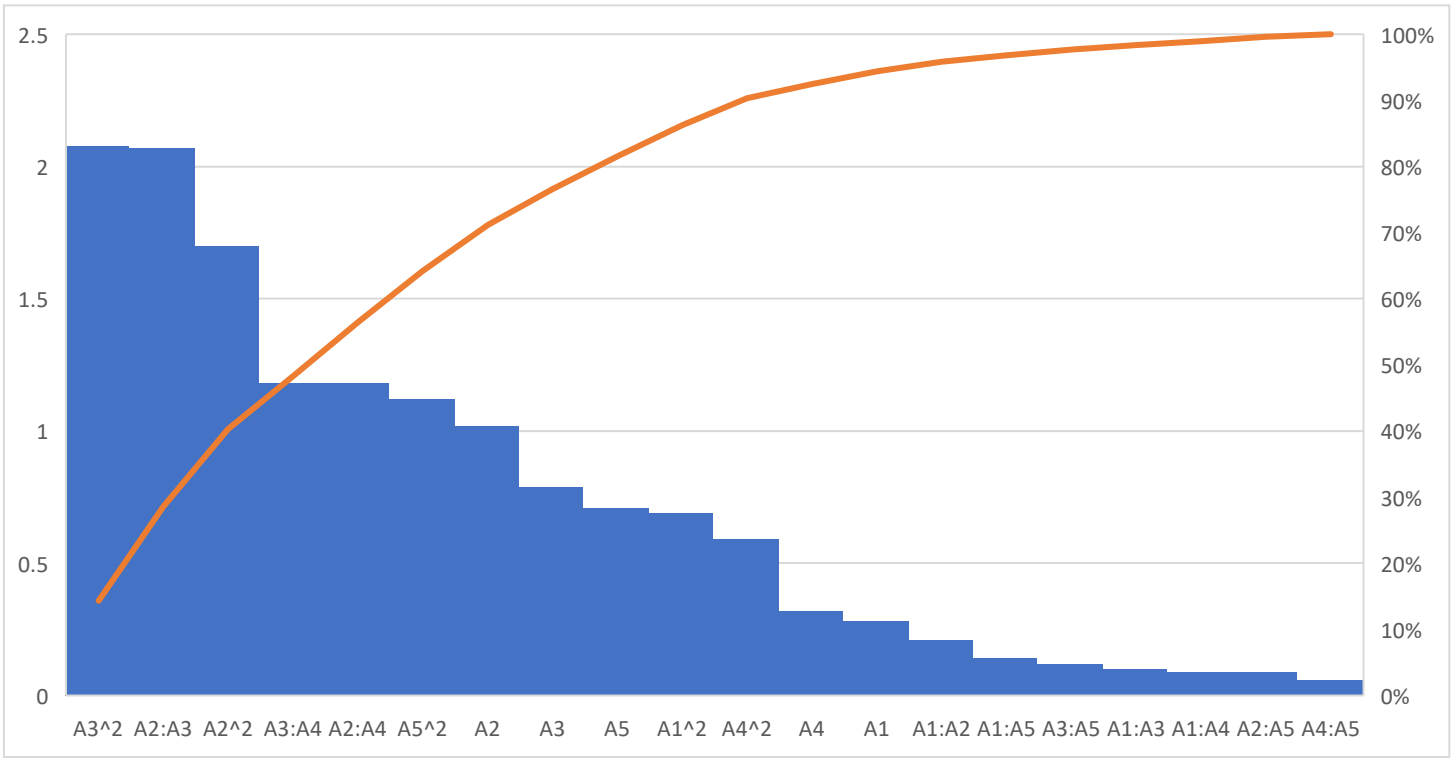

b

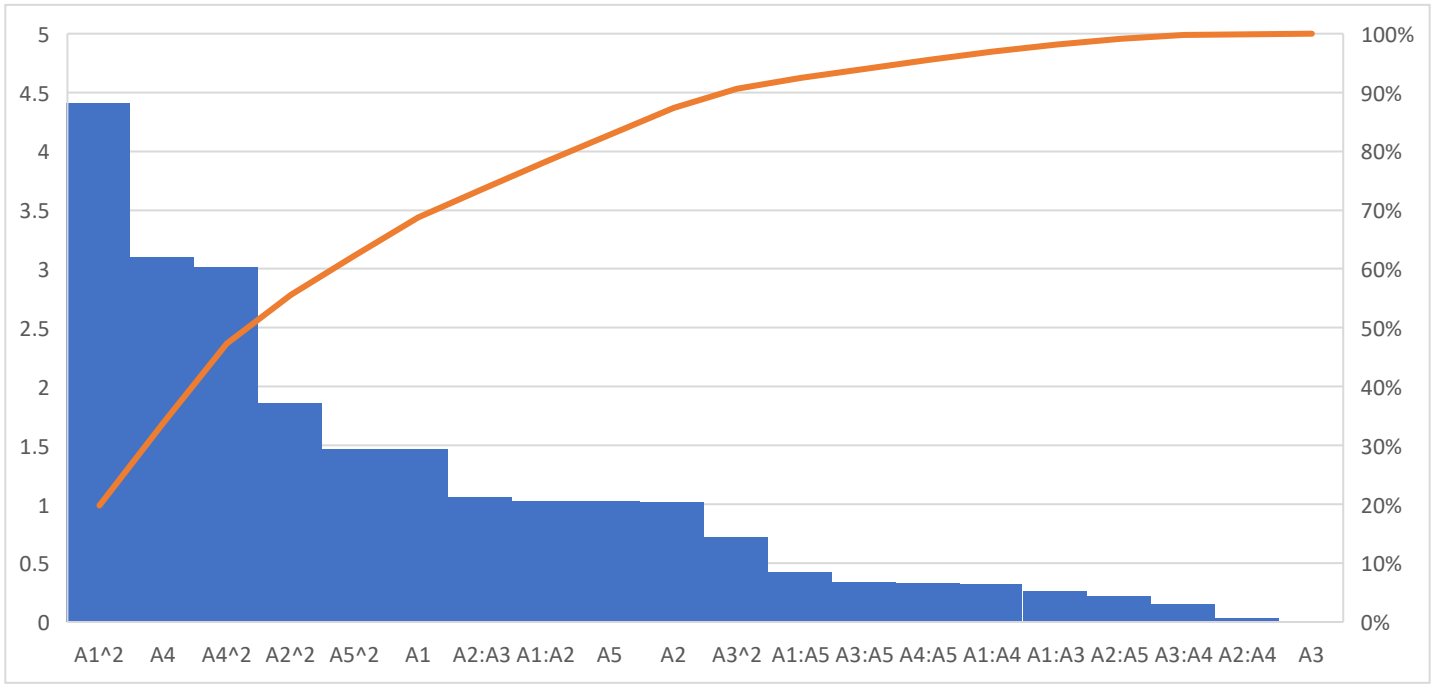

Figure 5.1: Pareto chart of standardised effects for the BBD for enzyme dosage (A1), feed percentage (A2), time (A3), temperature (A4), and pH (A5) for the hydrolysis of (a) starter feed and (b) grower feed with crude *T. harzianum* xylanase. Orange line represents p = 0.05.

5.4.1.2 Hydrolysis of starter and grower feeds with purified T. harzianum xylanase

Hydrolysis of the starter feed by the purified *T. harzianum* xylanase resulted in the highest amount of reducing sugars at run 12 (2.81 mg/ml) at the optimal enzyme dosage and pH and the other variables at their high levels (Table 5.1). There were other runs that produced similar high yields, however these were significantly different ($p \leq 0.05$). For the grower feed, run 24 (2.41 mg/ml) with all variables at their optimal levels resulted in the highest amount of reducing sugars. Run 12 also resulted in similar yields (2.31 U/ml) with feed percentage, time and temperature at their high levels. Table 5.3 represents the ANOVA results for the hydrolysis of the starter and grower feeds by the purified *T. harzianum* xylanase, the interactions between the enzyme dosage and time as well as the time and temperature, and the linear terms for time were significant as p-values were 0.05, 0.04, and 0.04, respectively. For treatment of the grower feed, the square ($p \leq 0.0003$) and linear terms ($p \leq 0.02$) for pH as well as the interactions between the enzyme dosage and feed ($p \leq 0.03$), and; time and temperature ($p \leq 0.02$) were significant. The Pareto charts of standardization histogram graphs (Figure 5.2) also showed that those terms were significant ($p \leq 0.05$), as they crossed the p-line (cumulative% = 50%).

Table 5.3: The ANOVA and regression coefficients of the response surface quadratic model for the response variables for optimizing reducing sugars by purified *T. harzianum* xylanase

Variable	Estimate		Std. Error		t value		p-value	
	Starter feed	Grower feed	Starter feed	Grower feed	Starter feed	Grower feed	Starter feed	Grower feed
Model	3.52	1.06	7.90	5.87	0.44	0.18	0.03*	0.03*
Dosage	0.08	-0.06	0.27	0.20	0.31	-0.29	0.76	0.77
Feed	0.50	-1.99	2.26	1.68	0.22	-1.19	0.83	0.24
Time	-0.27	-0.18	0.12	0.09	-2.22	-1.95	0.04*	0.06
Temperature	0.02	-0.08	0.15	0.11	0.16	-0.74	0.87	0.47
pH	-0.015	2.69	1.46	1.08	-0.01	2.48	0.99	0.02*
Dosage: Feed	-0.09	0.10	0.06	0.04	-1.45	2.25	0.16	0.03*
Dosage: Time	0.00	0.01	0.00	0.01	0.05	0.55	0.05*	0.59
Dosage: Temperature	0.00	0.01	0.00	0.02	0.25	0.33	0.80	0.74
Dosage: pH	-0.01	-0.01	0.03	0.02	-0.42	-0.30	0.68	0.77
Feed: Time	0.01	-0.01	0.02	0.01	0.64	-0.62	0.53	0.54
Feed: Temperature	0.01	0.02	0.02	0.01	0.32	1.39	0.75	0.18
Feed: pH	0.11	0.14	0.2	0.22	0.36	0.65	0.72	0.52
Time: Temperature	0.00	0.03	0.00	0.01	2.22	2.46	0.04*	0.02*
Time: pH	-0.00	-0.04	0.01	0.02	-0.41	-0.47	0.69	0.64
Temperature: pH	0.00	0.05	0.01	0.01	-0.30	0.49	0.77	0.63
Dosage^2	0.00	-0.03	0.00	0.02	0.32	-1.14	0.75	0.27
Feed^2	-0.38	-0.50	0.39	0.29	-0.97	-1.76	0.34	0.09
Time^2	0.00	-0.01	0.00	0.01	0.99	-0.38	0.33	0.71
Temperature^2	-0.00	-0.01	0.00	0.01	-1.11	-0.51	0.28	0.61
pH^2	-0.01	-0.30	0.10	0.07	-0.18	-4.10	0.86	0.0003*

* $p \leq 0.05$ shows significance, Lack of fit = 0.40, Lack of fit = 0.62

a

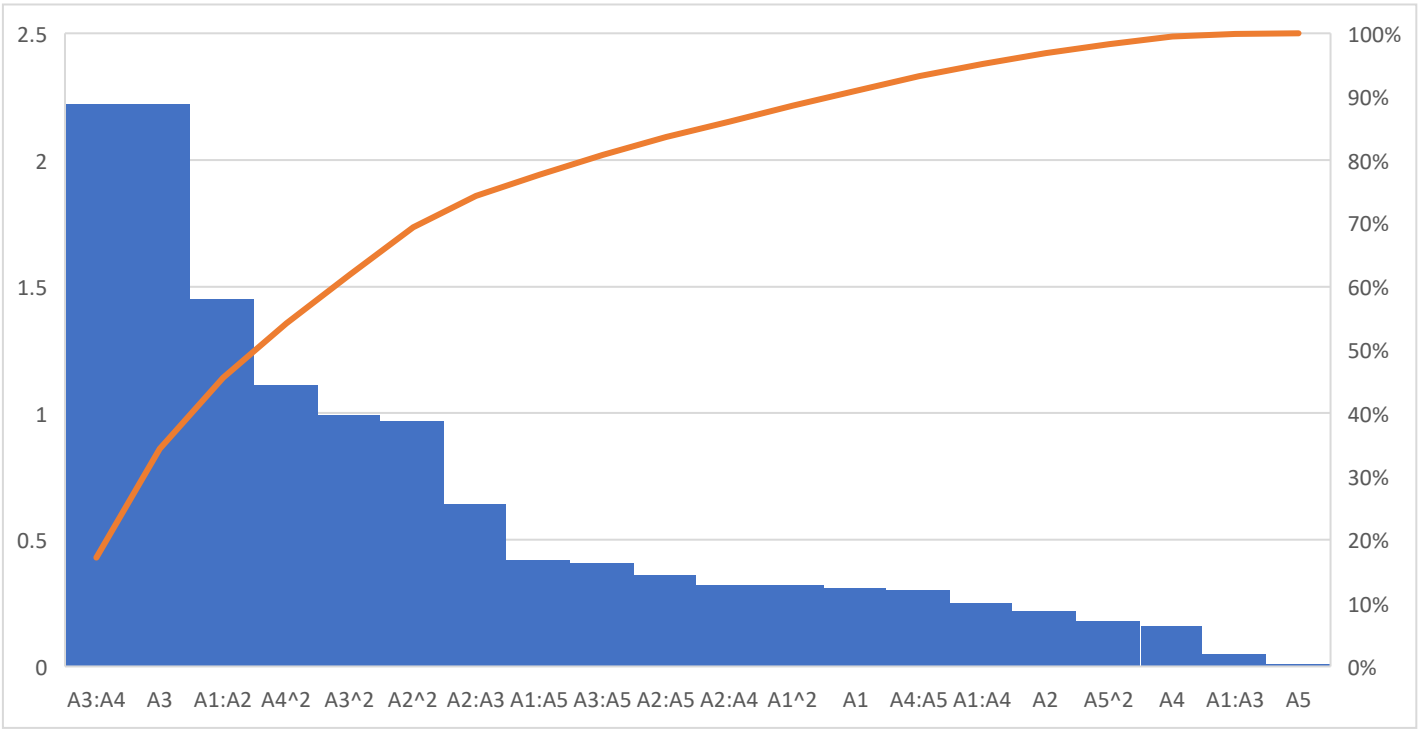

b

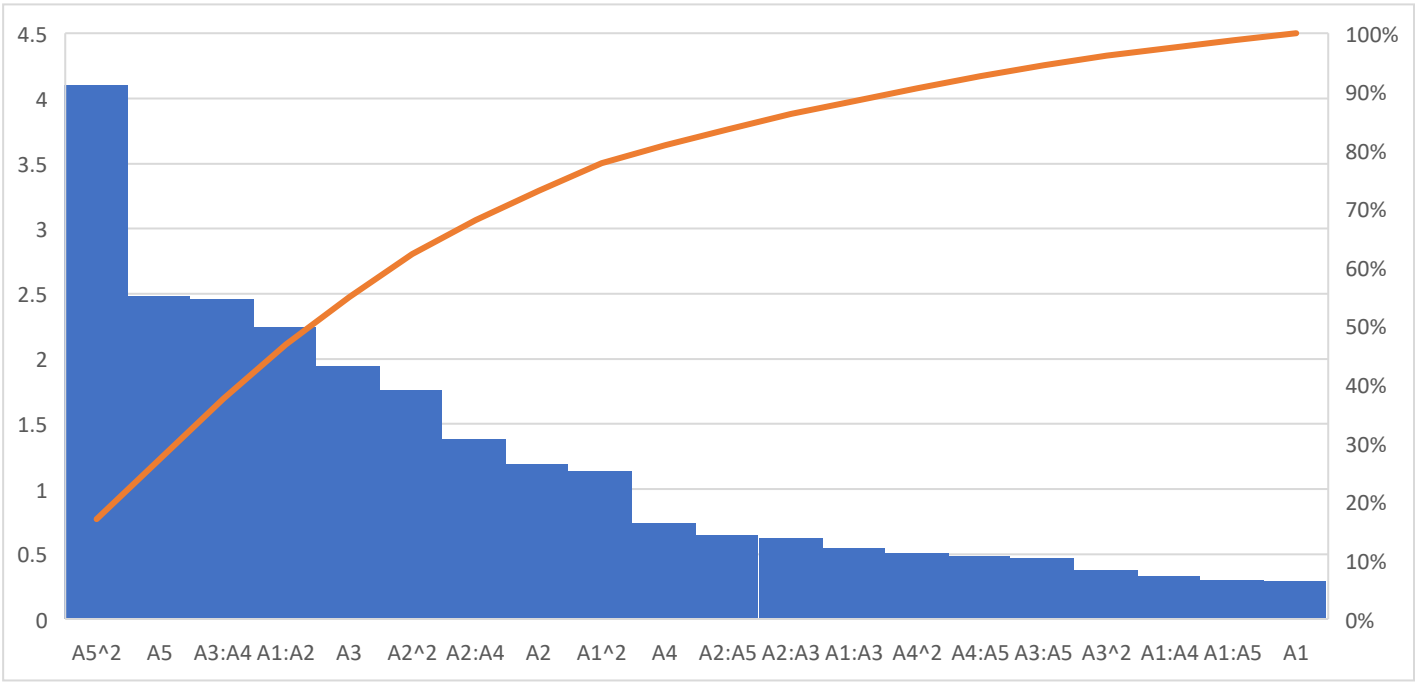

Figure 5.2: Pareto chart of standardised effects for the BBD for enzyme dosage (A1), feed percentage (A2), time (A3), temperature (A4), and pH (A5) for the hydrolysis of (a) starter feed and (b) grower feed with purified *T. harzianum* xylanase. Orange line represents p = 0.05.

5.4.1.3 Hydrolysis of starter and grower feeds with recombinant XT6 xylanase

The run that had the highest effect on starter feed, was run 12 (2.98 mg/ml) with enzyme dosage and pH at their optimal levels and the other variables at their high levels (Table 5.1). For the grower feed, run 12 (2.79 mg/ml) with enzyme dosage and pH at its optimal level, and the other variables at their high levels. There were similar yields for other runs, however, there was a significant ($p \leq 0.05$) difference between the runs. Overall, the starter feed hydrolysis by all three enzymes resulted in higher levels of reducing sugars compared to the hydrolysis of the grower feed. The starter feed with crude *T. harzianum* xylanase, had the highest effect on reducing sugars (8.05 mg/ml) and the grower feed with purified *T. harzianum* xylanase had the lowest effect on reducing sugars (2.41 mg/ml). Table 5.4 shows the interactions between the enzyme dosage and feed concentration including the time and temperature and their linear terms for time to be significant as p-values were 0.0004, 0.03, and 0.01, respectively. The square terms for the enzyme dosage ($p \leq 0.03$) and temperature ($p \leq 0.05$) were also significant. For the grower feed, results showed that the interaction between time and temperature (0.03) and the linear terms ($p \leq 0.02$) for time to be significant including the square term of pH ($p \leq 0.05$). The Pareto charts of standardization histogram graphs (Figure 5.3) also showed that those terms were significant ($p \leq 0.05$), as they crossed the p-line (cumulative% = 50%).

Table 5.4: The ANOVA and regression coefficients of the response surface quadratic model for the response variables for optimizing reducing sugars by purified recombinant XT6 xylanase.

Variable	Estimate		Std. Error		t value		p-value	
	Starter feed	Grower feed	Starter feed	Grower feed	Starter feed	Grower feed	Starter feed	Grower feed
Model	9.32	6.51	5.83	8.73	1.59	0.75	0.04*	0.04*
Dosage	-3.17	-1.28	1.98	2.96	-1.60	-0.43	0.12	0.67
Feed	-1.34	-8.30	1.67	2.49	-0.81	-0.33	0.43	0.74
Time	-2.48	-3.51	9.14	1.37	-2.71	-2.57	0.01*	0.02*
Temperature	-1.25	1.10	1.11	1.66	-1.13	0.07	0.27	0.95
pH	7.80	2.75	1.08	1.61	0.72	0.17	0.48	0.87
Dosage: Feed	1.03	-8.60	4.36	6.53	2.35	-0.13	0.03*	0.90
Dosage: Time	-2.21	-1.57	1.81	2.72	-1.22	-0.06	0.23	0.95
Dosage: Temperature	2.21	1.17	2.18	3.27	1.01	0.36	0.32	0.72
Dosage: pH	-3.85	7.88	2.18	3.27	-0.18	0.24	0.86	0.81
Feed: Time	1.59	1.40	1.48	2.22	1.07	0.63	0.29	0.53
Feed: Temperature	-2.30	-1.24	1.78	2.67	-0.13	-0.46	0.90	0.65
Feed: pH	7.25	2.54	2.18	3.27	0.33	0.78	0.74	0.44
Time: Temperature	4.04	4.43	1.32	1.97	3.07	2.25	0.004*	0.03*
Time: pH	-8.96	1.12	9.09	1.36	-1.00	0.82	0.92	0.42
Temperature: pH	8.51	1.85	1.09	1.63	0.78	1.13	0.44	0.27
Dosage^2	6.70	7.01	2.86	4.29	2.34	0.16	0.03*	0.87
Feed^2	-6.10	1.24	2.86	4.29	-0.21	0.29	0.83	0.77
Time^2	-7.93	-9.33	5.58	8.34	-0.14	-0.01	0.89	0.99
Temperature^2	-2.64	-1.66	8.03	1.20	-0.33	-1.38	0.05*	0.18
pH^2	-1.40	-2.09	7.16	1.07	-1.95	-1.95	0.06	0.05*

* $p \leq 0.05$ shows significance, Lack of fit = 0.17, Lack of fit =. 0.5

a

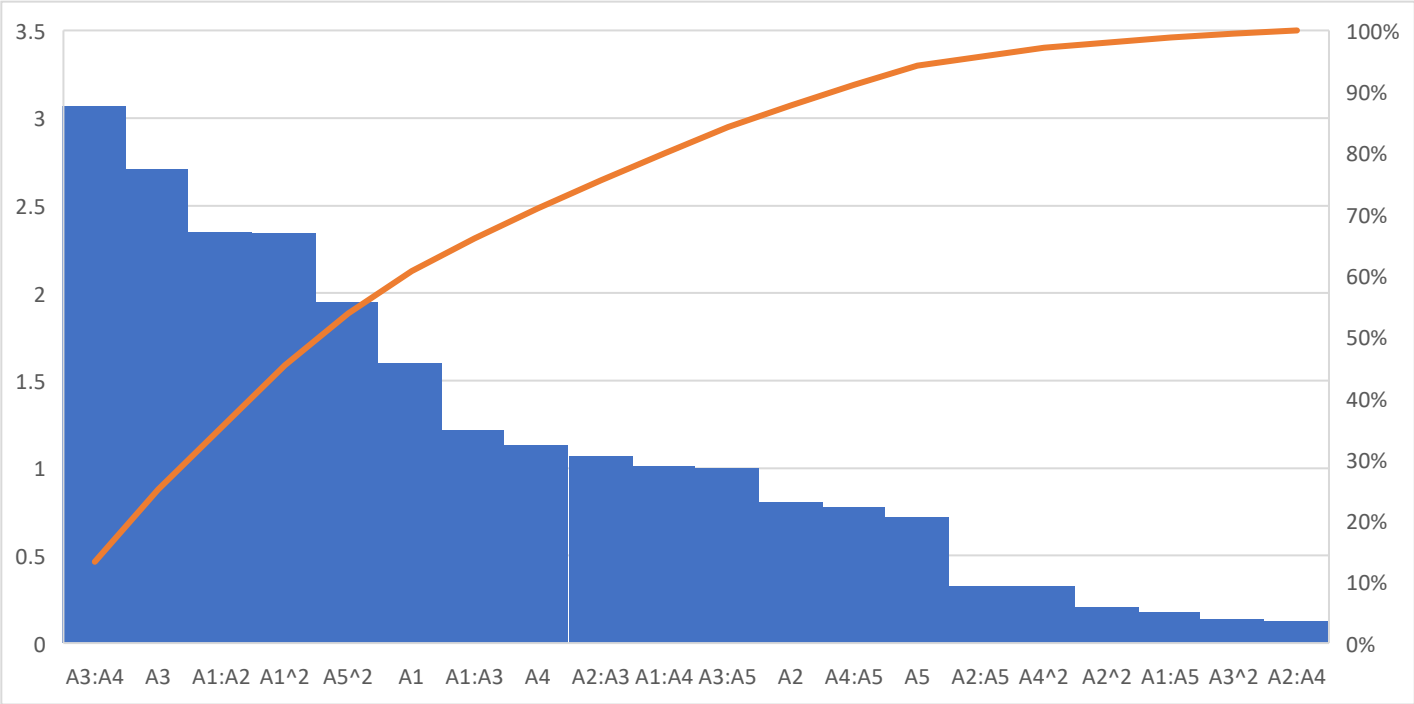

b

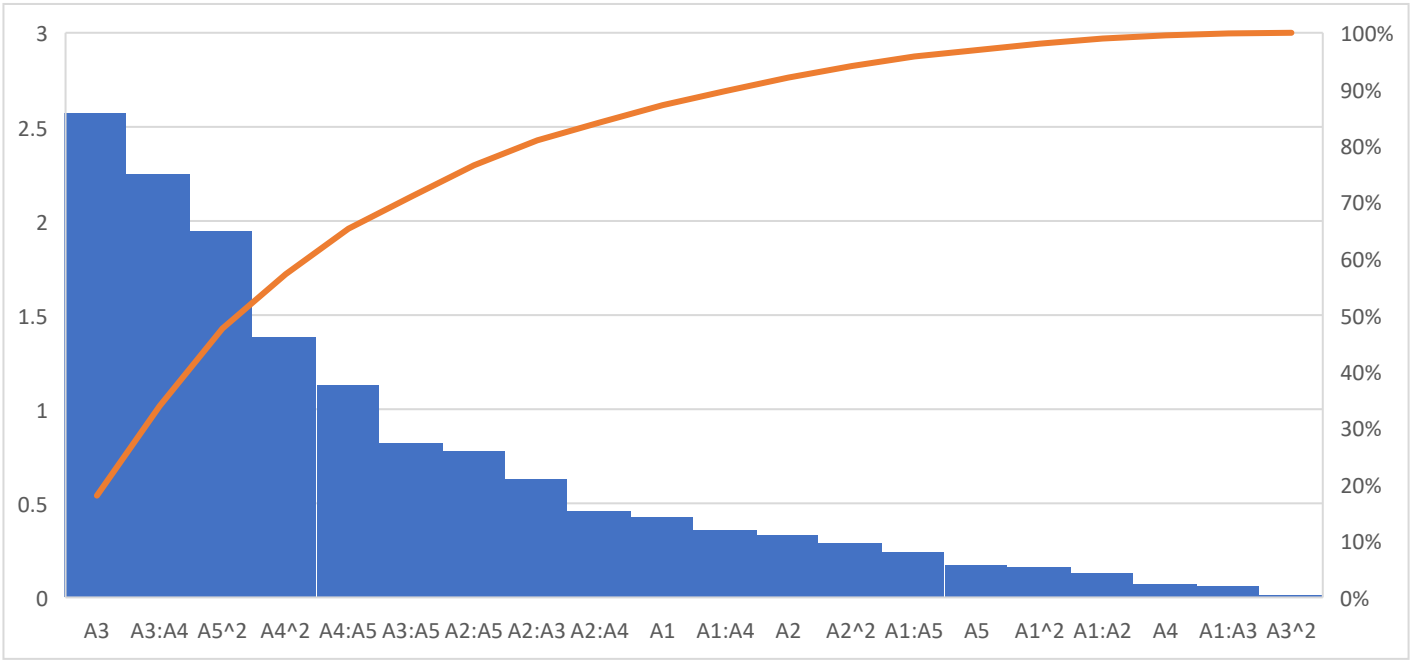

Figure 5.3: Pareto chart of standardised effects for the BBD for enzyme dosage (A1), feed percentage (A2), time (A3), temperature (A4), and pH (A5) for the hydrolysis of (a) starter feed and (b) grower feed with purified recombinant XT6 xylanase. Orange line represents p = 0.05.

5.4.2 Interaction of variables for feed hydrolysis

The relationship between the responses and the parameters for feed hydrolysis generated by the quadratic model and the optimum level of each variable was studied using three-dimensional (3D) response surface plots (Figures 5.4-5.8) (Appendix IV, supplementary Figures 1- 6) where the z-axis refers to reducing sugars versus any two variables, whilst the other variables are at their optimal levels.

5.4.2.1 Effect on reducing sugar yield of hydrolysis of starter and grower chicken feeds by the crude T. harzianum xylanase

The hydrolysis of the xylan in chicken feed can be influenced by the feed, enzyme dosage, time, temperature, and pH. The interactive effects of the variables were analysed for the crude *T. harzianum* xylanase in starter and grower chicken feeds (Figures 5.4a and b). For this analysis, the other parameter was kept constant at their zero (optimal) levels. The mutual interaction of these variables (feed: time and time: temperature) was significant ($p \leq 0.05$), indicating that there is a synergistic interaction favoring the production of reducing sugars by the crude *T. harzianum* xylanase on starter chicken feed. The highly elliptical response surface plot Figure 5.4a shows the highest reducing sugars yield (3 mg/ml) was produced when both variables, feed and time, were high. Chapa et al. [29] also observed similar results, showing as the incubation time increased there was a rise in reducing sugars. Ai et al. [30] reported 3.9 mg/ml of reducing sugars using xylanase of *Streptomyces olivaceoviridis* on pretreated corncobs after 24 h of reaction time. Feed concentration also plays an important role in the enzymatic hydrolysis [29]. Increasing the concentration of feed showed a substantial rise in reducing sugars while decreasing the feed concentration from 1.0% to 1.4% decreased the yield of reducing sugars. It is clear from Figure 5.4a that a higher feed concentration (>1.0%) is not advantageous to enhancing the yield of reducing sugars. The decrease in the yield of reducing sugars, using higher feed concentration may be due to the reduction of water content in the aqueous medium. A similar trend was also

observed by Yoon et al. [31]. Figure 5.4b shows a high yield with low temperatures and incubation time. For enzyme action, temperature is one of the most important parameters. The optimization of reaction temperature was necessary to achieve optimal functioning of the enzyme in the provided conditions because of the well-established facts of enzyme inhibition at lower temperatures and enzyme inactivation at higher temperatures [32]. As shown in Figure 5.4b, the yield of reducing sugars was significantly higher at 55°C and an incubation time of approximately 25 h. Production of reducing sugars was reduced at 70-75°C, this may be due to inactivation of the enzyme at higher temperatures during longer incubation time. The interactions of the variables on grower feed with crude *T. harzianum* xylanase were not significant ($p \leq 0.05$) (Appendix IV, supplementary Figures 1-2).

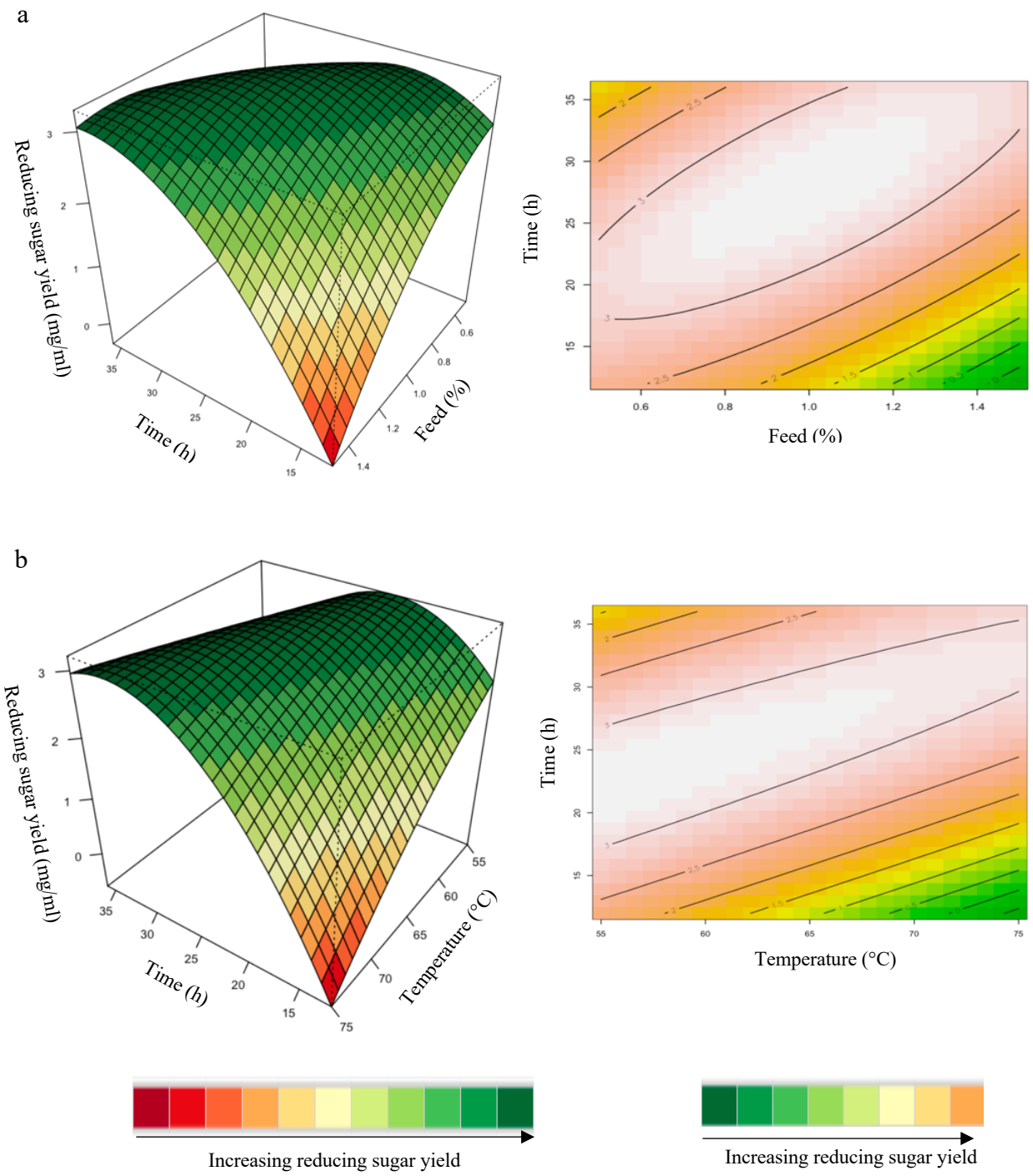

Figure 5.4: 3D- response surface plots and contour plots of the combined effects of feed and time (a) and time and temperature (b) on yield of reducing sugars by crude *T. harzianum* xylanase treatment of starter chicken feed.

5.4.2.2 Effect on reducing sugar yield of the hydrolytic activity of the purified T. harzianum xylanase on starter and grower chicken feeds

The mutual interaction of these variables (dosage: time and time: temperature) was significant ($p>0.05$), indicating that there is synergistic interaction favouring the production of reducing sugars by the purified *T. harzianum* xylanase on starter chicken feeds. Enzyme concentration plays a significant role in increasing the reducing sugars and XOS yield [33]. Enzyme doses in the range of 5–15 U/ml were used in the present study. Enhanced yield of reducing sugars was obtained at high incubation times and enzyme dosages (Figure 5.5a). The contour plot showed that an incubation time of approximately 30 h and 13 U/ml enzyme dosage, resulted in the highest yield of reducing sugars. Yang et al. [34] observed that an increase in xylanase dose from 5 to 10 U/ml increased the reducing sugar only up to 12 g/l from 11 g/l after 24 h of reaction time in their experiments. Enzymes can be more effective after a pre-treatment of the substrate since this increases the accessibility of the active sites of the enzyme to the substrate. The use of enzymes on a substrate without prior pre-treatment processes may be less effective since hydrolysable xylans are usually located at the periphery of the particles of substrates [33]. The interaction between time and temperature (Figure 5.5b) resulted in the highest yield of reducing sugars at high (75°C) temperatures and incubation time (35 h).

For the optimization of reducing sugars from hydrolysis of grower chicken feed, the yield was enhanced at high dosage and feed concentration (Figure 5.6a). For the interaction between time and temperature (Figure 5.6b), the reducing sugars yield was enhanced at high incubation time and temperature. The positive effects on the production of reducing sugars at a high temperature included the dissolution of a high concentration of xylan, the prevention of microbial contamination, and an increase in the reaction rate [35]. Other variables' interactions were insignificant, however, their interactions are shown in the supplementary figure (Appendix IV, supplementary Figures 3-4).

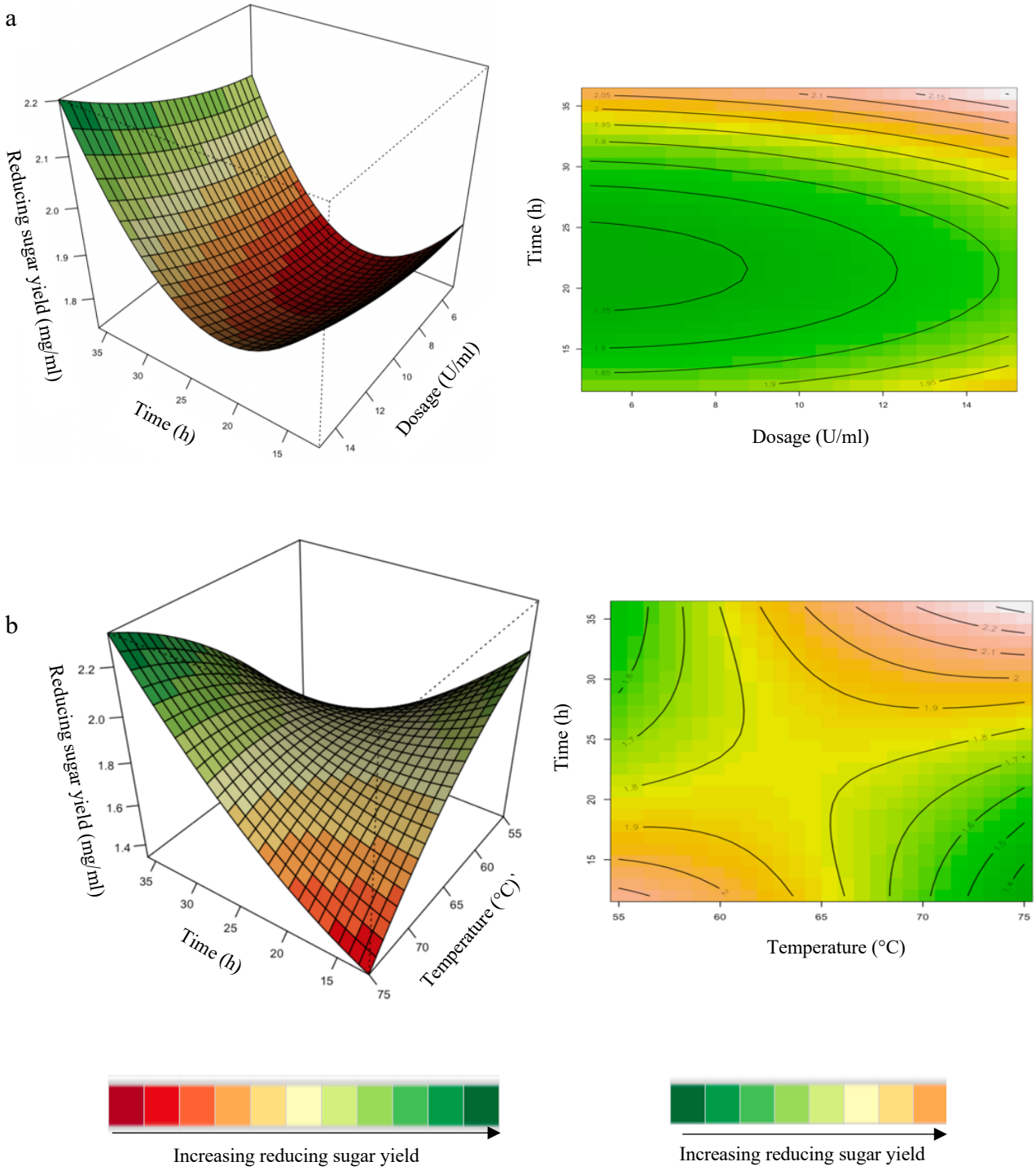

Figure 5.5: 3D- response surface plots and contour plots of the combined effects of dosage and time (a) and time and temperature (b) on yield of reducing sugars by purified *T. harzianum* xylanase treatment of starter chicken feed.

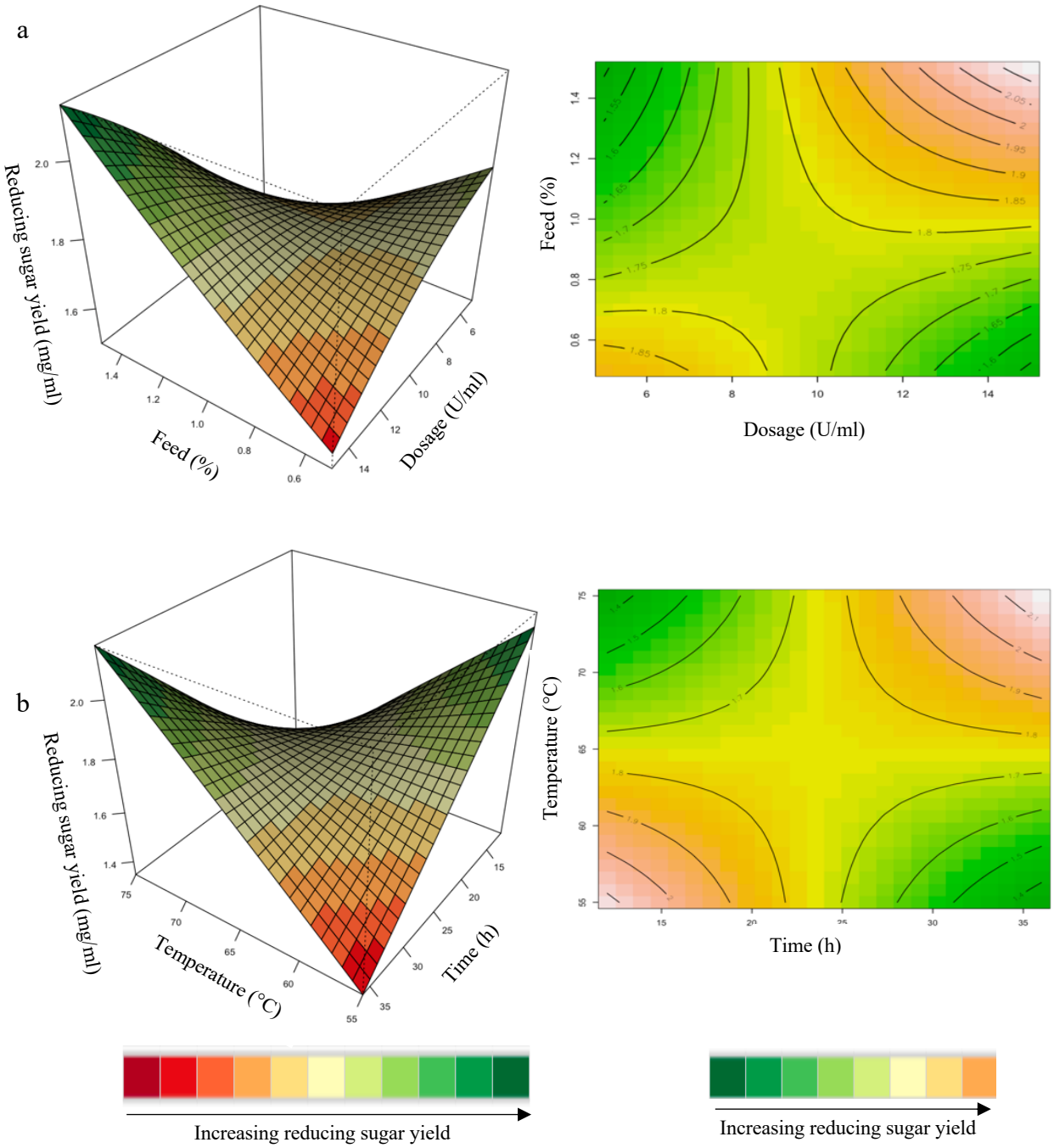

Figure 5.6: 3D- response surface plots and contour plots of the combined effects of dosage and feed (a) and time and temperature (b) on yield reducing sugars by purified *T. harzianum* xylanase treatment of grower chicken feed.

5.4.2.3 Effect on reducing sugar yield of the hydrolytic activity of the recombinant XT6 xylanase on starter and grower chicken feeds

The mutual interaction of these variables (dosage: feed and time: temperature) were significant ($p>0.05$), indicating that there is synergistic interaction favouring the production of reducing sugars by the purified recombinant XT6 on starter feed. Enhanced yield of reducing sugars was shown at high enzyme dosages and feed concentrations (Figure 5.7a). At high incubation time and temperatures, the yield of reducing sugars was enhanced (Figure 5.7b). Li et al. [36] reported, a *Streptomyces spp.* T7, which was used to produce XOS from corncob xylan at 60 °C with the highest yield of reducing sugars. Khangwal et al. [21] also reported a recombinant xylanase, SipoEnXyn10 (*Streptomyces ipomoeae* cloned and expressed in *E. coli*), was used to produce XOS from beechwood xylan at 65 °C with the highest yield of reducing sugars.

The interactive effect of time and temperature were examined, and the results are illustrated in Figures 5.8a and 5.8b. The mutual interaction of these variables (time: temperature) was significant ($p>0.05$), indicating that there is synergistic interaction favouring the production of reducing sugars by the purified recombinant XT6 on grower feed. Both high (35 h and 75°C) and low (15 h and 55°C) levels in BBD, enhanced the yield of reducing sugars.

a

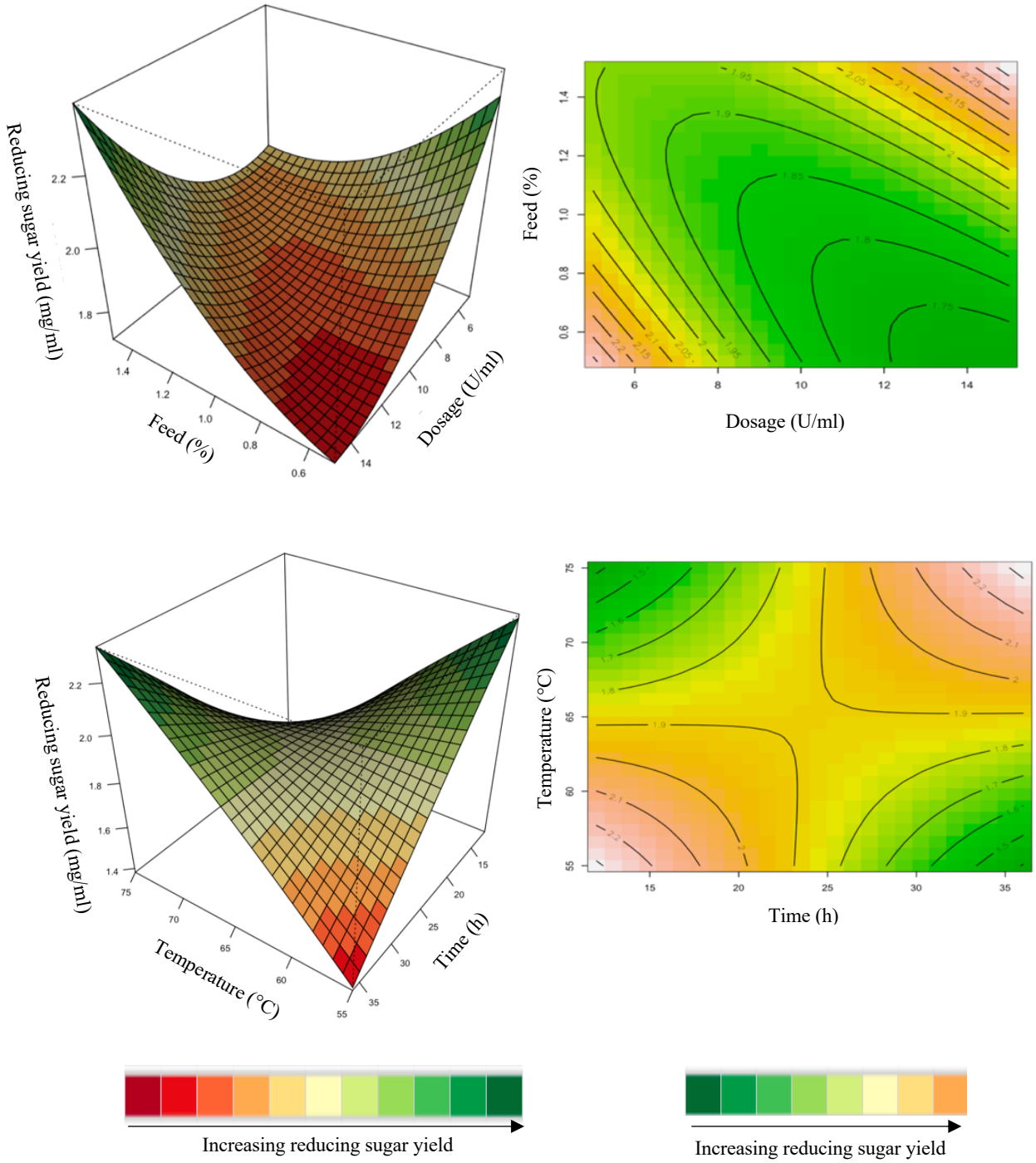

Figure 5.7: 3D- response surface plots and contour plots of the combined effects of dosage and feed (a) and time and temperature (b) on yield of reducing sugars by purified XT6 of starter chicken feed.

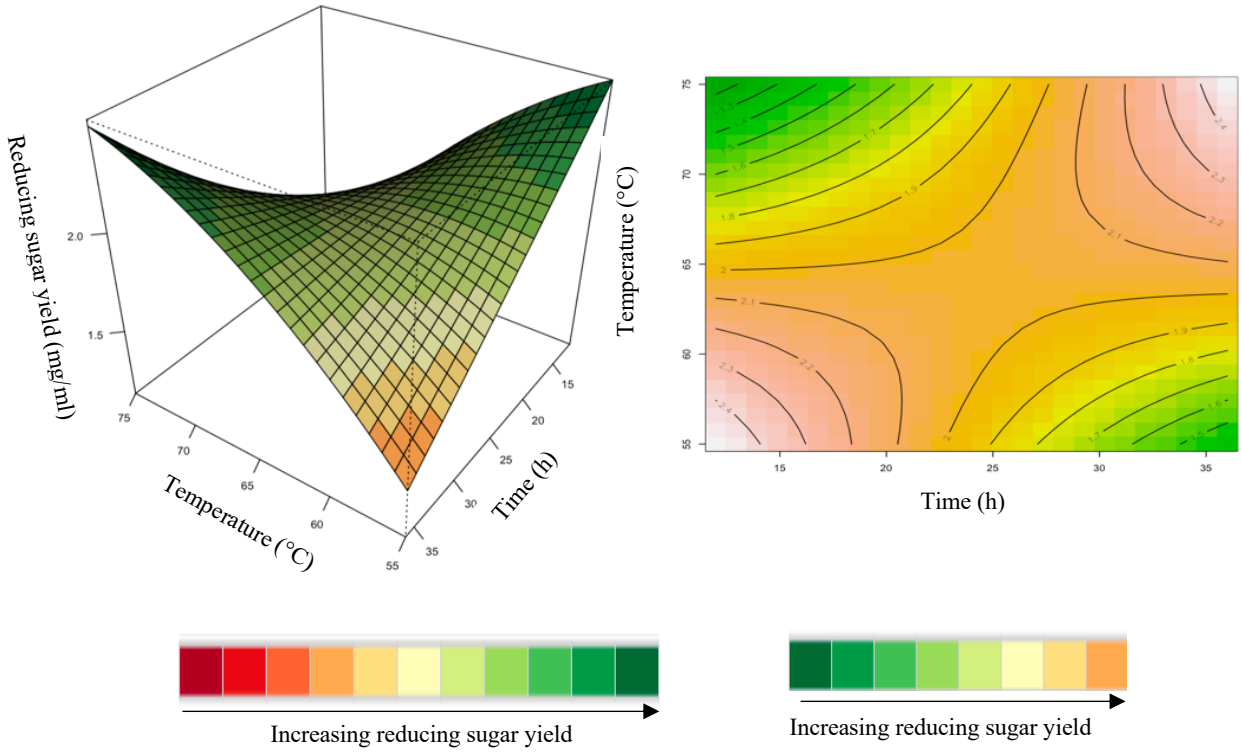

Figure 5.8: 3D- response surface plot and contour plot of the combined effects of time and temperature on yield of reducing sugars by purified XT6 of grower chicken feed.

5.4.3 TLC and HPLC analysis of feed hydrolysis products

Thin-layer chromatography was performed to visualize the monosaccharides and degree of polymerization (DP) of the XOS (and) produced following hydrolysis of the local chicken feeds by the three enzyme preparations (Figures 5.9a-d). After the optimal hydrolysis treatments of, 8.65 U/ml, 2.9 U/ml, and 3.63 U/ml reducing sugars were produced from starter feed substrates by the crude *T. harzianum* xylanase, purified *T. harzianum* xylanase, and recombinant XT6 xylanase, respectively. Hydrolysis of the grower chicken feed produced 2.5 U/ml, 3.96 U/ml, and 3.60 U/ml reducing sugars by the crude fungal xylanase, purified fungal xylanase, and recombinant xylanase, respectively. TLC analysis indicated the production of XOS of DP 2–6 (equivalent to X2-X6) in the enzymatic reactions. Hydrolysis of the chicken starter and grower feeds by the enzymes produced XOS which migrated between xylobiose, xylotriose, xylotetraose,

and xylopentose (Figure 5.9a-c). The substrate controls of the chicken feeds displayed some faint spots that corresponded to those of the hydrolysed samples. This may have been due to the decomposition of the substrates during the termination of the reaction (heating at 100°C). Figure 5.9d shows the monosaccharides glucose, and galactose following chicken feeds hydrolysis. One of the attractive features of the process was the production of only XOS and no xylose. The absence of xylose and the predominant production of xylobiose suggest a unique specificity and catalytic mechanism of the thermophilic xylanase. It indicates that the enzyme has a higher affinity for cleaving the glycosidic bonds at specific positions within the xylan substrate, resulting in the release of xylobiose as the primary product. The absence of xylose in our study was beneficial because previous research has indicated that xylose production can hinder the production of XOS [37]. Hegazy et al. [38] also reported non-competitive end product inhibition by xylose of a *G. stearothermophilus* derived xylanase, XT6.

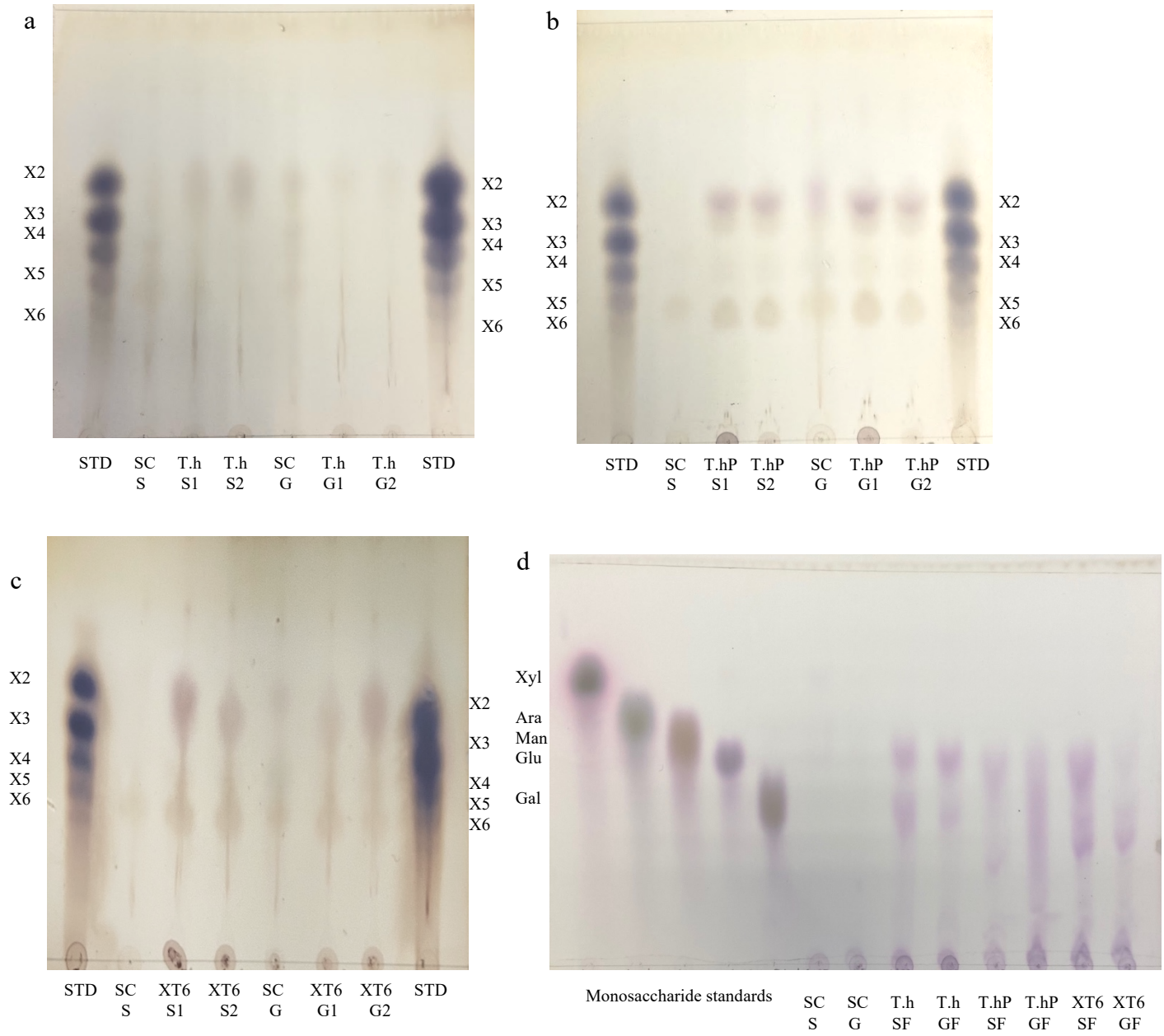

Figure 5.9: The TLC profile of XOS produced from chicken feed hydrolysis by crude (a) and purified (b) *T. harzianum* xylanases and the recombinant XT6 xylanase (c). Figure 5.9 (d) shows the TLC profile of monosaccharides produced from chicken feed hydrolysis by crude and purified *T. harzianum* xylanases and recombinant XT6 xylanase. STD - Xylooligosaccharides standards, SC (S) - substrate control (No xylanase) starter feed, SC (G)- Substrate control (no xylanase) grower feed, T.h S1 - starter feed with crude *T. harzianum* xylanase (sample 1), T.h S2- starter feed with crude *T. harzianum* xylanase (sample 2), T.h G1- grower feed with crude *T. harzianum* xylanase (sample 1) and T.h G2- grower feed with crude *T. harzianum* xylanase (sample 2). T.hP S1- starter feed with purified *T. harzianum* xylanase (sample 1), T.hP S2- starter feed with purified *T. harzianum* xylanase (sample 2), T.hP G1- grower feed with purified *T. harzianum* xylanase (sample 1) and T.hP G2- grower feed with purified *T. harzianum* xylanase (sample 2). X2 - Xylobiose; X3 - Xylotriose; X4 - Xylotetraose; X5 - Xylopentaose; X6 - Xylohexaose.

Monosaccharide standards; Xyl- xylose, Ara- arabinose, Man- mannose, Glu- glucose, and Gal- galactose. T.h SF - starter feed with crude *T. harzianum* xylanase, T.h GF - grower feed with crude *T. harzianum* xylanase, T.hP SF - starter feed with purified *T. harzianum* xylanase, T.hP GF - grower feed with purified *T. harzianum* xylanase, XT6 SF- recombinant XT6 xylanase with starter feed and XT6 GF- recombinant XT6 xylanase with grower feed.

In addition to, glucose and galactose observed on TLC (Figure 5.9d), hydrolysis of chicken feeds by the three enzyme preparations also produced mannose evident in HPLC chromatograms (Figure 5.10). Xylobiose (X2) was the only XOS observed by HPLC (Figure 5.10). Khangwal et al. [20] observed xylobiose as the major product from corncobs and *Moso bamboo.* The hydrolysis of grower chicken feed by the purified *T. harzianum* xylanase produced the highest concentration of xylobiose and the lowest concentration of xylobiose was observed by the hydrolysis of grower feed by crude *T. harzianum* xylanase. Overall, the hydrolysis by purified *T. harzianum* xylanase resulted in higher monosaccharides and xylobiose concentrations than the crude *T. harzianum* xylanase and recombinant XT6 xylanase. The yield of XOS with DP 3 and higher could not be measured due to the unresolved peaks in HPLC. However, the spots for X3, X4, and X5 were noted to be predominant on the TLC chromatograms.

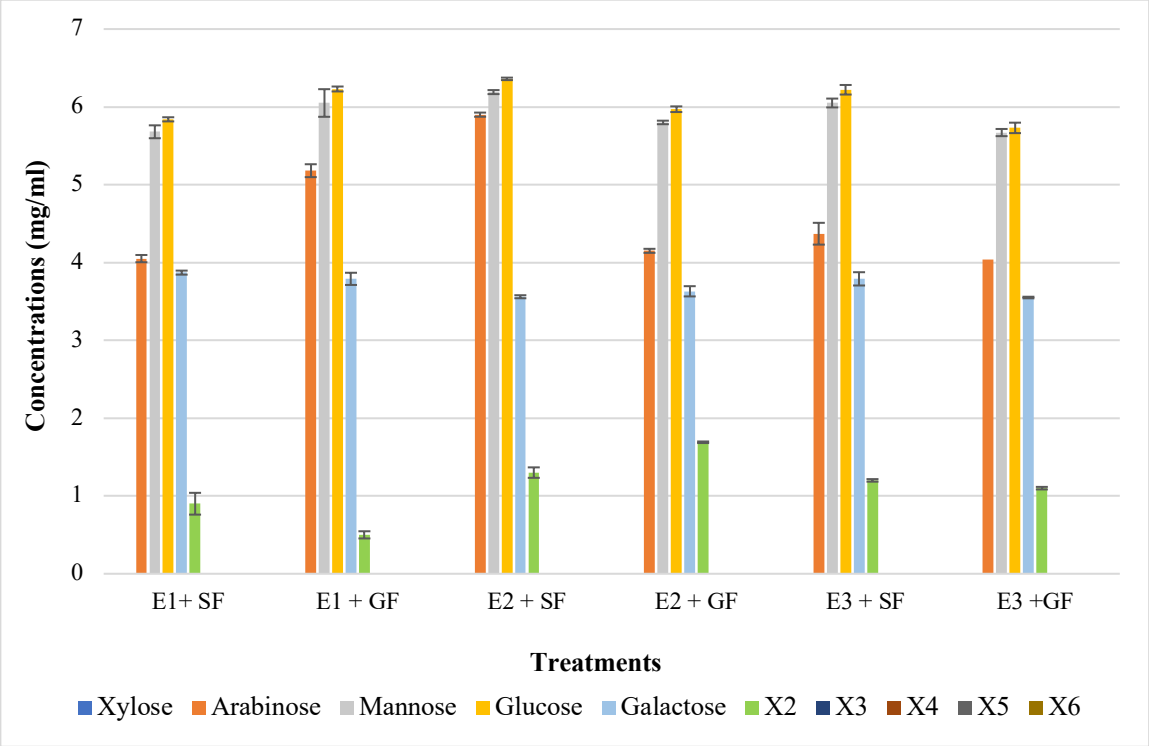

Figure 5.10: The HPLC profile on monosaccharides and xylooligosaccharides produced by chicken feed hydrolysis. E1+SF- crude *T. harzianum* xylanase used to hydrolyse starter chicken feed, E1+GF- crude *T. harzianum* xylanase used to hydrolyse grower chicken feed, E2+SF- purified *T. harzianum* xylanase used to hydrolyse starter chicken feed, E2+GF- purified *T. harzianum* xylanase used to hydrolyse grower chicken feed, E3+SF- purified recombinant XT6 xylanase used to hydrolyse starter chicken feed and E3+GF- purified recombinant XT6 xylanase used to hydrolyse grower chicken feed. Data points represent the mean values ± SD (n=3). (Standard curve is shown in Appendix IV, Supplementary Figure 7).

Lately, XOS (particularly xylobiose) has attracted interest as an effective prebiotic that has beneficial effects on animal and human digestion [40]. Xylanases are desirable for XOS production by biomass hydrolysis as TLC analysis revealed that hydrolysis of xylan biomass, produced short-chain (DP 2–6) XOS (Figure 5.9). Similar results were obtained in previous reports on xylanases [41, 42]. The production of XOS of similar DP at moderate temperatures highlights the suitability of xylanases in bioprocesses that are preferably performed with less (heat) energy input. Nonetheless, the HPLC-based estimation of XOS yield by the xylanases does not include the concentration of DP 3 and higher oligosaccharides, that are visible in TLC (Figures 5.9a-c). The XOS is reported to have the capability of proliferating the population of

beneficial gut microflora [44, 45]. Further, the XOS of this DP range (2-6) has enormous intestinal health potential and anti-cancerous prospects [7]. Hydrolysis of starter and grower feeds produced XOS that migrated in between the standards on TLC (Figure 5.9). This observation could be attributed to several factors. One possibility is the presence of XOS with chain lengths different from those represented by the standards used in the TLC analysis. This suggests the existence of additional XOS variants that were not included in the specific set of standards employed. Furthermore, the presence of structural isomers or impurities in the sample may also contribute to the observed migration behaviour. Analytical limitations, such as plate quality or the choice of solvent system, could also influence the migration pattern [44].

5.4.4 Effect of feed hydrolysates on cell viability

The potential toxic effects of the feed hydrolysates produced by the xylanolytic treatments were examined by the MTS assay on HEK293 cells. Using the standard curve of HEK293 cells at 490 nm (Appendix IV, supplementary Figure 7), the cell viability was determined. Cells were deemed to be viable at absorbances above 0.9 (also indicated by the red horizontal line in the Figures below) and samples were considered to be toxic to the HEK293 cells when the absorbance was below 0.9. The HEK293 cells were treated with different concentrations of each hydrolysis sample for 48 h and the results of cell viability (Figure 5.11) indicated that they were not toxic to HEK293 cells at dilutions ranging from 1:5 to 1:50 (0.5-2 mg/ml). In the MTS assay, a significant decrease in viability of HEK293 cells was observed for all the undiluted hydrolysates (Figure 5.11). In contrast, little or no cytotoxic effect was observed for the HEK293 cells for all the hydrolysate concentrations (0.5-2 mg/ml). In contrast some samples appeared to have a stimulatory effect on the cells, especially E1+GF, E2+GF and E3+GF. Batsalova et al. [45] performed cytotoxicity studies on human cell lines derived from healthy tissue (MRC-5 lung fibroblasts) and different cancer cell lines (A549 lung adenocarcinoma, HT-29 colon adenocarcinoma, and U-937 histiocytic lymphoma) with pure XOS. Their studies showed an

antitumor potential of the sample because XOS treatment led to stronger cytotoxic effects in tumour cell lines compared with the MRC-5 fibroblasts. The data showed that the higher the concentrations of XOS, the higher the inhibition of cells, which confirmed the tumour-specific cytotoxic effect of the XOS sample.

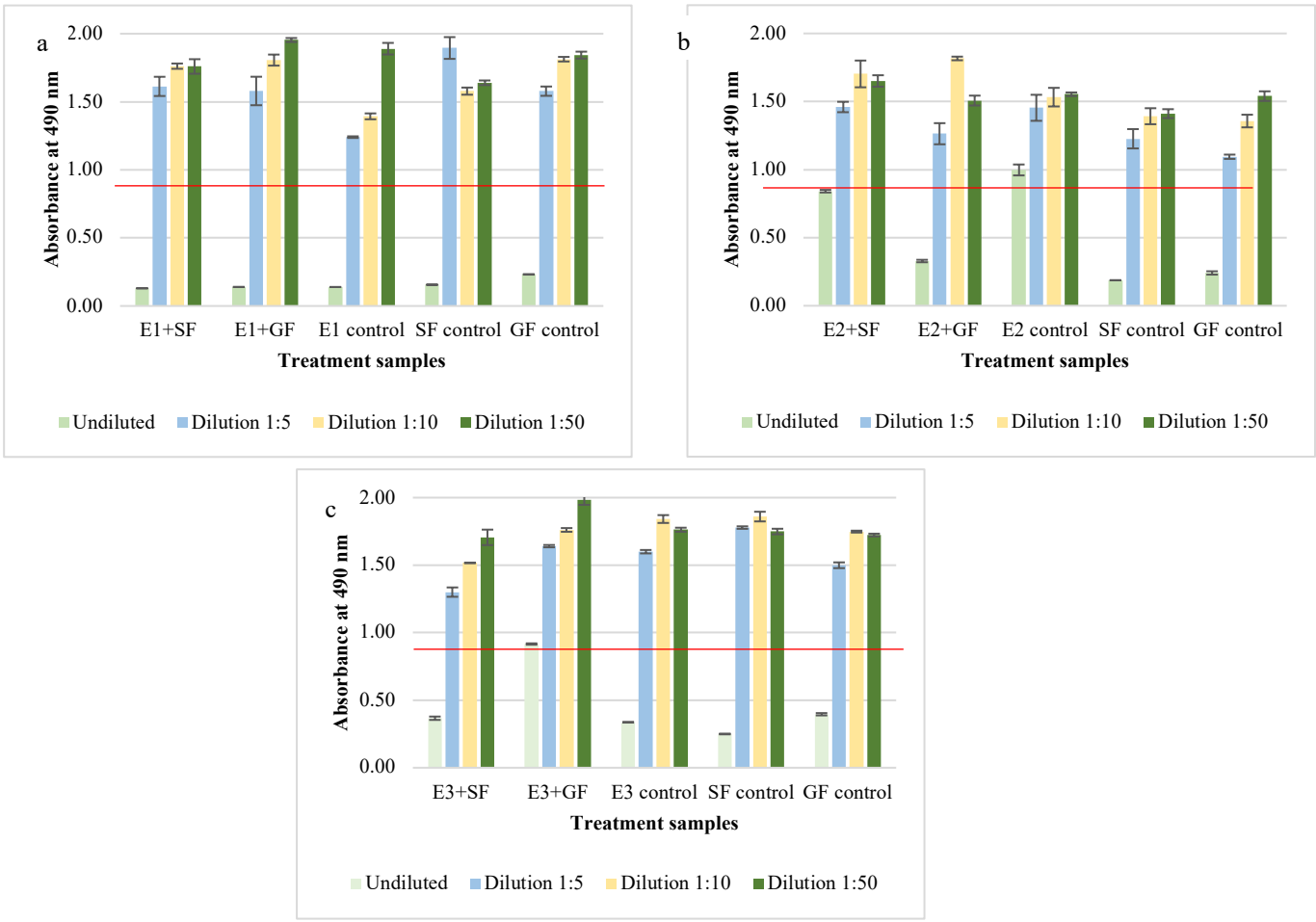

Figure 5.11: Cytotoxicity of hydrolysate products: crude *T. harzianum* xylanase (a), purified *T. harzianum* xylanase (b) and purified recombinant XT6 xylanase (c) on starter and grower chicken feeds with HEK293 cells, respectively, after 48 h of incubation with different hydrolysate concentrations. All experiments were performed in triplicate and the data expressed as mean ± SD.

5.5 Conclusions

The present study established the potential of native *T. harzianum* and recombinant *G. stearothermophilus* xylanases for an enhanced production of hydrolysate products, especially XOS from starter and grower chicken feeds. Starter feed hydrolysis resulted in higher yields of reducing sugars compared to grower feed. Overall, the purified *T. harzianum* xylanase resulted in a higher yield of reducing sugars compared to the crude *T. harzianum* xylanase and recombinant XT6 xylanase. The RSM efficiently optimized the yield of reducing sugars and quantified the interactive effects of the significant variables. The xylanases were efficient in releasing short-chain XOS (xylobiose, xylotriose, xylotetraose, and xylopentaose) and monosaccharides (glucose, galactose, and mannose), with xylobiose being the dominant product. All the undiluted hydrolysates were toxic to the HEK293 cells. The diluted hydrolysates on the other hand displayed an inverse concentration-dependent toxicity with a few displaying stimulatory effects on cell viability. This points to interesting prospects for future studies and application of XOS as prebiotics in the feed industry to reduce viscosity and improve the gut microbiota.

5.6 References

[1] McLoughlin, R.F., Berthon, B.S., Jensen, M.E., Baines, K.J., & Wood, L.G. (2017). Short-chain fatty acids, prebiotics, synbiotics, and systemic inflammation: A systematic review and meta-analysis. *The American Journal of Clinical Nutrition.* 106*,* 930–945.

[2] Passos, A.A. *et al.* (2015). Effect of dietary supplementation of xylanase on apparent ileal digestibility of nutrients, viscosity of digesta, and intestinal morphology of growing pigs fed corn and soybean meal-based diet. *Animal Nutrition*. 1*,* 19–23.

[3] Duarte, M.E., Zhou, F.X., Dutra, W.M., & Kim, S.W. (2019). Dietary supplementation of xylanase and protease on growth performance, digesta viscosity, nutrient digestibility, immune and oxidative stress status, and gut health of newly weaned pigs. *Animal Nutrition*. 5*,* 351–358.

[4] Duarte, M.E., Tyus, J., & Kim, S.W. (2020). Synbiotic effects of enzyme and probiotics on intestinal health and growth of newly weaned pigs challenged with enterotoxigenic F18+*Escherichia coli. Frontiers in Veterinary Science*. 7.

[5] Aragon, C.C. *et al.* (2018). Production of Xylo-oligosaccharides (XOS) by controlled hydrolysis of Xylan using immobilized Xylanase from *Aspergillus niger* with improved properties. *Integrative Food Nutrition and Metabolism.* 5.

[6] Donaldson, J. *et al.* (2021). A modern hybrid rye, as an alternative energy source for broiler chickens, improves the absorption surface of the small intestine depending on the intestinal part and xylanase supplementation. *Animals.* 11, 1349.

[7] Saini, R. *et al.* (2022). Recent advancements in prebiotic oligomers synthesis via enzymatic hydrolysis of lignocellulosic biomass. *Bioengineered*. 13(2): 2139-2172.

[8] Dong, C.D. *et al.* (2023). Bioprocess development for the production of xylooligosaccharides prebiotics from agro-industrial lignocellulosic waste. *Heliyon.* 9(7): 18316.

[9] Malgas, S., & Pletschke, B.I. (2019). The effect of an oligosaccharide reducing-end xylanase, BhRex8A, on the synergistic degradation of xylan backbones by an optimised xylanolytic enzyme cocktail. *Enzyme and Microbial Technology*. 122, 74-81.

[10] Carvalho, A.F.A., Neto, P.D.O., da Silva, D.F., & Pastore, G.M. (2013). Xylo-oligosaccharides from lignocellulosic materials: chemical structure, health benefits and production by chemical and enzymatic hydrolysis. *Food Research International.* 51, 75–85.

[11] Gurpilhares, D.D.B., Cinelli, L.P., Simas, N.K., Pessoa Jr, A., & Sette, L.D. (2019). Marine prebiotics: polysaccharides and oligosaccharides obtained by using microbial enzymes. *Food Chemistry*. 280, 175–186

[12] Zhang, J., Wang, Y.H., Wei, Q.Y., Du, X.J., & Qu, Y.S. (2018). Investigating desorption during ethanol elution to improve the quality and antioxidant activity of xylo- oligosaccharides from corn stalk. *Bioresource Technology.* 249, 342–347.

[13] Zhao, C. *et al.* (2017). Functional properties, structural studies and chemo-enzymatic synthesis of oligosaccharides. *Trends in Food Science and Technology*. 66, 135–145.

[14] Bertacchi, S., Jayaprakash, P., Morrissey, J.P., & Branduardi, P. (2022). Interdependence between lignocellulosic biomasses, enzymatic hydrolysis and yeast cell factories in biorefineries. *Microbial Biotechnology.* 15(3): 985-995.

[15] Shehata, A.A. *et al.* (2022). Probiotics, prebiotics, and phytogenic substances for optimizing gut health in poultry. *Microorganisms.* 10(2): 395.

[16] Morgan, N.K., Wallace, A., Bedford, M.R., & Choct, M. (2017). Efficiency of xylanases from families 10 and 11 in production of xylo-oligosaccharides from wheat arabinoxylans. *Carbohydrate Polymers*. 167, 290–296.

[17] Qian, S. *et al.* (2020). Evaluation of an efficient fed-batch enzymatic hydrolysis strategy to improve production of functional xylooligosaccharides from maize straws. *Industrial Crops and Products.* 157, 112920.

[18] Wu, W.J., & Ahn, B.Y. (2018). Statistical optimization of medium components by response surface methodology to enhance menaquinone-7 (vitamin k2) production by *Bacillus subtilis*. *Journal of Microbiology and Biotechnology.* 28(6): 902-908.

[19] Dhaver, P., Pletschke, B., Sithole, B., & Govinden, R. (2022). Optimization, purification, and characterization of xylanase production by a newly isolated *Trichoderma harzianum* strain by a two-step statistical experimental design strategy. *Scientific Reports.* 12(1): 17791.

[20] Joshi, N., Sharma, M. & Singh, S.P. (2020). Characterization of a novel xylanase from an extreme temperature hot spring metagenome for xylooligosaccharide production. *Applied Microbiology and Biotechnology.* 104, 4889–4901.

[21] Khangwal, I., Nath, S., Kango, N., Shukla, P. (2020). Endo-xylanase induced xylooligosaccharides production from corn cobs, its structural features, and concentration-dependent antioxidant activities. *Biomass Conversion and Biorefinery.* 12, 1-11.

.

[22] Georgeta-Simona, S. *et al.* (2016). HPLC method for quantification of five compounds in a parenteral form used in treatment of companion animals. *Journal of Chromatographic Science*. 54(9): 1567–1572.

[23] Pu, J., Zhao, X., Wang, Q., Wang, Y., & Zhou, H. (2016). Development and validation of a HPLC method for determination of degree of polymerization of xylo-oligosaccharides. *Food Chemistry.* 213, 654–659.

[24] Ghasemi, M., Turnbull, T., Sebastian, S., & Kempson, I. (2021). The MTT Assay: utility, limitations, pitfalls, and interpretation in bulk and single-cell analysis. *International Journal of Molecular Science*. 22(23): 12827.

[25] Stockert, J.C., Horobin, R.W., Colombo, L.L. & Blázquez-Castro, A. Tetrazolium salts and formazan products in Cell Biology: Viability assessment, fluorescence imaging, and labelling perspectives. *Acta Histochemica.* 120, 159–167.

[26] Tan, E., Chin, C.S.H., Lim, Z.F.S., & Ng, S.K. (2021). Hek293 cell line as a platform to produce recombinant proteins and viral vectors. *Frontiers in Bioengineering and Biotechnology*. 9: 796991.

[27] Perumal, P.O. *et al.* (2019). Cytoproliferative and anti-oxidant effects induced by tannic acid in human embryonic kidney (Hek-293) cells. *Biomolecules*. 9(12): 767.

[28] Ataei, D., Hamidi-Esfahani, Z., & Ahmadi-Gavlighi, H. (2020). Enzymatic production of xylooligosaccharides from date (*Phoenix dactylifera L.*) seed. *Food Science and Nutrition.* 8(12): 6699-6707.

[29] Chapa, D., Pandit, P., & Shah, A. (2012). Production of xylooligosaccharides from corncob xylan by fungal xylanase and their utilization by probiotics. *Bioresource Technology*. 115, 215-221.

[30] Ai, Z. *et al.* (2005). Immobilization of *Streptomyces olivaceoviridis* E-86 xylanase on Eudragit S-100 for xylo- oligosaccharide production. *Process Biochemistry*. 40, 2707–2714.

[31] Yoon, K.Y., Woodams, E.E., & Hang, Y.D. (2006). Enzymatic production of pentoses from the hemicellulose fraction of corn residues. *LWT-Food Science and Technology.* 39, 387–391.

[32] Sun, Q. *et al.* (2023). Optimization of pre-treatment and enzymatic hydrolysis coupled with ultrasonication for the production of xylooligosaccharides from corn cob. *Biomass Conversion and Biorefinery.* (2023).

[33] Gowdhaman, D., & Ponnusami, V. (2015). Production and optimization of xylooligosaccharides from corncob by *Bacillus aerophilus* KGJ2 xylanase and its antioxidant potential. *International Journal of Biology and Macromolecules.* 79: 595-600.

[34] Yang, R., Xu, S., Wang, Z., & Yang, W. (2005). Aqueous extraction of corncob xylan and production of xylooligosaccharides. *LWT - Food Science and Technology*. 38, 677–682.

[35] Yan, F. *et al.* (2022). Preparation and nutritional properties of xylooligosaccharides from agricultural and forestry by-products: A comprehensive review. *Frontiers in Nutrition.* 9: 977548.

[36] Li, Y. *et al.* (2022). Identification and characterization of a novel endo-β-1,4-xylanase from *Streptomyces* sp. T7 and its application in xylo-oligosaccharide production. *Molecules*. 27(8): 2516.

[37] Rahmani, N. *et al.* (2019). GH-10 and GH-11 Endo-1, 4-β-xylanase enzymes from *Kitasatospora* sp. produce xylose and xylooligosaccharides from sugarcane bagasse with no xylose inhibition. *Bioresource Technology*. 272, 315-325.

[38] Hegazy, U.M. *et al.* (2019). Revealing of a novel xylose-binding site of *Geobacillus stearothermophilus* xylanase by directed evolution. *The Journal of Biochemistry,* 165(2): 177-184.

[39] Rashin, R. & Sohail, M. (2022). Xylanolytic *Bacillus* species for xylooligosaccharides production: A critical review. *Bioresources and Bioprocessing.* 8(16): 2021.

[40] Su, Y. *et al.* (2021). Efficient production of xylooligosaccharides rich in xylobiose and xylotriose from poplar by hydrothermal pre-treatment coupled with post-enzymatic hydrolysis. *Bioresource Technology.* 342, 125955.

[41] Valladares-Diestra, K.K., de Souza Vandenberghe, L.P., & Soccol, C.R. (2022). Integrated xylooligosaccharides production from imidazole-treated sugarcane bagasse with application of in house produced enzymes. *Bioresource Technology*. 362*,* 127800.

[42] Finegold, S. *et al.* (2014). Xylooligosaccharides increases bifidobacteria but not lactobacilli in human gut microbiota. *Food and Function*. 5.

[43] De Maesschalck, C. *et al.* (2015). Effects of xylo-oligosaccharides on broiler chicken performance and microbiota. *Applied and Environmental Microbiology*. 81(17): 8-5880.

[44] Sithole, T. Cloning, expression, partial characterization and application of a recombinant GH10 xylanase, XT6, from *Geobacillus stearothermophilus* T6 as an additive to chicken feeds. (ORCID ID: 0000-00030-2058-5571) Master's thesis, Rhodes University, Grahamstown (EC), 2022.

[45] Batsalova, T., Georgiev, Y., Moten, D., Teneva, I., & Dzhambazov, B. (2022). Natural xylooligosaccharides exert antitumor activity via modulation of cellular antioxidant state and TLR4. *International Journal of Molecular Science*. 23(18): 10430.

[46] Biasato, I. *et al.* (2018). Modulation of intestinal microbiota, morphology and mucin composition by dietary insect meal inclusion in free-range chickens. *BMC Veterinary Research*. 14(1): 1-15.

[47] El-Deek, A.A. *et al.* (2020). Alternative feed ingredients in the finisher diets for sustainable broiler production. *Scientific Reports.* 10(1): 1-9.

[48] Saleh, E.A., Watkins, S.E., & Waldroup, P.W. (1997). Changing time of feeding starter, grower, and finisher diets for broilers 2. birds grown to 2.2 kg. *Journal of Applied Poultry Research.* 6(1): 64- 73.

[49] Dhaver, P., Pletschke, B., Sithole, B. & Govinden, R. Isolation, screening and partial optimization of thermostable xylanase production under submerged fermentation by fungi in Durban, South Africa. *Mycology.* 13(4): 271-292

[50] R Core Team. R: A language and environment for statistical computing. R Foundationfor Statistical Computing, Vienna, Austria. URL http://www.R-project.org/. (2020).

[51] Singh, N., Sithole, B., Kumar, A., & Govinden, R. (2023). A glucose tolerant β-glucosidase from a newly isolated *Neofusicoccum parvum* strain F7: production, purification, and characterization. *Scientific Reports.* 13(1): 5134.

CHAPTER SIX

GENERAL CONCLUSIONS AND FUTURE RECOMMENDATIONS

6.1 General conclusions

The enzymatic hydrolysis of xylan has become an attractive process due to its numerous biotechnological applications in industries such as food, animal feed, waste treatment, ethanol production, textile, and pulp and paper [1]. Xylanases have gained great significance in lignocellulosic biomass saccharification, as they aid cellulose hydrolysis by first hydrolysing and removing xylan, which may act as a barrier against cellulases, yielding industrially important products [2,3].

This research study successfully identified and achieved the production of a novel thermophilic xylanase from *T. harzianum* ZNH14, a South African strain. This not only expands our understanding of enzyme catalysis at high temperatures, but also offers several practical advantages. Thermophilic xylanases have immense potential in industrial applications, such as biofuel production, food processing, and paper manufacturing. Their stability and activity at elevated temperatures make them highly desirable for these processes.

Through optimization of fermentation conditions, statistical modelling, and purification techniques, the study successfully increased xylanase production to a specific activity of 254.63 U/mg. This improvement addresses another gap in the field, as previous studies have often not found it easy to achieve high levels of enzyme activity.

The expression of recombinant XT6 xylanase, using optimization techniques, also resulted in significant increases in enzyme activity. This brings new insights to the field by demonstrating effective strategies for enhancing enzyme activity through genetic engineering and optimization.

Furthermore, the study successfully scaled up xylanase production, achieving improved activity compared to lab scale studies (145.13 to 165.18 U/ml) on a large scale with a specific activity

(4388.55 U/mg) higher than commercial XT6 xylanase (12 U/mg). This addresses a common challenge in literature, as studies have struggled to achieve efficient and cost-effective production of enzymes on a larger scale. The improved yields provide exciting potential for enhancing hydrolysate product yield and the producing xylooligosaccharides (XOS), which are valuable products with various applications.

Importantly, this study demonstrated the efficiency of xylanases in releasing short-chain XOS and monosaccharides, with promising results for using XOS as prebiotics in the feed industry. Xylobiose, a disaccharide composed of two xylose units, has been shown to have prebiotic properties. It can serve as a source of nutrition for beneficial gut bacteria, promoting their growth and activity. This can have positive effects on the overall gut health and microbiome composition, which in turn can impact various aspects of animal and human health. This addresses the need for natural, functional ingredients in animal feed, a topic of increasing interest in the field. The absence of xylose and the dominant production of xylobiose from enzymatic hydrolysis is particularly interesting, as studies have shown that xylose production can hinder the production of XOS including the non-competitive end-product inhibition of a *G. stearothermophilus* derived xylanase, XT6, by xylose. This finding can provide valuable insights into the enzymatic activity and substrate specificity of thermophilic xylanases and their potential applications.

Overall, this study has not only contributed novel insights and advancements for xylanase production but also addressed key challenges identified in the field. The findings pave the way for further development and utilization of xylanases in various industries, offering potentially more efficient and sustainable processes.

6.2 Recommendations and future perspectives

Despite being an old and time-consuming method, OFAT experiments ensure that the optimal levels are not too far from the high and low levels. In addition, it is recommended to determine the optimal pH and temperature range of enzymes for industrial purposes, especially for those

used in biorefineries which require enzymes that are efficient at high temperatures, thus it will be worthwhile to revisit determination of the temperature optima as it seems that the enzyme can withstand higher temperatures.

Due to lower xylanase yields or the inability to scale up xylanases from *T. harzianum* and *G. stearothermophilus,* the previous experience and knowledge of using these enzymes have been limited. However, this study adopted a statistical approach of selectively optimizing xylanase enzymes on a small scale, which was later scaled up to achieve more desirable activities. The xylanases exhibited favourable characteristics that make them suitable for potential application in various commercial industries, including the biofuel industry. Using these enzymes could significantly reduce process costs by eliminating the expenses associated with purchasing commercial enzymes. Thus, we recommend using a more statistical approach to optimize yield of enzymes.

It is recommended that the *T. harzianum* xylanase be scaled up in a 5-l stirred tank bioreactor and the dissolved oxygen should be optimised for the recombinant XT6 xylanase and fermentation allowed to proceed for longer periods (more than 6 days) , till the enzyme yield is seen to decrease. Production should also be further scaled up in 20-l bioreactors once these parameters have been determined.

Analysis of the chemical composition of the feeds as well as structural analysis of the produced XOS should be conducted using mass spectrometry (MS) and nuclear magnetic resonance spectroscopy (NMR). This is crucial to characterise the XOS and their degree of substitution. These factors will contribute significantly to the prebiotic effects of the XOS, thus facilitating a deeper understanding of the XOS properties. The purification of XOS is of utmost importance due to its vast potential in applications beyond animal feed improvement.

In future studies, to avoid issues around cell lysis of *E. coli* cells to release the recombinant protein of interest from the *E. coli* cells and obtain a purified protein for downstream applications. r, cell lysis can be time-consuming and may result in low protein yields or degradation. Therefore,

researchers may seek alternative expression systems that allow for protein secretion or streamlined purification methods, eliminating the need for cell lysis. Exploring such approaches could enhance the efficiency and simplicity of recombinant protein expression, facilitating its adoption in diverse experimental settings. Future studies should incorporate molecular techniques such as cloning, and recombinant DNA technology to homologously overexpress the *T. harzianum* xylanase or heterologously overexpress it in eukaryotic systems such as *Saccharomyces cerevisiae* or *Pichia pastoris*, leading to higher enzyme production levels, which could then be evaluated for various applications in industry. Thermophilic xylanases, such as those produced by the *T. harzianum* and *G. stearothermophilus*, have the ability to tolerate high temperatures, making them well-suited for biomass conversion processes. The application of thermophilic xylanases in the biofuel industry is therefore of great importance for future studies, as it may provide a viable and sustainable solution for clean energy production while minimizing costs and improving overall process efficiency.

6.3 References

[1] Bhardwaj, N., Kumar, B., & Verma, P. (2019). A detailed overview of xylanases: an emerging biomolecule for current and future prospective. *Bioresources and Bioprocessing*. 6(40): 2019.

[2] Thakur, A. *et al.* (2021). Two-step saccharification of the xylan portion of sugarcane waste by recombinant xylanolytic enzymes for enhanced xylose production. *ACS Omega*. 6(17): 11772-11782.

[3] Bedford, M.R. (2018). The evolution and application of enzymes in the animal feed industry: the role of data interpretation. *British Poultry Science*, 59(5): 486-493.

APPENDIX I: CHAPTER TWO SUPPLEMENTARY DATA

Morphology of fungal isolates on potato dextrose agar (PDA) from three selected areas

Table 1: Morphology of fungal isolates on potato dextrose agar (PDA) from isolation area 1

Fungal isolates (Area 1: Soil)	Colony morphology
C1 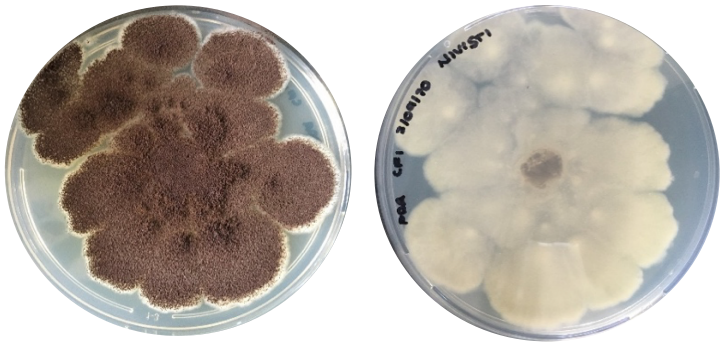	**Front:** Black colonies, with a fury off white outline and flat elevation. **Back:** Cream to light brown with white centres
C2 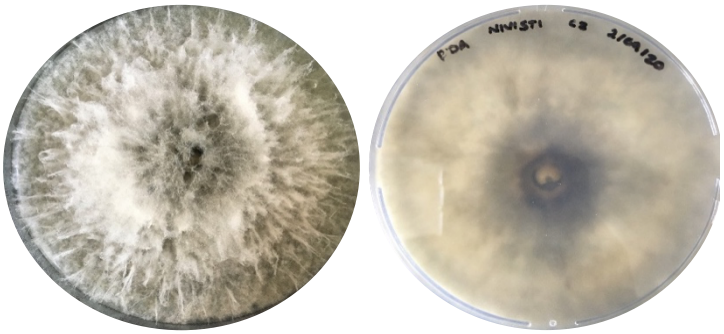	**Front:** white furry growth with dark grey centre, elevated. **Back:** cream outline with dark grey to black centre
C3 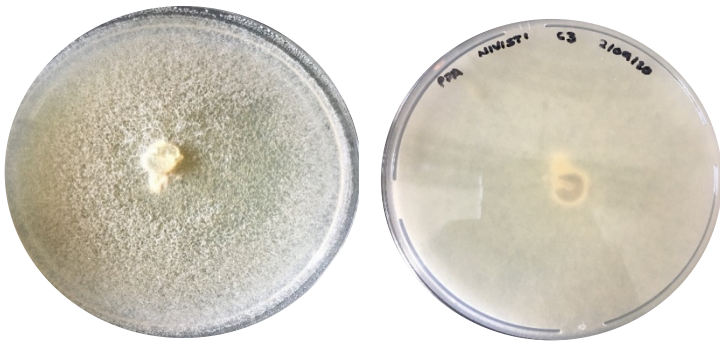	**Front:** White/light green colonies, , flat elevation. **Back:** Cream centre, white background
C4 	**Front:** White fluffy growth, elevated **Back:** Yellow colour agar, white lined surface

C5 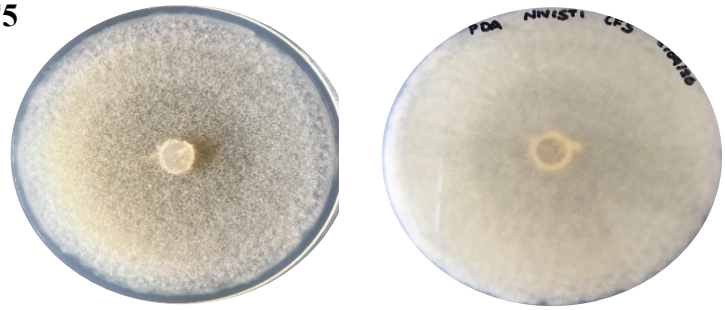		**Front:** White to light brown growth, flat elevation **Back:** Whitish brown colour with cream centre
C6 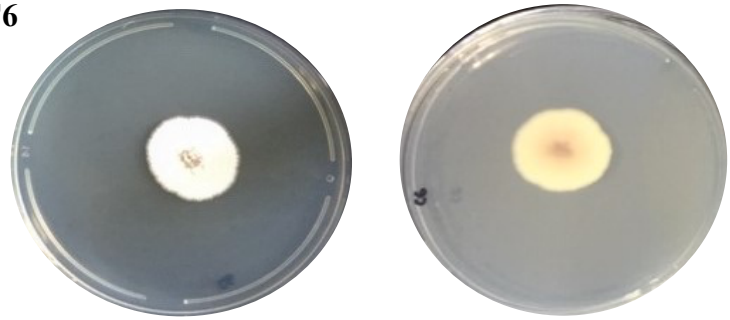		**Front:** White fluffy growth, elevated **Back:** cream colour outline, pinkish brownish centred
C7 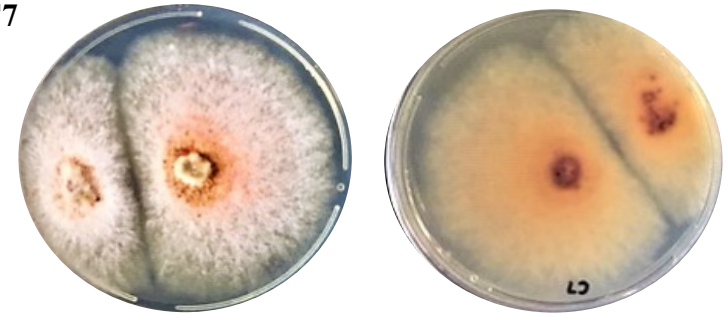		**Front:** White elevated growth with an inner pink growth and orange centres **Back:** Cream to light brown, pinkish orange centres

Fungal isolates (Area 1: Bark)	Colony morphology
CB1 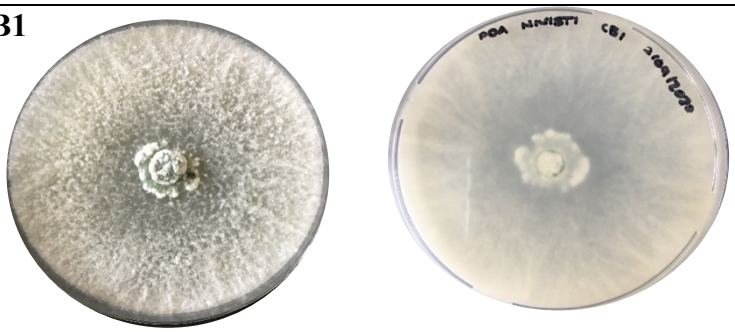	**Front:** White colonies, flat surface **Back:** White centre with cream outline
CB2 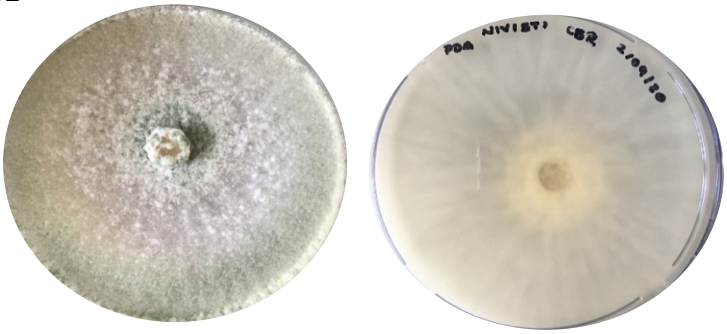	**Front:** Dark green colonies, white furry outline, flat elevation. **Back:** Yellow centre, cream outline
CB3 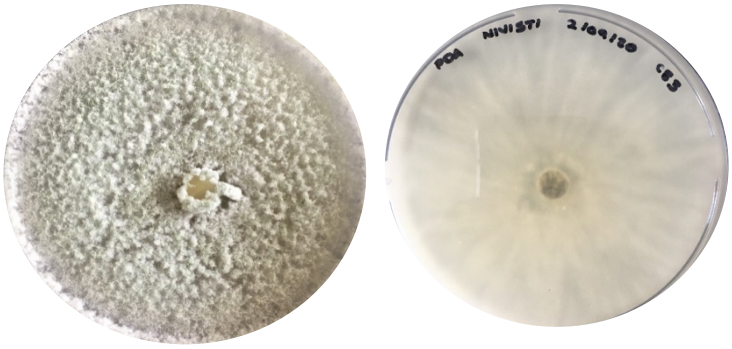	**Front:** Dark green colonies, white fluffy outline, elevated. **Back:** Grey centre, cream outline
CB4 	**Front:** Grey-green growth with cream outlines and flat surfaced **Back:** Dark yellow centres and light yellow to cream boarders

CB5 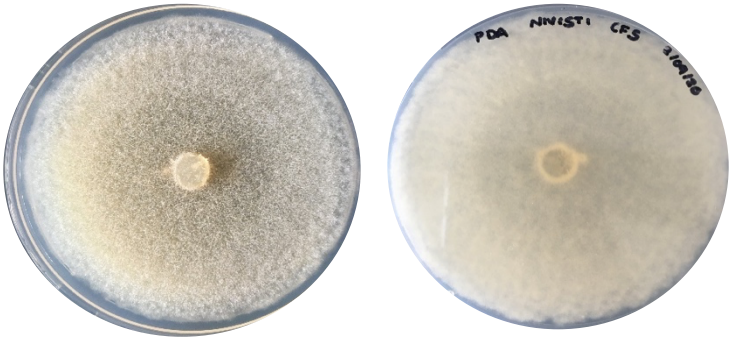	**Front:** White to light brown growth, flat elevation **Back:** Whitish brown colour with cream centre
CB6 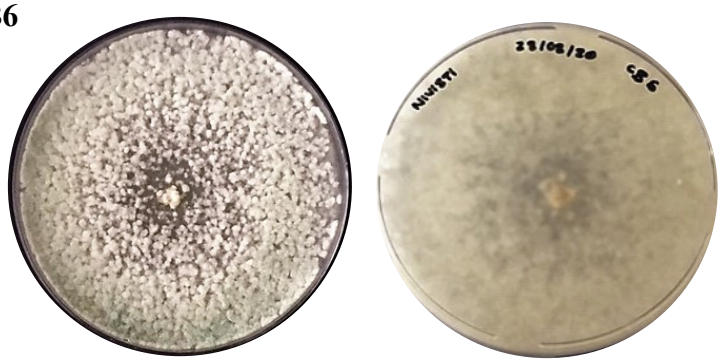	**Front:** White colonies, white fluffy circular like colonies, elevated. **Back:** Grey centre, cream outline
CB7 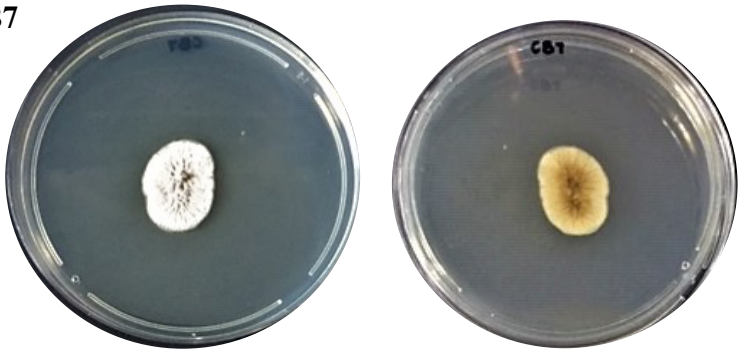	**Front:** White growth, elevated **Back:** cream colour outline, brown centred
CB8 	**Front:** White growth, elevated with grey centres **Back:** cream colour outline, brownish centred

CB9 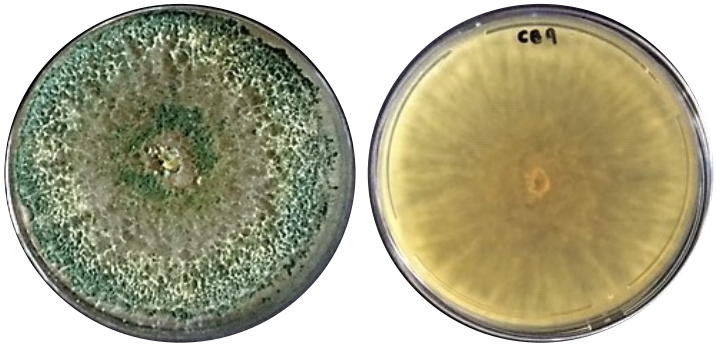	**Front:** Dark green colonies, white furry outline, flat elevation. **Back:** Yellow centre, cream outline
CB10 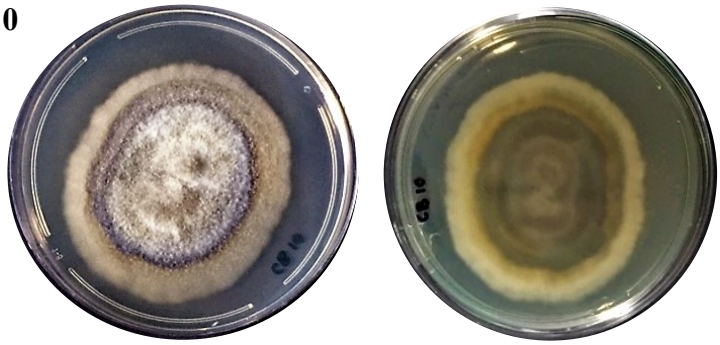	**Front:** White centre dark brown outline with a light brown boarder. **Back:** Dark brown centre with cream outline
CB11 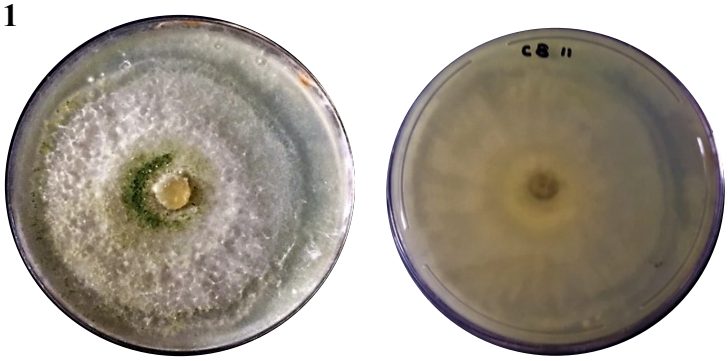	**Front:** white colonies, white furry outline, with green colonies flat elevation. **Back:** Cream centre, cream to white outline

Table 2: Morphology of fungal isolates on potato dextrose agar (PDA) from isolation area 2

Fungal isolates (Area 2: Soil)	**Colony morphology**
MS1 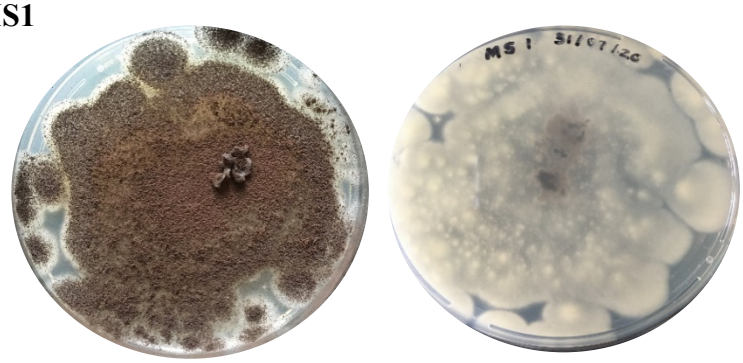	**Front:** Black colonies, with a fury off white outline and flat elevation. **Back:** Cream to light brown with white centres
MS2 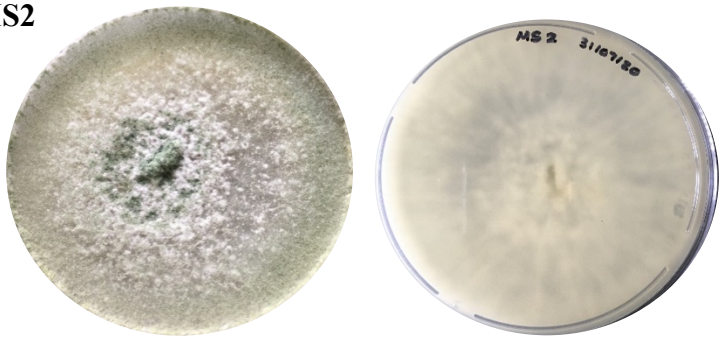	**Front:** Dark green colonies, white furry outline, flat elevation. **Back:** Yellow centre, cream outline
MS3 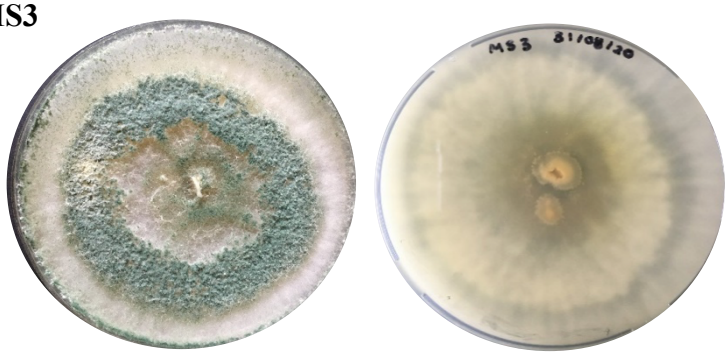	**Front:** Dark green colonies, white furry outline, flat elevation. **Back:** Yellow centre, cream outline
MS4 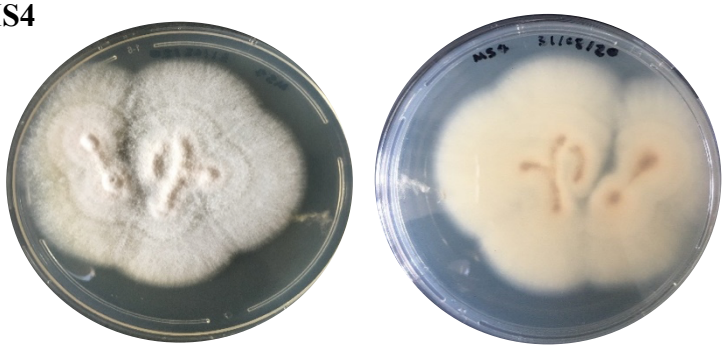	**Front:** White fluffy growth, elevated **Back:** cream colour outline, pinkish brownish centred

MS5 	**Front:** White fluffy growth towards boarder, elevated **Back:** Dark Yellow colour centre, with yellow boarder
MS6 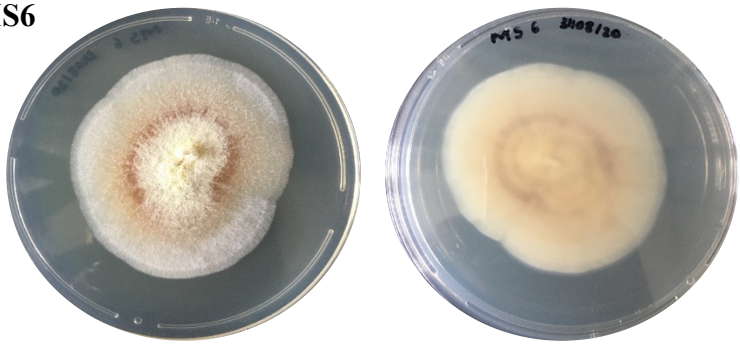	**Front:** White elevated centre with an inner pink outline and light brown boarder **Back:** Cream to light brown, pinkish centre
MS7 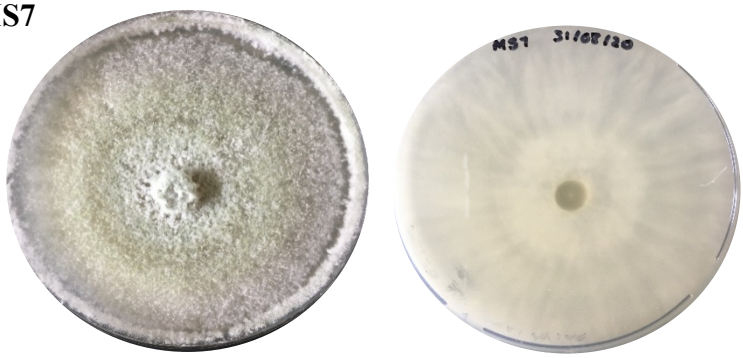	**Front:** White colonies, flat surface with white outer elevated surface **Back:** White centre with lines
MS8 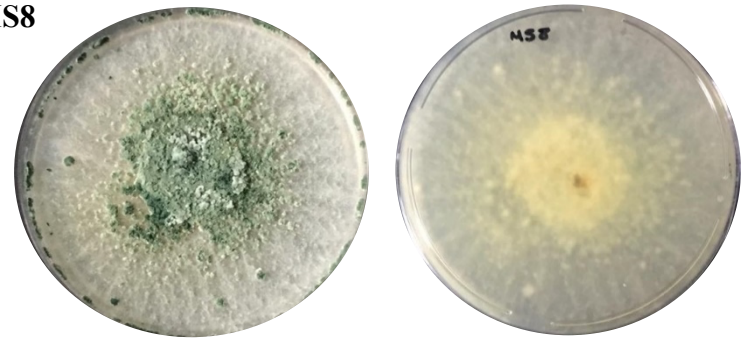	**Front:** Dark green colonies, white furry outline, flat elevation. **Back:** Yellow centre, cream outline

Fungal isolates (Area 2: Bark)	Colony morphology
MB1 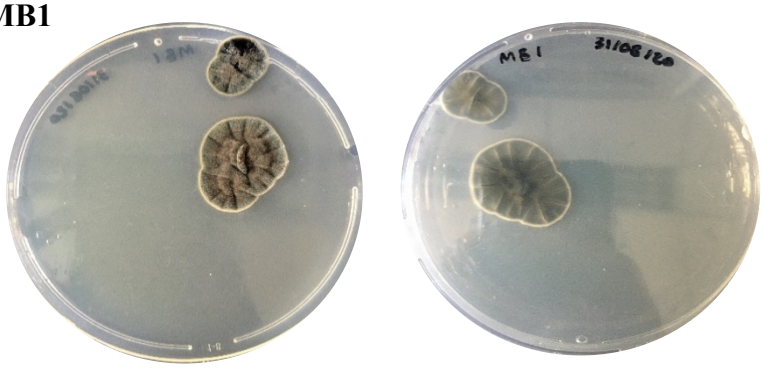	**Front:** Dark green colonies, with a fury off white outline and flat elevation. **Back:** Yellow with off white boarder
MB2 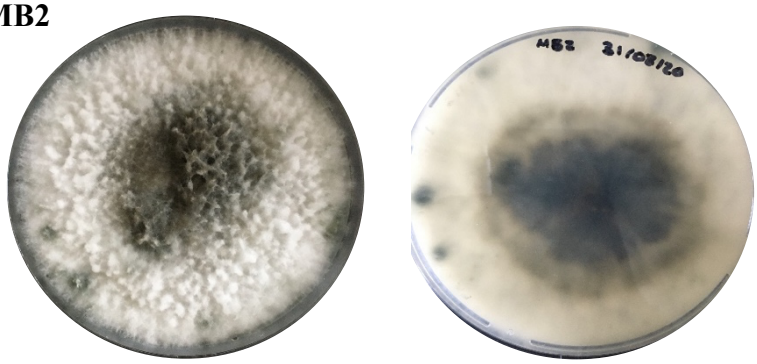	**Front:** Dark green colonies, white furry outline, flat elevation. **Back:** Yellow centre, cream outline
MB3 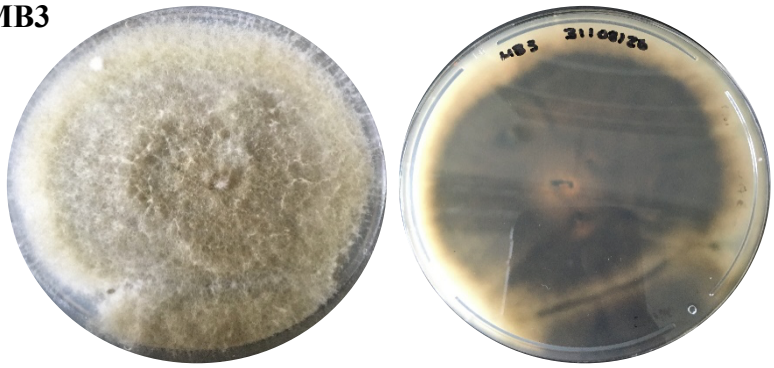	**Front:** Dark green colonies, white fluffy outline, elevated. **Back:** Yellow centre, cream outline
MB4 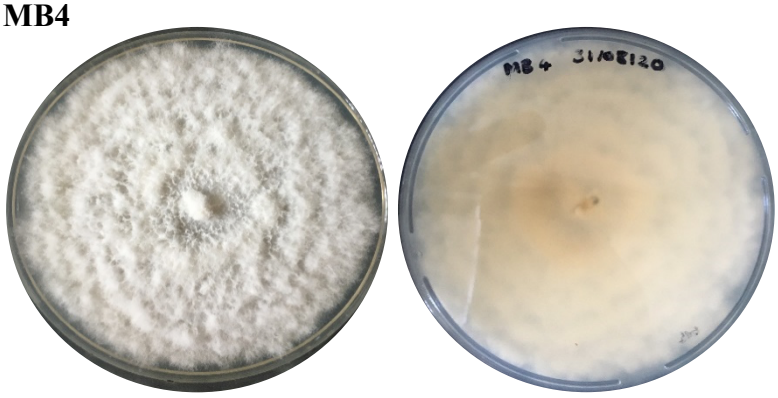	**Front:** Dark brown centre, light brown lining, fury surface, flat elevation. **Back:** Cream to light brown, dark grey centre

MB5 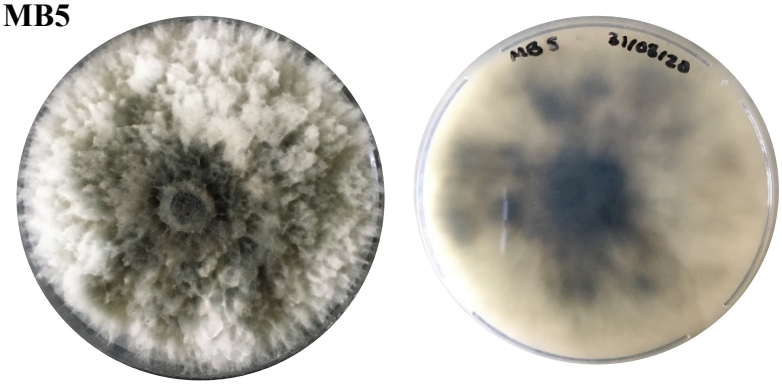	**Front:** Black centre and white margin with a raised elevation. **Back:** Cream growth with black patches.

Table 3: Morphology of fungal isolates on potato dextrose agar (PDA) from isolation area 3

Fungal isolates (Area 3: bark)	Colony morphology
PB1 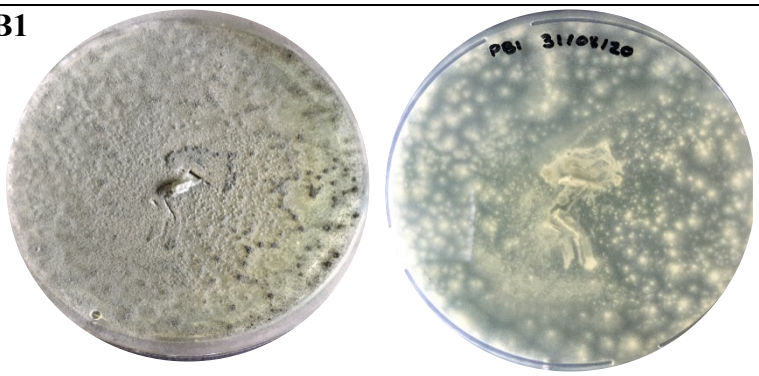	**Front:** Dark green colonies, with a powdery texture and flat elevation. **Back:** Yellow with off white
PB2 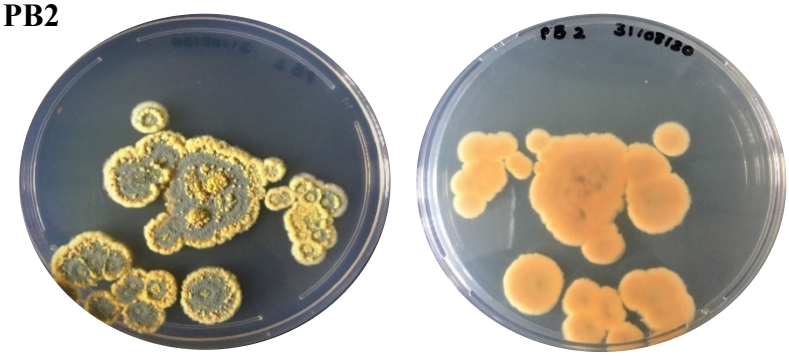	**Front:** Dark grey centres with a bright yellow elevated outline, flat surface **Back:** Dark orange with thin cream outline
PB3 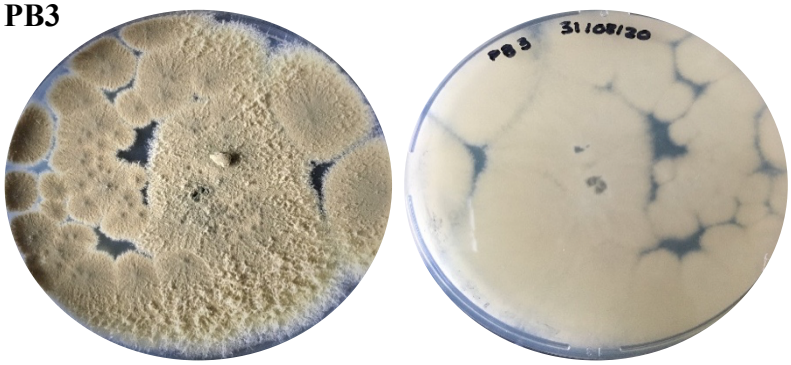	**Front:** Powdery greyish brown surface with off white outline **Back:** Off white smudged colour
PB4 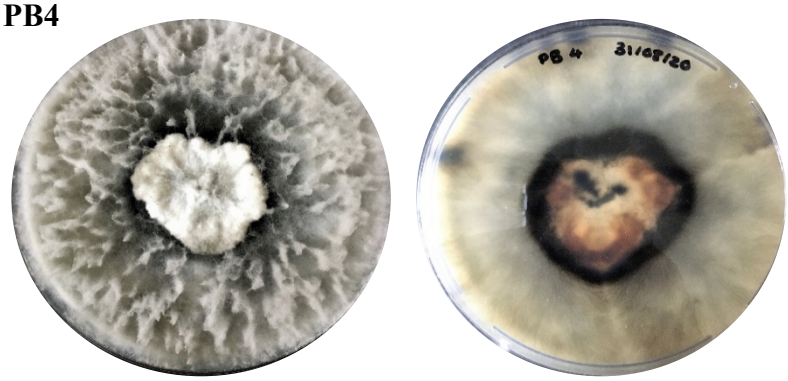	**Front:** white furry growth with white centre and a dark grey boarder, elevated. **Back:** cream outline with dark grey to black centre and pink inner

PB5 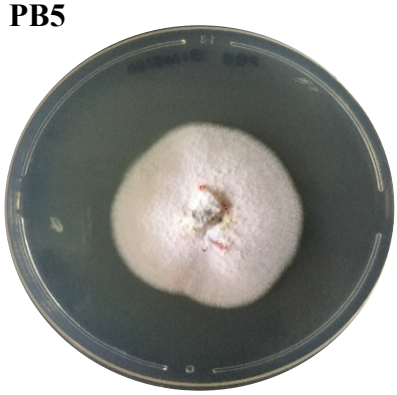 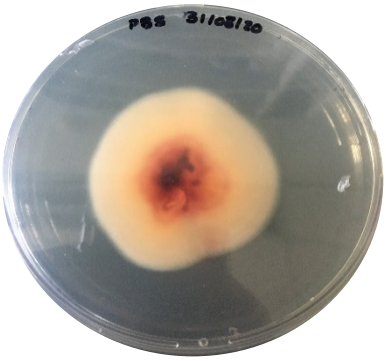	**Front:** White elevated centre with an inner pink outline and light brown boarder **Back:** Cream to light brown, pinkish centre
PB6 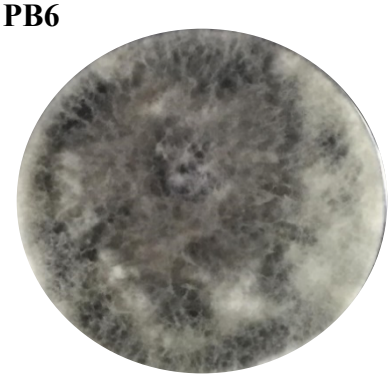 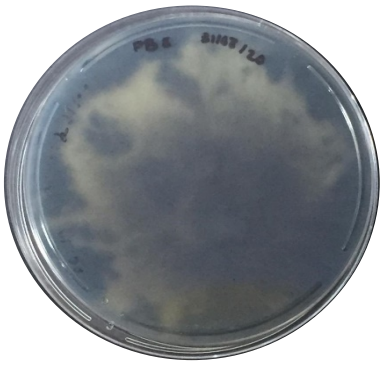	**Front:** White furry growth with white centre and a dark grey boarder, elevated. **Back:** Cream outline with dark grey to black centre
PB7 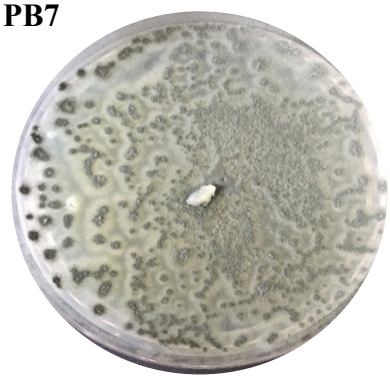 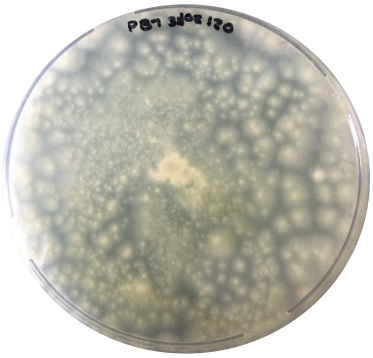	**Front:** Dark green colonies, with a powdery texture and flat elevation. **Back:** Yellow with off white
PB8 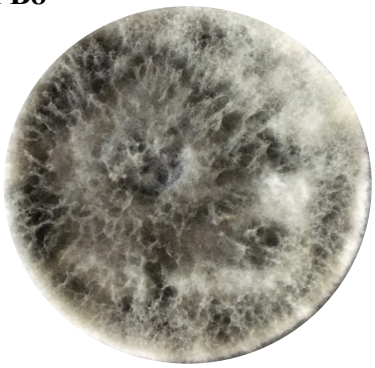 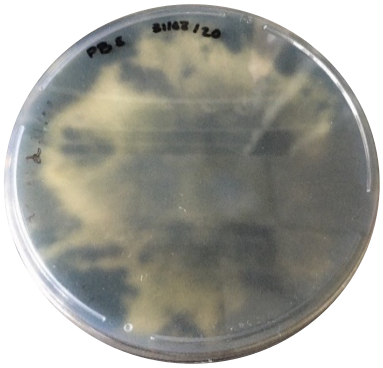	**Front:** White furry growth with white centre and a dark grey boarder, elevated. **Back:** Cream outline with dark grey to black centre

PB9 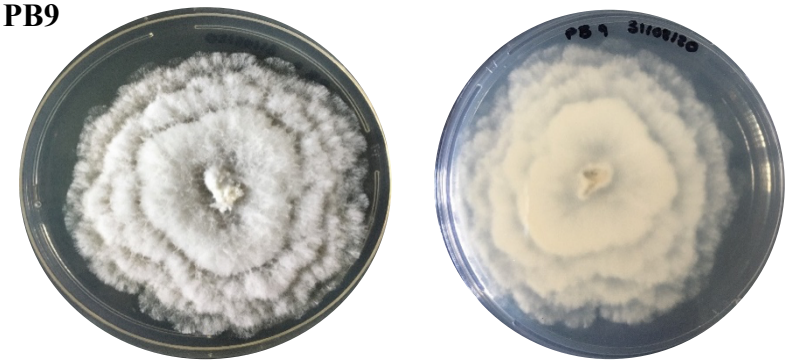	**Front:** White fluffy growth, elevated **Back:** cream colour outline, brownish centred
PB10 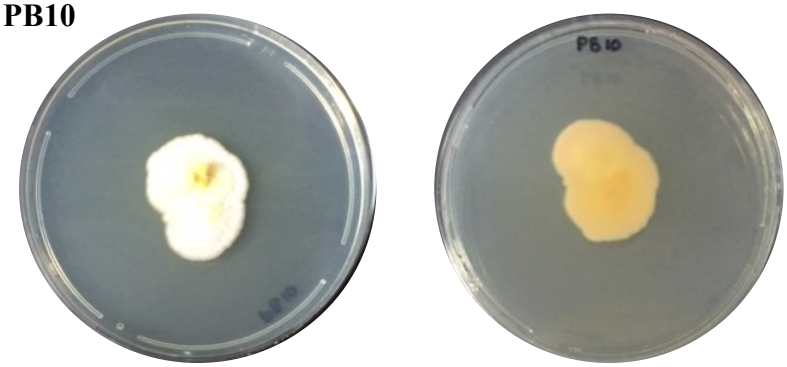	**Front:** White fluffy growth, elevated **Back:** Cream to yellow colour
PB11 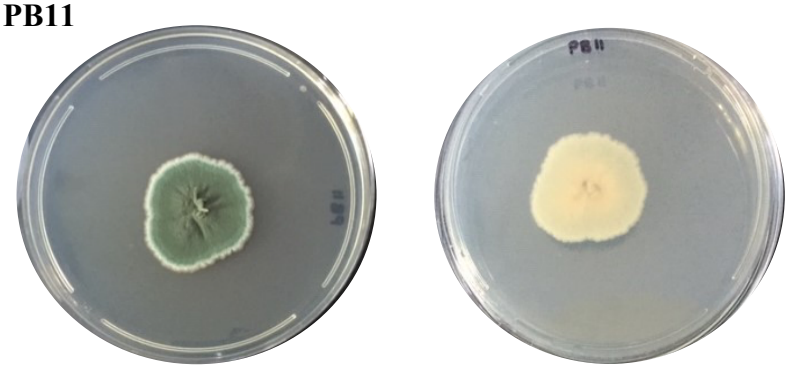	**Front:** Dark green with white outline flat surface **Back:** Cream with brownish centre

Fungal isolates (Area 3: Soil)	Colony morphology
PS1 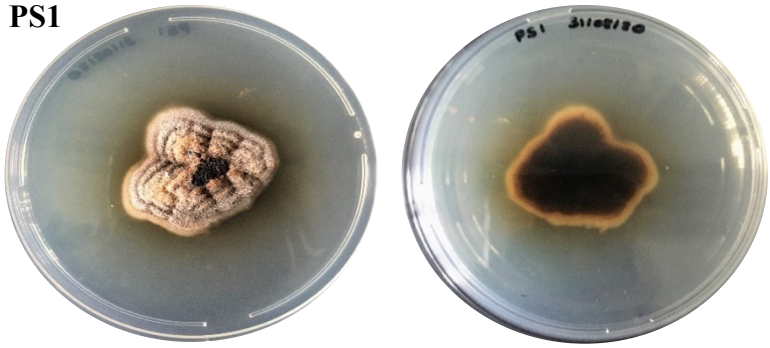	**Front:** Dark green colonies, with a fury off white outline and flat elevation. **Back:** Yellow with off white boarder
PS2 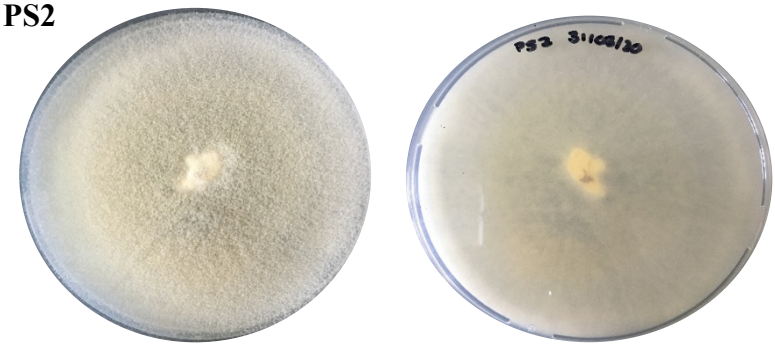	**Front:** Dark green colonies, white furry outline, flat elevation. **Back:** Yellow centre, cream outline
PS3 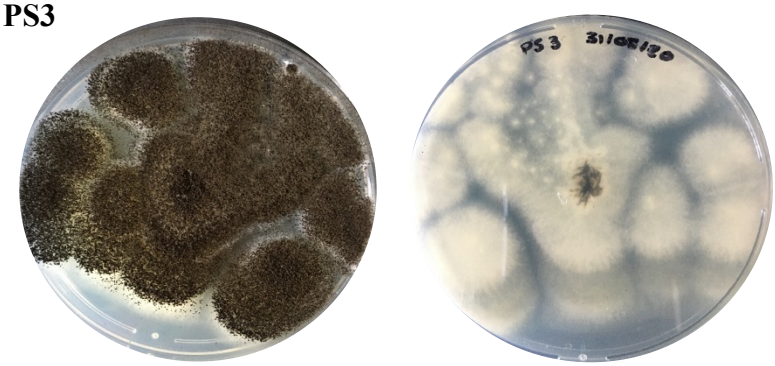	**Front:** Dark green colonies, white fluffy outline, elevated. **Back:** Yellow centre, cream outline
PS4 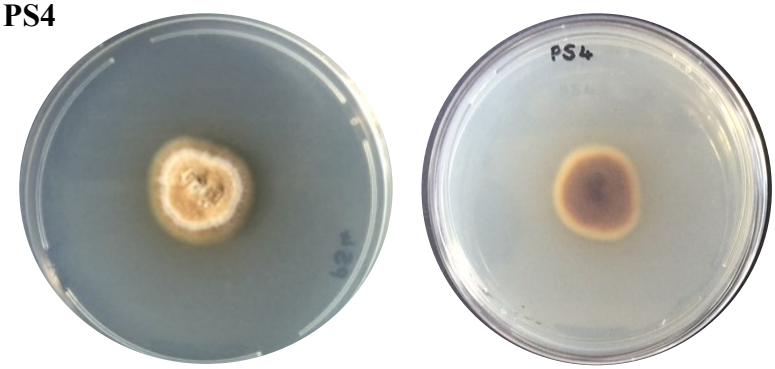	**Front:** Dark brown centre, light brown lining, fury surface, flat elevation. **Back:** Cream to light brown, dark grey centre

Xylan substrate agar plates primary and secondary screening of fungal isolates

Primary screening:

Table 4: Plate screening of fungi isolated from area 1 (Green highlight represents the isolates selected for the next screening)

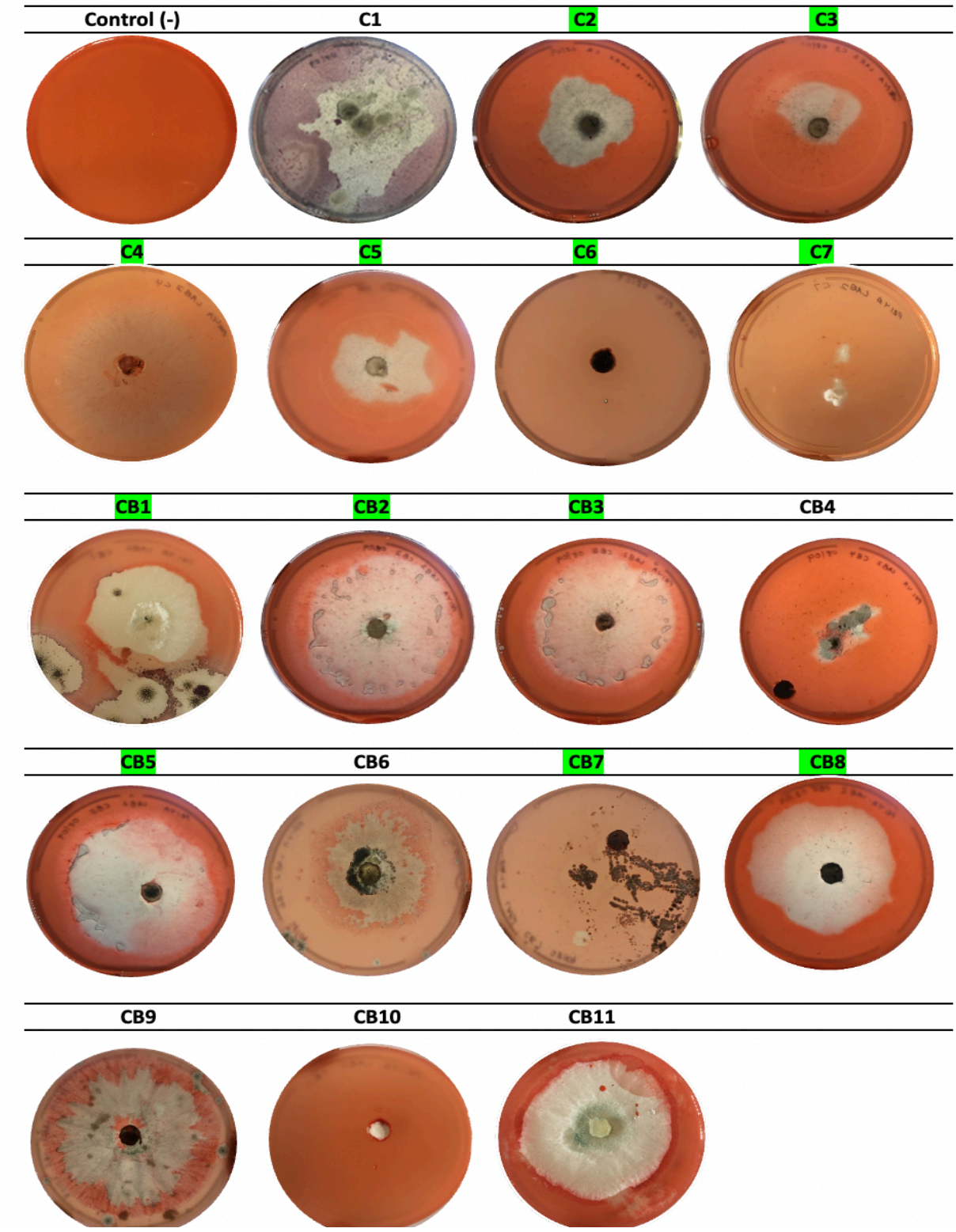

Table 5: Plate screening of fungi isolated from area 2 (Green highlight represents the isolates selected for the next screening)

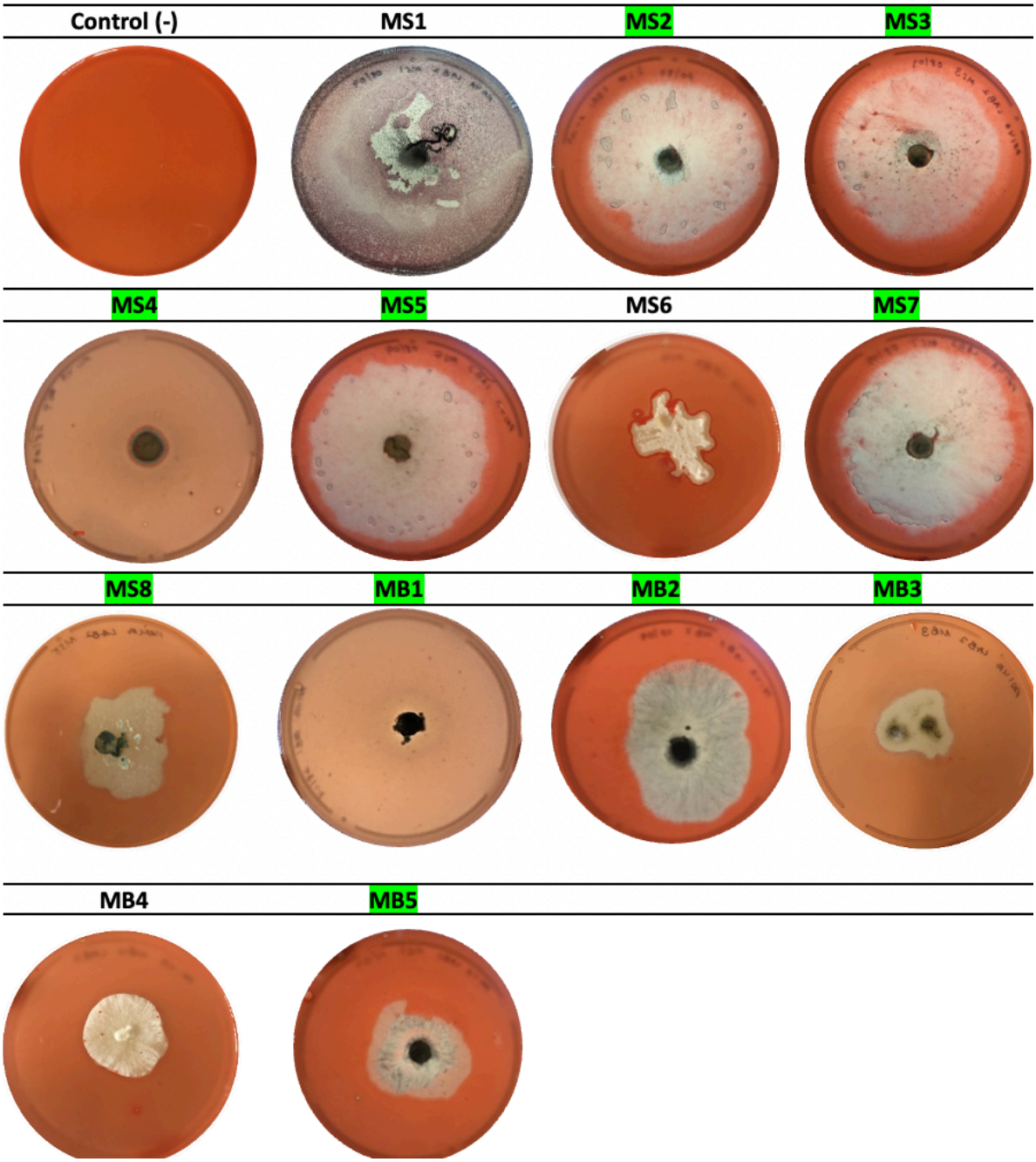

Table 6: Plate screening of fungi isolated from area 3 (Green highlight represents the isolates selected for the next screening)

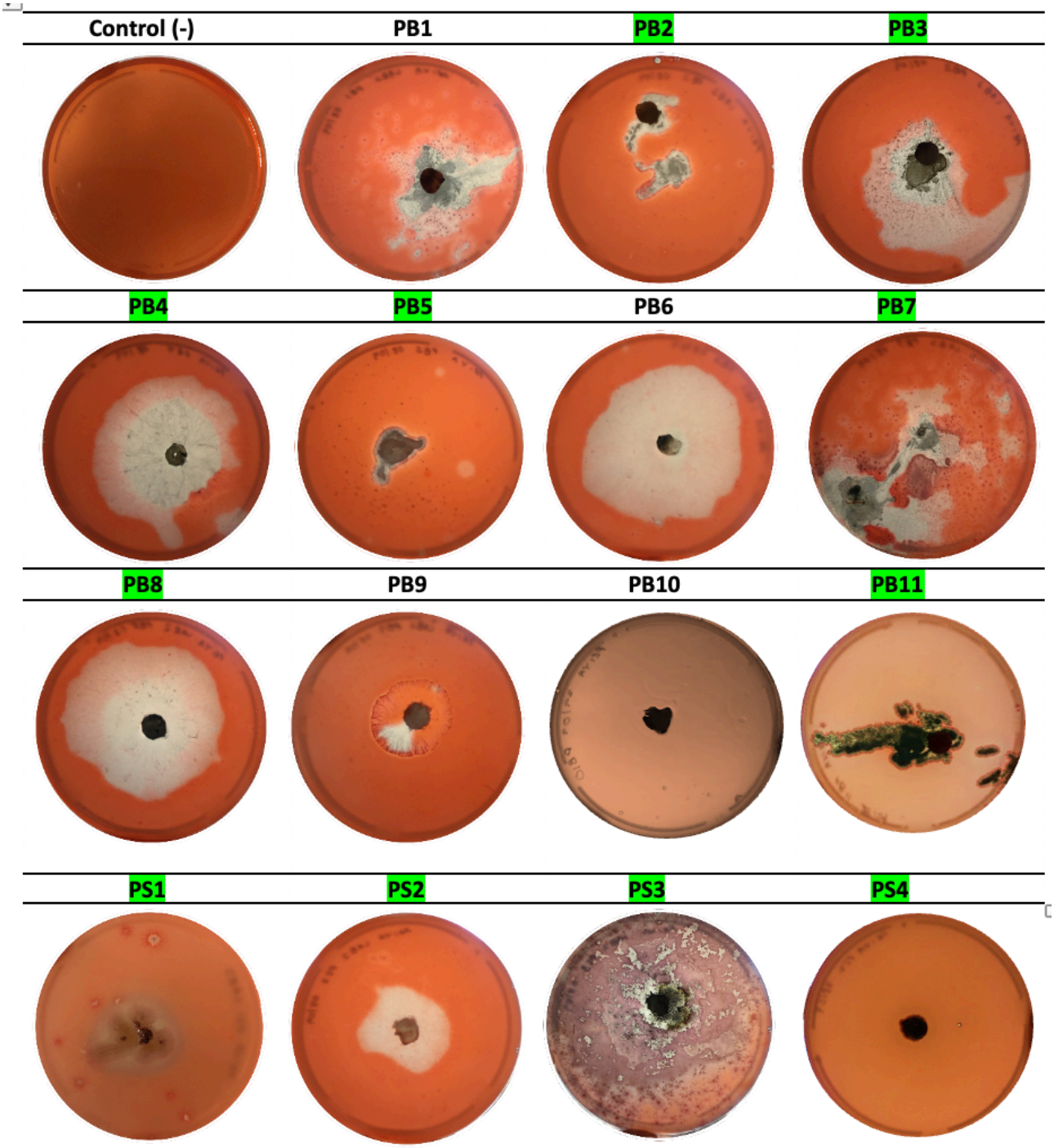

Table 7: Zones of clearance for secondary screening for area 1

Isolate	Activity
C1	–
C2	++
C3	++
C4	++
C5	++
C6	++
C7	++
CB1	++
CB2	++
CB3	++
CB4	+
CB5	++
CB6	+
CB7	++
CB8	++
CB9	+
CB10	-
CB11	-

Key: none (-), 1-2 mm (+), >2 (++)

Table 8: Zones of clearance for secondary screening for area 2

Isolate	Activity
MS1	–
MS2	++
MS3	++
MS4	++
MS5	++
MS6	+
MS7	++
MS8	++
MB1	++
MB2	++
MB3	++
MB4	+
MB5	++

Key: none (-), 1-2 mm (+), >2 (++)

Table 9: Zones of clearance for secondary screening for area 3

Isolate	Activity
PS1	++
PS2	++
PS3	++
PS4	++
PB1	+
PB2	++
PB3	++
PB4	++
PB5	++
PB6	+
PB7	++
PB8	++
PB9	+
PB10	+
PB11	++

Key: none (), 1-2 mm (+), >2 (++)

Secondary screening:

Table 10: Plate screening of fungi isolated from area 1 (Grey highlight represents the isolates selected for the next screening)

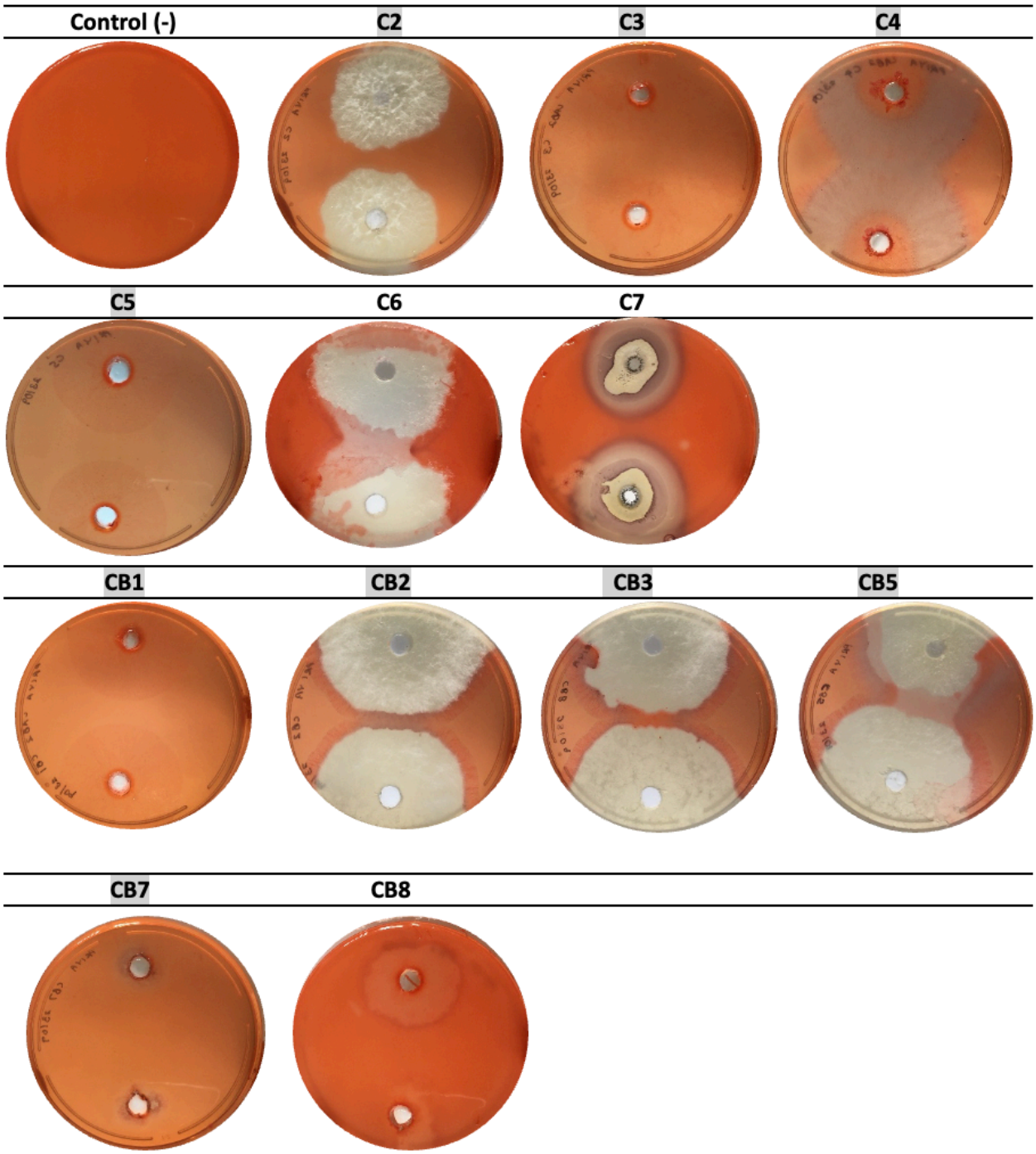

Table 11: Plate screening of fungi isolated from area 2 (Grey highlight represents the isolates selected for the next screening)

Control (-)	MS2	MS3	MS4
		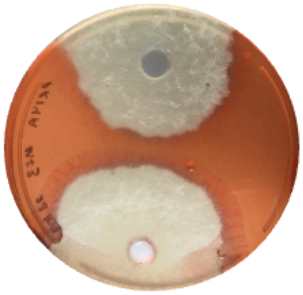	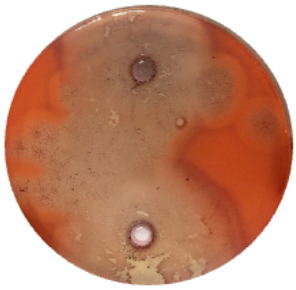
MS5	**MS7**	**MS8**	**MB1**
		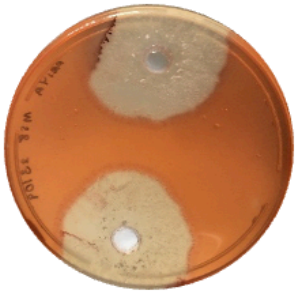	
MB2	**MB3**	**MB5**	
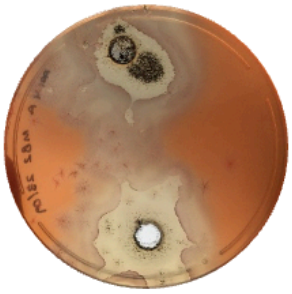			

Table 12: Plate screening of fungi isolated from area 3 (Grey highlight represents the isolates selected for the next screening)

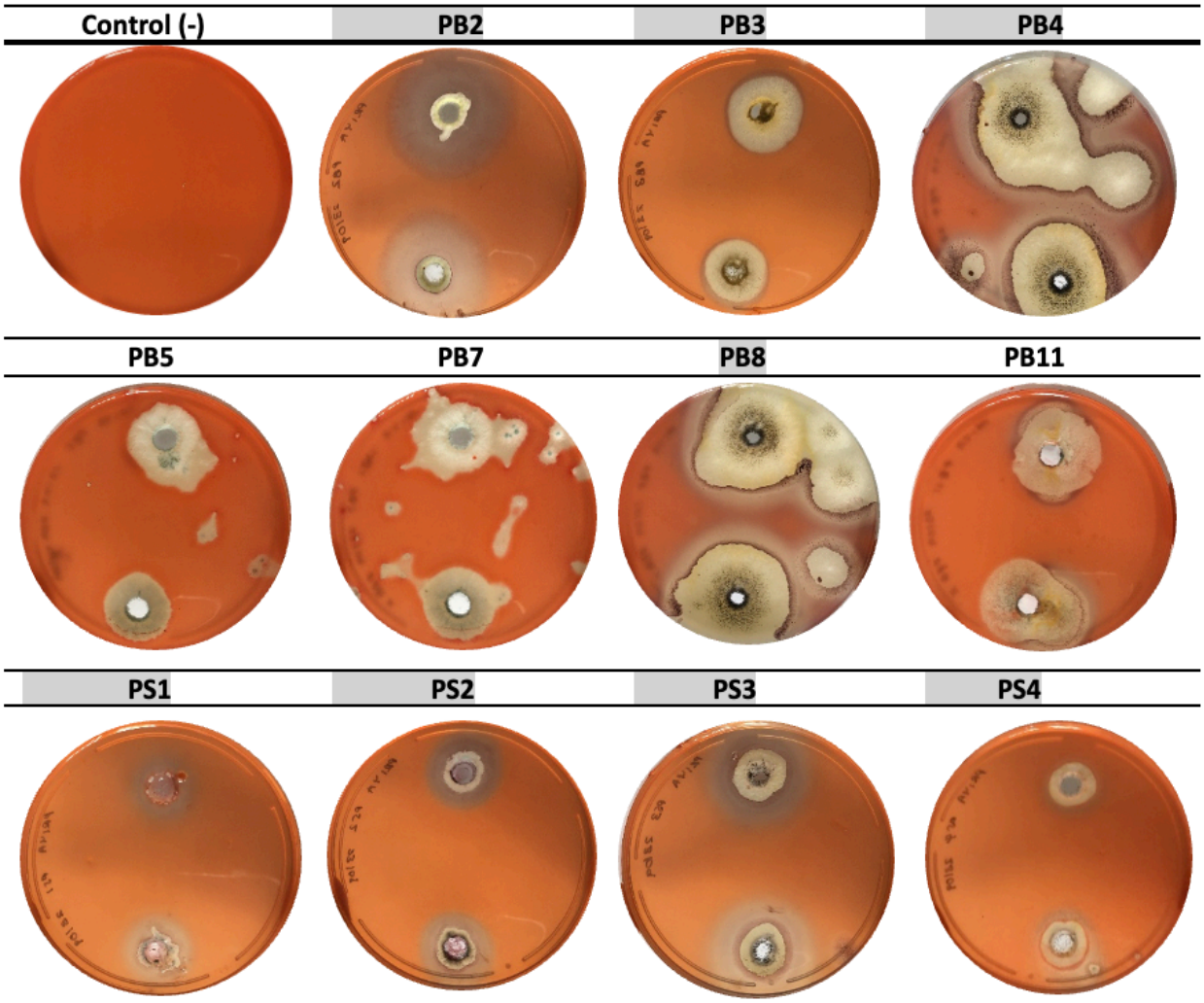

Table 13: Diameter of clearance zones representing xylanase activity for site 1 (29°49'01"S 30°56'41" E)

Isolate	Activity
C2	++
C3	++
C4	++
C5	++
C6	–
C7	–
CB1	++
CB2	++
CB3	++
CB5	++
CB7	++
CB8	–

Key: none (-), 1-2 mm (+), >2 (++)

Table 14: Diameter of clearance zones representing xylanase activity for site 2 (29º49'03"S 30º56'29" E)

Isolate	Activity
MS2	++
MS3	++
MS4	++
MS5	++
MS7	++
MS8	++
MB1	++
MB2	++
MB3	++
MB5	–

Key: none (-), 1-2 mm (+), >2 (++)

Table 15: Diameter of clearance zones representing xylanase activity for site 3 (29º16'13"S 31º22'06" E)

Isolate	Activity
PS1	++
PS2	++
PS3	++
PS4	++
PB2	++
PB3	++
PB4	++
PB5	–
PB7	++
PB8	++
PB11	++

Key: none (-), 1-2 mm (+), >2 (++)

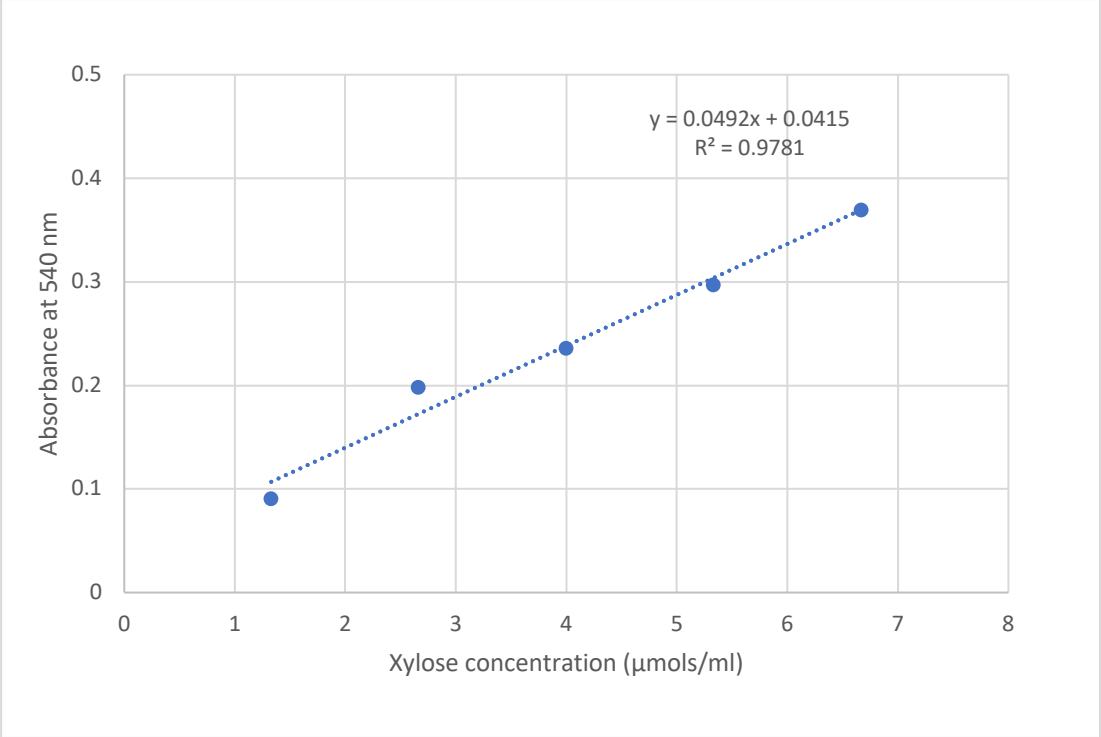

Figure 1: Xylanase enzyme standard curve for the determination of xylanase activity

APPENDIX II: CHAPTER THREE SUPPLEMENTARY DATA

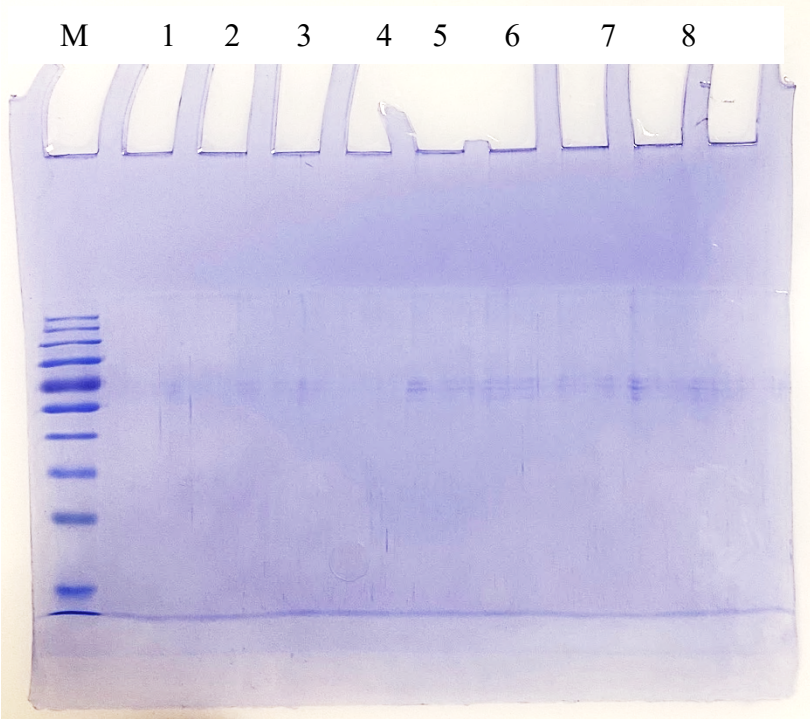

Figure 1: Original 12% SDS PAGE gel image representing lanes M: Molecular weight marker (Thermoscientific, USA), 1-4: 50, 60, 70 and 80% ammonium sulphate fractions purified (not concentrated), and 5-8: 50, 60, 70 and 80% ammonium sulphate fractions purified (concentrated). Lanes M, and 5-8 were cropped for the manuscript and are represented in chapter three, Figure 3.7a, Lanes M, and 5-8.

M 1 2 3 4 5 6 7 8

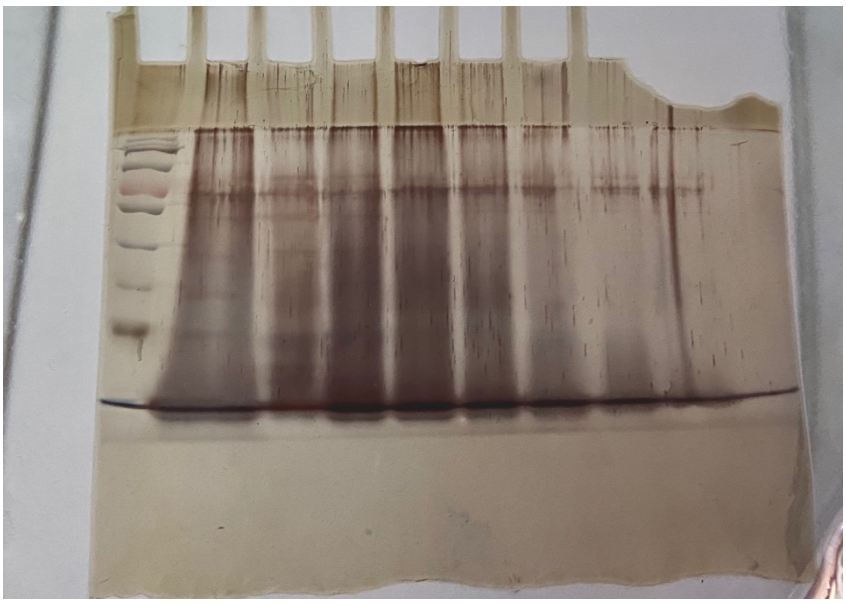

Figure 2: Original 12% SDS PAGE gel (silver stained) image representing lanes M: Molecular weight marker (Thermoscientific, USA), 1: crude, 2-8: 30, 40, 50, 60, 70, 80 and 90% ammonium sulphate fractions. Lanes 4-7 were cropped for the manuscript and are represented in chapter three, Figure 3.7a, Lanes 1-4.

Figure 3: Original native-substrate PAGE gel (stained) image representing lanes M: Molecular weight marker (Thermoscientific, USA), 1: crude, 2-8: 30, 40, 50, 60, 70, 80 and 90% ammonium sulphate fractions showing zones of clearance. Lane 5 was cropped for the manuscript and is represented in chapter three, figure 3.7b, Lane 1.

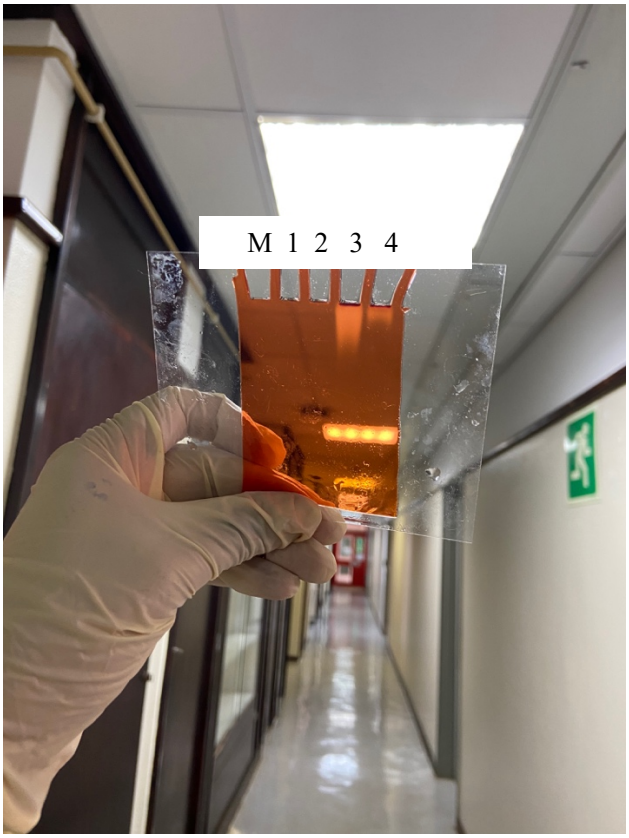

Figure 4: Original native-substrate PAGE gel (stained) image representing lanes M: Molecular weight marker (Thermoscientific, USA), 1: crude, (not concentrated), 2: purified 50% fraction (not concentrated), 3: crude (concentrated), and 4: purified 50% fraction showing zones of clearance. Lane 4 was cropped for the manuscript and is represented in chapter three, figure 3.9b, Lane 2.

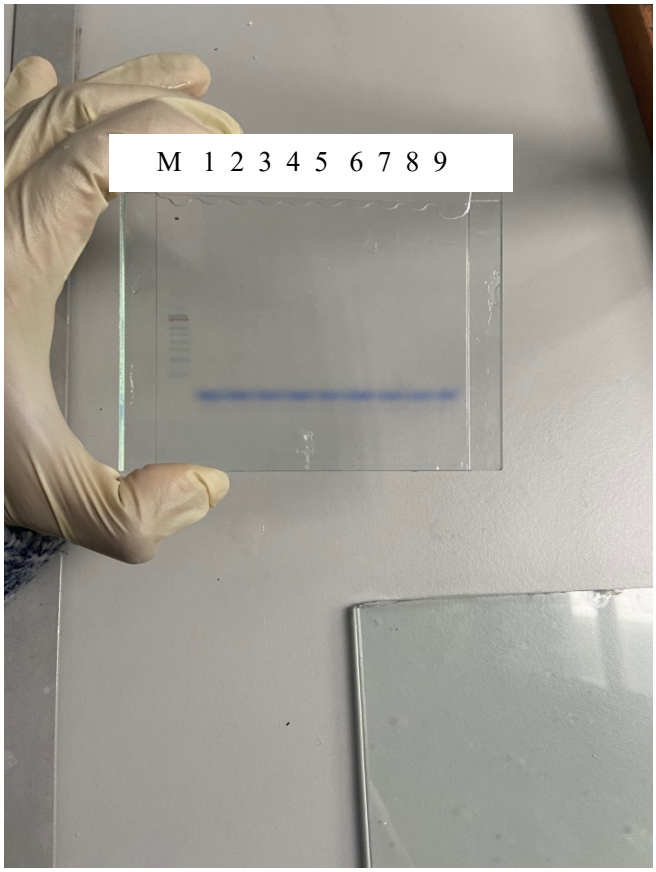

Figure 5: Original native-substrate PAGE gel (unstained) image representing lanes M: Molecular weight marker (Thermoscientific, USA), 1: crude, 2-9: 20, 30, 40, 50, 60, 70, 80 and 90% ammonium sulphate fractions. Lane M was cropped for the manuscript and is represented in chapter three, figure 3.9b, Lane M.

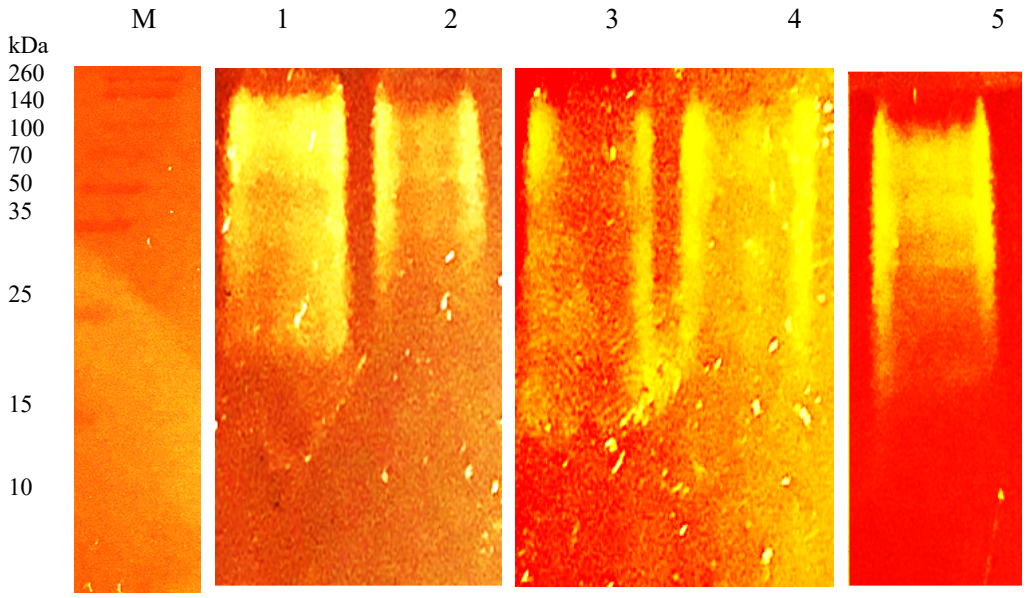

Figure 6: Native substrate PAGE gel (1% xylan) of the *T. harzianum* crude xylanases from runs 4, 6, 7, 8 and 12 from RSM. lane M: Spectra multicolour broad range marker (Thermo Scientific, USA), lane 1: crude extract, lane 2: Spectra multicolour broad range marker Thermo Scientific, USA) (stained with Congo red) and lane 3: crude xylanase extract showing zones of clearance.

APPENDIX III: CHAPTER FOUR SUPPLEMENTARY DATA

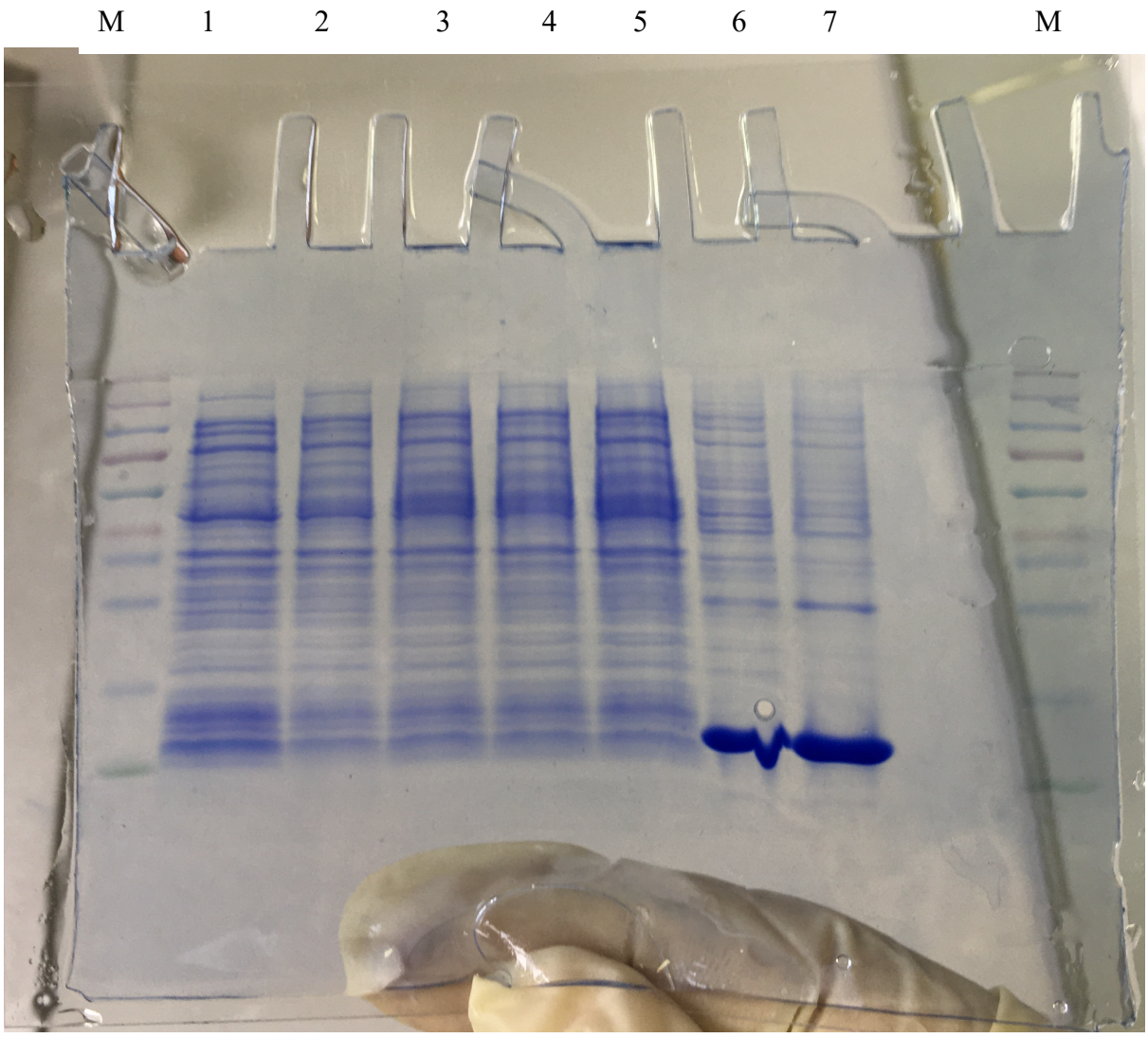

Figure 1: Original 12% SDS- PAGE gel image representing lanes M: Molecular weight marker (Thermoscientific, USA), l: uninduced fraction, 2-5: induction fractions at 1 to 4 h, and 6 and 7: BL21 cells without XT6 insert (positive control). Lane M and 1-5 were cropped and represented as figure 4.1 in chapter four.

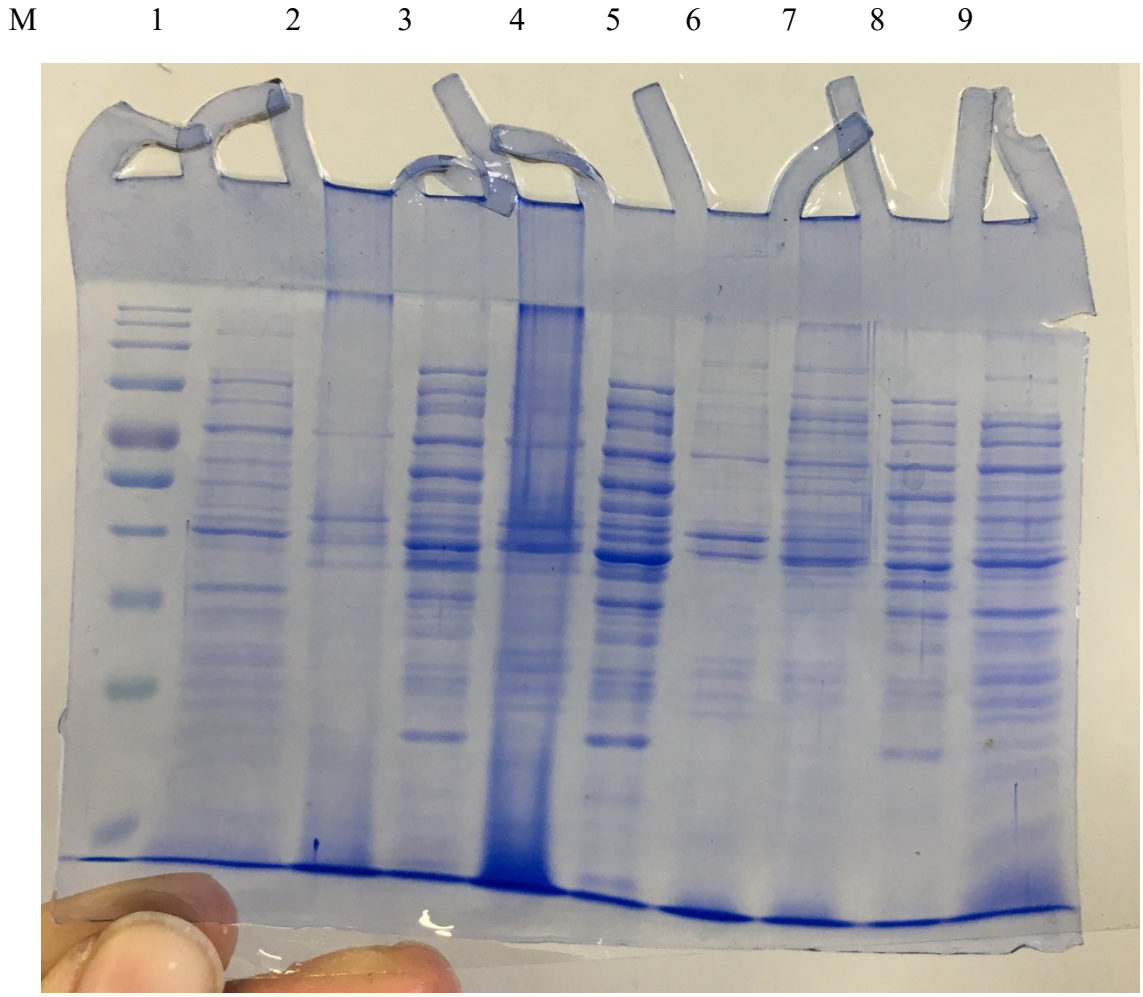

Figure 2: Original 12% SDS-PAGE gel image showing expression of the recombinant XT6 xylanase in *E. coli* BL21 (DE3) cells after various lysis techniques. Lane M: Molecular weight marker (Thermo Scientific, USA), Lane 1: uninduced sample, Lane 2 and 3: insoluble and soluble fractions tested with lysozyme + 1% TritonX-100, Lane 4 and 5: insoluble and soluble fractions tested with sonication in 0.05 M sodium phosphate (pH 6.0) buffer, Lane 6: insoluble fractions sonicated in 0.05 M Tris-HCl and 8M urea, Lane 7: soluble fraction sonicated in Tris-HCl buffer, Lane 8 and 9: insoluble and soluble fraction with lysozyme. This image was cropped and edited and is represented as figure 4.2 in chapter four.

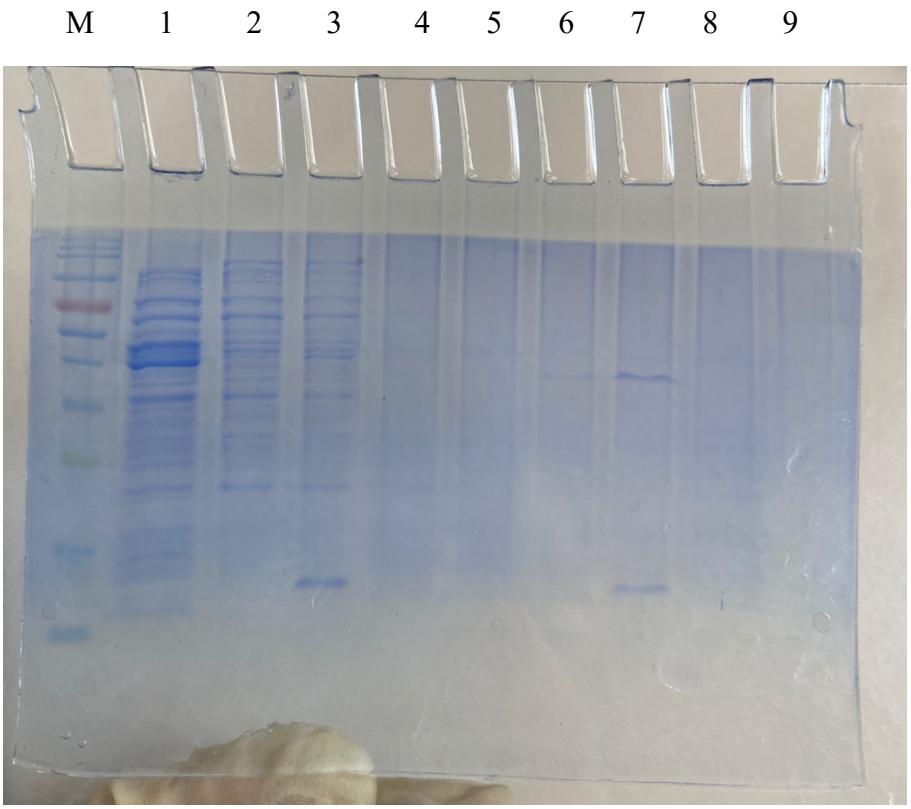

Figure 3: Original 12% SDS-PAGE gel image showing purification fraction profiles heterologously produced XT6 after affinity chromatography purification in a cobalt column. Lane M: Molecular weight marker (Thermo Scientific, USA), Lane 1: Crude (induced XT6), Lane 2: Flowthrough, Lane 3-5: Wash 1-3, Lane 6-8: Eluted fractions 1-3, and Lane 9: Wash 4. This image was neatly cropped and edited and shown as figure 4.9 in chapter four.

APPENDIX IV: CHAPTER FIVE SUPPLEMENTRAY DATA

a

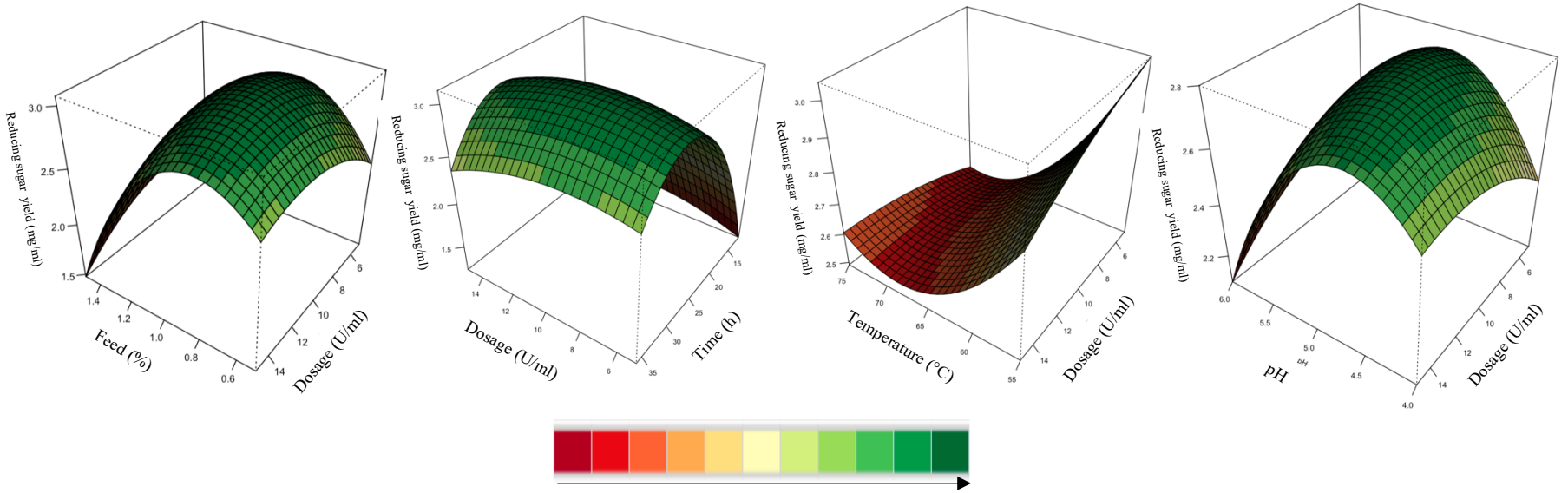

b

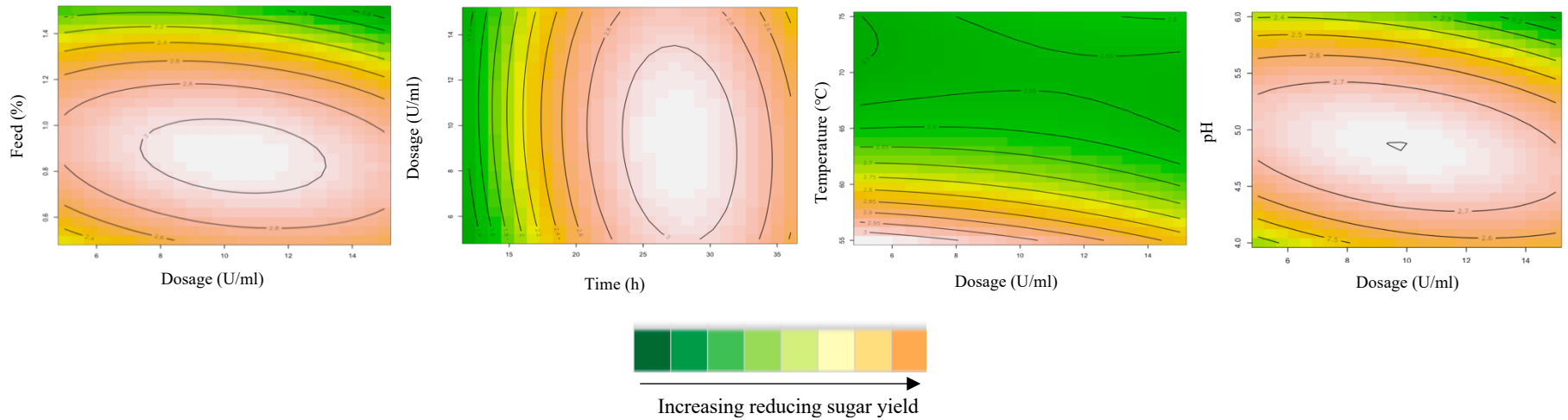

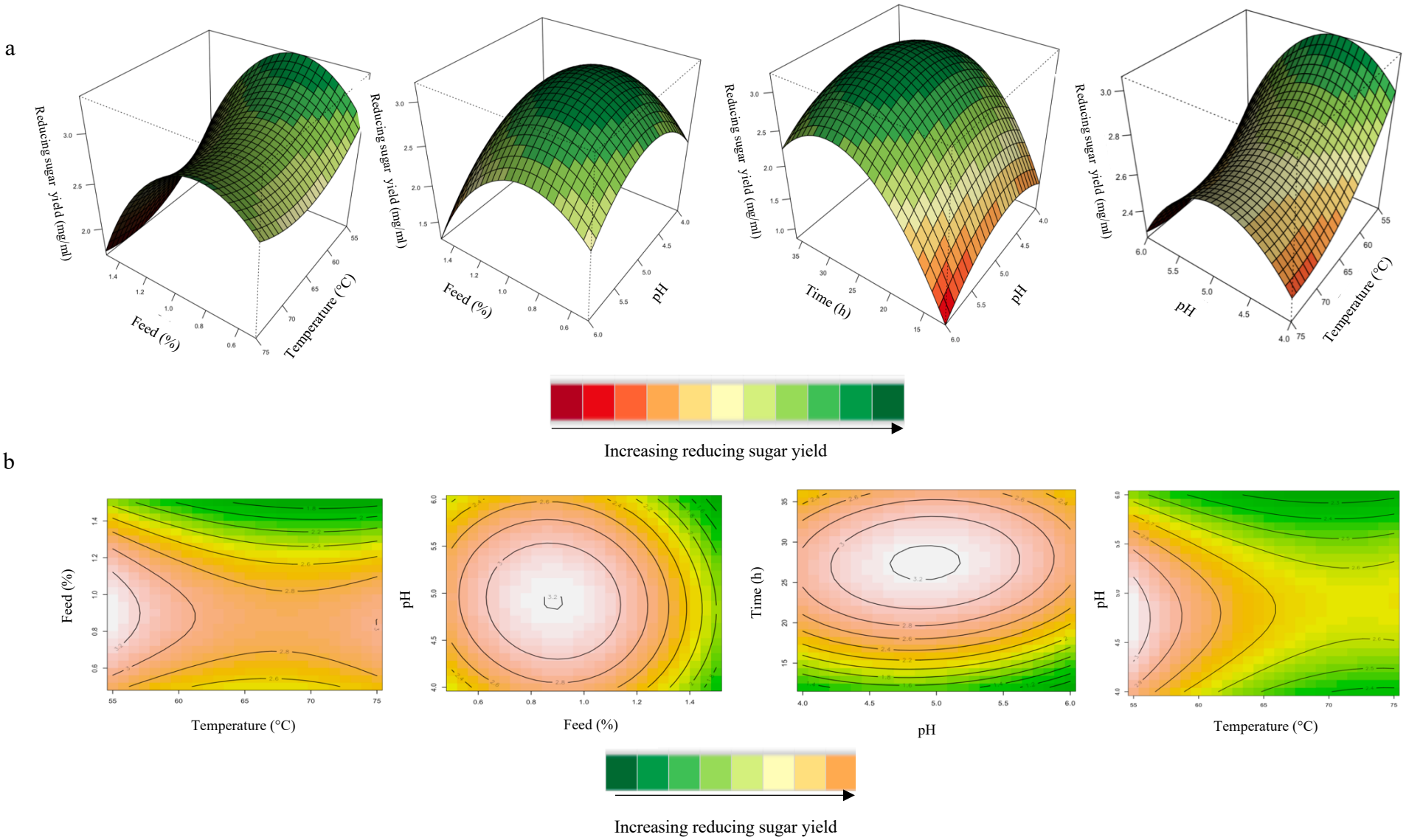

Figure 1: 3D- response surface plots (a) and contour plots (b) of the combined effects of variables on reducing sugar yield by crude *T. harzianum* xylanase of starter chicken feed.

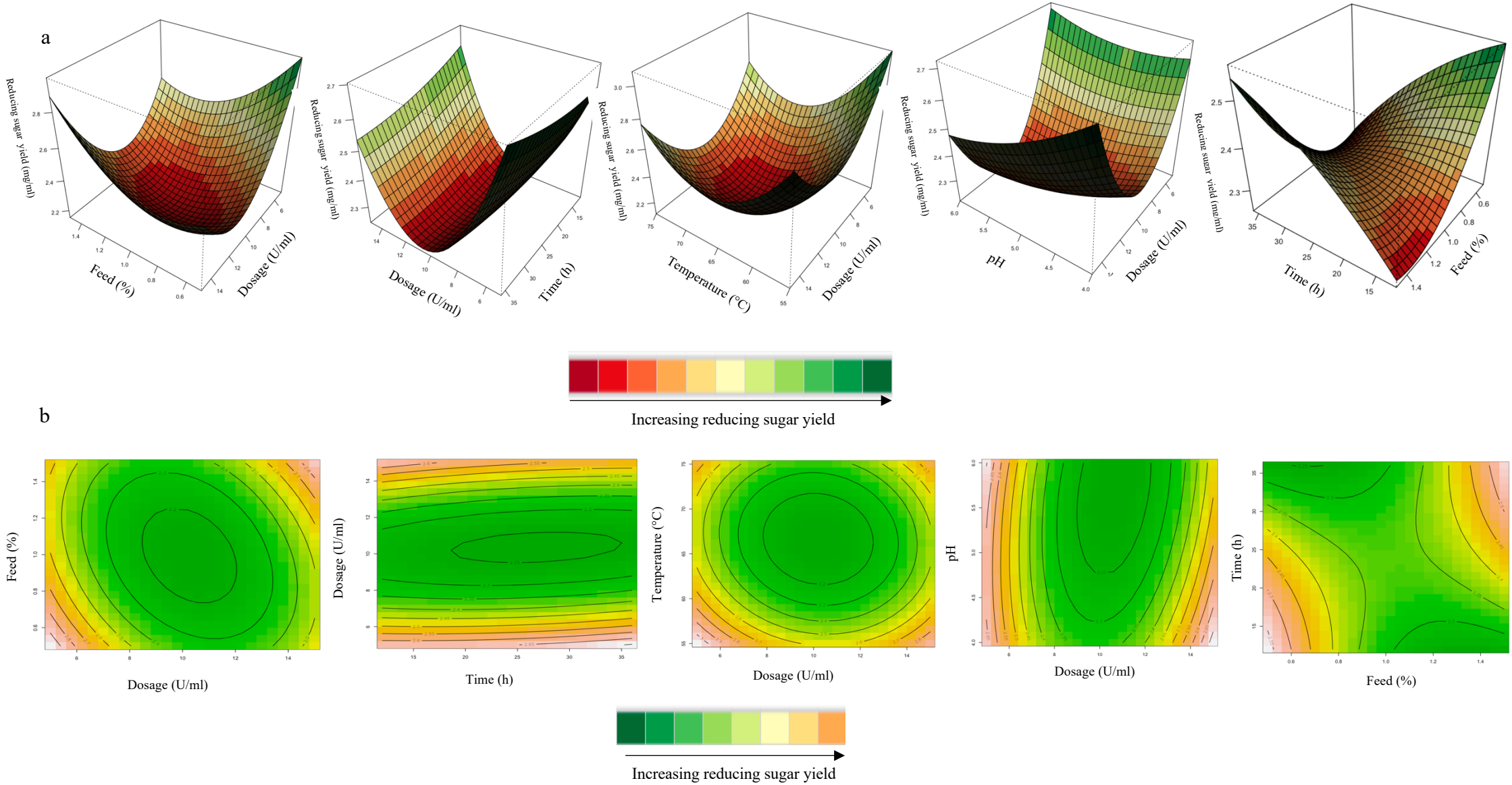
a
Reducing sugar yield (mg/ml)
Feed (%)
Dosage (U/ml)
Time (h)
Temperature (°C)
pH
Increasing reducing sugar yield
b
Dosage (U/ml)
Time (h)
Temperature (°C)
pH
Feed (%)
Increasing reducing sugar yield

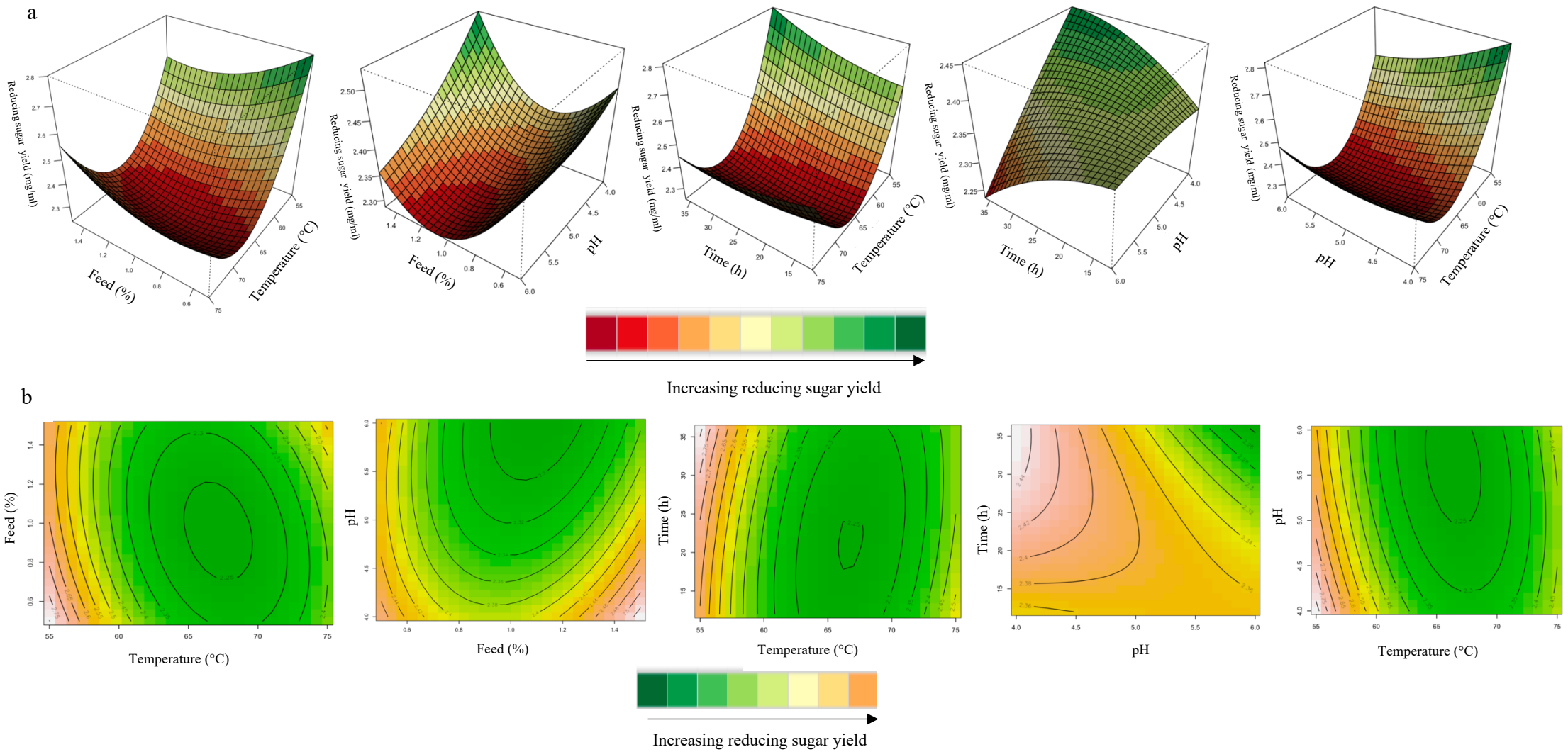

Figure 2: 3D- response surface plots (a) and contour plots (b) of the combined effects of variables on reducing sugar yield by crude *T. harzianum* xylanase of grower chicken feed.

a

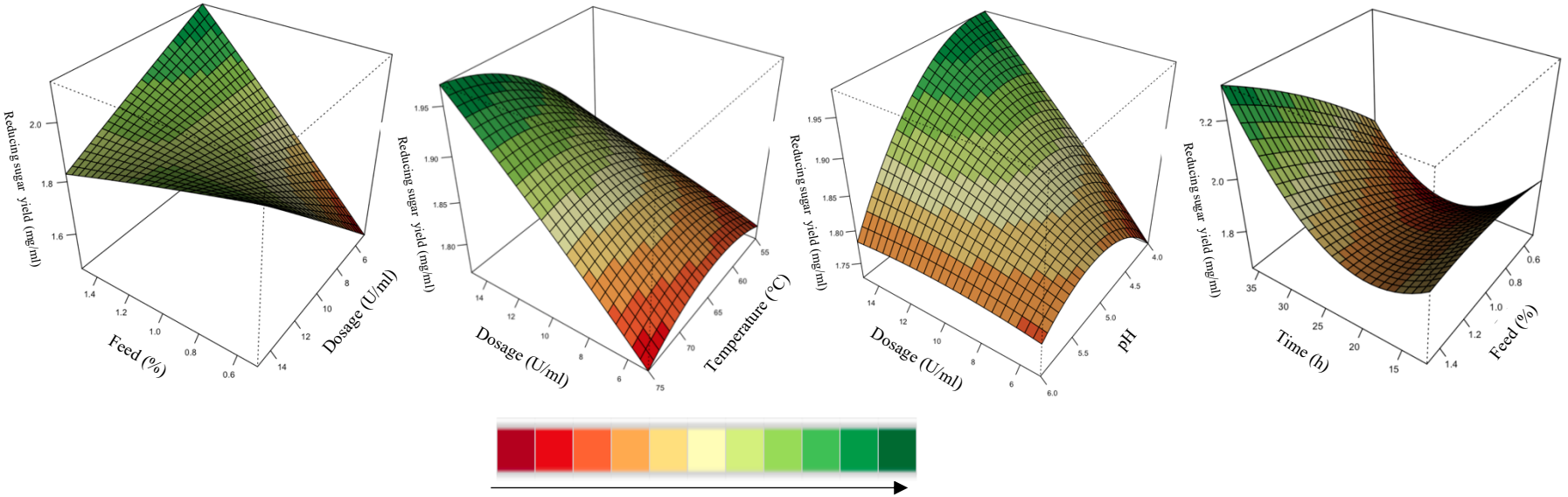
Reducing sugar yield (mg/ml)
Feed (%)
Dosage (U/ml)
Temperature (°C)
pH
Time (h)
Increasing reducing sugar yield

b

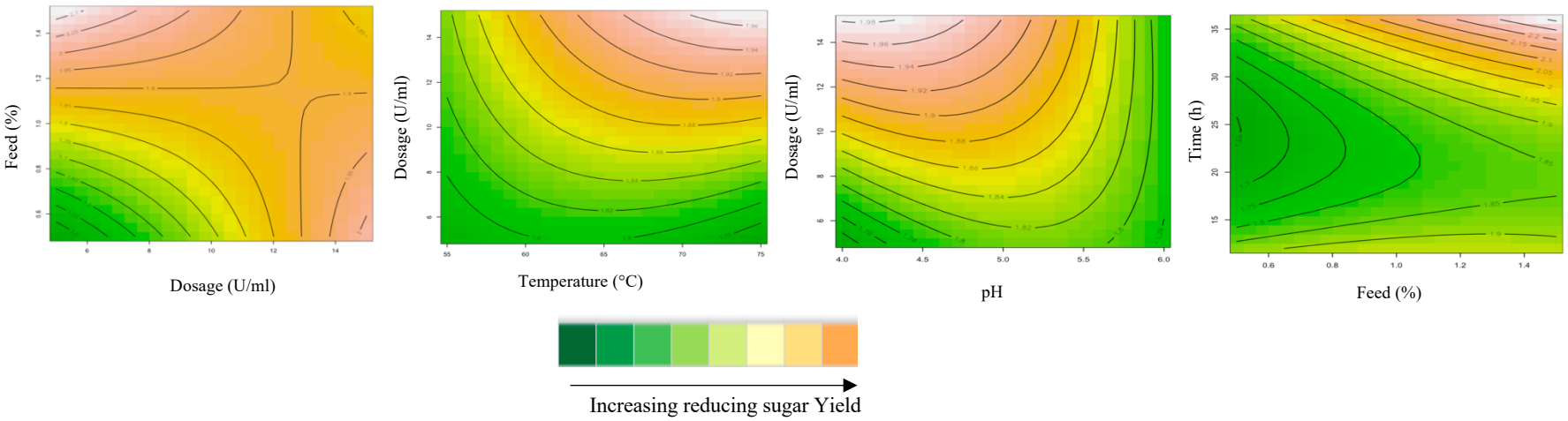
Feed (%)
Dosage (U/ml)
Temperature (°C)
pH
Time (h)
Increasing reducing sugar Yield

a

b

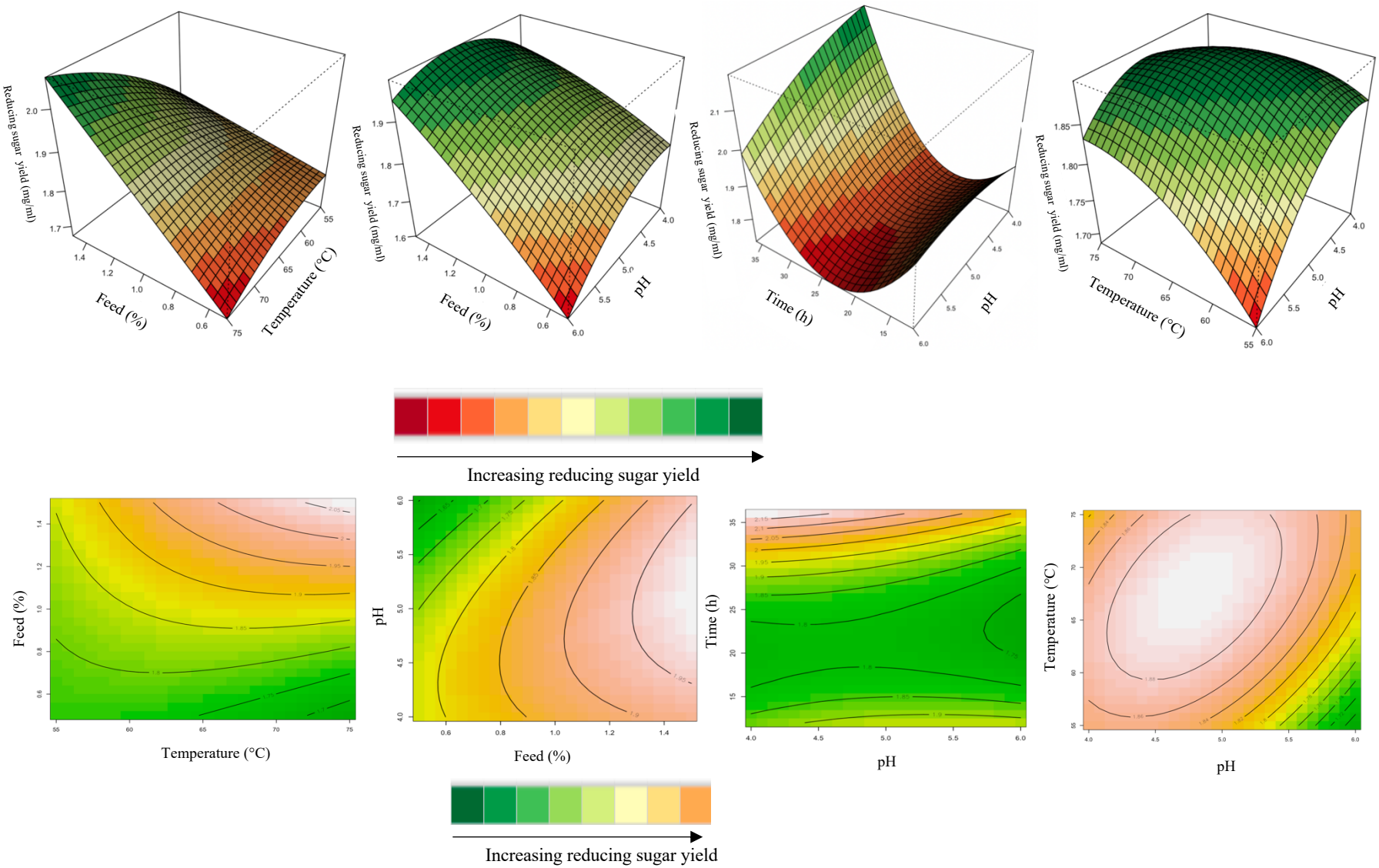

Figure 3: 3D- response surface plots (a) and contour plots (b) of the combined effects of variables on reducing sugar yield by purified *T. harzianum* xylanase of starter chicken feed.

a

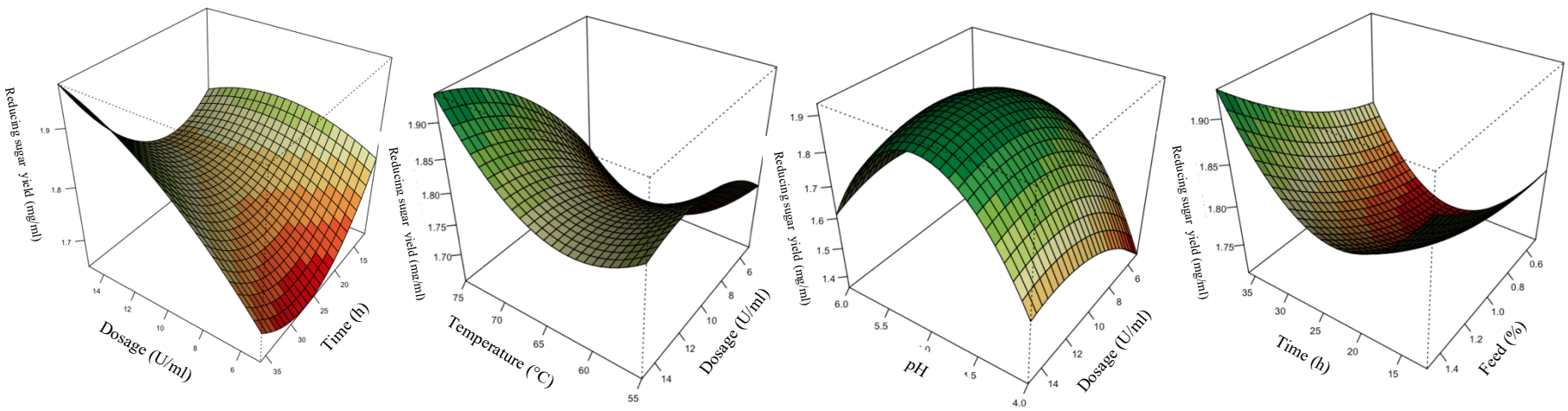

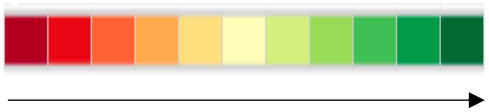

Increasing reducing sugar yield

b

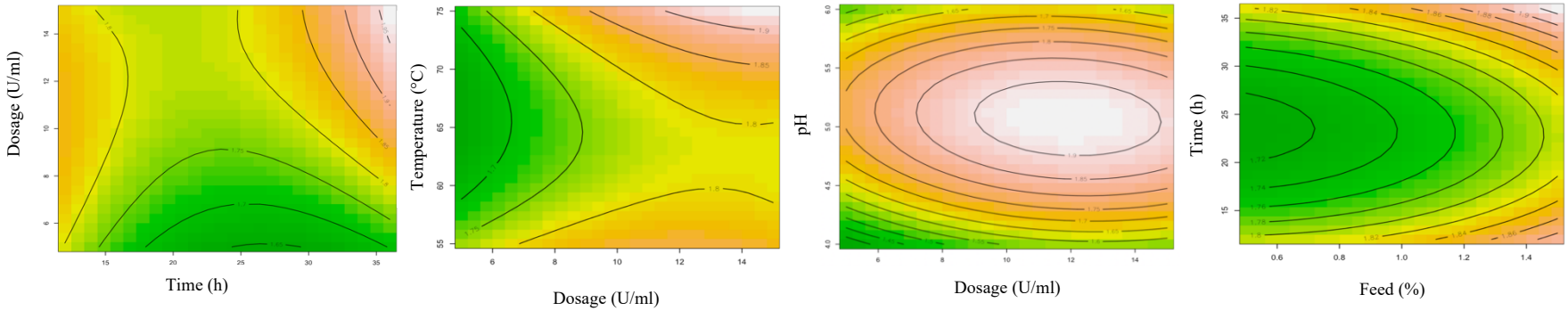

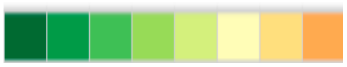

Increasing reducing sugar yield

a

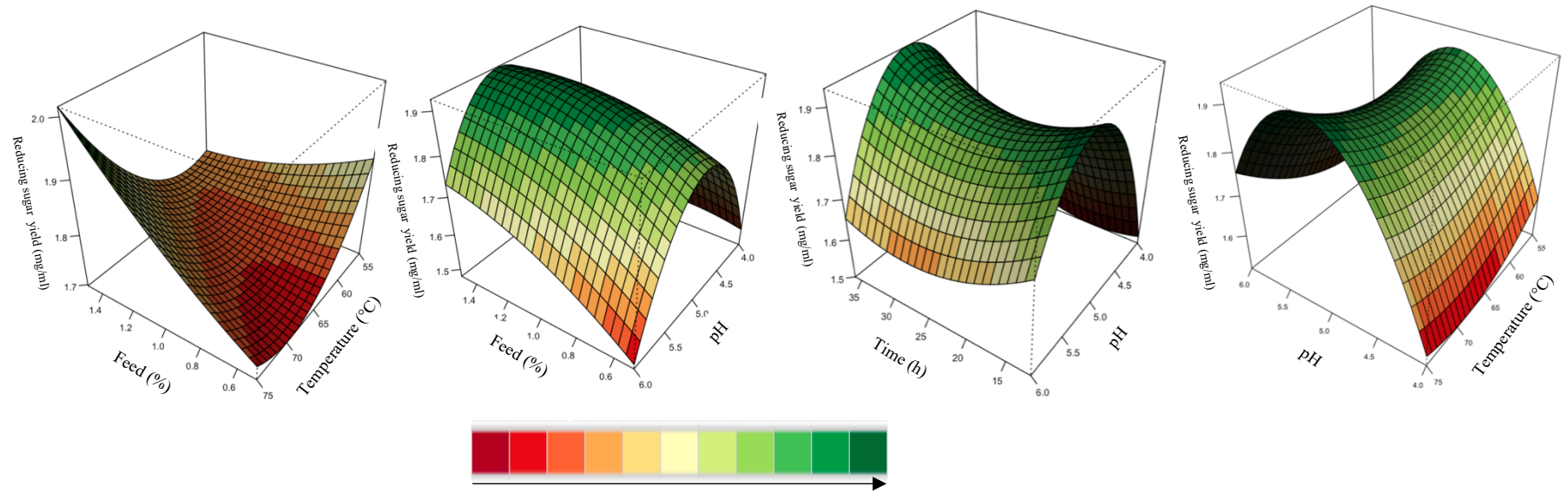

b

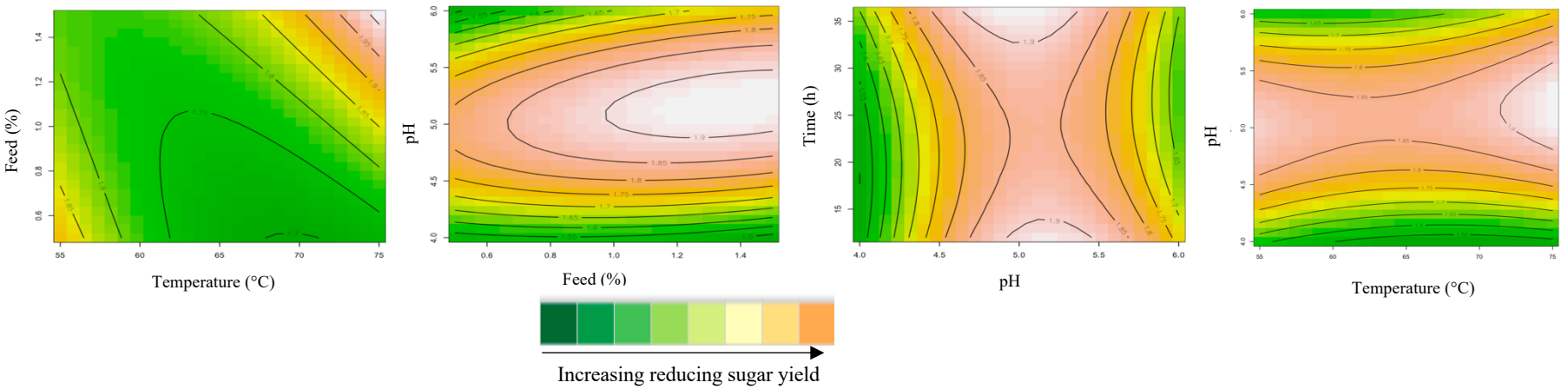

Figure 4: 3D- response surface plots (a) and contour plots (b) of the combined effects of variables on reducing sugar yield by purified *T. harzianum* xylanase of grower chicken feed.

a

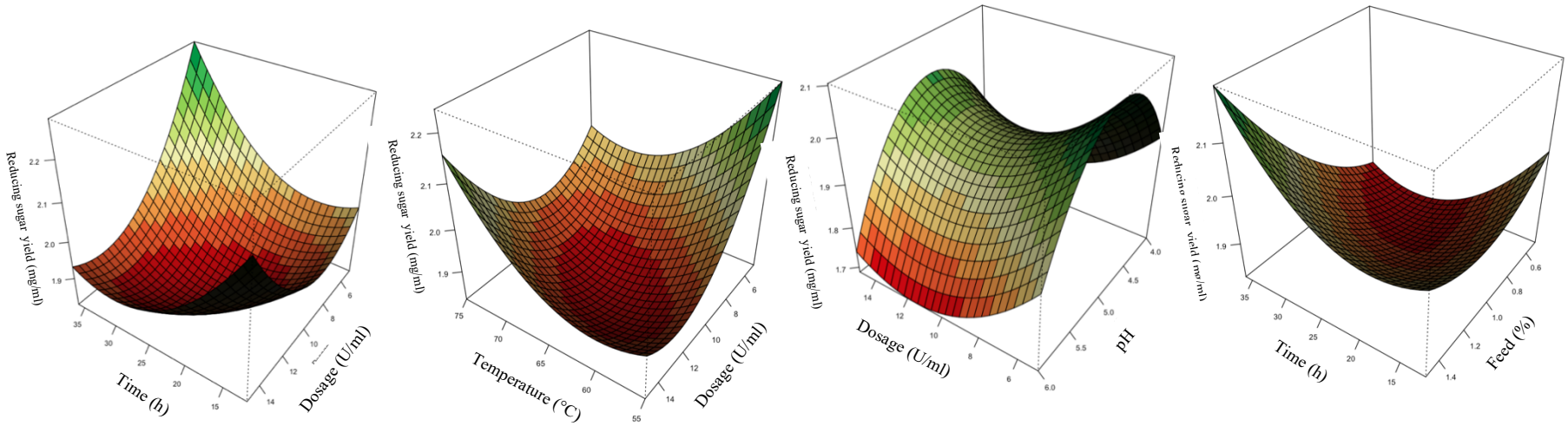
Reducing sugar yield (mg/ml)
Time (h)
Dosage (U/ml)
Temperature (°C)
pH
Feed (%)

b

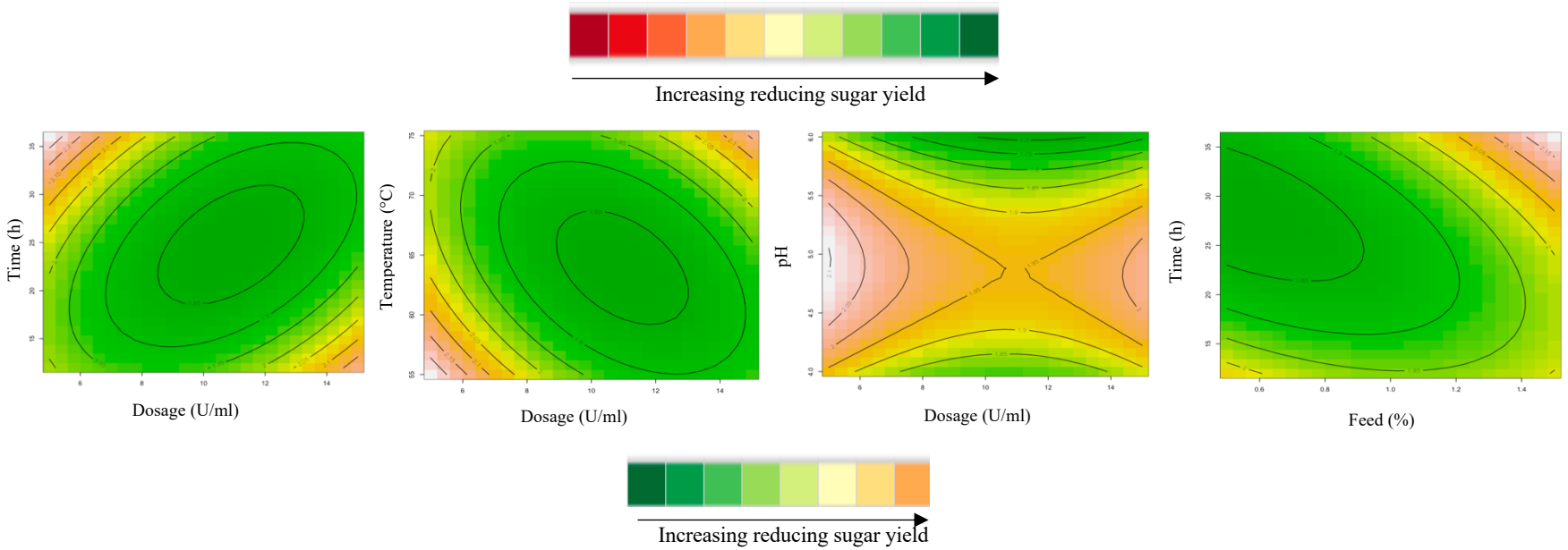
Increasing reducing sugar yield
Time (h)
Dosage (U/ml)
Temperature (°C)
pH
Feed (%)
Increasing reducing sugar yield

a

b

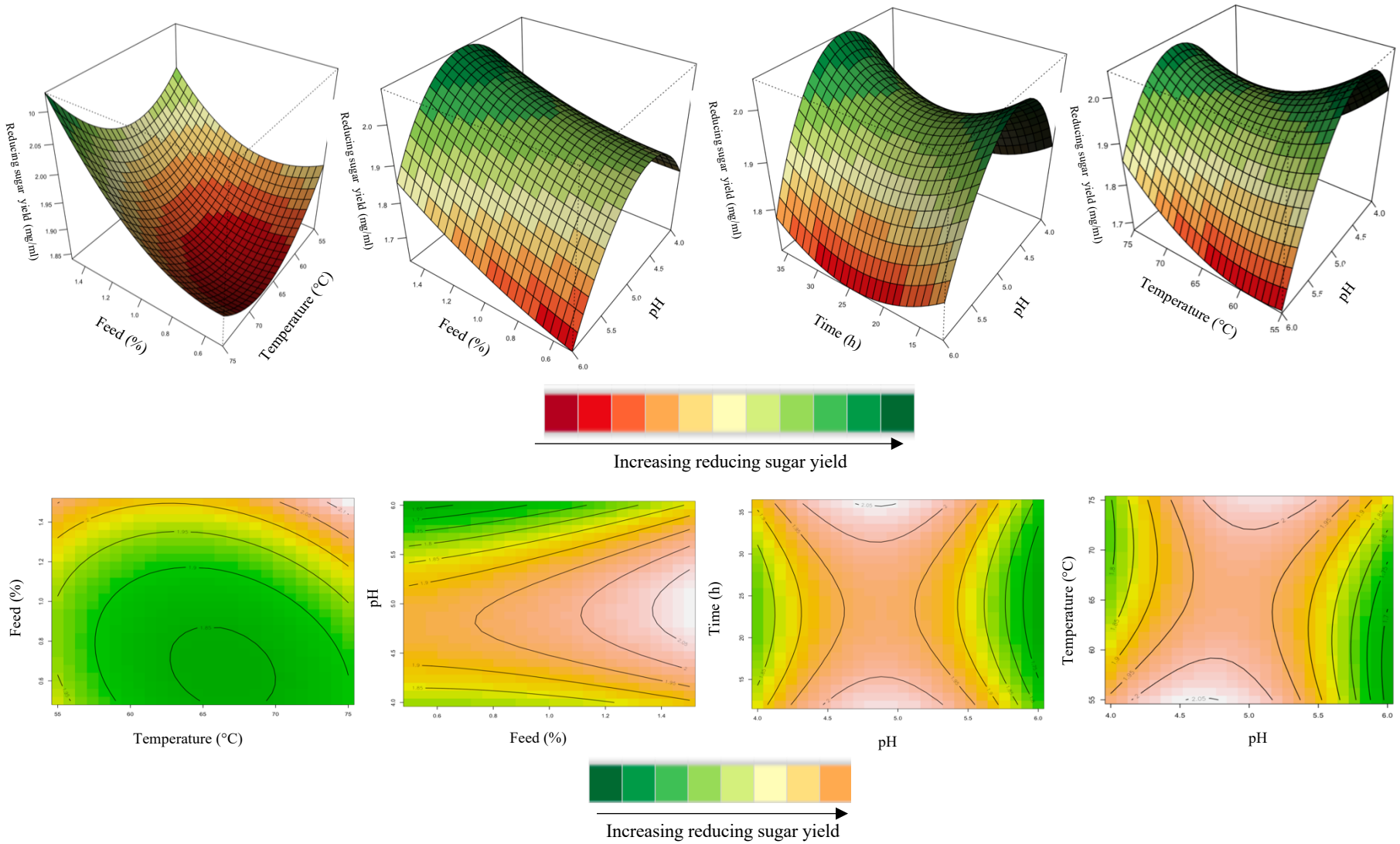

Figure 5: 3D- response surface plots (a) and contour plots (b) of the combined effects of variables on reducing sugar yield by purified XT6 of starter chicken feed.

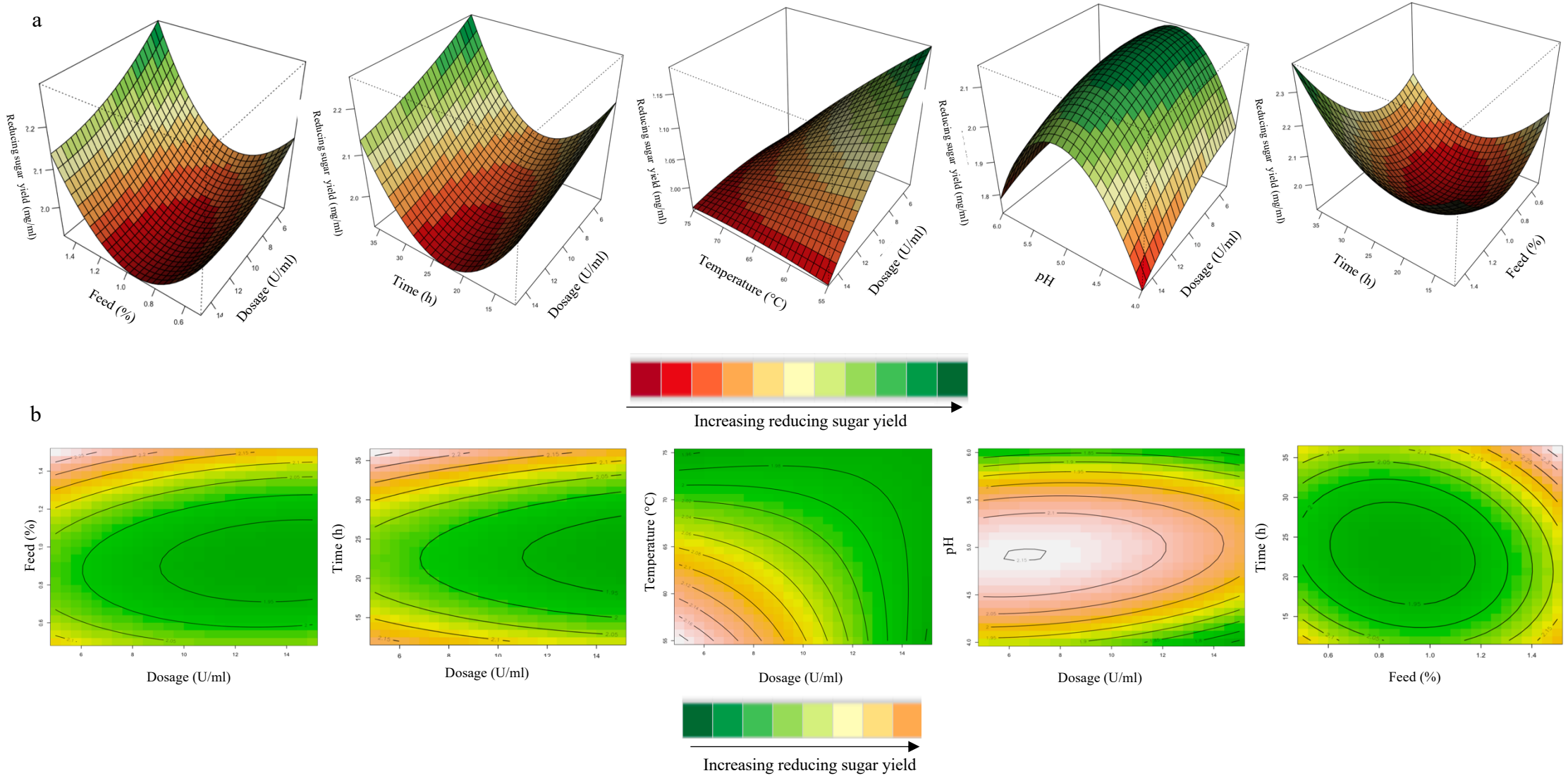
a
Reducing sugar yield (mg/ml)
Feed (%)
Dosage (U/ml)
Time (h)
Temperature (°C)
pH
Increasing reducing sugar yield
b
Feed (%)
Time (h)
Temperature (°C)
pH
Dosage (U/ml)
Increasing reducing sugar yield

a

b

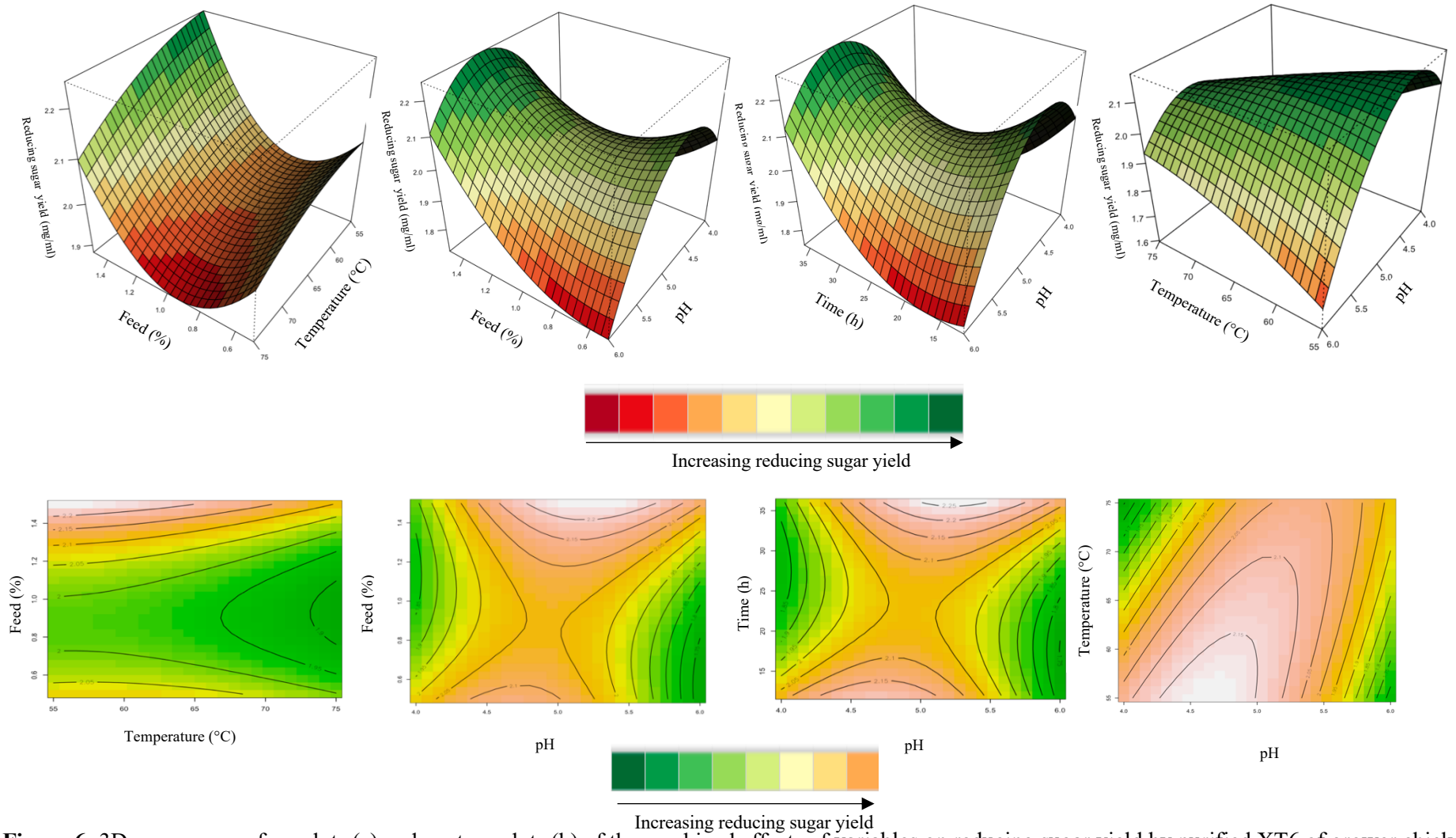

Figure 6: 3D- response surface plots (a) and contour plots (b) of the combined effects of variables on reducing sugar yield by purified XT6 of grower chicken feed.

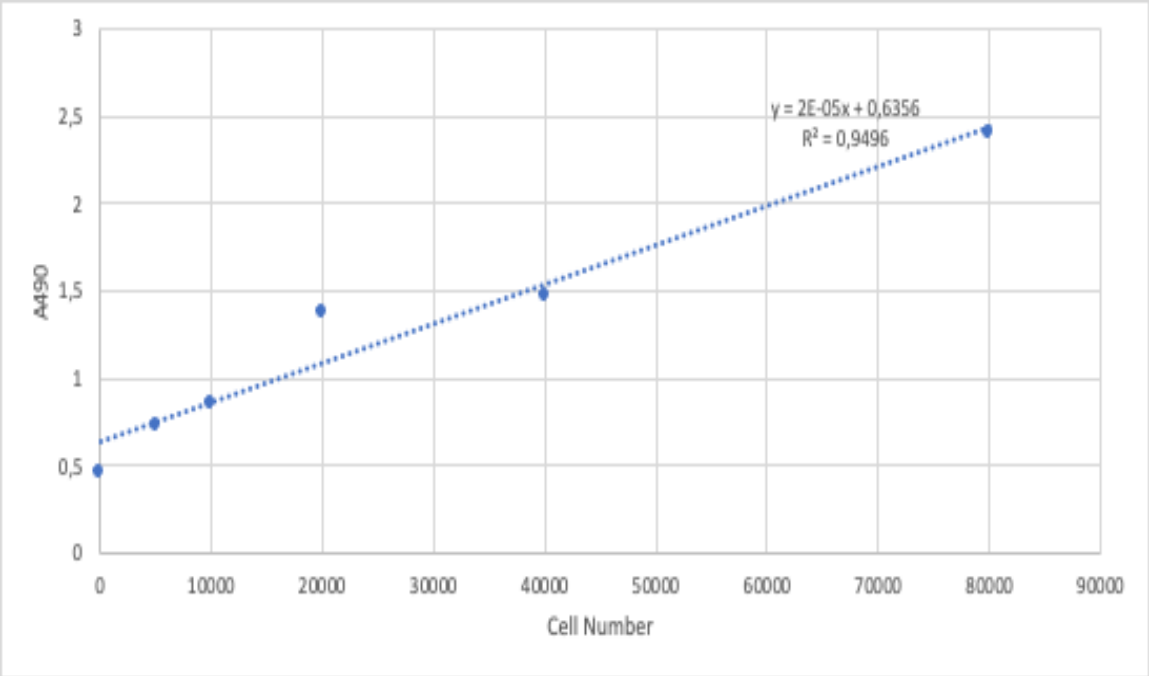

Figure 7: Standard curve of HEK293 cells at 490 nm

MYCOLOGY
https://doi.org/10.1080/21501203.2022.2079745

Isolation, screening, preliminary optimisation and characterisation of thermostable xylanase production under submerged fermentation by fungi in Durban, South Africa

Priyashini Dhaver[a], Brett Pletschke[b], Bruce Sithole[c,d] and Roshini Govinden[a]

[a]Discipline of Microbiology, School of Life Sciences, Westville Campus, University of KwaZulu-Natal, Durban, South Africa; [b]Enzyme Science Programme (ESP), Department of Biochemistry, Microbiology and Biotechnology, Rhodes University, Eastern Cape, South Africa; [c]Biorefinery Industry Development Facility, Council for Scientific and Industrial Research, Durban, South Africa; [d]Discipline of Chemical Engineering, University of KwaZulu-Natal, Durban, South Africa

ABSTRACT

Fungi are renowned for their ability to produce extracellular enzymes into their surrounding environment. Xylanases are hydrolytic enzymes capable of xylan degradation. The objectives of this study were to isolate, screen for potential xylanolytic fungi from soil and tree bark samples from three locations in South Africa and to determine their growth conditions for maximum xylanase production. Forty-six isolates were obtained based on clearing zone formation on xylan-enriched agar plates using Congo red indicator. Xylanase activity was quantified during submerged fermentation. Isolate MS5, identified as *Trichoderma harzianum* with the highest enzyme activity (38.17 U/ml) was selected for further studies based on thermophilic properties (70°C) and pH (5.0). The culture conditions; incubation period (5 days), agitation speed (160 rpm) wheat bran (1%) and ammonium sulphate (1.2%) were optimised further. Biochemical characterisation of the crude enzyme revealed two pH and temperature optima (pH 6.0 at 60°C and 70°C, pH 8.0 at 55°C and 75°C). The enzyme retained >70% activity after 4 h at pH 6.0 at 70°C. SDS-PAGE revealed multiple protein bands with a prominent band at 70 kDa. Substrate Native PAGE revealed multiple isoforms between 55 and 130 kDa. This enzyme will be beneficial for applications in the animal feed and biofuels industries.

ARTICLE HISTORY
Received 29 November 2021
Revised 18 April 2022
Accepted 15 May 2022

KEYWORDS
Fungi; xylanase; screening; isolation; xylan plate assay

1. Introduction

Lignocellulosic materials are widespread in nature and xylan is a polysaccharide found in the hemicellulose fraction of lignocellulose, a major component of the plant cell wall. Xylan is a significant resource of renewable biomass, suitable as a substrate for the production of many commodities such as biofuels, affordable energy sources for fermentation and improved animal feeds. However, xylan must be converted to xylose and xylo-oligosaccharides for most bioconversion processes. The conversion of xylan can be performed by acid hydrolysis or by xylanolytic enzymes (xylanases) that deconstruct plant structural material thus breaking down hemicellulose (Bhardwaj et al. 2019).

Xylanase production by fungi, bacteria, yeast, marine algae, etc. has been studied and reported by several authors, but the main sources of industrial enzymes are fungi and bacteria (Wong et al. 1988; Prade 1996; Mandla 2015; Lee et al. 2018) through intracellular or extracellular secretions by the microorganisms (Lee et al. 2018). Depending on the source, xylanases have different characteristics, which make them useful for several applications. Microbial enzymes are preferred in industrial applications due to their ability to be produced in large volumes over a short period (Adesina and Onilude 2013; Motta et al. 2013). Fungi are highly diverse in nature and have been recognised as an unrivalled target for enzyme screening (Nair and Shashidhar 2008). Filamentous fungi are producers of xylanases and other xylan degrading enzymes, with the noteworthy characteristics of secreting enzymes into the surrounding medium, thus avoiding the need for cell lysis, and with much higher activities compared to yeasts and bacteria (Nair and Shashidhar 2008). Thus, fungal enzymes are very attractive for various industrial processes (Prasad Uday et al. 2017). On an industrial scale, xylanases are produced mainly by *Aspergillus and*

CONTACT Roshini Govinden govindenr@gmail.com
Supplemental data for this article can be accessed online at https://doi.org/10.1080/21501203.2022.2079745

Trichoderma spp. in solid-state fermentation (SSF). *T. harzianum* is present in all soil types and are the most prevalent culturable fungi (Chen and Zhuang 2017).

The application of xylanases in industrial processes has had many limitations for its commercial feasibility due to several factors (Walia et al. 2013). These include the inaccessibility of substrate to the xylanases caused by physical limitations, the incomplete hydrolysis of xylan due to its diverse branched nature, the narrow pH optimum range, thermal instability of the enzymes, end-product inhibition, and cost of enzyme production (Walia et al. 2013). Fungal xylanases are effective in a pH range of 4.0–6.0 and temperatures below 50°C, thus their use in industrial applications is restricted. Previous studies also showed that mesophilic organisms are not ideal for xylanase production as these enzymes generally become denatured at temperatures above 55°C (Robledo et al. 2016). As a consequence, the efficiency of hydrolysis decreases during the catalytic application, requiring supplementation during the process or higher enzyme yields to overcome this problem, thus increasing the process costs. Therefore, the use of thermostable enzymes is essential for hydrolysis at high temperatures.

Xylanases have been used in the feed industry to reduce the viscosity of food and improve nutrient absorption in the digestive tracts of animals (Bedford 2018). The enzymes could be applied when the feeds are being processed, before the pellet process (70–95°C, pH 4–6), indicating the requirement for thermostable enzymes that are also active in acidic conditions (Collins et al. 2005; Pariza and Cook 2010). Numerous studies have been conducted to isolate thermophilic enzymes with superior enzyme stability from fungi (Haki and Rakshit 2003; Robledo et al. 2016). Thermophilic xylanases are characterised by temperature optima between 50°C and 80°C and are stable in this range (Haki and Rakshit 2003). Chadha et al. (2019) published a review on thermophilic fungal and bacterial xylanases that details that these enzymes have a multiplicity of isoforms (in excess of 15 for *Myceliophothora sepedonium*) in some instances that was revealed by transcriptomic and proteomic studies. However, due to the yield of enzymes required for large-scale applications, the search for microorganisms able to produce thermostable xylanases with high yields and characteristics desired for industrial applications is still ongoing. Considering the industrial importance of xylanase, the aim of this study was to isolate, screen, and identify fungal isolates from the soil and bark of trees from three locations in KwaZulu-Natal, South Africa (29°49′01″ S 30°56′41″ E; 29° 49′03″ S 30°56′29″ E and 29°16′13″ S 31°22′06″ E). This paper describes the isolation and screening of thermophilic xylanolytic fungi, as well as the growth parameters for optimal xylanase production by the highest xylanase producer. Selection was made based on the strain's ability to grow in thermophilic and acidic conditions but directed by the knowledge that if the organisms can grow under these conditions then the enzymes and proteins produced (adaptive evolution) likely function well under these conditions as well. As the xylanase, we were seeking was for an animal feed application requiring enzymes that could function in these conditions our focus remained on the *T. harzianum* strain as it met our requirements even though it is a much studied strain.

2. Materials and methods

2.1 Isolation, growth, and maintenance of bacteria and fungi

Soil and bark samples were collected from three local sites i.e. the University of KwaZulu-Natal (Westville) close to the Chemistry (29°49′01″ S 30°56′41″ E) and Microscopy (29°49′03″ S 30° 56′29″ E) disciplines and a town known as Darnall in the north coast region (29°16′13″ S 31° 22′06″ E) in KwaZulu-Natal, South Africa. Three tree species were selected for the tree bark samples; *Acer neguno* (29°49′01″ S 30°56′41″ E), *Juglans regia* (29°49′03″ S 30°56′29″ E) and *Citrus limon* (29°16′13″ S 31°22′06″ E). Soil microbial properties vary widely, both spatially and temporally. Therefore, soil still remains an attractive source of microorganisms with desirable properties. It is important to carefully collect soil samples for bioprospecting microbial enzyme

producers according to a given objective or hypothesis. However, in the interest of obtaining many different types of organisms isolation was conducted from soil and tree bark samples that were obtained from different sites as a simple random sampling technique (Lorenz and Dick 2011). Using sterile beakers and spatulas, 1 g of soil and bark samples were transferred to 10 ml sterile tubes. Ten-fold serial dilutions were performed, thereafter 0.1 ml aliquots from each dilution were spread plated on potato dextrose agar (PDA) and incubated at 30°C for 5 to 7 d. Pure isolates were obtained from each dilution plate (Mohammed 2013). Short term (working) stocks were prepared with fungal isolates at 4°C that were previously inoculated and grown for 5 day at 30°C. For the medium term stocks, PDA slants were prepared and left to solidify at room temperature in 15 ml falcon tubes. Fungal cultures were streaked onto the PDA slants, grown for 5 days at 30°C followed by addition of sterile mineral oil to cover the fungal mycelium and storage at 4°C. Long term stocks were prepared by washing fungal spores from the 5-day PDA plates with distilled water and adding 50% glycerol in a 1:1 ratio to the spore suspension and storing at −20°C and −80°C.

2.2 Screening for enzyme activity

The screening strategy used was based on a combination of approaches reported in literature (Gautam et al. 2015; da Silva Menezes et al. 2017).

2.2.1 Primary screening of isolates

Qualitative screening was conducted by first growing the fungi on substrate agar plates containing (g/L): 0.5 g NaCl, 1 g KH_2PO_4, 0.5 g $MgSO_4$, 0.01 g $MnSO_4$, 0.3 g NH_4NO_3, 0.01 g $FeSO_4$, 6 g bacteriological agar supplemented with 1% (w/v) beechwood xylan. Plates were inoculated in the centre with the microorganism and incubated at 30°C for 5 to 7 days, then stained with 0.1% Congo red for 10 min and destained with 1 M NaCl for 15 min to observe and measure halo diameters for xylanase activity (Mosina et al. 2017).

2.2.2 Secondary screening of isolates

The selected xylanase-producing isolates (after primary screening) were inoculated into potato dextrose broth and incubated at 30°C for 7 days at 200 rpm in a shaking incubator (New Brunswick Scientific, incubator shaker series, Innova 44). The cultured media were then centrifuged (Eppendorf Centrifuge 5418, Germany) at 1,6873 × *g* for 10 min. Using sterile pipette tips, 5 mm wells were made on substrate agar plates as prepared above. The supernatants containing the crude enzymes were dispensed into the wells and the plates incubated at 30°C for 2 to 3 days, after which they were stained, destained, and analysed as described previously in 2.2.1.

2.2.3 Tertiary (quantitative) screening of isolates

The isolates that showed high xylanase activity were subjected to quantitative screening after cultivation in a nutrient salt solution (NSS) medium [(g/L): 0.005 g CaCl, 0.23 g KH_2PO_4, 0.05 g $MgSO_4$, 0.005 g $NaNO_3$, 0.002 g $ZnSO_4$, 0.009 g $FeSO_4$, 0.23 g KCl, 7 g peptone, and 20 g wheat bran]. Erlenmeyer flasks (250 ml) containing 50 ml of the medium were each inoculated with two 5 mm fungal plugs from a 5-day-old plate culture and incubated at 30°C at 200 rpm for 7 d in a shaking incubator (New Brunswick Scientific, incubator shaker series, Innova 44, Germany). Cultured media were removed after the incubation period and the cell-free supernatant was recovered by centrifuging samples at 16,873 × *g* for 10 min (Eppendorf Centrifuge 5418, Germany). Xylanase activity was determined as described below 2.2.4.

2.2.4 Xylanase assay

Xylanase activity was quantified using the DNS assay for reducing sugars according to the method of Miller (1959). The reaction included 600 µl of 1% (w/v) beechwood xylan (1 g in 100 ml of citrate buffer, pH 5) which was placed in 15 ml test tubes and 66.67 µl of the enzyme was added. The reaction mixture was incubated in a water bath at 55°C for 15 min and terminated by adding 1 ml 3,5-dintrosalicylic acid (DNS) reagent to the reaction mixture and then heated for 5 min at 100°C in a water bath. The absorbance was read at 540 nm using a spectrophotometer (Shimadzu UV-1800, Japan) to determine the concentration of sugar released by the enzyme. One unit (U) of xylanase was defined as the

amount of enzyme that released 1 µmol xylose as reducing sugar equivalents per min under the specified assay conditions.

2.3 Identification of the unknown isolates

The identification of the unknown isolates was accomplished by: (2.3.1) isolation of the genomic DNA; and (2.3.2) amplification of the 18S rRNA ITS2 region; sequencing and BLAST analysis of the 18S rRNA gene.

2.3.1 Genomic DNA extraction

Genomic DNA isolation was performed using the ZR Soil Microbe DNA Miniprep™ kit (Zymo Research, USA) according to the instructions provided by the manufacturer. After extraction, gDNA samples were stored at −20°C. A gDNA concentration of 58.6 (CB1), 13.1 (CB2), 33.9 (PB7), 8.1 (PS3) and 44.7 µg/ml (MS5) was indicative of successful DNA extractions and was used as template DNA in PCR reactions.

2.3.2 Polymerase chain reaction amplification of the 18S ribosomal RNA ITS2 region and identification

Universal fungal primers for the ITS2 region of the 18S rRNA were used for the PCR reaction. The ITS primer pair used were: forward: ITS5F (5′-GGAAGTAAAAG TCGTAACAAGG–3′) and reverse: ITS4R (5′CTCCTCCGCTTATTGATATGC–3′) (White et al. 1990). The PCR reaction consisted of template DNA, 2.5 µM forward and reverse primers, 25 mM $MgCl_2$, 10 mM dNTPs, Taq DNA polymerase, 10 mM buffer (Thermo Scientific, USA). The reaction mixture was brought up to a volume of 50 µl using nuclease-free water. Amplification was conducted in a T100 Thermal Cycler (Bio-Rad, USA) under the following thermal cyclic conditions: initial denaturation at 95°C for 2 min followed by 25 cycles of denaturation at 95°C for 30 s, annealing at 53°C for 45 s, and extension at 72°C for 1 min. Thereafter, a final extension step was performed at 72°C for 8 min. The PCR products were then subjected to electrophoresis on a 1% agarose gel, which was run at 90 V for 45 min and then stained with ethidium bromide (0.5 µg/ml). The presence of the PCR amplicon was confirmed and sent to Inqaba BioTec for sequencing. The sequences was cleaned using DNA Man, and thereafter the consensus sequence was used to identify the isolates by BLAST analysis, using the NCBI database (Tuohy et al. 1993). The ITS2 region of the 18S ribosomal RNA was amplified as shown in Figure 1, in which an expected 600 bp amplicon was obtained.

2.4 Effect of pH and incubation temperature on xylanase production by MS5

The effect of pH and incubation temperature on xylanase production was studied according to Bhavsar et al. (2016) to aid in the selection of the most promising isolate. High temperatures could result in evaporation and drying of the wheat bran. This was avoided by using a larger total volume of medium and an equivalent inoculum size. The effect of pH on xylanase production was determined in NSS media prepared in buffers ranging from pH 4.0 to 10.0 by adjusting the pH using 1 M HCl and 1 M NaOH. Erlenmeyer flasks (250 ml) containing 50 ml of the medium were each inoculated with two 5 mm fungal plugs from 5-day-old plate cultures and incubated at 30°C at 200 rpm for 7 days in a shaking incubator (New Brunswick Scientific, incubator shaker series, Innova 44, Germany). The pH was not maintained however to verify that the pH was the same as the initial, the pH was measured towards the end of fermentation and compared to the initial pH (4.0–10.0).

The effect of temperature on xylanase production was studied by inoculating a 5-day-old culture into the NSS medium prepared with the pH buffer that resulted in the best enzyme activity determined previously and incubated at 20°C to 80°C for 7 days at 200 rpm. Xylanase assays were performed as described previously and results were reported. The catalytic temperature during the assays in was controlled by a CPS Controller (Shimadzu CPS-240A, Kyoto Japan) attached to the spectrophotometer. The isolate that resulted in the highest enzyme activity was selected for further studies.

2.5 Phylogenetic analysis and morphological studies of MS5

2.5.1 Phylogenetic analyses

The 18S rRNA sequence of the isolate was compared with other closely related strains using BLAST and NCBI GenBank database. Alignment and the

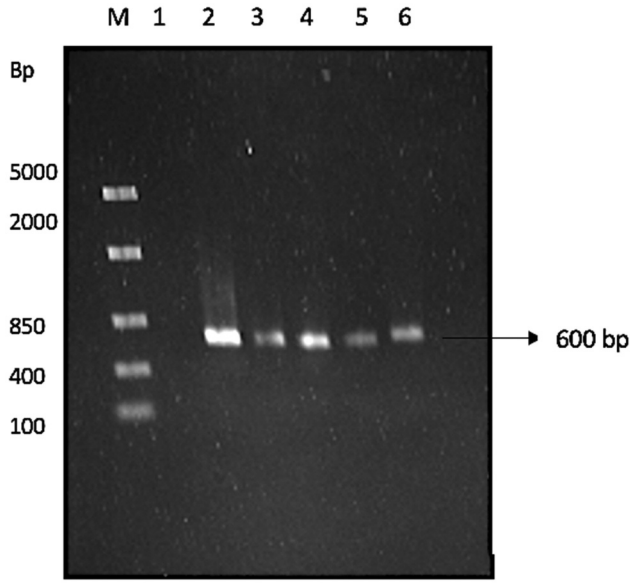

Figure 1 Agarose (1%) gel showing 18s rRNA amplicon. lane M: marker, FastRuler middle range molecular weight ladder (Thermo Sientific, USA), lane 1: negative control, lane 2: CB1, lane 3: CB2, lane 4: PB7, lane 5: PS3, and lane 6: MS5, 600 bp between ITS5 and ITS4 region.

phylogenetic tree were constructed using MEGA 11 software. The neighbour-joining (NJ) tree of the isolate was evaluated using 100 bootstrap replications (Tamura et al. 2011). The phylogenetic tree included 51 nucleotide sequences obtained from NCBI Blast (2.5.2). The phylogenetic tree was constructed using the neighbour-joining method (Telles et al. 2018) (Figure 2).

2.5.2 Morphological characterisation using light microscopy

The morphological characteristics of the *T. harzianum* strain were examined using a 5-day-old fungal culture. A lactophenol cotton blue wet mount slide was prepared using the method of Leck 1999. The slide was examined using a light microscope (Primostar 415,500–0057-000, Germany) to examine the structures. The photomicrographs were recorded with an iPhone 6s camera.

2.6 Time course for optimal enzyme production

To determine the time required for optimal enzyme production, 50 ml NSS (pH 5.0) was dispensed into 250 ml Erlenmeyer flasks, inoculated with two 5 mm plugs of a 5-day-old fungal culture, and incubated at 200 rpm at 70°C in a shaking incubator (New Brunswick Scientific, incubator shaker series, Innova 44, Germany). Samples were collected every 24 h and centrifuged at 1,6873 × *g* for 10 min and xylanase activity quantified. All experiments were carried out in duplicate and analytical assays on samples in duplicate yielding quadruplicate results (Cunha et al. 2018).

2.7 Effect of agitation on xylanase production

The effect of agitation conditions on xylanase production during submerged shake flask fermentation was studied in Erlenmeyer flasks (250 ml) containing 50 ml of the medium (pH 5.0) inoculated with two 5 mm fungal plugs from a 5 d old plate culture and incubated at 70°C in a shaking incubator (New Brunswick Scientific, incubator shaker series, Innova 44, Germany) at different rpm (120, 140, 160, 180 and 200). All experiments were carried out in duplicate and analytical assays on samples in duplicate yielding quadruplicate results (Cunha et al. 2018).

2.8 Effect of different carbon and nitrogen sources on xylanase production

The effect of carbon and nitrogen sources in the NSS was determined. Different carbon sources (1% w/v) such as wheat bran, glycerol (v/v), glucose, sucrose, maltose, and lactose (Okafor et al. 2007;

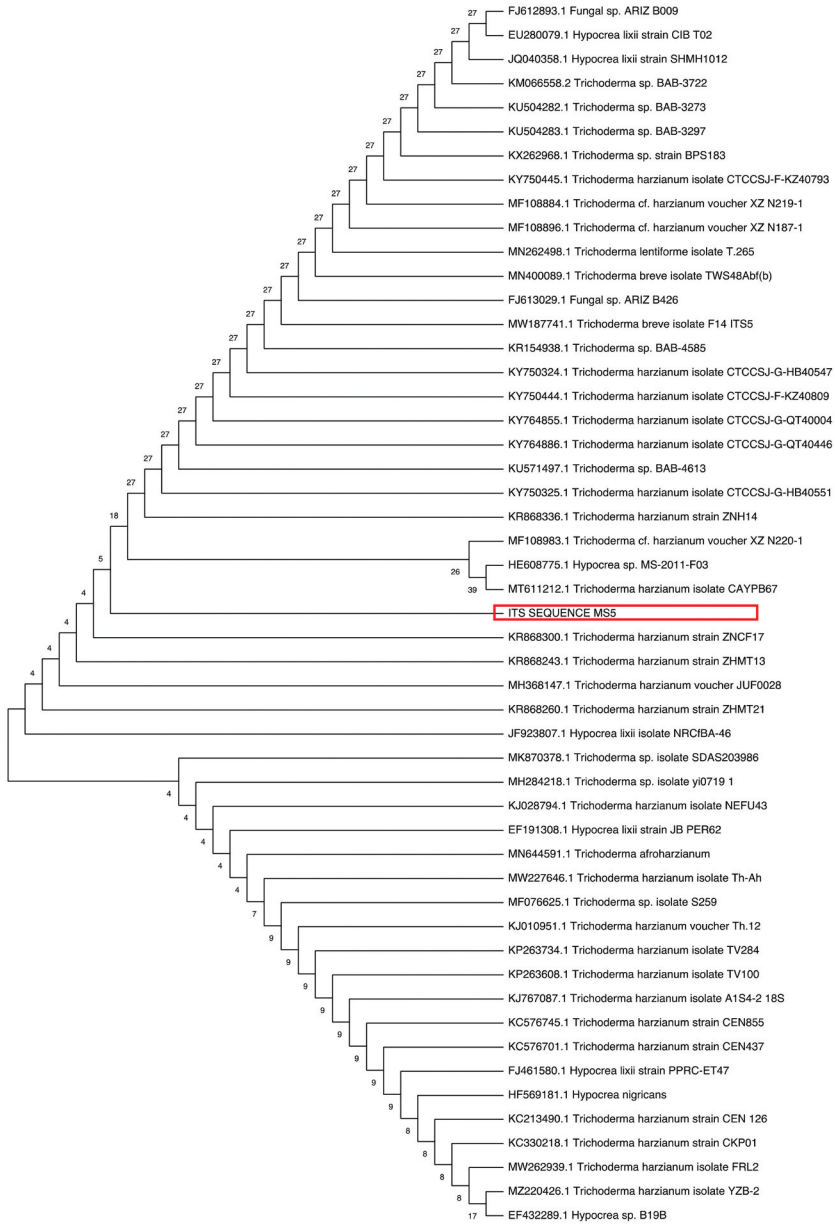

Figure 2 Phylogenetic analysis of the 50 isolates based on alignment of the nucleotide sequences of xylanases including the its sequence of selected MS5 isolate with Mega11. The microbial species, strain name and accession number are presented. Numbers on branches indicate bootstrap support.

Pandey et al. 2012) and different nitrogen sources (1% w/v) such as peptone, ammonium sulphate, ammonium acetate, casein, glycine, and yeast extract (Gomaa 2013; Ajijolakewu et al. 2017) were used to determine maximal enzyme production under optimised conditions for the other parameters. Once the optimal carbon and nitrogen sources were determined, concentrations between 0.5% and 2% (w/v) were used to determine the optimal concentration for maximum xylanase production.

2.9 Biochemical characterisation of crude enzyme

2.9.1 Determination of pH and temperature optima of crude xylanases

To determine the optimum pH values for xylanase activity, different pH buffers were required with 1% substrate for the enzyme reaction at 55°C. The following buffers were used: 0.1 M sodium citrate buffer (pH 3.0–5.0), 0.1 M potassium phosphate buffer (pH 6.0–8.0) and 0.1 M Glycine-NaOH buffer (pH 9.0–10.0) (Franco et al. 2004). All buffers were adjusted to the

required pH by using 0.1 M HCl and 0.1 M NaOH as the acid and base. Thereafter, the reaction was stopped by adding DNS and incubating assays at 100°C (Miller 1959).

The optimum temperature of xylanase activity was determined by incubating the enzyme with the optimum pH buffer (pH 6.0 and 8.0) and substrate (1%) in a temperature range between 40°C and 90°C for the reaction time. Thereafter, the enzyme was assayed using the DNS method (Miller 1959).

2.9.2 pH and temperature stability of crude xylanase

The pH stability of the enzyme was determined at both pH optima (pH 6.0 and 8.0) by incubating the enzyme in the respective buffers for 4 h at optimum temperature with aliquots removed every 30 min (Abo-Elmagd 2014). Thereafter, xylanase activity was assayed using the DNS method (Miller 1959) and reported as residual activity (%).

Temperature stability of xylanase was determined by preincubating the enzyme at the different temperature optima (55°C, 60°C, 70°C and 75°C) with aliquots collected every 30 min for 4 h for determination of residual activity that was reported as a mean (n = 3) ± SD.

2.9.3 SDS-PAGE

SDS-PAGE was carried out according to Laemmli (1970). A 12% denaturing polyacrylamide gel, which contained SDS was prepared. Following electrophoresis at 50 V for 4 h, the gel was stained with Coomassie Brilliant Blue for 15 min and destained overnight in a de-staining solution. In order to visualise the proteins and determine the molecular mass of the proteins using standard molecular weight markers. To allow for the protein to be more visible, silver staining was performed according to the manual instructions (SilverQuest^{TM} Silver Staining kit, Thermo Fisher Scientific, LC6070).

2.9.4 Substrate native PAGE

Native-PAGE was conducted at room temperature using a 15% polyacrylamide gel supplemented with 1% (w/v) beechwood xylan. Following electrophoresis at 50 V for 4 h, the xylan gel was incubated at optimum temperature (70°C) in pH 5.0 citrate buffer for 1 h. The gel was stained with 0.1% (w/v) Congo red for 15 min at room temperature and destained with 1 M NaCl for 10 min. The protein bands associated with xylanase activity were visualised as clearing zones against a background (Goluguri et al. 2016).

2.10. Statistical analysis

Data presented in this paper show the mean of four replicates with their standard deviation (mean ± SD). Results were analysed statistically by Microsoft Excel.

3. Results

3.1 Screening for enzyme activity

A total of 48 isolates were obtained from the three sites, with similar isolates obtained from soil and bark samples within the three sites. From all the isolates, 33 were selected for secondary screening based on the size of the clear zones on xylan agar plates (Supplementary Tables 1–3). The unhydrolysed, Congo red-stained xylan medium appeared dark red as seen in the negative control (Table 1). The 23 isolates (Supplementary Tables 4–6) with the largest zones of clearance (Figure 3) were selected for quantitative analysis. In Figure 3, isolates CB1 (21.67 U/ml), CB2 (16.98 U/ml), MS5 (22.98 U/ml), PS3 (15.64 U/ml) and PB7 (14.22 U/ml) produced the highest enzyme activity compared to the others. Fungal morphology on PDA and xylanase activity on substrate agar plates of the five isolates with the highest enzyme activity from Figure 3 are summarised in Table 1.

3.2 Effect of pH and incubation temperature on xylanase production

Five of the 23 isolates, with the highest activities (CB1, CB2, MS5, PS3, and PB7) were selected for pH and temperature studies in order to determine which isolate would be the best to select for future studies. To determine best conditions for enzyme production, the effect of pH was determined

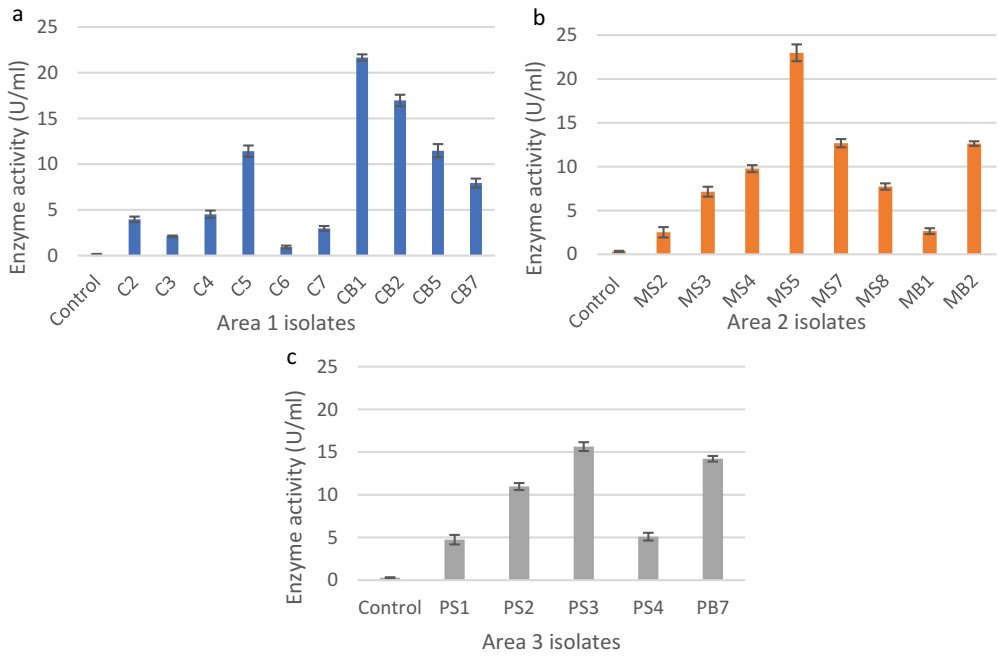

Figure 3 Xylanase activity of the fungal isolates from the different sample areas based on the 3,5-dintrosalicylic acid assay for reducing sugars. a: Area 1, b: Area 2, and c: Area 3.

Table 1. Fungal isolates substrate agar screening results for xylanase activity.

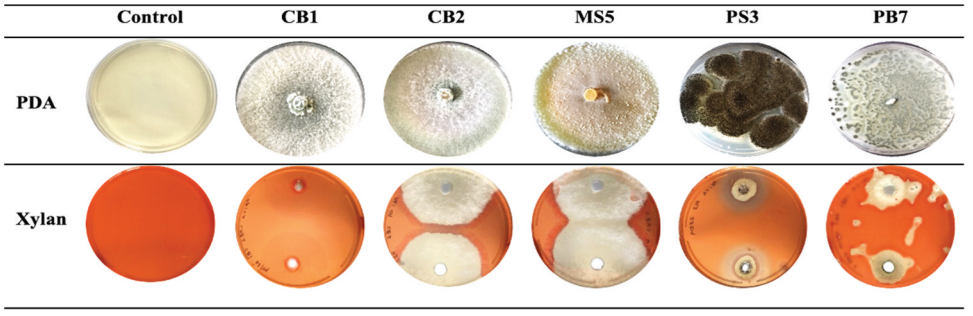

between pH 4.0 and 10.0 (Figure 4). Isolate CB1 produced the highest enzyme activity (38.32 ± 0.89 U/ml) when grown in the medium at pH 10, with elevated enzyme activity at pH 7.0 and 9.0. Isolates CB2 and MS5 produced the highest enzyme activities of 38.49 ± 1.16 U/ml and 38.50 ± 0.76 U/ml at pH 6.0 and 5.0, respectively. Isolate PB7, produced highest enzyme activity (38.12 ± 0.79 U/ml) at neutral pH. Lastly, for isolate PB7, the highest enzyme activity (36.96 ± 0.32 U/ml) was observed at pH 6.0.

The effect of temperature on enzyme production is shown in Figure 5. Temperatures between 20°C and 80°C were tested as this was the range tested in previous studies (Yadav et al. 2018). For isolate CB1, enzyme activity was highest (36.17 ± 1.65 U/ml) at 60°C and for isolates, CB2 and PB7, the highest activities of 37.77 ± 0.85 U/ml and 37.69 ± 0.82 U/ml, respectively, were observed at 50°C. Isolate MS5 produced the highest enzyme activity (38.17 ± 0.86 U/ml) at 70°C, and isolate PS3 appeared to be an extreme thermophile and produced the highest (35.96 ± 1.16 U/ml) enzyme activity at 80°C with similar activities at 40°C and 50°C (35.61 ± 0.84 U/ml and 35.01 ± 0.84 U/ml). Isolate MS5 was selected for further studies due to its thermophilic properties and acidic conditions.

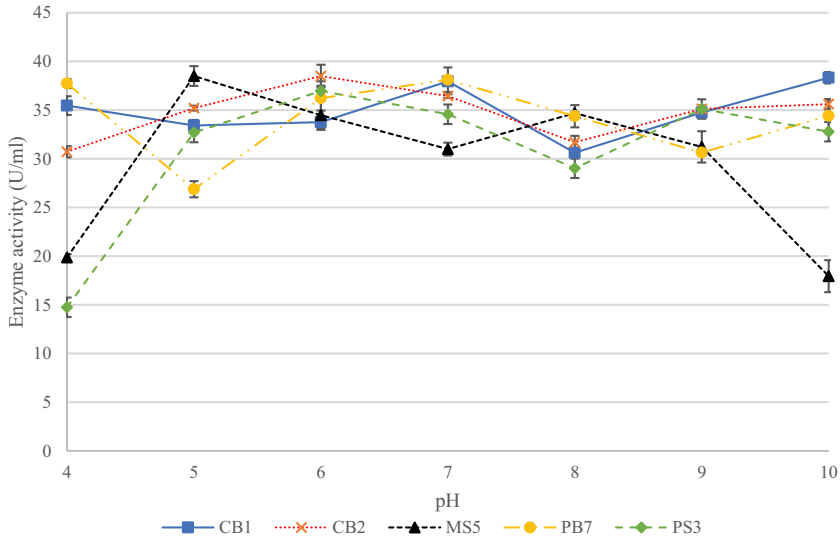

Figure 4 Effect of pH on xylanase production for the five selected fungal isolates, produced during submerged fermentation at 30°C and 200 rpm. Data points represent the means ± SD (n = 4).

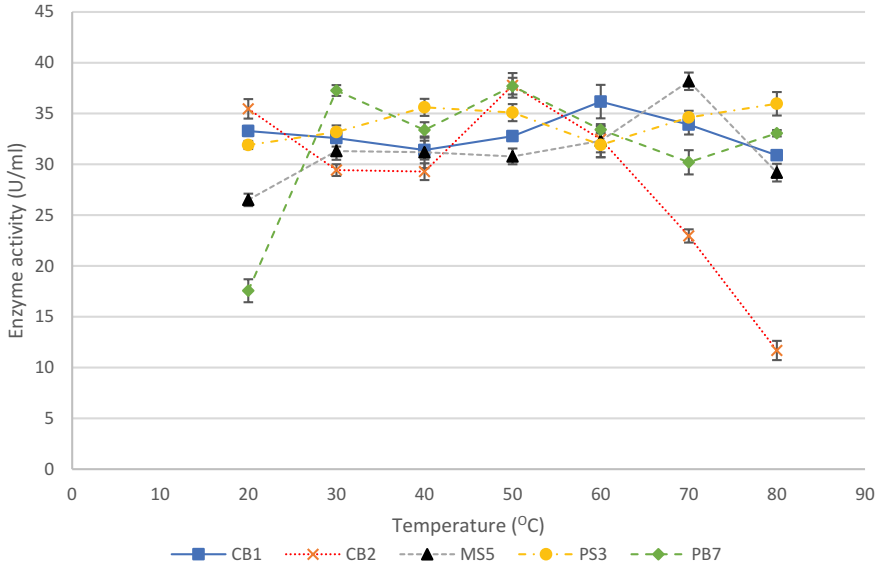

Figure 5 Effect of temperature on xylanase production by the five selected fungal isolates, during submerged fermentation at their optimum pH and 200 rpm. Data points represent the means ± SD (n = 4).

3.3 Identification of five fungal isolates and morphological studies of selected isolate

3.3.1 Identification of fungal isolates

The PCR amplicon was sent to Inqaba BioTec for sequencing and the consensus sequences were submitted to National Centre for Biotechnology Information (NCBI) database to determine the identity of the unknown isolates. Isolate CB1 had a 99.83% identity with *Hyprocrea lixxi* strain TU Graz 3TSM1 and CB2 a 100% identity to *Trichoderma atroviride* strain CUZFVG243. Isolates PB7 and PS3 are both *Aspergillus* sp. with a 99.49% and 99.83% identity to *Aspergillus fumigatus* CK392 and *Aspergillus welwitschiae* SFC102281, respectively. Although sequencing and BLAST analysis resulted in a low (45%) percentage coverage the ID of the unknown isolate MS5 was revealed to be *Trichoderma harzianum* strain with a 99.83% identity to the *Trichoderma harzianum* ZNH14 strain (Table 2).

Table 2. Identification of unknown isolates.

Isolate	Identity	Max score	Total score	% Coverage	E.value	% Identity	Accession number
CB1	*Hypocrea lixii* TU Graz 3TSM1	1096	2096	94	0	99.83	EU871017.1
CB2	*Trichoderma atroviride* CUZFVG243	1075	2107	96	0	100	KC884783.1
PB7	*Aspergillus fumigatus* CK392	1066	2111	98	0	99.49	MK439477.1
PS3	*Aspergillus welwitschiae* SFC102281	1068	2046	94	0	99.83	MH374611.1
MS5	*Trichoderma harzianum* ZNH14	1110	2129	45	0	99.83	KR868336.1

3.3.2 Phylogenetic analysis of isolate MS5

Phylogenetic analysis plays an important role in understanding the current research in biological processes (the evolution of species, populations and genes) and became an important data source for how traits evolve over time, the order in which interrelated traits evolve and the influence of an ecology on the evolution of traits. The evolutionary relationship between species is generally reflected in the form of phylogenetic trees (Chen and Zhuang 2017). There were 46 branches originating from the original root. All the *T. harzianum* isolates do not form a single taxon but form sister taxa with other *Trichoderma* species. The isolate reported in the current study forms sister taxa with 2 other *T. harzianum* strains as well as a third branch that splits into 2 sister taxa, one being a *Trichoderma* sp. and the other *T. lixii*.

3.3.3 Morphological studies of MS5

Microscopic examination of the 5-day-old culture using light microscopy showed septate hyphae, conidiospores and phialides (Figure 6). The morphological analysis indicates that isolate MS5 belongs to the *Trichoderma* genus.

3.4 Time course studies for optimal xylanase production by *T. harzianum*

The time required for maximal xylanase production was determined by growing the isolateat 70°C at 200 rpm for 1 to 8 days. The highest activity (39.01 ± 0.75 U/ml) was obtained after 5 days. A further increase in the incubation period resulted in a decrease in the enzyme production (Figure 7).

3.5 Effect of agitation on xylanase production by *T. harzianum*

The effect of agitation speeds on xylanase production was studied between 120 and 200 rpm at 70°C for 5 days. At the lower agitation rates tested, enzyme-production was directly proportional to agitation speed with the highest xylanase activity (39.19 ± 0.83 U/ml) observed at 160 rpm (Figure 8). However, a further increase in agitation speed resulted in a sharp and steady decrease in enzyme activity.

3.6 Effect of different carbon and nitrogen sources on xylanase production by *T. harzianum*

The effect of carbon (Figure 9a) and nitrogen sources (Figure 9b) in the growth medium were studied to order to maximise enzyme production. It was clear that the *T. harzianum* strain produced the highest xylanase levels when supplemented with glucose (36.76 ± 0.97 U/ml) compared to the control, followed by wheat bran (35.44 ± 0.86 U/ml) and sucrose (24.77 ± 0.71 U/ml). Glycerol had the smallest effect on enzyme production (6.86 ± 0.44 U/ml). Wheat bran was selected as the carbon source for further studies.

Of the nitrogen sources tested, peptone produced the highest enzyme activity (38.9 ± 0.67 U/ml) followed by ammonium sulphate (37.20 ± 1.15 U/ml) and casein (25.16 ± 0.77 U/ml) (Figure 9). The addition of glycine proved to be inhibitory (4.53 ± 0.38 U/ml) as it resulted in lower enzyme activity compared to the control (5.42 ± 0.44 U/ml). Ammonium sulphate was selected as the nitrogen source for further studies. A range of wheat bran and ammonium

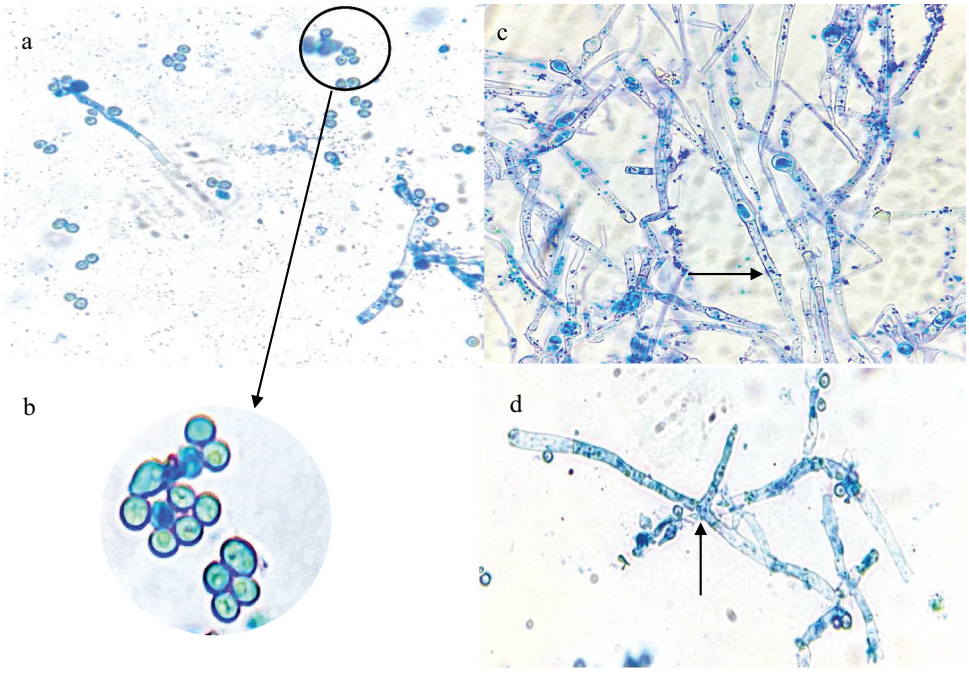

Figure 6 Photomicrographs of a lactophenol cotton blue strain preparation of the identified *Trichoderma harzianum* strain at 1000 x magnification. the black arrows represent, (a) conidia (b) an enlarged image of the conidiospores (c) hyphae, and (d) phialides.

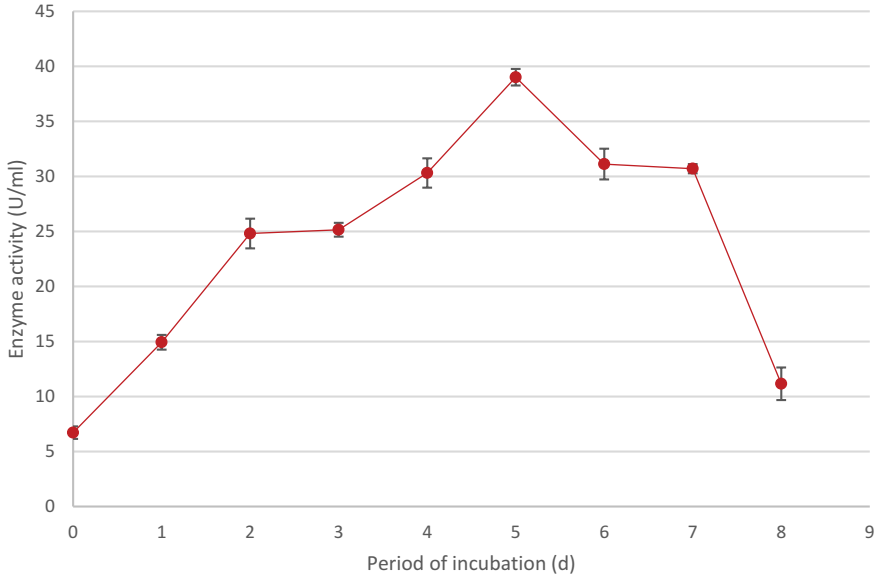

Figure 7 Time course studies showing the optimal period of incubation for maximum xylanase production by identified *Trichoderma harzianum* isolate during submerged fermentation at 70°C, pH 5.0 and standard agitation (200 rpm). Data points represent the means ± SD (n = 4).

sulphate concentrations were tested in order to establish best concentrations for enzyme production. As shown in (Figure 10) the highest xylanase levels were produced in 1% (w/v) wheat bran (35.49 ± 0.72 U/ml) and 1.2% (w/v) ammonium sulphate (37.01 ± 1.24 U/ml).

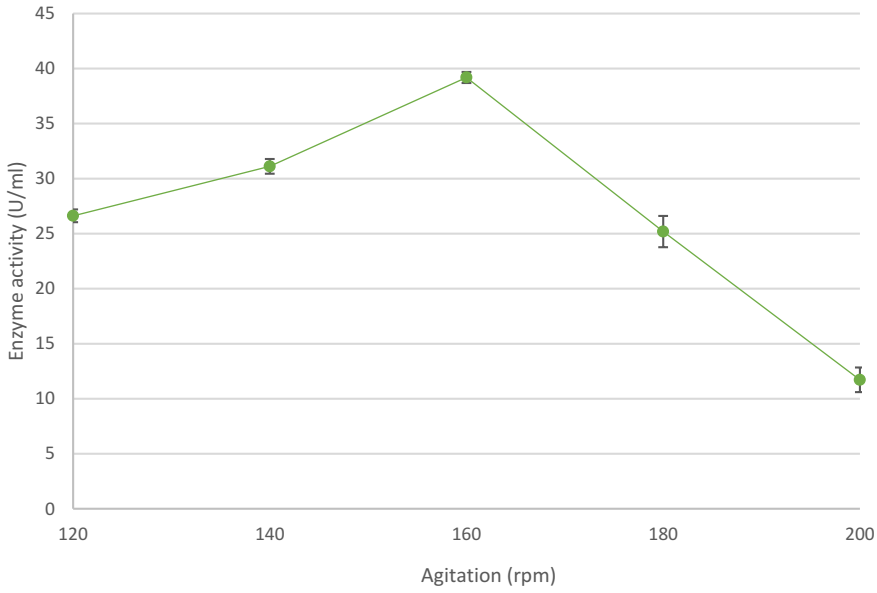

Figure 8 The effect of agitation on xylanase production by the identified *Trichoderma harzianum* isolate, produced during submerged fermentation at 70°C, pH 5.0 for 5 days. Data points represent the means ± SD (n = 4).

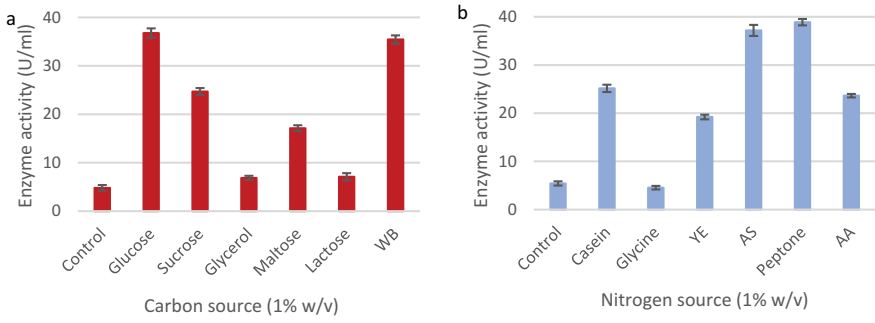

Figure 9 Effect of various carbon (a) and nitrogen (b) sources on xylanase production by identified *Trichoderma harzianum* isolate during submerged fermentation at 70°C, pH 5.0, for 5 days at 160 rpm. WB: wheat bran, YE: yeast extract, AS: ammonium sulphate, and AA: ammonium acetate. columns represent the means ± SD (n = 4)

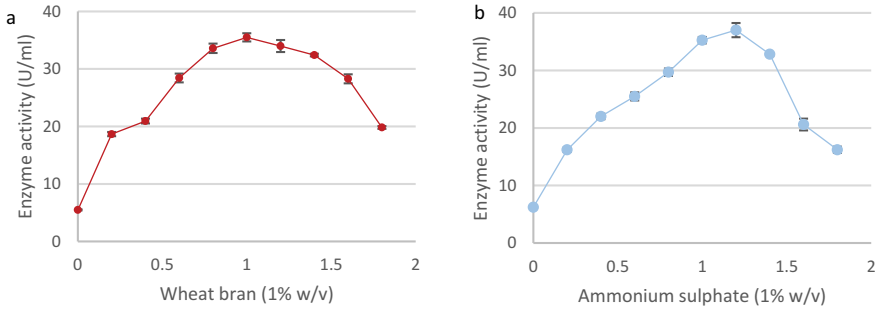

Figure 10 Effect of different wheat bran (a) and ammonium sulphate (b) concentrations (w/v) on xylanase production by the *Trichoderma harzianum* isolate during submerged fermentation at 70°C, pH 5.0, for 5 days at 160 rpm. Data points represent the means ± SD (n = 4).

3.7 Biochemical characterisation of crude xylanases

3.7.1 Determination of pH and temperature optima for enzyme activity

Various pH affected the activity of xylanase from *T. harzianum*. The highest xylanase activity was seen at pH 8.0 (37.80 ± 1.53 U/ml) and a second peak was observed at at pH 6.0 (36.13 ± 1.44 U/ml) (Figure 11a). Enzyme activity assays were performed at various temperatures at both pH optima. Figure 11b shows that the xylanase activity was the highest at 60°C (39.37 ± 0.86 U/ml) witha second peak at 70°C (31.66 ± 0.41 U/ml) at pH 6.0, whereas at pH 8.0, the xylanase activity was the highest at 75°C (39.08 ± 1.92 U/ml) and peaked again at 55°C (38.24 ± 2.11 U/ml).

3.7.2 Determination of pH and temperature f on enzyme stability

The *T. harzianum* xylanase retained >50% maximal activity at pH 6 after 4 h (Figure 12a) whereas at pH 8.0 the enzyme only retained activity for 0.5 h

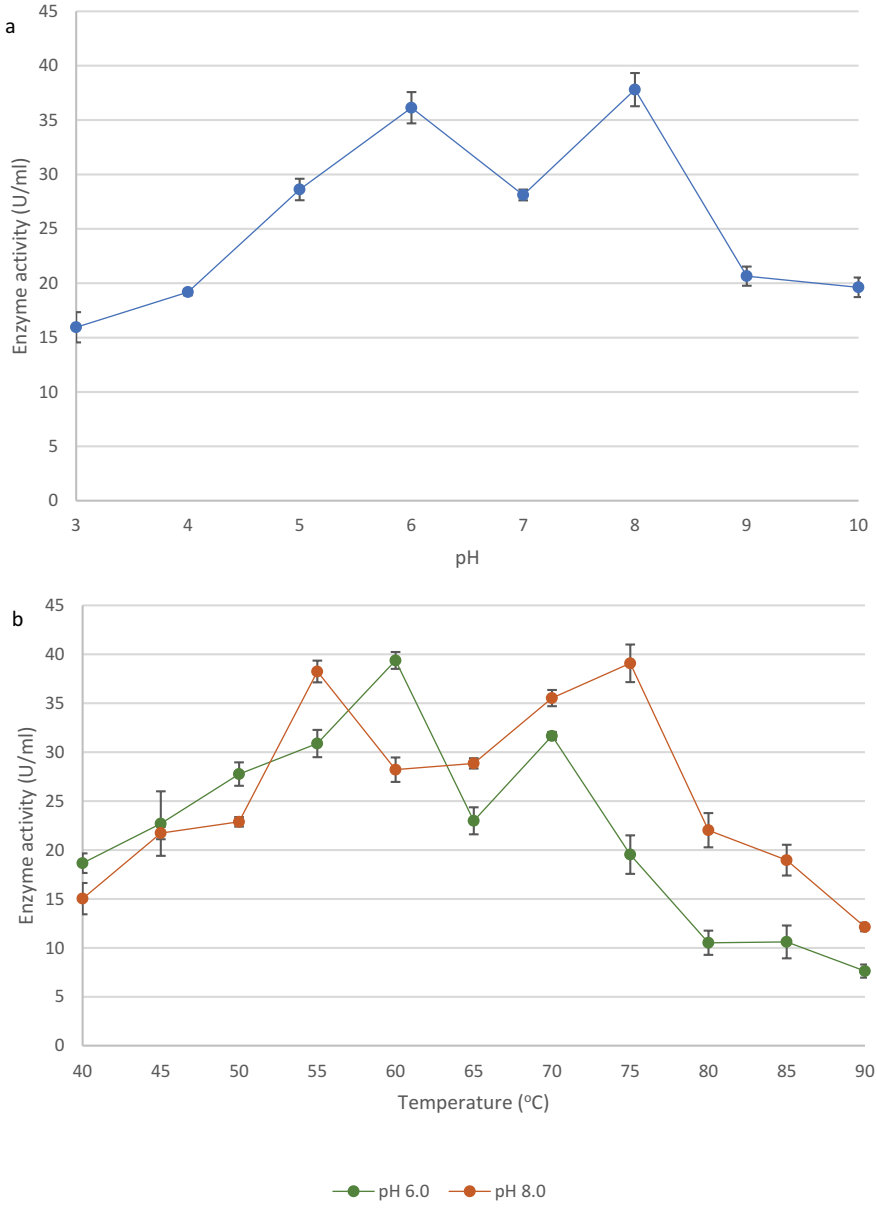

Figure 11 Effect of pH (a) and temperature (b: at pH 6.0 and pH 8.0)) on the activity of xylanase from the identified *Trichoderma harzianum* isolate crude extracellular supernatants. Data points represent the means ± SD (n = 3).

which gradually declined for 2.5 h with sharper decline in activity between 2.5 and 4 h. In Figure 12b, at pH 6.0, the enzyme retained >50% activity after 4 h at both 60°C and 70°C. At pH 8.0, the enzyme retained >50% activity at 75°C for 4 h and lost activity after 4 h at 55°C.

3.7.3 Polyacrylamide Gel Electrophoresis

The SDS PAGE gel of the crude xylanase enzyme (Figure 13) was stained using silver staining, which revealed multiple protein bands in the crude extract. A prominent band with a molecular weight of 70 kDa was observed. The native PAGE gel supplemented with 1% (w/v) beechwood xylan revealed hydrolysis of the substrate as evidenced by the areas with a slightly yellow hue. The majority of the xylanase activity corresponded to the mass of proteins in the top half of the gel between 34 and 130 kDa in molecular weight where brighter bands were observed at a higher molecular weight (55–130 kDa).

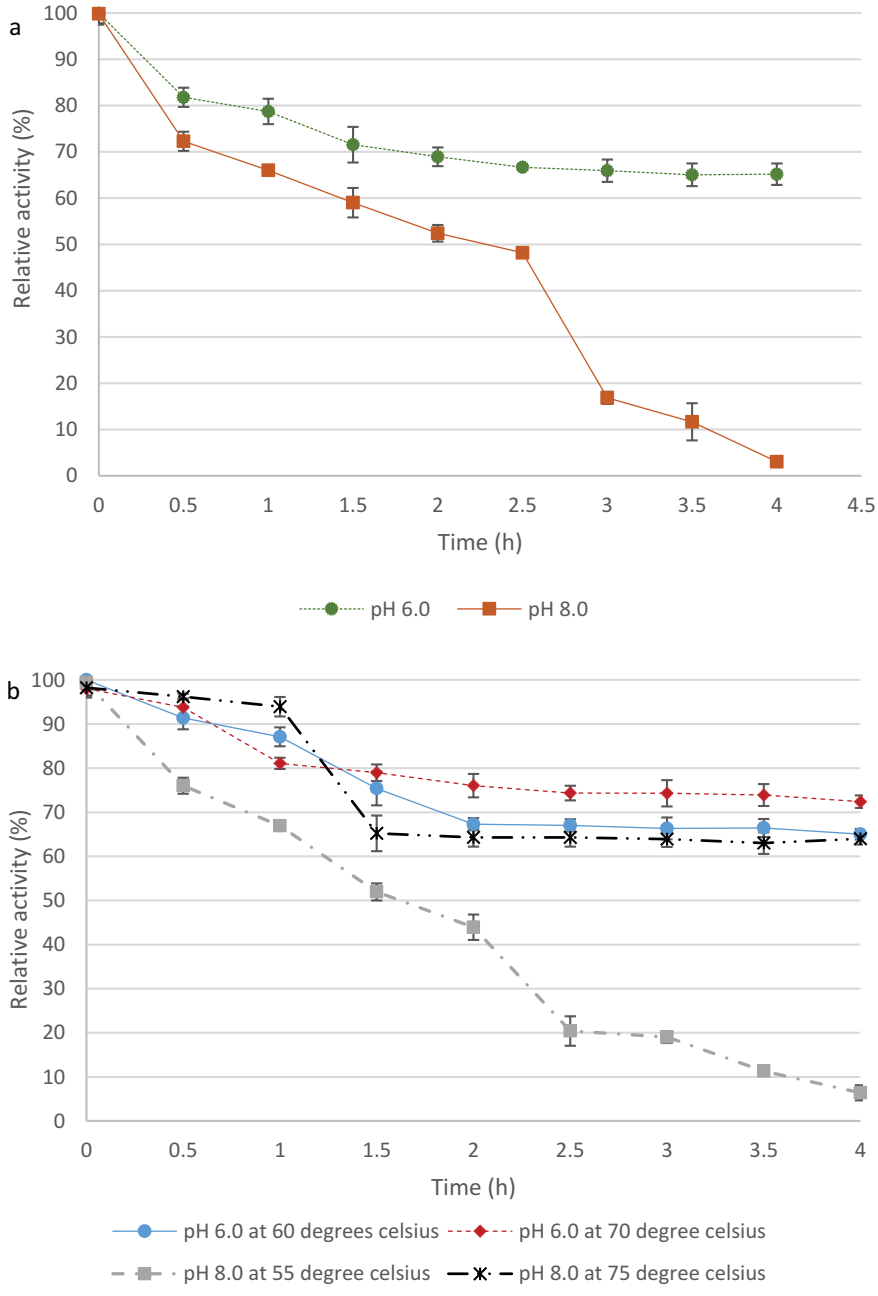

Figure 12 pH (A) and temperature (B) stability of crude xylanases produced by the *Trichoderma harzianum* isolate. Data points represent the means ± SD (n = 3).

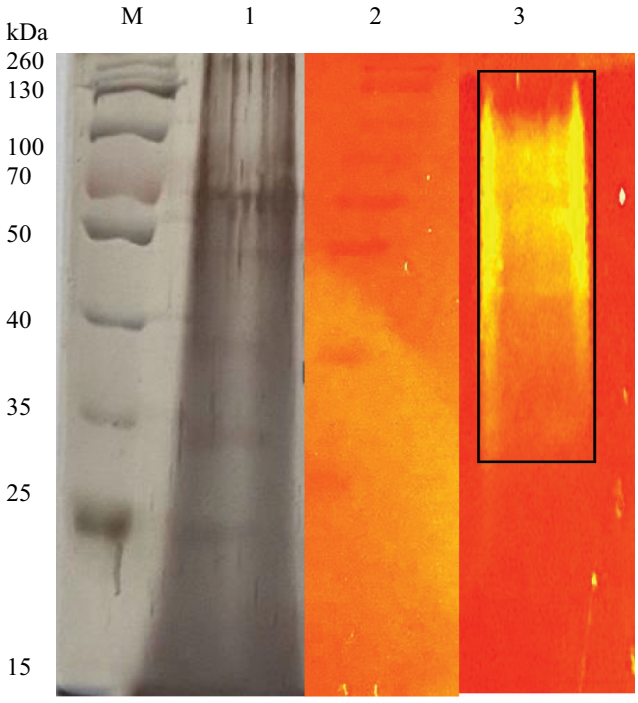

Figure 13 SDS PAGE gel (silver stained) and native substrate PAGE gel (1% xylan) of the *Trichoderma harzianum* crude xylanases. lane M: Spectra multicolour broad range marker (Thermo Scientific, USA), lane 1: crude extract, lane 2: Spectra multicolour broad range marker Thermo Scientific, USA) (stained with Congo red) and lane 3: crude xylanase extract showing zones of clearance.

4. Discussion

In spite of advanced knowledge of microbial xylanases garnered over the past decades, bioprospecting for organisms with xylanases with potentially ideal characteristics for industrial application is ongoing and to this end several factors (location, desired qualities, characteristics of microorganism, etc.) are still significant for the choice of such an organism. In the present study, 46 filamentous fungal isolates were obtained from soil and bark samples and screened for their xylanase activity under submerged fermentation. During the isolation, the growth of bacteria was not intentionally prevented, instead sub culturing was performed from the original plates to obtain pure fungal cultures. Primary screening using qualitative methods is a powerful tool that allows rapid and easy screening of microorganisms for enzyme production. This qualitative substrate agar test indicates positive or negative enzyme production and is invaluable when screening a large number of isolates and quantitative analysis is not required (Pointing 1999). The xylanase-producing isolates displayed clearing zones from a dark red to a light red colour representing efficient xylanase activity. The low enzyme activity displayed by some isolates may be due to the presence of contaminants or enzyme activities being too low for complete hydrolysis of the substrate for visualisation on the substrate agar (Singh et al. 2006). After screening, five isolates were selected for pH and incubation temperature studies for the fermentation medium.

The pH plays a crucial role in nutrient transport across the membrane and the functioning of the microorganism's enzyme systems and thus influences the growth rate and the levels of enzyme produced (Gupta and Kar 2009). The temperature of the fermentation medium is a vital factor that has a strong influence on product formation (Pathak et al. 2014). Isolate CB1 identified as *Hypocrea lixii* (is a teleomorph of *T. harzianum*), exhibited the highest activity at pH 10 with several other peaks indicating the organism, is possibly an alkaliphile that also produced isoforms with different pH and temperature optima. Temperatures between 20°C and 80°C were tested and all five isolates produced the highest activities at temperatures between 50°C and 70°C. Again, a second enzyme activity peak observed would indicate the presence of more than one isoform. de Oliveira et al. (2014) also reported the presence of isoforms at 55°C at pH 5.0 and at 44°C at pH 3.6 for xylanases produced by *H. lixii*. Isolate CB2, identified as *Trichoderma atroviride*, appeared to be an acidophile and produced the highest activity at pH 6.0. Grigorevski-Lima et al. (2009) reported similar results with optimal pH studies. Isolates PS3 and PB7 displayed highest activity at neutral pH and at pH 6.0, respectively, indicating that the latter could possibly be an acidophile. Both these isolates are *Aspergillus* spp. and Hombalimath et al. (2021) reported similar studies where optimal activity was obtained at pH 7.0. Isolate MS5 showed optimal results at pH 5.0 with a second peak at pH 8.0 representing isoforms was similar to a report by Amore et al. (2015) who obtained maximal activity at pH 7.0 and a second peak at pH 9.0. Most fungi can grow in a wide pH range of 5.0–10.0 (Singh et al. 2006;

Abubakar et al. 2013). Generally, the higher xylanase titres (2701 U/g substrate) in fungal systems have been reported to occur at pH 5.0 (Shah and Datta 2005). However, their reported activity was expressed per gram substrate utilised which was reported for lignocellulosic biomass whereas the current study reports it in the conventional manner (U/ml). In addition, many studies report on the purified enzymes or on recombinant enzymes thus activities are higher (Zhang et al. 2010; Yangyuan et al. 2015; Deshmukh et al. 2016). Xylanases produced by these isolates may have a potential for applications in different sectors, including food and feed, paper and pulp and textile industries that require enzyme to work at high temperatures. The highest xylanase titres in fungal systems have generally been reported to occur at temperatures that are optimal for the growth of cultures in submerged fermentation (Sanghvi et al. 2010). The majority of fungal isolates produce one to three xylanase isoforms (Polizeli et al. 2005; Gong et al. 2018). Lenartovicz et al. (2002) reported that three xylanase isoforms were produced by *Aspergillus fumigatus*. However, *Thermomyces stellatus* and *Scytalidium thermophilium* are reported to have 10 isoforms while *Pseudocercosporella* and *Myceliophthora themophilum* have 14 and 13 isoforms, respectively (Chadha et al. 2019). Multiple forms of xylanases differ in stability, catalytic efficiency, absorption, and activity on substrates (Liao et al. 2015). Badhan et al. (2007) reported that 10 different functionally diverse xylanases were resolved electrophoretically using PAGE/IEF from *Myceliophthora* sp. and they also showed characteristically different activity against unsubstituted xylans, arabinoxylans and methyl-glucouroxylan.

Isolate MS5 was selected for further studies due to its thermophilic properties (temperature optimum of 70°C) and acidic pH optimum of 5.0; these properties were deemed favourable for the conditions of its targeted application in the hydrolysis of animal feed (Rigoldi et al. 2018). The advantages of thermophilic enzymes for conducting biotechnological processes at elevated temperatures are; reducing the risk of contamination by mesophilic microorganisms, decreasing the viscosity of the reaction medium, increasing the bioavailability and solubility of organic compounds, increasing the diffusion coefficient of substrates and products resulting in higher reaction rates (Kambourova 2018).

Azimova et al. (2020) reported that the *T. harzianum* strain UzCF-28 produced xylanases, which was also confirmed by Abbas et al. (2012). The Blast analysis returned a low percentage coverage (45%); however, the ITS2 amplicon was of the recommended size, the E value (Table 2) is 0 despite the low percentage coverage, there was a 99.8% similarity to *T. harzianum* ZNH14 (Chamacho et al., 2009). Filamentous fungi that belong to the *Trichoderma* genus are attractive (Marecik et al. 2018) due to their inducible enzyme systems, the considerable quantities of enzymes secreted by these fungi, including cellulase and hemicellulase cocktails. As a result of their wide spectrum of metabolic activities, *Trichoderma* sp. fungi have found numerous practical applications such as enzyme producers, as biofungicides (Mulatu et al. 2021), and in the food industry (Harris and Ramalingam 2010).

Sequences were assembled and aligned using the Mega11 software. All species of the related taxa from Blast analysis were included in the phylogenetic tree, all *T. harzianum* isolates were not grouped together and the species were either scattered among the clades or showed separate terminal branches. Chen and Zhuang (2017) discovered several new *Trichoderma* sp. during a screening exercise conducted on several hundred soil samples in China. They reported that *T. harzianum* formed the largest clade among the green-spored groups that formerly contained 41 species.

The abbreviated tree was constructed using 50 different microorganisms, mostly *T. harzianum* strains. Two predominant sister clades emerge from the root. Both consist of strains of *T. harzianum* but with Hypocrea strains forming part of the same sister clades, such as *T. harzianum* strains as well as *T. lixii* NRCfBA-46 in terms of distance (Chen and Zhuang 2017). Chaverri and Samuels (2002) reported cultures derived from ascospores of *Hypocrea lixii* (*T. lixii*) cultures produced the morphological species *T. harzianum*. The *H. lixii* isolates were shown to group with isolates of *T. harzianum* based on

phylogenies of four genes, translation elongation factor-1 α, calmodulin, actin and ITS rDNA, and morphological and cultural data (Chaverri et al. 2003). This could explain the genetic link between the two morphs.

When grown on PDA, the *T. harzianum* strain initially produced a fast-growing white downy mycelium (Table 1) which then changed to yellowish-green and later deep green as it matured. The conidiation predominantly effuse which appeared powdery and granular due to dense conidiation producing woolly and floccose compact tufts and rings with green coloured spores fringed by sterile white mycelium (Gams and Bissett 2002). Microscopic examination of the 5-day-old culture using light microscopy showed septate hyphae, conidiospores and phialides (Figure 6). Conidiospores of *T. harzianum* were formed in pairs along the main branches and axis (Figure 6a). The hyphae were thin and branched (Figure 6c). The phialides branching patterns were verticillate, broad, and branching frequently at approximately 90° one branching verticillate had two to three phialides (Figure 6d). Phialides were characteristically elongate lageniform in shapes. At the end of the phialides, conidia were formed with a globose or subglobose shape to obvoid and are smooth-walled, subhyaline to pale green (Figure 6b). These structures are similar to those described in previous studies (Gams and Bissett 2002).

Production of microbial enzymes is dependent upon various cultural and nutritional factors such as fermentation incubation period, agitation, carbon and nitrogen sources and hence these were studied in order to optimise xylanase production by *T. harzianum*. For the optimal period for enzyme production, the fungal isolate was incubated for a period of 8 d at the optimal pH and temperature obtained previously. The highest enzyme activity (39.01 U/ml) was obtained after 5 days. Similar results were reported by Goyal et al. (2008) where optimal xylanase activity (139.82 U/ml) was obtained between 5 and 7 days of incubation for *T. viride*. After 5 days of incubation, the enzyme activity declined, this could be due accumulation of toxic products in the medium that inhibits fungal growth, repression of enzyme expression by metabolic products or by multiple regulatory mechanisms (Shulami et al. 2014).

Agitation is considered an important factor for microbial growth as it controls the transfer of oxygen, heat, and nutrients from the medium to the microorganism and prevents the clumping together of the mycelia (Ibrahim et al. 2015). Highest enzyme activity (39.19 U/ml) was observed at 160 rpm (Figure 8) with higher agitation speeds resulting in lower xylanase activity. These higher agitation levels may have aggravated cell damage which, in turn, could have led to enzyme production falling off (Zhu et al. 2012). Several reports link increased agitation speeds to high shear stress leading to mycelial rupture and destruction of cellular structures, which decreases both mycelial growth and enzyme production (Bhattacharyya et al. 2008; Singhania et al. 2011). At high agitation rates, laminar flows are generated in a flask, which do not allow absorption of oxygen into the medium although rpm is high, which may cause reduced growth and enzyme production. However, below a certain threshold, lower agitation rates result in reduced mixing of the medium and as a consequence lower oxygen supply to the microorganism, lower growth rates and thus enzyme production.

Carbon and nitrogen sources are necessary for the growth and metabolism of microorganisms. The use of affordable C and N sources is important as these can reduce the cost of production significantly. Surprisingly, the best carbon source for xylanase production from *T. harzianum* was glucose. Carbon catabolite repression (CCR) has to be overcome usually for expression of hydrolytic enzymes (Hu et al. 2021). Basal expression levels of xyn1 coding for xylanase are affected by glucose and repression is reported to be mediated by the binding of the catabolite repressor protein Cre1 to the promoter of xyn 1. Mutants with truncated cre1 escape CCR (Mach et al. 1996). AC et al. (2008) studied xylanase regulation in *Aspergillus phoenicis* by growing the organism in media supplemented with 1% glucose, xylan or xylose. In the first few hours, glucose repressed xylanase production but after 72 h the level of glucose in the culture medium had dropped below 0.05 mg/mL, and some xylanolytic activity was already detectable in this carbon-derepressed culture. We believe that the levels of xylanase obtained on our study

were done during the de-repressed phase. The next best substrate was wheat bran while glycerol resulted in the lowest xylanase levels. Low activity could be due to the inability of the fungus to metabolise some substrates. Seyis and Aksoz (2005) tested xylanase production by *T. harzianum* 1073 D3 and reported maximum activity on melon peel (26.5 U/mg of protein) Wheat bran was selected as the carbon source as glucose is not cost-effective. Other enzyme production studies have also shown that wheat bran is a good carbon source for maximal xylanase production (Biswas et al. 2019).

The organic nitrogen source, peptone resulted in the maximum yield of xylanase from *T. harzianum* followed by ammonium sulphate (Figure 9) while xylanase production decreased in the presence of glycine. A review of the literature showed that ammonium sulphate (37.2 U/ml) is an appropriate source of nitrogen for *T. harzianum*, so it was selected as peptone (38.9 U/ml) is not cost-effective (Abdullah et al. 2015; Biswas et al. 2019). Glycerol had the greatest catabolic repression as the carbon source due to its minimal enzyme activity (6.86 U/ml). da Silva Delabona et al. (2016) reported that the use of glycerol to bulk up biomass is a good strategy followed by induction for cellulase production. Glycine as the nitrogen source had the greatest catabolic repression as minimal enzyme activity (4.53 U/ml) was observed.

Biochemical characterisation of xylanase revealed an enzyme with promising properties (high enzyme activity at various pH and temperatures) for future studies. The crude xylanase from *T. harzianum* demonstrated two pH optima: at 6.0 and 8.0 meaning that at least two different isoforms are present. The enzyme displayed greater stability at pH 6.0 and retained more than 50% of its activity over 4 h. However, it was not very stable at pH 8.0, as it lost activity after 1.5 h. These results are similar to those reported by Costa et al. (2019) and Sharma et al. (2016) for xylanase from *T. viride* and thermostable *Fusarium* sp. XPF5. Abo-Elmagd (2014) found that the xylanase from *T. harzianum* MH-20 had optimum activity at pH 5.5 and was stable from pH 5.5–6.5. Temperature can influence reaction rate of an enzyme. Thermal stability of the enzyme was observed at higher temperatures than expected with the xylanase retaining >50% of its activity at 60°C, 70°C and 75°C.

Thermostable and neutrally stable xylanases are beneficial for large scale production as the process would be simplified and save cooling time as well as reduce the problems of possible contamination (Liang et al. 2010) thus reducing costs. However, the target enzyme in the current study is produced under mildly acidic conditions, yet the cost impact may be minimised if acid lysed lignocellulose is used as the carbon source. The multiple high activities at various temperature and pH optima observed suggests that this organism produces multiple xylanases. This has been reported previously (Raj et al. 2013) who also reported multiple xylanases and endoglucanases produced by *Simplicillium obclavatum* MTCC 9604 during growth on wheat bran. Each xylanase may have diverse structures, physicochemical properties and rate of activities.

Several bands at approximately at 70 kDa, 49 kDa, 39 kDa, and 25 kDa (Figure 13) were apparent for the crude *T. harzianum* xlanase de Paula Silveira et al. (1999) and Silva et al. (2015) reported xylanase at 14–19 kDa from *T. inhamatum* and *T. harzianum*. Nathan et al. (2017) reported molecular weights between 14 and 66 kDa for xylanases from *T. viride* VKF3. Native substrate PAGE was performed using a native gel supplemented with xylan substrate and stained with Congo red. This approach and zymogram analysis are widely used for confirmation of xylanolytic activity and to identify the fractions that possess the activity during purification. A range of isoforms were detected (55–130 kDa) as the crude enzyme migrated through the Native PAGE gel and hydrolysed the xylan forming bands of hydrolysis. Nathan et al. (2017) reported xylanase activity at 14 kDa and between 43 and 66 kDa.

T. harzianum xylanases with various pH and temperature optima and activities have been studied previously, e.g. one with a lower temperature optimum (22°C) (Azzouz et al. 2020). Bhalla et al. (2015) reported maximal xylanase activity from *Geobacillus* sp. strain WSUCF1 at 60°C (pH 6.0). However, the current study is the first report of a *T. harzianum* strain isolated in South Africa with thermophilic isoforms displaying high activities and different pH optima, which are suitable for applications in animal feed improvement

and biofuels production. The isoform produced at acidic optimum (pH 5.0) was targeted in this study for future applications in the feed industry.

The growth conditions of the isolate in submerged fermentation has been performed to find the best conditions for highest xylanase production. Future studies using statistical experiment design (Plackett-Burman and Response Surface Methodology), scaled up production in bioreactors, purification and characterisation of the pure enzyme will be conducted.

Acknowledgements

This work was supported by a DST grant managed by the Technology Innovation Agency (TIA) DST/CON/0177/2018: SIIP: ENZYME AND MICROBIAL TECHNOLOGIES (EMT) grant and the Biorefinery Industry Development Facility (BIDF) at the Council for Scientific and Industrial Research (CSIR), Durban, South Africa.

Disclosure statement

No potential conflict of interest was reported by the author(s).

Funding

This work was supported by the Department of Science DST [DST/CON/0177/2018]. and Technology and managed by the Technology Innovation Agency (TIA).

References

Abbas A, Ahmad S, Mushtaq Z, Jamil A. 2012. Partial purification and characterization of a xylanase from *Trichoderma harzianum*. J Chem Soc Pak. 34 (6):1455–1459.

Abdullah R, Nisar K, Aslam A, Iqtedar M, Naz S. 2015. Enhanced production of xylanase from locally isolated fungal strain using agro-industrial residues under solid-state fermentation. Nat Prod Res. 29(11):1006–1011. doi:10.1080/14786419.2014.968157.

Abo-Elmagd HI. 2014. Optimization and biochemical characterization of exracellular xylanase from *Trichoderma harzianum* MH-20 under solid state fermentation. Life Sci J. 11 (3):188–195.

Abubakar A, Suberu HA, Bello IM, Abdulkadir R, Daudu OA, Lateef AA. 2013. Effect of pH on mycelial growth and sporulation of *Aspergillus parasiticus*. J Plant Sci. 1 (4):64–67.

AC SR, F ZF, MC B, SC P-N, HF T, J J, M DL, T DMP. 2008. Regulation of xylanase in *Aspergillus phoenicis*: a physiological and molecular approach. J Ind Microbiol Biotechnol. 35(4):237–244. doi:10.1007/s10295-007-0290-9.

Adesina FC, Onilude AA. 2013. Isolation, identification, and screening of xylanase and glucanase-producing micro fungi from degrading wood in Nigeria. Afr J Agric Res. 8 (34):4414–4421. doi:10.5897/AJAR2013.6993.

Ajijolakewu AK, Leh CP, Wan Abdullah WN, Lee CK. 2017. Optimization of production conditions for xylanase production by newly isolated strain *Aspergillus niger* through solid state fermentation of oil palm empty fruit bunches. Biocatal Agric Biotechnol. 11:239–247. doi:10.1016/j.bcab.2017.07.009.

Amore A, Parameswaran B, Kumar R, Birolo L, Vinciguerra R, Marcolongo L, Ionate E, La Cara F, Pandey A, Faraco V. 2015. Application of a new xylanase activity from *Bacillus amyloliquefaciens* XR44A in brewer's spent grain saccharification. J Chem Technol Biotechnol. 90(3):573–581. doi:10.1002/jctb.4589.

Azimova NS, Khamidova KM, Turaeva BI, Karimov HK, Shakirov ZS. 2020. Properties of the cellulase and xylanase enzyme complexes of *Trichoderma harzianum* UzCF-28. Eurasia J Biosci. 14:5803–5808.

Azzouz Z, Bettache A, Boucherba N, Amghar Z, Benallaoua S. 2020. Optimization of xylanase production by newly isolated strain *Trichoderma afroharzianum* isolate AZ 12 in solid state fermentation using response surface methodology. Cellul Chem Tech. 54 (5–6):451–462. doi:10.35812/CelluloseChemTechnol.2020.54.46.

Badhan AK, Chadha BS, Kaur J, Saini HS, Bhat MK. 2007. Production of multiple xylanolytic and cellulolytic enzymes by thermophilic fungus *Myceliophthora* sp. IMI 387099. Bioresour Technol. 98:504–510. doi:10.1016/j.biortech.2006.02.009.

Bedford MR. 2018. The evolution and application of enzymes in the animal feed industry: the role of data interpretation. Br Poult Sci. 59(5):486–493. doi:10.1080/00071668.2018.1484074.

Bhalla A, Bischoff KM, Sani KR. 2015. Highly thermostable xylanase production from a thermophilic *Geobacillus* sp. strain WSUCF1 utilizing lignocellulosic biomass. Front Bioeng Biotechnol. 3:84. doi:10.3389/fbioe.2015.00084.

Bhardwaj N, Kumar B, Verma P. 2019. A detailed overview of xylanases: an emerging biomolecule for current and future prospective. Bioresour Bioprocess. 6:40.

Bhattacharyya MS, Singh A, Banerjee UC. 2008. Production of carbonyl reductase by *Geotrichum candidum* in a laboratory scale bioreactor. Bioresour Technol. 99(18):8765–8770. doi:10.1016/j.biortech.2008.04.035.

Bhavsar NH, Raol BV, Raol GG, Bhatt PR. 2016. Isolation, screening, and optimization of xylanase-producing fungi from compost pit. Ijir. 2(11):44–68.

Biswas P, Bharti AK, Kadam A, Dutt D. 2019. Wheat bran as substrate for enzyme production and its application in the bio-deinking of mixed office waste (MOW) paper. BioRes. 14 (3):5788–5806.

Camacho C, Coulouris G, Avagyan V, et al.$3$2 2009. BLAST+: architecture and applications. BMC Bioinform. 10:421. doi:10.1186/1471-2105-10-4212009

Chadha BS, Kaur B, Basotra N, Tsang A, Pandey A. 2019. Thermostable xylanases from thermophilic fungi and bacteria: current perspective. Bioresource Technol. 277 (2019):195–203. doi:10.1016/j.biortech.2019.01.044.

Chaverri P, Samuels G. 2002. *Hypocrea lixii*, the teleomorph of *Trichoderma harzianum*. Mycol Prog. 1(3):283–286. doi:10.1007/s11557-006-0025-8.

Chaverri P, Castlebury L, Samuels G, Geiser D. 2003. Multilocus phylogenetic structure within the *Trichoderma harzianum/ Hypocrea lixii* complex. Mol Phylogenet Evol. 27(2):302–313. doi:10.1016/S1055-7903(02)00400-1.

Chen K, Zhuang WY. 2017. Discovery from a large-scaled survey of *Trichoderma* in soil of China. Sci. 7:9090.

Collins T, Gerday C, Feller G. 2005. Xylanases, xylanase families and extremophilic xylanases. FEMS Microbiol Rev. 29 (1):3–23. doi:10.1016/j.femsre.2004.06.005.

Costa A, Cavalheiro G, Vieira E, Gandra J, Goes R, Fonseca P, LeiteR G. 2019. Catalytic properties of xylanases produced by *Trichoderma piluliferum* and *Trichoderma viride* and their application as additives in bovine feeding. Biocatal Agric. 19:101–161.

Cunha L, Martarello R, Monteiro de Souza P, Medeiros de Freitas M, Vanio Gomes Barros K, Ximenes Ferreira Filho E, Homem-de-Mello M, Magalhaes PO. 2018. Optimization of xylanase production from *Aspergillus foetidus* in soybean residue. Hindawi Enzyme Res. 2018(2):1–7. doi:10.1155/2018/6597017.

da Silva Delabona P, Deise JL, Diogo R, Rabelo SC, Farinas CS, da Cruz Pradella JG. 2016. Enhanced cellulase production by *Trichoderma harzianum* by cultivation on glycerol followed by induction on cellulosic substrates. J Ind Microbiol Biotechnol. 43(2016):617–626. doi:10.1007/s10295-016-1744-8.

da Silva Menezes B, Rossi DM, Ayub MA. 2017. Screening of filamentous fungi to produce xylanase and xylooligosaccharides in submerged and solid-state cultivations on rice husk, soybean hull, and spent malt as substrates. World J Microbiol Biotechnol. 3(3):58. doi:10.1007/s11274-017-2226-5.

de Paula Silveira F, de Sousa M, Ricart C, de Medeiros Milagres, AMF. 1999. A new xylanase from a *Trichoderma harzianum* strain. J Ind Microbiol Biotech. 23(1):682–685. doi:10.1038/sj.jim.2900
682

Deshmukh RA, Jagtap S, Mandal MK, Mandal SK. 2016. Purification, biochemical characterization and structural modelling of alkali-stable β-1,4-xylan xylanohydrolase from *Aspergillus fumigatus* R1 isolated from soil. BMC Biotechnol. 16(1):11. doi:10.1186/s12896-016-0242-4.

Franco PF, Ferreira HM, Filho EX. 2004. Production and characterization of hemicellulase activities from *Trichoderma harzianum* strain T4. Biotechnol Appl Biochem. 40 (3):255–259. doi:10.1042/BA20030161.

Gams W, Bissett J. 2002. Morphology and identification of *Trichoderma*. In: Christian PK, Gary GH, editors. *Trichoderma and Gilocladium*. basic biology, taxonomy and genetics, Vol. 1. Taylor and Francis London; p. 3–31.

Gautam A, Kumar A, Dutt D. 2015. Production of cellulase-free xylanase by *Aspergillus flavus* ARC- 12 using pearl millet stover as the substrate under solid-state fermentation. J Adv Enzym Res. 1:1–9.

Goluguri TC, Addepally U, Shetty PR. 2016. Novel alkali-thermostable xylanase from *Thielaviopsis basicola* (MTCC 1467): purification and kinetic characterization. Int J Biol Macromol. 82:823–829. doi:10.1016/j.ijbiomac.2015.10.055.

Gomaa EZ. 2013. Optimization and characterization of alkaline protease and carboxymethyl-cellulase produced by *Bacillus pumillus* grown on *Ficus nitida* wastes. Braz J Microbiol. 44 (2):529–537. doi:10.1590/S1517-83822013005000048.

Gong W, Dai L, Zhang H, Zhang L, Wang L. 2018. A highly efficient xylan-utilization system in *Aspergillus niger* an76: a functional-proteomics study. Front Microbiol. 9:430. doi:10.3389/fmicb.2018.00430.

Goyal M, Kalra K, Sareen V and Soni G. (2008). Xylanase production with xylan rich lignocellulosic wastes by a local soil isolate of Trichoderma viride. Braz. J. Microbiol. 39(3), 535–541. 10.1590/S1517-83822008000300025

Gupta U, Kar R. 2009. Xylanase production by thermotolerant *Bacillus* species under solid state and submerged fermentation. Braz Arch Biol Technol. 52(6):1363–1371. doi:10.1590/S1516-89132009000600007.

Haki GD, Rakshit SK. 2003. Developments in industrially important thermostable enzymes: a review. Bioresour Technol. 89 (1):17–34. doi:10.1016/S0960-8524(03)00033-6.

Harris AD, Ramalingam C. 2010. Xylanases and its application in food industry: a review. J Exp Sci. 1(7):1–11.

Hombalimath VS, Achappa S, Patil LR, Shet AR, Desai SV. 2021. Optimization of xylanase production from *Aspergillus* spp. under solid-state fermentation using lemon peel as substrate. J Pharm Res Int. 33(47B):35–43. doi:10.9734/jpri/2021/v33i47B33094.

Hu Y, Li M, Liu Z, Song X, Qu Y, Qin Y. 2021. Carbon catabolite repression involves physical interaction of the transcription factor CRE1/CreA and the Tup1–Cyc8 complex in *Penicillium oxalicum* and *Trichoderma reesei*. Biotechnol for Biofuels. 14 (1):244. doi:10.1186/s13068-021-02092-9.

Ibrahim D, Weloosamy H, Lim S. 2015. Effect of agitation speed on the morphology of *Aspergillus niger* HFD5A-1 hyphae and its pectinase production in submerged fermentation. World J Biol Chem. 6(3):265–271. doi:10.4331/wjbc.v6.i3.265.

Kambourova M. 2018. Thermostable enzymes and polysaccharides produced by thermophilic bacteria isolated from Bulgarian hot springs. Eng Life Sci. 18(11):758–767. doi:10.1002/elsc.201800022.

Leck A. 1999. Preparation of lactophenol cotton blue slide mounts. Community Eye Health. 12(30):1–24.

Lee SH, Lim V, Lee CK. 2018. Newly isolate highly potential xylanase producer strain from various environmental sources. Biocatal Agric Biotechnol. 16:669–676. doi:10.1016/j.bcab.2018.09.024.

Lenartovicz V, Marques De Souza G, Moreira F, Peralta R. 2002. Temperature effect in the production of multiple xylanases by *Aspergillus fumigatus*. J Basic Microbiol. 42(6):388–395. doi:10.1002/1521-4028(200212)42:6<388::AID-JOBM388>3.0.CO;2-H.

Liang Y, Feng Z, Yesuf J, Blackburn JW. 2010. Optimization of growth medium and enzyme assay conditions for crude cellulases produced by a novel thermophilic and cellulolytic bacterium *Anoxybacillus* sp. 527. Appl Biochem Biotechnol. 160(6):1841–1852. doi:10.1007/s12010-009-8677-x.

Liao H, Zheng H, Li S, Wei Z, Mei X, Ma H, Shen Q, Xu Y. 2015. Functional diversity and properties of multiple xylanases from *Penicillium oxalicum* GZ-2. Sci Rep. 5(1):12631. doi:10.1038/srep12631.

Lorenz N, Dick R. 2011. Sampling and pretreatment of soil before enzyme analysis. Methods Soil Enzymol 9 . 85–100.

Mach RL, Strauss J, Zeilinger S, Schindler M, Kubicek CP. 1996. Carbon catabolite repression of xylanase I (xyn1) gene expression in *Trichoderma reesei*. Mol Microbiol. 21 (6):1273–1281. doi:10.1046/j.1365-2958.1996.00094.x.

Mandla A. 2015. Review on microbial xylanases and their applications. Int J Life Sci. 4(3):178–187.

Marecik R, Błaszczyk L, Biegańska-Marecik R, Piotrowska-Cyplik A. 2018. Screening and identification of *Trichoderma* strains isolated from natural habitats with potential to cellulose and xylan degrading enzymes production. Pol J Microbiol. 67 (2):181–190. doi:10.21307/pjm-2018-021.

Miller GL. 1959. Use of dinitrosalicylic acid reagent for determination of reducing sugar. Anal Chem. 31(3):426–428. doi:10.1021/ac60147a030.

Mohammed IJ. 2013. Screening of fungi isolated from *environmental samples* for xylanase and cellulase production. Int Sch Res Notices: Microbiol. 2013:283423.

Mosina NL, Naidu Krishna SB, Ramnath L, Govinden R. 2017. Screening, production, and partial characterization of xylanases from woodchips fungi with potential application in bioethanol production. Curr Trends Biotechnol Pharm. 11 (4):2230–7303.

Motta FL, Andrade CCP, Santana MHA. 2013. A review on xylanase production by the fermentation of xylan: classification, characterization, and applications. In: Sustainable degradation of lignocellulosic biomass – techniques, applications and commercialization. InTechOpen: Croatia; p. 251–266.

Mulatu A, Alemu T, Megersa N, Vetukuri RR. 2021. Optimization of culture conditions and production of bio-fungicides from *Trichoderma* species under solid-state fermentation using mathematical modeling. Microorganisms. 9(8):1675. doi:10.3390/microorganisms9081675.

Nair SG, Shashidhar S. 2008. Fungal xylanase production under solid-state and submerged fermentation conditions. Afr J Microbiol Res. 2(4):82–86.

Nathan V, Mary R, Gunaseeli R, Dhiraviam K. 2017. Low molecular weight xylanase from T*richoderma viride* vkf3 for bio-bleaching of newspaper pulp. Bioresources. 12(3). doi:10.15376/biores.12.3.5264-5278.

Okafor UA, Okochi O-OBM VI, Nwodo-Chinedu S. 2007. Xylanase production by *Aspergillus niger* ANL 301 using agro-wastes. Afr J Biotechnol. 6:1710–1714.

Pandey S, Shahid M, Srivastra M, Sharma A, Singh A, Kumar V, Srivasthava, Y. 2012. Isolation and optimized production of xylanase under solid-state fermentation condition from *Trichoderma* sp. Int J Adv Res. 2(3):263–273.

Pariza MW, Cook M. 2010. Determining the safety of enzymes used in animal feed. Regul Toxicol Pharmacol. 56 (3):332–342. doi:10.1016/j.yrtph.2009.10.005.

Pathak P, Bhardwaj NK, Singh AK. 2014. Production of crude cellulase and xylanase from *Trichoderma harzianum* PPDDN10 NFCCI-2925 and its application in photocopier waste paper recycling. Appl Biochem Biotechnol. 172(8):3776–3797. doi:10.1007/s12010-014-0758-9.

Pointing SB. 1999. Qualitative methods for the determination of lignocellulosic enzyme production by tropical fungi. Fungal Divers. 2:17–33.

Polizeli MLTM, Rizzatti ACS, Monti R, Terenzi HF, Jorge JA, Amorim DS. 2005. Xylanases from fungi: properties and industrial applications. Appl Microbiol Biotechnol. 67 (5):577–591. doi:10.1007/s00253-005-1904-7.

Prade RA. 1996. Xylanases, from biology to biotechnology. Biotechnol Genet Eng Rev. 13(1):101–131. doi:10.1080/02648725.1996.10647925.

Prasad Uday US, Bandyopadhyay TK, Goswami S, Bhunia B. 2017. Optimization of physical and morphological regime for improved cellulase free xylanase production by fed batch fermentation using *Aspergillus niger* (KP874102.1) and its application in bio-bleaching. Bioengineered. 8(2):137–146. doi:10.1080/21655979.2016.1218580.

Raj A, Kumar S, Singh KS, Kumar M. 2013. Characterization of a new *providencia* sp. strain x1 producing multiple xylanases on wheat bran. Sci World J. 6(1):1–10. doi:10.1155/2013/386769.

Rigoldi F, Donini S, Redaelli A, Parisini E, Gautieri A. 2018. Review: engineering of thermostable enzymes for industrial applications. APL Bioeng. 2(1):011501. doi:10.1063/1.4997367.

Rizzatti ACS, Freitas FZ, Bertolini MC, Peixoto-Noguiera SC, Terenzi HF, Jorge JA, Moraes Polizeli MdLT. 2008. Regulationof *Aspergillus phoenicis*: a physiological and moleculr approach. J Ind Microbiol Biotechnol. 35(4): 237–244. doi:10.1007/s10295-007-0290-9.

Robledo A, Aguilar CN, Belmares-Cerda RE, Flores-Gallegos AC, Contreras-Esquivel JC, Montanez JC, Mussatto SL. 2016. Production of thermostable fungal strains isolated from maize silage. J Food. 14(2):302–308.

Sanghvi GV, Koyani RD, Rajput KS. 2010. Thermostable xylanase production and partial purification by solid-state fermentation using agricultural waste wheat straw. Mycology. 1

(2):106–112. Regulation of xylanase in *Aspergillus phoenicis*: a physiological and molecular approach. doi:10.1080/21501203.2010.484029.

Seyis I, Aksoz N. 2005. Effect of carbon and nitrogen sources on xylanase production by *Trichoderma harzianum* 1073 D3. Int Biodeterior. 55(2):115–119. doi:10.1016/j.ibiod.2004.09.001.

Shah A, Datta M. 2005. Xylanase production under solid-state fermentation and its characterization by an isolated strain of *Aspergillus foetidus* in India. World J Microbiol Biotechnol. 21(3):233–243. doi:10.1007/s11274-004-3622-1.

Sharma P, Kaushik N, Sharma S, Kumar V. 2016. Isolation, screening, characterization and optimization of xylanase production from thermostable alkalophillic *Fusarium* sp. X J Biochem Tech. 7(3):1089–1092.

Shulami S, Shenker O, Langut Y, Lavid N, Gat O, Zaide G, Zehavi A, Sonenshein AL, Shoham Y. 2014. Multiple regulatory mechanisms control the expression of the *Geobacillus stearothermophilus* gene for extracellular xylanase. J Biol Chem. 289(37):25957–25975. doi:10.1074/jbc.M114.592873.

Silva LAO, Terrasan F, Rafael C, Carmona E. 2015. Purification and characterization of xylanases from *Trichoderma inhamatum*. Electronic J. 18(4):307–313.

Singh R, Gupta V, Kumar V, Gupta R. 2006. A simple activity staining protocol for lipases and esterases. J Appl Microbiol Biotechnol. 70(6):679–682. doi:10.1007/s00253-005-0138-z.

Singhania RR, Sukumaran RK, Rajasree KP, Mathew A, Gottumukkala L, Pandey A. 2011. Properties of a major β-glucosidase-BGL1 from *Aspergillus niger* NII-08121 expressed differentially in response to carbon sources. Process Biochem. 46(7):1521–1524. doi:10.1016/j.procbio.2011.04.006.

Tamura K, Peterson D, Peterson N, Stecher G, Nei M, Kumar S. 2011. MEGA5: molecular evolutionary genetics analysis using maximum likelihood, evolutionary distance and maximum parsimony methods. Mol Biol Evol. 28(10):9–2731. doi:10.1093/molbev/msr121.

Telles GP, Araújo GS, Walter M, Brigido MM, Almeida NF. 2018. Live neighbor-joining. BMC Bioinform. 19(1):172. doi:10.1186/s12859-018-2162-x.

Tuohy MG, Puls J, Claeyssens M, Anská MVR, Coughlan MP. 1993. The xylan-degrading enzyme system of *Talaromyces emersonii*: novel enzymes with activity against aryl β - d - xylosides and unsubstituted xylans. Biochem J. 290 (2):515–523. doi:10.1042/bj2900515.

Walia A, Mehta P, Chauhan A, Shirkot CK. 2013. Optimization of cellulase-free xylanase production by alkalophilic *Cellulosimicrobium* sp. CKMX1 in solid-state fermentation of apple pomace using central composite design and response surface methodology. Ann Microbiol. 63(1):187–198. doi:10.1007/s13213-012-0460-5.

White TJ, Bruns T, Lee SB, Taylor J. 1990. Amplification and direct sequencing of fungal ribosomal RNA genes for phylogenetics. PCR protocols: a guide to methods and application. New York (NY): Academic Press.

Wong KKY, Tan LUL, Saddler JN. 1988. The multiplicity of β-1,4-xylanase in micro-organisms: functions and applications. Microbiol Rev. 52(3):305–317. doi:10.1128/mr.52.3.305-317.1988.

Yadav P, Maharjan J, Korpole S, Prasad GS, Sahni G, Bhattarai T, Sreerama L. 2018. Production, purification, and characterization of thermostable alkaline xylanase from *Anoxybacillus kamchatkensis* NASTPD13. Front bioeng biotechnol. 6:65. doi:10.3389/fbioe.2018.00065.

Yang-yuan L, Kai-xin Z, Ai-hong H, Dan-ni L, Li-zhi C, Shu-de X. 2015. High-level expression and characterization of a thermostable xylanase mutant from *Trichoderma reesei* in *pichia pastoris*. Protein Expr Purif. 108:90–96. doi:10.1016/j.pep.2014.11.014.

Zhang M, Jiang Z, Yang S, Hua C, Li L. 2010. Cloning and expression of a *Paecilomyces thermophila* xylanase gene in *E. coli* and characterization of the recombinant xylanase. Bioresour Technol. 101(2):688–695. doi:10.1016/j.biortech.2009.08.055.

Zhu H, Liu W, Tian B, Zhang C. 2012. Fluid flow induced shear stress affects cell growth and total flavone production by *Phellinus igniarius* in stirred-tank bioreactor. Chiang Mai J Sci. 39:69–75.

scientific reports

Check for updates

OPEN

Optimization, purification, and characterization of xylanase production by a newly isolated *Trichoderma harzianum* strain by a two-step statistical experimental design strategy

Priyashini Dhaver[1]✉, Brett Pletschke[2], Bruce Sithole[3,4] & Roshini Govinden[1]

Xylanases are hydrolytic enzymes with a wide range of applications in several industries such as biofuels, paper and pulp, food, and feed. The objective of this study was to optimize the culture conditions and medium components for maximal xylanase production from a newly isolated *Trichoderma harzianum* strain using the Plackett–Burman Design (PBD) and Box Behnken Design (BBD) experimental strategies. Xylanase production was enhanced 4.16-fold to 153.80 U/ml by BBD compared to a preliminary one-factor-at-a-time (OFAT) activity of 37.01 U/ml and 2.24-fold compared to the PBD (68.70 U/ml). The optimal conditions for xylanase production were: 6 days of fermentation, incubation temperature of 70 °C, pH 5.0, agitation of 160 rpm, and 1.2% wheat bran and ammonium sulphate. The experimental design effectively provided conditions for the production of an acidic-thermostable enzyme with exciting potential for application in animal feed improvement. The acidic-thermostable xylanase was purified from the submerged culture and SDS-PAGE analysis revealed a molecular weight of 72 kDa. This protein had maximum xylanolytic activity at pH 6.0 and 65 °C and was stable for 4 h retaining > 70% activity and exhibited substrate specificity for beechwood xylan with a K_m of 5.56 mg/ml and V_{max} of 1052.63 µmol/min/mg. Enzyme activity was enhanced by Fe^{2+}, Mg^{2+}, and Zn^{2+}. There was an absence of strong inhibitors of xylanase activity. Overall, these characteristics indicate the potential for at least two industrial applications.

After cellulose, hemicellulose is the second most abundant terrestrial polysaccharide composed of ß-1,4-D-xylopyranoside residues and ß-1,4-xylan as main constituents with arabinosyl and acetyl side chains[1]. Hemicellulose is a short crosslinked polymer compared to cellulose, which is a long straight-chain homopolymer. Xylans have a β-(1,4) linked backbone made of D-xylose and there are three subtypes of xylan based on the side chain. The subtypes are homoxylan, glucuronoxylan, and arabinoxylan. Homoxylan is only found in two or three types of plants and is mostly cross-linked by β-(1,4)-glycosidic bonds. Xylan is a renewable biomass resource that has potential as a substrate in many production processes. However, it must be hydrolysed to xylose and xylo-oligosaccharides which can be accomplished by xylanolytic enzymes. Among them, xylanases deserve special attention as they degrade the major hemicellulosic polysaccharides by catalyzing the hydrolysis of xylopyranosyl linkages of ß-1,4-xylan[2]. The main enzymes involved are endo-1,4-β-xylanases which make random cuts in the xylan backbone and β-xylosidases which are exoglycosidases with the ability to degrade the non-reducing ends of xylooligosaccharides into xylose. The side groups in xylans are cleaved by α-L-arabinofuranosidases (EC 3.2.1.55), α-glucuronidases (EC 3.2.1.139), and acetyl xylan esterases (EC 3.1.1.72)[3]. The most common microbial xylanases that would hydrolyze all types of xylan are grouped based on amino acid similarities and structural

[1]Discipline of Microbiology, School of Life Sciences, Westville Campus, University of KwaZulu-Natal, Durban 4000, South Africa. [2]Enzyme Science Programme (ESP), Department of Biochemistry and Microbiology, Rhodes University, Makhanda (Grahamstown), Eastern Cape, South Africa 6139. [3]Biorefinery Industry Development Facility, Council for Scientific and Industrial Research, Durban 4000, South Africa. [4]Discipline of Chemical Engineering, University of KwaZulu-Natal, Durban 4000, South Africa. ✉email: pdhaver10@gmail.com

characteristics, into glycoside hydrolase (GH) families 10 or 11 in the Carbohydrate-Active enzyme (CAZy) database (http://www.cazy.org)[4]. GH10 families are able to catalyze the hydrolysis of a wide range of xylans, while GH11 families are known to cleave unsubstituted regions of arabinoxylan[4]. However, both GH10 and GH11 xylanases have applications in various industries such as food and feed[5], biofuel production[6], paper and pulp[7], and medical and pharmaceutical[8]. Xylanases are also found in GH families 30, 8, and 5. The complete degradation of heterogeneous xylan into simple sugars requires the synergistic action of several inducible hemicellulases[9].

Microbes such as bacteria, fungi, and actinomycetes are ubiquitous in nature[10] and several endogenous and exogenous microbial enzymes have been widely explored, resulting in a variety of microorganisms commonly regarded as the most significant and convenient producers of large quantities of enzymes in a short period on inexpensive feedstock. Xylanases are produced by microbial biosynthesis for industrial applications[11,12]. Thermophilic fungi in particular are promising candidates for biotechnological applications due to their strong ability to degrade plant polysaccharide components and their robustness under harsh environmental conditions[2]. Many of the filamentous fungi that have been studied produce several xylanases and have high xylan-degrading ability. *Trichoderma* sp. and *Aspergillus* sp. are most frequently employed for industrial applications[9] including the bioconversion of plant biomass into animal feed[5], plant fertilizers, and chemicals for the food industry[9].

The production of enzymes is costly, thus, to meet industrial demand, a low-cost growth medium is required for microbial growth and enzyme production. There are two possible cultivation methods for microbial xylanase production: solid-state and submerged fermentation[13]. Submerged fermentation technology has the advantage of short production periods to achieve high yields at low costs. Both the nutrient medium composition and culture conditions have a strong influence on xylanase production. The physical and chemical factors known to influence xylanase production are temperature, pH, incubation period, carbon and nitrogen sources and concentration, and agitation speed[14]. Temperature effects on enzyme production are predominantly related to the growth of the organism (mesophilic, psychrophilic, or thermophilic). The pH is one of the most important factors governing microbial growth due to their sensitivity to the hydrogen ion concentration in the medium[15]. It is also key to enzyme activity as it can alter the ionic charges on the molecule, which could cause changes to the enzyme's shape (they may denature), and that usually leads to a reduction or loss of the catalytic properties of the enzymes and cessation of metabolic activity[16].

Supplementation of the growth medium with carbon and nitrogen sources usually increases enzyme production as this provides an enriched environment for microbial growth[17]. Therefore, screening of the most influential factors and optimization of the growth conditions are essential to ensure maximal enzyme production, potentially significantly reducing production costs for xylanases[18]. There are two approaches to optimize the fermentation process classical and statistical. The classical approach is based on the testing of "one-factor-at-a-time (OFAT)" and the statistical approach includes the Plackett–Burman design (PBD) and response surface methodologies (RSM).

The OFAT approach is a conventional single-dimensional investigation that involves changing one independent variable at a time while the others remain at their optimal level[19,20]. This is the main strategy used for selecting optimal conditions, which continues to be widely used in preliminary optimization studies[21]. The main disadvantages of OFAT are the partial explanation regarding the effect of the factors on the response and the absence of the interaction effects between the variables[22]. This method also involves a relatively high number of experiments, which makes it laborious and time-consuming[21]. Moreover, it may lead to unreliable results and inaccurate conclusions.

To resolve this problem, optimization studies can be carried out by using multivariate statistical methods[21], PBD and RSM can potentially eliminate the limitations of the OFAT optimization process[23]. PBD is a powerful statistical technique for screening medium components in shake flask fermentation and reduces the total number of experiments[24]. This technique is useful and has been widely used as the first step of an optimization procedure, however, it cannot determine the interaction effects[23] but allows the evaluation of the importance of each factor in moderately few experiments[25]. RSM using a Box–Behnken Design (BBD) is an effective optimization tool. The RSM design can provide the dependence of enzyme production on independent variables, predicted results for responses, and levels for independent variables in the form of mathematical models[26,27].

Hydrolysis of xylan and hemicellulosic materials to various xylooligosaccharides has been accomplished using crude xylanases. However, to meet the desired requirements of some applications, robust xylanases (resistant to metal ions and chemicals, displaying pH, and thermostability) with specific biochemical properties for pH and temperature optima as well as, high specific activity are required, which would require purification of appropriate candidate enzymes[28]. Purification of xylanases is necessary to remove contamination by proteins and other enzymes in the culture medium, such as cellulases, as well as compounds derived from hydrolysis of the substrate. These contaminants can complicate activity assays, protein quantification, and physicochemical assays[29]. Purification and physicochemical characterization (activity and stability at various pH and temperatures) of pure xylanases provide information on the enzyme's structural and functional features, which may be used to assess its application potential[29]. Purification should be centred on attaining the highest yield while retaining the highest possible enzymatic activity and purity[30].

Xylanases are required in large quantities for industrial-level applications because they not only have application in several processes but possess the necessary characteristics to withstand harsh conditions during these industrial processes. As a result, there is a need to select microorganisms that produce high levels of xylanases with appropriate properties, followed by optimization of growth which would lead to higher levels of enzymes[19]. There are several reports available on the optimization of media components and the physical growth parameters for the production and purification of xylanases for various applications using different substrates[8,12,21]. Xylanase production by *Trichoderma reesei* SAF3[31] and *Trichoderma stromaticum* AM7[32] was increased by optimization. While there are reports on multiple other species, there were very few reports on thermostable *Trichoderma harzianum* xylanases in literature.

Variables	Symbol code	Units	Experimental values	
			Low level (− 1)	High level (+ 1)
Incubation temperature	X_1	°C	40	80
Incubation time	X_2	Days (d)	2	6
pH	X_3	–	4	8
Agitation	X_4	rpm	140	180
Wheat bran (carbon source)	X_5	%	0.8	1.2
Ammonium sulphate (nitrogen source)	X_6	%	1.0	1.4

Table 1. Experimental variables and levels used in the PBD for optimal xylanase production by the *Trichoderma harzianum* strain.

Therefore, in the present study, a recently isolated and characterized fungal strain, *T. harzianum*, producing a thermophilic and acidic xylanase was the subject of study. The major focus of this study was to employ statistical design strategies to optimize xylanase production. Although this is not a novel approach, its application to a novel thermophilic and acidic xylanase is. We also report on the purification and characterization of the *T. harzianum* xylanase, to determine its applicability for future studies in animal feed improvement.

Materials and methods

Microbial strain. The *T. harzianum* strain was selected from a previous screening study as the candidate for xylanase production[33]. Fungal cultures were streaked on the PDA plates and slants, grown for 5 days at 30 °C followed by the addition of sterile mineral oil to cover the fungal mycelium and storage at 4 °C. Long-term stocks were prepared by washing fungal spores from the 5-day PDA plates with distilled water and adding 50% glycerol in a 1:1 ratio to the spore suspension and storing at − 20 °C and − 80 °C.

Medium and cultivation. Nutrient salt solution (NSS) used for xylanase production comprised [(g/L): (0.005 g) CaCl, (0.23 g) KH_2PO_4, (0.05 g) $MgSO_4$, (0.005 g) $NaNO_3$, (0.002 g) $ZnSO_4$, (0.009 g) $FeSO_4$, (0.23 g) KCl, (7 g) peptone, and (20 g) wheat bran]. Erlenmeyer flasks (250 ml) containing 50 ml of the medium were each inoculated with two 5 mm fungal plugs from a 5-day-old plate culture and incubated at 30 °C at 200 rpm for 7 days in a shaker (New Brunswick Innova 44, Germany). Cultured media were removed after the incubation period and the cell-free supernatant was recovered by centrifuging samples at 16,873 × *g* for 10 min (Eppendorf centrifuge 5418, Germany). Xylanase activity was determined as described below in the xylanase assay method ("Xylanase assay").

Xylanase assay. Xylanase activity was quantified using the 3,5-dintrosalicylic acid (DNS) assay for reducing sugars according to the method by Miller[34]. The reaction included 600 µl of 1% (w/v) of beechwood xylan (1 g in 100 ml of 50 mM citrate buffer pH 5.0) in 15 ml test tubes to which 66.67 µl of the culture supernatant was added. The reaction mixture was incubated in a water bath at 55 °C for 15 min and terminated by the addition of 1 ml DNS reagent followed by heating for 5 min at 100 °C in a water bath. One unit (U) of xylanase was defined as the amount of enzyme that released 1 µmol xylose as reducing sugar equivalents per min under the specified assay conditions.

Optimization of xylanase production: one factor at a time (OFAT). To optimize the growth parameters, OFAT was used to evaluate the effect of a single parameter at a time performed in earlier study[33]. The enzyme activity was obtained to determine the optimal yield and was reported in previous studies[33].

Statistical optimization, experimental design, and data analysis. *Plackett–Burman design (PBD).* Six variables were selected for this study: Incubation temperature (X_1), Incubation time (X_2), pH (X_3), Agitation (X_4), Wheat bran (X_5), and Ammonium sulphate (X_6) (Table 1). The total number of experimental runs carried out for the six variables was twelve[35]. Each variable was represented by a high level denoted by '+' and a low level denoted by '–'. The high level of each variable was sufficiently far from the low level so that any significant effect would be observed. The experimental runs were performed in duplicate and an average of the results was reported Table 2 represents the PBD based on the first-order polynomial model Eq. (1):

$$Y = \beta_0 \sum \beta_i X_i, \tag{1}$$

where Y is defined as the response (peak area and retention factor), β_0 is the model intercept, β_i is the linear coefficient and X_i is the level of the independent variable. The PBD was analyzed using R studio software[36] to estimate the significant factors. ANOVA was performed to determine the *p*-values as well as the R coefficients to check the significance and fit of the regression model. Screened parameters were represented on a Pareto chart of standardized effects. The effect of each variable was analyzed and the ones with the highest influence on the production of xylanase were selected for the second level optimization by BBD of RSM.

Run no	Variable level						Enzyme activity (U/ml)	
	X_1	X_2	X_3	X_4	X_5	X_6	Observed	Predicted
1	80 (+)	6 (+)	4 (−)	180 (+)	1.2(+)	1.4 (+)	27.1	32.3
2	40 (−)	6 (+)	8 (+)	140 (−)	1.2 (+)	1.4 (+)	68.7	68.4
3	80 (+)	2 (−)	8 (+)	180 (+)	0.8 (−)	1.4 (+)	19.3	17.5
4	40 (−)	6 (+)	4 (−)	180 (+)	1.2 (+)	1.0 (−)	29.3	27.8
5	40 (−)	2 (−)	8 (+)	140 (−)	1.2 (+)	1.4 (+)	32.5	32.6
6	40 (−)	2 (−)	4 (−)	180 (+)	0.8 (−)	1.4 (+)	8.8	9.9
7	80 (+)	2 (−)	4 (−)	140 (−)	1.2 (+)	1.0 (−)	25.6	20.5
8	80 (+)	6 (+)	4 (−)	140 (−)	0.8 (−)	1.4 (+)	23.1	18.2
9	80 (+)	6 (+)	8 (+)	140 (−)	0.8 (−)	1.0 (−)	16.2	21.2
10	40 (−)	6 (+)	8 (+)	180 (+)	0.8 (−)	1.0 (−)	34.8	30.0
11	80 (+)	2 (−)	8 (+)	180 (+)	1.2 (+)	1.0 (−)	16.7	18.3
12	40 (−)	2 (−)	4 (−)	140 (−)	0.8 (−)	1.0 (−)	9.8	15.2

Table 2. Plackett–Burman design matrix for screening of six medium components for xylanase production by the *Trichoderma harzianum* strain. X_1: Incubation temperature. X2: Incubation time. X_3: pH. X_4: Agitation. X_5: Wheat bran. X_6: Ammonium sulphate.

Variables	Symbol code	Experimental values		
		Low (−1)	Zero (0)	High (+1)
Incubation time (d)	X_2	4	5	6
pH	X_3	4	5	6
Carbon source Wheat bran (%)	X_5	0.8	1	1.2

Table 3. Experimental codes and levels of independent variables in the RSM for optimal xylanase production by the *Trichoderma harzianum* strain.

Optimization of the significant variables using response surface methodology (RSM). The BBD was used to elucidate the main interaction and quadratic effects of the three significant variables arising from the PBD, with replicated centre points[21]. The experimental design and statistical analysis were performed using R Studio[36]. A three-level three-factor BBD was used to evaluate the combined effect of the three significant independent variables, Incubation time (X_2), pH (X_3), and wheat bran (X_5) (Table 3). The design consisted of 16 combinations, including three replicates of the centre point as shown in Table 4. After the experimental runs were completed, the average xylanase activities were taken as the response (Y). A multiple regression analysis of the data was carried out to obtain an empirical model that relates the response measured to the independent variables[37]. The second-order polynomial Eq. (2) is shown below:

$$Y = \beta_0 + \sum \beta_1 X_1 + \sum \beta_2 X_2 + \sum \beta_{12} X_1 X_2, \quad (2)$$

where Y represents the response variable (peak area), β_0 is the interception coefficient, β_1 is the coefficient for the linear effects, β_2 is the coefficient for the quadratic effect, β_{12} are interaction coefficient and X_1 X_2 is the coded independent variables that influence the response variable Y. The response in each run was the average of duplicates. In this experimental design, data were analyzed by one-way ANOVA with Tukey's multiple comparison test ($p \leq 0.05$) using R studio[36], and ggplot2 was used for the generation of 3D response surface and contour plots[38].

Scaled-up production in the optimized medium. The optimized parameters for each factor from the statistical design experiments were implemented for the scaled-up production of the xylanases. The nutrient salt solution was prepared as previously described ("Medium and cultivation") and supplemented with the optimized wheat bran and ammonium sulphate concentrations. Erlenmeyer flasks (2 l) containing 400 ml of the medium were each inoculated with two 5 mm fungal plugs from a 5-day-old plate culture and incubated at the optimized parameters in a shaker (New Brunswick Innova 44, Germany). Cultured media were removed after the incubation period and the cell-free supernatant was recovered by centrifuging samples at 16,873 × *g* for 10 min (Eppendorf centrifuge 5418, Germany). Xylanase activity was determined as described in "Xylanase assay".

Purification of xylanase. All purification steps were carried out at 4 °C. Partial purification of the xylanase was carried out by ammonium sulphate precipitation (20–80%). The pellets were dissolved in 50 mM citrate buffer pH 5.0 and subjected to dialysis overnight in the same buffer. The fraction that resulted in the highest activity, was concentrated in 3 kDa Amicon centrifugal tubes, the protein precipitate dissolved in 50 mM citrate buffer pH 5.0 buffer and loaded onto an anion exchange column (HiTrap Q FF 5 ml) which was connected to

Run order	Experimental value (coded value)			Enzyme activity (U/ml)	
	Incubation time (d)	pH	Wheat bran %	Observed	Predicted
1	4 (−)	4 (−)	1 (0)	97.09	86.35
2	6 (+)	4 (−)	1 (0)	89.76	87.11
3	4 (−)	6 (+)	1 (0)	98.65	107.01
4	6 (+)	6 (+)	1 (0)	109.22	102.35
5	4 (−)	5 (0)	0.8 (−)	90.82	97.68
6	6 (+)	5 (0)	0.8 (−)	101.32	108.72
7	4 (−)	5 (0)	1.2 (+)	103.37	88.34
8	6 (+)	5 (0)	1.2 (+)	153.80	134.75
9	5 (0)	4 (−)	0.8 (−)	60.01	58.78
10	5 (0)	6 (+)	0.8 (−)	66.92	74.32
11	5 (0)	4 (−)	1.2 (+)	82.99	69.65
12	5 (0)	6 (+)	1.2 (+)	116.74	64.98
13	5 (0)	5 (0)	1 (0)	29.68	37.85
14	5 (0)	5 (0)	1 (0)	33.23	37.85
15	5 (0)	5 (0)	1 (0)	27.38	37.85
16	5 (0)	5 (0)	1 (0)	42.30	37.85

Table 4. Experimental design for the BBD model for three significant independent variables (Incubation time, pH, and wheat bran) tested and predicted and observed responses for xylanase production.

the AKTA Purifier (AKTA Purifier, GE Healthcare Bio-Science, AB75184, Uppsala Sweden). Before loading the sample, the column was equilibrated with 20 mM Tris buffer, (pH 8.0). The enzyme was eluted using a 0–2 M sodium chloride gradient at a flow rate of 1.5 ml/min. Fractions were collected and those displaying xylanase activity were pooled, concentrated, and dialyzed against a 50 mM citrate buffer (pH 5.0), to be used for further characterization of the enzyme. Protein concentration was measured by the Bradford method[39] using bovine serum albumin as the standard. The samples were separated on a 12% SDS-polyacrylamide gel according to Laemmli[40]. Native PAGE was performed with 1% xylan as the substrate. Once electrophoresis was completed, the gel was incubated in 50 mM citrate buffer pH 5.0 at the optimum temperature (70 °C) for 20 min and thereafter stained with 0.1% Congo red solution for 30 min and destained in 1 M NaCl until clearance bands representing xylanase activity were obtained.

Characterization of purified xylanase. *Effect of pH and temperature on xylanase activity.* The pH optimum was determined by measuring enzyme activity between pH 4.0 and 10.0 The following buffers were used: 0.1 M sodium citrate buffer (pH 3.0–5.0), 0.1 M potassium phosphate buffer (pH 6.0–8.0) and 0.1 M Glycine NaOH buffer (pH 9.0–10.0)[41]. Enzyme assays were conducted as previously described ("Xylanase assay"). For determination of the optimum temperature, the reactions were carried out at the optimum pH between 40 to 80 °C with intervals of 5 °C.

pH and thermostability. The pH stability of the enzyme was determined by incubating the enzyme in the optimal pH buffer for 4 h at 55 °C with aliquots removed every 30 min. A substrate control was also incubated for 4 h. Thereafter, xylanase activity was assayed using the DNS method and reported as residual activity (%). Temperature stability was determined by incubating the enzyme in the optimal pH buffer at optimal temperature for 4 h with aliquots collected every 30 min. The activity was assayed and reported as residual activity (%).

Effect of metallic ions and different solvents on xylanase activity. The effect of metallic ions ($CaCl_2$, $CoCl_2$, $FeSO_4$, $MgSO_4$, $MnSO_4$, and $ZnSO_4$) and chemical agents (SDS, DMSO, and EDTA) on enzyme activity was evaluated at two concentrations: 2 mM and 10 mM. The residual activity was measured using the standard assay conditions. The activity in the absence of metallic ions or inhibitors was taken as the control (100%)[42].

Substrate specificity. The specificity of the purified xylanase was verified by assaying the activity using various substrates, viz., beechwood xylan, birchwood xylan, xylan from Larchwood, wheat arabinoxylan (soluble and insoluble), carboxymethylcellulose (CMC) and Avicel. Substrates (1% w/v) were suspended in 50 mM citrate buffer (pH 6.0) and incubated with the purified enzyme at 65 °C for 15 min and thereafter the xylanase activity was determined by the DNS method as described previously ("Xylanase assay")[43].

Kinetic parameters. The K_m and V_{max} values for the xylanase were determined by measuring the enzymatic activity using different concentrations of the xylan substrate (1–20 mg/ml). The activity was measured under standard assay conditions as described previously. The Michaelis-Menton and Lineweaver- Burk plots were acquired to determine K_m and V_{max}.

	df	Sum of squares	Mean square	F-value	*p*-value
Model	6	2521.08	420.18	12.59	0.00700*
Incubation temperature (X_1)	1	119.1	119.1	3.992	0.10220
Incubation time (X_2)	1	610.6	610.6	20.473	0.00626*
pH (X_3)	1	280.1	280.1	9.392	0.02796*
Agitation (X_4)	1	166.0	166.0	5.566	0.06481
Wheat bran (X_5)	1	1277.7	1277.7	42.839	0.00125*
Ammonium sulphate (X_6)	1	66.3	66.3	2.222	0.19622
Residuals	5	166.92	33.39		

Table 5. Analysis of variance (ANOVA) for six variables by PBD experiment. *df* degree of freedom. *Significant *p*-value at $p \leq 0.05$. Adjusted R^2 (mean coefficient of determination) = 0.97.

Equipment and settings. Neither image acquisition tools nor image processing software packages were used for the figures in this study. For Fig. 7, processing such as changing brightness and contrast was applied equally across the entire image and applied equally to the controls. The contrast does not allow for any data to disappear. There were no excessive manipulations, such as processing to emphasize one region in the image at the expense of others.

Results and discussion

Screening of significant medium constituents for xylanase production. The rows in Table 2 represent the twelve different experiments. The data obtained from the PBD runs indicate a wide variation in xylanase activity from 9.8 to 68.7 U/ml across the twelve runs. This variation demonstrated that the effect of the medium and culture conditions on the production of xylanase was significant ($p < 0.05$). The R^2, or coefficient of determination, is the percentage of response variance that can be ascribed to the model rather than a random error[44]. According to Xie et al.[45], R^2 should be at least 90% for a model to fit well. The determination coefficient (R^2) indicates that the independent variables were responsible for 97 percent of the sample variance in xylanase output, and just roughly 3% of the overall variation was not explained by the model. The greater the correlation between experimental and anticipated values, the closer R (correlation coefficient) is to 1. The value of R (0.97) indicated that the experimental data and the theoretical values predicted by the model equation were in close agreement. As indicated in Table 5, the *p*-value was used to verify the significance of each of the coefficients. The incubation period (X_2), pH (X_3), and wheat bran (X_5) were all shown to have a significant ($p < 0.05$) effect on xylanase activity. The Pareto chart of standardization (Fig. 1) confirmed that these three factors significantly influenced xylanase production ($p < 0.05$), as they crossed the *p*-line. However, the other independent factors ($p > 0.05$) were generally considered insignificant.

There is a 97% chance that the model explains the measured variations in response. The magnitude and direction of the factor coefficient in the equation clarify the influence of the six variables for xylanase production. The higher magnitude indicated a large effect on the response. The corresponding response of xylanase activity was expressed in terms of the following regression Eq. (3) derived from the Unstandardized Beta values (Table 6):

$$Y = X_1 + X_2 + X_3 + X_4 + X_5 + X_6, \tag{3}$$

$$Y = 20.58 - 0.47X_1 + 4.28X_2 + 1.51X_3 - 0.16X_4 + 23.99X_5 + 4.56X_6,$$

where Y is defined as the peak area, X_1 refers to the incubation temperature, X_2 is the incubation time, X_3 is the pH, X_4 is the agitation, X_5 is the wheat bran and X_6 is the ammonium sulphate.

Optimization of significant variables for xylanase production. *Box Behnken design.* A total of 16 runs were performed to determine the conditions for optimal xylanase production by *T. harzianu*m. A matrix was run with the three significant variables that emerged from the PBD experiments. The results for the BBD runs (Table 4) show that the lowest activity of 27.38 U/ml was obtained under zero-level conditions (5 days, pH 5.0, and 1% wheat bran) in run 15 while run 8 resulted in the highest xylanase activity of 153.80 U/ml under the following conditions: 6 days of incubation, pH 5.0, and 1.2% wheat bran. This was significantly and markedly (over four-fold)_higher ($p \geq 0.05$) than the highest enzyme activities obtained during OFAT (38.50 U/ml). Long et al.[21] confirmed a similar but lower influence of optimized parameters on xylanase production (174.46–266.70 U/ml) by *Trichoderma orientalis*. Using the quadratic equation, the predicted values were determined (Table 4). The R^2 or coefficient of determination (0.9647, close to 1) confirmed the validity of the model, i.e., that 96.47% of the variability of the response can be expressed by the model. The value of the coefficient of adjusted determination, adjusted R^2, was 0.9112 confirming that the actual values were close to the predicted values[46,47]. The correlation was confirmed by plotting the actual value curve as a function of the predicted values (Fig. 2) which shows the points distributed around the regression line. Figure 2 shows that the actual response values agreed well with the predicted response values, thus the predicted xylanase production is within the limits of the experimental factors. Therefore, the model is considered of sufficient quality[46] with a 96.47% chance that it explains the measured variations in response.

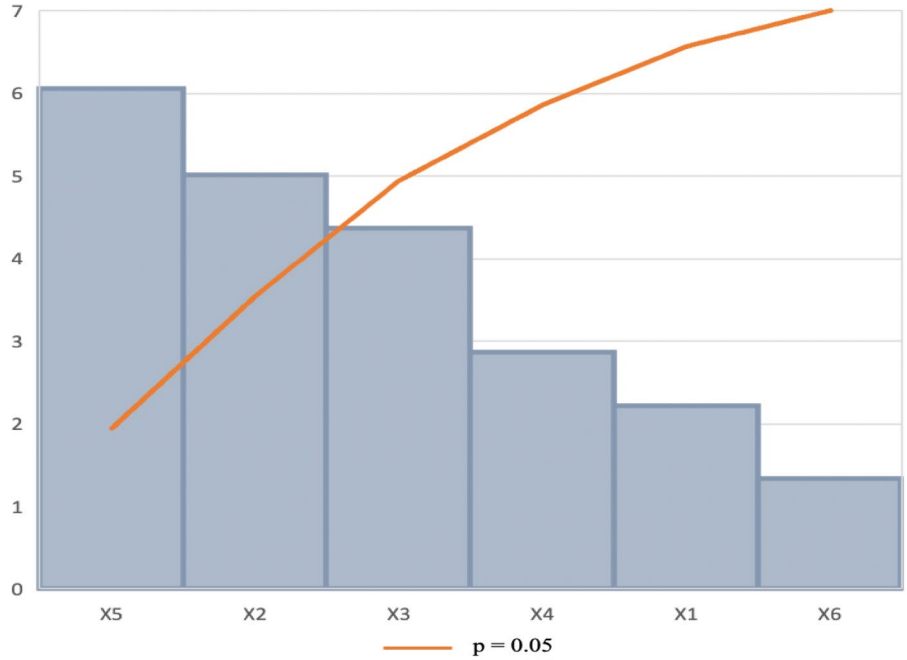

Figure 1. Pareto chart of standardized effects for the production of xylanase. Incubation temperature (X_1), incubation time (X_2), pH (X_3), agitation (X_4), wheat bran (X_5), ammonium sulphate (X_6).

	Unstandardized beta	Coefficients Std.Error	Standardized coefficients beta	t-value
Model	20.58	14.45		1.42
Incubation temperature (X_1)	− 0.47	0.11	− 0.61	− 2.22
Incubation time (X_2)	4.28	0.85	0.57	5.02
pH (X_3)	1.51	0.68	0.25	4.37
Agitation (X_4)	− 0.16	0.06	− 0.33	− 2.87
Wheat bran (X_5)	23.99	3.96	0.80	6.06
Ammonium sulphate (X_6)	4.56	3.41	0.15	1.34

Table 6. Effect estimates for xylanase production from the results of PBD.

Maximum xylanase production (153.80 U/ml) by the *T. harzianum* strain occurred in BBD run 8 under acidic conditions (pH 5.0), the higher wheat bran (1.2%), and a 5-day incubation period. Lightly lower activity can be observed for run 12 (116.74 U/ml) where the incubation period was 5 days, the wheat bran was 1.2% and the pH was 6.0. Even lower but similar enzyme activities were obtained for runs 6 (101.32 U/ml) and 7 (103.37 U/ml) where either the incubation time (4 or 6 days) or wheat bran (0.8 or 1.2%) was at their low or high levels, respectively compared to run 8 where both these parameters were at their high levels (6 days and 1.2%). This may be due to the presence of two isoforms that are maximally produced under acidic conditions. The presence of isoforms requires different periods of incubation for maximal xylanase activity and various wheat bran concentrations. In the presence of xylan, most microorganisms can produce multiple types of xylanases. Fungi are well-known for producing a wide range of xylanases (up to 30 multiple forms)[5,48]. Zhang et al.[49] reported that three xylanase isoforms were produced by *Aspergillus fumigatus*. Multiple forms of xylanases differ in stability, catalytic efficiency, absorption, and activity on substrates[50]. Okafor et al.[51] isolated a strain of *Penicillium chrysogenum* PCL501 from wood wastes and found that after 4 days of fermentation, wheat bran produced the highest xylanase activity of 6.47 U/ml. Abdel-Sater et al.[52] obtained maximum xylanase production from *T. harzianum* after 8 days of fermentation whereas, Thomas et al.[53] achieved maximum xylanase production in 4 days of fermentation by an *Aspergillus* sp.

The production of multiple forms of xylanases can be influenced by many factors, including the presence of various alleles of the same gene, variable mRNA processing, proteolytic digestion post secretion, and post-translational modifications such as glycosylation and autoaggregation[54]. Because xylanases have varying catalytic efficiencies, the production of several xylanases is particularly beneficial for the complete hydrolysis of hemicellulosic substances[55]. Generally, xylanase production is directly proportional to the duration of the fermentation time up to a certain level and then decreases, thus, incubation time affects xylanase production by fungi[56].

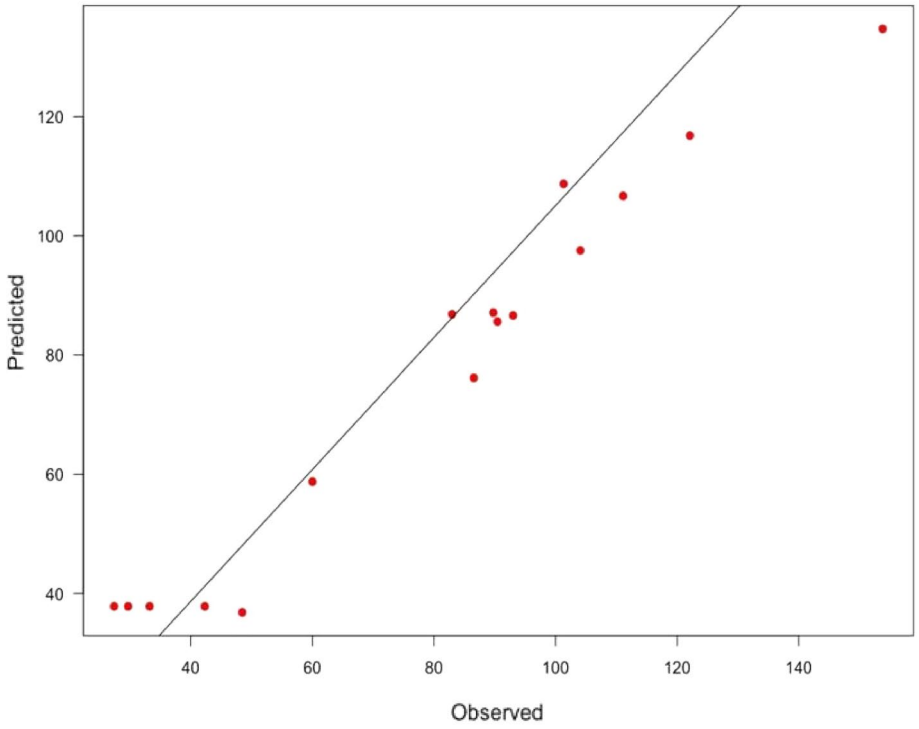

Figure 2. Graphical representation of the minimal difference between the actual (straight line) and predicted responses (circles) for the Response Surface Methodology Design for optimal xylanase activity.

	Estimate	Std. Error	t value	*p*-value
Model	2736.80	227.41	12.03	0.00001*
Incubation time (X_2)	− 555.80	43.97	− 12.64	0.00001*
pH (X_3)	− 178.57	49.62	− 3.60	0.01137*
Wheat bran (X_5)	− 1897.16	219.83	− 8.63	0.00013
Incubation time (X_2): pH (X_3)	4.48	3.78	1.18	0.28169
Incubation time (X_2): Wheat bran (X_5)	12.08	25.78	0.47	0.65598
pH (X_3): Wheat bran (X_5)	33.55	18.92	1.77	0.02042*
Incubation time $(X_2)^2$	52.50	4.17	12.59	0.00005*
pH $(X_3)^2$	13.04	4.17	3.13	0.12655
Wheat bran $(X_5)^2$	887.04	104.24	8.51	0.00014

Table 7. Analysis of variance (ANOVA): and regression coefficients of the response surface quadratic model for the response variables for xylanase production by *Trichoderma harzianum* strain. *Significant *p*-value at $p \leq 0.05$. Adjusted $R^2 = 0.9117$. Lack of fit *p*-value = 0.3741.

Second-order regression and prediction. The second-order regression equation provides the xylanase activity produced by the *T. harzianum* strain as a function of incubation time (X_2), pH (X_3), and wheat bran (X_5) which can be presented in the following Eq. (4):

$$Y = 44.91 - 0.004X_2 + 0.012X_3 + 42.09X_5 - 0.004X_{22} + 0.012X_{32} + 42.09X_{52} + X_2X_3 + X_2X_5 + X_3X_5, \quad (4)$$

where Y is the peak area, X_2 is the incubation time, X_3 is the pH and X_5 is the wheat bran concentration. The statistically insignificant parameters ($p > 0.05$) and their interactions were omitted from the equation. The model constants and coefficients were generated using the unstandardized beta values.

ANOVA and Pareto chart. The "Lack of fit *p*-value" (Table 7) was insignificant as the *p*-value was greater than 0.05, however, literature shows this *p*-value (> 0.05) is considered acceptable[57]. According to Bezerra et al.[58], significant regression and a non-significant lack of fit present in the model were well-fitted to the experiments. Based on this, the regression equation can be validated[59]. ANOVA was performed to determine the *p*-values (Table 7). This showed the model, the linear and square terms for X_2 (Incubation time), and the interaction between X_3 (pH) and X_5 (Wheat bran) as well as the linear terms of X_3 (pH) to be significant as the *p*-values were 0.00001, 0.0001, 0.00005, 0.02042 and 0.01137, respectively. The Pareto chart of standardization histogram graph

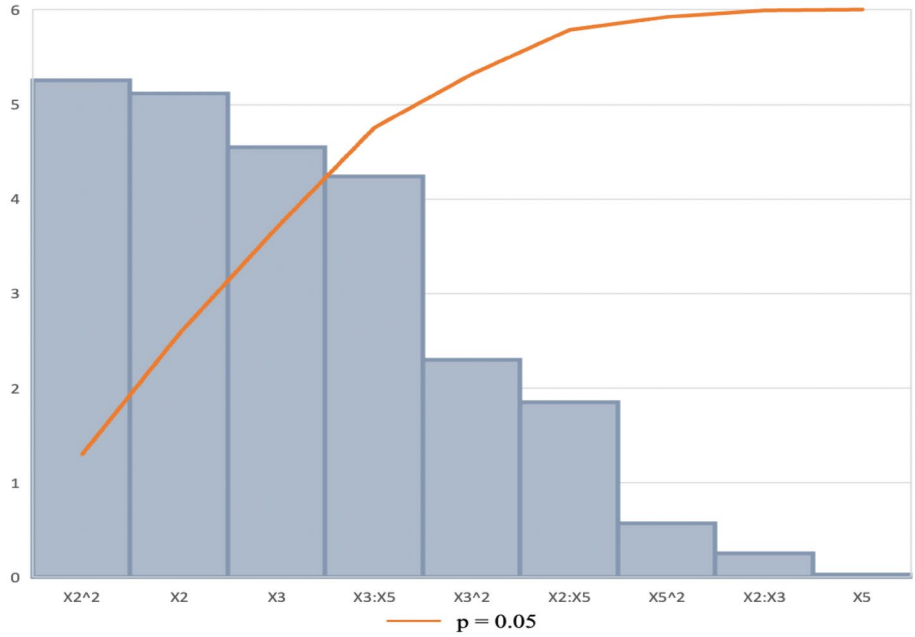

Figure 3. Pareto chart standardized effects of nine interactive factors affecting the production of xylanase optimization. Incubation temperature (X_1), incubation time (X_2), pH (X_3), agitation (X_4), wheat bran (X_5), ammonium sulphate (X_6).

(Fig. 3) also showed that Incubation time (X_2, X_2^2), the interaction between pH and wheat bran (X_3, X_5), and pH (X_3) was significant ($p < 0.05$), as it crosses the *p*-line.

Interaction of variables. The relationship between the parameters and the responses can be understood by studying the three-dimensional (3D) response surface plots for xylanase activity generated from the quadratic model. The 3D response surface plot can also be used to determine the optimum level of each variable for xylanase activity (Figs. 4, 5, 6). While maintaining other variables at their optimal level, the Z-axis (referring to xylanase activity) versus any two variables was constructed in the response surface plot.

Figure 4a,b illustrate the combined effects of incubation time and pH xylanase activity increases at a high pH and shorter incubation time. Figure 4b illustrates the contour plot, which shows that high enzyme activity was obtained at the shortest (4 days) and longest period (6 days) of incubation in acidic (4.0–6.0) conditions. Yadav et al.[29], reported similar pH conditions for optimization of xylanse production from *Anoxybacillus kamchatkensis* NASTPD13.

Figure 5a,b show that xylanase production is directly proportional to incubation time and wheat bran. This could be due to higher levels of degradation of xylan present in the wheat bran by *T. harzianum*. In Fig. 5b, it is apparent that the xylanase activity is highest at high concentrations of wheat bran with the shortest (4 days) and longest period (6 days) of incubation. Previous studies showed the time course during the OFAT approach, being favourable at 4 days and 6 days of incubation with the optimum being at 5 days[33]. The RSM plots correspond with the OFAT results, as the plots show the highest xylanase activity obtained at high wheat bran between 4 and 6 days. Simultaneously, it was highlighted by Beg et al.[60] that wheat bran could effectively induce higher xylanase production by *Aspergillus awamori.* Li et al.[61] also reported the importance of the substrate concentrations for xylanase production by *A. awamori.* The facts mentioned here, correspond to the reports by Cui and Zhao[62], as they mention that the enzymes, which are involved in substrate degradation, were generally mostly inducible. These were formed only when the substrate it correlates with, was present in the nutrient salt solution.

Figure 6 shows the highest xylanase activity obtained with high wheat bran and the entire pH range tested. However, at lower wheat bran concentrations, higher xylanase activity can be observed at the pH extremes tested (at approximately pH 4 and pH 6). Figure 6b illustrates, at high wheat bran concentration and over a wide pH range with the highest activity obtained at the highest pH and wheat bran concentration. The interaction between the pH and wheat bran (130 U/ml) and between incubation time and wheat bran (130 U/ml) had the highest effect on xylanase activity compared to the interaction between incubation time and pH (120 U/ml).

The study successfully demonstrated a notable increase in enzyme activity using the statistically designed experiments compared to OFAT. It was also demonstrated that multiple forms of xylanase were produced (isoforms) based on variations in the growth and media conditions. Based on Table 4, there could potentially be 5 different isoforms. High xylanase activity was observed for runs 4, 6, 7, 8, and 12. Supplementary Fig. 6 representing these RSM runs indicates the presence of isoforms by several zones of clearance on the substrate native PAGE gels.

Multiple forms of xylanases with different pH optima could be beneficial for animal feed improvement[13]. Xylanase is used to reduce the viscosity of the feed and improve the absorption of nutrients in the digestive

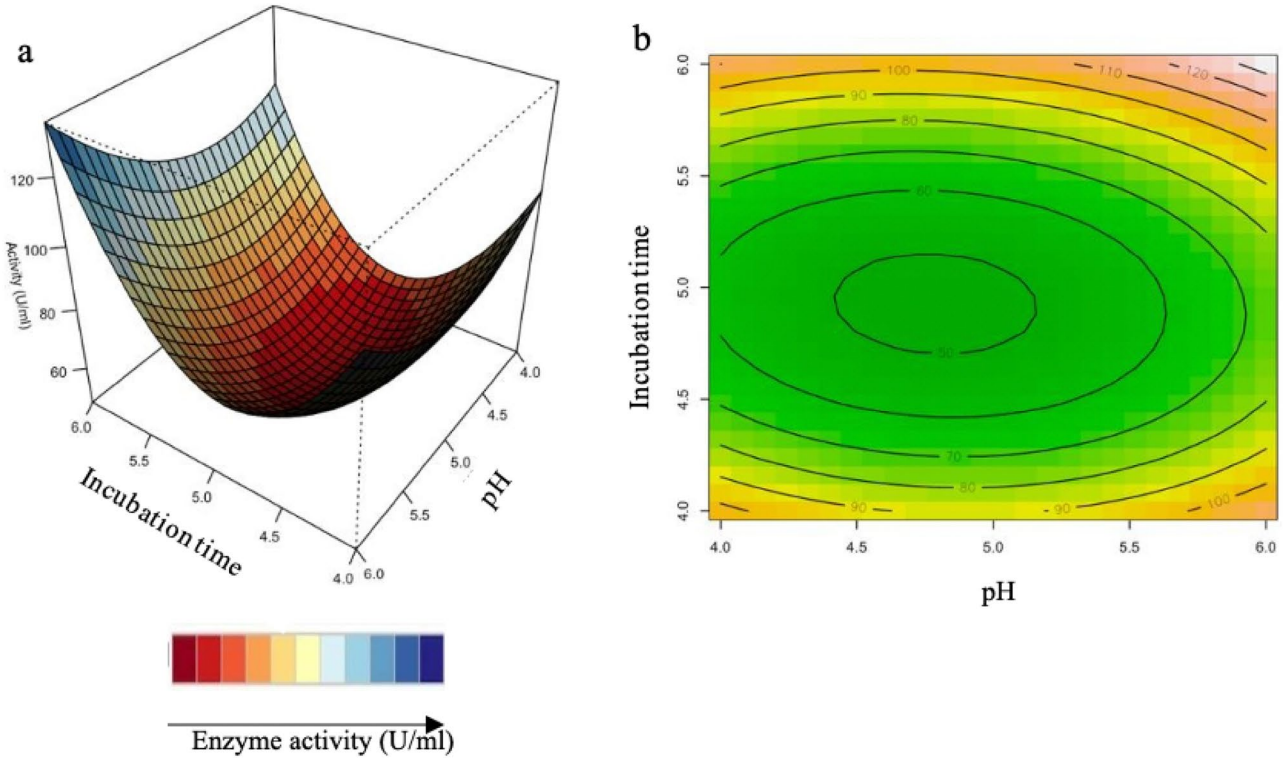

Figure 4. 3D-response surface plots (**a**) and contour plots (**b**) of the combined effects of Incubation time (X_2) and pH (X_3) on xylanase production by *Trichoderma harzianum* strain.

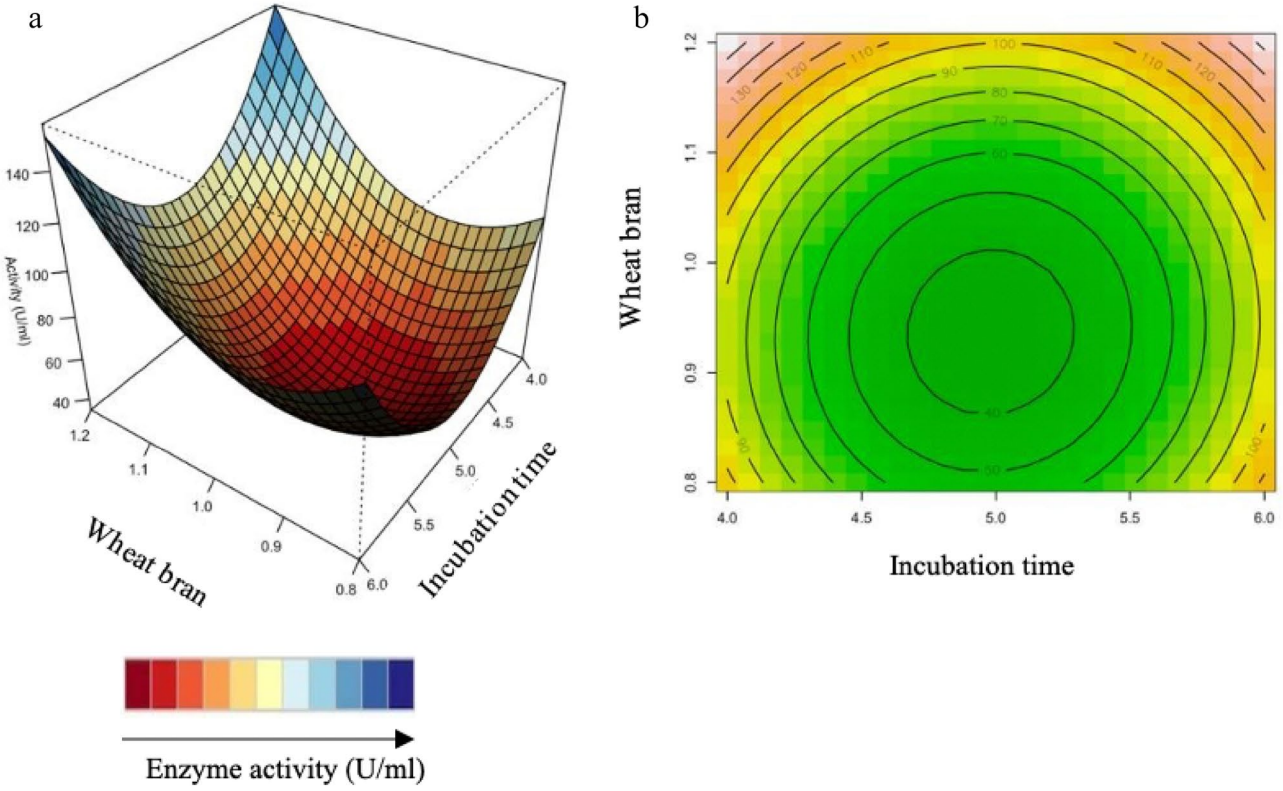

Figure 5. 3D-response surface plots (**a**) and contour plots (**b**) of the combined effects of Incubation time (X_2) and wheat bran (X_5) on xylanase production by *Trichoderma harzianum* strain.

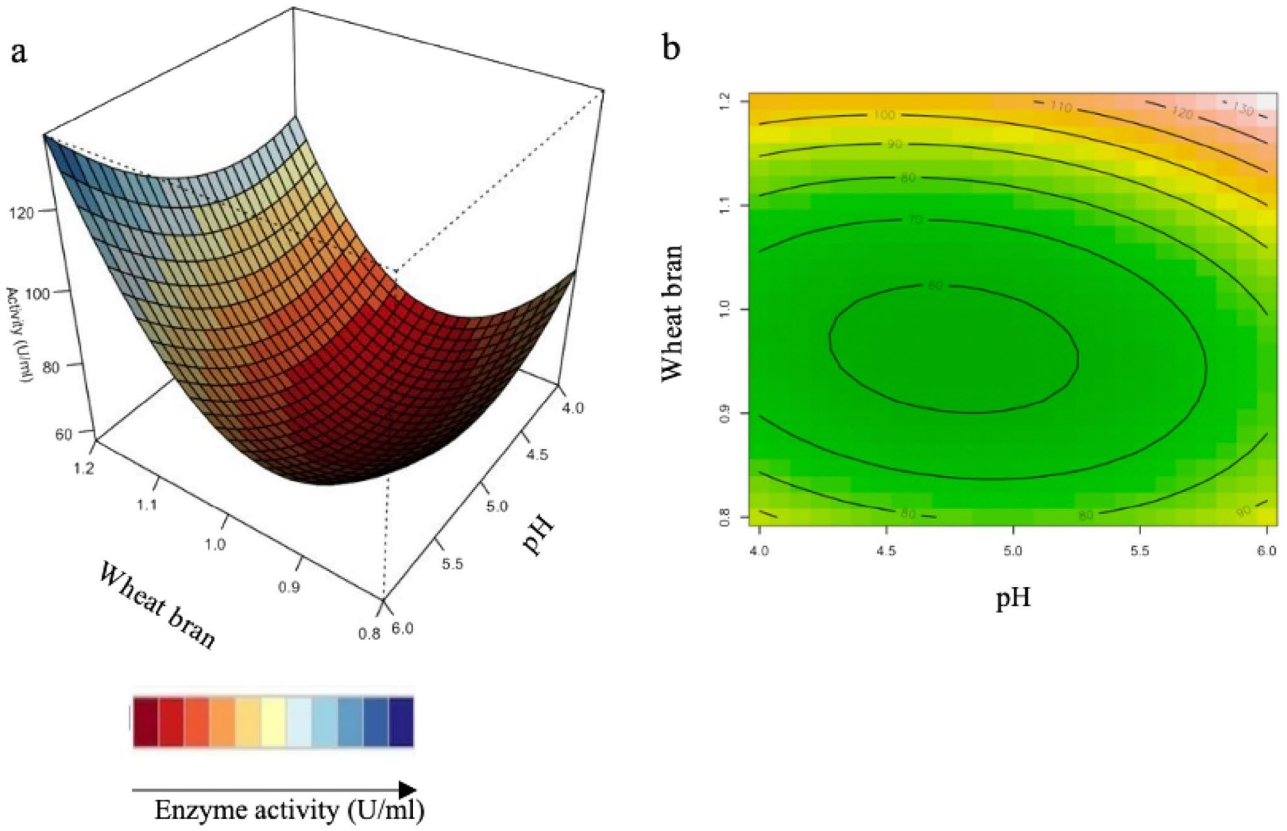

Figure 6. 3D-response surface plots (**a**) and contour plots (**b**) of the combined effects of pH (X_3) and wheat bran (X_5) on xylanase production by *Trichoderma harzianum* strain.

tract of animals. The enzymes could be applied before the pelleting process, which operates between pH 4.0 and 6.0 thus requiring enzymes that are active within this pH range. Most xylanases reported to date are optimally active in the acidic or neutral pH range. Xylanases with acidic pH optima could potentially also be useful for applications containing waste, as a method of waste management, and as a feedstock for fermentable sugars[63].

Scaled-up fermentation in optimized conditions for further studies. The xylanase enzyme was produced on a larger scale for further studies. The enzyme was produced at pH 5.0 for 6 days of incubation and with 1.2% wheat bran. The enzyme activity was determined in order to compare the activities to the smaller scale production. The enzyme activity obtained was 152.78 U/ml which was similar to the enzyme production on a smaller scale (153.80 U/ml).

Purification of xylanase from the *T. harzianum* isolate and zymography. The xylanase from *T. harzianum* was purified using ammonium sulphate precipitation, dialysis, and chromatographic methods in combination. Table 8 summarizes the purification stages. The enzyme was fractionated with the following ammonium sulphate saturations: (0–19%, 20–29%, 30–39%, 40–49%, 50–59%, 60–69% and 70–79%). The 70–79% saturation fraction resulted in significantly high xylanase activity with a recovery of 20.31% enzyme activity. The 50–59%, 60–69%, and fractions also showed relatively high recovery of enzyme activity (18.73%, and 17.48%, respectively) whereas 10.42% enzyme was recovered in the 40–49% fraction (Table 8) therefore these fractions were further studied to confirm if they were isoforms. The active fractions were then dialyzed at 4 °C overnight to remove the salts, and the enzyme was loaded onto DEAE Sephadex for further purification. A 0–2 M sodium chloride concentration gradient was used to elute the bound protein. Xylanase activity was measured in both bound and unbound protein fractions. The primary peak eluted at 0.5 M sodium chloride and the corresponding fraction had a specific activity of 254.62 mol/mg, and a 2.52-fold purity. Furthermore, a single band with a molecular weight of 72 kDa was evident on SDS-PAGE gels of the purified enzyme (50%) (Fig. 7a). The other ammonium sulphate fractions (60–79%) also have the same molecular weight protein (72 kDa). To assess the activity/purity, the purified xylanase was subjected to zymogram analysis by substrate native-PAGE (1% beechwood xylan). The xylanolytic activity of the enzyme was indicated by clear zones in the gel after Congo-red staining (Fig. 7b). Purified preparations of enzymes are a requisite for their application as well as elucidating their basic characteristics and mechanisms. Based on the high molecular weight of the purified enzyme, it can be tentatively inferred that it may belong to the GH10 family since enzymes belonging to this family feature a larger molecular weight[63]. Enzymes are also classified based on their catalytic reactions. Based on the sequence similarities of amino acids, xylanases are classified into glycosyl hydrolase (GH) families 10

AS fraction (%)	Total protein (mg)	Total activity (U)	Specific Activity (U/mg)	Yield (%)	Fold purity
Crude extract	95	9593	101.21	100	1.0
Ammonium sulphate fraction					
50–59%	12.77	2394.51	187.53	24.96	1.85
60–69%	10.45	1796.44	171.91	18.73	1.70
70–79%	10.11	1676.73	165.85	17.48	1.64
80–89%	7.02	1947.93	277.48	20.31	2.74
Anion exchange chromatography					
50–59%	0.40	999.90	2499.75	10.42	24.70
60–69%	0.28	636.88	2274.57	6.64	22.47
70–79%	0.16	313.67	1960.44	3.27	19.37
80–89%	0.32	700.60	2189.38	7.30	21.63

Table 8. Purification table for xylanase from *Trichoderma harzianum* strain.

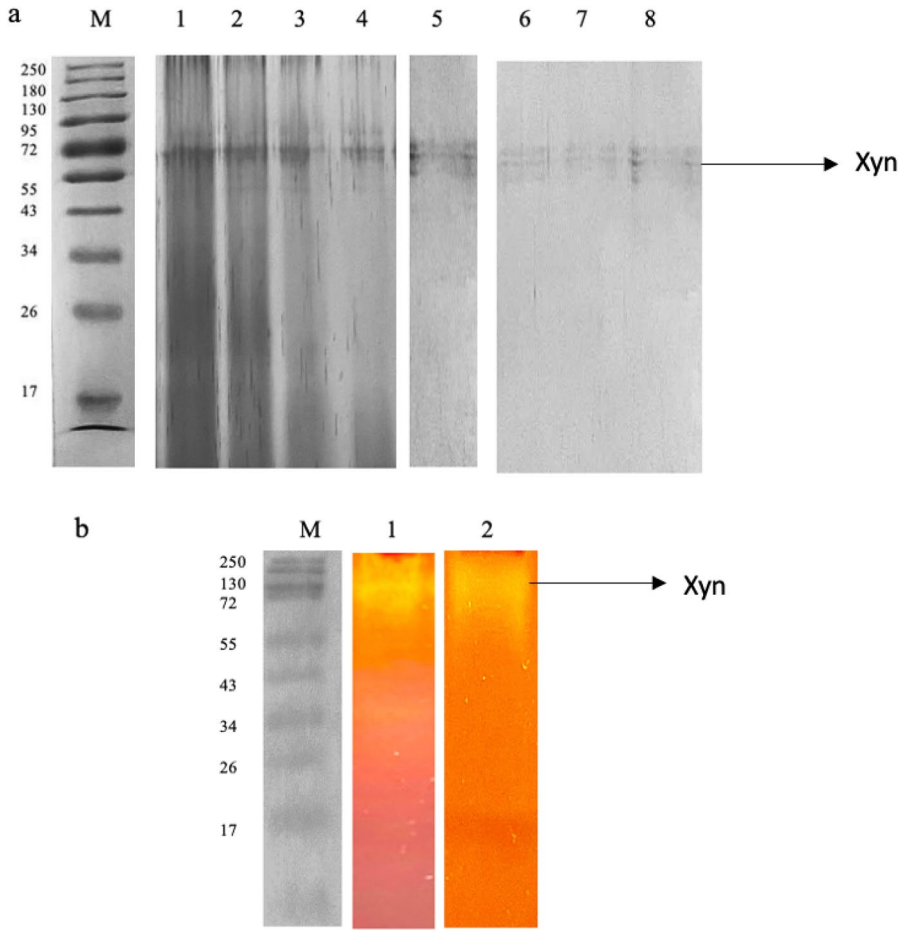

Figure 7. A 12% SDS PAGE (**a**) and Native substrate-PAGE (**b**) analysis of purified xylanase. 12% SDS PAGE (cropped) represents Lane M: Molecular weight marker (Thermoscientific, USA), 1–4: 50, 60, 70, and 80% ammonium sulphate fractions (Coomassie-stained), and 5–8: Purified xylanase from *Trichoderma harzianum* (Xyn). Native substrate-PAGE (cropped) represents Lane M: Molecular weight marker (Thermoscientific, USA), 1: 50% Ammonium sulphate fraction showing zone of clearance, and Lane 2: Purified xylanase (Xyn) from *Trichoderma harzianum* on native substrate gel showing zone of clearance. The original gels are presented in Supplementary Figs. 1–5.

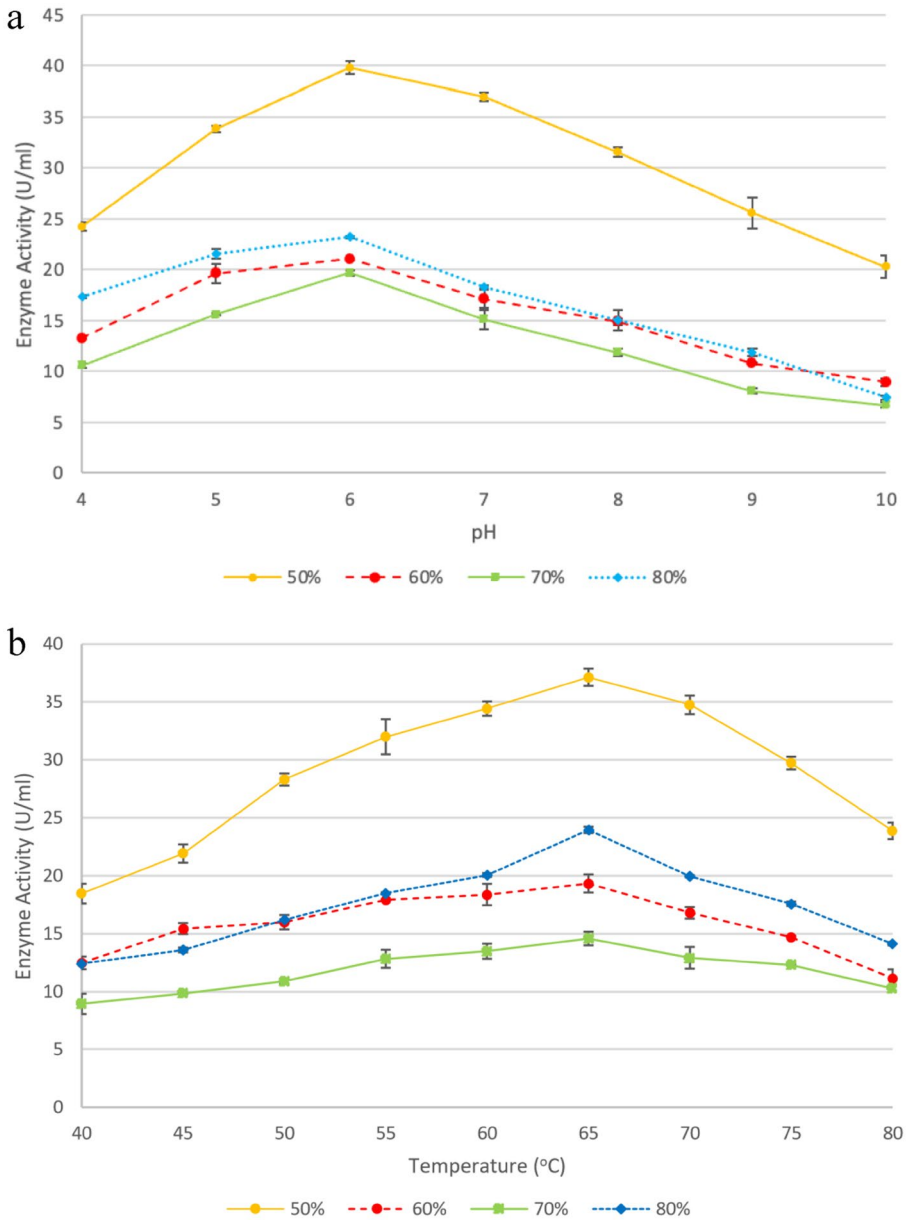

Figure 8. Effect of pH (**a**) and temperature (**b**) on the activity of purified xylanases (50%, 60%, 70%, and 80% ammonium sulphate fractions). Data points represent the means ± SD (n = 4).

(GH10) and 11 (GH11)[2]. Family GH10 contains xylanases of high molecular mass (> 30 kDa) with a $(\beta/\alpha)_8$ barrel structure and acidic *pI* values, while GH11 include are the low-molecular-weight endoxylanases which are divided into alkaline *pI* and acidic *pI* xylanases[2].

Characterization of xylanase. *pH optimum and stability.* The enzyme activity is greatly affected by pH because substrate binding and catalysis are dependent on the charge distribution of both the substrate and the enzyme molecules. The reaction pH was adjusted to 4.0–10.0 with various buffers as described above. The optimum pH of *T. harzianum* xylanase is pH 6.0 with an activity of 40 U/ml (Fig. 8a). The enzyme is fairly stable at pH 6.0 and remains active (Fig. 9) retaining > 70% of its activity over 4 h. Souza et al.[64] reported that the xylanase from *Thermoascus aurantiacus* expressed in *E. coli* showed optimum activity and stability at a similar pH. Yadav et al.[29] reported that xylanase from *Anoxybacillus kamchatkensis* NASTPD13 showed high activity between pH 6.0 to 9.0 and at pH 6.0, the enzyme retained 71% of its activity over 24 h. The purified 60–79% ammonium sulphate fraction was further confirmed to contain the same protein as that purified in the 50% fraction as it displayed the same pH optimum and size (pH 6.0) (Fig. 8a). Thus, the purified fractions of the 50–79% ammonium sulphate fractions can be combined to increase the yield (%).

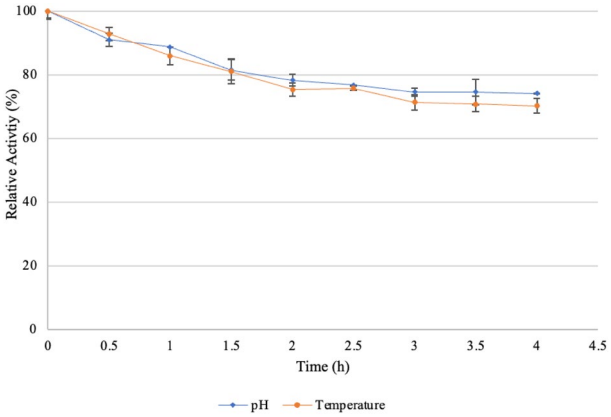

Figure 9. pH and temperature stability of purified xylanases (50% ammonium sulphate fraction) produced by the *Trichoderma harzianum* isolate. Data points represent the means ± SD (n = 4).

	Concentration (mM)	
Metal ions	2.0	10.0
None	100	100
CaCl	84.71	104.27
$CoCl_2$	100.20	104.59
$FeSO_4$	97.62	110.89
$MgSO_4$	96.56	109.44
$MnSO_4$	101.77	100.96
$ZnSO_4$	94.05	108.55
KH_2PO_4	101.98	110.91
NaCl	101.11	98.76

Table 9. Effect of metal ions on purified xylanase activity (relative activity %).

Optimum temperature and thermal stability. The experiment was carried out at different reaction temperatures ranging from 40 to 79 °C to find the optimal temperature of the xylanase. The highest activity of xylanase was observed at 65 °C (Fig. 8b). Thermal stability data illustrated in Fig. 9 shows that the enzyme retained > 70% activity at 65 °C for 4 h. A similar result was reported by de Oliveira Simões et al.[65]. However, in that study, the enzyme was subjected to treatment for 24 h and was stable for 1 h. The purified 60–79% ammonium sulphate fraction contained the same purified protein as the 50% fraction, with the same molecular weight, pH and temperature optima obtained (65 °C) (Fig. 8b). This confirms that these fractions are not isoforms of the xylanase produced. However, the shape of the curve for the 50% ammonium sulphate fraction is different from the other fractions, which seem to show an optimum rather than a broad bell shape.

The advantages of enzymes that prefer high temperatures are well known because the solubility of the reagents and products is increased, the viscosity is reduced, and the mass transfer rate is higher[66]. When looking for enzymes for industrial uses, stability, and activity at high temperatures are highly desirable.

Effect of metal ions and inhibitors. The effects of 8 metal ions (Ca^{2+}, Co^{2+}, Fe^{2+}, Mg^{2+}, Mn^{2+}, Zn^{2+}, K^+, and Na^+) at a final concentration of 2 mM and 10 mM on xylanase activity were determined (Table 9) at the optimal pH and temperature (6.0 and 65 °C). Enzyme activity was slightly increased by 2 mM $Mn2^+$, K^+, and Na^+ (101.11–101.77 U/ml) whereas the enzyme activity was slightly but significantly higher with 10 mM Ca^{2+}, Co^{2+}, Fe^{2+}, Mg^{2+}, Zn^{2+} (104.27–110.89 U/ml) ($p \geq 0.05$) and thus, these ions act as cofactors for the enzyme. Maximum enhancement was observed for Fe^{2+} (10.88%) followed by Mg^{2+} (9.43%) and Zn^{2+} (8.43%) at 10 mM. Fu et al.[43] reported similar findings for xylanase from *Trichoderma* sp. TPS-36.

Inhibitory effects were observed for Fe^{2+} (15.29%), Mg^{2+} (3.44%), Zn^{2+} (5.95%) at 2 mM and Na^+ (1.24%) at 10 mM, however, this inhibition of xylanase was weak (< 50%). Co^{2+} and Ca^{2+} had no effect on xylanase activity (100%) at either concentrations.

Fu et al.[43] also reported weak (< 50%) inhibition of xylanase with the same ions and that Co^{2+} and Ca^{2+} had no effect on xylanase activity (100%) at either concentrations.

Substrate specificity of purified xylanase. To determine the substrate specificity of the xylanase for polysaccharide degradation, potential substrates, including birchwood xylan, beechwood xylan, wheat arabinoxylan

Substrates	Relative activity
Beechwood xylan	100
Birchwood xylan	174.07
Xylan from Larchwood	131.03
Wheat arabinoxylan (soluble)	70.54
Wheat arabinoxylan (Insoluble)	46.62
CMC	ND
Avicel	ND

Table 10. Substrate specificity of the purified xylanase. Each data point represents mean ± SD (n = 3) ND is not detected.

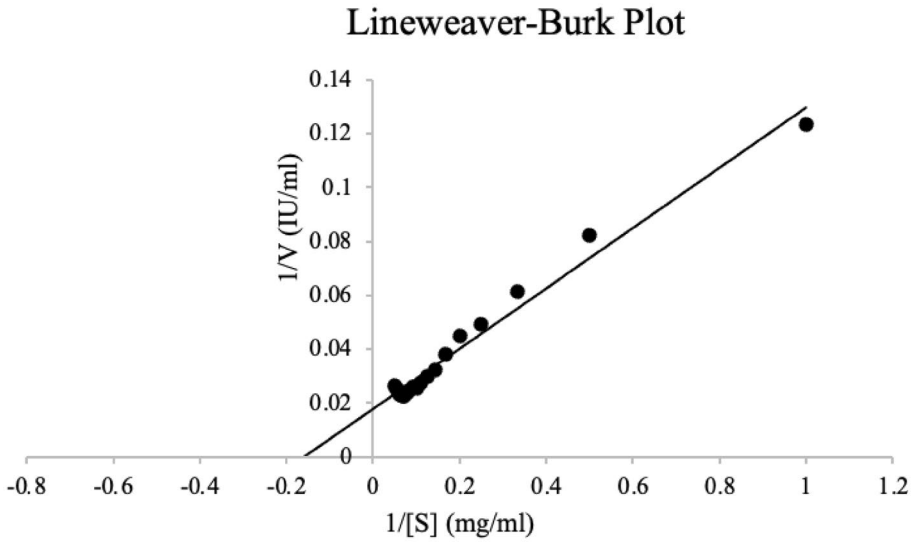

Figure 10. Double reciprocal plot of the purified (50% ammonium sulphate fraction) xylanase from *Trichoderma harzianum* on beechwood xylan. Data points represent the means ± SD (n = 3).

(soluble and insoluble), xylan from Larchwood, CMC and Avicel were tested under optimal conditions (pH 6.0 and temperature 65 °C) using the purified xylanase. Higher hydrolytic activity was observed for the xylans from beechwood, birchwood, and Larchwood compared to wheat arabinoxylan (Table 10). The xylanase most actively degraded birchwood xylan (174.07%), followed by Larchwood xylan (131.03%), and presented the lowest activity towards wheat arabinoxylan (soluble 70.54% and insoluble 46.62%). The purified xylanase exclusively hydrolyzed xylans, with no activity on CMC and Avicel. This suggested that xylanase's substrate-binding domain has a high affinity for xylans from softwood (birchwood and beechwood)[67]. This might be due to differences in xylan polymer structures and the presence of reactive groups on the surface that are more readily bound. The purified xylanase exhibited significant hydrolytic activity on the diverse xylan substrates, indicating that it might be classified as an endo-1,4-xylanase[68].

Kinetic analysis. The Michaelis constant, K_m, may be determined by measuring the substrate concentration at half the maximum velocity. K_m is a constant that remains fixed for every given enzyme and substrate combination. As a result, a low K_m improves the enzyme's affinity for the substrate[69] The concentration range of the substrate under investigation was 1–20 mg/ml, the study revealed K_m and V_{max} were 5.56 mg/ml and 1052.63 µmol/min/mg (Fig. 10). The value of K_m is within the range of fungal xylanases reported in literature (0.14–14 mg/ml). Raj et al.[70] obtained similar values (4.96 mg/ml and lower V_{max} 402 µmol/mg/ml) for xylanase from alkaliphilic *Bacillus licheniformis*. Fu et al.[43] reported high V_{max} (1250 µmol/min/mg) similar to this study. Because xylanase has a high V_{max} value and a low K_m value, it has a high affinity for the substrate, beechwood xylan, and can catalyze it more efficiently and quickly than other substrates. Xylanases from *Caldicoprobacter algeriensis* sp. nov. strain TH7C1T were shown to have high selectivity for beechwood xylan[42].

Conclusion

The current study describes the successful optimization of xylanase production via statistical modelling using PBD and BBD by a *T. harzianum* strain in submerged fermentation. The most influential independent variables were identified and optimized—resulting in a 4.16-fold and 2.24-fold increase in enzyme activity with BBD

compared to the OFAT and PBD, respectively. PBD allowed for the consideration of various variables and avoided loss of information, which might be essential in the optimization of the fermentation process. The predictions of the mathematical models were validated by experimental results. Quadratic models with three independent variables were shown to accurately define xylanase production, with high R^2 values for correlations between the actual and predicted values of the response variables. Results showed high enzyme activities obtained within a high pH range which indicates the potential of the xylanase for use over a wide range of applications. Acidic-thermostable xylanase was purified with a 10.42% recovery and 2.52-fold purity. The specific activity of purified xylanase was 254.63 U/mg. The acidic-thermostability of *T. harzianum* xylanase is advantageous for animal feed manufacturing. Future studies will include scaling up the production of xylanase from *T. harzianum* under optimized conditions, which include the factors and their variables that resulted in the highest xylanase activity (RSM, run 8). Studies will also include sequencing the xylanase protein to understand the structure-guided function of this enzyme.

Data availability

The datasets used and/or analysed during the current study are available from the corresponding author upon reasonable request. Other data generated or analysed during this study are included in this article [and its supplementary information file].

Received: 6 September 2022; Accepted: 18 October 2022
Published online: 22 October 2022

References

1. Broeker, J. *et al.* The hemicellulose-degrading enzyme system of the thermophilic bacterium *Clostridium stercorarium*: Comparative characterization and addition of new hemicellulolytic glycoside hydrolases. *Biotechnol. Biofuels.* **11**, 229 (2018).
2. Bagewadi, Z. K., Mulla, S. I. & Ninnekar, H. Z. Purification, characterization, gene cloning and expression of GH-10 xylanase (*Penicillium citrinum* isolate HZN13). *3 Biotech.* **6**, 169 (2016).
3. Tenkanen, M. *et al.* Xylanase XYN IV from *Trichoderma reesei* showing exo- and endo-xylanase activity. *FEBS J.* **280**(1), 285–301 (2013).
4. Katsimpouras, C. *et al.* A novel fungal GH30 xylanase with xylobiohydrolase auxiliary activity. *Biotechnol. Biofuels.* **12**, 120 (2019).
5. Polizeli, M. D. L. T. D. M. *et al.* Xylanases from fungi: properties and industrial applications. *Appl. Microbiol. Biotecnol.* **67**(5), 577–591 (2005).
6. Li, X., Dilokpimol, A., Kabel, M. A. & de Vries, R. P. Fungal xylanolytic enzymes: Diversity and applications. *Bioresour. Technol.* **344**, 126290 (2022).
7. Dar, F. M., & Dar, P. M. Fungal xylanases for different industrial applications. In *Industrially Important Fungi for Sustainable Development*. 515–539 (Springer, 2021).
8. Bhardwaj, N., Agrawal, K., & Verma, P. Xylanases: An overview of its diverse function in the field of biorefinery. *Bioenergy Res. Commer. Oppor. Chall.* 295–317 (2021).
9. Yi, Z. *et al.* Xylan deconstruction by thermophilic *Thermoanaerobacterium bryantii*, hemicellulases is stimulated by two oxidoreductases. *Catalysts* **12**, 182 (2022).
10. Golgeri, M. D. B. *et al.* A systematic review on potential microbial carbohydrases: Current and future perspectives. *Crit. Rev. Food Sci. Nutr.* (2022).
11. Chadha, B. S., Kaur, B., Basotra, N., Tsang, A. & Pandey, A. Thermostable xylanases from thermophilic fungi and bacteria: Current perspective. *Bioresour. Technol.* **277**, 195–203 (2019).
12. Intasit, R., Cheirsilp, B., Suyotha, W. & Boonsawang, P. Synergistic production of highly active enzymatic cocktails from lignocellulosic palm wastes by sequential solid state submerged fermentation and co-cultivation of different filamentous fungi. *Biochem. Eng. J.* **173**, 108086 (2021).
13. Walia, A., Guleria, S., Mehta, P., Chauhan, A. & Parkash, J. Microbial xylanases and their industrial application in pulp and paper biobleaching: A review. *3 Biotech.* **7**, 11 (2017).
14. Kereh, H., Mubarik, N. R., Palar, R., Santoso, P. & Yopi.,. Optimization of process parameters and scale-up of xylanase production using corn cob raw biomass by marine bacteria *Bacillus subtilis* LBF M8 in stirred tank bioreactor. *PJBT.* **15**(3), 707–714 (2018).
15. Jain, P. & Pundir, R. K. Effect of fermentation medium, pH and temperature variations on antibacterial soil fungal metabolite production. *J. Agric. Technol.* **7**(2), 247–269 (2011).
16. Kurrataa, Y. & Meryandini, A. Characterization of xylanase activity produced by *Paenibacillus* sp. XJ18 from TNBD Jambi, Indonesia. *J. Biosci.* **22**, 20–26 (2015).
17. Wang, X. *et al.* Growth strategy of microbes on mixed carbon sources. *Nat. Commun.* **10**, 1279 (2019).
18. Nasr, S., Soudi, M. R., Hatef Salmanian, A. & Ghadam, P. Partial optimization of endo-1, 4-B-xylanase production by *Aureobasidium pullulans* using agro-industrial residues. *Iran. J. Basic Med. Sci.* **16**(12), 1245–1253 (2013).
19. Uhoraningoga, A., Kinsella, G. K., Henehan, G. T. & Ryan, B. J. The goldilocks approach: A review of employing design of experiments in prokaryotic recombinant protein production. *Bioeng.* **5**(4), 89 (2018).
20. Khusro, A. & Aarti, C. Molecular identification of newly isolated *Bacillus* strains from poultry farm and optimization of process parameters for enhanced production of extracellular amylase using OFAT method. *Res. J. Microbiol.* **10**(9), 393–420 (2015).
21. Long, C., Liu, J., Gan, L., Zeng, B. & Long, M. Optimization of xylanase production by *Trichoderma orientalis* using corn cobs and wheat bran via statistical strategy. *Waste Biomass Valoriz.* **10**(1), 1277–1284 (2019).
22. Zhang, H. & Wu, J. Statistical optimization of aqueous ammonia pre-treatment and enzymatic hydrolysis of corn cob powder for enhancing sugar production. *Biochem. Eng. J.* **174**, 108106 (2021).
23. Irfan, M. *et al.* Statistical optimization of saccharification of alkali pre-treated wheat straw for bioethanol production. *Waste Biomass Valoriz.* **7**(6), 1289–1296 (2016).
24. Ekpenyong, M. G., Antai, S. P., Asitok, A. D. & Ekpo, B. O. Plackett–Burman Design and response surface optimization of medium trace nutrients for glycolipopeptide biosurfactant production. *Iran. Biomed. J.* **21**(4), 249–260 (2017).
25. Sun, T. *et al.* The optimization of fermentation conditions for *Pichia pastoris* GS115 producing recombinant xylanase. *Eng. Life Sci.* **20**, 216–228 (2019).
26. Wu, W. J. & Ahn, B. Y. Statistical optimization of medium components by response surface methodology to enhance menaquinone-7 (vitamin k2) production by *Bacillus subtilis*. *J. Microbiol. Biotechnol.* **28**(6), 902–908 (2018).
27. Momeni, M. M., Kahforoushan, D., Abbasi, F. & Ghanbarian, S. Using chitosan/chpatc as a coagulant to remove colour and turbidity of industrial wastewater: Optimization through RSM design. *J. Environ. Manag.* **211**, 347–355 (2018).

28. Kiran, E. U., Akpinar, O. & Bakir, U. Improvement of enzymatic xylooligosaccharides production by the co-utilization of xylans from different origins. *Food Bioprod. Process.* **91**, 565–574 (2013).
29. Yadav, P. *et al.* Production, purification, and characterization of thermostable alkaline xylanase from *Anoxybacillus kamchatkensis* NASTPD13. *Front. Bioeng. Biotechnol.* **6**, 65 (2018).
30. Periyasamy, K., Santhalembi, L. & Mortha, G. Production, partial purification and characterization of enzyme cocktail from *Trichoderma citrinoviride* AUKAR04 through solid-state fermentation. *Arab. J. Sci. Eng.* **42**, 53–63 (2017).
31. Kar, S. S. *et al.* Process optimization of xylanase production using cheap solid substrate by *Trichoderma reesei SAF3* and study on the alteration of behavioural properties of enzyme obtained from SSF and SmF. *Bioprocess Biosyst. Eng.* **36**, 57–68 (2012).
32. Carvalho, E. A. *et al.* Optimization of Xylanase production by *Trichoderma stromaticum* in solid state fermentation. *Proceedings.* 3, (2017).
33. Dhaver, P., Pletschke, B., Sithole, B. & Govinden, R. Isolation, screening and partial optimization of thermostable xylanase production under submerged fermentation by fungi in Durban, South Africa. *Mycology.* (2022).
34. Miller, G. L. Use of dinitrosalicylic acid reagent for determination of reducing sugar. *Anal. Chem.* **31**, 426–428 (1959).
35. Ghosh, P. & Ghosh, U. Statistical optimization of laccase production by isolated strain *Aspergillus flavus* PUF5 utilizing ribbed gourd peels as the substrate and enzyme application on apple juice clarification. *Indian J. Chem. Eng.* **61**, 1–12 (2019).
36. R Core Team. *R: A Language and Environment for Statistical Computing.* (R Foundation for Statistical Computing, 2020). http://www.R-project.org/.
37. Coman, G. & Bahrim, G. Optimization of xylanase production by *Streptomyces* sp. P12–137 using response surface methodology and central composite design. *Ann. Microbiol.* **61**(4), 773–779 (2011).
38. Wickham, H. *Ggplot2: Elegant Graphics for Data Analysis*. 2nd ed. (Springer, 2009). https://doi.org/10.1007/978-0-387-98141-3.
39. Bradford, M. M. A rapid and sensitive method for the quantitation of microgram quantities of protein utilizing the principle of protein-dye binding. *Anal. Biochem.* **72**(12), 248–254 (1976).
40. Laemmli, U. K. Cleavage of structural proteins during the assembly of the head of bacteriophage T4. *Nature* **227**, 680–685 (1970).
41. Franco, P. F., Ferreira, H. M. & Filho, E. X. Production and characterization of hemicellulase activities from *Trichoderma harzianum* strain T4. *Biotechnol. Appl. Biochem.* **40**(3), 255–259 (2004).
42. Amel, B. D. *et al.* Characterization of a purified thermostable xylanase from *Caldicoprobacter algeriensis* sp. Nov. strain TH7C1. *Carbohydr. Res.* **419**, 60–68 (2016).
43. Fu, L. H. *et al.* Purification and characterization of an endo-xylanase from *Trichoderma* sp., with xylobiose as the main product from xylan hydrolysis. *World J. Microbiol. Biotechnol.* **35**, 171 (2019).
44. Said, K. & Afizal, M. Overview on the response surface methodology (RSM) in extraction processes. *J. Appl. Sci. Process Eng.* **2**, 1 (2016).
45. Xie, Y. *et al.* Collaborative optimization of ground source heat pump-radiant ceiling air conditioning system based on response surface method and NSGA-II. *Renew. Energy.* **147**(1), 249–264 (2019).
46. Azzouz, Z., Bettache, A., Boucherba, N., Amghar, Z. & Benallaoua, S. Optimization of xylanase production by newly isolated strain *Trichoderma afroharzianum* isolate AZ12 in solid-state fermentation using Response Surface Methodology. *Cellulose* **54**, 451–462 (2020).
47. Chicco, D., Warrens, M. J. & Jurman, G. The coefficient of determination R squared is more informative than SMAPE, MAE, MAPE, MSE, and RMSE in regression analysis evaluation. *PeerJ Comput. Sci.* **7**, 623 (2021).
48. Roy, S., Dutta, T., Sarkar, T. S. & Ghosh, S. Novel xylanases from *Simplicillium obclavatum* MTCC 9604: Comparative analysis of production, purification, and characterization of enzyme from submerged and solid state fermentation. *Springerplus* **2**, 382 (2013).
49. Zhang, S. *et al.* Synergistic mechanism of GH11 xylanases with different action modes from *Aspergillus niger* An76. *Biotechnol. Biofuels.* **14**, 118 (2013).
50. Liao, H. *et al.* Functional diversity and properties of multiple xylanases from *Penicillium oxalicum* GZ-2. *Sci. Rep.* **5**, 12631 (2015).
51. Okafor, U. A., Okochi, V. I., Onyegeme-okerenta, B. M. & Nwodo-Chinedu, S. Xylanase production by *Aspergillus niger* ANL 301 using agro-wastes. *AJB.* **6**, 1710–1714 (2007).
52. Abdel-Sater, M. A. & El-Said, A. H. M. Xylan-decomposing fungi and xylanolytic activity in agricultural and industrial wastes. *Int. Biodeterior. Biodegrad.* **47**, 15–21 (2001).
53. Thomas, L., Parameswaran, B. & Pandey, A. Hydrolysis of pre-treated rice straw by an enzyme cocktail comprising acidic xylanase from *Aspergillus* sp. for bioethanol production. *Renew. Energy.* **98**, 9–15 (2016).
54. Maity, C. *et al.* Xylanase isozymes from the newly isolated *Bacillus* sp. CKBx1D and optimization of its deinking potentiality. *Appl. Biochem. Biotechnol.* **167**(5), 1208–1219 (2012).
55. Choudhury, B. *et al.* Biobleaching of nonwoody pulps using xylanase of *Bacillus brevis* BISR-062. *Appl. Biochem. Biotechnol.* **128**, 159–169 (2006).
56. Ribeiro Sales, M. *et al.* Cellulase and xylanase production by *Aspergillus* species. *Ann. Microbiol.* **61**, 917–924 (2011).
57. Abu, M. L., Nooh, H. M., Oslan, S. N. & Salleh, A. B. Optimization of physical conditions for the production of thermostable T1 lipase in *Pichia guilliermondii* strain SO using response surface methodology. *BMC Biotechnol.* **17**, 78 (2017).
58. Bezerra, M. A., Santelli, R. E., Oliveira, E. P., Villar, L. S. & Escaleira, L. A. Response surface methodology (RSM) as a tool for optimization in analytical chemistry. *Talanta* **76**(5), 965–977 (2018).
59. He, X. *et al.* Efficient degradation of azo dyes by a newly isolated fungus *Trichoderma tomentosum* under non-sterile conditions. *Ecotoxicol. Environ. Saf.* **150**, 232–239 (2018).
60. Beg, Q. K., Bhushan, B., Kapoor, M. & Hoondal, G. S. Production and characterization of thermostable xylanase and pectinase from *Streptomyces* sp. QG-11-3. *J. Ind. Microbiol. Biotechnol.* **23**, 396–402 (2000).
61. Liu, W., Lu, Y. L. & Ma, G. R. Induction and glucose repression of endo-beta-xylanase in the yeast *Trichosporon cutaneum* SL409. *Process Biochem.* **34**, 67–72 (1999).
62. Cui, F. & Zhao, L. Optimization of xylanase production from *Penicillium* sp. WX-Z1 by a two-step statistical strategy: Plackett–Burman and Box–Behnken experimental design. *Int. J. Mol. Sci.* **13**(8), 10630–10646 (2012).
63. Bhardwaj, N., Kumar, B. & Verma, P. A detailed overview of xylanases: An emerging biomolecule for current and future prospective. *Bioresour. Bioprocess.* **6**, 40 (2019).
64. Souza, A. R. *et al.* Engineering increased thermostability in the GH-10 endo-1, 4-β-xylanase from *Thermoascus aurantiacus* CBMAI 756. *Int. J. Biol. Macromol.* **93**, 20–26 (2016).
65. de Oliveira Simões, L. C. *et al.* Purification and physicochemical characterization of a novel thermostable xylanase secreted by the fungus *Myceliophthora heterothallica* F.2.1.4. *Appl. Biochem. Biotechnol.* **188**(4), 991–1008 (2019).
66. Vieille, C. & Zeikus, G. J. Hyper thermophilic enzymes: Sources, uses, and molecular mechanisms for thermostability. *MMBR.* **65**(1), 1–43 (2001).
67. Yin, L., Lin, H., Chiang, Y. & Jiang, S. T. Bio properties and purification of xylanase from *Bacillus* sp. YJ6. *J. Agric. Food Chem.* **58**(1), 557–562 (2010).
68. Fang, Z., Smith, J., Richard, L. & Tian, X. Isolation, purification, and potential applications of xylan. *Sustain. Biomass Resour.* **9**(1), 3–35 (2019).
69. Deshmukh, R. A. *et al.* Purification, biochemical characterization and structural modelling of alkali-stable β-1,4-xylan xylanohydrolase from *Aspergillus fumigatus* R1 isolated from soil. *BMC Biotechnol.* **16**, 11 (2016).

70. Raj, A. S., Kumar, S., Singh, S. K. & Prakash, J. Production and purification of xylanase from alkaliphilic *Bacillus licheniformis* and its pre-treatment of eucalyptus kraft pulp. *Biocatal. Agric. Biotechnol.* **15**, 199–209 (2018).

Acknowledgements
This work was supported by the Technology Innovation Agency (TIA) managed DST/CON/0177/2018: SIIP: ENZYME AND MICROBIAL TECHNOLOGIES (EMT) grant and the Biorefinery Industry Development Facility (BIDF) at the Council for Scientific and Industrial Research (CSIR), Durban, South Africa.

Author contributions
This study was carried out by P.D. and supervision was undertaken by R.G., B.S., and B.P. The manuscript was written by P.D. and all authors reviewed, edited and proof checked the manuscript. The study was supported by B.S. and T.I.A. and C.S.I.R.

Competing interests
The authors declare no competing interests.

Additional information
Supplementary Information The online version contains supplementary material available at https://doi.org/10.1038/s41598-022-22723-x.

Correspondence and requests for materials should be addressed to P.D.

Reprints and permissions information is available at www.nature.com/reprints.

Publisher's note Springer Nature remains neutral with regard to jurisdictional claims in published maps and institutional affiliations.

scientific reports

Check for updates

OPEN

Enhanced production of a recombinant xylanase (XT6): optimization of production and purification, and scaled-up batch fermentation in a stirred tank bioreactor

Priyashini Dhaver[1], Tariro Sithole[2], Brett Pletschke[2]✉, Bruce Sithole[3,4] & Roshini Govinden[1]

The endoxylanase XT6 produced by *Geobacillus stearothermophilus* is a desirable candidate for industrial applications. In this study, the gene encoding XT6 was cloned using the pET-28a expression vector and expressed in *Escherichia coli* BL21 (DE3) cells. Recombinant XT6 production was improved by optimizing cell lysis (sonication, chemical, and enzymatic lysis) and expression conditions. Sonication in a 0.05 M sodium phosphate (pH 6.0) buffer resulted in the highest xylanase activity (16.48 U/ml). Screening and optimization of induction conditions using the Plackett–Burman Design and Box-Behnken Design (BBD) approaches revealed that cell density pre-induction ($OD_{600\,nm}$), post-induction incubation time, and IPTG concentration significantly ($p < 0.05$) influenced the expression levels of XT6 (16.48 U/ml to 40.06 U/ml) representing a 3.60-fold increase. BBD resulted in a further 8.74-fold increase in activity to 144.02 U/ml. Batch fermentation in a 5-l stirred tank bioreactor at 1 vvm aeration boosted recombinant xylanase production levels to 165 U/ml suggesting that heterologous expression of the XT6 enzyme is suitable for scaled-up production. The pure enzyme with a molecular weight of 43 kDa and a 15.69-fold increase in purity was obtained using affinity chromatography and a cobalt column. Future studies will include application of the purified recombinant xylanase to animal feed.

Problem statement: Interest in xylan-degrading enzymes has escalated over the last few years due to their applications in pulp processing and the biodegradation of lignocellulosic materials[1]. Hemicellulose, which makes up 30–40% of lignocellulosic biomass, is mainly constituted of xylan[1]. Xylan is a polysaccharide made up of β-1,4-xylose units or β-1,4-mannose units with arabinose, methylglucuronic acid, and acetate substitutions[2,3]. The complex chemical composition of xylan requires the concerted action of several enzymes, collectively known as hemicellulases, including endo-β-D-xylanases, β-xylosidases, α-L-arabinofuranosidases, α-D-glucuronidases, acetyl xylan esterases, ferulic and *p*-coumaric acid esterases. These enzymes work together to produce xylooligosaccharides (XOS) and xylose, which are the end products of their synergistic action on the linear and side chains[4]. Endo-1,4-β-xylanase is an important enzyme that operates on the xylan backbone of hemicellulose with high specificity, minimum substrate loss, and few side products[2] compared to the commonly used chemical hydrolysis techniques. Xylanase acts synergistically in conjunction with other accessory enzymes to degrade xylan to component sugars.

Current state of the art: In nature, filamentous fungi such as *Aspergillus* spp.[5] and *Trichoderma* spp.[6] produce xylanases rapidly. Some bacteria, such as *Bacillus stearothermophilus, Bacillus subtilis*[7], and *Paenibacillus* spp., produce extracellular thermostable xylanase enzymes[8]. These thermostable xylanases are more suitable for

[1]Discipline of Microbiology, School of Life Sciences, University of KwaZulu-Natal, Westville Campus, Durban 4000, South Africa. [2]Enzyme Science Programme (ESP), Department of Biochemistry and Microbiology, Rhodes University, Makhanda (Grahamstown), 6140, Eastern Cape, South Africa. [3]Biorefinery Industry Development Facility, Council for Scientific and Industrial Research, Durban 4000, South Africa. [4]Discipline of Chemical Engineering, University of KwaZulu-Natal, Durban 4000, South Africa. ✉email: b.pletschke@ru.ac.za

industrial bioprocesses than those produced by mesophilic bacteria[3]. The genus *Geobacillus* has been widely examined among numerous thermophilic bacteria studied for xylanase production due to its ability to produce highly thermostable enzymes and ability to use a variety of carbon sources[9]. In thermophilic niches, the genus evolved several species, whose genomes encode highly thermostable enzymes that can be applied in several industrial bioprocesses such as in lignocellulosic biomass hydrolysis[6], pulp and paper production[10], bioethanol production[11], etc. In recent years, xylanases with specific properties have been identified from bacterial and fungal sources, and numerous strategies have been developed to engineer xylanases for specific industrial applications[12]. Due to product inhibition and catabolite repression, microbial xylanases are produced in low titres.

Recent proposed strategies: Researchers have introduced recombinant DNA technology to solve this challenge which has led to the development of xylanolytic enzymes that are more appropriate for industrial applications. To attain overproduction of the enzyme to suit commercial purposes, the xylanase-encoding genes have been cloned into homologous and heterologous hosts[13]. *Escherichia coli* is the first-line system for the heterologous production of particularly non-glycosylated proteins[14]. Cloning of genes in *E. coli* is considered advantageous for high enzyme production levels as it can be easily grown and rapidly on inexpensive substrates to high cell density under favorable growth conditions to achieve high-level expression of the desired recombinant protein[15]. Moreover, *E. coli* can be easily manipulated and has several available cloning and expression vectors, and is amenable to various cultivation techniques[14]. In view of these advantages, *E. coli* can be a suitable host for the large-scale manufacturing of heterologous proteins[14] in bioreactors that provide a well-controlled culture environment[16]. One of the most significant disadvantages of using *E. coli* to produce desired products is that these bacteria do not ordinarily release proteins into the environment[17]. Proteins produced remain confined within the constraints of the cellular framework requiring disruption of the cell walls for the release of proteins into the surrounding environment. Techniques such as sonication, chemical lysis, enzymatic lysis, bead milling, and high-pressure homogenization are reported to be effective for the recovery of proteins from *E. coli* cells[18].

The reaction of cells to their surroundings can also influence the host's expression level[19]. As a result, fermentation factors such as temperature, cell density, induction period, and inducer concentrations must be optimized for the host cells, to maintain favorable conditions to ensure high enzyme activity and protein production efficiency[14]. The traditional method for optimizing the fermentation process is the one-factor-at-a-time (OFAT) approach, where one parameter is varied, while the others are kept constant. However, this approach is laborious due to many factors and the inability to identify the interactions between variables, which can cause misinterpretation of the results[20]. Such challenges may be overcome by using statistical approaches. Plackett Burman Design (PBD) and Rresponse Ssurface Methodology (RSM) approaches were used in this study to optimize the expression of the *G. stearothermophilus* XT6 in *E. coli* to produce high yields of the functional recombinant XT6 protein. Significant steps in the production of a recombinant protein after cloning include fermentation to produce high biomass yields, cell lysis to release intracellular proteins, and the recovery of the protein of interest using a targeted separation technique such as Immobilized Affinity Chromatography (IMAC). All steps are paramount for the success and economic viability of the process.

Aims and objectives: This study aimed to optimize cell lysis (sonication, chemical lysis, and enzymatic lysis) which is critical to achieving the highest possible yield of soluble protein, the expression of XT6 by *E. coli* in shake flask studies, and the scaled-up of production in large-scale bioreactors. The expressed recombinant XT6 protein was then purified and used in further application studies to improve the digestibility of animal feed and assess the effect of the recombinant XT6 xylanase on the hydrolysis of feed substrates.

Materials and methods

Obtaining *E. coli* with pET28(+)/XT6 and expression of recombinant XT6 xylanase

E. coli BL21(DE3) cells were transformed with the pET28(+)-XT6 plasmid DNA[22]. The recombinant cells were grown on 2 × YT plates containing 50 µg/ml kanamycin (SIGMA, China) and were incubated (Heraeus B6120 Incubator, Gemini BV) for 24 h at 37 °C[22].

Single colonies of the recombinant *E. coli* cells harboring XT6 were cultured in 5 ml of 2 × YT broth (50 µg/ml kanamycin) and incubated at 37 °C for 24 h. The culture was transferred into fresh 2 × YT broth (50 µg/ml kanamycin) and grown at 37 °C until the mid-log phase at $OD_{600\ nm}$ was between 0.4 and 0.7. Protein expression was induced by the addition of 1 mM isopropyl-β-Dthiogalactopyranoside (1 M IPTG) (Glentham Life Science, Corsham). Samples were taken every hour for up to 4 h, and the $OD_{600\ nm}$ readings of the bacterial cells were recorded each hour. Collected samples were centrifuged (Eppendorf centrifuge 5418, Germany) at 16 060×*g* for a minute. The supernatant was discarded, and the pellet resuspended in 2 × SDS sample buffer (0.004% (v/v) bromophenol blue, 10% (v/v) 2-mercaptoethanol, 20% (v/v) glycerol, 4% (v/v) SDS and 0.125 mM Tris-HCl, Sigma, South Africa). The volume of sample buffer used to resuspend the pellet was obtained using the formula: [resuspension volume (ml) = $OD_{600\ nm}$/6]. Samples were boiled for 5 min and then incubated on ice before SDS-PAGE analysis[22]. All chemicals and reagnts were obtained from Sigma, Merck.

Optimization of cell lysis

Lysis is a critical stage in the purification of intracellular bioproducts. There are several factors and challenges to consider when selecting the correct lysis protocol as there is no standard procedure applicable for the recovery of all types of recombinant proteins[18]. It is thus, advisable to thoroughly study and test various lysis protocols to ensure the highest possible recovery of the desired product. The different lysis protocols that were tested to maximize recovery of the intracellular recombinant xylanase from the *E. coli* expression host are described below.

Enzymatic lysis (lysozymes)
After induction, the cells were harvested by centrifugation (Eppendorf Centrifuge 5418, Germany) (10,000×*g* at 4 °C for 10 min), and the pellet was resuspended in phosphate-buffered saline (PBS) buffer (20 ml/g of cells). Lysozyme (1 mg/ml) (Sigma, Switzerland) was added to the cell suspension and incubated with shaking at room temperature for 2 h. Samples were stored at − 80 °C overnight and thereafter centrifuged as described above, and the protein was obtained in the supernatant (soluble fraction)[18].

Enzymatic and chemical lysis
The procedure described above in 2.3.1.1 was followed. However, TritonX-100 (1% v/v) (Merck chemicals, England) was used in conjunction with lysozyme, as TritonX-100 is reported to assist in the disruption of the cellular membrane leading to enhanced cell lysis[23].

Sonication
The harvested cells were centrifuged, and the pellets resuspended in 0.05 M sodium phosphate (pH 6.0), 0.05 M Tris–HCl (pH 8.0) buffer, and 0.05 M Tris-HCl (pH 8.0) with 8 M urea. The cell suspensions were lysed using a probe sonicator (OMNI Sonic Ruptor 400, 220 V 6A, 18-200, United Kingdom) at 50 kHz for 30 s. The samples were kept on ice to prevent heating and denaturation during sonication. The lysate was centrifuged for 10 min at 10,000×*g* at 4 °C. The soluble fraction was expected to contain the target protein[18].

Quantification of the extent of lysis

There are several techniques which can be used to quantify the extent of cell lysis. These can be categorized as direct and indirect analyses of cellular lysis.

Direct cellular analysis: optical density at 600 nm
The extent of the lysis of *E. coli* cells can be determined by measuring and comparing the $OD_{600\ nm}$ before and after cell lysis treatments[24].

Indirect analysis (quantification of cellular products)
The indirect techniques of cellular lysis quantification are based on separating several cellular products resulting from cell lysis.

Quantification of total protein. The total protein content was determined using the Bradford technique using bovine serum albumin (BSA) (Sigma, USA) as the standard at values ranging from 0 to 50 mg/ml. In a reaction vessel, aliquots of 1 ml Bradford reagent (Sigma, USA) were well mixed with 33.33 µl of protein and allowed to stand for 5 min at room temperature. A spectrophotometer was used to detect the absorbance at 595 nm (Shimadzu UV-1800, Japan). The blank was comprised of 33.33 µl of distilled water mixed with Bradford reagent[26]. The degree of cell lysis was evaluated by measuring the concentration of proteins in the supernatant of lysate samples before and after lysis.

Xylanase protein quantification. The concentration of the xylanase protein was determined before and after cell lysis using a spectrophotometer (Nanodrop 2000c spectrophotometer, Thermo Scientific). The molar extinction coefficient used was 80 790 M^{-1} cm^{-1} at 280 nm, with a theoretical molecular weight of 46 763 Da for the enzyme[25].

Quantification of xylanase activity. Xylanase activity was quantified using the 3,5-dinitro salicylic (DNS) (Sigma, India) acid assay for reducing sugars[27]. The reaction included 600 µl of 1% (w/v) of beechwood xylan (1 g in 100 ml of citrate buffer, pH 5) (Sigma, India), to which 66.67 µl of the enzyme was added and incubated in a water bath at 55 °C for 15 min. The reaction was terminated by adding 1 ml DNS acid reagent to the reaction mixture and then heated for 5 min at 100 °C in a water bath. The absorbance was read at 540 nm using a spectrophotometer (Shimadzu UV-1800, Japan) to determine the concentration of sugar released by the enzyme. One unit (U) of xylanase was defined as the amount of enzyme that released 1 µmol xylose as reducing sugar equivalents per min under the specified assay conditions. All enzyme assays were performed in triplicate.

SDS-PAGE. The molecular weight of the recombinant XT6 xylanase was confirmed by 12% SDS-PAGE[28]. The gel was run at a constant voltage (50 V) (BioRad, Power Pac™ HV, USA) until the dye front reached the bottom of the gel. Following electrophoresis, the gel was stained in Coomassie Brilliant Blue (Merck, Germany) for 15 min and destained overnight in a destaining solution (10% acetic acid (Merck, Germany), 20% methanol (Merck, Germany), and 70% dH_20) to visualize the proteins and determine the molecular weight of the proteins using standard molecular weight markers. To determine the degree of lysis samples representing the total lysate proteins, both the insoluble phase (pellet), and lysate supernatant (soluble phase) were run on the gel The greater the number of proteins (represented by the number of bands as well as the intensity of bands) released to the soluble phase, the greater the cellular lysis efficiency.

Experimental design and optimization of cultivation parameters

OFAT optimization of the production of the recombinant XT6 xylanase
The factors tested included cell density pre-induction ($OD_{600\ nm}$)[31], induction temperature[30], time[13], IPTG concentration[13], as well as yeast extract, and tryptone concentration[29].

Statistical optimization, experimental design, and data analysis

Plackett–Burman design (PBD). Six variables were selected for this study as shown in Table 1: Incubation temperature (X1), cell density pre-induction ($OD_{600\,nm}$) (X2), post-induction time (X3), yeast extract concentration (X4), tryptone concentration (X5), and IPTG concentration (X6). The total number of experimental runs carried out for the six variables was twelve[32]. Each variable was represented by a high level denoted by '+' and a low level denoted by '–'. The high level of each variable was sufficiently far from the low level so that any significant effect would be observed. The experimental runs were performed in duplicate, and an average of the results was reported. Table 1 represents the PBD based on the first-order polynomial model Eq. (1).

$$Y = \beta_0 \sum \beta_i X \tag{1}$$

where Y is the response (peak area and retention factor), β_0 is the model intercept, βi is the linear coefficient, and X_i is the level of the independent variable. The PBD was analyzed using R studio software[33] to estimate the significant factors. Analysis of variance (ANOVA) was performed to determine the *p* values and the *R* coefficients to check the significance and fit of the regression model. Screened parameters were represented on a Pareto chart of standardized effects. The effect of each variable was analyzed, and the variables with the highest influence on the production of xylanase were selected for the second-level optimization by BBD of Response Surface Methodology (RSM).

Optimization of significant variables using Response Surface Methodology (RSM). The BBD was used to elucidate the primary interaction and quadratic effects of the three significant variables arising from the PBD, with replicated centre points. The experimental design and statistical analysis were performed using R Studio[33]. Table 2 represents a three-level, three-factor BBD was used to evaluate the combined effect of the three independent variables, cell density pre induction ($OD_{600\,nm}$) (X2), post-induction time (X3), and IPTG concentration (X6). The design consisted of 16 combinations, including three replicates of the centre point. After the experimental runs, the average xylanase activities were taken as the response (Y). A multiple regression analysis of the data was carried out to obtain an empirical model relating the response to the independent variables.

The second-order polynomial equation is shown below in Eq. (2):

$$Y = \beta_0 + \sum \beta_i X_1 + \sum \beta_{ii} X_2 + \sum \beta_{ij} X_1 X_2 \tag{2}$$

where Y represents the response variable (peak area), β_0 is the interception coefficient, β_i is the coefficient for the linear effects, β_{ii} is the coefficient for the quadratic effect, β_{ij} are interaction coefficient, and X_1 X_2 is the coded independent variables that influence the response variable Y. The response in each run was the average. In this experimental design, data were analyzed by one-way ANOVA with Tukey's multiple comparison tests ($p < 0.05$) using R studio[33], and ggplot2 was used for the generation of 3D response surface and contour plots.

Scaled-up enzyme production in a stirred tank bioreactor

This study was carried out in a Sartorius BioStat®B-DCU fermenter with a working volume of 3-l with 2 × YT medium supplemented with kanamycin (50 µg/ml) in a UniVessel® Glass 5 L (260 mm diameter and 690 mm

Symbol code		Units	Experimental values	
			Low level (– 1)	High level (+ 1)
Induction temperature	X1	°C	25	37
Cell density pre-induction ($OD_{600\,nm}$)	X2	–	0.4	0.6
Post induction time	X3	Hours (h)	3	5
Yeast extract	X4	%	0.5	1.5
Tryptone	X5	%	1	2
IPTG	X6	mM	0.5	2.5

Table 1. Experimental variables and levels used in the Plackett Burman Design for optimal recombinant XT6 xylanase production.

Variables	Symbol code	Experimental values		
		Lower (– 1)	Zero (0)	Higher (+ 1)
Cell density pre-induction ($OD_{600\,nm}$)	X2	0.4	0.5	0.6
Post-induction time (h)	X3	3	4	5
[IPTG] (mM)	X6	0.5	1.5	2.5

Table 2. Experimental codes and levels of independent variables in the RSM for optimal recombinant XT6 xylanase production.

height). The fermenter was sterilized at 121 °C for 15 min. Optimal conditions from the lab-scale production were used to set up fermentation in the bioreactor. A BioStat®B twin control tower with MFCS was used to monitor all the relevant parameters and data. The pH and Dissolved Oxygen (DO) probes were first calibrated according to the standard procedure given by the manufacturer. Fermentation was carried out at 30 °C, 200 rpm with one impeller (Rushton blade disc impeller). Three different aeration rates: 0.5, 1, and 2 volume of air per volume of liquid per min (vvm) were tested. Growth was monitored every 30 min and after 2 h, cells reached the expected $OD_{600\,nm}$ (0.5), and IPTG was added to the fermentation. After 4 h of fermentation, the content of the bioreactor was harvested, and down streaming was carried out with the separation of the pellet and supernatant using the centrifuge (Beckman Coulter™, Avanti® J-26XPI, USA) at 4 °C, 16 873×*g* for 10 min.

Specific growth rate

The specific growth rate is the most important parameter to be determined during fermentation, as it represents the dynamic behavior of microorganisms. The specific growth rate period is defined as the rate of increase of biomass of a cell population per unit of biomass concentration. This can be determined by obtaining the gradient of the growth curve shown in Fig. 8B[34], Eq. (3).

$$\text{Specific growth rate}(\mu) = \frac{\text{ODx} - \text{ODy}}{\text{Tx} - \text{Ty}} \tag{3}$$

Productivity

Productivity is defined as the final product concentration divided by the time from inoculation to batch delivery. This is determined by the final biomass concentration subtracted from the inoculum concentration divided by the cultivation time (h), Eq. (4).

$$P_o = (X_F - X_O)/t_c \tag{4}$$

where X_F is the final biomass concentration (g/l), X_o is the inoculum (g/l), and t_c is the cultivation time (h).

Biomass yield coefficient

The biomass yield coefficient could be defined as the mass of microorganisms produced per mass of a substrate utilized, known as the growth yield coefficient[35], Eq. (5).

$$\text{Yield coefficient} = \frac{\text{Biomass produced}}{\text{Substrate utilized}} \tag{5}$$

Purification of recombinant XT6 xylanase

Purification was conducted using affinity chromatography. A column was packed with the appropriate amount of HisPur cobalt resin, and gravity flow allowed the storage buffer to drain from the resin. Two resin bed volumes of the equilibration/wash buffer (50 mM NaH_2PO_4, 300 mM NaCl, 0.03% (w/v) sodium azide, 10 mM imidazole, and 50 mM Na_2HPO_4, pH 8.0) were added. The buffer was allowed to drain from the resin at a flow rate of 0.5–1 ml/min. Two resin bed volumes of the prepared protein extract (supernatant) were loaded directly into the column containing the HisPur cobalt resin (SIGMA, USA). The flow-through was collected and reapplied to maximize the yield. The supernatant was decanted and kept as the flow-through fraction (FT-unbound protein sample). The resin was washed with two resin-bed volumes of equilibration/wash buffer to remove all non-specifically bound proteins on the resin. This was repeated until the absorbance of the flow-through fraction, at 280 nm, reached baseline. The flow-through was collected each time in a new collection tube and labeled as the "wash" fractions (W1–W3). Two-resin bed volumes of elution buffer (50 mM NaH_2PO_4, 300 mM NaCl, 0.03% (w/v) sodium azide, 250 mM imidazole, and 50 mM Na_2HPO_4, pH 8.0, SIGMA, USA) were added to the resin and repeated three times (E1–E3), to elute His-tagged proteins and any remaining protein. A final wash step (W4) was conducted to remove residual imidazole using the wash buffer from the column. The three elution fractions were pooled together and concentrated using 30 kDa Amicon filters by centrifugation (4000×*g* at 4 °C for 20 min) (Eppendorf centrifuge 5418, Germany). The concentrate was then constituted in a final glycerol concentration of 20% (v/v) for XT6 stabilization during storage at -20°C. To store the cobalt column appropriately for regeneration, it was washed with ten resin-bed volumes of 20 mM 2-(N-morpholino)ethanesulfonic acid (MES) buffer (SIGMA, South Africa), 0.05 M NaCl, pH 5.0, followed by ten resin-bed volumes of ultrapure water and stored in 30% ethanol at 4 °C.

Results and discussion

Expression of the recombinant XT6 xylanase

Induction and expression of the recombinant XT6 xylanase were performed by growing the cells until the $OD_{600\,nm}$ was between 0.4 and 0.6, then adding 1 mM IPTG, followed by hourly sampling (1 to 4 h). The insoluble fractions were analyzed using 12% SDS-PAGE and illustrated in Fig. 1, with the uninduced cell lysate serving as a control. More highly contrasted bands of 43 kDa were observed in the cell lysate of samples after induction, while less contrasted bands were observed for the control (uninduced), indicating successful expression of the cloned XT6 gene. Gomez Garcia et al. reported a similar molecular weight (45 kDa) for a xylanase from *Geobacillus* sp. DUSELR13[6].

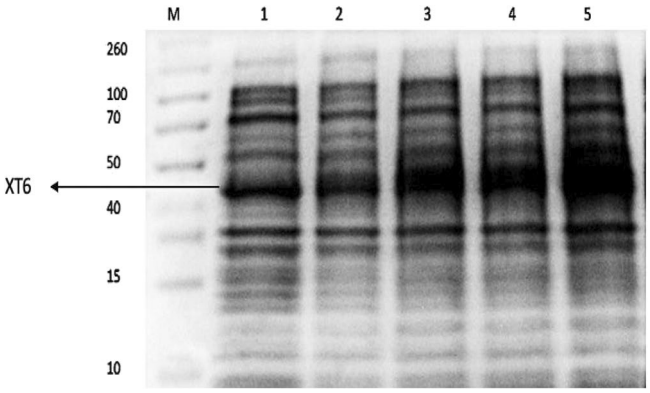

Figure 1. 12% SDS-PAGE gel showing expression of the recombinant *G. stearothermophilus* xylanase (XT6) in *E. coli* BL21 (DE3) cells. Lane M: Molecular weight marker (Thermo Scientific, USA), Lane 1: uninduced sample, and Lanes 2–5: Induction samples at 1–4 h, respectively. (Original image shown in supplementary Fig. 1).

Optimization of cell lysis

A series of experiments were performed to determine the most efficient method for lysing the recombinant *E. coli* cells. The SDS-PAGE gel in Fig. 2 showed that sonication with a 0.05 M sodium phosphate (pH 6.0) buffer resulted in the highest protein concentrations compared to the other lysis procedures. Figure 3 shows the various direct and indirect analysis methods to monitor cell lysis. Sonication with 0.05 M sodium phosphate buffer (pH 6.0) was effective as higher enzyme activity was obtained after cell lysis (16.48 U/ml) compared to the other techniques (9.40, 9.36, 9.03, and 9.53 U/ml) ($p < 0.05$). There was a significant difference ($p < 0.05$) between the "Before" and "After" cell lysis fractions for each analysis and method of lysis.

Sonication has been shown to be an effective method for lysing bacterial cell walls[21]. Sonication, using a probe to generate sound energy, usually within a range of 20–50 kHz, can disrupt the structure of cells through the formation of violent implosions of small bubbles and cavitation within the sample. The energy of the sonic waves can disrupt the intramolecular forces that provide the integrity for the cellular wall[21]. Tris-HCl has an effective pH range of 7.0 to 9.0 and can be used to extract soluble cytoplasmic proteins. However, the preferred pH of the enzyme in this study is pH 6.0; thus, this may be a reason for the low enzyme activity. The components of cell disruption buffers are critical for efficient disruption and will affect subsequent purification steps, including targeting the stability and recovery of the protein. Criteria such as pH, ionic strength, additives to prevent degradation and improve stability, and the buffer-to-cell weight ratio, are required to achieve efficient cell disruption. The pH selected for the lysis buffer should be one pH unit below or above the protein isoelectric point, as this will maintain a positive or negative charge on the protein and prevent isoelectric precipitation[36]. The ionic strength inside the cytoplasm of a typical cell is 0.15–0.2 M, with high concentrations of charged biomolecules available for ionic protein interaction. The lysis buffer should contain at least 0.05–0.1 M NaCl; if the ionic strength of the

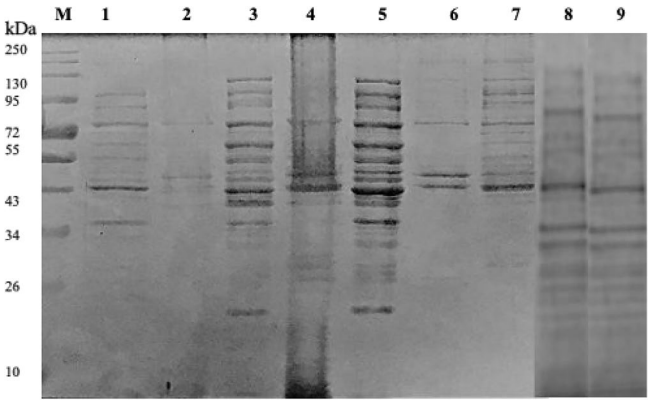

Figure 2. 12% SDS-PAGE gel showing the recombinant XT6 expressed in *E. coli* BL21 (DE3) cells after various lysis techniques. Lane M: Molecular weight marker (Thermo Scientific, USA), Lane 1: uninduced sample, Lanes 2 and 3: insoluble and soluble fractions after lysis with lysozyme + 1% TritonX-100, Lanes 4 and 5: insoluble and soluble fractions following sonication in 0.05 M sodium phosphate (pH 6.0) buffer, Lane 6: insoluble fraction sonicated in 0.05 M Tris–HCl and 8 M urea, Lane 7: soluble fraction sonicated in Tris–HCl buffer, and Lanes 8 and 9: insoluble and soluble fraction treated with lysozyme. (Original image shown in supplementary Fig. 2).

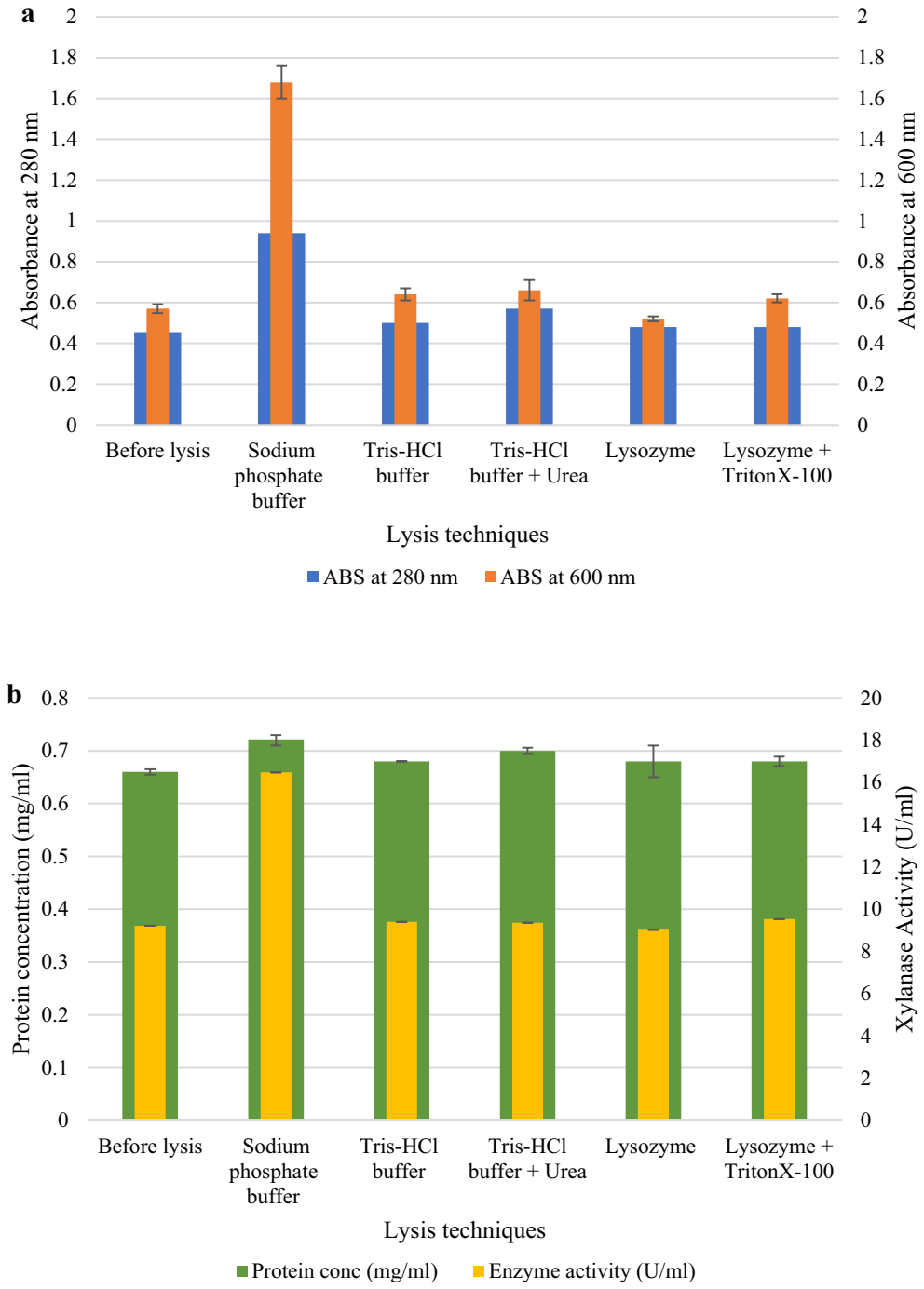

Figure 3. Analysis of the lysis methods to assess the efficiency of lysis of recombinant *E. coli* cells expressing the XT6 xylanase representing (**a**) $OD_{280\ nm}$ and $OD_{600\ nm}$, and (**b**) protein concentration, and xylanase activity after different lysis techniques.

lysis buffer is increased, it will reduce the ionic interactions[36]. The isoelectric point of XT6 is 9, and therefore at lower pH values, the enzyme will have a positive net charge[22,37]. However, the cell lysis was most effective with 0.05 M sodium phosphate buffer at pH 6.0 compared to Tris-HCl (+/− 8 M urea) at pH 8.0.

The synergistic effect of lysozyme and TritonX-100 has previously been shown to increase the amount of cellular lysis substantially; however, in this study, it was not observed[23]. Lysozymes break down the polysaccharide chains of peptidoglycan, which surround the inner membrane of *E. coli* cells[18]. Gram-positive bacteria can be directly exposed to lysozyme; however, the outer membrane of the Gram-negative bacteria needs to be removed before exposing the peptidoglycan layer to the enzyme. TritonX-100 is a non-ionic detergent that can solubilize the outer and inner membranes of *E. coli* cells[38]. The cost of purchasing lysozymes may be a deterrent

to enzymatic lysis, as this additional cost may make the operating costs unfeasible. Thus, sonication of cells resuspended in 0.05 M sodium phosphate buffer (pH 6.0) is recommended for cells lysis in future studies.

Statistical optimization of recombinant XT6 xylanase production in batch fermentation

Screening of significant medium constituents for recombinant XT6 xylanase production

Each row in Table 3 represents one of twelve experiments, and each column has a different variable tested at high (+) and low (−) levels. The data obtained from the PBD runs indicate a wide variation in xylanase activity from 13.97 to 40.06 U/ml across the twelve runs. ANOVA demonstrated that this variation due to the effect of the medium and culture conditions on xylanase production was significant ($p < 0.05$). The R^2, or coefficient of determination, is the proportion of variation in the response attributed to the model rather than to random error[39]. A previous study suggested for a good fit of a model[40], R^2 should be at least 90%. The determination coefficient (R^2) implies that the sample variation of 94% for xylanase production was attributed to the independent variables, and only about 7% of the total variation could not be explained by the model. The closer R (correlation coefficient) value is to 1, the better the correlation between the experimental and predicted values. Here, the R value (0.94) shown in Table 4 indicated a close agreement between the experimental results and the theoretical values predicted by the model equation.

The p value served as a tool for checking the significance of each of the coefficients, as is shown in Table 4, and indicates that cell density pre- induction ($OD_{600\ nm}$) (X_2), post-induction time (X_3), and IPTG concentration (X_6) had a significant effect ($p < 0.05$) on xylanase production. The Pareto chart of standardization illustrated in Fig. 4 confirmed that these three factors significantly influenced xylanase production ($p < 0.05$) as the factors crossed the p-line. However, the other independent factors ($p > 0.05$) were considered insignificant. It has been previously demonstrated in a previous study that the four most relevant variables influencing recombinant protein expression are cell density pre- induction ($OD_{600\ nm}$), IPTG concentration, post-induction temperature, and duration of induction[20].

There was a 94% chance that the model explained the measured variations in response. The magnitude and direction of the factor coefficient in the equation clarified the influence of the six variables for xylanase production. The higher magnitude indicated a large effect on the response. The corresponding response of xylanase

Variable level							Enzyme activity (U/ml)	
Run no	X1	X2	X3	X4	X5	X6	Observed	Predicted
1	25 (−)	0.4 (−)	3 (−)	1.5 (+)	1 (−)	2.5 (+)	25.88	14.61
2	37 (+)	0.6 (+)	3 (−)	0.5 (−)	1 (−)	2.5 (+)	18.81	11.58
3	37 (+)	0.4 (−)	3 (−)	0.5 (−)	2 (+)	0.5 (−)	28.30	15.41
4	25 (−)	0.6 (+)	3 (−)	1.5 (+)	2 (+)	0.5 (−)	17.82	10.32
5	25 (−)	0.6 (+)	5 (+)	1.5 (+)	1 (−)	0.5 (−)	23.65	12.73
6	37 (+)	0.6 (+)	5 (+)	0.5 (−)	1 (−)	0.5 (−)	20.73	13.56
7	37 (+)	0.4 (−)	5 (+)	1.5 (+)	2 (+)	0.5 (−)	31.36	18.19
8	25 (−)	0.4 (−)	5 (+)	0.5 (−)	2 (+)	2.5 (+)	13.97	8.06
9	25 (−)	0.4 (−)	3 (−)	0.5 (−)	1 (−)	0.5 (−)	40.06	32.70
10	37 (+)	0.6 (+)	3 (−)	1.5 (+)	2 (+)	2.5 (+)	21.35	12.22
11	25 (−)	0.6 (+)	5 (+)	0.5 (−)	2 (+)	2.5 (+)	16.83	8.89
12	37 (+)	0.4 (−)	5 (+)	1.5 (+)	1 (−)	2.5 (+)	27.07	16.47

Table 3. PBD matrix for screening of six medium components. X1: Induction temperature. X2: Cell density pre- induction ($OD_{600\ nm}$). X3: Post-induction time. X4: Yeast extract. X5: Tryptone. X6: IPTG.

	df	Sum of squares	Mean square	F-value	*p*-value
Model	6				
Induction temperature	1	70.71	70.71	3.44	0.1126
Cell density pre- induction ($OD_{600\ nm}$)	1	149.46	149.46	7.82	0.0429*
Post Induction time	1	300.63	300.63	14.65	0.0123*
[Yeast extract]	1	19.89	19.89	0.96	0.3701
[Tryptone]	1	26.08	26.08	1.27	0.3108
[IPTG]	1	136.74	136.74	6.66	0.0494*
Residuals	5	102.62	102.62		

Table 4. Analysis of variance (ANOVA) for six variables by PBD. df: degree of freedom. *Significant p value at $p < 0.05$. R^2(mean coefficient of determination) = 0.9419.

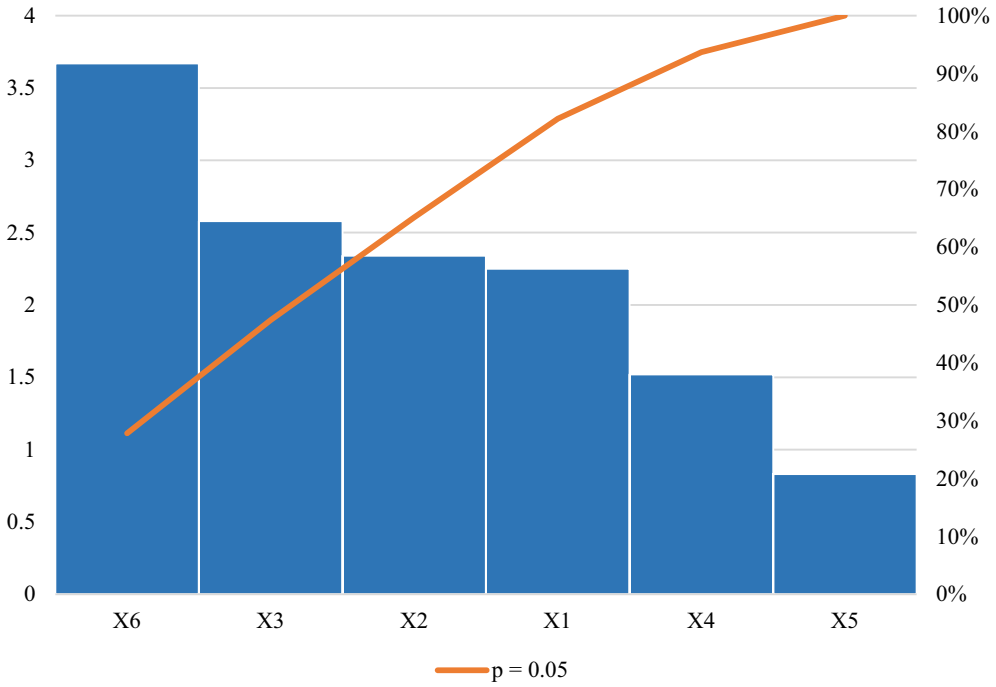

Figure 4. Pareto chart of standardized effects for the production of the recombinant xylanase by *E. coli* BL21. Induction temperature (X1), Cell density pre-induction ($OD_{600\ nm}$) (X2), post-induction time (X3), yeast extract concentration (X4), tryptone concentration (X5), IPTG concentration (X6).

production was expressed in terms of the following regression Eq. (6) derived from the Unstandardized Beta values shown in Table 5:

$$\begin{aligned} Y &= X_1 + X_2 + X_3 + X_4 + X_5 + X_6 \\ Y &= 48.49 - 0.28X_1 - 33.37X_2 - 3.74X_3 - 4.93X_4 - 2.35X_5 - 0.98X_6 \end{aligned} \quad (6)$$

Optimization of significant variables using RSM for recombinant XT6 xylanase production

BBD. A total of 16 runs were performed to determine the conditions for optimal xylanase production. A matrix was run with the three significant variables as per PBD. The results for the BBD matrix runs in Table 6 showed that run 13 resulted in the highest xylanase activity of 144.02 U/ml under the following conditions: Cell density pre-induction ($OD_{600\ nm}$) 0.5, post-induction time of 4 h, and 1.5 mM IPTG, while the lowest activity of 10.18 U/ml was obtained under conditions (cell density pre-induction ($OD_{600\ nm}$) of 0.5, post-induction time of 3 h and 0.5 mM IPTG) in run 9. This was markedly higher ($p > 0.05$) compared to the highest enzyme activities obtained during OFAT (16.48 U/ml). Farliahati et al.[41] confirmed a similar influence of optimized parameters on the enhanced xylanase production by recombinant *E. coli* DH5α (1.526–2.655 U/ml).

For the regression analysis of the experimental data, a quadratic equation was generated for the BBD for optimal xylanase production, as shown in Eq. (7):

$$Y = \beta 0 + X_2 + X_3 + X_5 + X_{22} + X_{32} + X_{52} + X_2X_3 + X_2X_5 + X_3X_5 \quad (7)$$

Unstandardized beta	Coefficient std. error		Standardized coefficient beta	t-value
Model	48.49	9.57		5.66
Induction temperature (X1)	0.28	0.13	0.36	2.25
$OD_{600\ nm}$ (X2)	− 33.37	14.25	− 0.40	− 2.34
Post-induction time (X3)	− 3.74	1.45	0.46	− 2.58
[Yeast extract] (X4)	− 4.93	3.24	− 0.28	− 1.52
[Tryptone] (X5)	− 2.35	2.84	− 0.14	− 0.83
[IPTG] (X6)	− 0.98	0.27	− 0.60	− 3.67

Table 5. Effect estimates for xylanase production from the results of PBD.

Run no	Experimental value (Coded value)			Enzyme activity (U/ml)	
	X2	X3	X6	Observed	Predicted
1	0.4 (−)	3 (−)	1.5 (0)	44.72	47.24
2	0.6 (+)	3 (−)	1.5 (0)	10.96	10.45
3	0.4 (−)	5 (+)	1.5 (0)	11.65	10.09
4	0.6 (+)	5 (+)	1.5 (0)	31.42	28.51
5	0.4 (−)	4 (0)	0.5 (−)	13.42	12.55
6	0.6 (+)	4 (0)	0.5 (−)	51.37	50.02
7	0.4 (−)	4 (0)	2.5 (+)	71.59	64.28
8	0.6 (+)	4 (0)	2.5 (+)	26.23	27.68
9	0.5 (0)	3 (−)	0.5 (−)	10.18	9.85
10	0.5 (0)	5 (+)	0.5 (−)	16.24	14.45
11	0.5 (0)	3 (−)	2.5 (+)	101.37	118.01
12	0.5 (0)	5 (+)	2.5 (+)	86.27	86.11
13	0.5 (0)	4 (0)	1.5 (0)	144.02	151.50
14	0.5 (0)	4 (0)	1.5 (0)	127.84	127.47
15	0.5 (0)	4 (0)	1.5 (0)	131.77	126.93
16	0.5 (0)	4 (0)	1.5 (0)	120.72	124.70

Table 6. Experimental design obtained for the BBD model for three independent variables tested and predicted responses for recombinant xylanase production by *E. coli* BL21. X2: Cell density pre- induction ($OD_{600\ nm}$). X3: post-induction time. X6: IPTG concentration.

The predicted values were determined using the regression equation (Table 6). The R^2 or coefficient of determination (0.9357, close to 1) confirmed the model's validity, i.e., that the model can express 93.57% of the variability of the response. The coefficient of adjusted determination, adjusted R^2, was 0.9383, confirming that the actual values were close to the predicted values[42,43]. The correlation was established by plotting the actual value curve as a function of the predicted values (Fig. 5), which shows the points distributed around the regression line.

Figure 5 shows that the actual response values agreed well with the predicted response values. Thus the predicted xylanase production was within the limits of the experimental factors. Therefore, the model was considered of sufficient quality[42] with a 93.57% chance that it explained the measured variations in response. Maximum xylanase production (144.02 U/ml) by the recombinant XT6 xylanase occurred in BBD run 13 under optimal conditions (Cell density pre- induction ($OD_{600\ nm}$) 0.5, 4 h post-induction time, and 1.5 mM IPTG concentration).

Second-order regression and prediction. The second-order regression equation provides the xylanase activity produced by XT6 from *G. stearothermophilus* as a function of cell density pre- induction ($OD_{600\ nm}$) (X_2), post-induction time (X_3), and IPTG concentration (X_6) which is presented in Eq. (8):

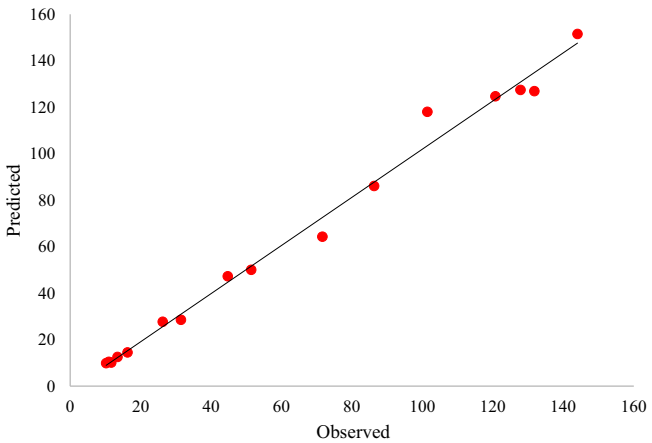

Figure 5. Graphical representation of the minimal difference between the actual (straight line) and predicted responses (circles) for the RSM for optimal recombinant xylanase activity.

$$Y = 50.26 - 26.75X_2 - 2.71X_3 + X_6 + X_2^2 + X_3^2 + X_6^2 + X_2X_3 + X_2X_6 + X_3X_6 \quad (8)$$

where Y is the peak area, X_2 is the $OD_{600\,nm}$, X_3 is the post-induction time, and X_6 is the IPTG concentration. The statistically insignificant parameters ($p > 0.05$) and the interactions were omitted from the equation. The model constants and coefficients were generated using the unstandardized beta values.

ANOVA and Pareto chart. The "Lack of fit p-value" represented in Table 7, was insignificant as the p value was greater than 0.05; in accordance with literature (> 0.05)[44] and also that significant regression and a non-significant lack of fit of the model were well-fitted to the experiments[44]. The regression equation was validated on this basis[45] and ANOVA performed to determine the p values. As evident in Table 7. This showed the model, the linear and square terms for X_2 (Cell density pre-induction ($OD_{600\,nm}$)), X_3 (post-induction time), and X_6 (IPTG concentration) to be significant as p values were 0.0018261, 0.0164311, 0.0138398, 0.0009394, 0.0032260 and 0.0207146, respectively. The Pareto chart of standardization histogram graph (Fig. 6) also showed that terms were significant ($p < 0.05$), as the factors crossed the p-line (cumulative % = 50%).

Interaction of variables. The interaction effects of the variables on xylanase production were also studied by plotting response surface plots and 3D-contour plots against any two independent variables while having another

Variable	Estimates	Std. Error	t value	*p* value
Model	− 2109.82	364.36	− 5.79	0.0011614*
X2 ($OD_{600\,nm}$)	5713.49	1077.59	5.30	0.0018261*
X3 (Post-induction time)	312.47	94.72	3.30	0.0164311*
X6 [IPTG]	241.99	70.27	3.44	0.0137398*
X2:X3	133.83	98.88	1.35	0.2247133
X3:X6	− 208.28	98.88	− 2.11	0.0797899
X2:X6	− 5.29	9.89	− 0.54	0.6119137
$X2^2$	− 5963.13	988.86	− 6.03	0.0009394*
$X3^2$	− 46.77	9.89	− 4.73	0.0032260*
$X6^2$	− 30.80	9.89	− 3.12	0.0207146*

Table 7. ANOVA for the response surface methodology parameters for the recombinant xylanase. *Significant p value at $p < 0.05$. Adjusted $R^2 = 0.9357$. Lack of fit p value = 0.0694.

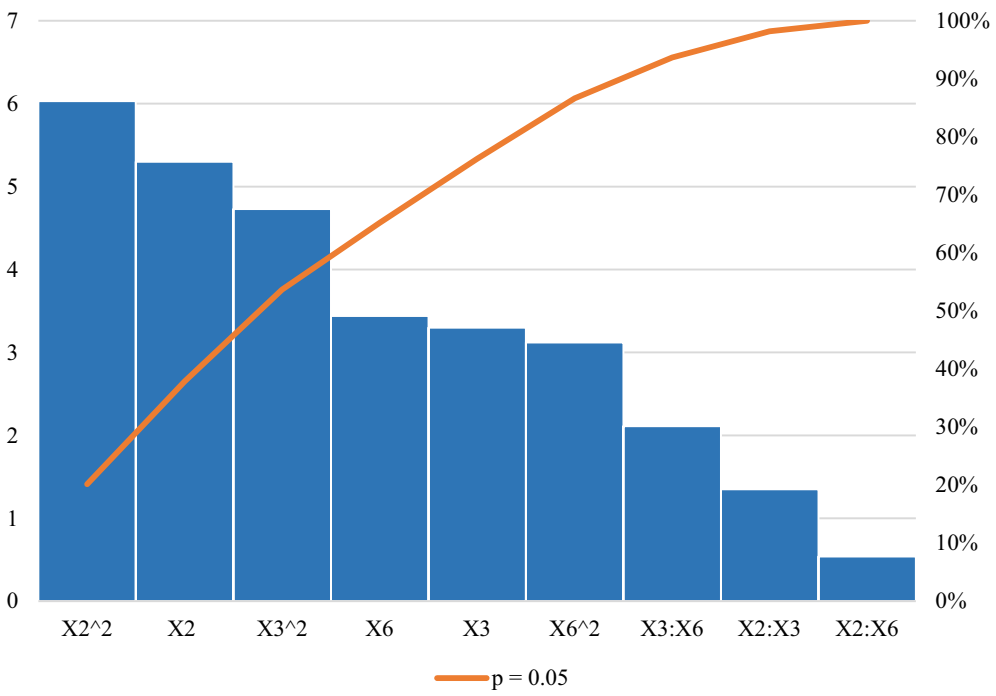

Figure 6. Pareto chart of standardized effects for the nine interactive factors affecting the optimization of xylanase production. Interactions, linear and square terms for cell density (X2), post-induction time (X3), and IPTG concentration (X6).

variable at its central level. These plots were drawn to illustrate the combined effect of each independent variable on the response variable and is shown in Fig. 7. The Z-axis refers to the xylanase activity versus any two variables.

Effect of cell density pre- induction ($OD_{600\ nm}$) and post-induction time The overexpression of the recombinant XT6 xylanase was influenced by the post-induction time and pre-induction cell density ($OD_{600\ nm}$)[20,46]. The interactive effect of cell density pre-induction ($OD_{600\ nm}$) (X_2) and post-induction time (X_3) was examined, and the results are illustrated in Figs. 7a,b. For this analysis, the other parameter was kept constant at a zero levels. The mutual interaction of both factors (X_2X_3) was not significant ($p > 0.05$), indicating that there is no synergistic interaction favoring the expression of recombinant XT6. The highly elliptical response surface plot Fig. 7a shows the highest activity (110 U/ml) of the recombinant XT6 when both variables, cell density pre-induction ($OD_{600\ nm}$) (X_2) and post-induction time (X_3), were close to the central values, cell density pre- induction ($OD_{600\ nm}$) of 0.5 and 4 h, respectively. The findings accentuated that post-induction time was a key factor influencing the expression of XT6 xylanase. In the present study, the post-induction time of 4 h optimally induced production of active recombinant XT6 presumably because this duration was suitable for the correct folding and accumulation of the of recombinant XT6 in *E. coli*. This finding is in accordance with previous reports[20,47,48].

Effect of post-induction time and IPTG concentration Considering that IPTG is costly and is potentially toxic to cells, it is essential to determine the optimum concentration for induction[49]. The interactive effect of post-induction time (X_3) and IPTG concentration (X_6) was examined, and the results are illustrated by both surface and contour plots as illustrated in Fig. 7c,d. The mutual interaction of both factors (X_2X_3) was not significant ($p > 0.05$), indicating that there is no synergistic interaction favoring the expression of recombinant XT6 xylanase. The expression of the recombinant XT6 increased with time up to 4 h and IPTG concentration up to its midpoint (1.5 mM), reaching the highest xylanase activity of 100 U/ml.

Effect of pre-induction cell density ($OD_{600\ nm}$) and IPTG concentration The dependency of the recombinant XT6 xylanase production on IPTG concentration (mM) and cell density pre-induction is presented in Fig. 7e,f. The interaction between these two parameters was insignificant based on the high *p* value (0.6119) represented in Table 6. At the zero levels (optimal levels) of cell density ($OD_{600\ nm}$) and IPTG concentration, the production of recombinant XT6 xylanase will improve as depicted by Fig. 7e. Figure 7f illustrated that with a higher IPTG concentration; the xylanase activity was the highest (110 U/ml) demonstrating that the induction of recombinant XT6 in the middle log phase leads to higher protein expression levels. In this phase, most recombinant bacteria are growing rapidly, and cells are in an ideal environment for the expression of recombinant proteins. A previous study by Batumalaie et al.[20], also reported that induction at the mid-log phase led to overexpression of lipase KV1 in *E. coli*.

Scaled-up production of the recombinant XT6 xylanase

Similar or higher enzyme activities are expected when scaling up the production of enzymes from shake flasks to bioreactors[50]. This was observed for the 5-l stirred tank bioreactor run using the same production parameters. The bioreactor maintains a more consistent and homogenous environment with more efficient aeration rates, pH, better mixing, and heat transfer[51]. Table 8 compares xylanase production in shake flask and a stirred tank bioreactor (at different aeration rates). In stirred tank bioreactors, agitation and aeration are essential operational parameters in scaling up aerobic biosynthesis systems and industrial bioprocess development[52]. In aerobic fermentation, the presence of oxygen influences enzyme secretion, which may be attributed to increased metabolic activities of the organism[53] as has been reported that amylase production by *Bacillus* spp. is strongly affected by the presence of dissolved oxygen.

Consequently, providing air to the fermentation medium using a compressor under sterile conditions is more efficient by combining agitation with aeration[54]. Higher aeration rates implies improved oxygen supply in the fermenter thus enhanced growth of bacteria and enzyme production. Higher xylanase activities were obtained in the 5-l bioreactor at all the oxygen transfer rates tested [(146.32 U/ml (0.5 vvm), 165.18 U/ml (1 vvm) and 159.44 U/ml (2 vvm)], compared to shake flask studies (145.83 U/ml) under the same production parameters (30 °C, cell density pre- induction ($OD_{600\ nm}$) 0.5, 4 h post-induction time, 1% yeast extract, 1.5% tryptone, and 1.5 mM IPTG). Overall, at 1 vvm aeration, the xylanase activity was observed to be the highest (165.18 U/ml). A similar study reported optimal xylanase activity from *Bacillus amyloliquifaciens* at 1 vvm (56.80 U/ml) in a stirred tank bioreactor[48]. Another study showed aeration rates to be a significant factor for high enzyme yields in a stirred tank bioreactor[55].

Effect of aeration rates on pH, dissolved oxygen, biomass, and xylanase activity

Figure 8 shows the fermentation kinetics at 200 rpm and the different aeration rates (0.5, 1, and 2 vvm). Increasing the aeration rate increased biomass, and xylanase production rates and decreased dissolved oxygen. There was more of a change in the fermentation media pH during the growth phase as aeration rates increased. After 6 h, the pH changed from an initial value of 7.00 to 6.42, 6.38 and 6.62 with aeration rates of 0.5, 1, and 2 vvm (Fig. 8a-c), respectively. This can be attributed to higher growth and metabolism rates at the higher aeration rates[56,57]. DO% at 2 h was 63.4, 71.3, and 78.65% at 0.5, 1, and 2 vvm, respectively, and then decreased after 4 h (at 6 h on graph) of expression to 1.1, 0.6 and 2.3% at 0.5, 1, and 2 vvm, respectively shown in Figs. 8a–c. However, as mentioned earlier this had no effect on xylanase activity in the bioreactor. Given the low solubility of oxygen in aqueous solutions[58], DO in the broth can be limiting, so it is an important influencing factor in aerobic microbial fermentations and can be manipulated up to a point by agitation and aeration rates. The drop

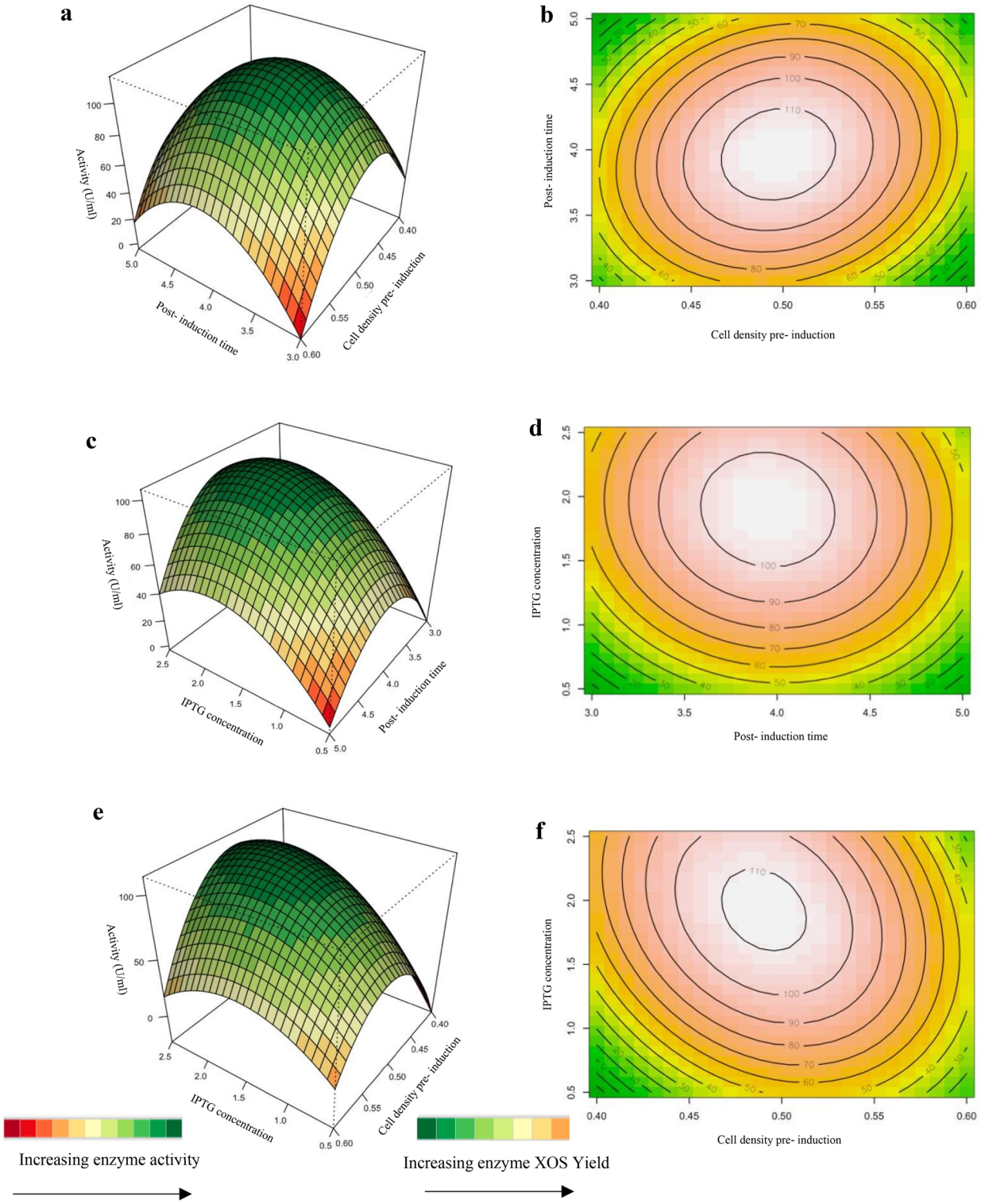

Figure 7. Response surface plots (**a**, **c**, **e**) and contour plots (**b**, **d**, **f**) of the combined effects of; (**a**) and **b**) Cell density pre-induction ($OD_{600\,nm}$) (X2) and post-induction time (X3), (**c**) and (**d**): Post-induction time (X3) and IPTG concentration (X6) and (**e**) and (**f**): Cell density pre- induction ($OD_{600\,nm}$) (X2) and IPTG concentration (X6) on recombinant xylanase production.

in DO levels is due to the active growth phase of the culture when it rapidly consumes oxygen, thus decreasing the oxygen levels in the reactor. While the shake flask culture system allowed oxygen transfer, it was expected to be lower than the 1 vvm achieved in the bioreactor.

Samples	Protein concentration activity (mg/ml)	Enzyme activity (U/ml)	Specific activity (U/mg)
Expression in shake flasks	3.01	145.13	48.22
Expression in a 5-l bioreactor (0.5 vvm)	1.57	146.32	93.20
Expression in a 5-l bioreactor (1 vvm)	0.50	165.18	330.36
Expression in a 5-l bioreactor (2 vvm)	1.14	159.44	139.86

Table 8. Analysis of protein concentration, enzyme activity and specific activity of XT6 produced in batch shake flask and in bioreactor fermentations at different aerations rates.

Effect of aeration rate on specific growth rate, productivity and yield coefficient

Table 9 demonstrates that an increase in the aeration rate resulted in improvements in the specific growth rate, biomass productivity, and yield coefficient. Higher aeration increases the oxygen available to cells, which promotes respiration and the efficient use of the oxidative phosphorylation pathway for energy generation and growth which naturally manifests in a higher growth rate and more significant biomass formation. A change in the aeration rate from 0.5 to 2 vvm resulted in a 1.44-fold increase in the specific growth rate. A similar trend was also observed with the productivity and yield coefficient; however, at 2 vvm, the productivity and yield coefficient decreased. This indicates that the optimum aeration rate for xylanase production in the stirred tank bioreactor is 1 vvm. Similar findings were obtained by Ronda et al.[59]. The highest aeration rate at 2 vvm most likely increased the shear stress on the bacterium, leading to lower biomass productivity and yield coefficient.

Purification of recombinant XT6 xylanase

The T-7-based pET vector for the *E. coli* expression system was selected for the production of the recombinant XT6 xylanase, as this expression system has been reported to be fast-growing and produces a high yield of the target protein[20]. This vector is recognized for its expression efficiency and, most importantly, for facilitating purification due to the presence of the His6- tag sequence. The recombinant XT6 xylanase was then purified to homogeneity by HisPur cobalt resin affinity chromatography. SDS-PAGE in Fig. 9 showed that the expressed protein band was 43 kDa in size.

These findings were consistent with a previous study[60] that optimized recombinant protein expression and purification. The His6-tag sequence aids in the selective binding of the expressed protein to the cobalt beads without impact on protein structure[61]. Therefore, the results from the present study are in accordance with the well-established concept that *E. coli* BL21 (DE3)/pET28a is an excellent expression host/system[15,25,62]. The specific activity of the purified recombinant XT6 xylanase was 4388.55 U/mg (Table 10), 28.97-fold higher than that of the crude lysate (151.50 U/mg) with a 67.04% recovery of the enzyme.

The higher purification fold (28.97) compared to the recombinant crude lysate shows that the recombinant tagged protein remained in its active conformation[24]. The commercial endo-1,4-β-xylanase (*Bacillus stearothermophilus* T6) has a specific activity of 12–65 U/mg on wheat arabinoxylan, according to Megazyme (CAS number: 9025-57-4). This study yielded a xylanase with a 67.5 to 365-fold higher specific activity (4388.55 U/mg) albeit on beechwood xylan.

Conclusions

Multiple lysis techniques were tested in this study to release the intracellular protein, including sonication and synergistic lysis with lysozyme and TritonX-100. Based on our analysis, a mechanical technique; sonication of cells resuspended in 0.05 M sodium phosphate (pH 6.0) buffer was recommended for further studies as in resulted in 3.21 fold increase compared to the other lysis techniques. In this study, optimization of the expression of the recombinant XT6 xylanase using PBD and RSM was successfully carried out as these statistical designs showed that under the optimized induction conditions of an induction temperature of 30 °C, cell density pre- induction ($OD_{600\ nm}$) at 0.5, post-induction time of 4 h, yeast extract concentration of 1% (w/v), tryptone concentration of 1.5% (w/v), and IPTG concentration of 1.5 mM, the enzyme activity increased from 16.48 U/ml to 144.02 U/ml. The large-scale production of xylanase was successful at 1 vvm aeration and improved the production of the recombinant XT6 xylanase. Compared to commercial XT6 xylanase from megazyme, the specific activity obtained from the scaled-up production is 5.23 fold higher.. Future applications involving this enzyme will include testing on animal feed substrates for the production of xylooligosaccharides, which are used as prebiotics in the feed industry, to reduce the feed viscosity and improve the gut microbiota.

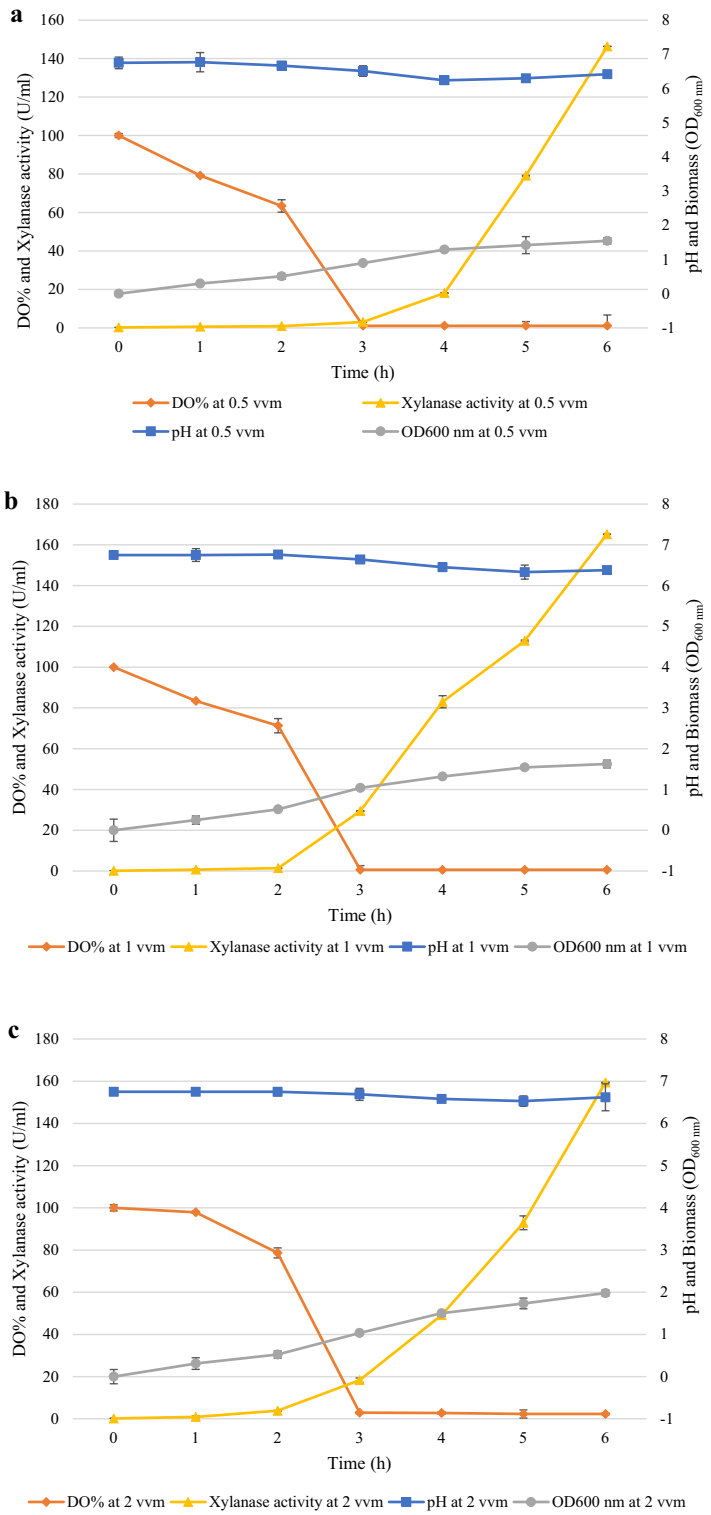

Figure 8. Analysis of pH, dissolved oxygen (DO%), biomass, and xylanase activity at 0.5 vvm (**a**), 1vvm (**b**), and 2 vvm (**c**) aeration rates, during batch fermentation in a stirred tank bioreactor at 200 rpm. 0–2 h represents the time before induction.

Aeration rates (vvm)	Specific growth rate (h^{-1})	Productivity ($g/l.h^{-1}$)	Yield coefficient
0.5	0.25	66	2.71
1	0.27	78	2.82
2	0.36	34	1.28

Table 9. Effect of aeration rates on specific growth rate, biomass yield, and productivity.

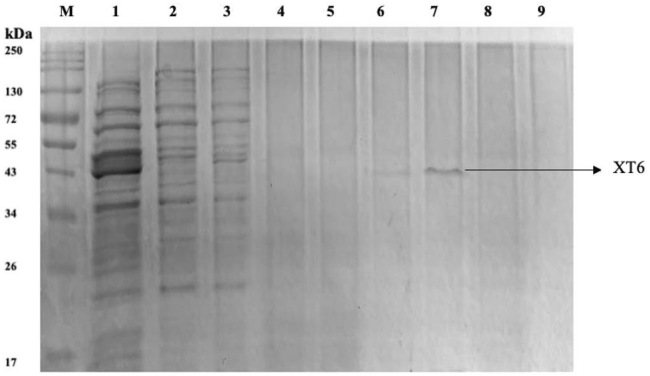

Figure 9. 12% SDS PAGE gel of purification fractions of the heterologously produced *G. stearothermophilus* XT6 after affinity chromatography purification in a cobalt column. Lane M: Molecular weight marker (Thermo Scientific, USA), Lane 1: Crude (induced XT6), Lane 2: Flow-through, Lanes 3–5: Wash 1–3, Lanes 6–8: Eluted fractions 1–3, and Lane 9: Wash 4. (Original image shown in supplementary as Fig. 3).

Purification step	Total protein (mg)	Total activity (U)	Specific activity (U/mg)	Yield (%)	Fold purity
Recombinant crude lysate	9.50	1440.20	151.50	100.0	1.0
Cobalt column	1.35	1038.15	769.00	72.08	5.08
Ultrafiltration	0.22	965.48	4388.55	67.04	28.97

Table 10. Purification of the recombinant XT6 xylanase.

Data availability

The datasets used and/or analysed during the current study are available from the corresponding author upon reasonable request. Other data generated or analysed during this study are included in this article [and its supplementary information file].

Received: 15 August 2023; Accepted: 23 November 2023
Published online: 28 November 2023

References

1. Chen, Z. *et al.* Exploitation of lignocellulosic-based biomass biorefinery: A critical review of renewable bioresource, sustainability and economic views. *Biotechnol Adv.* **69**, 108265 (2023).
2. Marcolongo, L. *et al.* Properties of an alkali-thermo stable xylanase from *Geobacillus thermodenitrificans* A333 and applicability in xylooligosaccharides generation. *World J. Microbiol. Biotechnol.* **31**, 633–648 (2015).
3. Bhalla, A., Bischoff, K. M. & Sani, R. K. Highly thermostable xylanase production from a thermophilic *Geobacillus* sp. strain WSUCF1 utilizing lignocellulosic biomass. *Front. Bioeng. Biotechnol.* **3**, 84 (2015).
4. Linares-Pasten, J. A., Aronsson, A. & Karlsson, E. N. Structural considerations on the use of endo-xylanases for the production of prebiotic xylooligosaccharides from biomass. *Curr. Protein Pept. Sci.* **19**(1), 48–67 (2018).
5. Cunha, L., Martarello, R., Souza, P. & Freitas, M. Optimization of xylanase production from *Aspergillus foetidus* in soybean residue. *Enzyme Res.* **12**, 10–17 (2018).
6. Gómez García, R. *et al.* Production of a xylanase by *Trichoderma harzianum (Hypocrea lixii)* in solid-state fermentation and its recovery by an aqueous two-phase system. *Can. J. Biotechnol.* **2**(9), 108–115 (2018).
7. Bibra, M., Kunreddy, V. R. & Sani, R. K. Thermostable xylanase production by *Geobacillus* sp. strain DUSELR13, and its application in ethanol production with lignocellulosic biomass. *Microorganisms* **6**(3), 93 (2018).
8. Wang, L. *et al.* Identification and characterization of a thermostable GH11 xylanase from *Paenibacillus campinasensis* NTU-11 and the distinct roles of its carbohydrate-binding domain and linker sequence. *Colloid Surf. B Biointerfaces* **209**(1), 112167 (2019).
9. Carlson, C., Singh, N. K., Bibra, M., Sani, R. K. & Venkateswaran, K. Pervasiveness of UVC 254-resistant *Geobacillus* strains in extreme environments. *Appl. Microbiol. Biotechnol.* **102**, 1869–1887 (2018).
10. Gupta, G. K. *et al.* Xylanolytic enzymes in pulp and paper industry: New technologies and perspectives. *Mol. Biotechnol.* **64**, 130–143 (2022).

11. Raita, M., Ibenegbu, C., Champreda, V. & Leak, D. J. Production of ethanol by thermophilic oligosaccharide utilizing *Geobacillus thermoglucosidasius* TM242 using palm kernel cake as a renewable feedstock. *Biomass Bioenergy* **95**, 45–54 (2016).
12. Walia, A. *et al.* Microbial xylanases and their industrial application in pulp and paper biobleaching: A review. *Biotech* **7**, 11 (2013).
13. Zafar, A. *et al.* Cloning, expression, and purification of xylanase gene from *Bacillus licheniformis* for use in saccharification of plant biomass. *Appl. Biochem. Biotechnol.* **178**, 294–311 (2016).
14. Zare, H., Mir Mohammad Sadeghi, H. & Akbari, V. Optimization of fermentation conditions for reteplase expression by *Escherichia coli* using response surface methodology. *AJMB* **11**(2), 162–168 (2019).
15. Choi, T. G. & Geletu, T. T. High-level expression and purification of recombinant flounder growth hormone in *E. coli*. *JGEB* **16**, 347–355 (2018).
16. Tripathi, N. K. & Shrivastava, A. Recent developments in bioprocessing of recombinant proteins: Expression hosts and process development. *Front. Bioeng. Biotechnol.* **7**, 420 (2019).
17. Kleiner-Grote, G., Risse, J. M. & Friehs, K. Secretion of recombinant proteins from *E. coli*. *Eng. Life Sci.* **18**(8), 532–550 (2018).
18. Shehadul Islam, M., Aryasomayajula, M. & Selvaganapathy, P. R. A review on macroscale and microscale cell lysis methods. *Micromachines* **8**(3), 83 (2018).
19. Dehnavi, E., Ranaei Siadat, S. O., Fathi Roudsari, M. & Khajeh, K. Cloning and high-level expression of beta-xylosidase from *Selenomonas ruminantium* in *Pichia pastoris* by optimizing pH, methanol concentration and temperature conditions. *Protein Expr. Purif.* **124**, 55–61 (2016).
20. Batumalaie, K., Khalili, E., Mahat, N. A., Huyop, F. Z. & Wahab, R. A. A statistical approach for optimizing the protocol for over-expressing lipase KV1 in *Escherichia coli*: Purification and characterization. *Biotechnol. Biotechnol. Equip.* **32**(1), 69–87 (2018).
21. Kwon, Y. C. & Jewett, M. High-throughput preparation methods of crude extract for robust cell-free protein synthesis. *Sci. Rep.* **5**, 8663 (2015).
22. Sithole, T. Cloning, expression, partial characterization and application of a recombinant GH10 xylanase, XT6, from *Geobacillus stearothermophilus* T6 as an additive to chicken feeds. (ORCID ID: 0000-00030-2058-5571) Master's thesis, Rhodes University, Grahamstown (EC) (2022).
23. Grigorov, E., Kirov, B., Marinov, M. B. & Galabov, V. Review of microfluidic methods for cellular lysis. *Micromachines* **12**(5), 498 (2021).
24. Newton, J. M., Schofield, D., Vlahopoulou, J. & Zhou, Y. Detecting cell lysis using viscosity monitoring in *E. coli* fermentation to prevent product loss. *Biotechnol. Prog.* **32**(4), 1069–1076 (2016).
25. Lu, Y. *et al.* High-level expression of improved thermostable alkaline xylanase variant in *Pichia pastoris* through codon optimization, multiple gene insertion and high-density fermentation. *Sci. Rep.* **6**, 37869 (2016).
26. Bradford, M. M. A rapid and sensitive method for the quantitation of microgram quantities of protein utilizing the principle of protein-dye binding. *Anal. Biochem.* **72**(12), 248–254 (1976).
27. Miller, G. L. Use of dinitrosalicylic acid reagent for determination of reducing sugar. *Anal. Chem.* **31**, 426–428 (1959).
28. Laemmli, U. K. Cleavage of structural proteins during the assembly of the head of bacteriophage *T4*. *Nature* **227**, 680–685 (1970).
29. Zhang, Z., Xiaoqiong, P. & Wu, Z. D. Novo synthesis and expression of a thermostable xylanase from *Geobacillus stearothermophilus* in *Escherichia coli*. *Chin. J. Appl. Environ. Biol.* **2**, 271–275 (2010).
30. Mühlmann, M. *et al.* Optimizing recombinant protein expression via automated induction profiling in microtiter plates at different temperatures. *Microb. Cell Factories* **16**, 220 (2017).
31. Kaur, J., Kumar, A. & Kaur, J. Strategies for optimization of heterologous protein expression in *E. coli*: Roadblocks and reinforcements. *Int. J. Biol. Macromol.* **106**, 803–822. https://doi.org/10.1016/j.ijbiomac.2017.08.080 (2018).
32. Ghosh, P. & Ghosh, U. Statistical optimization of laccase production by isolated strain *Aspergillus flavus* PUF5 utilizing ribbed gourd peels as the substrate and enzyme application on apple juice clarification. *Indian J. Chem. Eng.* **61**, 1–12 (2019).
33. R Core Team (2020). R: A language and environment for statistical computing. R Foundation for Statistical Computing, Vienna, Austria. Available online: URL http://www.R-project.org/.
34. Zwietering, M. H., Jongenburger, I., Romburts, F. M. & Van't Riet, K. Modeling the bacterial growth curve. *Appl. Environ. Microbiol.* **56**, 1875–1881 (1990).
35. Kahm, M., Hasenbrink, G., Lichtenberg-Fraté, H., Ludwig, J. & Kschischo, M. Fitting biological growth curves with R. *J. Stat. Softw.* **33**, 1–21 (2010).
36. Tokmakov, A. A., Kurtani, A. & Sato, K. I. Protein pI and intracellular localization. *Front. Mol. Biosci.* **29**(8), 775736 (2021).
37. Fishman, A., Berk, Z. & Shoham, Y. Large-scale purification of xylanase T-6. *Appl. Microbiol. Biotechnol.* **44**, 88–93 (1995).
38. Orwick-Rydmark, M., Arnold, T. & Linke, D. The use of detergents to purify membrane proteins. *Curr. Protoc. Protein Sci.* **8**, 4481–4835 (2016).
39. Said, K. & Afizal, M. Overview on the response surface methodology in extraction processes. *J. Appl. Sci. Process Eng.* **2**, 1 (2016).
40. Xie, Y. *et al.* Collaborative optimization of ground source heat pump-radiant ceiling air conditioning system based on response surface method and NSGA-II. *Renew. Energy* **147**(1), 249–264 (2019).
41. Farliahati, M. R. *et al.* Enhanced production of xylanase by recombinant *Escherichia coli* DH5α through optimization of medium composition using Response Surface Methodology. *Ann. Microbiol.* **60**, 279–285 (2010).
42. Azzouz, Z., Bettache, A., Boucherba, N., Amghar, Z. & Benallaoua, S. Optimization of xylanase production by newly isolated strain *Trichoderma afroharzianum* isolate AZ12 in solid-state fermentation using Response Surface Methodology. *Cellul. Chem. Technol.* **54**(5–6), 451–462 (2020).
43. Chicco, D., Warrens, M. J. & Jurman, G. The coefficient of determination R squared is more informative than SMAPE, MAE, MAPE, MSE, and RMSE in regression analysis evaluation. *PeerJ Comput. Sci.* **7**, 623 (2021).
44. Bezerra, M. A., Santelli, R. E., Oliveira, E. P., Villar, L. S. & Escaleira, L. A. Response surface Methodology (RSM) as a tool for optimization in analytical chemistry. *Talanta.* **76**(5), 965–977 (2018).
45. He, X. *et al.* Efficient degradation of Azo dyes by a newly isolated fungus *Trichoderma tomentosum* under non-sterile conditions. *Ecotoxicol. Environ. Saf.* **150**, 232–239 (2018).
46. Akbari, V. *et al.* Optimization of a single-chain antibody fragment overexpression in *Escherichia coli* using response surface methodology. *Res. Pharm. Sci.* **10**(1), 75–83 (2015).
47. Kanno, A. I. *et al.* Optimization and scale-up production of Zika virus ΔNS1 in *Escherichia coli:* Application of response surface methodology. *AMB Express* **10**(1), 1 (2019).
48. Kumar, S., Gulati, P. & Singha, T. Kinetic study and optimization of recombinant human tumor necrosis factor-alpha (rhTNF-α) production in *Escherichia coli*. *Prep. Biochem. Biotechnol.* **51**(3), 267–276 (2020).
49. Gomes, L., Monteiro, G. & Mergulhão, F. The impact of IPTG induction on plasmid stability and heterologous protein expression by *Escherichia coli* biofilms. *Int. J. Mol. Sci.* **21**(2), 576 (2020).
50. Kereh, H. & Mubarik, N. Optimization of process parameters and scale-up of xylanase production using corn cob raw biomass by marine bacteria *Bacillus subtilis* LBF M8 in stirred tank bioreactor. *PJBT* **15**, 707–714 (2018).
51. Kumar, S., Sharma, N. & Pathania, S. Optimization of process parameters and scale-up of xylanase production from *Bacillus Amyloliquifaciens* Sh8 in a stirred tank bioreactor. *Cellul. Chem. Technol.* **51**(5–6), 403–415 (2015).
52. Bandaiphet, C. & Prasertsan, P. Effect of aeration and agitation rates and scale-up on oxygen transfer coefficient, KLa in exopolysaccharide production from *Enterobacter cloacae* WD7. *Carbohydr. Polym.* **66**(2), 216–228 (2015).

53. Zotta, T., Parente, E. & Ricciardi, A. Aerobic metabolism in the genus *Lactobacillus:* Impact on stress response and potential applications in the food industry. *J. Appl. Microbiol.* **122**(4), 857–869 (2017).
54. Elmansy, E. A., Asker, M., El-Kady, E. M., Hassanein, S. M. & El-Beih, F. M. Production and optimization of α-amylase from thermo-halophilic bacteria isolated from different local marine environments. *BNRC* **42**(1), 31 (2018).
55. Núñez, E. G. *et al.* Influence of aeration-homogenization system in stirred tank bioreactors, dissolved oxygen concentration and pH control mode on BHK-21 cell growth and metabolism. *Cytotechnology.* **66**(4), 605–617 (2014).
56. Abdella, A., Mazeed, T. E. S., Yang, S. T. & El-Baz, A. F. Production of β-glucosidase by *Aspergillus niger* on wheat bran and glycerol in submerged culture: Factorial experimental design and process optimization. *Curr. Biotechnol.* **3**(2), 197–206 (2014).
57. Kumar, V. & Shukla, P. Extracellular xylanase production from *T. lanuginosus* VAPS24 at pilot scale and thermostability enhancement by immobilization. *Process Biochem.* **71**, 53–60 (2018).
58. Gomes, J. *et al.* Production of a high level of cellulase-free xylanase by the thermophilic fungus *Thermomyces lanuginosus* in laboratory and pilot scales using lignocellulosic materials. *Appl. Microbiol. Biotechnol.* **39**, 700–707 (1993).
59. Garcia-Ochoa, F. & Gomez, E. Bioreactor scale-up and oxygen transfer rate in microbial processes: An overview. *Biotechnol. Adv.* **27**(2), 153–176 (2009).
60. Ronda, S. R., Bokka, C. S., Ketineni, C., Rijal, B. & Allu, P. R. Aeration effect on Spirulina platensis growth and γ-Linolenic acid production. *Braz. J. Microbiol.* **43**(1), 12–20 (2012).
61. Rosano, G. L. & Ceccarelli, E. A. Recombinant protein expression in *Escherichia coli*: Advances and challenges. *Front. Microbiol.* **5**, 172 (2017).
62. Kielkopf, C. L., Bauer, W. & Urbatsch, I. L. Expressing cloned genes for protein production, purification, and analysis. *Cold Spring Harb. Protoc.* **2**, 43–69 (2020).
63. Shilling, P. J. *et al.* Improved designs for pET expression plasmids increase protein production yield in *Escherichia coli*. *Commun. Biol.* **3**, 214 (2020).

Acknowledgements

This research was funded by University of Kwa-Zulu Natal and the Technology Innovation Agency (TIA) managed DST/CON/0177/2018: SIIP: ENZYME AND MICROBIAL TECHNOLOGIES (EMT) grant and the Biorefinery Industry Development Facility (BIDF) at the Council for Scientific and Industrial Research (CSIR), Durban, South Africa. TS was funded by the TIA-managed SIIP grant (2018/FUN/0180) and Rhodes University.

Author contributions

Experimental research, conceptualization, methodology, software validation, formal analysis, data curation, writing, P.D.; experimental research (cloning), T.S; review and editing, R.G.; B.P.; supervision, R.G.; B.P.; B.S.; funding acquisition, B.S. The study was supported by BS, TIA, and CSIR.

Competing interests

The authors declare no competing interests.

Additional information

Supplementary Information The online version contains supplementary material available at https://doi.org/10.1038/s41598-023-48202-5.

Correspondence and requests for materials should be addressed to B.P.

Reprints and permissions information is available at www.nature.com/reprints.

Publisher's note Springer Nature remains neutral with regard to jurisdictional claims in published maps and institutional affiliations.

International Journal of
Molecular Sciences

MDPI

Article

Optimization of Xylooligosaccharides Production by Native and Recombinant Xylanase Hydrolysis of Chicken Feed Substrates

Priyashini Dhaver [1], Brett Pletschke [2], Bruce Sithole [3,4] and Roshini Govinden [1,*]

[1] Discipline of Microbiology, School of Life Sciences, Westville Campus, University of KwaZulu-Natal, Durban 4000, South Africa; pdhaver10@gmail.com
[2] Enzyme Science Programme (ESP), Department of Biochemistry and Microbiology, Rhodes University, Makhanda (Grahamstown) 6140, South Africa; b.pletschke@ru.ac.za
[3] Biorefinery Industry Development Facility, Council for Scientific and Industrial Research, Durban 4000, South Africa; bbsithole@hotmail.com
[4] Discipline of Chemical Engineering, University of KwaZulu-Natal, Durban 4000, South Africa
* Correspondence: govindenr@ukzn.ac.za; Tel.: +27-31-260-8281

Abstract: Poultry production faces several challenges, with feed efficiency being the main factor that can be influenced through the use of different nutritional strategies. Xylooligosaccharides (XOS) are functional feed additives that are attracting growing commercial interest due to their excellent ability to modulate the composition of the gut microbiota. The aim of the study was to apply crude and purified fungal xylanases, from *Trichoderma harzianum*, as well as a recombinant glycoside hydrolase family 10 xylanase, derived from *Geobacillus stearothermophilus* T6, as additives to locally produced chicken feeds. A Box–Behnken Design (BBD) was used to optimize the reducing sugar yield. Response surface methodology (RSM) revealed that reducing sugars were higher (8.05 mg/mL, 2.81 mg/mL and 2.98 mg/mL) for the starter feed treated with each of the three enzymes compared to the treatment with grower feed (3.11 mg/mL, 2.41 mg/mL and 2.62 mg/mL). The hydrolysis products were analysed by thin-layer chromatography (TLC), and high-performance liquid chromatography (HPLC) analysis and showed that the enzymes hydrolysed the chicken feeds, producing a range of monosaccharides (arabinose, mannose, glucose, and galactose) and XOS, with xylobiose being the predominant XOS. These results show promising data for future applications as additives to poultry feeds.

Keywords: xylooligosaccharides; chicken feed; lignocellulosic biomass; response surface methodology; xylanase

Citation: Dhaver, P.; Pletschke, B.; Sithole, B.; Govinden, R. Optimization of Xylooligosaccharides Production by Native and Recombinant Xylanase Hydrolysis of Chicken Feed Substrates. *Int. J. Mol. Sci.* **2023**, *24*, 17110. https://doi.org/10.3390/ijms242317110

Academic Editors: Salvatore Fusco and Patrizia Contursi

Received: 25 October 2023
Revised: 28 November 2023
Accepted: 29 November 2023
Published: 4 December 2023

1. Introduction

Xylan is the second most common renewable terrestrial polysaccharide in nature after cellulose. Non-starch polysaccharides (NSPs) like xylan cannot be hydrolysed by endogenous enzymes in monogastric animals like poultry [1]. This leads to an environment favourable for these NSPs to encapsulate the other nutrients, thus acting as a barrier in the small intestine and resulting in the increased viscosity of the digesta [2]. Recent studies [3,4] have shown that a decreased growth performance due to increased digesta viscosity has been commonly seen in chickens that ingest diets containing high levels of NSPs.

In response to this, livestock producers have incorporated exogenous enzymes such as xylanases into poultry feeds in order to degrade the xylan into short-chain sugars, thereby reducing intestinal viscosity and enhancing the digestive utilization of nutrients [5]. Research suggests that the presence of certain enzymes, such as xylanase, or the combination of enzymes with dietary components, like xylanase with hybrid rye, can have an impact on the integrity of the chicken intestinal barrier, specifically affecting the tight junction proteins [6].

Xylan, derived from lignocellulosic biomass, can be hydrolysed through the use of exogenous chemicals and enzymatic processes to generate a mixture of xylooligosaccharides (XOSs) and monosaccharides [7,8]. The resulting XOS mixture is recognized as a prebiotic [1]. XOS are oligosaccharides made up of repeating xylose units linked by β-(1–4)-linkages—examples include xylobiose, xylotriose, xylotetraose, xylopentaose, and xylohexaose [9]. XOS have a promising market potential as food additives, feed additives, health care products, and pharmaceuticals [10] because of their prebiotic [11], antioxidant [12], and anticancer activity [13]. Hemicelluloses are efficiently hydrolysed into monosaccharides or XOS with minimal enzyme loading which is important for the lignocellulosic bioenergy and biorefinery industry [8].

Lignocellulosic biomass is the most cost-efficient and sustainable natural resource available globally. It is comprised of terrestrial vegetation like shrubs and grasses, as well as agricultural biomass by-products like corn stover, straw, saw-dust wastes, paper mill discards, and energy-yielding vegetation [14]. Its hydrolysis products have been widely adopted as prebiotics and carbohydrases in feed additives in broiler chickens, to enhance intestinal health and stimulate performance [15]. However, hydrolysis conditions affect the production of hydrolysis products. Therefore, it is vital to understand the effects of enzyme dosage, feed substrate loading, incubation time, temperature, and pH during hydrolysis [16,17]. An efficient way to understand the impact of various process variables and their interactions on the process's outcome and to identify the ideal conditions for maximizing the process output is to use the Response Surface Methodology (RSM), a mathematical and statistical technique [18]. The RSM, using a Box Behnken Design (BBD), is an effective optimization tool. The RSM design can provide the dependence of enzyme activity on independent variables (enzyme dosage, feed loading, incubation time, pH, and incubation temperature), predicted results for responses, and levels for independent variables in the form of mathematical models [19].

Following optimization to enhance yields, analysis of the hydrolysates is usually carried out using two techniques: thin-layer chromatography (TLC) and high-performance liquid chromatography (HPLC) [20–22]. HPLC employs detectors [such as refractive index (RI) and diode array detector (DAD)] for the determination of total component sugars produced after hydrolysis [23,24].

The addition of xylanases to chicken cereal feed diets can enhance NSP hydrolysis and the production of prebiotic XOSs. Considering the potential market demand for XOSs in the agricultural and pharmaceutical industry, the aim of the present study was to optimize the hydrolysis of starter and grower chicken feed using crude [25] and purified [19] *Trichoderma harzianum* xylanases and the recombinant *Geobacillus stearothermophilus* XT6 xylanase [26] obtained from previous studies, to enhance the production of reducing sugars. XOSs and monosaccharides were monitored qualitatively and quantitatively using chromatographic techniques to analyse the feed hydrolysate profiles.

2. Results and Discussion

2.1. Optimization of Feed Hydrolysis for Enhanced Reducing Sugars

2.1.1. Hydrolysis of Starter and Grower Feeds with Crude *T. harzianum* Xylanase

This study focused on the conditions favouring the hydrolysis of chicken feeds. Production of XOS from various sources of xylan such as wheat bran, birchwood, corncob, tobacco stalk, etc., using commercial xylanases has been reported previously [27,28]. However, relatively few studies have involved the xylanases from *T. harzianum* and the recombinant XT6 xylanase. The runs that produced the highest reducing sugars for the starter feed with the crude *T. harzianum* xylanase was run 45 (8.05 mg/mL) with all variables at their optimal levels (Table 1).

Table 1. Experimental design for the Box Behnken Design (BBD) model for five independent variables tested for reducing sugar production from two chicken feed types.

Variable Level						Reducing Sugars (mg/mL)					
						Starter Chicken Feed			Grower Chicken Feed		
Run Order	X1 (U/mL)	X2 (%)	X3 (h)	X4 (°C)	X5 (pH)	Crude *T. harzianum* Xylanase	Purified *T. harzianum* Xylanase	Recombinant XT6 Xylanase	Crude *T. harzianum* Xylanase	Purified *T. harzianum* Xylanase	Recombinant XT6 Xylanase
1	**5 (−)**	**0.5 (−)**	**24 (0)**	**65 (0)**	5 (0)	3.16	0.82	2.36	3.21	2.09	2.37
2	15 (+)	0.5 (−)	24 (0)	65 (0)	5 (0)	3.10	1.90	1.68	2.92	1.59	2.17
3	5 (−)	1.5 (+)	24 (0)	65 (0)	5 (0)	2.78	1.99	2.12	2.56	1.73	2.62
4	15 (+)	1.5 (+)	24 (0)	65 (0)	5 (0)	1.95	2.22	2.46	2.96	2.21	2.34
5	5 (−)	1 (0)	12 (−)	65 (0)	5 (0)	2.02	2.23	2.10	2.85	1.68	2.20
6	15 (+)	1 (0)	12 (−)	65 (0)	5 (0)	2.74	2.25	2.57	2.84	1.93	2.14
7	5 (−)	1 (0)	36 (+)	65 (0)	5 (0)	2.86	2.15	2.03	2.69	1.49	2.22
8	15 (+)	1 (0)	36(+)	65 (0)	5 (0)	3.23	2.21	1.97	2.50	1.97	2.12
9	10 (0)	0.5 (−)	12 (−)	55 (−)	5 (0)	2.60	1.87	2.18	2.46	2.00	2.16
10	10 (0)	1.5 (+)	12 (−)	55 (−)	5 (0)	2.82	2.13	2.05	2.51	2.10	2.45
11	10 (0)	0.5 (−)	36 (+)	75 (+)	5 (0)	2.21	2.11	2.27	2.40	2.17	2.53
12	10 (0)	1.5 (+)	36 (+)	75 (+)	5 (0)	2.93	**2.81**	**2.98**	2.83	2.31	**2.79**
13	10 (0)	1 (0)	24 (0)	55 (−)	4 (−)	2.74	2.05	2.17	2.79	1.85	2.62
14	10 (0)	1 (0)	24 (0)	75 (+)	4 (−)	2.68	2.00	1.97	2.59	1.73	1.99
15	10 (0)	1 (0)	24 (0)	55 (−)	6 (+)	2.38	1.68	1.67	2.57	1.55	1.81
16	10 (0)	1 (0)	24 (0)	75 (+)	6 (+)	2.56	1.80	1.81	2.60	1.65	1.92
17	10 (0)	0.5 (−)	24 (0)	65 (0)	4 (−)	2.60	1.88	1.71	2.28	1.29	1.94
18	10 (0)	1.5 (+)	24 (0)	65 (0)	4 (−)	2.52	1.78	1.71	2.46	1.03	1.69
19	10 (0)	0.5 (−)	24 (0)	65 (0)	6 (+)	2.50	1.80	1.57	2.28	1.65	1.73
20	10 (0)	1.5 (+)	24 (0)	65 (0)	6 (+)	2.08	1.91	1.72	2.31	1.68	1.99
21	10 (0)	1 (0)	24 (0)	65 (0)	5 (0)	1.92	2.01	1.86	1.95	1.81	1.41
22	10 (0)	1 (0)	24 (0)	65 (0)	5 (0)	2.32	1.88	1.92	1.82	1.92	2.44
23	10 (0)	1 (0)	24 (0)	65 (0)	5 (0)	2.21	2.13	1.94	1.77	1.91	1.95
24	10 (0)	1 (0)	24 (0)	65 (0)	5 (0)	2.18	2.27	2.10	2.46	**2.41**	2.11
25	5 (−)	1 (0)	24 (0)	55 (−)	5 (0)	3.03	1.78	2.20	3.07	1.77	1.92
26	15 (+)	1 (0)	24 (0)	55 (−)	5 (0)	2.66	1.59	1.64	2.63	1.60	1.73
27	5 (−)	1 (0)	24 (0)	75 (+)	5 (0)	2.56	1.63	1.85	2.45	1.89	1.75
28	15 (+)	1 (0)	24 (0)	75 (+)	5 (0)	2.51	1.60	1.73	2.22	1.87	1.80
29	5 (−)	1 (0)	24 (0)	65 (0)	4 (−)	2.33	1.86	1.87	2.16	1.25	1.65
30	15 (+)	1 (0)	24 (0)	65 (0)	4 (−)	2.47	1.91	1.86	2.36	1.63	1.51
31	5 (−)	1 (0)	24 (0)	65 (0)	6 (+)	2.41	1.90	1.89	2.22	1.51	1.89
32	15 (+)	1 (0)	24 (0)	65 (0)	6 (+)	2.05	1.71	1.80	2.13	1.76	1.90
33	10 (0)	0.5 (−)	12 (−)	65 (0)	5 (0)	2.36	1.78	1.74	2.03	1.70	2.13
34	10 (0)	1.5 (+)	12 (-)	65 (0)	5 (0)	−5.86	1.71	1.89	1.76	1.85	2.24
35	10 (0)	0.5 (−)	36 (+)	65 (0)	5 (0)	2.28	1.90	1.69	1.58	1.72	1.91
36	10 (0)	1.5 (+)	36(+)	65 (0)	5 (0)	2.48	2.16	1.92	2.10	1.89	2.48
37	10 (0)	0.5 (−)	24 (0)	55 (−)	5 (0)	2.97	1.80	1.84	2.89	1.96	2.03
38	10 (0)	1.5 (+)	24 (0)	55 (−)	5 (0)	4.45	1.60	2.07	2.56	1.79	1.92
39	10 (0)	0.5 (−)	24 (0)	75 (+)	5 (0)	2.51	1.52	1.79	2.31	1.35	1.59
40	10 (0)	1.5 (+)	24 (0)	75 (+)	5 (0)	2.61	1.49	1.66	2.22	1.91	1.36
41	10 (0)	1 (0)	12 (−)	65 (0)	4 (−)	2.49	1.60	1.67	2.24	1.71	1.93
42	10 (0)	1 (0)	36 (+)	65 (0)	4 (−)	2.40	1.80	1.69	2.48	1.77	1.60
43	10 (0)	1 (0)	12 (−)	65 (0)	6 (+)	2.07	1.77	1.67	2.21	1.74	1.61

Table 1. *Cont.*

Variable Level						Reducing Sugars (mg/mL)					
						Starter Chicken Feed			Grower Chicken Feed		
Run Order	X1 (U/mL)	X2 (%)	X3 (h)	X4 (°C)	X5 (pH)	Crude *T. harzianum* Xylanase	Purified *T. harzianum* Xylanase	Recombinant XT6 Xylanase	Crude *T. harzianum* Xylanase	Purified *T. harzianum* Xylanase	Recombinant XT6 Xylanase
44	10 (0)	1 (0)	36 (+)	65 (0)	6 (+)	2.41	1.73	1.64	2.22	1.60	1.83
45	10 (0)	1 (0)	24 (0)	65 (0)	5 (0)	**8.05**	1.60	1.65	1.98	1.75	2.03
46	10 (0)	1 (0)	24 (0)	65 (0)	5 (0)	4.91	1.51	1.80	1.81	1.75	2.16
47	10 (0)	1 (0)	24 (0)	65 (0)	5 (0)	1.90	1.52	1.74	1.62	1.89	2.29
48	10 (0)	1 (0)	24 (0)	65 (0)	5 (0)	7.84	1.95	2.11	1.96	2.18	2.33

For the grower feed, the highest reducing sugars was produced in run 1 (3.21 mg/mL) with the enzyme dosage (5 U/mL) and feed percentage (0.5%) at their low levels and incubation time, pH, and incubation temperature at their optimal levels. Run 25 also produced similar high yields of reducing sugars (3.07 mg/mL), with the only difference being that the feed percentage was at its optimal level (1%) and the incubation temperature was at its low level (55 °C). Analysis of Variance (ANOVA) was performed to determine the *p*-values. The model was significant ($p \leq 0.05$) for all enzymatically treated feed samples. Table 2 shows the results for the starter feed treatment with crude *T. harzianum* xylanase, the interactions between the feed loading and incubation time as well as the incubation time and incubation temperature ($p \leq 0.05$), and the square terms for feed loading and incubation time ($p \leq 0.03$), which were significant. Similarly, for the grower feed treatment, the square terms for enzyme dosage ($p \leq 0.0001$) and incubation temperature ($p \leq 0.005$) were significant as well as the linear terms for incubation temperature ($p \leq 0.004$). The Pareto charts of standardization histogram graphs (Figure 1) corroborate these findings ($p \leq 0.05$), as they crossed the p-line (cumulative% = 50%).

Table 2. Analysis of Variance (ANOVA) and regression coefficients of the response surface quadratic model for the response variables for optimizing chicken feed hydrolysis by crude *T. harzianum* xylanase.

Variable	Estimate		Std. Error		*t* Value		*p*-Value	
	Starter Feed	Grower Feed	Starter Feed	Grower Feed	Starter Feed	Grower Feed	Starter Feed	Grower Feed
Model	−23.24	27.40	49.43	8.95	−0.47	3.06	0.05 *	0.005 *
Enzyme Dosage (U/mL)	0.48	−0.45	1.68	0.30	0.28	−1.47	0.78	0.15
Feed Loading (%)	14.41	−2.59	14.11	2.55	1.02	−1.02	0.32	0.32
Incubation Time (h)	−0.61	−0.01	0.77	0.14	−0.79	−0.01	0.43	0.99
Incubation Temperature (°C)	0.30	−0.53	0.94	0.17	0.32	−3.10	0.75	0.004 *
pH	6.51	−1.70	9.13	1.65	0.71	−1.03	0.48	0.31
Enzyme Dosage (U/mL): Feed Loading (%)	−0.08	0.07	0.37	0.07	−0.21	1.03	0.84	0.31
Enzyme Dosage (U/mL): Time (h)	−0.01	−0.01	0.02	0.02	−0.10	−0.26	0.92	0.80
Enzyme Dosage (U/mL): Temperature (°C)	0.01	−0.01	0.02	0.01	0.09	0.32	0.93	0.75
Enzyme Dosage (U/mL): pH	−0.02	−0.01	0.18	0.03	−0.14	−0.43	0.89	0.67
Feed Loading (%): Incubation Time (h)	0.26	0.02	0.13	0.02	2.07	1.06	0.03 *	0.30
Feed Loading (%): Incubation Temperature (°C)	−0.18	0.00	0.15	0.02	−1.18	0.03	0.25	0.98
Feed Loading (%): pH	−0.17	−0.07	1.84	0.33	−0.09	−0.22	0.93	0.83
Incubation Time (h): Incubation Temperature (°C)	0.01	−0.01	0.01	0.01	1.18	−0.15	0.05 *	0.88
Incubation Time (h): pH	0.01	−0.01	0.08	0.01	0.12	−0.34	0.91	0.73
Temperature (°C): pH	0.01	0.01	0.09	0.02	0.06	0.33	0.95	0.74
Enzyme Dosage (U/mL)^2	−0.02	0.02	0.02	0.01	−0.69	4.41	0.50	0.0001 *
Feed Loading (%)^2	−4.12	0.81	2.43	0.44	−1.70	1.86	0.04 *	0.07
Incubation Time (h)^2	−0.01	0.01	0.01	0.01	−2.08	0.72	0.03 *	0.48
Incubation Temperature (°C)^2	−0.01	0.03	0.01	0.01	−0.59	3.02	0.56	0.005 *
pH^2	−0.68	0.02	0.61	0.11	−1.12	1.47	0.27	0.15

* $p \leq 0.05$ shows significance. Lack of fit = 0.98. Lack of fit = 0.16.

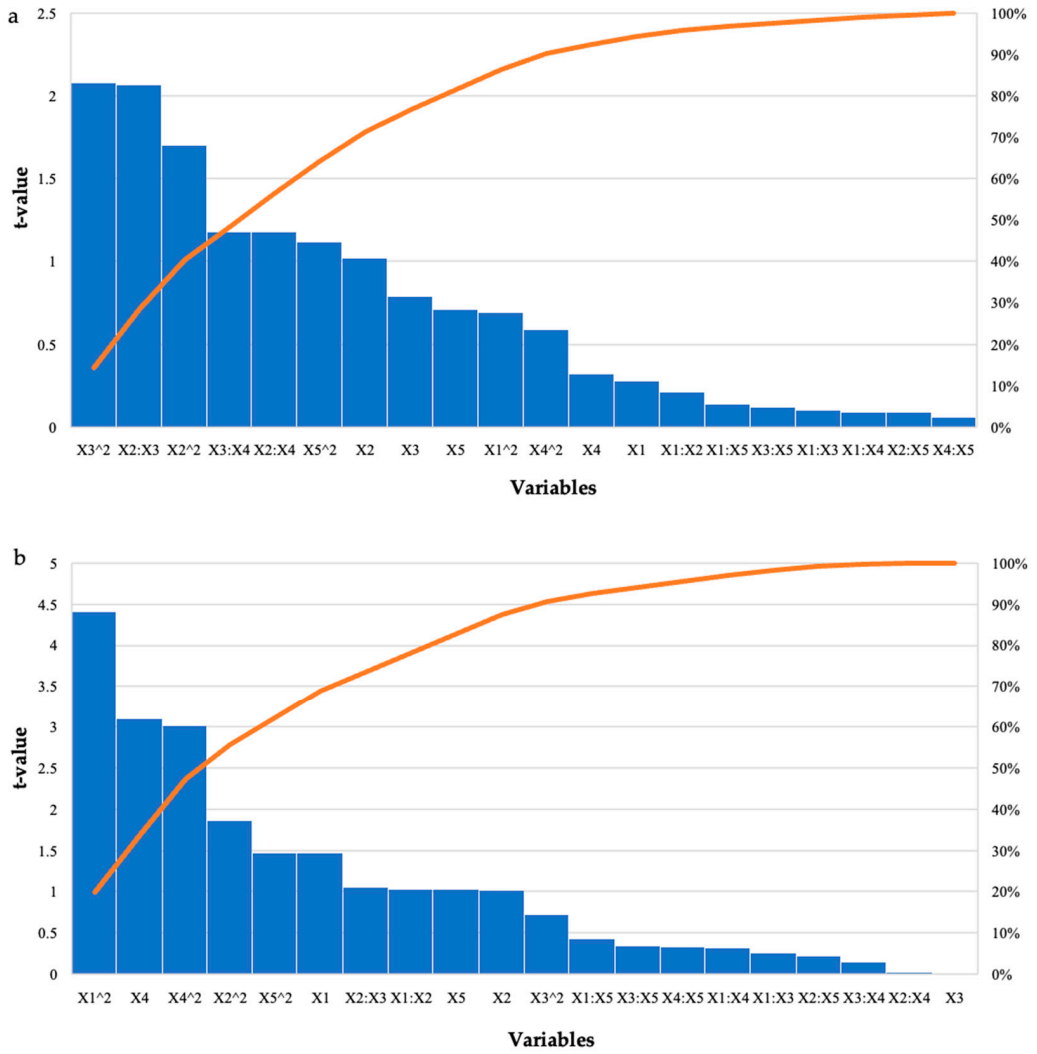

Figure 1. Pareto chart of standardized effects for the BBD for enzyme dosage (X1), feed loading (X2), incubation time (X3), incubation temperature (X4), and pH (X5) for the hydrolysis of (**a**) starter feed and (**b**) grower feed with crude *T. harzianum* xylanase. The orange line represents $p = 0.05$.

2.1.2. Hydrolysis of Starter and Grower Feeds with Purified *T. harzianum* Xylanase

Hydrolysis of the starter feed by the purified *T. harzianum* xylanase resulted in the highest amount of reducing sugars in run 12 (2.81 mg/mL) at the optimal enzyme dosage and pH with the other variables at their high levels (Table 1). There were other runs that produced similar high yields; however, these were significantly different ($p \leq 0.05$). For the grower feed, run 24 (2.41 mg/mL) with all variables at their optimal levels resulted in the highest amount of reducing sugars. Run 12 also resulted in similar yields (2.31 mg/mL) with feed loading, incubation time, and temperature at their high levels. Table 3 represents the ANOVA results for the hydrolysis of the starter and grower feeds by the purified *T. harzianum* xylanase, the interactions between the enzyme dosage and incubation time, as well as the incubation time and incubation temperature. The linear terms for time were significant (p-values were 0.05, 0.04, and 0.04), respectively. For treatment of the grower feed; the square ($p \leq 0.0003$) and linear terms ($p \leq 0.02$) for pH; as well as the interactions between the enzyme dosage and feed ($p \leq 0.03$); and time and temperature ($p \leq 0.02$) were significant. The Pareto charts of standardization histogram graphs (Figure 2) also showed that those terms were significant ($p \leq 0.05$), as they crossed the p-line (cumulative% = 50%).

Table 3. ANOVA and regression coefficients of the response surface quadratic model for the response variables for optimizing chicken feed hydrolysis by the purified *T. harzianum* xylanase.

Variable	Estimate		Std. Error		*t* Value		*p*-Value	
	Starter Feed	Grower Feed	Starter Feed	Grower Feed	Starter Feed	Grower Feed	Starter Feed	Grower Feed
Model	3.52	1.06	7.90	5.87	0.44	0.18	0.03 *	0.03 *
Enzyme Dosage (U/mL)	0.08	−0.06	0.27	0.20	0.31	−0.29	0.76	0.77
Feed Loading (%)	0.50	−1.99	2.26	1.68	0.22	−1.19	0.83	0.24
Incubation Time (h)	−0.27	−0.18	0.12	0.09	−2.22	−1.95	0.04 *	0.06
Incubation Temperature (°C)	0.02	−0.08	0.15	0.11	0.16	−0.74	0.87	0.47
pH	−0.015	2.69	1.46	1.08	−0.01	2.48	0.99	0.02 *
Enzyme Dosage (U/mL): Feed Loading (%)	−0.09	0.10	0.06	0.04	−1.45	2.25	0.16	0.03 *
Enzyme Dosage (U/mL): Time (h)	0.00	0.01	0.00	0.01	0.05	0.55	0.05 *	0.59
Enzyme Dosage (U/mL): Temperature (°C)	0.00	0.01	0.00	0.02	0.25	0.33	0.80	0.74
Enzyme Dosage (U/mL): pH	−0.01	−0.01	0.03	0.02	−0.42	−0.30	0.68	0.77
Feed Loading (%): Incubation Time (h)	0.01	−0.01	0.02	0.01	0.64	−0.62	0.53	0.54
Feed Loading (%): Incubation Temperature (°C)	0.01	0.02	0.02	0.01	0.32	1.39	0.75	0.18
Feed Loading (%): pH	0.11	0.14	0.2	0.22	0.36	0.65	0.72	0.52
Incubation Time (h): Incubation Temperature (°C)	0.00	0.03	0.00	0.01	2.22	2.46	0.04 *	0.02 *
Incubation Time (h): pH	−0.00	−0.04	0.01	0.02	−0.41	−0.47	0.69	0.64
Temperature (°C): pH	0.00	0.05	0.01	0.01	−0.30	0.49	0.77	0.63
Enzyme Dosage (U/mL)^2	0.00	−0.03	0.00	0.02	0.32	−1.14	0.75	0.27
Feed Loading (%)^2	−0.38	−0.50	0.39	0.29	−0.97	−1.76	0.34	0.09
Incubation Time (h)^2	0.00	−0.01	0.00	0.01	0.99	−0.38	0.33	0.71
Incubation Temperature (°C)^2	−0.00	−0.01	0.00	0.01	−1.11	−0.51	0.28	0.61
pH^2	−0.01	−0.30	0.10	0.07	−0.18	−4.10	0.86	0.0003 *

* $p \leq 0.05$ shows significance. Lack of fit = 0.40. Lack of fit = 0.62.

2.1.3. Hydrolysis of Starter and Grower Feeds with Recombinant XT6 Xylanase

The run that had the highest effect on starter feed was run 12 (2.98 mg/mL), with enzyme dosage and pH at their optimal levels and the other variables at their high levels (Table 1). For the grower feed, run 12 (2.79 mg/mL) had enzyme dosage and pH at their optimal levels, and the other variables at their high levels. There were other runs that produced similar high yields; however, these were significantly different ($p \leq 0.05$). Overall, higher levels of reducing sugars were obtained for the starter feed hydrolysis by all three enzymes compared to the grower feed. Hydrolysis of the starter feed with the crude *T. harzianum* xylanase produced the highest yield of reducing sugars (8.05 mg/mL). The lowest yield (2.41 mg/mL) was obtained for the grower feed hydrolysed by purified *T. harzianum* xylanase. Table 4 shows that the interactions between the enzyme dosage and feed loading, as well as incubation time and temperature, and the linear terms for time were significant as *p*-values were 0.0004, 0.03, and 0.01, respectively. The square terms for the enzyme dosage ($p \leq 0.03$) and incubation temperature ($p \leq 0.05$) were also significant. For the grower feed, the interaction between incubation time and temperature (0.03) and the linear terms ($p \leq 0.02$) for the incubation time were significant, as well as the square term for pH ($p \leq 0.05$). The Pareto charts of standardization histogram graphs (Figure 3) also showed that those terms were significant ($p \leq 0.05$), as they crossed the p-line (cumulative% = 50%).

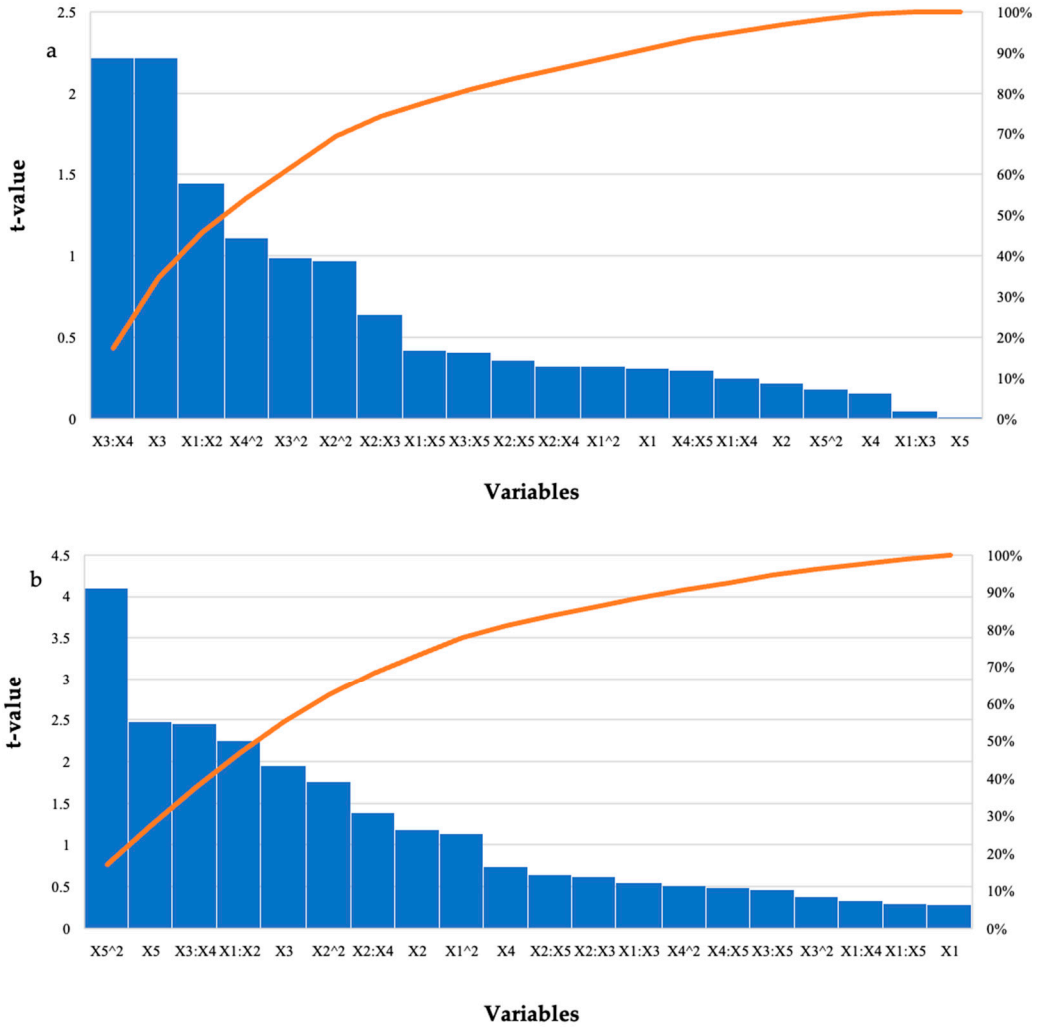

Figure 2. Pareto chart of standardised effects for the BBD for enzyme dosage (X1), feed loading (X2), incubation time (X3), incubation temperature (X4), and pH (X5) for the hydrolysis of (**a**) starter feed and (**b**) grower feed with purified *T. harzianum* xylanase. The orange line represents $p = 0.05$.

Table 4. ANOVA and regression coefficients of the response surface quadratic model for the response variables for optimizing chicken feed hydrolysis by the purified recombinant XT6 xylanase.

Variable	Estimate		Std. Error		*t* Value		*p*-Value	
	Starter Feed	Grower Feed	Starter Feed	Grower Feed	Starter Feed	Grower Feed	Starter Feed	Grower Feed
Model	9.32	6.51	5.83	8.73	1.59	0.75	0.04 *	0.04 *
Enzyme Dosage (U/mL)	−3.17	−1.28	1.98	2.96	−1.60	−0.43	0.12	0.67
Feed Loading (%)	−1.34	−8.30	1.67	2.49	−0.81	−0.33	0.43	0.74
Incubation Time (h)	−2.48	−3.51	9.14	1.37	−2.71	−2.57	0.01 *	0.02 *
Incubation Temperature (°C)	−1.25	1.10	1.11	1.66	−1.13	0.07	0.27	0.95
pH	7.80	2.75	1.08	1.61	0.72	0.17	0.48	0.87
Enzyme Dosage (U/mL): Feed Loading (%)	1.03	−8.60	4.36	6.53	2.35	−0.13	0.03 *	0.90
Enzyme Dosage (U/mL): Time (h)	−2.21	−1.57	1.81	2.72	−1.22	−0.06	0.23	0.95
Enzyme Dosage (U/mL): Temperature (°C)	2.21	1.17	2.18	3.27	1.01	0.36	0.32	0.72
Enzyme Dosage (U/mL): pH	−3.85	7.88	2.18	3.27	−0.18	0.24	0.86	0.81
Feed Loading (%): Incubation Time (h)	1.59	1.40	1.48	2.22	1.07	0.63	0.29	0.53
Feed Loading (%): Incubation Temperature (°C)	−2.30	−1.24	1.78	2.67	−0.13	−0.46	0.90	0.65
Feed Loading (%): pH	7.25	2.54	2.18	3.27	0.33	0.78	0.74	0.44
Incubation Time (h): Incubation Temperature (°C)	4.04	4.43	1.32	1.97	3.07	2.25	0.004 *	0.03 *
Incubation Time (h): pH	−8.96	1.12	9.09	1.36	−1.00	0.82	0.92	0.42
Temperature (°C): pH	8.51	1.85	1.09	1.63	0.78	1.13	0.44	0.27

Table 4. *Cont.*

Variable	Estimate		Std. Error		*t* Value		*p*-Value	
	Starter Feed	Grower Feed	Starter Feed	Grower Feed	Starter Feed	Grower Feed	Starter Feed	Grower Feed
Enzyme Dosage (U/mL)^2	6.70	7.01	2.86	4.29	2.34	0.16	0.03 *	0.87
Feed Loading (%)^2	−6.10	1.24	2.86	4.29	−0.21	0.29	0.83	0.77
Incubation Time (h)^2	−7.93	−9.33	5.58	8.34	−0.14	−0.01	0.89	0.99
Incubation Temperature (°C)^2	−2.64	−1.66	8.03	1.20	−0.33	−1.38	0.05 *	0.18
pH^2	−1.40	−2.09	7.16	1.07	−1.95	−1.95	0.06	0.05 *

* $p \leq 0.05$ shows significance. Lack of fit = 0.40. Lack of fit = 0.62.

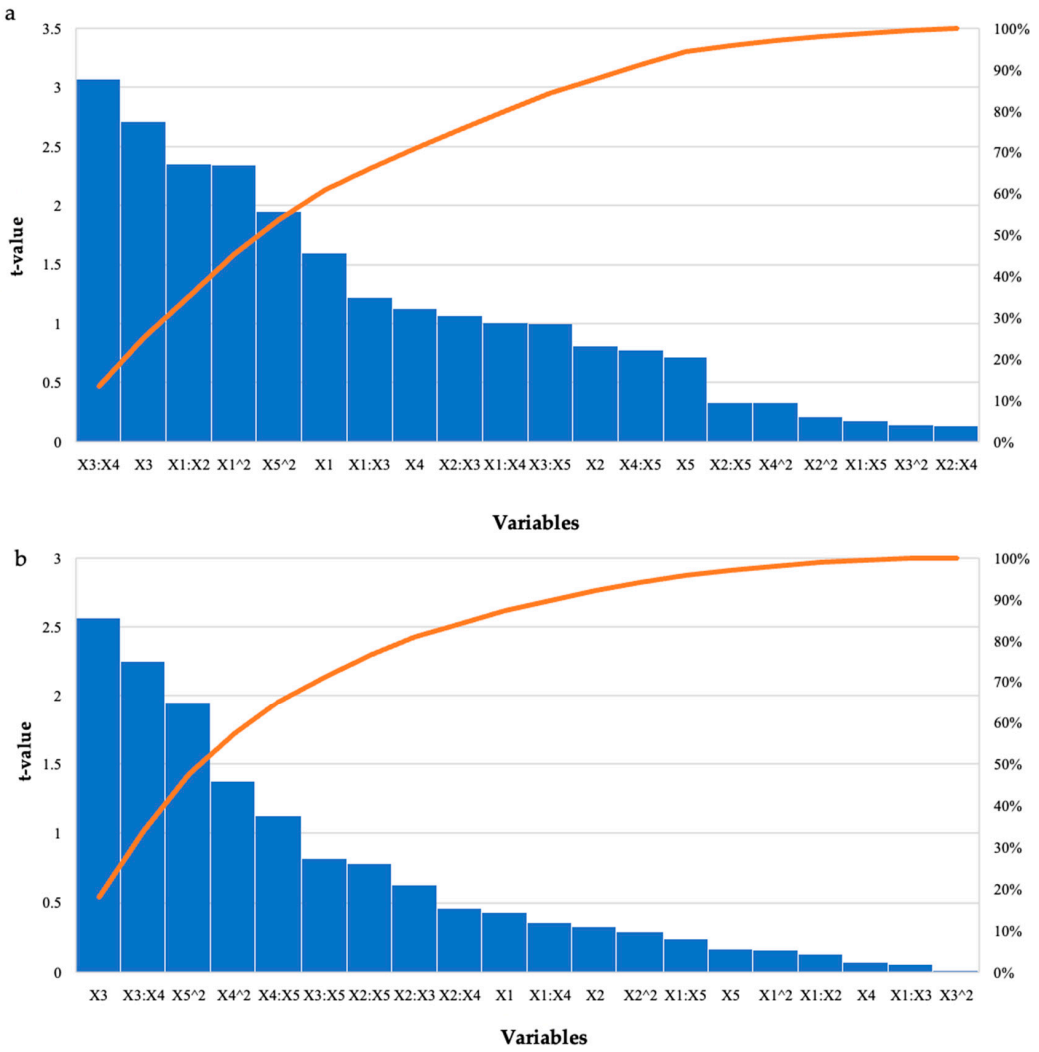

Figure 3. Pareto chart of standardised effects for the BBD for enzyme dosage (X1), feed loading (X2), incubation time (X3), incubation temperature (X4), and pH (X5) for the hydrolysis of (**a**) starter feed and (**b**) grower feed with purified recombinant XT6 xylanase. The orange line represents $p = 0.05$.

2.1.4. Interaction of Variables for Feed Hydrolysis

The relationship between the responses and the parameters for feed hydrolysis generated by the quadratic model and the optimum level of each variable were studied using three-dimensional (3D) response surface plots (Figures 4–8) (Supplementary Figures S1–S6), where the *z*-axis refers to reducing sugars versus any two variables, whilst the other variables are at their optimal levels 3.

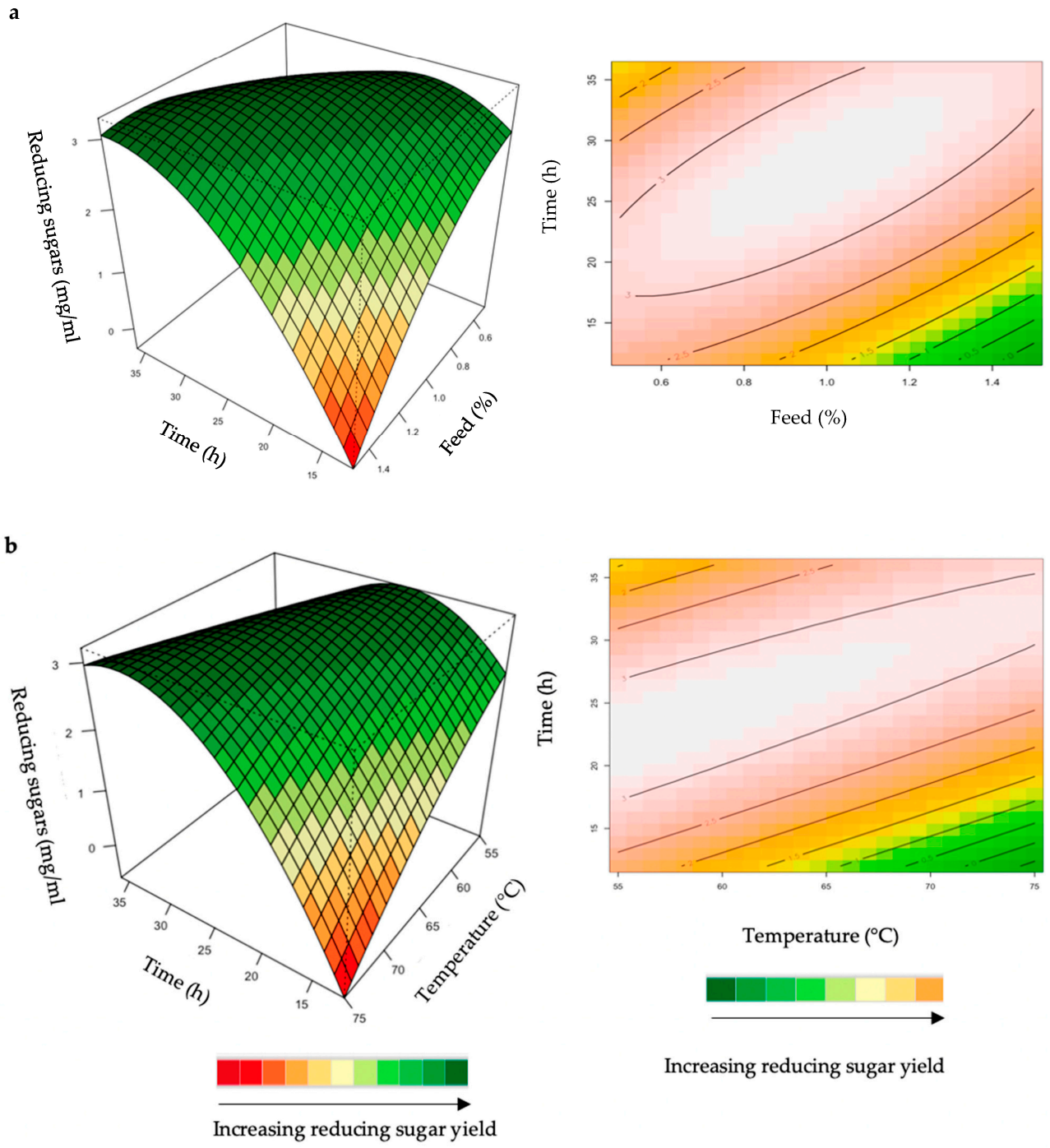

Figure 4. 3D-response surface plots and contour plots of the combined effects of feed loading and incubation time (**a**) and incubation time and temperature (**b**) on the yield of reducing sugars from the hydrolysis of starter chicken feed by the crude *T. harzianum* xylanase.

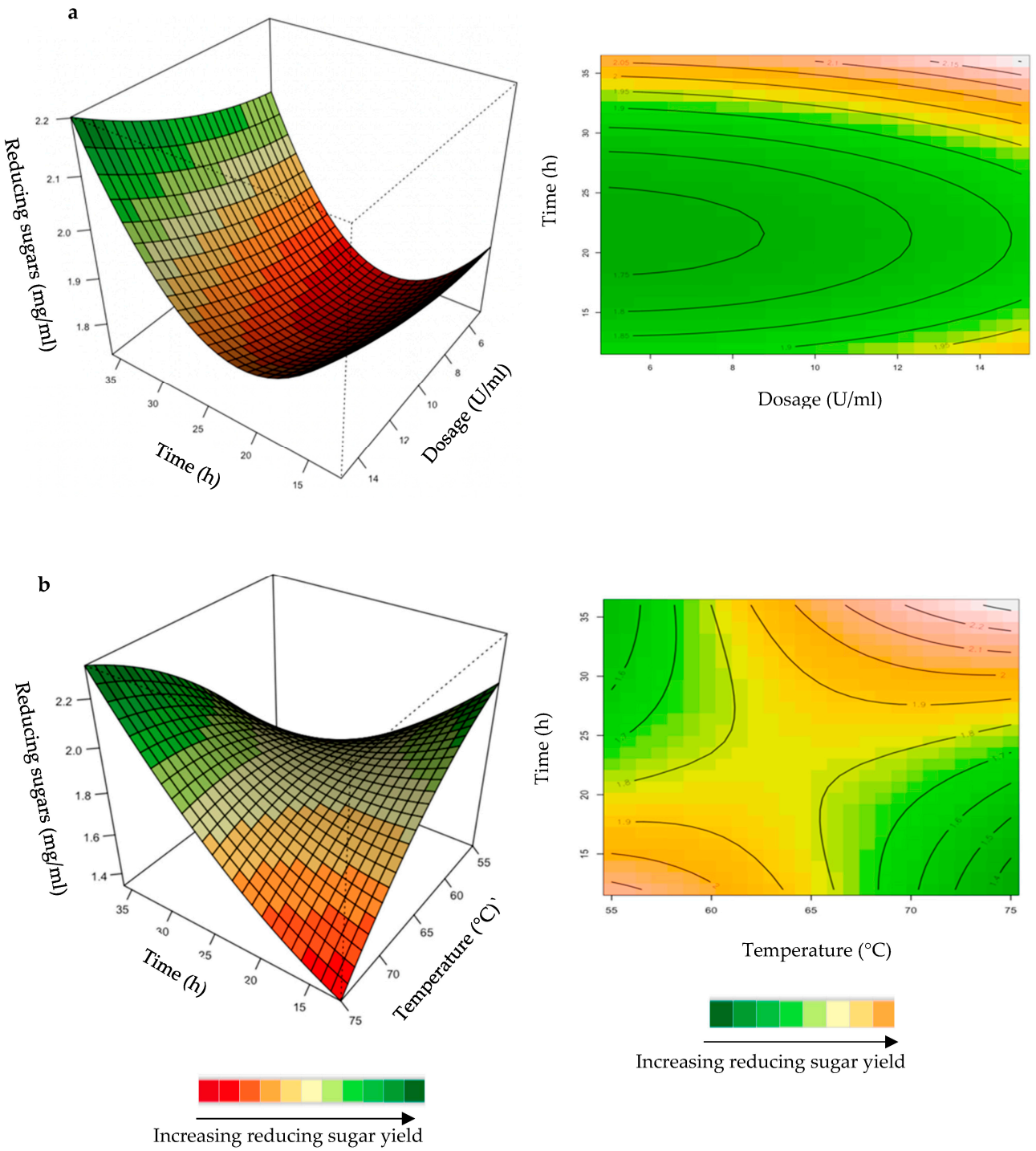

Figure 5. 3D-response surface plots and contour plots of the combined effects of enzyme dose and incubation time (**a**) and incubation time and temperature (**b**) on the yield of reducing sugars from starter chicken feed hydrolysed by the purified *T. harzianum* xylanase.

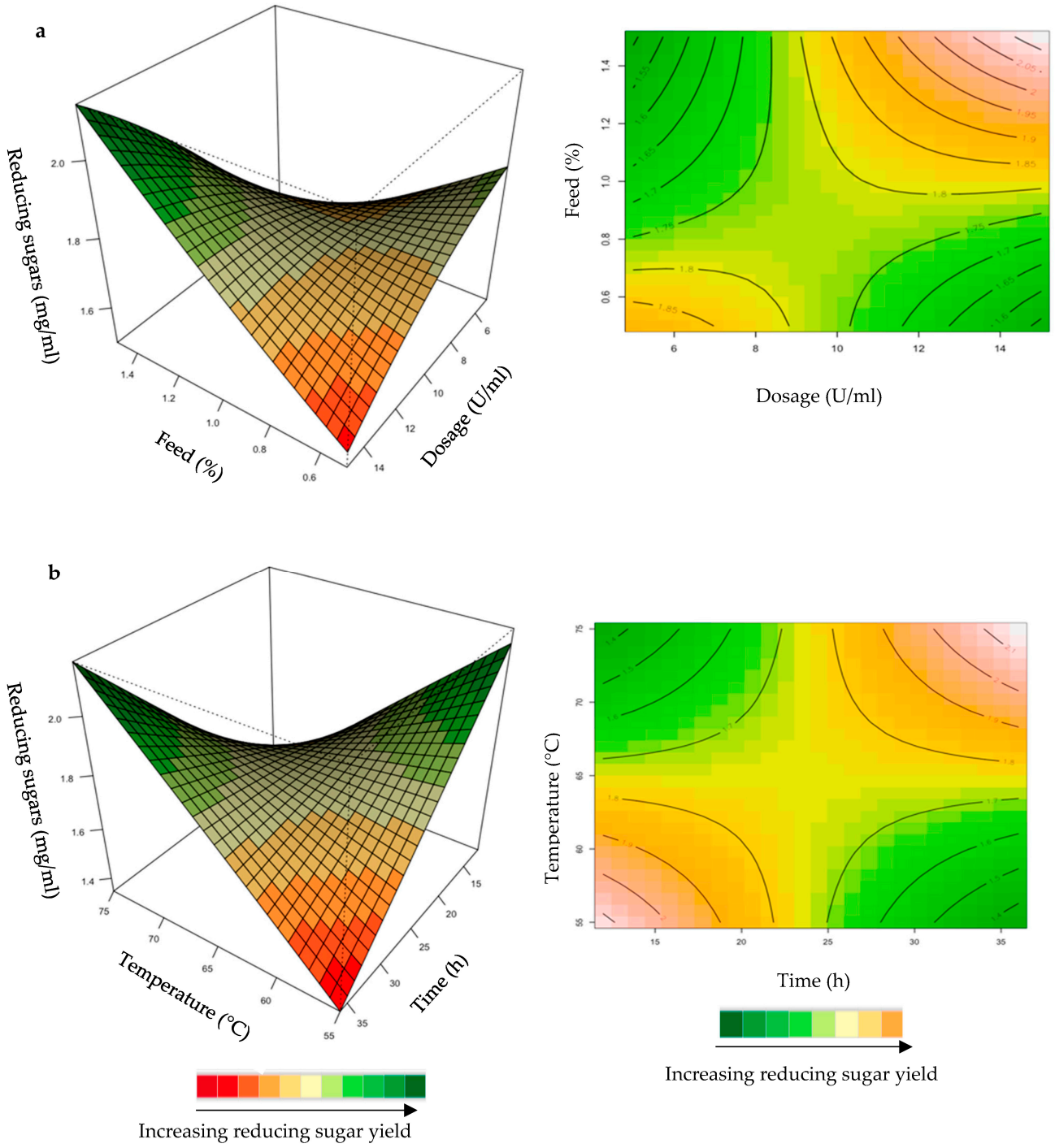

Figure 6. 3D-response surface plots and contour plots of the combined effects of enzyme dose and feed loading (**a**) and incubation time and temperature (**b**) on the yield of reducing sugars from grower chicken feed hydrolysed by the purified *T. harzianum* xylanase.

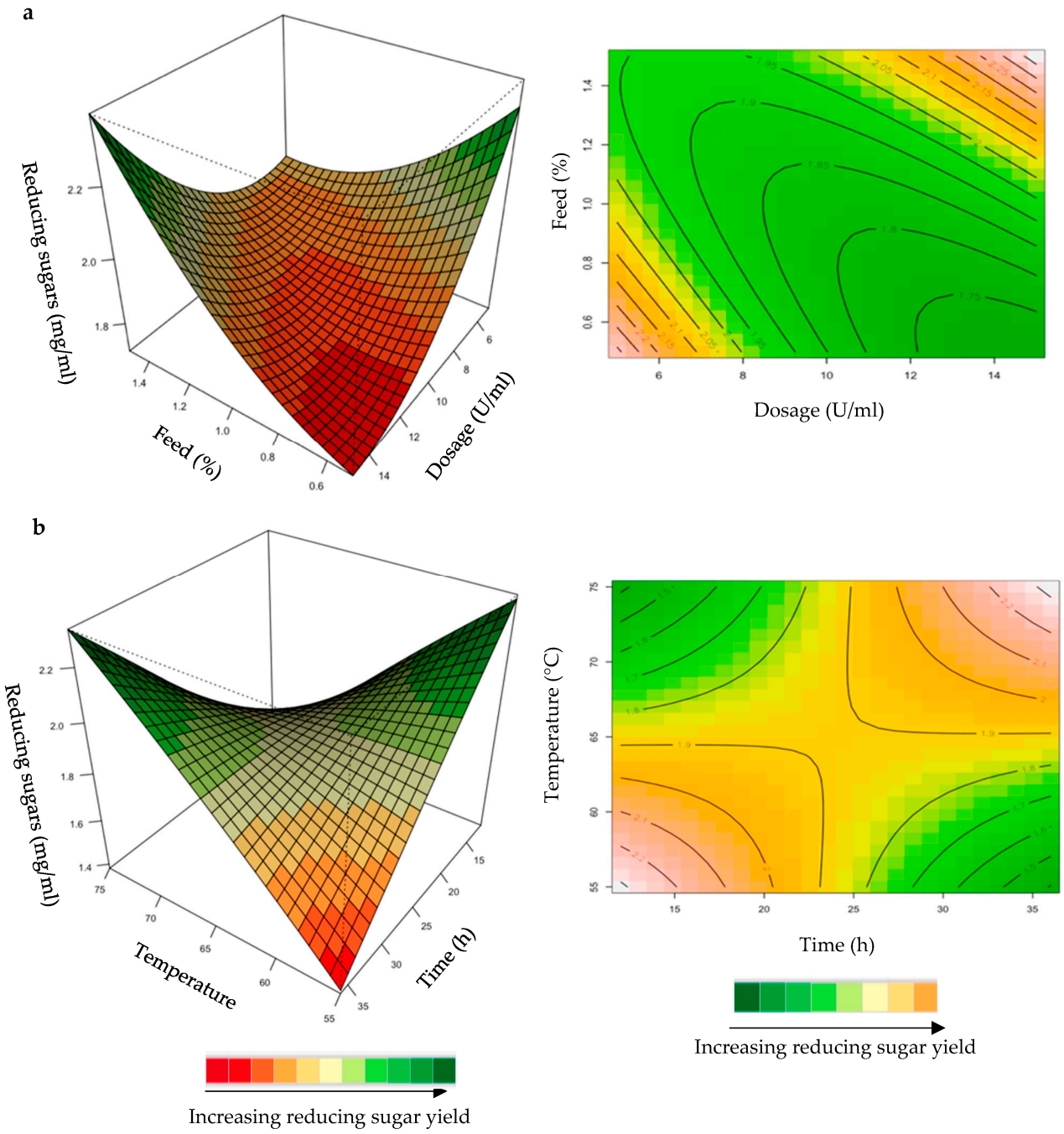

Figure 7. 3D-response surface plots and contour plots of the combined effects of dose and feed loading (**a**) and incubation time and temperature (**b**) on the yield of reducing sugars from the starter chicken feed hydrolysed by the purified recombinant XT6.

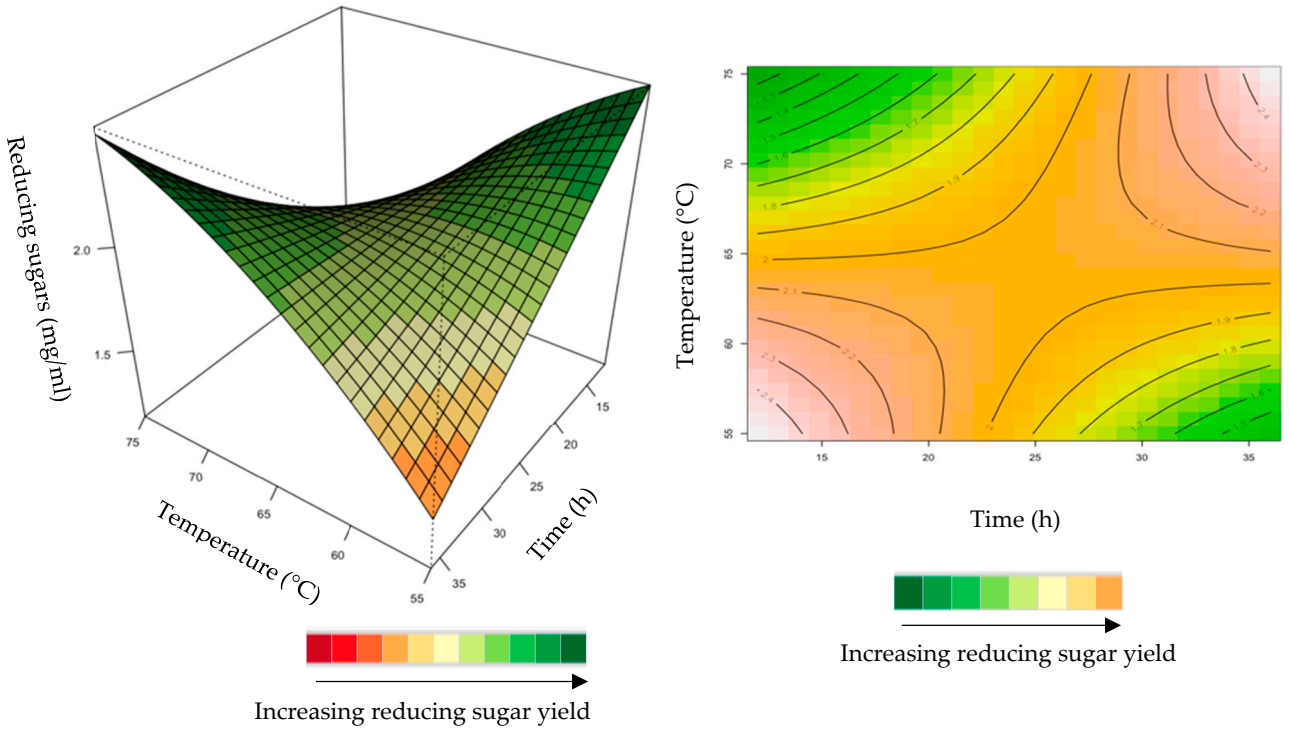

Figure 8. 3D-response surface plot and contour plot of the combined effects of incubation time and temperature on the yield of reducing sugars from the grower chicken feed hydrolysed by the purified recombinant XT6.

Effect of the Crude *T. harzianum* Xylanase on Reducing Sugar Yield Following Hydrolysis of Starter and Grower Chicken Feeds

The hydrolysis of the xylan in chicken feed can be influenced by the feed loading, enzyme dosage, incubation time, incubation temperature, and pH. The interactive effects of the variables were analysed for hydrolysis of the starter and grower chicken feeds by the crude *T. harzianum* xylanase (Figure 4a,b). For this analysis, the other parameters were kept constant at their zero (optimal) levels. The mutual interaction of the variables (feed loading: incubation time; incubation time: incubation temperature) were significant ($p \leq 0.05$), indicating that there is a synergistic interaction favouring the production of reducing sugars by the crude *T. harzianum* xylanase from starter chicken feed. The highly elliptical response surface plot in Figure 4a shows the that highest reducing sugars yield (3 mg/mL) was produced when both variables, feed loading and incubation time, were high. Chapa et al. [29] also obtained similar results, demonstrating that as the incubation time increased there was an increase in reducing sugars. Ai et al. [30] reported 3.9 mg/mL of reducing sugars from pretreated corncobs hydrolysed for 24 h by the *Streptomyces olivaceoviridis* xylanase. Feed loading also plays an important role in enzymatic hydrolysis [29]. Increasing the concentration of feed showed a substantial increase in reducing sugars, while decreasing the feed loading from 1.0% to 1.4% decreased the yield of reducing sugars. It is clear from Figure 4a that a higher feed loading (>1.0%) does not enhance the yield of reducing sugars. The lower yield of reducing sugars from higher feed loads could be attributed to the reduced availability of water in the aqueous medium. This trend was also observed by Yoon et al. [31]. Figure 4b shows a high yield at low incubation temperatures and times. Temperature is one of the most important parameters for enzyme activity. The optimization of reaction temperature was necessary to achieve optimal functioning of the enzyme in the provided conditions because of the well-established facts of enzyme inhibition at lower temperatures and enzyme inactivation at higher temperatures [32]. Figure 4b shows that the yield of reducing sugars was significantly higher at 55 °C and an incubation time of approximately 25 h. The production of reducing sugars was reduced at 70–75 °C, which

may be due to inactivation of the enzyme at these higher temperatures and longer incubation times. The interactions of the variables for the hydrolysis of grower feed by the crude *T. harzianum* xylanase were not significant ($p \leq 0.05$) (Supplementary Figures S1 and S2).

Effect of the Purified *T. harzianum* Xylanase on Reducing Sugar Yield Following Hydrolysis of Starter and Grower Chicken Feeds

The mutual interaction of the variables (enzyme dosage: incubation time; incubation time: temperature) was significant ($p \leq 0.05$), indicating that there is synergistic interaction favouring the production of reducing sugars by the activity of the purified *T. harzianum* xylanase on starter chicken feeds. Enzyme dose plays a significant role in increasing the reducing sugars and XOS yield [33]. Enzyme doses in the range of 5–15 U/mL were used in the present study. Enhanced yield of reducing sugars was obtained for long incubation times and high enzyme doses (Figure 5a). The contour plot showed that an incubation time of approximately 30 h and a 13 U/mL enzyme dosage resulted in the highest yield of reducing sugars. Yang et al. [34] observed that an increase in xylanase dose from 5 to 10 U/mL increased the reducing sugar to 12 g/L from 11 g/L after 24 h of incubation in their experiments. Enzymes can be more effective after a pre-treatment of the substrate, since this increases the accessibility of the active sites of the substrate to the enzyme. The decreased effectiveness of enzyme activity on untreated substrates could be attributed to the location of the hydrolysable xylans, which are usually located at the periphery of the particles of substrates [33]. The interaction between incubation time and temperature (Figure 5b) resulted in the highest yield of reducing sugars at high (75 °C) temperatures and prolonged incubation times (35 h).

For the optimization of reducing sugars from hydrolysis of grower chicken feed, the yield was enhanced at high dosage and feed loading (Figure 6a). For the interaction between time and temperature (Figure 6b), the reducing sugars yield was enhanced at long incubation times and high temperatures. The positive effects of high temperatures on the production of reducing sugars is the dissolution of xylan, the prevention of microbial contamination, and an increase in the reaction rate [35]. The interactions of the other variables were insignificant (Supplementary Figures S3 and S4).

Effect of the Recombinant XT6 Xylanase on Reducing Sugar Yield Following Hydrolysis of Starter and Grower Chicken Feeds

The mutual interaction of the variables (enzyme dose: feed loading; incubation time: temperature) were significant ($p \leq 0.05$), indicating that there is synergistic interaction favouring the production of reducing sugars by the purified recombinant XT6 on starter feed. An enhanced yield of reducing sugars was evident at high enzyme doses and feed loading (Figure 7a). At high incubation temperatures and long incubation times, the yield of reducing sugars was enhanced (Figure 7b). Li et al. [36] reported a *Streptomyces* spp. T7 which was used to produce XOSs from corncob xylan at 60 °C, with the highest yield of reducing sugars. Khangwal et al. [21] also reported a recombinant xylanase, SipoEnXyn10 (*Streptomyces ipomoeae* cloned and expressed in *E. coli*), which was used to produce XOS from beechwood xylan at 65 °C with the highest yield of reducing sugars.

The interactive effect of time and temperature were examined, and the results are illustrated in Figure 8. The mutual interaction of these variables (time: temperature) was significant ($p > 0.05$), indicating that there is synergistic interaction favouring the production of reducing sugars by the purified recombinant XT6 on grower feed. Both high (35 h and 75 °C) and low (15 h and 55 °C) levels in BBD enhanced the yield of reducing sugars.

2.2. Thin Layer Chromatography (TLC) and High Performance Liquid Chromatography (HPLC) Analysis of Feed Hydrolysis Products

The TLC was performed to visualize the monosaccharides/XOS and the degree of polymerization (DP) of the XOS produced following the hydrolysis of the local chicken feeds by the three enzyme preparations (Figure 9a–d). After the optimal hydrolysis treatments, 2.9 U/mL, 8.65 U/mL, and 3.63 U/mL reducing sugars were produced from starter

feed hydrolysed by the crude *T. harzianum* xylanase, purified *T. harzianum* xylanase, and recombinant XT6 xylanase, respectively. Hydrolysis of the grower chicken feed produced 2.5 U/mL, 3.96 U/mL, and 3.60 U/mL reducing sugars by the crude fungal xylanase, purified fungal xylanase, and recombinant xylanase, respectively. The TLC analysis indicated the production of XOS of DP 2–6 (equivalent to X2–X6) in the enzymatic reactions. The substrate controls displayed some faint spots that corresponded to those of the hydrolysed samples. This may have been due to their breakdown during the termination of the reaction (heating at 100 °C). Figure 9d shows the monosaccharides glucose and galactose following chicken feed hydrolysis. One of the attractive features of the process was the production of only XOS and no xylose. The absence of xylose and the predominant production of xylobiose suggest a unique specificity and catalytic mechanism of the thermophilic xylanase. This indicates that the enzyme has a higher affinity for cleaving the glycosidic bonds at specific positions within the xylan substrate, resulting in the release of xylobiose as the primary product. The absence of xylose in our study was beneficial because previous research has indicated that xylose production can hinder the production of XOS [37]. Hegazy et al. [38] also reported non-competitive end product inhibition by xylose of a *G. stearothermophilus* derived xylanase, XT6.

In addition to glucose and galactose observed on TLC (Figure 9d), hydrolysis of chicken feeds by the three enzyme preparations also produced mannose evident in HPLC chromatograms (Figure 10). Xylobiose (X2) was the only XOS observed by HPLC (Figure 10). Khangwal et al. [21] observed xylobiose as the major product from corncobs and *Moso bamboo.* The hydrolysis of grower chicken feed by purified *T. harzianum* xylanase produced the highest concentration of xylobiose and the lowest concentration was observed by the hydrolysis of grower feed hydrolysed by the crude *T. harzianum* xylanase. Overall, hydrolysis using the purified *T. harzianum* xylanase resulted in higher monosaccharides and xylobiose concentrations than the crude *T. harzianum* xylanase and recombinant XT6 xylanase. The yield of XOS with DP 3 and higher could not be measured due to the unresolved HPLC peaks. However, the spots for X3, X4, and X5 were noted to be predominant as shown on TLC chromatograms.

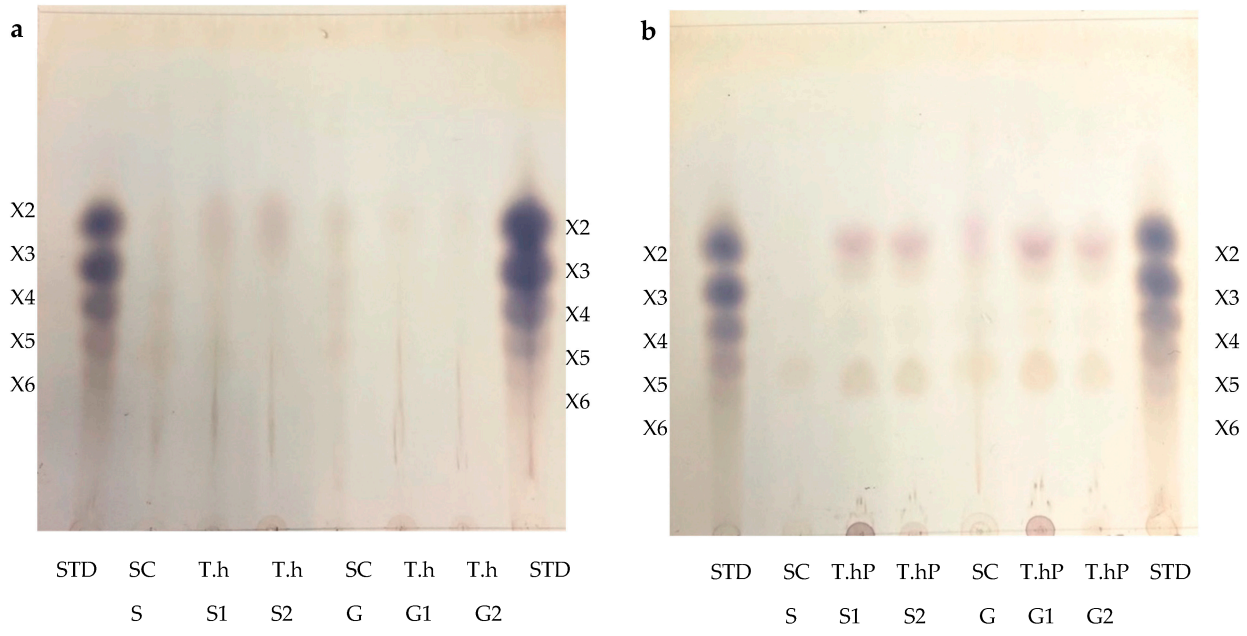

Figure 9. *Cont.*

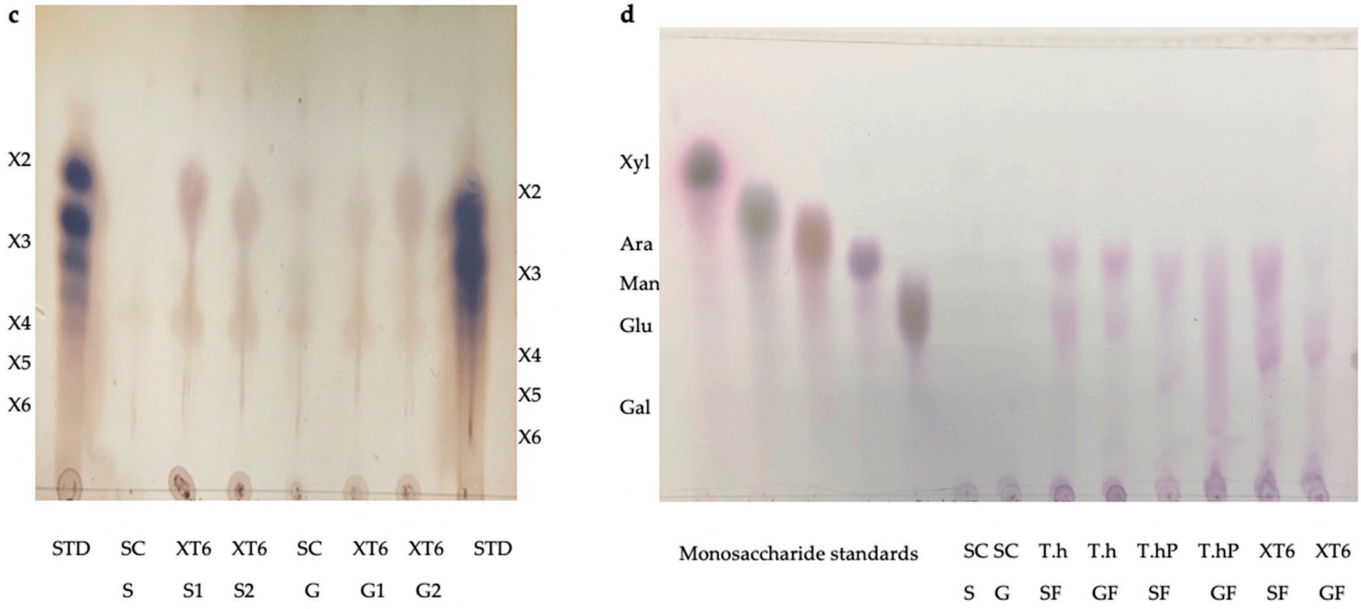

Figure 9. Thin Layer Chromatography (TLC) profile of XOS produced from chicken feed hydrolysis by the crude (**a**) and purified (**b**) *T. harzianum* xylanases and the recombinant XT6 xylanase (**c**). (**d**) shows the TLC profile of the monosaccharides resulting from chicken feed hydrolysis by the three enzyme preparations. STD—Xylooligosaccharides standards, SC (S)—substrate control (no xylanase) starter feed, SC (G)–Substrate control (no xylanase) grower feed, T.h S1—starter feed with crude *T. harzianum* xylanase (sample 1), T.h S2—starter feed with crude *T. harzianum* xylanase (sample 2), T.h G—grower feed with crude *T. harzianum* xylanase (sample 1) and T.h G2—grower feed with crude *T. harzianum* xylanase (sample 2). T.hP S1—starter feed with purified *T. harzianum* xylanase (sample 1), T.hP S2—starter feed with purified *T. harzianum* xylanase (sample 2), T.hP G1–grower feed with purified *T. harzianum* xylanase (sample 1) and T.hP G2—grower feed with purified *T. harzianum* xylanase (sample 2). X2—Xylobiose; X3—Xylotriose; X4—Xylotetraose; X5—Xylopentaose; X6—Xylohexaose. Monosaccharide standards; Xyl—xylose, Ara–arabinose, Man—mannose, Glu—glucose, and Gal—galactose. T.h SF—starter feed with crude *T. harzianum* xylanase, T.h GF—grower feed with crude *T. harzianum* xylanase, T.hP SF—starter feed with purified *T. harzianum* xylanase, T.hP GF—grower feed with purified *T. harzianum* xylanase, XT6 SF—recombinant XT6 xylanase with starter feed and XT6 GF–recombinant XT6 xylanase with grower feed.

Lately, XOS (particularly xylobiose) has attracted interest as an effective prebiotic that has beneficial effects on animal and human digestion [39]. Xylanases are desirable for XOS production from biomass hydrolysis. TLC analysis revealed that the hydrolysis of xylan biomass produced short-chain (DP 2–6) XOS (Figure 9). Similar results were obtained in previous reports on xylanases [40,41]. The production of XOS of similar DP at moderate temperatures highlights the suitability of xylanases for the bioprocessing industries that are preferably performed with less (heat) energy input. Nonetheless, the HPLC-based estimation of XOS yield by xylanases does not include the DP 3 and higher oligosaccharides that are evident in TLC chromatograms (Figure 9a–c). XOS is reported to have the capability of aiding in the proliferation of the population of beneficial gut microflora [42,43]. Further, the XOS of this DP range (2–6) has enormous intestinal-health potential and anti-cancerous prospects [7]. Hydrolysis of starter and grower feeds produced XOS that transitioned between the standards on TLC (Figure 9). This observation may have been due to the substitution of the arabinoxylan in the feeds, which led to the formation of a suspension of feeds in the buffer and, thus, did not result in the release of soluble xylans [44].

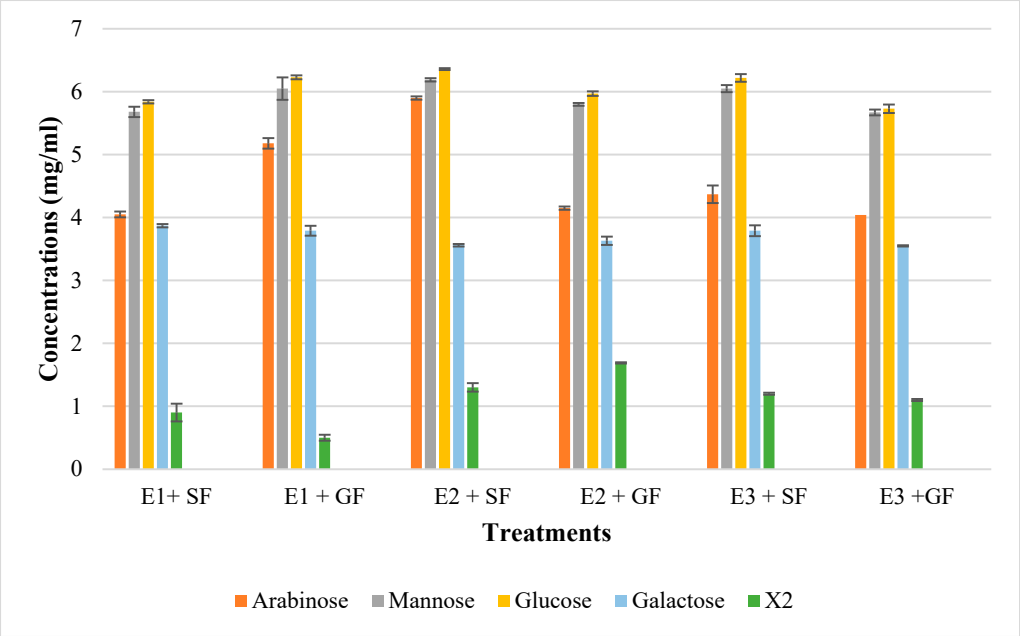

Figure 10. The High-Performance Liquid Chromatography (HPLC) profile of monosaccharides and xylooligosaccharides resulting from chicken feed hydrolysis. E1 + SF Crude *T. harzianum* xylanase + starter chicken feed, E1 + G—crude *T. harzianum* xylanase + grower chicken feed, E2 + S—purified *T. harzianum* xylanase + starter chicken feed, E2 + G—purified *T. harzianum* xylanase + grower chicken feed, E3 + S—purified recombinant XT6 xylanase + starter chicken feed and E3 + G—purified recombinant XT6 xylanase + grower chicken feed. Data points represent the mean values ± SD (n = 3).

3. Materials and Methods

3.1. Feed Samples and Enzymes

Chicken starter and grower feed substrates were obtained from Rhodes University, Grahamstown, Eastern Cape. According to Biasato et al. [45], the feeds for monogastric animals such as chickens and pigs in South Africa primarily consist of corn as the main energy source and soybean as the main protein source. Studies by El-Deek et al. [46] and Saleh and Watkins [47] have reported that the formulations of starter and grower feeds for broilers often vary in terms of the ratio of corn to soybean. It was observed that starter feeds generally contain more soybean and less corn compared to grower feeds [44]. Table 5 represents the composition of the feeds used in this study. A crude and purified *T. harzianum* xylanase was previously studied and included in this study [19,25]. A recombinant XT6 xylanase previously optimized and purified [26] and was included in this study.

Table 5. Feed composition of the starter and grower feeds for broilers.

Composition (%)	Starter Feed	Grower Feed
Methionine	0.23	0.10
Lysine	0.10	0.16
Kynofos 21 (Mono dicalcium phosphate (MDCP))	1.15	0.80
Salt	0.36	0.30
Premix	0.30	0.30
Feed lime	1.46	2.34
Maize bran	4.00	6.00
Soybean	35.00	20.00
Maize	57.40	70.00

3.2. Optimization of the Hydrolysis of Feed Using the Crude and Pure Fungal T. harzianum and Pure Recombinant XT6 Xylanases

The crude and purified *T. harzianum* xylanases and purified recombinant XT6 xylanase were used in this study to hydrolyse xylan in starter and grower chicken feeds. The RSM using the BBD was used to study the influence of five variables on the hydrolysis of chicken feeds by xylanases and to statistically determine the optimum combination of enzyme dosage, feed loading, incubation time, pH, and incubation temperature for enhanced hydrolysis, which was achieved by monitoring reducing sugars (mg/mL) as the endpoint. This was achieved using the 3,5-Dinitrosalicylic acid (DNS) assay. The main interactions and the quadratic effects of the variables on enzymatic hydrolysis of the feed were also assessed, and a five-factor, three-level design was applied to investigate the quadratic response surfaces and construct secondary polynomial models. Each variable was coded and run at three independent levels, (−), (0), and (+) levels. The significant relationships in the model were assessed and all the statistical analyses were carried out using R Studio software (http://www.R-project.org/ (accessed on 15 March 2023)) [48]. The effect of each factor and their interactions on the dependent variables was assessed by the two-way Analysis of variance (ANOVA) technique [19,49]. The optimization data were analysed to determine the regression coefficients to arrive at the regression equation. The regression model containing coefficients, including the linear and quadratic effect of factors and the linear effect of interactions, was assumed to describe relationships between response (Y) and the experimental factors (X1, X2, X3, X4, and X5).

The second-order polynomial equation is shown below in Equation (1):

$$Y = \beta 0 + \sum \beta i\ X1 + \sum \beta ii\ X2 + \sum \beta ij\ X1 \times 2 \quad (1)$$

where β0 is the constant coefficient, βi is the linear coefficient of main factors, βii is the quadratic coefficient for main factors, and βij is the second-order interaction coefficient. The response variable was assigned at low and high of the observed values for the desirability of 0 and 1, respectively, to obtain the overall desirability [29].

3.3. Chromatographic Analysis of Hydrolysed Products

The qualitative and quantitative analyses of monosaccharides and XOS resulting from the feed hydrolysis were carried out using 2 µL aliquots from each hydrolysate for TLC and HPLC. The hydrolysate samples were applied to Silica Gel 60 F254 TLC plates (Merck, Darmstadt, Germany), which were then developed in a 1-butanol: acetic acid: water (2:1:1, *v*/*v*/*v*) mobile phase. The plates were left to air dry for 1 h and were then stained by soaking in Molisch's Reagent (0.3% (*w*/*v*) α-naphthol dissolved in a sulfuric acid: methanol solution (5:95, *v*/*v*)). The sugars developed on the plates were finally visualized by heating the plates at 110 °C in an oven (Heraeus B6120 Incubator, Gemini BV, Apeldoorn, The Netherlands) for 15 min. An XOS standard containing a mixture of xylobiose (X2), xylotriose (X3), xylotetraose (X4), xylopentaose (X5), and xylohexaose (X6)) was obtained from Professor Kugen Perumal at Durban University of Technology. Monosaccharide standards (xylose, arabinose, mannose, glucose, and galactose) were purchased from Sigma, Aldrich, Modderfontein, South Africa). The yield of monosaccharides and XOS were estimated by HPLC. The supernatant fractions from the hydrolysates were filtered using a 0.2 µm filter. The XOS and monosaccharides in the samples were quantified with a Shimadzu RID-20A HPLC system (Shimadzu Scientific Instruments, Southern California, CA, USA) using a BioRad Aminex HPX-87H column (Bio-Rad, Transgenomic, Inc., Omaha, NE, USA) at 50 °C with a mobile phase of 5 mM H_2SO_4 and a flow rate of 0.5 mL/min and samples were analysed with a refractive index (RI) detector.

4. Conclusions

The present study established the potential of native *T. harzianum* and recombinant *G. strearothermophilus* xylanases for the enhancement of the hydrolysate product and the production of XOS from starter and grower chicken feeds. Starter feed hydrolysis re-

sulted in higher yields of reducing sugars compared to grower feed. Overall, the purified *T. harzianum* xylanase resulted in a higher yield of reducing sugars compared to the crude *T. harzianum* xylanase and recombinant XT6 xylanase. The RSM efficiently optimized the yield of reducing sugars and quantified the interactive effects of the significant variables. The xylanases were efficient in releasing short-chain XOSs (xylobiose, xylotriose, xylotetraose, and xylopentaose) and monosaccharides (glucose, galactose, and mannose), with xylobiose being the dominant product. This shows interesting prospects for future studies using XOS as prebiotics in the feed industry and to reduce viscosity and improve the gut microbiota.

Supplementary Materials: The supporting information can be downloaded at: https://www.mdpi.com/article/10.3390/ijms242317110/s1.

Author Contributions: Experimental research, conceptualization, methodology, software validation, formal analysis, data curation, writing, P.D.; review and editing, R.G. and B.P.; supervision, R.G., B.P. and B.S. All authors have read and agreed to the published version of the manuscript.

Funding: Funding acquisition, B.S. The study was supported by BS and TIA and CSIR. This research was funded by the University of KwaZulu-Natal and the Technology Innovation Agency (TIA) managed DST/CON/0177/2018: SIIP: ENZYME AND MICROBIAL TECHNOLOGIES (EMT) grant and the Biorefinery Industry Development Facility (BIDF) at the Council for Scientific and Industrial Research (CSIR), Durban, South Africa.

Institutional Review Board Statement: Not applicable.

Data Availability Statement: The datasets used and/or analysed during the current study are available from the corresponding author upon reasonable request. Other data generated or analysed during this study are included in this article [and its supplementary information file].

Conflicts of Interest: The authors declare no conflict of interest.

References

1. McLoughlin, R.F.; Berthon, B.S.; Jensen, M.E.; Baines, K.J.; Wood, L.G. Short-chain fatty acids, prebiotics, synbiotics, and systemic inflammation: A systematic review and meta-analysis. *Am. J. Clin. Nutr.* **2017**, *106*, 930–945. [CrossRef] [PubMed]
2. Passos, A.A.; Park, I.; Ferket, P.; von Heimendahl, E.; Kim, S.W. Effect of dietary supplementation of xylanase on apparent ileal digestibility of nutrients, viscosity of digesta, and intestinal morphology of growing pigs fed corn and soybean meal-based diet. *Anim. Nutr.* **2015**, *1*, 19–23. [CrossRef]
3. Duarte, M.E.; Zhou, F.X.; Dutra, W.M.; Kim, S.W. Dietary supplementation of xylanase and protease on growth performance, digesta viscosity, nutrient digestibility, immune and oxidative stress status, and gut health of newly weaned pigs. *Anim. Nutr.* **2019**, *5*, 351–358. [CrossRef] [PubMed]
4. Duarte, M.E.; Tyus, J.; Kim, S.W. Synbiotic effects of enzyme and probiotics on intestinal health and growth of newly weaned pigs challenged with enterotoxigenic F18+*Escherichia coli*. *Front. Vet. Sci.* **2020**, *7*. [CrossRef] [PubMed]
5. Aragon, C.C.; Ruiz-Matute, A.I.; Corzo, N.; Monti, R.; Guisán, J.M.; Mateo González, C. Production of Xylo-oligosaccharides (XOS) by controlled hydrolysis of xylan using immobilized xylanase from *Aspergillus niger* with improved properties. *Integr. Food Nutr. Metab.* **2020**, *5*, 1–9. [CrossRef]
6. Donaldson, J.; Świątkiewicz, S.; Arczewka-Włosek, A.; Muszyński, S.; Szymańczyk, S.; Arciszewski, M.B.; Siembida, A.Z.; Kras, K.; Piedra, J.L.V.; Schwarz, T.; et al. Modern hybrid rye, as an alternative energy source for broiler chickens, improves the absorption surface of the small intestine depending on the intestinal part and xylanase supplementation. *Animals* **2021**, *11*, 1349. [CrossRef]
7. Saini, R.; Patel, A.K.; Saini, J.K.; Chen, C.W.; Varjani, S.; Singhania, R.R.; Di Dong, C. Recent advancements in prebiotic oligomers synthesis via enzymatic hydrolysis of lignocellulosic biomass. *Bioengineered* **2022**, *13*, 2139–2172. [CrossRef]
8. Dong, C.D.; Tsai, M.L.; Nargotra, P.; Kour, B.; Chen, C.W.; Sun, P.P.; Sharma, V. Bioprocess development for the production of xylooligosaccharides prebiotics from agro-industrial lignocellulosic waste. *Heliyon* **2023**, *9*, 18316. [CrossRef]
9. Malgas, S.; Pletschke, B.I. The effect of an oligosaccharide reducing-end xylanase, BhRex8A, on the synergistic degradation of xylan backbones by an optimised xylanolytic enzyme cocktail. *Enzyme Microb. Technol.* **2019**, *122*, 74–81. [CrossRef]
10. Carvalho, A.F.A.; Neto, P.D.O.; da Silva, D.F.; Pastore, G.M. Xylo-oligosaccharides from lignocellulosic materials: Chemical structure, health benefits and production by chemical and enzymatic hydrolysis. *Food Res. Int.* **2023**, *51*, 75–85. [CrossRef]
11. Gurpilhares, D.D.B.; Cinelli, L.P.; Simas, N.K.; Pessoa, A., Jr.; Sette, L.D. Marine prebiotics: Polysaccharides and oligosaccharides obtained by using microbial enzymes. *Food Chem.* **2019**, *280*, 175–186. [CrossRef] [PubMed]

12. Zhang, J.; Wang, Y.H.; Wei, Q.Y.; Du, X.J.; Qu, Y.S. Investigating desorption during ethanol elution to improve the quality and antioxidant activity of xylo-oligosaccharides from corn stalk. *Bioresour. Technol.* **2018**, *249*, 342–347. [CrossRef] [PubMed]
13. Zhao, C.; Wu, Y.; Liu, X.; Liu, B.; Cao, H.; Yu, H.; Sarker, S.D.; Nahar, L.; Xiao, J. Functional properties, structural studies and chemo-enzymatic synthesis of oligosaccharides. *Trends Food Sci. Technol.* **2017**, *66*, 135–145. [CrossRef]
14. Bertacchi, S.; Jayaprakash, P.; Morrissey, J.P.; Branduardi, P. Interdependence between lignocellulosic biomasses, enzymatic hydrolysis and yeast cell factories in biorefineries. *Microb. Biotechnol.* **2022**, *15*, 985–995. [CrossRef] [PubMed]
15. Shehata, A.A.; Yalçın, S.; Latorre, J.D.; Basiouni, S.; Attia, Y.A.; Abd El-Wahab, A.; Visscher, C.; El-Seedi, H.R.; Huber, C.; Hafez, H.M.; et al. Probiotics, prebiotics, and phytogenic substances for optimizing gut health in poultry. *Microorganisms* **2022**, *10*, 395. [CrossRef] [PubMed]
16. Morgan, N.K.; Wallace, A.; Bedford, M.R.; Choct, M. Efficiency of xylanases from families 10 and 11 in production of xylo-oligosaccharides from wheat arabinoxylans. *Carbohydr. Polym.* **2017**, *167*, 290–296. [CrossRef] [PubMed]
17. Qian, S.; Zhou, J.; Chen, X.; Ji, W.; Zhang, L.; Hu, W.; Lu, Z. Evaluation of an efficient fed-batch enzymatic hydrolysis strategy to improve production of functional xylooligosaccharides from maize straws. *Ind. Crops Prod.* **2020**, *157*, 112920. [CrossRef]
18. Wu, W.J.; Ahn, B.Y. Statistical optimization of medium components by response surface methodology to enhance menaquinone-7 (vitamin k2) production by *Bacillus subtilis*. *J. Microbiol. Biotechnol.* **2018**, *28*, 902–908. [CrossRef]
19. Dhaver, P.; Pletschke, B.; Sithole, B.; Govinden, R. Optimization, purification, and characterization of xylanase production by a newly isolated *Trichoderma harzianum* strain by a two-step statistical experimental design strategy. *Sci. Rep.* **2022**, *12*, 17791. [CrossRef]
20. Joshi, N.; Sharma, M.; Singh, S.P. Characterization of a novel xylanase from an extreme temperature hot spring metagenome for xylooligosaccharide production. *Appl. Microbiol. Biotechnol.* **2020**, *104*, 4889–4901. [CrossRef]
21. Khangwal, I.; Nath, S.; Kango, N.; Shukla, P. Endo-xylanase induced xylooligosaccharides production from corn cobs, its structural features, and concentration-dependent antioxidant activities. *Biomass Convers. Biorefinery* **2022**, *12*, 5707–5717. [CrossRef]
22. Stan, G.S.; Badea, I.A.; Aboul-Enein, H.Y. HPLC method for quantification of five compounds in a parenteral form used in treatment of companion animals. *J. Chromatogr. Sci.* **2016**, *54*, 1567–1572. [CrossRef] [PubMed]
23. Pu, J.; Zhao, X.; Wang, Q.; Wang, Y.; Zhou, H. Development and validation of a HPLC method for determination of degree of polymerization of xylo-oligosaccharides. *Food Chem.* **2016**, *213*, 654–659. [CrossRef] [PubMed]
24. Debebe, A.; Temesgen, S.; Redi-Abshiro, M.; Chandravanshi, B.S.; Ele, E. Improvement in analytical methods for determination of sugars in fermented alcoholic beverages. *J. Anal. Methods Chem.* **2018**, *8*, 4010298. [CrossRef]
25. Dhaver, P.; Pletschke, B.; Sithole, B.; Govinden, R. Isolation, screening and partial optimization of thermostable xylanase production under submerged fermentation by fungi in Durban, South Africa. *Mycology* **2022**, *13*, 271–292. [CrossRef]
26. Dhaver, P.; Sithole, T.; Pletschke, B.; Sithole, B.; Govinden, R. Enhanced production of a recombinant xylanase (XT6): Optimization of production and purification, and scaled-up batch fermentation in a stirred tank bioreactor. *Sci. Rep.* **2023**, *13*, 20895. [CrossRef]
27. Chen, Y.; Xie, Y.; Ajuwon, K.M.; Zhong, R.; Li, T.; Chen, L.; Zhang, H.; Beckers, Y.; Everaert, N. Xylo-oligosaccharides, preparation and application to human and animal health: A review. *Front. Nutr.* **2021**, *8*, 731930. [CrossRef]
28. Ataei, D.; Hamidi-Esfahani, Z.; Ahmadi-Gavlighi, H. Enzymatic production of xylooligosaccharides from date (*Phoenix dactylifera* L.) seed. *Food Sci. Nutr.* **2020**, *8*, 6699–6707. [CrossRef] [PubMed]
29. Chapa, D.; Pandit, P.; Shah, A. Production of xylooligosaccharides from corncob xylan by fungal xylanase and their utilization by probiotics. *Bioresour. Technol.* **2012**, *115*, 215–221. [CrossRef]
30. Ai, Z.; Jiang, Z.; Li, L.; Deng, W.; Kusakabe, I.; Li, H. Immobilization of *Streptomyces olivaceoviridis* E-86 xylanase on Eudragit S-100 for xylo-oligosaccharide production. *Process Biochem.* **2005**, *40*, 2707–2714. [CrossRef]
31. Yoon, K.Y.; Woodams, E.E.; Hang, Y.D. Enzymatic production of pentoses from the hemicellulose fraction of corn residues. *LWT* **2006**, *39*, 387–391. [CrossRef]
32. Sun, Q.; Patil, P.J.; Singh, A.K.; Teng, C.; Zhou, M.; Zhou, Y.; Fan, G. Optimization of pre-treatment and enzymatic hydrolysis coupled with ultrasonication for the production of xylooligosaccharides from corn cob. *Biomass Convers. Biorefinery* **2023**, *2023*. [CrossRef]
33. Gowdhaman, D.; Ponnusami, V. Production and optimization of xylooligosaccharides from corncob by *Bacillus aerophilus* KGJ2 xylanase and its antioxidant potential. *Int. J. Biol. Macromol.* **2015**, *79*, 595–600. [CrossRef] [PubMed]
34. Yang, R.; Xu, S.; Wang, Z.; Yang, W. Aqueous extraction of corncob xylan and production of xylooligosaccharides. *LWT* **2005**, *38*, 677–682. [CrossRef]
35. Yan, F.; Tian, S.; Du, K.; Xue, X.A.; Gao, P.; Chen, Z. Preparation and nutritional properties of xylooligosaccharides from agricultural and forestry by-products: A comprehensive review. *Front. Nutr.* **2022**, *9*, 977548. [CrossRef] [PubMed]
36. Li, Y.; Zhang, X.; Lu, C.; Lu, P.; Yin, C.; Ye, Z.; Huang, Z. Identification and characterization of a novel endo-β-1,4-xylanase from *Streptomyces* sp. T7 and its application in xylo-oligosaccharide production. *Molecules* **2022**, *27*, 2516. [CrossRef] [PubMed]
37. Rahmani, N.; Kahar, P.; Lisdiyanti, P.; Lee, J.; Prasetya, B.; Ogino, C.; Kondo, A. GH-10 and GH-11 Endo-1, 4-β-xylanase enzymes from *Kitasatospora* sp. produce xylose and xylooligosaccharides from sugarcane bagasse with no xylose inhibition. *Bioresour. Technol.* **2019**, *272*, 315–325. [CrossRef] [PubMed]
38. Hegazy, U.M.; El-Khonezy, M.I.; Shokeer, A.; Abdel-Ghany, S.S.; Bassuny, R.I.; Barakat, A.Z.; Salama, W.H.; Azouz, R.A.M.; Fahmy, A.S. Revealing of a novel xylose-binding site of *Geobacillus stearothermophilus* xylanase by directed evolution. *J. Biochem.* **2019**, *165*, 177–184. [CrossRef]

39. Rashin, R.; Sohail, M. Xylanolytic *Bacillus* species for xylooligosaccharides production: A critical review. *Bioresour. Bioprocess.* **2021**, *8*, 16. [CrossRef]
40. Su, Y.; Fang, L.; Wang, P.; Lai, C.; Huang, C.; Ling, Z.; Sun, S.; Yong, Q. Efficient production of xylooligosaccharides rich in xylobiose and xylotriose from poplar by hydrothermal pre-treatment coupled with post-enzymatic hydrolysis. *Bioresour. Technol.* **2021**, *342*, 125955. [CrossRef]
41. Valladares-Diestra, K.K.; de Souza Vandenberghe, L.P.; Soccol, C.R. Integrated xylooligosaccharides production from imidazole-treated sugarcane bagasse with application of in house produced enzymes. *Bioresour. Technol.* **2022**, *362*, 127800. [CrossRef]
42. Finegold, S.M.; Li, Z.; Summanen, P.H.; Downes, J.; Thames, G.; Corbett, K.; Dowd, S.; Krak, M.; Heber, D. Xylooligosaccharides increases bifidobacteria but not *lactobacilli* in human gut microbiota. *Food Funct.* **2014**, *5*, 436–445. [CrossRef] [PubMed]
43. De Maesschalck, C.; Eeckhaut, V.; Maertens, L.; De Lange, L.; Marchal, L.; Nezer, C.; De Baere, S.; Croubels, S.; Daube, G.; Dewulf, J.; et al. Effects of xylo-oligosaccharides on broiler chicken performance and microbiota. *Appl. Environ. Microbiol.* **2015**, *81*, 5880–5888. [CrossRef] [PubMed]
44. Sithole, T. Cloning, Expression, Partial Characterization and Application of a Recombinant GH10 Xylanase, XT6, from *Geobacillus stearothermophilus* T6 as an Additive to Chicken Feeds. Master's Thesis, Rhodes University, Grahamstown, South Africa, 2022.
45. Biasato, I.; Ferrocino, I.; Biasibetti, E.; Grego, E.; Dabbou, S.; Sereno, A.; Gai, F.; Gasco, L.; Schiavone, A.; Cocolin, L.; et al. Modulation of intestinal microbiota, morphology and mucin composition by dietary insect meal inclusion in free-range chickens. *BMC Vet. Res.* **2018**, *14*, 383. [CrossRef] [PubMed]
46. El-Deek, A.A.; Abdel-Wareth, A.A.; Osman, M.; El-Shafey, M.; Khalifah, A.M.; Elkomy, A.E.; Lohakare, J. Alternative feed ingredients in the finisher diets for sustainable broiler production. *Sci. Rep.* **2020**, *10*, 17743. [CrossRef]
47. Saleh, E.A.; Watkins, S.E.; Waldroup, P.W. Changing time of feeding starter, grower, and finisher diets for broilers 2. birds grown to 2.2 kg. *J. App. Poul. Res.* **1997**, *6*, 64–73. [CrossRef]
48. R Core Team. *R: A Language and Environment for Statistical Computing*; R Foundation for Statistical Computing: Vienna, Austria, 2020; Available online: http://www.R-project.org/ (accessed on 15 March 2023).
49. Singh, N.; Sithole, B.; Kumar, A.; Govinden, R. A glucose tolerant β-glucosidase from a newly isolated *Neofusicoccum parvum* strain F7: Production, purification, and characterization. *Sci. Rep.* **2023**, *13*, 5134. [CrossRef]

UNIVERSITY OF KWAZULU-NATAL
INYUVESI YAKWAZULU-NATALI

COLLEGE OF AGRICULTURE, ENGINEERING AND SCIENCE

PRIS 2022

POSTGRADUATE RESEARCH AND INNOVATION SYMPOSIUM 2022

Third Prize

Awarded to

Priyashini Dhaver

School of Life Sciences

For Presentation of Research: Flash (poster) Category

[redacted]

Professor Neil A. Koorbanally
College Dean of Research
08 - 09 December 2022

INSPIRING GREATNESS

UNIVERSITY OF KWAZULU-NATAL™
INYUVESI YAKWAZULU-NATALI

COLLEGE OF AGRICULTURE, ENGINEERING AND SCIENCE

First Prize

Awarded to

Priyashini Dhaver

School of Life Sciences

For Presentation of Research: Flash (poster) Category

[redacted]

Professor Neil A. Koorbanally
College Dean of Research

02 and 03 November 2023

DATE

INSPIRING GREATNESS